ADVANCED COMBUSTION ENGINE TECHNOLOGIES

VEHICLE TECHNOLOGIES PROGRAM

Less dependence on foreign oil today, and transition to a petroleum-free, emissions-free vehicle tomorrow.

2007

annual progress report

U.S. Department of Energy
Energy Efficiency and Renewable Energy
Bringing you a prosperous future where energy is clean, abundant, reliable, and affordable

U.S. Department of Energy
1000 Independence Avenue, S.W.
Washington, D.C. 20585-0121

FY 2007 PROGRESS REPORT FOR ADVANCED COMBUSTION ENGINE TECHNOLOGIES

Energy Efficiency and Renewable Energy
Office of Vehicle Technologies

Approved by Gurpreet Singh
Team Leader, Advanced Combustion Engine R&D
Office of Vehicle Technologies

December 2007

Acknowledgement

We would like to express our sincere appreciation to Alliance Technical Services, Inc. and Oak Ridge National Laboratory for their technical and artistic contributions in preparing and publishing this report.

In addition, we would like to thank all the participants for their contributions to the programs and all the authors who prepared the project abstracts that comprise this report.

Table of Contents

I. INTRODUCTION

I. Introduction

DEVELOPING ADVANCED COMBUSTION ENGINE TECHNOLOGIES

On behalf of the Department of Energy's Office of Vehicle Technologies, we are pleased to introduce the Fiscal Year (FY) 2007 Annual Progress Report for the Advanced Combustion Engine R&D Sub-Program. The mission of the Vehicle Technologies (VT) Program is to develop more energy-efficient and environmentally friendly highway transportation technologies that enable the United States to use less petroleum. The Advanced Combustion Engine R&D Sub-Program supports this mission and the President's initiatives by removing the critical technical barriers to commercialization of advanced internal combustion engines for light-, medium-, and heavy-duty highway vehicles that meet future Federal emissions regulations. The primary goal of the Advanced Combustion Engine R&D Sub-Program is to improve the brake thermal efficiency of internal combustion engines:

- for passenger vehicles, from 30% (2002 baseline) to 45% by 2010, and
- for commercial vehicles, from 40% (2002 baseline) to 55% by 2013,

while meeting cost, durability, and emissions constraints. R&D activities include work on combustion technologies that increase efficiency and minimize in-cylinder formation of emissions, aftertreatment technologies that further reduce exhaust emissions, as well as the impacts of these new technologies on human health. Research is also being conducted on approaches to produce useful work from waste engine heat through the development and application of thermoelectrics, electricity generation from exhaust-driven turbines, and incorporation of energy-extracting bottoming cycles.

Advanced internal combustion engines are a key element in the pathway to achieving the goals of the President's FreedomCAR and Fuel Partnership for transportation. Advanced engine technologies being researched will allow the use of hydrogen as a fuel in highly efficient and low-emission internal combustion engines, providing an energy-efficient interim hydrogen-based powertrain technology during the transition to hydrogen/fuel-cell-powered transportation vehicles. Hydrogen engine technologies being developed have the potential to provide diesel-like engine efficiencies with near-zero air pollution and greenhouse gas emissions.

This introduction serves to outline the nature, recent progress, and future directions of the Advanced Combustion Engine R&D Sub-Program. The research activities of this Sub-Program are planned in conjunction with the FreedomCAR and Fuel Partnership and the 21st Century Truck Partnership (CTP) and are carried out in collaboration with industry, national laboratories, and universities. Because of the importance of clean fuels in achieving high efficiency and low emissions, R&D activities are closely coordinated with the relevant activities of the Fuel Technologies Sub-Program, also within the Office of Vehicle Technologies.

BACKGROUND

Advanced combustion engines have great potential for achieving dramatic energy efficiency improvements in light-duty vehicle applications, where it is suited to both conventional and hybrid-electric powertrain configurations. Light-duty vehicles with advanced combustion engines can compete directly with gasoline engine hybrid vehicles in terms of fuel economy and consumer-friendly driving characteristics; also, they are projected to have energy efficiencies that are competitive with hydrogen fuel cell vehicles when used in hybrid applications. The primary hurdles that must be overcome to realize increased use of advanced combustion engines in light-duty vehicles are the higher cost of these engines compared to conventional engines and compliance with the U.S. Environmental Protection Agency's (EPA's) Tier 2 regulations which are phasing in from 2004-2009. The Tier 2 regulations require all light-duty vehicles to meet the same emissions standards, regardless of the powertrain. Compliance can be achieved with advanced combustion engines through the addition of catalytic emission control technologies, though these technologies are much less mature than gasoline engine catalysts and are severely affected by sulfur from the fuel and lubricant. Even the recent reduction

of diesel fuel sulfur content to below 15 ppm does not assure that catalytic emission control devices will be durable and cost-effective. The Advanced Combustion Engine R&D Sub-Program focuses on developing technologies for light-, medium-, and heavy-duty internal combustion (ICE) engines operating in advanced combustion regimes, including homogeneous charge compression ignition (HCCI) and other modes of low-temperature combustion (LTC), which will increase efficiency beyond current advanced diesel engines and reduce engine-out emissions of nitrogen oxides (NOx) and particulate matter (PM) to near-zero levels.

The heavy-duty diesel engine is the primary engine for commercial vehicles because of its high efficiency and outstanding durability. However, the implementation of more stringent heavy-duty engine emission standards, which were phased in starting 2007 (100% implementation in 2010), is anticipated to cause a reduction in fuel efficiency due to the exhaust emission control devices needed to meet emissions regulations for both NOx and PM. Heavy-duty vehicles using diesel engines also have significant potential to employ advanced combustion regimes and a wide range of waste heat recovery technologies that will both improve engine efficiency and reduce fuel consumption.

Advanced engine technologies being researched and developed by the Advanced Combustion Engine R&D Sub-Program will also allow the use of hydrogen as a fuel in ICEs and will provide an energy-efficient interim hydrogen-based powertrain technology during the transition to hydrogen/fuel-cell-powered transportation vehicles.

Given these challenges, the Advanced Combustion Engine Technologies Sub-Program is working toward achieving the following objectives:

- Advance fundamental combustion understanding to enable design of engines with inherently lower emissions, and eventually advanced engines operating predominantly in low-temperature or HCCI combustion regimes. The resulting technological advances will reduce the size and complexity of emission control devices and minimize any impact these devices have on vehicle fuel efficiency. A fuel-neutral approach is being taken, with research addressing gasoline-based LTC engines as well as diesel-based advanced engines.
- Increase overall engine efficiency through fundamental improvements such as advanced combustion processes, reduction of parasitic losses, and recovery of waste heat.
- Improve the effectiveness, efficiency, and durability of engine emission control devices to enable these engines to achieve significant penetration in the light-duty market and maintain their application in heavy-duty vehicles.
- Develop highly efficient hydrogen engine technologies with near-zero NOx, PM and greenhouse gas emissions.
- Identify that any potential health hazards associated with the use of new vehicle technologies being developed by VT will not have adverse impacts on human health through exposure to toxic particles, gases, and other compounds generated by these new technologies.
- Develop advanced thermoelectric technologies for recovering engine waste heat and converting it to useful energy that will significantly increase vehicle fuel economy.

Technology Status

Recent advances in fuel injection systems have made the diesel engine very attractive for light-duty vehicle use by reducing the combustion noise associated with diesel engines, and consumers are discovering that diesel engines offer outstanding driveability and fuel economy. The change-over to ultra-low-sulfur diesel fuel enables catalytic exhaust treatment devices that virtually eliminate the offensive odors associated with diesel engines and further improve their prospects for wider use in light-duty vehicles. Mercedes-Benz has started selling a diesel passenger car that is certified to Tier 2 Bin 8 in the U.S. using a NOx adsorber and diesel particulate filter (DPF) and has added diesel engine options for its SUVs.

In early 2007, The U.S. Environmental Protection Agency (EPA) finalized its guidance document for using selective catalytic reduction (SCR) employing urea for regeneration (urea-SCR) technology for NOx control in light- and heavy-duty diesel vehicles and engines. This opens the door for the

introduction of SCR technology in Tier 2 light-duty vehicles, 2010 heavy-duty engines, and in other future diesel engine applications in the United States. Mercedes-Benz is offering a limited number of urea-SCR 2007 diesel vehicles in California that meet the Tier 2 Bin 5 standard. In 2008, Mercedes-Benz plans to expand availability of these vehicles to all 50 states. Volkswagen, Audi, and BMW also plan to incorporate urea-SCR technology into some of their diesel vehicles in 2008 with some Volkswagen models using NOx adsorber technology. In 2009, Honda plans to introduce a diesel passenger car to the U.S. that meets the Tier 2, Bin 5 standard using NOx adsorber technology and a particulate filter. These products are the direct result of regulation to reduce fuel sulfur content and R&D to develop advanced emission control technologies.

Current heavy-duty diesel engines have efficiencies in the range of 43-45%. These engines have significantly improved efficiency over engines produced just a few years ago. Improvements are being made in a wide variety of engine components such that engines a few years from now may have efficiencies between 47 and 48% without employing waste heat recovery.

In 2007, heavy-duty diesel engines for on-highway commercial trucks have been equipped with DPFs to meet particulate emissions standards. This will be the first very broad application of aftertreatment devices in the trucking industry. In some cases, DPFs are paired with oxidation catalysts to facilitate passive or active regeneration. DPFs are typically capable of reducing PM emissions by 95% or more. For NOx control, aftertreatment devices are not likely to be needed in the heavy-duty sector until 2010 emissions regulations take effect.

Among the options for NOx aftertreatment for diesel engines, urea-SCR is the clear leader because of its performance and superior fuel sulfur tolerance. The U.S. EPA has put regulations in place to assure that users of urea-SCR vehicles don't operate them without replenishing the urea. Using urea-SCR, light-duty manufacturers will be able to meet Tier 2, Bin 5 which is the "gold standard" at which diesel vehicle sales do not have to be offset by sales of lower emission vehicles. Heavy-duty diesel vehicle manufacturers will be attracted to urea-SCR since it has a broader temperature range of effectiveness than competing means of NOx reduction and allows the engine/emission control system to achieve higher fuel efficiency.

The other technology being considered for NOx control from diesel engines is lean-NOx traps (LNTs), also known as NOx adsorbers. LNTs appear to be favored by light-duty manufacturers (as witnessed by the 2007 Dodge Ram light-duty trucks with the Cummins 6.7-liter diesel engine using a LNT and DPF for emission control, and Volkswagen's and Honda's announcements of their intent to use LNTs with their diesel engines in 2008 and 2009, respectively) since overall fuel efficiency is less of a concern than for heavy-duty manufacturers, and because urea replenishment represents a larger concern for light-duty customers than for heavy-duty vehicle users. Other drawbacks to LNT use on heavy-duty vehicles are that they are larger in relation to engine displacement (being over twice as large as those required for light-duty vehicles), the "not-to-exceed" operating conditions generate higher exhaust temperatures which degrade durability, and the fuel used for regeneration adds to operating costs. Research on LNTs has decreased this fuel "penalty," but it is still in the range of five percent of total fuel flow. This problem is exacerbated by the need to periodically drive off accumulated sulfur (even using ultra-low-sulfur fuel) by heating the adsorber to high temperatures, again by using fuel (desulfation). In addition, the high temperature of regeneration and desulfation has been shown to cause deterioration in catalyst effectiveness. LNTs additionally require substantial quantities of platinum group metals, and the cost of these materials has been rising at a concerning rate.

An optimum solution to diesel engine emissions would be to alter the combustion process in ways that produce emissions at levels that don't need ancillary devices for emissions control, or greatly reduce the requirements of these systems, yet maintain or increase engine efficiency. This is the concept behind advanced combustion regimes such as HCCI, pre-mixed charge compression ignition (PCCI) and other modes of LTC, which result in greatly reduced levels of NOx and PM emissions (emissions of hydrocarbons and carbon monoxide still exist and must also be controlled – the lower exhaust temperatures associated with these combustion modes can make hydrocarbon and carbon monoxide control difficult). Significant progress is being made in these types of combustion systems, and performance has been demonstrated over increasingly larger portions of the engine speed/load map. In recent years, DOE has adopted the term "high-efficiency clean combustion" (HECC) to

include these various combustion modes since the boundaries among them are difficult to define. The major issues of this R&D include fuel mixing, control of air intake flow and its temperature, control of combustion initiation, and application over a wider portion of the engine operating range. Control of valve opening independent of piston movement appears to be highly desirable for such engines. Most heavy-duty engine manufacturers are employing some sort of HECC in engines designed to meet the 2010 emission standards. Ford has announced that it intends to release a light-duty diesel engine employing HECC before 2012 which may not include any NOx aftertreatment devices.[1] General Motors has demonstrated two driveable concept vehicles, a 2007 Saturn Aura and Opel Vectra, with light-duty HCCI engines using gasoline.[2]

Complex and precise engine and emission controls will require sophisticated feedback systems employing new types of sensors. NOx, PM, and combustion sensors are in the early stages of development and require additional advances to be cost-effective and reliable, but are essential to control systems for these advanced engine/aftertreatment systems. Much progress has been made, but durability and cost remain as the primary issues with these sensors. Start-of-combustion sensors have been identified as a need, and several development projects are underway.

Advanced fuel formulations and fuel quality are also crucial to achieving higher energy efficiencies and meeting emissions targets. The EPA rule mandating that the sulfur content of highway diesel fuel be reduced to less than 15 ppm is a great benefit to the effectiveness, efficiency, and durability of emission control devices. Since October 15, 2006, diesel fuel being sold for highway use in most of the country has less than 15 ppm sulfur (complete phase-in is anticipated by 2010 as small refiner exemptions are phased out). The addition of non-petroleum components such as biodiesel can have beneficial effects on emissions while providing lubricity enhancement to ultra-low-sulfur diesel fuel. Recent tests have shown that biodiesel lowers the regeneration temperature of particulate traps and increases the rate of regeneration with the potential for avoiding or reducing the need for active regeneration and its associated fuel economy penalty. On the other hand, biodiesel use has resulted in some operational problems as well. Fuel filter plugging has been reported under cold conditions for fuels with as little as 2% biodiesel because the biodiesel was not made to specification for blending with diesel fuel. Biodiesel is certain to become more prevalent in diesel fuel due in part to the recent expansion of the Renewable Fuel Standard, which calls for 0.5 billion gallons in 2009 increasing to 1.0 billion gallons by 2012.

Waste heat recovery is being implemented in heavy-duty diesel vehicles. New engines being introduced by Daimler Trucks in late 2007 include turbo compounding technology that uses a turbine to extract waste energy and add to engine power output. The addition of turbo compounding and other engine changes result in a claimed 5% improvement in vehicle fuel economy. Testing has shown that waste heat recovery has the potential to improve vehicle fuel economy by 10% and heavy-duty engine efficiency also by 10%.

Future Directions

Internal combustion engines have a maximum theoretical fuel conversion efficiency that is similar to that of fuel cells; it approaches 100%. The primary limiting factors to approaching these theoretical limits of conversion efficiency start with the high irreversibility in traditional premixed or diffusion flames, but include heat losses during combustion/expansion, untapped exhaust energy, and mechanical friction. Multiple studies agree that combustion irreversibility losses consume more than 20% of the available fuel energy and are a direct result of flame front combustion. Analyses of how "advanced combustion regimes" might impact the irreversibility losses have indicated a few directions of moderate reduction of this loss mechanism, but converting the preserved availability to work will require compound cycles or similar measures of exhaust energy utilization. The engine hardware changes needed to execute these advanced combustion regimes include variable fuel injection geometries, turbo and super charging to produce very high manifold pressures, compound compression and expansion cycles, variable compression ratio, and improved sensors and control methods. Larger reductions in

[1] "Ford, PSA Developing HCCI Diesel" by William Diem, WardsAuto.com, Oct. 11, 2006.
[2] "GM Demonstrates Gasoline HCCI On the Road" Green Car Congress, 24 August 2007.

combustion irreversibility will require a substantial departure from today's processes but are being examined as a long-range strategy.

The other areas where there is large potential for improvements in internal combustion engine efficiency are losses from the exhaust gases and heat transfer losses. Exhaust losses are being addressed by analysis and development of compound compression and expansion cycles achieved by valve timing, use of turbine expanders, regenerative heat recovery, and application of thermoelectric generators. Employing such cycles and devices has been shown to have the potential to increase heavy-duty engine efficiency by 10% to as high as 55%, and light-duty vehicle fuel economy by 10%. Heat transfer losses may be reduced by HECC, and interest in finding effective thermal barriers remains valid.

Fuels can also play an important role in reducing combustion irreversibility losses. Preliminary analyses show that combustion irreversibility losses per mole of fuel are considerably less for hydrogen than for hydrocarbon fuels. This finding is consistent with the understanding that combustion irreversibility losses are reduced when combustion is occurring nearer equilibrium (high temperature), since hydrogen has the highest adiabatic flame temperature of the fuels studied to date. This bodes well for the development of highly efficient hydrogen-fueled internal combustion engines.

Emission control devices for diesel engines to reduce PM and NOx will become widespread over the next few years. Much work still needs to be done to make these devices more durable and to lessen their impact on fuel consumption. Information about how best to employ these emission control devices also continues to evolve with new developments leading to more efficient operation. As engine combustion becomes cleaner, the requirements of the emission control devices will change as well.

Thermoelectric devices that convert waste engine heat to electricity have great potential to improve both engine efficiency and vehicle fuel economy. The electricity generated can be used to drive engine accessories, operate emission control equipment, or used directly to propel the vehicle. The challenges facing implementation of thermoelectric devices include scale-up, manufacturing techniques, and durability to withstand extremes of heat and vibration typical of vehicle environments.

Goals and Challenges

The Advanced Combustion Engine R&D Sub-Program has two activities:

- Combustion and Emission Control R&D
- Solid State Energy Conversion

Combustion and Emission Control R&D

The Combustion and Emission Control R&D activity focuses on enabling technologies for energy-efficient, clean vehicles powered by advanced combustion engines using clean hydrocarbon-based and non-petroleum-based fuels and hydrogen. R&D has been focused on developing technologies for light-, medium-, and heavy-duty engines and is being transitioned to developing technologies for advanced engines operating in combustion regimes that will further increase efficiency and reduce emissions to near-zero levels.

Fuel efficiency improvement is the overarching focus of this activity, but resolving the interdependent emissions challenges is a critical integrated requirement. (Penetration of even current-technology diesel engines into the light-duty truck market would reduce fuel use by 30-40% per gasoline vehicle replaced.) The major challenges facing diesel emission control systems across all three platforms are similar: durability, cost, and fuel penalty (or in the case of urea-SCR, urea infrastructure development). Full-life durability in full-scale systems suitable for 2010 regulations has yet to be demonstrated for either light- or heavy-duty systems, with the exception of very recent announcements by Cummins of a 2007 chassis certified heavy-duty diesel engine certified to the 2010 emission regulations. This is indicative of the progress achieved in the last ten years.

The VT technical targets for advanced combustion engines suitable for passenger vehicles (cars and light trucks), as well as to address technology barriers and R&D needs that are common between passenger and commercial (heavy-duty) vehicle applications of advanced combustion engines include:

- By 2010, for passenger vehicles, develop the understanding of novel low-temperature engine combustion regimes needed to simultaneously enable engine efficiency of 45 percent with a fuel efficiency penalty of less than 1 percent while meeting prevailing EPA emissions standards.
- By 2013, increase the thermal efficiency of heavy truck engines to 55 percent while meeting prevailing EPA emissions standards.

Presented in the following tables are the technical targets (consistent with the goals) for the Combustion and Emission Control R&D activity. The FreedomCAR and Fuel Partnership goals for both hydrocarbon- and hydrogen-fueled ICEs are shown in Table 1. These apply to passenger vehicles (cars and light trucks). The technical targets for heavy truck engines for commercial vehicles are shown in Table 2.

TABLE 1. Technical Targets for Passenger Vehicle Engines

Characteristics	Fiscal Year		
	2007	2009	2010
Reference peak brake thermal efficiency[a], %	32	34	35
Powertrain cost[b,c], $/kW	35	30	30
FREEDOMCAR AND FUEL PARTNERSHIP GOALS			
ICE Powertrain			
Peak brake thermal efficiency, % (Diesel/H_2–ICE) (H_2–ICE)			45/45 45 (2015)
Cost, $/kW - (Diesel/$H_2$–ICE) ($H_2$–ICE)			30/45 30 (2015)
Target peak brake thermal efficiency/part-load brake thermal efficiency (2 bar BMEP[d] @1500 rpm), %	42/29	44/30	45/31
Emissions[e], g/mil	Tier 2, Bin 5	Tier 2, Bin 5	Tier 2, Bin 5
Durability[e], hrs	5,000	5,000	5,000
Thermal efficiency penalty due to emission control devices[f], %	<3	<1	<1

[a] Current production, EPA-compliant engine.
[b] High-volume production: 500,000 units per year.
[c] Constant out-year cost targets reflect the objective of maintaining powertrain (engine, transmission, and emission control system) system cost while increasing complexity.
[d] Brake mean effective pressure.
[e] Projected full-useful-life emissions for a passenger car/light truck using advanced petroleum-based fuels as measured over the Federal Test Procedure as used for certification in those years.
[f] Energy used in the form of reductants derived from the fuel, electricity for heating and operation of the devices, and other factors such as increased exhaust back-pressure, reduce engine efficiency. A cycle average thermal efficiency loss of 1 to 2% is equivalent to a 3 to 5% fuel economy loss over the combined Federal Test Procedure drive cycle.

TABLE 2. Technical Targets for Heavy Truck Diesel Engines

Characteristics	Year			
	2002 baseline	2006	2009	2013
Engine thermal efficiency, %	>40	50	51	55
NOx emissions,[a] g/bhp-hr	<2.0	<0.20	<0.20	<0.20
PM emissions,[a] g/bhp-hr	<0.1	<0.01	<0.01	<0.01
Stage of development	Commercial	Prototype	Prototype	Prototype

[a] Using 15-ppm sulfur diesel fuel

Recovery of waste energy from the engine exhaust represents a potential for 10% or more improvement in overall engine thermal efficiency. Turbochargers strongly influence engine efficiency in several ways, including recovery of part of the exhaust energy. Turbochargers currently have efficiencies of around 50 to 58%, which could be increased to 72 to 76% with enhancements such as variable geometry. Turbocompounding can be configured to produce mechanical shaft power or electric power for additional waste heat recovery. Direct thermal-to-electric conversion could also improve the overall thermal efficiency. Bulk semiconductor thermoelectric devices are currently 6 to 8% efficient. Recent developments in quantum well thermoelectrics suggest a potential improvement to over 20% is possible. A Rankine bottoming cycle for heat recovery is being used in one of the heavy truck engine efficiency projects.

Enabling technologies being developed by the Combustion and Emission Control R&D activity focus on fuel systems, engine control systems, and engine technologies. Fuel systems R&D focuses on injector controls and fuel spray development. The fuel injection system pressure and fuel spray development influence the spray penetration and fuel-air mixing processes and thus combustion and emissions formation within the combustion chamber. Engine control systems R&D focuses on developing engine controls that are precise and flexible for enabling improved efficiency and emission reduction in advanced combustion engines. These control system technologies will facilitate adjustments to parameters such as intake air temperature, fuel injection timing, injection rate, variable valve timing, and exhaust gas recirculation to allow advanced combustion engines to operate over a wider range of engine speed/load conditions. Engine technologies development will be undertaken to achieve the best combination that enables advanced combustion engines to meet maximum fuel economy and performance requirements. These include variable compression ratio, variable valve timing, variable boost, advanced sensors, and exhaust emission control devices (to control hydrocarbon emissions at idle-type conditions) in an integrated system.

The Combustion and Emission Control R&D activity performs the critical role of elevating potential health issues related to advanced combustion engine technologies to the attention of industry partners and DOE/VT management. This portion of the activity ensures that the development of new vehicle technologies, rather than just enabling compliance with existing standards, also considers the possibility of causing negative health impacts:

- To provide a sound scientific basis underlying any unanticipated potential health hazards associated with the use of new powertrain technologies, fuels and lubricants in transportation vehicles.
- To ensure that vehicle technologies being developed by VT for commercialization by industry will not have adverse impacts on human health through exposure to toxic particles, gases, and other compounds generated by these new technologies.

Solid State Energy Conversion

The Solid State Energy Conversion activity focuses on developing advanced thermoelectrics for converting waste heat from engines into useful energy (e.g., electrical energy) to improve overall vehicle energy efficiency and reduce emissions. Effective use of waste heat from combustion engines would significantly increase vehicle fuel economy. In current production passenger vehicles, roughly over 70 percent of the fuel energy is lost as waste heat from an engine operating at full power. About 35 to 40 percent is lost in the exhaust gases and another 30 to 35 percent is lost to the engine coolant. There is an opportunity to recover some of the engine's waste heat using thermoelectric materials that will convert it directly to electricity for operating vehicle auxiliaries and accessories.

The goal of this activity is to develop advanced thermoelectric technologies for recovering engine waste heat and converting it to useful energy that will improve overall engine thermal efficiency to 55 percent for Class 7 and 8 trucks, and 45 percent for passenger vehicles while reducing emissions to near-zero levels. More specifically,

- By 2012, achieve at least 25 percent efficiency in advanced thermoelectric devices for waste heat recovery to potentially increase passenger and commercial vehicle fuel economy by a nominal 10 percent.

This activity also supports the overall engine efficiency goals of the FreedomCAR and Fuel Partnership, and 21st CTP. The technical targets for Solid State Energy Conversion are shown in Table 3.

TABLE 3. Solid State Energy Conversion Technical Targets

Characteristics	Year		
	2003 Status	2008	2010
Thermoelectric Devices			
Efficiency, % • bulk semiconductor • quantum well	5–7	– >15	– >20
Projected cost/output, $/kW (250,000 production volume)	--	500	180
Passenger Vehicle Application			
Fuel economy improvement, %	<4	>7	>12
Power, kW	<0.8	>1.0	>2.0
Projected component life, hours	<10	>5,000	>10,000
Commercial Vehicle Application			
Fuel economy improvement, %	<3	>8	>10
Power, kW	<10	>18	>20
Projected component life, hours	<10	>5,000	>20,000

Achieving these targets requires reduction in the cost of thermoelectrics, scaling them up into practical devices, and making them durable enough for vehicle applications.

PROJECT HIGHLIGHTS

The following projects highlight progress made in the Advanced Combustion Engine R&D Sub-Program during FY 2007.

Advanced Combustion and Emission Control Research for High-Efficiency Engines

A. Combustion and Related In-Cylinder Processes

The objective of these projects is to identify how to achieve more efficient combustion with reduced emissions from advanced technology engines.

- Argonne National Laboratory's (ANL) first single-shot measurements of sprays were performed and published. These measurements showed that important features of the spray are remarkably reproducible from one spray event to the next. ANL developed a new data analysis technique that allows for the calculation of the average velocity of the fuel in a spray as a function of time. This is one of the few experimental techniques that can measure spray velocity, and can do so in the very-near-nozzle region. In addition, ANL demonstrated that X-ray measurements of full-production 6-hole nozzles can be performed without sacrificing data quality. (Powell, ANL)
- Sandia National Laboratories (SNL) completed their automotive LTC facility upgrade incorporating a GM 1.9-liter production diesel head into an optically-accessible, single-cylinder engine. In addition, a new exhaust gas recirculation (EGR) simulation was installed capable of simulating EGR with H_2O, CO_2, N_2, O_2, CO, unburned hydrocarbons (UHCs) and other trace components. SNL evaluated optical engine performance and emissions for a wide range of operating conditions characterizing both high-dilution and late-injection LTC operating regimes. Lastly, SNL identified operating conditions of interest for future optical studies focusing on the sources of CO and UHC emissions. (Miles, SNL)

- SNL optical experiments showed conclusively that over-mixed fuel near the injector yields significant UHC emissions when ignition occurs after the end of injection because it does not achieve complete combustion. Computer models show improved agreement with experiments at LTC conditions. SNL also initiated a parallel experimental and modeling study of effects of bowl geometry, spray angle, and swirl ratio on in-cylinder LTC processes. (Musculus, SNL)
- SNL quantified the extent of liquid-phase penetration for typical early-injection LTC conditions with various injection durations, nozzle sizes, injection pressures and number of injections. This provides an understanding needed to prevent liquid wall impingement and its negative impacts on emissions and combustion efficiency. SNL also showed that the extent of liquid penetration depends upon the injected mass for short injections less than the steady-state liquid length, rather than the nozzle size or injection pressure. In addition, it was demonstrated that small nozzles actually form more soot than larger nozzles when the injection duration is adjusted such that the mass injected is constant. (Pickett, SNL)

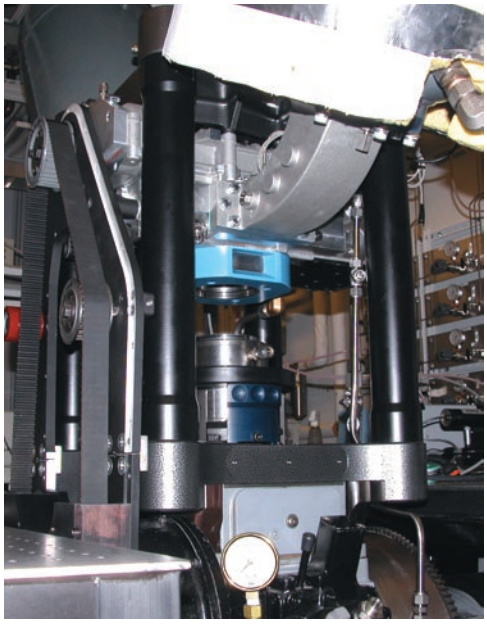

SNL Optically-Accessible Engine with GM 1.9-Liter Cylinder Head

- Oak Ridge National Laboratory (ORNL) demonstrated an increase in speed-load range for HECC operation of a light-duty diesel engine. Mixed-source EGR for controlling intake temperature was characterized and, correspondingly, emissions and efficiency. ORNL explored the relationship between brake specific fuel consumption and combustion noise for HECC operation and commissioned and mapped a modern light-duty diesel engine. (Wagner, ORNL)

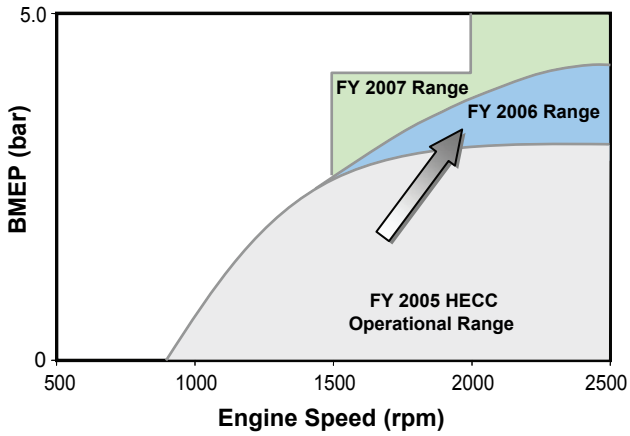

Expansion of HECC Speed-Load Range Accomplished by ORNL with Improved Control of Intake Mixture Temperature

- SNL completed infrastructure and preprocessor modifications to make calculations routine and performed systematic model validation of two fundamental combustion models in collaboration with the DOE Office of Science. SNL continued the sequence of calculations focused on the Combustion Research Facility optical hydrogen internal combustion engine in collaboration with C. White and S. Kaiser and systematically extended effort toward treatment of LTC engine processes. (Oefelein, SNL)
- Lawrence Livermore National Laboratory (LLNL) developed methodologies for experimental measurement of 40 hydrocarbon species in HCCI engine exhaust. LLNL demonstrated high fidelity modeling of the SNL HCCI engine, including unprecedented prediction of 40 measured intermediate hydrocarbon species. Innovative control strategies were demonstrated and applied to the Caterpillar 3406 experimental HCCI engine, showing optimum engine performance and fast transient response. (Aceves, LLNL)
- SNL determined the effects of EGR/residuals and its constituents on combustion phasing for single- and two-stage fuels. SNL showed how HCCI combustion progresses through various phases of autoignition, main combustion, and burnout using a combination of chemiluminescence

spectroscopy and chemical-kinetic analysis. Several fuel-stratification techniques were investigated to improve combustion efficiency at low loads, using a combination of metal-engine performance data and fuel planar laser induced fluorescence imaging. (Dec, SNL)

- SNL installed negative valve overlap (NVO) cams in an automotive HCCI engine. Tests were conducted to establish the operating range of recompression operation and they tested protocols to allow rapid and safe startup in the optical engine. SNL also created a 1-D cycle-simulation model to aid the selection of stable NVO operating conditions and adapted SNL's linear-eddy model to provide detailed, stochastic predictions of turbulent mixing in the HCCI engine. The model provided valuable insights into the effect of spatial fuel distribution on HCCI combustion and emissions. (Steeper, SNL)
- ORNL developed a data-based method to estimate global kinetic parameters from combustion measurements and form the basis of a low-order dynamic model to be used for prediction and control. Also developed was a Wiebe-based combustion metric to be used for feedback control as well as improving model estimates of global kinetic parameters. (Wagner, ORNL)
- The parallelization of KIVA-4 was tested by Los Alamos National Laboratory (LANL) in realistic geometries including 4-valve pentroof and 3-valve engine geometries. The collocated version of KIVA-4 was parallelized and run in parallel in a vertical valve engine geometry. The University of Wisconsin's chemistry and spray submodels were implemented in KIVA-4 and tested in a 2-D sector geometry and Reaction Design's chemistry package was interfaced with KIVA-4. Converters were developed for the TrueGrid and ICEM software programs. Remapping capability was demonstrated in a cylindrical tetrahedral mesh and reduced spray dependence was achieved by using the grid overset method in KIVA-4. (Torres, LANL)
- LLNL developed a chemical kinetic model for n-hexadecane, a primary reference fuel for diesel fuel, and a realistic representation of n-alkanes in diesel fuels. Also developed was the understanding of the chemical kinetics that control HCCI combustion under boosted conditions using LLNL surrogate fuel models and SNL HCCI engine data. Finally, LLNL developed a chemical kinetic model for methyl decanoate, a realistic component to represent methyl esters contained in biodiesel. (Pitz, LLNL)
- ORNL achieved and demonstrated the 2007 FreedomCAR goal of 42% peak break thermal efficiency on two light-duty diesel engines and completed the installation of a modern engine platform donated to ORNL by General Motors. Thermodynamic analysis methods were developed for use with engine simulation codes as well as experimental data to evaluate potential opportunities for waste heat recovery. ORNL demonstrated a potential of advanced combustion operation for achieving Tier 2 Bin 5 emissions regulations. (Wagner, ORNL)
- SNL developed a linear alternator/multi-level converter configuration calculated to exceed 30 kW power output charging a battery at greater than 95% conversion efficiency. It was determined with collaborators that the opposed piston concept is preferred for hybrid vehicle applications due to its capability to operate independently of other units (due to self balance). (Van Blarigan, SNL)
- ANL characterized the influence of injection timing on engine efficiency and emissions in direct injection operation and determined that nozzle design significantly influences brake thermal efficiency and emissions (2% increase in brake thermal efficiency and 47% decrease in NOx emissions) at low engine load with changed nozzle design. Multiple injection strategy images were captured and refined spectroscopic gas temperature measurements were performed. ANL installed a new cylinder head with central

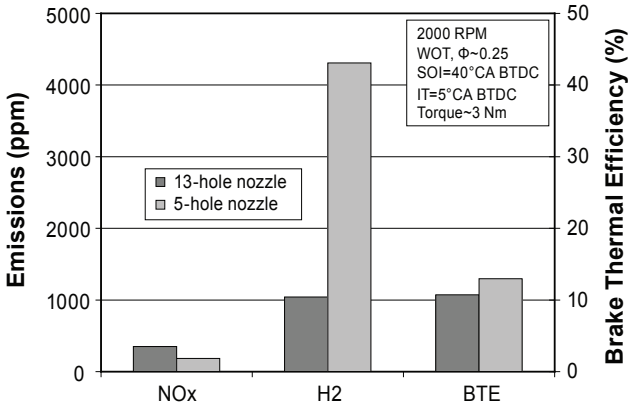

The Effect of Nozzle Design on Hydrogen Direct Injection Engine Emissions in Testing Conducted by ANL

and side injector locations – specific injector nozzles designed and manufactured for either location. (Wallner, ANL)

- Quantitative, instantaneous two-dimensional images of equivalence ratio and corresponding high-quality velocity measurements were made by SNL during the compression stroke with and without direct hydrogen injection. Analysis of the velocity field revealed that the observed substantial fuel stratification for late injection is favored by a relatively stable counter-flow situation created by jet-wall interaction. (Kaiser, SNL)
- Cummins demonstrated 12% fuel economy improvement on their ISB engine and 7% on their ISX engine. The combustion strategy employed to achieve high efficiency is a mixed mode that relies on extending the early PCCI combustion mode to encompass as much of the engine operating range as possible while implementing lifted flame diffusion controlled combustion for the remainder of the higher load operating range. (Stanton, Cummins)
- Caterpillar completed the Phase 2 optical diagnostic experiments and the single-cylinder engine fuels testing on low-cetane diesel boiling-range fuels. A prototype fuel injection system was developed and tested on the single-cylinder engine demonstrating ultra-low NOx and smoke emissions. An advanced multi-cylinder engine with compression ratio flexibility was developed and tested demonstrating benefits for emissions, efficiency and controls. (Milam, Caterpillar)
- International Truck and Engine Corporation demonstrated LTC combustion up to 1,500 RPM and 6 bar BMEP, with plans to extend to the full range of engine operation. NOx levels were limited to below 0.2 g/bhp-hr with soot levels below 2 mg/mm^3. Fuel efficiencies are comparable to 'conventional' operation. (de Ojeda, International)
- GE Global Research demonstrated an advanced fuel injection system to minimize fuel consumption, while meeting Tier 2 emissions levels on a locomotive engine. Changes in nozzle geometry have been proven to allow for further engine performance benefits. For the range studied, the number of holes seemed to have the strongest effect on PM, followed by rail pressure and nozzle flow. Changing the spray cone angle was found to have monotonic but opposing trends for specific fuel consumption and PM. (Primus, GE Global Research)
- ORNL designed and constructed a bench-top experimental apparatus for demonstrating low-irreversibility combustion based on the concept referred to as counterflow-preheat with near-equilibrium reaction (CPER). ORNL continued exploring better ways for recuperating exhaust heat and utilizing compound cycles for extracting work, as well as exercising engine and combustion models to identify combustion modifications that would mitigate exergy losses. (Graves, ORNL)
- Detroit Diesel Corporation (DDC) successfully completed the first part of the Near Zero Emissions at 50% Thermal Efficiency (NZ-50) project. DDC demonstrated 50.2% thermal efficiency with integrated experimental and analytical technologies at EPA 2010 emissions levels at a single operating condition in a multi-cylinder engine configuration. DDC also successfully launched the second part of the NZ-50 project in March of 2007, which focuses on high efficiency clean combustion. (Zhang, DDC)

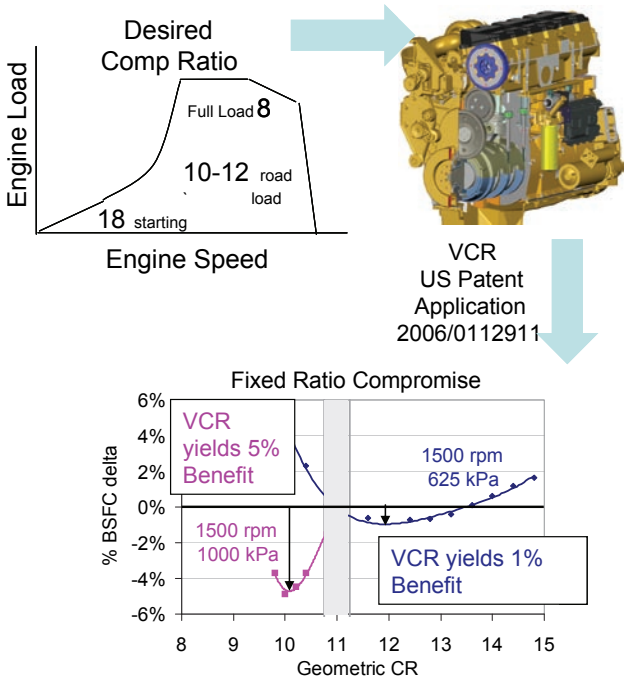

Caterpillar Implemented Variable Compression Ratio to Facilitate HCCI Combustion

- GM developed and demonstrated prototype gasoline and diesel engine hardware which enables operation of HCCI combustion for improved fuel efficiency and emissions performance. Both "two-step" and fully variable valve actuation systems were developed and tested.

B. Energy-Efficient Emission Controls

The following project highlights summarize the advancements made in emission control technologies to both reduce emissions and reduce the energy needed for emission control system operation.

- Using a one-of-a-kind very high field nuclear magnetic resonance instrument at Pacific Northwest National Laboratory (PNNL), the nucleation sites for Ba on the γ-alumina catalyst support material have been identified. The chemical form and stability of barium carbonate species formed during stored NOx removal in the presence of CO_2 has been determined. Studies of the effects of water on the decomposition of the deactivating $BaAl_2O_4$ phase show how treatments may be devised to restore performance after deactivation. Also, the relative performance of all alkaline earth oxide storage materials has been determined. (Peden, PNNL)
- PNNL observed a decrease in Pt accessibility for H_2 chemisorption with increasing reduction temperature without a corresponding change in Pt particle size, implying that BaO covers at least part of the Pt surface during reduction. Also observed was an increase in NOx storage capacity up to a reduction temperature of 500°C, which strongly suggests that there is a promotional effect of this (Pt-BaO) interaction on NOx storage. (Peden, PNNL)
- ORNL analyzed model and commercial LNT catalysts on a full-scale engine system with in-cylinder regeneration techniques and measured NH_3 emissions from LNTs and determined the effect of ceria on NH_3 control. They disseminated the data through Cross-Cut Lean Exhaust Emissions Reduction Simulations (CLEERS) to improve models. (Parks, ORNL)
- SNL completed construction and optimization of a thermodynamically consistent reaction mechanism for the precious metal sites on a benchmark LNT catalyst. Tentative mechanisms for the NOx storage and oxygen storage sites on the catalyst were formulated and the corresponding thermodynamic constraints were assembled. Using the combined reaction mechanism together with a Chemkin-based transient plug flow code and the Sandia APPSPACK optimization software, SNL carried out a preliminary evaluation of the storage parameters by fitting simulations of full LNT cycles to experiment
- ORNL with their International T amples in a OR activity is the key parameter limiting low-

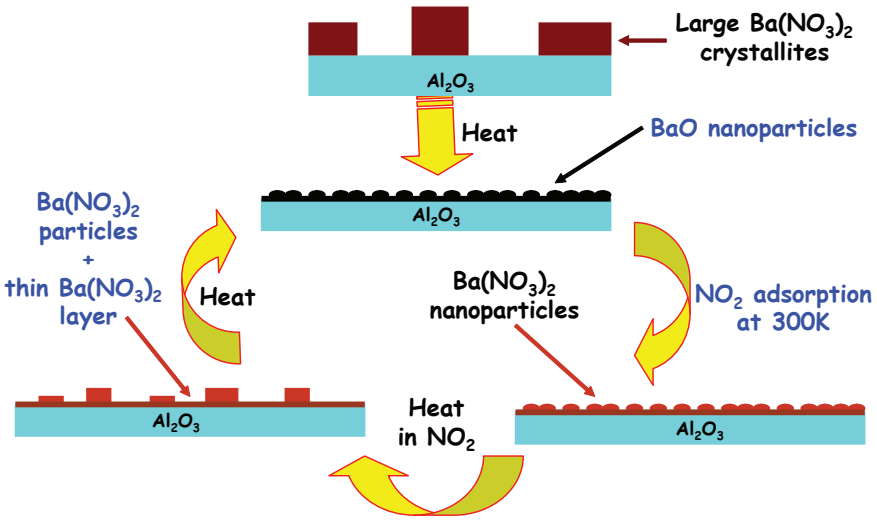

Cycle Of Morphology Changes Taking Place during NO_2 Uptake and Release on BaO/Al_2O_3 NOx Storage/Reduction Materials (PNNL)

temperature performance of the catalysts studied, established trends in NOx conversion and product selectivity with temperature, space velocity, lean-rich cycle time, and reductant species, and provided input for calibration of operating strategies. (Toops, ORNL)

- ORNL is working to provide a better understanding of the fundamental deactivation mechanisms that result during regeneration and desulfation of LNTs. They recently presented their efforts at the 20th North American Meeting, 2007 AIChE National Meeting, and the DOE Advanced Combustion Engine Merit Review. ORNL also submitted a paper to Catalysis Today. A full sulfation study on model catalysts and a full sulfation study on a commercial LNT were completed (Toops, ORNL)
- ORNL demonstrated real-time on-engine measurements of oil dilution by fuel using a diagnostic and showed that results trend with more conventional but slower-feedback off-line measurements. Also, the impact of sulfation on the spatial nature of various LNT catalyst reactions was characterized and used the results to develop a conceptual model of LNT sulfation which explains integral catalyst performance. (Partridge, ORNL)
- ORNL compared emissions and fuel efficiency for lean-NOx trap catalysis with three combustion modes: no EGR, production level EGR, and HECC. (Parks, ORNL)
- ORNL continued co-leading the CLEERS Planning Committee and facilitation of the SCR, LNT, and DPF Focus Group teleconferences with strong domestic and international participation. Additionally, ORNL continued co-leading the LNT Focus Group and refinement of the standard LNT materials protocol. Key R&D priorities were identified from the CLEERS community, including coordination of the R&D priorities survey with response from 14 DOE Diesel Crosscut Team companies and their partners in January, 2007. (Daw, ORNL)
- ORNL continued refinement and validation of the LNT material characterization protocol in conjunction with the LNT Focus Group, SNL, and PNNL and collaborating suppliers. Benchmarking of Umicore commercial reference LNT material for sulfation and desulfation characteristics was initiated. ORNL continued the in-depth study of the global kinetics of LNT regeneration, with specific emphasis on formation of byproduct N_2O and NH_3, effective fuel penalty, and potential coupling of LNT with SCR. Also, DRIFTS measurements of the fundamental mechanisms involved in S poisoning and desulfation of LNTs was continued. (Daw, ORNL)
- PNNL added catalytic chemistry to their micro-scale DPF models. Side-by-side loading and regeneration experiments were carried out with individual uncatalyzed and platinum-catalyzed DPF channels. Techniques for loading individual filter walls with aerosolized salt particles for fundamental filtration studies were developed. PNNL also participated in monthly CLEERS teleconferences and coordinated the calls focused on DPF technology. (Stewart, PNNL)

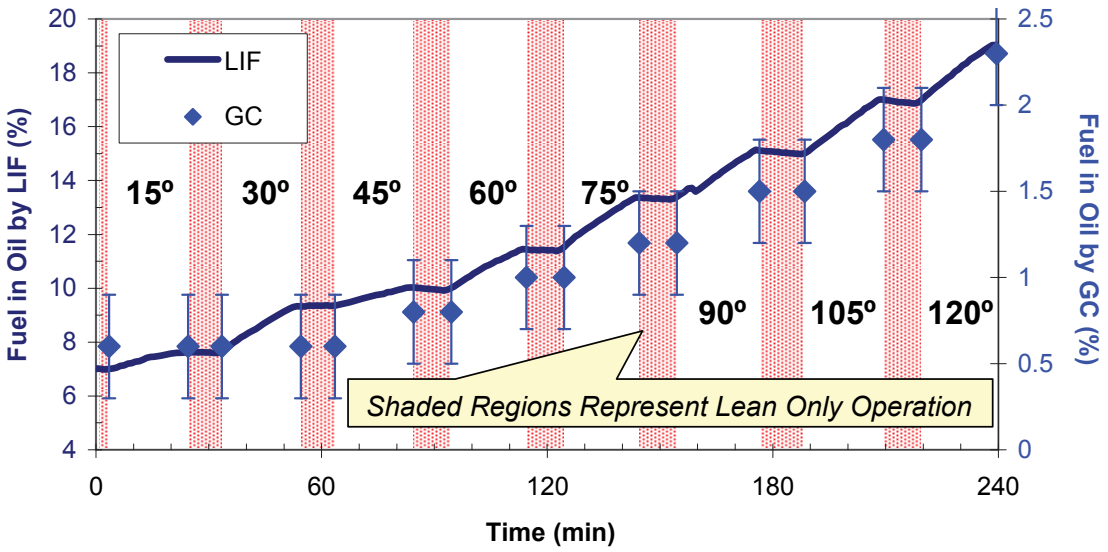

Comparison of Laser-Induced Fluorescence (LIF) Spectroscopy versus Gas Chromatograph Techniques Conducted by ORNL to Measure Fuel in Oil Dilution in Real Time

- GM tested over 8,000 catalyst materials for NOx reduction potential, conducted detailed engine testing, completed phosphorus poisoning studies, and developed specific formulations for lean gasoline applications. (Blint, GM)
- GM developed a DPF regeneration technology using external application of heat that reduces fuel consumption compared with injecting fuel to initiate regeneration.

C. Critical Enabling Technologies

Variable valve actuation (VVA), variable compression ratio, and combustion sensors are enabling technologies for achieving more efficient engines with very low emissions. The following highlights show the progress made during FY 2007.

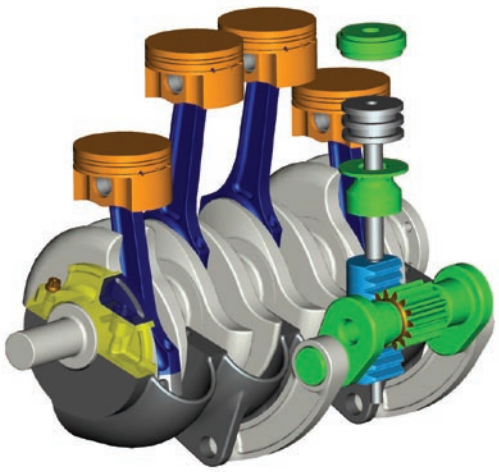

Variable Compression Ratio Mechanism Developed by Envera LLC

- An optimal, cost-effective, VVA system for advanced low-temperature diesel combustion processes was designed and tested. (Gutterman, Delphi)
- Hydraulic pressures in Envera LLC's actuator system were reduced by 86% through system optimization. The reduction in pressure significantly relaxes the demands that will be placed on the hydraulic system and enables cost to be reduced. A test rig was designed and built for evaluating actuator response. Test results indicate that compression ratio can be reduced from 18:1 to 8.5:1 in ~0.35 seconds, and increased from 8.5:1 to 18:1 in ~0.70 seconds. (Mendler, Envera LLC)
- An all-new planar type voltammetric NOx gas sensor was designed by Streamline Automation, LLC and they modified their existing monolithic cermet micro-arrays with new solder-less leads for long-term high-temperature operation. A new ruggedized stainless steel package was designed and prototyped. A new high-speed differencing voltammetry algorithm was engineered and employed for chemical characterization. Also, gas voltammetry was successfully applied to both commercial gas sensors (three) and to experimental gas micro-arrays (two). (Vogt, Streamline Automation, LLC)
- Two engines of same model line/different serial number were tested by TIAX LLC to verify engine-to-engine repeatability of their start of combustion sensor system (a potential drawback of accelerometer-based systems). TIAX also developed an array of algorithms to translate the accelerometer signal into the desired start of combustion value. A library of data has been generated relating engine cylinder pressure to accelerometer events, and the algorithms are being evaluated on the accelerometer data. (Smutzer, TIAX LLC)
- Westport Power, Inc. confirmed that the vertical acceleration of the main bearing caps has the best correlation with the start of combustion timing. An algorithm to obtain the timing for the start of combustion using accelerometers was developed. The targeted start of combustion error standard deviation is 0.5 crank angle degrees (CAD). The current results have largely exceeded this target for all the testing modes. The averaged engine-to-engine variation over all modes is 0.32 CAD with 98.9% confidence level. (Mumford, Westport Power, Inc.)
- John Deere is exploiting the flexibility of electrical coupling to the turbocharger to optimize system performance as a function of both engine speed and load. A smaller, higher performing turbo generator has been designed that exhibits considerable simplification. A series turbocharger system that provides improved performance and range was also successfully designed and modeled. (Vuk, John Deere)
- Cummins Inc. completed a system thermodynamic analysis across the engine's operating map to define the architecture of the waste heat recovery (WHR) system. The analysis results eliminated engine coolant and charge air as potential recovery sources and focused our efforts on waste energy

recovery from EGR and the engine's main exhaust gas stream. Also completed was a first generation component analysis and design for an on-engine system which will recover heat from the engine's EGR stream, thereby relieving the engine's jacket water system of this heat load and providing 6% fuel efficiency improvement (model-based results). (Nelson, Cummins)

- Through simulation, Volvo has demonstrated an engine efficiency increase of 8.2% when operating over a road cycle and 10.5% during steady-state operation over the European Standard Cycle at U.S. 2010 NOx levels (0.2 g/bhp-hr). Added investment for the continuously variable transmission and energy recovery devices will be returned in less than 1.5 years assuming fuel prices of $2.50 per gallon. (Habibzdeh, Volvo)

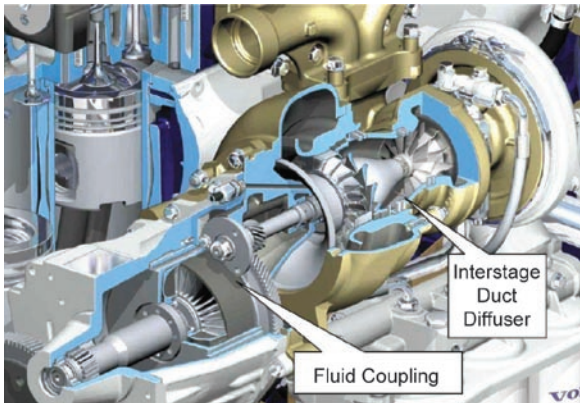

Schematic Close-Up of the Volvo D12 500 HP Engine Showing the Turbocharger, Interstage Duct Diffuser and Turbocompound Device

- Caterpillar Inc. designed, procured, and tested a novel nozzled/divided turbine stage, demonstrating a 5% improvement in turbine efficiency over standard production turbines. Caterpillar also designed, procured, and gas-stand tested a novel mixed-flow turbine stage, demonstrating the ability to shape the turbine efficiency characteristic to better match engine requirements. Lastly, Caterpillar designed, procured, and gas-stand tested a high efficiency compressor stage, demonstrating a 2-3% improvement in compressor efficiency over standard production compressors. (Kruiswyk, Caterpillar)
- Volvo Powertrain's Air-Power-Assist (APA) engine experimental setup was completed. In addition, the APA engine was made functional and preliminary testing was completed. (Kang, Volvo)

D. Health Impacts

The Health Impacts activity studies potential health issues related to new powertrain technologies, fuels, and lubricants to ensure that they will not have adverse impacts on human health. The following are highlights of the work conducted in FY 2007.

- ORNL measured mobile source air toxics (MSATs) from the European Saab Biopower vehicle that is optimized for performance with E85 (85% ethanol and 15% gasoline) fuel to provide information on the health impact of ethanol fuel introduction. Additionally, ORNL characterized MSATs from HECC on a diesel engine to determine any health impacts of advanced diesel combustion modes. (Parks, ORNL)
- The National Renewable Energy Laboratory (NREL) obtained support from the American Chemistry Council Petroleum Additives Product Approval Protocol Task Group to provide new and aged engine lubricating oils for all vehicles that will be tested. The scope of the project was increased to include medium-duty vehicles and E10 and biodiesel fuel testing as part of the overall project. (Lawson, NREL)
- Lovelace Respiratory Research Institute (LRRI) evaluated the health effects of inhaled nanoparticles from new and used diesel crankcase oil, and sulfate. It was discovered that oil and sulfate nanoparticles had little lung toxicity, but altered responses of immune cells elsewhere in the body. LRRI also completed

Saab 9-5 Biopower Vehicle on a Chassis Dynamometer Tested by ORNL

analysis of results from a comprehensive study of the effects of repeated inhalation exposure to laboratory-generated gasoline emissions. It was discovered that inhaled nitrogen oxide and carbon monoxide can duplicate some effects of gasoline emissions on blood vessels outside the lung. (Mauderly, LRRI)

- The Health Effects Institute (HEI) received four test engines from participating engine manufacturers at Southwest Research Institute (SwRI) and finalized the 16-hour test day cycle developed by West Virginia University based on a combination of Federal Test Procedure and California Air Resources Board cycles. Additionally, the emissions characterization protocol was finalized with the CRC ACES Panel and the investigators' team at SwRI and approved a revised testing plan from SwRI. (Greenbaum, HEI)

Solid State Energy Conversion

Several projects are being pursued to capture waste heat from advanced combustion engines in both light- an heavy-duty vehicles using thermoelectrics. Following are highlights of the development of these technologies during FY 2007.

- General Motors Research & Development Center (GM) found that existing bulk thermoelectric (TE) materials in an exhaust generator can meet the minimum 350 W requirement; the exhaust TE waste heat recovery has higher, but not significantly higher, cost than the existing fuel economy improving technologies. GM also found that low quality heat at the radiator makes recovering significant heat cost prohibitive using existing materials, and requires both TE figure of merit enhancement and cost reduction. Material selections for the exhaust TE waste heat recovery subsystem were finalized. (Yang, GM)
- A fractional BiTe thermoelectric generator module (TGM) has been built by BSST and tested that produced 130 watts of electric power. A full-scale BiTe TGM was built and tested that produced over 500 watts of electric power. A fractional high temperature TGM has been built using PbTe/TAGS that produced 20 watts electric power.
  A fractional high temperature TGM has been built using PbTe/TAGS/BiTe that demonstrated 10% conversion efficiency. (LaGrandeur, BSST)
- Systems for material synthesis, powder processing, hot pressing, leg preparation, material mechanical and thermoelectric property characterization, and couple fabrication have been demonstrated at Michigan State University (MSU). Systems are in place to produce a 40 W module in one week. Using the measured properties of known materials for the temperature range of operation, MSU estimates that a segmented couple can provide a conversion efficiency of over 12%. (Schock, MSU)

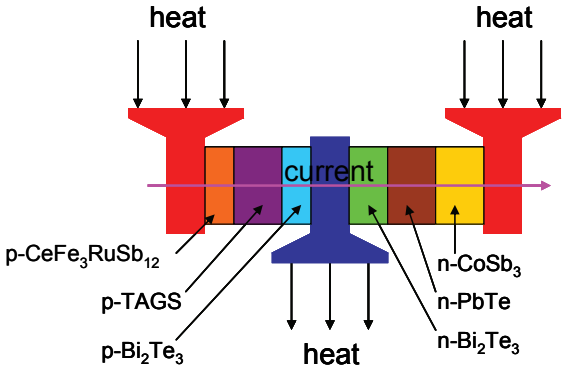

BSST "Y" configuration

BSST High Density Thermoelectric Subassembly

University Research

- Multi-cylinder supercharged engine operation for high-load limit extension has been demonstrated at the University of Michigan (UM) using port fuel injection. Initial experiments up to 1.7 bar intake pressure have shown proportional load increases. Combustion control is provided by an intake air cooler/flow splitter arrangement. Single-cylinder experiments have achieved low-load extension by fuel injection during negative valve overlap. Further, varying the timing of the injection affects the combustion phasing and shows promise as a control tool. (Assanis, UM)
- The University of Wisconsin-Madison has formulated combustion models and reaction mechanisms and has applied them to analyze and optimize low emissions diesel engine operation. In-cylinder

optical diagnostics have been developed for H_2O species, and temperature and turbulence dissipation measurements, for use in chemistry and turbulence model validation. A two-stage combustion strategy has been formulated and demonstrated with modeling and experiments to achieve 2010 emissions levels with low-temperature combustion operation. (Reitz, University of Wisconsin-Madison)

- West Virginia University (WVU) implemented simple models for LTC and diesel engines to obtain the pressure and temperature data required for the evaluation of efficiency for each type of engine. Values of energy losses in the LTC engine were compared with energy losses of a diesel engine with half the displacement of the LTC engine. Energy losses assessed in this model include friction, auxiliaries and heat transfer. A model to evaluate the total cooling burden was developed to assess the impact of the energy losses in the fan energy requirements, which is also powered by the engine. Model results showed that the total cooling burden on a LTC engine with higher displacement and lower power density was 15.6% lower than the diesel engine for the same amount of energy addition in the case of high load (43.57 mg fuel/cycle). (Clark, WVU)
- The University of Houston carried out a comprehensive experimental study of the steady-state behavior of the NO/H_2 and $NO/H_2/O_2$ reaction systems on model Pt and Pt/Ba monolith catalysts. Integral conversion and selectivity data were obtained over a range of temperatures, feed compositions, and catalyst loadings (Pt, BaO). The analytical system was upgraded to include a mass spectrometer, enabling the measurement of N_2 and H_2 in addition to the remaining species measured by Fourier transform infrared spectroscopy. (Harold, University of Houston)
- Bench reactor tests were performed at the University of Kentucky on a series of model monolith catalysts, in which the concentrations of the four main active components, Pt, Rh, CeO_2 (or CeO_2-ZrO_2) and BaO were systematically varied. From the resulting data, catalyst activity-composition (and in some cases selectivity-composition) correlations were derived. An automated catalyst aging cycle has been implemented for the accelerated aging of model monolithic catalysts. Under lean-rich cycling conditions, ceria was found to exert significant effects on the intra-catalyst chemistry, as demonstrated by the analysis of rich phase intra-catalyst H_2 concentration profiles. (Crocker, University of Kentucky)
- Texas A&M University developed an engine cycle simulation to determine the effects of compression ratio and expansion ratio on engine performance and second law performance. The results showed that increases of compression ratio beyond about 10:1 do provide significant thermodynamic gains. The use of a greater expansion stroke compared to the compression stroke ("Atkinson cycle") was most effective for wide-open-throttle conditions. The use of a greater expansion stroke had modest effects on the second law parameters. The simulation was modified to be able to consider diesel engine operations. Preliminary results were obtained and compared to

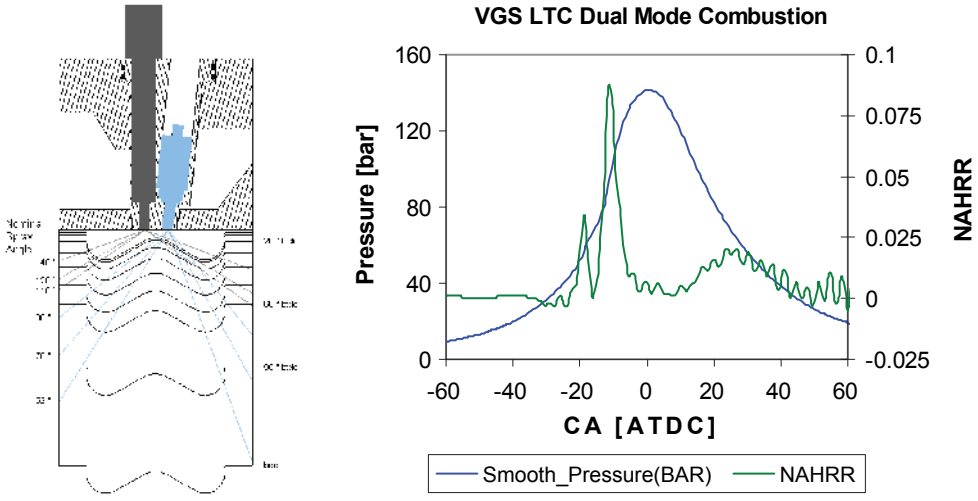

University of Wisconsin-Madison Variable Geometry Spray (VGS) Arrangement with High and Low Pressure Injectors and Two-Stage Combustion Results

experimental results for a 1.7-liter, direct-injection, Isuzu engine. (Caton, Texas A&M University)

- A fluidic rectifier with area ratio of 8, length of 5 mm and extension of 5 mm was fabricated and integrated into a forward/backward mass air flow sensor prototype and was characterized in the unsteady air intake flow facility and tested with robust, automotive hotwires at MSU. High-speed visualization of fuel air mixing and in-cylinder flame distribution was achieved to reveal the spray distribution, flame propagation, and fuel impingement in the optical engine. (Schock, MSU)
- A diesel engine and dynamometer rig for testing particulate matter sensors was designed and set up in the University of Texas (UT) Engine Combustion Laboratory. A particulate filter measurements system was designed and assembled to allow the sensors to be calibrated for non-volatile mass emissions of particulate matter. Using this system, the engine's PM emissions were determined as a function of engine operating condition. New sensor designs were developed, tested, and calibrated. (Hall, UT at Austin)

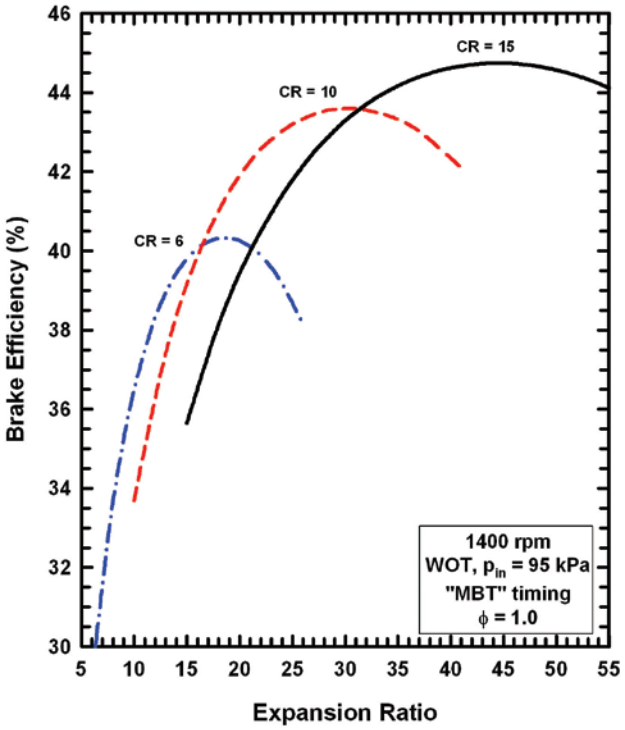

Effect of Expansion Ratio on Brake Thermal Efficiency at Different Compression Ratios as Determined by Texas A&M

FUTURE DIRECTIONS

Advanced Combustion and Emission Control Research for High-Efficiency Engines

A. Combustion and Related In-Cylinder Processes

The focus in FY 2008 for combustion and related in-cylinder processes will continue to be on advancing the fundamental understanding of combustion processes in support of achieving efficiency and emissions goals. This will be accomplished through modeling of combustion, in-cylinder observation using optical and other imaging techniques, and parametric studies of engine operating conditions. Several labs and universities plan to adopt a common engine research platform that will span optical single-cylinder through multi-cylinder experiments. Achievement of 43% peak efficiency for the 2008 FreedomCAR goal is expected to be validated at ORNL with this engine.

- ANL will increase the relevance of their measurements by studying sprays under conditions even closer to those of modern diesel engines. ANL plans to upgrade their fuel system to the latest generation of fuel injection equipment, and use full-production injectors that can also be run in the GM-Fiat 1.9-liter engine running in Argonne's Engine and Emissions group. ANL will also improve the measurement technique. While useful results are presented, improvements to the measurement technique will increase its applicability and accessibility in the future. Such improvements include faster data acquisition, processing, and analysis, improved X-ray detector systems, increased X-ray intensity, and greater automation. (Powell, ANL)
- SNL will develop an optical diagnostic technique for visualizing the in-cylinder spatial distribution of CO and apply optical techniques to investigate sources of UHC and CO emissions in highly dilute, LTC regimes. SNL will also evaluate the effect of engine boost on low-temperature

combustion systems and on the fuel conversion efficiency loss typically observed with high dilution levels. In addition, SNL will examine how trace components in simulated EGR influence the combustion and emissions formation processes. (Miles, SNL)

- SNL will apply optical diagnostics for other LTC conditions and maintain modeling collaboration with the University of Wisconsin to improve computer model performance for LTC conditions. SNL will develop a simple mixing model of end-of-injection mixing processes and continue to extend the conceptual model of diesel combustion to LTC conditions. (Musculus, SNL)
- SNL will investigate the location of evaporation for end of injection mixing near the nozzle and its impact on UHC. SNL will determine how multiple injections can be used to affect ignition timing and minimize UHC at LTC conditions. Direct measurements of mixing (equivalence ratio) at the time of the premixed burn in constant-injection-duration diesel fuel jets for various EGR levels and multiple injection strategies will be performed. This investigation will show how mixing between injections affects the equivalence ratio and location of the premixed burn. (Pickett, SNL)
- ORNL will explore advanced combustion operation on a GM 1.9-L engine including efficiency, emissions, noise, and stability with a high-pressure loop EGR system. The effect of intake mixture temperature and composition on advanced combustion operation will be characterized. ORNL will also investigate acoustic and vibration energy transmission paths for diagnostics and control of conventional combustion and advanced combustion modes. (Wagner, ORNL)
- SNL will continue development of high-fidelity simulations of the optical hydrogen internal combustion engine and systematically extend them to HCCI engine experiments. In addition, SNL will continue leveraging between DOE Office of Science and Energy Efficiency and Renewable Energy activities. (Oefelein, SNL)
- LLNL will validate KIVA3V-MZ-MPI against experimental data under partially stratified conditions by working with engine researchers at SNL to conduct validations of the code at PCCI conditions. LLNL will use KIVA3V-MZ-MPI as a predictive tool for engine geometry and fuel injection optimization and analyze spark-assisted HCCI experiments. (Aceves, LLNL)
- SNL will conduct an investigation of the potential of EGR/residuals for slowing the pressure-rise rate at high loads to further extend the upper-load limit of HCCI. The development of thermal stratification and its distribution in the bulk gases during the latter-compression and early-expansion strokes will be investigated. SNL will complete a detailed exhaust-speciation study over a range of fueling rates and for mixture stratification at low loads for iso-octane and gasoline and determine the effects of ethanol and/or ethanol-gasoline blends on HCCI performance for well-mixed and mixture-stratified operation. (Dec, SNL)
- SNL will complete the operating-range tests of recompression-HCCI combustion and investigate the use of alternative injection strategies, including injection during the recompression period, to accomplish advanced fuel-air mixing strategies. SNL will apply a PLIF diagnostic to characterize engine performance under these conditions and examine spark-assisted HCCI operation to understand its potential role for widening the HCCI operating range. (Steeper, SNL)
- ORNL will baseline and map SI-HCCI regions of operation on a multi-cylinder engine located at Delphi Automotive Systems. Detailed kinetics simulations will be performed of the SI-HCCI transition to improved physical understanding of multiple combustion modes and inter-mode switching. Simulations will be performed in-house as well as in collaboration with LLNL. ORNL will also improve the low-order combustion model for use in the development of fast diagnostics and control strategies. (Wagner, ORNL)
- LANL will continue with the validation of KIVA-4 in unstructured geometries and in parallel simulations of realistic engine geometries. LANL will implement LLNL's multi-zone combustion model into KIVA-4 and develop the capability to perform turbulent calculations with the large eddy simulation turbulence model in KIVA-4. (Torres, LANL)
- LLNL will extend model capabilities to additional new classes of fuel components, including hepta-methyl-nonane which is a primary reference fuel for diesel fuel and represents iso-alkanes in diesel fuel. LLNL will further validate their chemical kinetic model for n-hexadecane and continue the development of increasingly complex surrogate fuel mixtures to represent fuels for HCCI and diesel engines. (Pitz, LLNL)

- ORNL will characterize the thermodynamic availability of engine system components over the speed-load range of the engine and evaluate the potential efficiency benefits of bottoming cycles for waste heat recovery from the EGR system, exhaust system, etc. Low-temperature combustion approaches on the GM 1.9-L engine for reducing aftertreatment needs and improving overall system efficiency will be investigated. (Wagner, ORNL)
- SNL will fabricate and construct a two-stroke cycle, opposed piston research engine utilizing optimized coupling of Magnequench linear alternators as a proof-of-concept tool. The battery charging application will be optimized for higher power-to-weight ratio. Also, SNL will operate the research experiment fueled by hydrogen to measure indicated efficiency in a continuous operation regime and demonstrate flexibility and multi-fuel capability by operating on alternative fuels at various operating conditions (compression ratios, equivalence ratios). (Van Blarigan, SNL)
- ANL plans to expand engine testing to include central direct injection in addition to the current side injection location. ANL will evaluate newly designed injector nozzles for performance and emissions benefits and analyze the potential of water injection. Test runs at higher engine speed conditions will be conducted to evaluate the high-flow performance of the improved injectors. (Wallner, ANL)
- SNL will measure the velocity field in the vertical (axial) plane during the intake stroke to validate pre-injection accuracy of the companion simulation. Simultaneous two-dimensional measurements of velocity/equivalence ratio will be implemented. SNL will also install a new engine head, supplied by Ford R&D, featuring central injection and central ignition. Engine geometry will then be identical to that of collaborating labs at Ford and ANL. (Kaiser, SNL)
- Cummins will conduct multi-cylinder engine testing of advanced turbomachinery (electronic boosting, 2-stage turbocharging, and supercharging), advanced EGR cooling systems (EGR pump, 2-stage cooling, variable displacement pumps, etc.), and evaluate VVA including cylinder deactivation. (Stanton, Cummins)
- Caterpillar will continue optical engine tests to further develop fundamental understanding of low-temperature combustion and make improvements to further advanced fuel system capability and demonstration of those benefits. Additional fuels effects testing will be performed to discern fuel property effects. Control strategies will be refined and implemented on advanced multi-cylinder engines. (Milam, Caterpillar)
- International will complete the engine builds and benchmark the attributes of their variable compression ratio and VVA prototypes. KIVA3V combustion simulations will be conducted to further optimize combustion hardware. International will continue to conduct steady-state testing to optimize combustion hardware for U.S. 2010 heavy-duty emission regulations; special emphasis will be on fuel economy. Also, International will develop a prototype engine control unit to handle in-cylinder combustion diagnostics and feedback. (de Ojeda, International)
- GE Global Research will optimize the combination of post and pilot injections for the most favorable hardware combination, and expand the studies over the entire engine duty cycle. (Primus, GE Global Research)
- ORNL will shakedown and experimentally demonstrate low-irreversibility combustion in the CPER bench-top apparatus and continue analyses of data from CPER experiments to determine efficiency implications and appropriate ways to model exergy losses under different operating modes. Additionally, better ways for recuperating exhaust heat and utilizing compound cycles for extracting work will be explored. (Graves, ORNL)
- DDC will procure an advanced next generation fuel injection system including variable nozzles that can greatly enhance fuel injection flexibility. A master plan on consolidation of fuel injection strategy and dual combustion modes to minimize cylinder-out emissions will be developed. DDC will also continue steady-state advanced combustion development. (Zhang, DDC)
- GM will continue development and testing of their prototype gasoline and diesel engine hardware which enables operation of HCCI combustion for improved fuel efficiency and emissions performance. Both “two-step” and fully variable valve actuation systems will be further developed and tested.

B. Energy-Efficient Emission Controls

In FY 2008, work will continue on LNTs and selective catalytic reduction using urea (urea-SCR) to reduce NOx emissions. The focus of activities will be on making these devices more efficient, more durable, and less costly. For PM control, the focus will be on more efficient methods of filter regeneration to reduce impact on engine fuel consumption.

- PNNL will continue the studies of CO_2 and H_2O effects on BaO morphology changes and NOx storage properties. Characterization of the roles (especially with respect to deactivation) and material properties of promoter species will be detailed. PNNL will also initiate studies of interactions between multiple emission control devices (e.g., how to optimize LNT regeneration for NH_3 production if a downstream urea-SCR catalyst system is present). (Peden, PNNL)
- PNNL will further refine function-specific measures of 'aging' and validate the most-suitable function-specific measures on samples incrementally 'aged' under realistic conditions. PNNL will apply developed techniques to the commercial fresh and 'aged' samples in the monolith form and continue to improve mechanistic understanding of the sulfur removal processes. (Peden, PNNL)
- ORNL will conduct experiments to analyze the potential benefit of NH_3 emissions from LNT catalysts for downstream selective catalytic reduction, evaluate lower precious metal LNT catalysts to study possibilities for cost reduction (a key limitation to introduction of the technology), and examine LNT catalysts for lean gasoline engine applications. (Parks, ORNL)
- SNL will complete parameter optimization for the combined storage/regeneration mechanism, re-evaluating kinetic constants for the precious metal sites if necessary. SNL will also use the validated reaction mechanisms to investigate coupling between an LNT and other devices in the aftertreatment train. (Larson, SNL)
- ORNL will refocus efforts on the impacts of NH_3 storage on selective catalytic reduction catalyst performance, particularly at low temperatures and for aged catalysts. (Toops, ORNL)
- ORNL will investigate fast desulfation to potentially drive off weakly bound sulfates before they convert to strongly bound sulfates and determine sulfation/desulfation behavior of mixed model catalysts. Effects of doping storage phase with other alkali/alkaline components will be investigated to affect sulfate stability. (Toops, ORNL)
- ORNL will quantify engine-system non-uniformities and mitigation strategies as well as selected LNT sulfation effects. Selected nitrogen-selectivity issues related to LNT regeneration and hybrid catalyst systems will be investigated. (Partridge, ORNL)
- ORNL will continue engine-based studies to assess a combination of LNT catalysis for HECC and traditional modes. The ability of catalysts to control increased carbon monoxide and hydrocarbon emissions from advanced combustion modes will also be examined (Parks, ORNL)
- ORNL will continue co-leading the CLEERS planning committee and co-leading the LNT Focus Group, and support the DPF and SCR Focus Groups as needed. ORNL will also continue providing standard reference LNT materials and data for Focus Group evaluation and continue assisting in refinement of CLEERS technical priorities, especially in regard to the balance between LNT and urea-SCR R&D and synergies between these two technology areas. ORNL will organize the 11th CLEERS workshop in the spring of 2008 and continue maintenance and expansion of the CLEERS web site. (Daw, ORNL)
- ORNL will continue the expansion of the bench-flow and micro-reactor capabilities and continue the development and demonstration of methods for utilizing LNT protocol data to generate global reaction kinetics and simulate device-scale performance. ORNL will also continue the characterization of the Umicore LNT reference catalyst over a range of conditions relevant to both diesel and lean gasoline engine exhaust and transmit results to the LNT Focus Group as they become available. (Daw, ORNL)
- PNNL will conduct research into the design and optimization of 4-way devices which address soot, hydrocarbons, CO, and NOx in a single unit. Exploration of issues surrounding nano-particulate emissions, including nano-particle detection, identification by size and composition, and prediction of nano-particle formation and behavior in after-treatment systems will also be investigated. Filtration and regeneration experiments and simulations will be conducted to improve prediction

of global reaction rates during active and passive regeneration and estimation of device state from sensor data. (Stewart, PNNL)

C. Critical Enabling Technologies

The critical enabling technologies activities in FY 2008 include work on VVA, variable compression ratio systems, and combustion sensors.

- Delphi will refine their VVA system using finite element analysis and computational fluid dynamics (CFD). Accelerated durability testing of mechanism and dynamometer engine testing while monitoring exhaust emissions will verify the benefits predicted by CFD modeling. (Gutterman, Delphi)
- Envera LLC will optimize their variable compression ratio hydro-mechanical system for improved performance and manufacturability. The existing/optimized variable compression ratio engine will be installed and tested in a test vehicle. (Mendler, Envera LLC)
- The immediate future work for Streamline Automation, LLC is to take the engineering lessons learned from the design of the new stainless steel package, and of high-temperature interconnects, and complete the final construction of the new planar-type NOx sensor. During the next phase characterization, the differencing algorithm will be refined for real-time operation, and the identification and quantification portions of the signature processing will be integrated into that algorithm so that all processing is completed in real-time by an engine controller-type embedded computer. (Vogt, Streamline Automation, LLC)
- Testing will continue at TIAX LLC to generate further combustion sensor data at more speed and load points, and this data will be tested in the algorithms. Low-temperature combustion is planned to evaluate the sensor for HCCI engine operation (current data has been measured in diesel mode). The sensor package will also be tried on the second engine setup to determine the engine-to-engine repeatability of the algorithms. (Smutzer, TIAX LLC)
- Westport Power, Inc. will study sensor-to-sensor variation on two Cummins ISB engines as well as study the effectiveness of the current compensation methods in dealing with sensor-to-sensor variation. A charge amplifier for gain compensation will be investigated to further improve robustness using signals from non-adjacent bearing caps. (Mumford, Westport Power, Inc.)
- John Deere will perform vehicle testing to better define actual operating fuel savings. Emphasis will be primarily on the truck, since this is where there is most interest. Commercialization potential needs to be defined. More detailed cost analysis and projections are required. Volume projections will be important here, so knowing the nature of the benefits over a range of applications will be required. (Vuk, John Deere)
- Cummins will proceed to laboratory-based, engine-integrated system testing with an EGR-only WHR system and develop and tune the control system of the WHR system to provide optimum performance integrated with the engine and driveline systems. Cummins will also acquire, incorporate and test components necessary for main exhaust stream energy recovery and create specifications and initiate procurement of a second-generation hardware set appropriate for installation in-vehicle. (Nelson, Cummins)
- Volvo will test advanced compressors and turbines in special rigs and build a prototype of the high efficiency turbocompound device. Additional turbocompound device and turbocharger testing will be conducted in order to verify theoretical performance. Volvo will also demonstrate the engine and continuously variable transmission system in a test cell to determine system efficiency. (Habibzadeh, Volvo)
- Caterpillar plans an on-engine demonstration of a 4 to 4.5% improvement in thermal efficiency using advanced turbocharger technologies, intercooling, and insulated exhaust ports. Additionally, Caterpillar will conduct a bench demonstration of the performance of the Brayton bottoming cycle components, worth another 3 to 4% improvement in thermal efficiency. (Kruiswyk, Caterpillar)
- Volvo will conduct analysis of test results with simulation results and develop an advanced hybrid engine control strategy. (Kang, Volvo)

D. Health Impacts

The focus of the activities in Health Impacts is to identify and quantify the health hazards associated with exhaust from advanced combustion engines and put them in proper context with other air quality hazards, and to assess the relative hazards of emissions from different fuel, engine, and emission reduction technologies.

- ORNL will evaluate the impact of butanol fuel addition to ethanol-gasoline fuel mixtures on emissions and determine the efficiency of catalytic aftertreatment for reduction of mobile source air toxics from high efficiency clean combustion diesel operation. (Parks, ORNL)
- NREL will test a variety of light-, medium-, and heavy-duty vehicles over different driving test cycles at room temperature (72°F) and cold temperature (20°F) on chassis dynamometers in support of the Collaborative Lubricating Oil Study on Emissions (CLOSE) Program. (Lawson, NREL)
- The subproject of the Health Impacts activity will be completed by LRRI in early FY 2008. Wrap-up will include examining effects of nanoparticles and emission gases at lower concentrations, and publishing results. Future effort in this area will focus on evaluating emerging technologies. (Mauderly, LRRI)
- HEI will complete emissions characterization of the third and fourth 2007-compliant engines at SwRI and finalize the engine selection criteria described in the Initial Plan for Engine Selection with the ACES Oversight and Steering Committees. HEI will continue to work with LRRI, CRC, and the engine manufacturers to determine appropriate specifications for the LRRI engine facility. (Greenbaum HEI)

Solid State Energy Conversion

Research will continue in FY 2008 on thermoelectrics for capturing and utilizing waste heat from advanced combustion engines. Research will focus on development of practical systems that are suitable for future production.

- GM will finalize the TE waste heat recovery subsystem design and provide initial production-ready TE modules for application-based testing. GM will start TE exhaust waste heat recovery subsystem prototype construction and develop cost-effective thermoelectric materials and modules. (Yang, GM)
- BSST will complete the build of a full-scale high temperature TGM and perform a bench test including the primary heat exchanger and power conversion system subsystems. (LaGrandeur, BSST)
- MSU will conduct design and analysis of the power conditioning system to optimize thermoelectric system performance, including fault remediation and refine leg fabrication methods (e.g. wet milling/dry milling, hot pressing) for improving mechanical properties and microstructural characteristics. Additional refinement of fabrication techniques for scaleable couple/thermoelectric modules will also take place. Analytical studies will be finalized on the full engine system including coupling current simulations to the 3-D heat transfer studies to provide efficiency gains for the optimum thermoelectric generator-engine configurations. (Schock, MSU)

University Research

In FY 2008, our university partners will continue their fundamental research into combustion and the chemistry of emission control devices.

- UM will carry out single- and multi-cylinder experimental investigations of upper and lower load combustion limits with supercharging/turbocharging and fast thermal management of intake temperature. Valve actuation and supercharging/turbocharging implementations with the GT-Power® system model will be explored and performance and fuel economy benefits will be evaluated. UM will develop a model of spark-assisted HCCI and explore potential benefits of the technology from the point of view of control and range extension. (Assanis, UM)

- The University of Wisconsin-Madison will provide guidelines to the engine and energy industries for achieving optimal low-temperature combustion operation, and low emissions engine design concepts will be proposed and evaluated. (Reitz, University of Wisconsin-Madison)
- WVU will continue their activities in the following areas: (1) modeling to demonstrate the benefits of the "two fuels" approach in managing in-cylinder combustion, (2) determination of the optimal use of pre- and post-turbocharger heat from a system perspective, (3) design of the integrated heat exchanger and reformer, and (4) addressing the complete system design and control through modeling. (Clark, WVU)
- The University of Houston will conduct bench-scale experiments on the role of Rh and CeO_2 on the performance of their LNT. Focus will be placed on the effect of Pt/Ba interfacial coupling through bench-scale and temporal analysis of products (TAP) reactor experiments that quantify the effect of Pt/Ba interfacial perimeter on the activity and product distribution. Additionally, selected TAP experiments will be carried out using monolith catalysts, enabling a direct comparison of bench-scale and TAP data. (Harold, University of Houston)
- The University of Kentucky will complete accelerated aging of model monolithic catalysts (repeated sulfation/desulfation cycles). Aged catalysts will be characterized using standard physico-chemical techniques, in tandem with bench reactor tests, in order to correlate catalyst aging characteristics with washcoat composition. Additionally, *in situ* diffuse reflectance infrared Fourier transform spectroscopy and on-line mass spectrometry measurements will be performed on model powder catalysts in order to gain improved insights into the chemistry of catalyst desulfation. (Crocker, University of Kentucky)
- Texas A&M University will continue to use their engine cycle simulation to study diesel engines and initiate studies to examine novel engines such as the "iso-engine" (which uses an isothermal compression process). The on-going study of EGR for spark ignition engines will be completed. (Caton, Texas A&M University)
- MSU will correct the oscillation tracking deficiency in present automotive hotwire technology for improved frequency compensation methods through development of new, fast-response, yet robust sensor technology. The large eddy simulation model validation will be completed as well as performance testing of the HECC engine. (Schock, MSU)
- UT at Austin will evaluate new sensor designs to further improve sensor durability and complete the analysis of the effects of exhaust gas velocity on sensor output. Additionally, testing will begin on the sensor in a model-year 2007 6.7-liter Cummins diesel engine that will be installed in the UT Combustion Laboratory. (Hall, UT at Austin)

HONORS AND SPECIAL RECOGNITIONS

1. Paul Miles, Invited Lecture: *2007 SAE Homogeneous Charge Compression Ignition Combustion Symposium,* September 12–14, Lund.

2. 2006 SAE Russell S. Springer Award to Cherian Idicheria for best technical paper by author less than 36 years of age. (SAE 2006-01-3434).

3. Salvador M. Aceves invited to deliver a seminar at the SAE 2007 symposium on HCCI, September 2007, Lund, Sweden.

4. Daniel Flowers invited to deliver a seminar at the SAE 2007 symposium on HCCI, September 2007, Lund, Sweden.

5. Robert Wagner, Oak Ridge National Laboratory, FreedomCAR Technical Highlight in 2007.

6. John Dec, Plenary lecture at the SAE/NA 8th International Conference on Engines for Automobiles, Capri, Italy, September 2007.

7. John Dec, Invited presentation at the SAE HCCI Symposium, Lund, Sweden, September 2006.

8. Magnus Sjöberg, SAE Russell S. Springer Award, presented at 2007 SAE Congress.

9. John Dec, SAE Lloyd Withrow Distinguished Speaker Award, presented at 2007 SAE Congress.

10. 2007 Science & Technology highlight for the Energy & Engineering Sciences directorate at ORNL.

11. Robert Wagner, Oak Ridge National Laboratory, DOE EERE Weekly Report.

12. Robert Wagner, Oak Ridge National Laboratory, ACEC Technical Team summary to USCAR Board of Directors.

13. Robert Wagner, Oak Ridge National Laboratory, ACEC Technical Team highlight.

14. Robert Wagner, Oak Ridge National Laboratory, FreedomCAR Technical Highlight in 2007.

15. Letter from Dr. John C. Wall, Cummins Vice President and Chief Technical Officer: "The knowledge and tools developed in our CRADA were critical to the R&D efforts that culminated in the release of the aftertreatment technology that meets the 2010 environmental standards in 2007."

16. First Place Winner of the "DuBose-Crouse Award for Unique, Unusual and New Techniques in Microscopy"; 40th Annual IMS/ASM 2007 International Meeting, Fort Lauderdale, FL: Saenz, N., H.E. Dillon, S. Carlson and G.D. Maupin. *Advanced Meatallographic Techniques Applied to Diesel Particulate Filters.*

17. J. Yang, GM Research & Development Center - The John M. Campbell Award (outstanding contributions to pure or applied science).

18. Ron Graves, Oak Ridge National Laboratory, Fellow Grade of Membership, Society of Automotive Engineers, April 2007.

INVENTION AND PATENT DISCLOSURES

1. J. B. Green, C. S. Daw, R. M. Wagner, Oak Ridge National Laboratory, "Combustion Diagnostic for Active Engine Feedback Control"; United States patent number 7,277,790 B1.

2. Dec, J. E. and Sjöberg, M., U.S. Patent number 7,128,046 B1, "Fuel Mixture Stratification as a Method for Improving Homogeneous Charge Compression Ignition Operation," issued October 31, 2006.

3. Oak Ridge National Laboratory, "A method for diagnosing and controlling combustion instabilities in internal combustion engines operating in or transitioning to homogeneous charge compression ignition modes", IDEAS 05-156, patent pending.

4. Streamline Automation, LLC, Provisional Patent filed – Voltammetry-Enhanced Multiple Gas Emissions Sensing, application number 60944156.

5. Streamline Automation, LLC, Provisional Patent filed – Aerodynamically-Efficient High-Performance Adapter for Exhaust Gas Sensors, application number 60944272.

6. Streamline Automation, LLC, Provisional Patent filed – Miniature Multi-Channel Potentiostat for Gas Voltammetry, application number 60950336.

7. Streamline Automation, LLC, Provisional Patent Application pending – Gas-Selective Filter for Automotive Exhaust Gas Sensors.

8. The University of Texas at Austin, Patent Pending: 2443 - A Sensor to Measure Time-Resolved Particulate (soot) Exhaust Emissions from Internal Combustion Engines has been patented with coverage in the US in the form of a PCT that was nationalized in the US. Provisional: 7/19/2002, PCT conversion: 7/18/2003, Nationalization in the US: 1/19/2005.

9. Westport Power, Inc., Patent application in progress for algorithm developed during this period.

10. Cummins Inc., Patent No. US7,211,793 B2; Date of Patent May 1, 2007; Neal W. Currier and Aleksey Yezerets, Mass spectrometry system and method.

11. Caterpillar, Ignition Timing Control with Fast and Slow Control Loops (IVP and EGR).

12. Caterpillar, Mixed High and Low Pressure EGR in HCCI Engine.

13. Caterpillar, Strategy for Extending the HCCI Operation Range using Low Cetane Number Diesel Fuel and Cylinder Deactivation.

14. Caterpillar, Recipe for High Load HCCI Operation.

15. Caterpillar, Power Balancing Cylinders in HCCI Engine.

16. Marc Allain and Min Sun, Detroit Diesel Corporation, "Method and System of Diesel Engine Setpoint Compensation for Transient Operation of a Heavy-Duty Diesel Engine", U.S. Patent No. 7,281,518, October 16, 2007.

17. Guangsheng Zhu and Houshun Zhang, Detroit Diesel Corporation, "Invention of Squish-Induced Mixing-Intensified Low Emission Combustion (SIMILECOM)." Record of invention was submitted on August 16, 2007.

18. John Deere, 17307, Turbo Generator Control with Variable Valve Actuation

19. John Deere, 18117, Circumferential Dual-Vane Turbine Inlet

20. Mike Kass and Bill Partridge, Oak Ridge National Lab, US Patent "Integrated Self-Cleaning Window Assembly for Optical Transmission in Combustion Environments," Patent No. U.S. 7,247,383 B1, Date of Patent July 24, 2007.

21. Delphi Variable Valve Actuation Provisional Patents submitted:

1. System for Continuously Varying Engine Valve Duration.
2. Continuously Variable Valve Actuation System.
3. Electro-hydraulically actuated Variable Valve Duration System.

22. GM has submitted over forty invention disclosures related to their externally heated particulate filter regeneration device. Numerous patent applications are in process.

The remainder of this report highlights progress achieved during FY 2007 under the Advanced Combustion Engine R&D Sub-Program. The following 63 abstracts of industry, university, and national laboratory projects provide an overview of the exciting work being conducted to tackle tough technical challenges associated with R&D of higher efficiency, advanced internal combustion engines for light-duty, medium-duty, and heavy-duty vehicles. We are encouraged by the technical progress realized under this dynamic Sub-Program in FY 2007, but we also remain cognizant of the significant technical hurdles that lay ahead, especially those to further improve efficiency while meeting the EPA Tier 2 emission standards and heavy-duty engine standards for the full useful life of the vehicles.

Gurpreet Singh
Team Leader,
Advanced Combustion Engine R&D
Office of Vehicle Technologies

Roland M. Gravel
Office of Vehicle Technologies

Kenneth C. Howden
Office of Vehicle Technologies

John W. Fairbanks
Office of Vehicle Technologies

James Eberhardt
Chief Scientist,
Office of Vehicle Technologies

II. ADVANCED COMBUSTION AND EMISSION CONTROL RESEARCH FOR HIGH-EFFICIENCY ENGINES

A. Combustion and Related In-Cylinder Processes

II.A.1 Light-Duty Diesel Spray Research Using X-Ray Radiography

Christopher F. Powell (Primary Contact),
Jin Wang
Argonne National Laboratory
9700 S. Cass Avenue
Argonne, IL 60439

DOE Technology Development Manager:
Gurpreet Singh

Objectives

- Study the mechanisms of spray atomization by making detailed, quantitative measurements in the near-nozzle region of sprays from light-duty diesel injectors.
- Perform these measurements under conditions as close as possible to those of modern diesel engines.
- Utilize the results of our unique measurements in order to advance the state-of-the-art in spray modeling.

Accomplishments

- A collaborative paper between Argonne and Robert Bosch GmbH was published in September 2007, based on X-ray measurements of near-production nozzles.
- Our first single-shot measurements of sprays were performed and published in 2007. These measurements showed that important features of the spray are remarkably reproducible from one spray event to the next.
- In FY 2007, we developed a new data analysis technique that allows us to calculate the average velocity of the fuel in a spray as a function of time. This is one of the few experimental techniques that can measure spray velocity, and can do so in the very-near-nozzle region.
- In FY 2007 we published an article in the Journal of Automobile Engineering's Special Issue on Engine Diagnostics. Our paper was one of only seven chosen for publication in this important special issue.
- FY 2007 saw the continuation of an important collaboration with General Motors (GM) and the Engine Research Center (ERC) at the University of Wisconsin. One week of X-ray measurements in FY 2007 was dedicated to this collaboration.
- In FY 2007, we demonstrated that X-ray measurements of full-production six-hole nozzles can be performed without sacrificing data quality.

Future Directions

- Increase the relevance of our measurements by studying sprays under conditions even closer to those of modern diesel engines. We have made steady progress over the course of the project, continually increasing the ambient pressure and enabling the use of production nozzles. We plan to upgrade our fuel system to the latest generation of fuel injection equipment, and use full-production injectors that can also be run in the GM-Fiat 1.9-liter engine running in Argonne's Engine and Emissions group.
- Increase the impact of our work by fostering collaboration with outside groups. Our collaborations with modeling groups allow our work to increase the fundamental understanding of the mechanics of the spray event, while our collaborations with industry enable us to develop a technique that is useful as a diagnostic for injection system manufacturers. Both of these expand the impact of our research, and help to meet the program objectives of decreased emissions and increased efficiency.
- Improve the measurement technique. While we produce useful results today, improvements to the measurement technique will increase its applicability and accessibility in the future. Such improvements include faster data acquisition, processing, and analysis, improved X-ray detector systems, increased X-ray intensity, and greater automation.

Introduction

Fuel injection systems are one of the most important components in the design of combustion engines with high efficiency and low emissions. A detailed understanding of the fuel injection process and the mechanisms of spray atomization can lead to better engine design. This has spurred considerable activity in the development of optical techniques (primarily using lasers) for measurements of diesel fuel injection systems. Some of these optical techniques have become commercially available and can be readily applied to the testing and development of modern injection systems. Despite significant advances in spray diagnostics over the last 30 years, scattering of light

from the large number of droplets surrounding the spray prevents penetration of visible light and limits such measurements to the periphery of the spray. This is especially true in the near-nozzle region of the spray, which is considered to be the most important region for developing a comprehensive understanding of spray behavior. Existing models of spray structure have only been compared with data acquired in the region relatively far from the nozzle. It is unknown how well these models apply in the crucial near-nozzle region. The limitations of visible light in the near-nozzle region of the spray have led us to develop the X-ray absorption technique for the study of fuel sprays. X-rays are highly penetrative, and measurements are not complicated by the effects of scattering. The technique is non-intrusive, quantitative, highly time-resolved, and allows us to make detailed measurements of the spray, even in the dense droplet region very near the nozzle.

Approach

This project studies the sprays from commercially-available light-duty diesel fuel injectors. Our approach is to make detailed measurements of the sprays from these injectors using X-ray absorption. This will allow us to make detailed measurements of the fuel distribution in these sprays, extending the existing knowledge into the near-nozzle region. The X-ray measurements were performed at the 1BM-C station of the Advanced Photon Source at Argonne National Laboratory. A schematic of the experimental setup is shown in Figure 1; detailed descriptions of the experimental methods are given in references [1] and [2]. The technique is straightforward; it is similar to absorption or extinction techniques commonly used in optical analysis. However, the X-ray technique has a significant advantage over optical techniques in the measurement of sprays: because the measurement is not complicated by the effects of scattering, there is a simple relation between the measured X-ray intensity and the mass of fuel in the path of the X-ray beam. For a monochromatic (narrow wavelength bandwidth) X-ray beam, this relation is given by

$$I/I_0 = \exp(-\mu_M M)$$

where I and I_0 are the transmitted and incident intensities, respectively; μ_M is the mass absorption constant; and M is the mass of fuel. The constant μ_M is measured in a standard cell, and the incident and transmitted intensities are measured as a function of time by the X-ray detector. This allows direct determination of the mass of fuel at any position in the spray as a function of time. It is the goal of our work to use the X-ray technique to measure sprays from our light-duty fuel injector at different injection pressures, different ambient pressures, and using different nozzle geometries. This will enable us to quantify how each of these variables affects the structure of the spray. We will also collaborate with spray modelers to incorporate this previously unknown information about the near-nozzle region of the spray into new models. This will lead to an increased understanding of the mechanisms of spray atomization and will facilitate the development of fuel injection systems designed to improve efficiency and reduce pollutants.

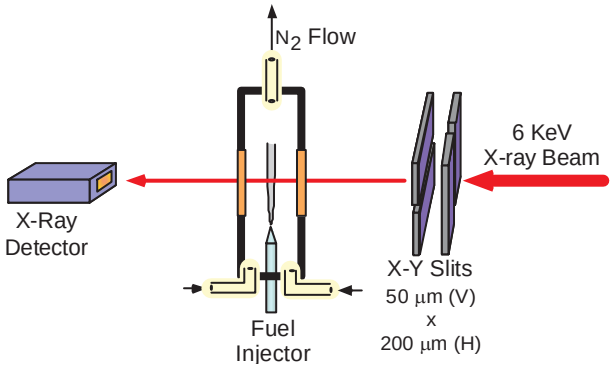

FIGURE 1. Schematic of the Experimental Setup

Results

In 2007 we made significant advances to make measurements of sprays under conditions similar to those in a real engine. For the first time, X-ray measurements were performed using a full-production six-hole nozzle. These measurements demonstrated that we could isolate a single spray from this nozzle, and study it without interference from neighboring sprays. This is a significant step, as most of our previous work has used single-hole nozzles, which may generate sprays that differ in structure from true production nozzles. The measurements of production nozzles enable the results to be directly applied to modern engines and computational models.

A new analysis technique for the X-ray spray measurements was developed in FY 2007 that allows us to calculate the average velocity of the fuel in a spray as a function of time. This is one of the few experimental techniques that can measure spray velocity, and can do so in the very-near-nozzle region. The fuel velocity is an extremely important quantity in spray modeling, as it directly influences aerodynamic breakup. Yet, few reliable measurements of velocity in the spray core have been published, and modelers often must assume or 'tune' the velocity, reducing the reliability of the models. Figure 2 shows the axial velocity of the fuel over the course of the injection event. Note that a significant amount of time is required for the fuel to reach its maximum velocity, while most spray models assume a constant speed over the entire spray event. With this new analysis, we can now provide modelers with

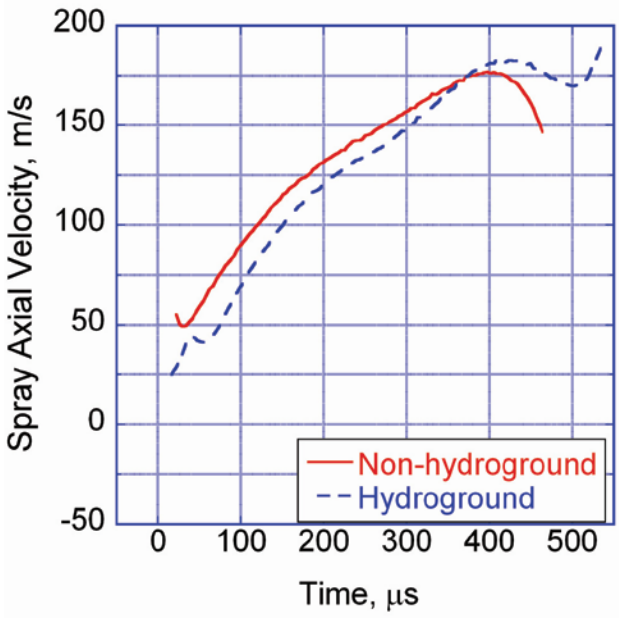

FIGURE 2. Average Spray Axial Velocity as a Function of Time for Two Different Nozzles at 250 Bar Injection Pressure

accurate measurements of the average speed of the fuel, resulting in improved spray modeling.

Our first single-shot measurements of sprays were performed and published in 2007. Previously, all of our published results were averaged over many sprays. The new X-ray monochromator which became operational in FY 2006 increased our X-ray flux by a factor of 50, and enabled us to make meaningful measurements from a single spray event. Figure 3 shows the projected density of fuel as a function of time for four individual spray events (red points) and for the average of 32 spray events (black curve). These measurements showed that important features of the single-shot measurements remarkably reproducible, and are preserved in the average measurements, while the noise is significantly reduced. Therefore, conclusions about spray structure which have been made based on averaged data are likely applicable to single-shot events as well.

Our group's collaboration with Robert Bosch GmbH had another milestone in FY 2007; a joint paper was published based on research completed in FY 2006. This paper detailed the measurements of near-production nozzles at high spray chamber densities. In order to build on the results of this paper, Bosch has requested that additional collaborative measurements be performed in FY 2008, with Bosch providing state-of-the-art injection equipment and technical support. This has all been accomplished based on a handshake agreement with engineers at Bosch Corporate Research, Stuttgart. Bosch has supported our work over the last two years with approximately $50,000 of in-kind contributions, and the work has been freely publishable and available to our memorandum of understanding partners.

FY 2007 saw the continuation of an important collaboration with GM and the ERC at the University of Wisconsin. One week of X-ray measurements in FY 2007 was dedicated to this collaboration. Measurements were performed at ambient pressures up to 30 bar for several different nozzle geometries. The analysis of the results is being performed by students and faculty at ERC with funding from GM. The collaboration will continue in the future, and the experiments and analysis will form the Ph.D. thesis of Amaury Malave at the University of Wisconsin.

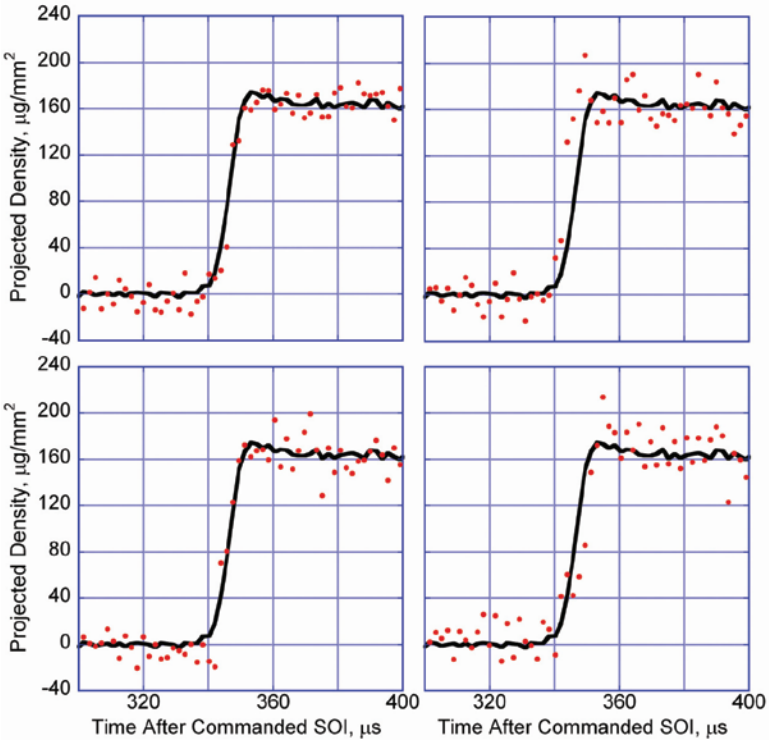

FIGURE 3. Projected Density of Fuel Versus Time at the Apparent Start of Injection for Four Individual Spray Events (Red Points) and the Average of 32 Spray Events (Black Curve)

Conclusions

- The X-ray technique can be used to observe subtle changes in the spray structure resulting from different nozzle geometries. These changes are not apparent using other imaging techniques. This is a very useful diagnostic tool to fuel system manufacturers when designing and testing new injection systems.
- The time-dependent mass measurements provide unique information to spray modelers, and allow them to test their models in the near-nozzle region of the spray, something that was impossible previously. This data is crucial for the development of accurate spray models and for the detailed understanding of spray behavior. The quantitative measurements that we have provided may help to elucidate the mechanisms of spray atomization. This could ultimately lead to the design of cleaner, more efficient engines.
- The impact of our work on the engine community is shown by the expanding list of collaborators and by the significant in-kind contributions to our work that are being made by fuel system and engine manufacturers.

References

1. C. F. Powell, Y. Yue, R. Poola, and J. Wang, J. Synchrotron Rad. 7:356-360 (2000).

2. C. F. Powell, Y. Yue, R. Poola, J. Wang, M.-C. Lai, J. Schaller, SAE 2001-01-0531, (2001).

FY 2007 Publications/Presentations

1. "Measurement Of Diesel Spray Axial Velocity X-Ray Radiography", A. Kastengren, C. F. Powell, J. Wang, S.-K. Cheong, Y. Wang, K.-S. Im, X. Liu, J. Wang, Presentation to the Combustion MOU Partners, Sandia National Laboratory, February 2007.

2. "Fuel Spray Research Using Advanced Photon Sources", C. F. Powell, Presentation at DOE Merit Review and Peer Evaluation, Arlington, VA, June, 2007.

3. "Effect of Ambient Pressure on Diesel Spray Axial Velocity and Internal Structure", A. L. Kastengren, C. F. Powell, K.-S. Im, Y. Wang, J. Wang, DEER Conference, Detroit, MI, August 2007.

4. "Improved Method to Determine Spray Axial Velocity Using X-Ray Radiography", A. Kastengren, C. F. Powell, T. Riedel, S. –K. Cheong, Y. Wang, K. –S. Im, X. Liu, J. Wang. 20th Annual Conference on Liquid Atomization and Spray Systems, Chicago, IL, May 2007.

5. "Fuel Spray Characterization Using Ultra-Fast X-Ray Radiography", C. F. Powell, Presentation to the Graduate School of Mechanical Engineering, University of Illinois at Chicago, March 2007.

6. "X-Ray Measurements of the Mass Distribution in the Dense Primary Break-Up Region of the Spray from a Standard Multi-Hole Common-Rail Diesel Injection System" P. Leick, T. Riedel, G. Bittlinger, C.F. Powell, A.L. Kastengren, J. Wang, Proceedings of the 21st ILASS - Europe Meeting, Muğla, Turkey, September 2007.

7. "Spray Density Measurements Using X-Ray Radiography" A. L. Kastengren, C. F. Powell, Journal of Automotive Engineering, Volume 221, Number 6, 2007, pp. 653-662.

8. "Determination of Diesel Spray Axial Velocity Using X-Ray Radiography" A. Kastengren, C. F. Powell, T. Riedel, S. –K. Cheong, Y. Wang, K. –S. Im, X. Liu, J. Wang, Society of Automotive Engineers, Paper 2007-01-0666 (2007).

II.A.2 Low-Temperature Automotive Diesel Combustion

Paul Miles
Sandia National Laboratories
PO Box 969
Livermore, CA 94551-0969

DOE Technology Development Manager:
Gurpreet Singh

Subcontractors:
University of Wisconsin Engine Research Center,
Madison, WI

Objectives

- Provide the physical understanding of the in-cylinder combustion processes needed to meet future diesel engine emissions standards while retaining the inherent efficiency and low CO_2 emissions of the direct-injection diesel engine.
- Improve the multi-dimensional models employed in engine design and optimization and validate the model predictions against in-cylinder measurements and tailpipe emissions.
- Investigate the effect of various combustion system parameters on engine performance and emissions, thereby generating a knowledge base for optimization efforts.

Accomplishments

- Completed automotive low-temperature combustion (LTC) facility upgrade incorporating a General Motors (GM) 1.9-liter production diesel head into an optically-accessible, single-cylinder engine. Installed new exhaust gas recirculation (EGR) simulation capabilities permitting simulated EGR with H_2O, CO_2, N_2, O_2, CO, unburned hydrocarbon (UHC), and other trace components.
- Established correspondence between optical and traditional metal engine performance and emissions, through close comparison of pressure-based performance metrics as well as engine-out emissions for a range of combustion system parameters.
- Evaluated optical engine performance and emissions for a wide range of operating conditions characterizing both high-dilution and late-injection LTC operating regimes. Identified operating conditions of interest for future optical studies focusing on the sources of CO and UHC emissions.
- Examined sources of UHC emissions and their cyclic-variability through time-resolved measurements obtained with a fast flame ionization detector.
- Identified a "best-fit" modeling constant that matches the measured turbulent kinetic energy and its dissipation rate to data obtained in a motored engine.
- Demonstrated the ability of multi-dimensional engine combustion models to predict the influence of swirl on soot formation and oxidation in heavy-duty diesel engines, and employed the model to understand asymmetries in soot formation with respect to the fuel jets.

Future Directions

- Develop optical diagnostic technique for visualizing the in-cylinder spatial distribution of CO.
- Apply optical techniques to investigate sources of UHC and CO emissions in highly dilute, LTC regimes.
- Evaluate the effect of engine boost on low-temperature combustion systems and on the fuel conversion efficiency loss typically observed with high dilution levels.
- Examine how trace components in simulated EGR influence the combustion and emissions formation processes.
- Assess the impact of strain and rotation dependent model coefficients on the modeling of the turbulent kinetic energy dissipation in flows with bulk compression.

Introduction

Direct injection diesel engines have the highest fuel conversion efficiency and the lowest CO_2 emissions of any reciprocating internal combustion engine technology. However, this efficiency often comes at the expense of high NOx or particulate matter (soot) emissions. Through adoption of LTC techniques–relying on lower compression ratios, large quantities of cooled EGR, and unconventional injection timing and/or strategies–soot and NOx can often be dramatically reduced. Unfortunately, the low combustion temperatures beneficial for inhibiting soot and NOx formation can also lead to significant CO and UHC emissions, due to the slower oxidation of these species and to the more stringent mixing requirements imposed by the low O_2 concentration in the intake charge. Failure to rapidly oxidize CO and UHC can also result in

a substantial penalty in fuel consumption. Reduction of CO and UHC emissions, and recovery of fuel economy, is imperative if these engines are to achieve widespread acceptance. Only then can they contribute to our energy security and help reduce the CO_2 emissions associated with personal transportation.

Identifying the dominant in-cylinder processes influencing CO and UHC emissions, understanding the relevant physics controlling these processes, and developing a predictive modeling capability are crucial steps toward the development and optimization of clean, fuel-efficient engines utilizing LTC systems. Each of these components is represented in the research described in the following.

Approach

The research approach consists first of establishing an optically-accessible research engine with characteristics and operating conditions that allow it to closely match the combustion and engine-out emissions behavior of traditional, all-metal test engines. Detailed measurements of in-cylinder flows, fuel and pollutant spatial distributions, and other thermo-chemical properties are subsequently obtained, and employed both to identify the dominant physical processes governing combustion and emission formation and to formulate and validate multi-dimensional computer models. These measurements are closely coordinated and compared with engine-out emissions and with the predictions of numerical simulation efforts.

The experimental and numerical efforts are mutually complementary. Detailed measurements of flow variables permit the evaluation and refinement of the computer models, while the model results can be used to clarify the flow physics–a process that is difficult if only limited measurements are employed. Jointly, these approaches address the principal goals of this project: development of the physical understanding to guide, and the modeling tools to refine, the design of optimal, clean, high-efficiency combustion systems.

Results

Research efforts in this fiscal year were divided among four main areas: completion of the facility upgrades to incorporate a GM production diesel engine head into our optically-accessible engine and to improve our EGR simulation capabilities; careful matching of all-metal test engine performance and emissions data to establish the relevance of the optical engine measurements; benchmarking engine performance and emissions over a broad range of operating conditions to establish the foundation for future optical studies; and assessment of the performance of various aspects of turbulent combustion modeling in engines.

The upgraded optical engine is shown in Figure 1. In addition to incorporating the GM 1.9-liter production head, the optical access was improved significantly. By recessing the upper liner into the cylinder head, a clear view into the squish volume can be achieved even with the piston at top dead center (TDC). The large top-ring land height further allows imaging of the full-bowl depth at crank angles ±30° on either side of TDC. Moreover, a concave surface on the bottom of the optical piston acts as a negative lens, and allows imaging of the squish volume from below to within 3 mm of the cylinder wall.

Because the optical engine is skip-fired, there is no natural source of undiluted exhaust gas and EGR must be simulated. Concurrent with the engine upgrade, we also improved our ability to simulate EGR. The EGR system now incorporates a boiler that allows the addition of H_2O to our previous mixture of CO_2 and N_2. We have also added the capability to include CO and UHC, as well as other trace species in our simulated EGR. These species influence the combustion process through their thermophysical properties, their impact on the chemical kinetics of the ignition process, and through their intrinsic heating value. At high EGR rates, EGR characterized by large CO and UHC mole fractions contains a significant quantity of chemical energy, and impacts the amount of fuel required to obtain a given load significantly.

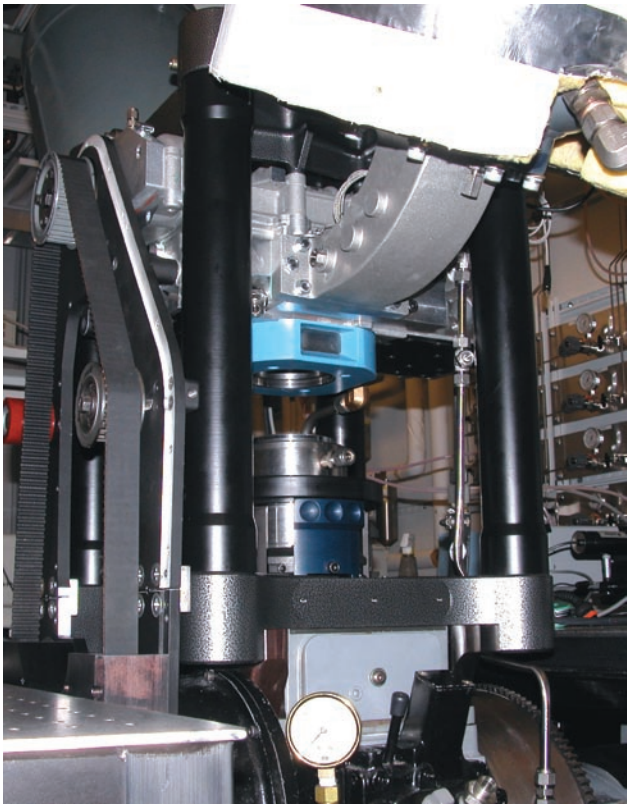

FIGURE 1. The Optically-Accessible Engine Incorporating the GM 1.9-Liter Head

To ensure that the data acquired in the optical engine accurately represents the combustion process occurring in all-metal engines, we have carefully matched the near-TDC thermodynamic conditions of the metal test engine by closely matching the composition of the intake gases, the near-TDC pressure of a motored metal engine trace (obtained with hot combustion chamber surfaces and representative EGR and residual concentrations), and the ignition delay. The same fuel batch was used in both the metal and optical engine tests to ensure that the ignition delay can be used as an accurate thermometer. A comparison of the apparent heat release rate observed in the metal and the optical engines is shown in Figure 2. Note that the timing of the main heat release is quite sensitive to intake temperature. With an intake temperature of 72°C, both the timing and the magnitude of the peak heat release are well matched. The breadth of the heat release measured in the metal engine is greater, however, and the optical engine heat release exhibits greater post-TDC fluctuations. Modeling of the optical engine extended piston as an oscillating spring-mass system suggests that these differences may be attributed to deformation of the optical piston.

A comparison of the UHC and CO emissions measured in both engines for a start of injection (SOI) sweep is presented in Figure 3. The magnitude, the location of the minima, and the trends in the emissions match well when the full complement of EGR gases is employed in the optical engine. When only N_2 and CO_2 are used to simulate EGR the magnitude of the emissions is higher. While running these tests, the injected fuel quantity was held constant. Hence, the differences observed cannot be attributed to reduced fueling when the simulated EGR contains UHC and CO. Away from the minimum, the relative increase in CO emissions is well matched, while the UHC emissions increase more rapidly in the optical engine. We believe this is due to a greater sensitivity of UHC emissions to wall temperature differences between the two engines. The existence of a distinct minimum in UHC and CO emissions (as well as indicated specific fuel consumption) is also noteworthy. A similar minimum was identified in a previous engine build, and shown to be associated with an optimal fuel distribution that best utilizes the available air [1]. The duplication of this behavior demonstrates the general applicability of this earlier work.

We have also investigated the ability of multi-dimensional engine combustion models to duplicate and explain the behavior of soot distributions in swirl-supported, heavy-duty diesel engines. Experimentally, soot observed during the expansion stroke is found to be rotating in a counter-clockwise direction, characterized by a positive vorticity (Figure 4). This vorticity, as well as the temporal evolution of the soot cloud, mark the soot-containing fluid as the remnants of the windward (with respect to swirl) side of the fuel jet head vortex. Because the swirl might be expected to transport fresh air into the windward side–thereby enhancing mixing–higher soot levels in this region are not expected. The predictions of multi-dimensional simulations performed at the University of Wisconsin, also shown in Figure 4, both reproduce and help explain this phenomenon. In the presence of swirl, the initial premixed heat release occurs predominantly on the leeward side of the jet. Combustion-induced flows subsequently lead to better mixing and reduced soot formation in this area. The higher soot concentrations on the windward side of the jet are thus predominantly due to higher rates of soot formation in this region just after the premixed combustion event.

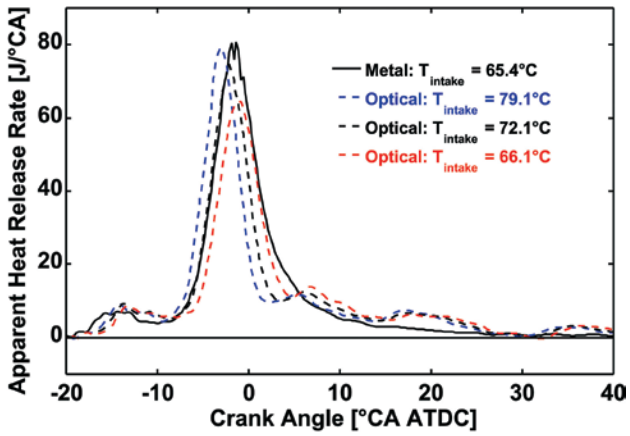

FIGURE 2. A comparison of the apparent heat release rate observed in the optical and the all-metal test engines at 2,000 RPM, a load of 6 bar indicated mean effective pressure, SOI = -41.7°, and a 9% O_2 concentration. Metal engine results courtesy of Prof. David Foster, GM-University of Wisconsin collaborative research laboratory.

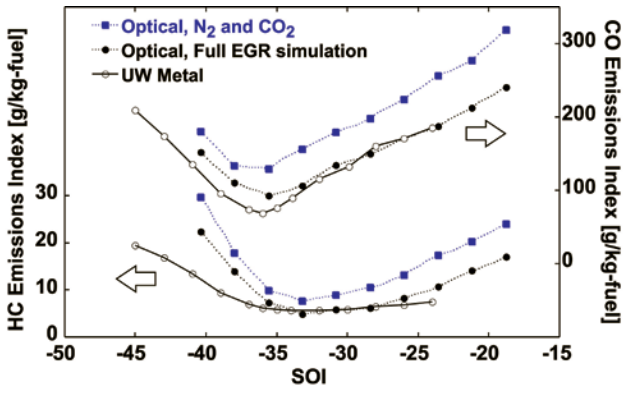

FIGURE 3. UHC and CO Emissions Obtained in an SOI Sweep, for the Same Conditions Identified in Figure 2

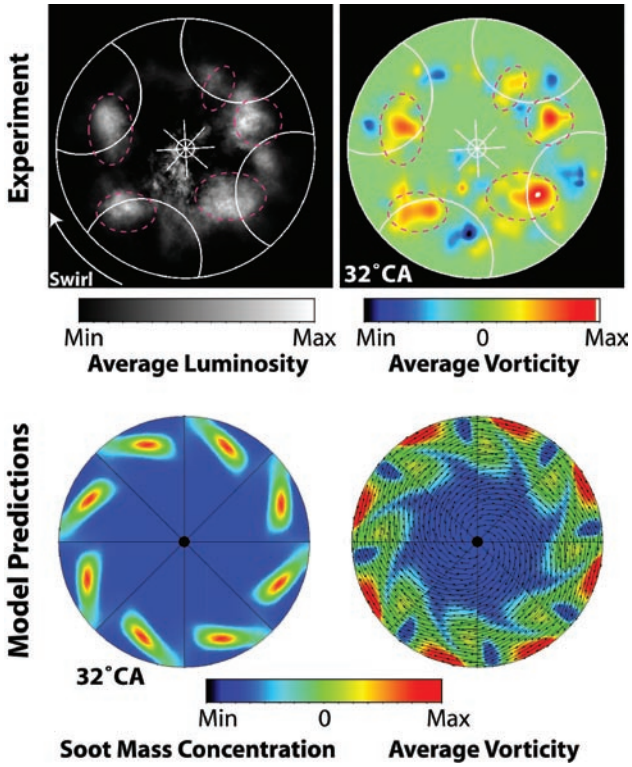

FIGURE 4. The upper row presents the mean distribution of soot luminosity and the axial component of vorticity (flow rotation) measured in a heavy-duty diesel engine with a swirl ratio of 1.7. Model predictions of these quantities are shown in the lower row. The model correctly predicts the approximate location of the soot and its correlation with positive vorticity.

Conclusions

- An upgrade to the optical engine and improved EGR simulation facilities have been completed and offer new capabilities for investigation the sources of emissions and inefficiencies in LTC systems.
- Careful matching of operating conditions allows both the combustion performance and the emissions behavior to be well-matched between optical and traditional metal engines, ensuring the relevance of data obtained from the optical engine.
- Performance and emission behavior has been mapped over a wide range of operating conditions, providing the foundation for future optical studies of emission sources and their mitigation in LTC regimes.
- The ability of multi-dimensional simulations to predict and explain the soot distributions observed in swirl-supported heavy-duty engines has been examined. The simulations reproduce the experimental results and show that enhanced mixing during the premixed heat release on the leeward side of the jet reduces the formation of soot as compared to the windward side of the jet.

References

1. Miles, PC (2005) US Department of Energy, Office of FreedomCar and Vehicle Technology, 2005 Annual Progress Report.

FY 2007 Publications/Presentations

1. Fife ME., Miles PC, Bergin MJ, Reitz, RD, and Torres, DJ. (2008) The impact of a non-linear turbulent stress relationship on simulations of flow and combustion in an HSDI diesel engine, *Submitted to* ***SAE 2008 World Congress***, Offer: 08PFL-992.

2. Colban WF, Kim D, Miles PC, Opat R, Krieger R, Foster D, Durrett R, Gonzalez M. (2008) A detailed comparison of emissions between optical and metal single-cylinder diesel engines at low-temperature combustion conditions, *Submitted to* ***SAE 2008 World Congress***, Offer: 08PFL-602.

3. Bergin M, Reitz RD. (2008) Optimization of injector spray configurations for an HSDI diesel engine at high load, *Submitted to* ***ASME J. Gas Turbines and Power.***

4. Colban WF, Miles PC, Oh S. (2007) Effect of intake pressure on emissions from an automotive diesel engine operating in low-temperature combustion regimes," ***SAE Powertrain, Fuels and Lubricants meeting***, Oct. 29-31, Chicago, SAE Paper: 2007-01-4063.

5. Miles PC, RempelEwert BH, Reitz RD (2007) Assessment of Reynolds-averaged dissipation modeling in engine flows. ***8th Int'l. Conference on Engines for Automobiles–ICE2007***, Sept. 16-20, Capri-Naples. SAE Paper: 2007-24-0046. *Selected for SAE Transactions.*

6. Miles, PC. (2007) On sources of CO and UHC emissions in low-temperature diesel combustion regimes, *Invited presentation:* ***2007 SAE Homogeneous Charge Compression Ignition Combustion Symposium***, Sept. 12–14, Lund.

7. Miles, PC. (2007) Sources and mitigation of CO and UHC emissions in low-temperature diesel combustion regimes: insights obtained via homogeneous reactor modeling. ***13th Diesel Engine Efficiency and Emissions Research Conference (DEER 2007)***, Aug. 13-16, Detroit.

8. Colban WF, Miles PC, Oh S. (2007) On the cyclic variability and sources of unburned hydrocarbon emissions in low-temperature diesel combustion systems, ***JSAE/SAE 2007. International Fuels and Lubricants meeting***, July 23-26, Kyoto. SAE Paper: 2007-01-1837. *Also presented at* ***DOE/OFCVT Advanced Engine Combustion Meeting***, February 6–7, 2007.

9. Miles PC. (2007) Automotive low-temperature combustion research, ***DOE EERE/OFCVT Merit Review***, June 18-19, Arlington.

10. Bergin M, Reitz RD, Oh S, Miles PC, Hildingsson L, Hultqvist A. (2007) Fuel injection and mean swirl effects on combustion and soot formation in heavy-duty diesel engines," ***SAE 2007 World Congress***, April 16-19, Detroit. SAE Paper: 2007-01-0912. *Selected for SAE Transactions.*

11. Miles PC, Hildingsson L, Hultqvist A (2007) The influence of fuel injection and heat release on bulk flow structures in a direct-injection, swirl-supported diesel engine. ***Exp. In Fluids***, **43:** 273-283. *Revised and expanded version of paper presented at* ***13th Int. Symp. on Applications of Laser Tech. to Fluid Mech****., June 26–29, 2006.*

12. Miles PC, Collin R, Hildingsson L, Hultqvist A, Andersson Ö (2007) Combined measurements of flow structure, partially-oxidized fuel, and soot in a high-speed, direct injection diesel engine. ***Proc .of the Combustion Institute,*** **31**: 2963–2970.

13. Bergin MJ, Reitz RD, Oh S, Miles PC, Hildingsson L, Hultqvist A. (2007) Fuel injection and mean swirl effects on combustion and soot formation in heavy-duty diesel engines, ***DOE/OFCVT Advanced Engine Combustion Meeting,*** Feb. 6–7.

14. Yu R, Bai XS, Hildingsson L, Hultqvist A, Miles PC (2006) Numerical and experimental investigation of turbulent flows in a diesel engine, ***SAE 2006 Fall Powertrain and Fluid Systems***, Oct. 17–19. SAE Paper: 2006-01-3436.

15. Mullin AS, Miles PC (2007) Chemistry and physics of new fuels in novel combustion regimes, Contribution to: ***DOE/BES workshop report on Basic Research Needs for Clean and Efficient Combustion of 21st Century Fuels,*** Oct. 29–Nov. 1, Arlington.

16. Miles PC (2007) Low-temperature automotive diesel combustion. ***DOE OFCVT Annual Report.***

Special Recognitions & Awards

Invited Lecture: *2007 SAE Homogeneous Charge Compression Ignition Combustion Symposium*, Sept. 12–14, Lund.

II.A.3 Heavy-Duty Low-Temperature and Diesel Combustion Research and Heavy-Duty Combustion Modeling

Mark P. B. Musculus
Combustion Research Facility
Sandia National Laboratories
P.O. Box 969, MS9053
Livermore, CA 94551-0969

DOE Technology Development Manager:
Gurpreet Singh

Objectives

The overall FreedomCAR and Vehicle Technologies (FCVT) goal for this project is to develop fundamental understanding of advanced low-temperature combustion (LTC) technologies. The specific goals for FY 2007 include:

- Understand LTC unburned hydrocarbon (UHC) emissions (Sandia)
  - This is a response to a specific industry request to understand why UHC emissions increase dramatically when ignition occurs after the end of fuel injection.
  - It is also consistent with the overall FCVT goal of understanding UHC emissions for low-load LTC.
- Improve LTC diesel computer models (Sandia and University of Wisconsin)
  - Improve predictions of diesel flame lift-off and soot formation at LTC conditions.
  - Understand how mixing, combustion, and pollutant formation are affected by engine design parameters, including 1) piston bowl geometry, 2) swirl ratio, and 3) spray targeting.
  - Validate/improve modeling of LTC mixing, combustion, and pollutant formation processes.
- Continue to refine conceptual model for LTC conditions (Sandia)
  - This is a long-term goal with continuous effort to update our understanding of in-cylinder LTC processes as more data becomes available.

Accomplishments

- Optical experiments showed conclusively that over-mixed fuel near the injector yields significant UHC emissions when ignition occurs after the end of injection because it does not achieve complete combustion.
  - Persistent formaldehyde fluorescence and absence of OH fluorescence shows that near-injector mixtures do not burn to completion when ignition occurs after the end of injection.
  - Direct equivalence ratio measurements by toluene fluorescence show that the mixtures *rapidly* become fuel lean, and that they are stagnant, remaining near the injector late in the cycle.
  - The total amount of over-mixed fuel in the near-injector region that does not achieve complete combustion follows trends and magnitude of measured UHC emissions.
- After refinement to include cool-flame reactions, computer models show improved agreement with experiments at LTC conditions.
  - Skeletal chemical kinetics mechanisms were modified to include cool-flame reactions to better simulate flame lift-off at LTC conditions.
  - With better lift-off simulation, prediction of soot formation was also improved.
- Initiated a parallel experimental and modeling study of effects of bowl geometry, spray angle, and swirl ratio on in-cylinder LTC processes
  - Preliminary computer models predict that spray targeting is the most significant factor affecting LTC performance and emissions, though swirl is important as well.
  - Will acquire large optical dataset of mixing, combustion, and pollutant formation with ranges of bowl diameter, spray angle, and swirl ratio to understand effects of design factors and to validate model predictions of in-cylinder phenomena.

Future Directions

- Apply optical diagnostics for other LTC conditions
  - Compare single and split/pilot injection schemes for conventional and LTC combustion using multiple imaging diagnostics.
- Maintain modeling collaboration with the University of Wisconsin to improve computer model performance for LTC conditions.
  - Analyze large optical dataset of parametric variation in bowl geometry, injector spray angle, and swirl ratio.
  - Use experimental data to validate and improve computer models.

- Develop simple mixing model of end-of-injection mixing processes.
  - Improve understanding of physical processes affecting liquid- and vapor-fuel mixing after end of injection.
  - Predict effect of injection rate shapes on mixture formation.
- Continue to extend the conceptual model of diesel combustion to LTC conditions.

Introduction

Although LTC strategies can achieve very low emissions of nitrogen oxides (NOx) and particulate matter (PM) at high efficiency, they typically have increased emissions of other pollutants, including UHCs. The UHC emissions often increase with longer ignition delays (ID) [1,2], particularly when the ID exceeds the injection duration. As part of a specific request for insight into in-cylinder processes causing high UHC emissions, Cummins Inc. provided UHC data from a wide range of diesel engine operating conditions. Figure 1 shows that the UHC emissions become very high for conditions with positive "ignition dwell," defined as the time between the end of injection (EOI) and the start of combustion. UHC emissions for LTC conditions with large, positive ignition dwells are likely dependent on in-cylinder phenomena occurring near or after EOI.

The primary goal of this project for FY 2007 is verify the existence of over-lean mixtures near the injector that do not achieve complete combustion when the ignition dwell is positive, and to assess the importance of these mixtures to UHC emissions. This primary goal is consistent with the overall FCVT goal of understanding UHC emissions for low-load LTC conditions. A second goal is to improve LTC diesel computer models (in collaboration with the University of Wisconsin) to better predict diesel flame lift-off and soot formation at LTC conditions, as well as to understand the influence of engine design parameters on mixing, combustion, and pollutant formation.

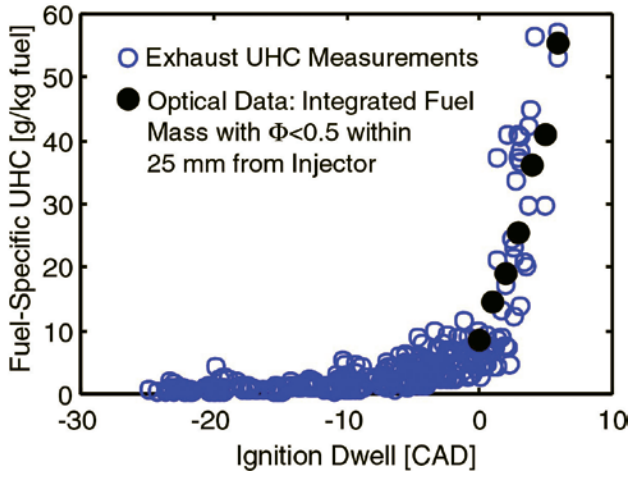

FIGURE 1. Exhaust UHC for a wide range of diesel engine operating conditions (open blue circles) and in-cylinder fuel mass in mixtures with $\Phi<0.5$ within 25 mm of the injector (filled black circles) at various ignition dwells. Exhaust emissions data is from Cummins Inc.

Approach

This project uses an optically-accessible, heavy-duty, direct-injection diesel engine (Figure 2). Imaging access is through a window in the bowl of an extended piston. Windows in the cylinder wall and in the piston bowl-wall are for the laser diagnostics. Figure 2 also shows the setup of the optical diagnostics, which use three cameras. The progress of vapor-fuel combustion is inferred from simultaneous images of planar laser-induced fluorescence (PLIF) of formaldehyde (H_2CO) and hydroxyl radical (OH) under LTC conditions with varying ignition dwells. Quantitative measurements of the in-cylinder vapor-fuel concentration using PLIF of a toluene fuel-tracer are compared to engine-out UHC emissions. The engine operating condition simulates exhaust gas recirculation dilution to 12.6% intake oxygen (by volume), and the engine load is near 4 bar indicated mean effective pressure, with injection near top-dead center.

The modeling work uses a version of the Los Alamos KIVA computer code that has been improved at the University of Wisconsin. Instead of using full detailed chemistry, the model uses a reduced kinetic mechanism for n-heptane ignition and combustion so that solutions can be completed in a reasonable time. Based on sensitivity analysis of a more complex full chemistry mechanism [3], the reduced mechanism was recently improved to include cool-flame reactions that are important for predicting the diesel flame lift-off length at LTC conditions. Also, a multi-objective genetic algorithm [4] was implemented in the KIVA computer model to predict an optimal set of piston bowl designs and spray geometries, which will be studied and validated experimentally in FY 2008.

Results

Simultaneous images of H_2CO fluorescence (red) and OH fluorescence (green) under conditions with ignition dwells that are short (top row) and long (bottom row) are shown in Figure 3. The images were acquired (1) near the peak in the first-stage ignition heat release, (2) near the peak in the second-stage ignition heat release, and (3) late in the cycle, when combustion was essentially complete. For each image in Figure 3, the

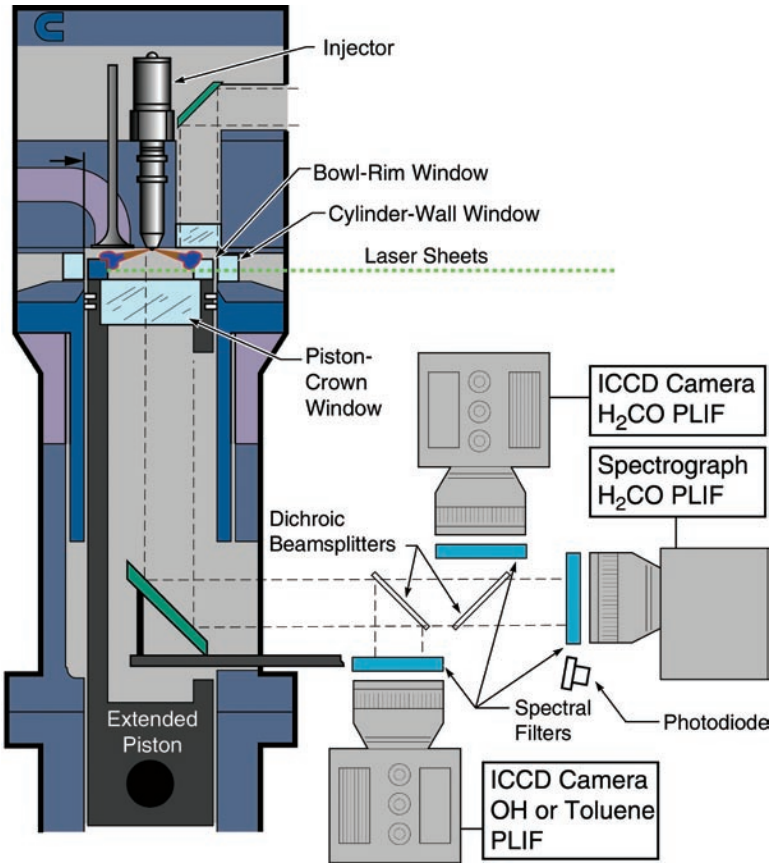

FIGURE 2. Schematic Diagram of the Optically Accessible Direct Injection Diesel Engine and Optical Setup

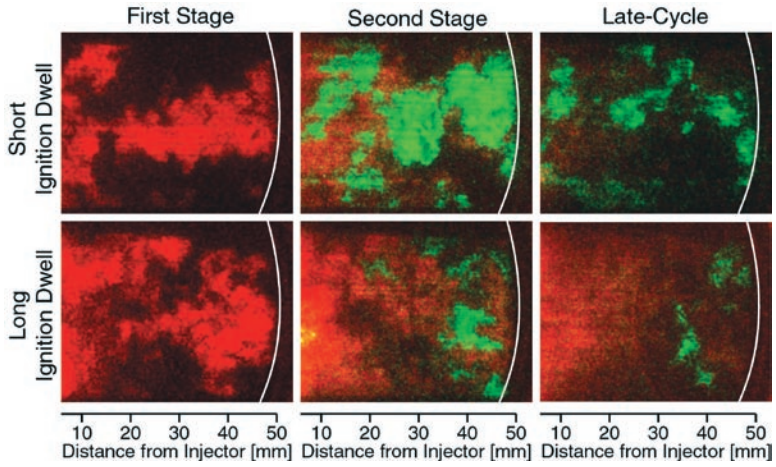

FIGURE 3. Representative composite images of H_2CO PLIF (red) and OH PLIF (green) for the shorter-ID (top row) and longer-ID (bottom row) operating conditions. Images were acquired shortly after first-stage ignition (left column), second-stage ignition (middle column), and late in the cycle (right column). The curved white line represents the piston bowl, and the distance from the fuel injector is indicated below the images.

view is through the piston-crown window (see Figure 2), and the curved white line represents the piston bowl-rim. One of the eight fuel jets, which penetrates horizontally from left to right from the perspective of the camera, is captured in the images. The injector is about 6 mm to the left of the field of view, as indicated by the scale at the bottom of the images.

For both operating conditions, H_2CO PLIF first appears throughout the horizontal jet during the first stage of ignition, and the OH initially appears during the second stage of ignition, in the downstream region of the jet, near the piston bowl-rim. H_2CO fluorescence indicates regions that have completed the first stage of ignition, but have not yet reached complete combustion, while OH indicates regions that have transitioned to the second stage of ignition, where combustion is largely complete.

For the shorter ignition dwell condition (top row), OH fluorescence also appears upstream, near the injector. Late in the cycle, some OH fluorescence (green) is apparent in pockets throughout the combustion chamber, while H_2CO fluorescence (red) is very weak or absent. By contrast, for the long ignition dwell, OH fluorescence almost never appears upstream, and H_2CO fluorescence persists late in the cycle. Although some H_2CO fluorescence is detectable downstream, the strongest fluorescence is typically upstream, within about 25 mm from the injector. The persistent H_2CO fluorescence indicates that combustion is incomplete, and chemical kinetics simulations predict that over-mixing of the fuel to overly lean mixtures is the most likely cause for incomplete combustion.

Figure 4 shows direct measurements of the in-cylinder vapor-fuel equivalence ratio using toluene fluorescence, and the data confirms that the mixtures near the injector indeed become very fuel-lean shortly after the end of injection. In Figure 4, the injector was rotated from its orientation in Figure 3, so that one of the jets that intersected the laser sheet penetrated upward and to the right (2 o'clock position), and another penetrated down and to the right (4 o'clock position).

At EOI, which is 0° after the end of injection (AEI), the mixtures on the jet centerline are fuel-rich throughout the jet, with the richest mixtures near the injector, as is typical of conventional quasi-steady diesel jets. But rapidly after the end of injection, the mixtures near the injector become fuel-lean. By only 0.25° AEI, the axial equivalence ratio distribution is relatively flat. By 1° AEI, the upstream mixtures, near the injector, are clearly leaner than the downstream mixtures. By 3.5° AEI, the mixtures are near stoichiometric within 25 mm from the injector. At 5° AEI, which is the start of the main combustion, the mixtures near the injector are very fuel-lean, which is consistent with the predictions of over-lean mixtures by the chemical kinetics simulation to explain the persistent H_2CO fluorescence. Also, downstream mixtures that showed strong OH fluorescence (Figure 3) are near-stoichiometric (Figure 4), and should achieve complete combustion. At later times, the jets become indistinct, and the residual jet momentum does not carry the fuel-lean mixtures downstream; rather, they stagnate near the injector, do not achieve complete combustion, and go on to contribute to UHC emissions. Indeed, as shown in Figure 1, the total in-cylinder fuel in mixtures with equivalence ratios less than 0.5 within 25 mm from the injector (filled black circles) agrees very well with exhaust UHC measurements (open blue circles). This agreement indicates that incomplete combustion in over-lean mixtures near the injector is likely responsible for much of the UHC emissions for conditions with long positive ignition dwell.

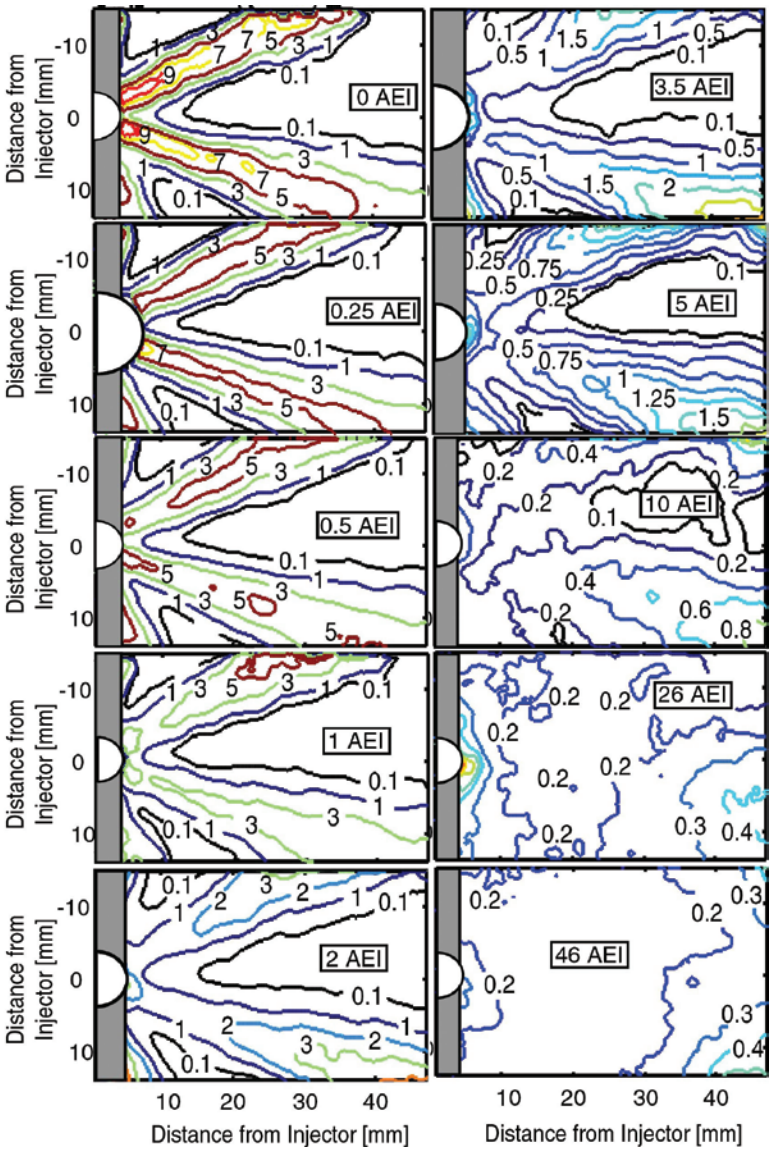

FIGURE 4. Equivalence ratio contours measured by toluene fluorescence. The time in crank-angle degrees after the end of injection (AEI) is indicated in each of the plots. The injector is on the middle left edge of each image, and two of the eight fuel jets fall within the field of view (see Figure 3 for field of view). The white half circle and vertical gray rectangle masks represent areas of residual laser flare off the injector and firedeck surface, respectively, where fuel vapor measurements are not viable.

Figure 5 shows a comparison of diesel jet lift-off lengths under LTC conditions from measurements in a constant-volume combustion vessel (squares), predictions from the KIVA computer model using the original chemical kinetics mechanism with no cool flame reactions (circles), and predictions with several critical cool-flame reactions added to the mechanism (triangles). Addition of the cool-flame reactions that were identified through a sensitivity analysis of a complex detailed chemistry mechanism [3] clearly improves the agreement between the model predictions (triangles) and experimental measurements (squares). These improved predictions of flame lift-off translate to better prediction of soot formation in the diesel jets under LTC conditions (not shown here).

Finally, Figure 6 shows the results of a design optimization using genetic algorithms with the KIVA computer model. The technique [4] identifies a set of optimum designs (the Pareto citizens, in blue triangles) that have the best performance over a range of emissions and efficiency criteria, plotted on the axes. The "Pareto surface" of the blue triangles is useful because rather than producing only a single optimum design as in previous optimization approaches, different optimal engine designs may be selected from the Pareto surface depending on the relative importance of the performance criteria to the engine designer.

Conclusions

- This project uses an optical engine to study in-cylinder phenomena coupled with modeling collaborations to improve simulation capabilities for LTC conditions.
- Multiple imaging diagnostics showed that over-mixed fuel near the injector yields significant UHC emissions because it does not achieve complete combustion when ignition occurs after the end of injection.
- Using experimental data for validation, the accuracy of computer model predictions was improved.
- FY 2007 activity transfers results to industry to address a specific request for information about dramatic increase UHC emissions for LTC conditions.
- Future work will explore multiple injection strategies and combustion chamber design parameters with both experiments and simulations.

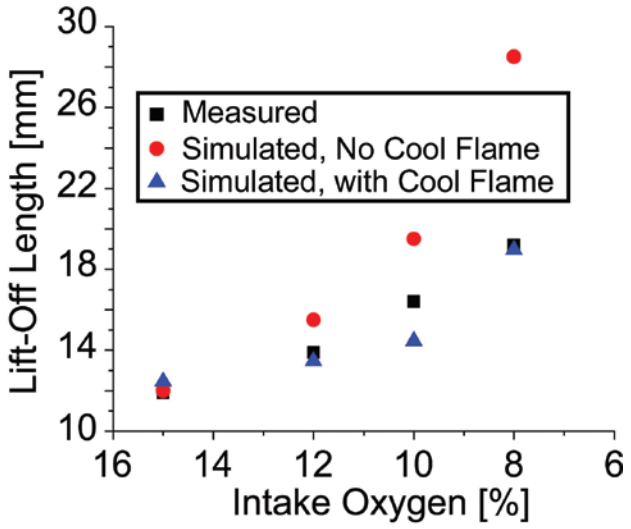

FIGURE 5. Lift-Off Measurements (Black Squares) and Predictions with (Blue Triangle) and without (Red Circle) Cool-Flame Reactions in the n-Heptane Reduced Mechanism

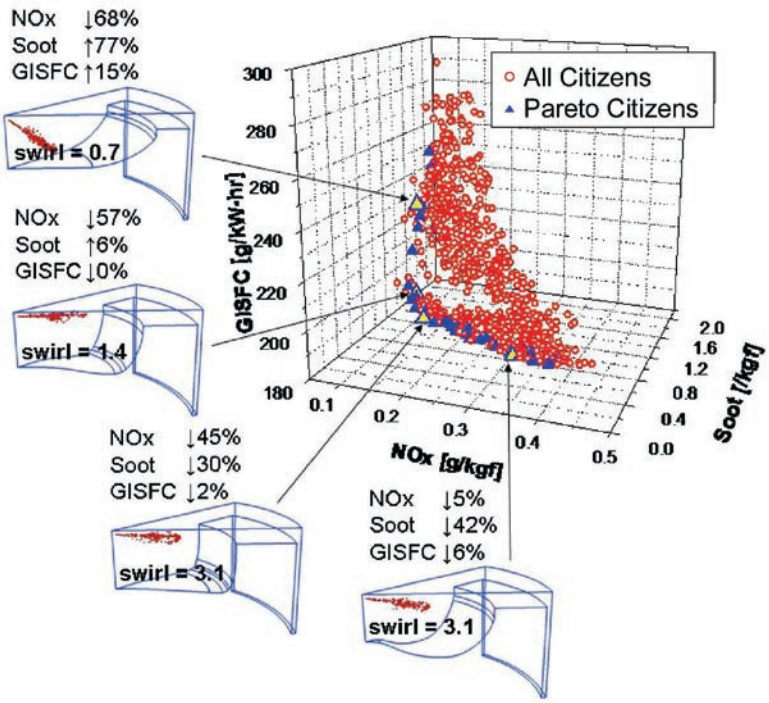

FIGURE 6. Predicted emissions and fuel consumption performance for simulations with different piston bowl geometry, fuel spray angle, and swirl ratio at a LTC condition. The optimal "Pareto surface" citizens (blue triangles) are a subset of the full set of configurations tested (red circles).

References

1. Kanda, T., Hakozaki, T., Uchimoto, T., Hatano, J., Kitayama, N., and Sono, H., "PCCI Operation with Early Injection of Conventional Diesel Fuel," SAE Paper 2005-01-0378, 2005.

2. Okude, K., Mori, K., Shiino, S., and Moriya, T., "Premixed Compression Ignition (PCI) Combustion for Simultaneous Reduction of NOx and Soot in Diesel Engine," SAE Paper 2004-01-1907, 2004.

3. Maroteaux, F. and Noel, L., "Development of a Reduced n-Heptane Mechanism for HCCI Combustion Modeling," Combustion and Flame 146, pp. 246-267, 2006.

4. Coello Coello, C.A. and Pulido, G.T., "A Micro-Genetic Algorithm for Multiobjective Optimization," First International Conference on Evolutionary Multi-Criterion Optimization, Lecture notes in Computer Science no. 1993, pp. 126-140, 2001.

FY 2007 Publications/Presentations

Publications

1. "End-of-Injection Over-Mixing and Unburned Hydrocarbon Emissions in Low-Temperature-Combustion Diesel Engines," M. Musculus, T. Lachaux, L. Pickett, and C. Idicheria, SAE Paper 2007-01-0907, 2007 SAE International Congress and Exposition, April 2007.

2. "In-Cylinder Unburned Hydrocarbon Visualization During Low-Temperature Compression-Ignition Engine Combustion Using Formaldehyde PLIF," T. Lachaux and M. Musculus, Proceedings of the Combustion Institute Vol. 31, pp. 2921-2929, Presented August 2006, Published late 2006.

3. "A Computational Investigation into the Effects of Spray Targeting, Swirl Ratio

and Bowl Geometry for Low-Temperature Combustion in a Heavy-Duty Diesel Engine," C. Genzale, D. Wickman and R.D. Reitz, SAE paper 2007-01-0119, 2007 SAE International Congress and Exposition, April 2007.

4. "Numerical Predictions of Diesel Flame Lift-off Length and Soot Distributions under Low Temperature Combustion Conditions," G. Vishwanathan and R.D. Reitz, Submitted SAE Congress, 2008.

5. "Evaluation of the Equivalence Ratio-Temperature Region of Diesel Soot Precursor Formation Using a Two-Stage Lagrangian Model," L. Pickett, J. Caton, M. Musculus, and A. Lutz., International Journal of Engine Research Vol. 7, No. 5, pp. 349-370, December 2006.

6. "Validation of Engine Combustion Models Using Detailed In-Cylinder Optical Diagnostics Data for a Heavy-Duty Compression-Ignition Engine," S. Singh, R. Reitz, M. Musculus and T. Lachaux, International Journal of Engine Research, Vol. 8, No. 1, pp. 97-126, Jan. 2007.

7. "Two-Stage Ignition and Unburned Fuel Emissions for Heavy-Duty Diesel Low-Temperature Combustion of Neat n-Heptane," M. Musculus and T. Lachaux, 5th US Combustion Meeting, San Diego, March 25-28, 2007.

8. "Gradient Effects on Two-Color Soot Optical Pyrometry in a Heavy-Duty DI Diesel Engine," M. Musculus, S. Singh, and R. Reitz, submitted to Combustion and Flame, May 2007.

9. "Optical Diagnostics Of a Late Injection Low-Temperature Combustion In a Heavy Duty Diesel Engine," T. Lachaux, M. Musculus, S. Singh and R. Reitz, submitted to ASME Internal Combustion Engine Division 2007 Fall Technical Conference, 2007.

10. "In-Cylinder and Exhaust Soot in Low-Temperature Combustion Using a Wide-Range of EGR in a Heavy-Duty Diesel Engine," E. Huestis, P. Erickson, and M. Musculus, submitted to 2007 SAE Powertrain and Fluid Systems Conference.

11. Invited by Woodhead Publishing of Cambridge to contribute book chapter to "Direct Injection Combustion Engines and Their Fuels for Automotive Applications in 21st Century".

Presentations

1. "Quantitative Laser Diagnostics Issues in Transient, High-Pressure Environments of Engines," M. Musculus, L. Pickett, P. Miles, Third International Conference on Lasers and Diagnostics, City University, London, UK, May 23, 2007.

2. "Diesel Jet Mixing in Conventional and Low-Temperature Diesel Combustion," M. Musculus, J. Dec, and T. Lachaux, presented at 10th International Conference on Present and Future Engines for Automobiles, Rhodes Island, Greece, May 30, 2007.

3. "Liquid-Phase Fuel Penetration in Diesel Sprays at the End of Injection," M. Musculus and T. Lachaux, Advanced Engine Combustion Working Group Meeting, June 2006.

4. "Vapor-Phase Fuel-Air Mixing in Diesel Jets at the End of Injection," T. Lachaux, M. Musculus, L. Pickett and C. Idicheria, Advanced Engine Combustion Working Group Meeting, June 2006.

5. "Visualization of UHC Emissions for Low-Temperature Diesel Engine Combustion," M. Musculus and T. Lachaux, Diesel Engine-Efficiency and Emissions Reduction Conference, Detroit MI, August 21, 2006.

6. "Unburned Hydrocarbon Emissions from End-of-Injection Over-Mixing for LTC Diesel Combustion," M. Musculus, T. Lachaux, L. Pickett, and C. Idicheria, Advanced Engine Combustion Working Group Meeting, February 2007.

7. "What's New in Engine Research," M. Musculus, SoCal Science Café, Newport Beach, CA, April 7, 2007.

8. "Laser-Based Imaging of Combustion Processes in the Next Generation of Engines," M. Musculus and J. Dec, USC Viterbi School of Engineering Undergraduate Honors Colloquium, March 9, 2007.

II.A.4 Low-Temperature Diesel Combustion Cross-Cut Research

Lyle M. Pickett
MS 9053
Sandia National Laboratories
P.O. Box 969
Livermore, CA 94551-9053

DOE Technology Development Manager:
Gurpreet Singh

Objectives

- Determine the history of liquid penetration at conditions typical of early-injection low-temperature diesel combustion.
- Investigate the timing and amount of soot formation for short-injection events at high-exhaust gas recirculation (EGR) low-temperature combustion (LTC) conditions.
- Show how multiple injections affect liquid-phase penetration.

Accomplishments

- Quantified the extent of liquid-phase penetration for typical early-injection LTC conditions with various injection durations, nozzle sizes, injection pressures and number of injections. Provides an understanding needed to prevent liquid wall impingement and its negative impacts on emissions and combustion efficiency.
- Showed that the extent of liquid penetration depends upon the injected mass for short injections less than the steady-state liquid length, rather than the nozzle size or injection pressure.
- Demonstrated that small nozzles actually form more soot than larger nozzles when the injection duration is adjusted such that the mass injected is constant.

Future Directions

- Investigate the location of evaporation for end-of-injection mixing near the nozzle and its impact on unburned hydrocarbons.
- Determine how multiple injections can be used to affect ignition timing and minimize unburned hydrocarbons (UHC) at LTC conditions.
- Perform direct measurements of mixing (equivalence ratio) at the time of the premixed burn in constant-injection-duration diesel fuel jets for various EGR levels and multiple injection strategies. This investigation will show how mixing between injections affects the equivalence ratio and location of the premixed burn.

Introduction

Avoiding liquid impingement upon the cylinder liner and preventing excessive impingement on the piston bowl are considered to be key technologies for successful implementation of diesel LTC combustion. Cylinder-liner impingement causes oil dilution and piston impingement may cause high UHC emissions, poor fuel-air mixing, and low combustion efficiency. Unfortunately, prevention of liquid impingement is difficult because the early-injection timing (-50° to -20° crank-angle degrees, CAD), required to induce sufficient fuel-air premixing, also creates charge-gas conditions where liquid impingement is likely (i.e., low charge-gas temperature and density). A low charge-gas temperature will result in little fuel evaporation, and a low density will allow rapid penetration with little momentum and mass exchange with the spray. Alternatively, if injection phasing is retarded closer to top dead center (TDC), there will be less time available for mixing prior to ignition and fuel-rich mixtures forming both nitrogen oxides and soot may be produced. Overall, there is a strong need to understand the effects of injector variables such as nozzle size, injection pressure, injection duration, and number of injections on liquid phase penetration and combustion in LTC engines.

Approach

With the ability to carefully control the charge-gas temperature and density, a constant-volume vessel was utilized to quantify the extent of liquid penetration and soot formation while the thermodynamic and injector conditions were varied. Experiments using a Bosch second-generation common-rail injector with various single-hole nozzles of the same shape (KS1.5/86) are reported here. A more detailed description of the facility may be found in [1].

Mie-scattering and shadowgraph images were simultaneously acquired using high-speed cameras to define the spray liquid and vapor phases, respectively, for a given set of conditions as shown in Figure 1. Mie-scatter images were acquired at a rate of 50 kHz. A survey of the literature shows typical premixed compression-ignition timing ranges from (-40° to -20° CAD) *for conventional spray included angles and nozzle sizes*. Table 1 shows the expected thermodynamic conditions for these injection timings with other

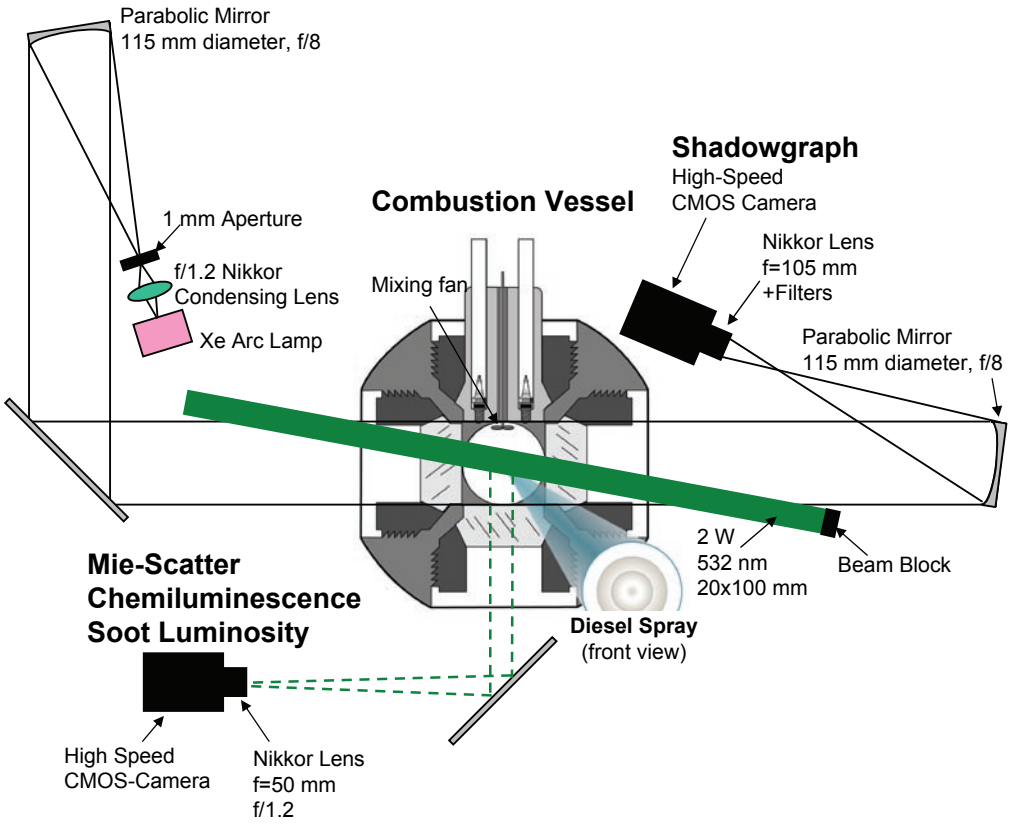

FIGURE 1. Combustion Vessel and High-Speed Imaging Setup (Mirror spacing not to scale.)

assumptions listed on the table. Finally, a #2 diesel fuel (T_{90} = 573 K) and kerosene fuel (T_{90} = 523 K) were compared to assess the effect of fuel type.

TABLE 1. Calculated Charge-Gas Conditions for a Given Crank-Angle (CA)

Assumptions: T_{BDC} = 340 K; P_{BDC} = 1 atm; Compression Ratio = 16; γ = 1.35;					
CAD [°ATDC]	-40	-35	-30	-25	-20
Temperature [K]	601	637	677	721	768
Density [kg/m^3]	5.2	6.2	7.3	8.8	10.5

Results

Figure 2 shows the transient liquid penetration for a long-injection event (solid) and a short-injection event with a 250 μs injection duration (dotted). The liquid length is the longest axial distance of any measurable elastic scatter from droplets, defining the axial boundary between liquid and vapor phases of the spray. The long-injection event shows the expected trend of decreased liquid penetration with injection timing retarded towards TDC. The long-injection-duration sprays eventually reach a "steady-state" liquid length as has been demonstrated in the past [2]. The -40 CAD timing

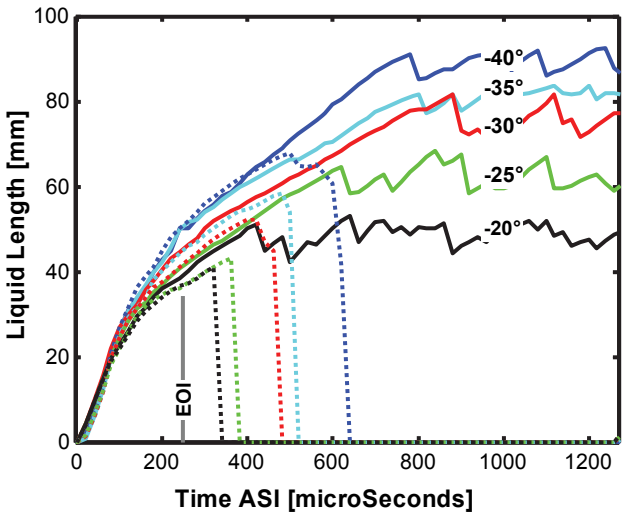

FIGURE 2. Transient Liquid Penetration for Long (Solid) and Short (Dashed) Injection Durations (Thermodynamic conditions for the simulated crank-angle of injection given in Table 1. Fuel, kerosene; T_{fl} = 373 K; d = 0.180 mm; DP_{inj} = 110 MPa.)

has a steady liquid length of approximately 90 mm, which would likely impinge liquid on the cylinder liner. However, shortening the injection duration to 250 μs

significantly decreases the maximum liquid penetration, particularly for the problematic, earlier injection timings. These findings suggest that short injection durations are less likely to experience wall impingement, and therefore could be used for successful LTC operation. However, the amount of fuel injected is small, which would limit the operating load. This is consistent with known trends for LTC operation in engines.

Figure 3 compares the effect of fuel type on the transient liquid history. A lower boiling-point fuel is shown to be effective in reducing the maximum liquid penetration, as well as shortening the time before the fuel completely evaporates after the end of injection. This behavior is expected to be favorable for LTC operation.

An alternative to the use of a lower-boiling point fuel to limit the liquid penetration is to use multiple short injections, as demonstrated in Figure 4. Shadowgraph images, marking the vapor phase, are shown at the right of Figure 4. Blue lines overlaid on the image mark the boundary of the liquid phase obtained from Mie-scatter images. The image sequence shows the first two injections of a four-injection event (equal injection durations). During the first injection, the liquid and vapor phases overlap, indicating low evaporation rates. After the end of injection (0.411 ms), liquid and vapor coincide at the head of the jet, but a vaporized fuel region remains near the nozzle. The second injection begins as liquid vaporizes at the head of the jet. This new injection quickly reaches the vapor region at the head of the jet as it flows through the "wake" left behind by the first injection.

The maximum penetration distance of the liquid and vapor phases is shown at the left of Figure 4 for the entire four-injection event. The vapor phase separates from the liquid phase after the end of the first injection and continues to penetrate across the chamber. The maximum penetration of the liquid phase of the second injection is longer than the first because of mixing with cooler gas vaporized by the first injection and faster penetration by moving through the wake of the first injection. Following injections (second and third) penetrate approximately the same as the second injection. In addition, the maximum liquid penetration remains much less than that of a single, continuous injection with a long injection duration (red curve). Therefore, pulsation of the injector is shown to be effective in limiting liquid penetration and possibly preventing wall wetting.

The dependency of the maximum liquid penetration distance upon injection duration was investigated further by examining the effects nozzle diameter and injection duration with the same total mass injected. It is well known that reducing the injection pressure or nozzle size will reduce the rate of liquid penetration, but the injection duration must be increased in order to reach the same injected mass. For short, transient injections, the question is which strategy minimizes

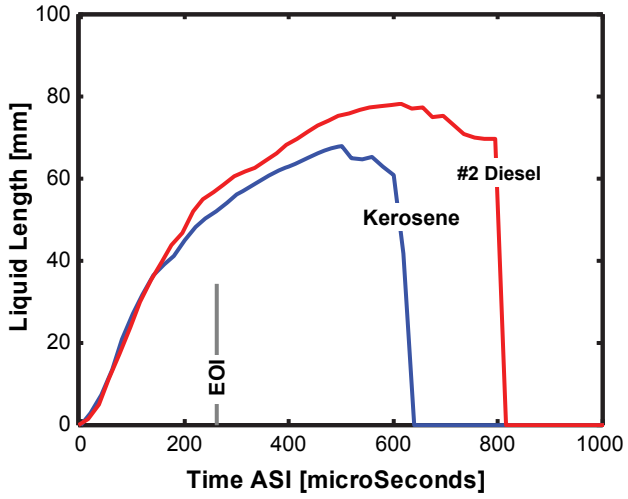

FIGURE 3. Transient Liquid Penetration for Diesel Fuel Compared to Kerosene at -40 CAD Thermodynamic Conditions and a 250 μs Injection Duration (Other conditions the same as Figure 2.)

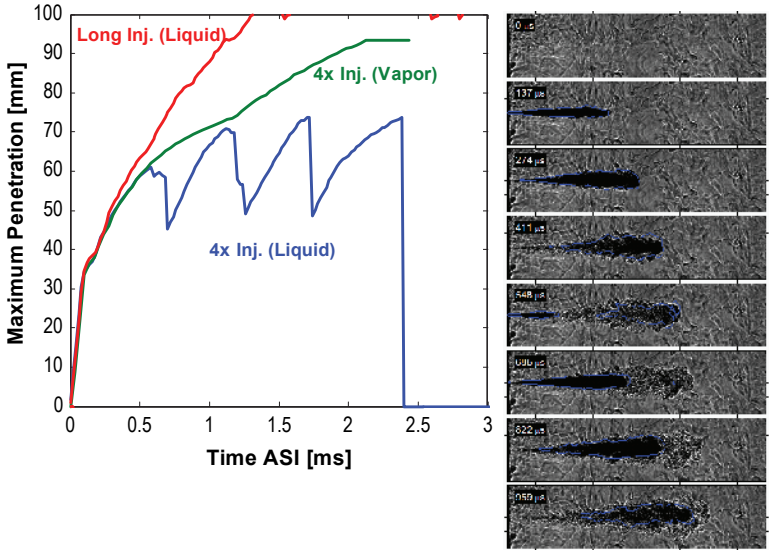

FIGURE 4. Transient Penetration of Liquid (Blue) and Vapor (Green) Phases for a Four-Injection Event (Injection duration for each injection is 0.2 ms. A long injection duration [2 ms] is shown for reference [red]. -40 CAD simulated conditions, Fuel = #2 diesel; T_{fl} = 373 K; d = 0.110 mm; DP_{inj} = 110 MPa.)

liquid penetration. Figure 5 shows the maximum measured liquid penetration for a range of nozzle sizes with the same injection pressure. The major conclusion is that nozzle size does not affect the maximum liquid penetration, indicating that the maximum liquid penetration tends to collapse for given injection mass. Note that this result is restricted to transient injections where the maximum liquid penetration is less than a steady-state value. For example, the steady-state liquid length scales linearly with nozzle diameter and this would eventually dominate if smaller nozzle diameters were used. A study of injection pressure effects confirmed the result that the maximum liquid was the same when the same mass was injected. The collapse of maximum liquid penetration with injection mass may be one contributing factor that limits LTC combustion to low-load conditions.

Similarly, it is well known that reducing the nozzle diameter increases the rate of mixing relative to the fuel injection rate, but again the injection duration must be increased to deliver the same total amount of fueling. Figure 6 shows that the longer injection duration actually causes *more* soot formation for smaller nozzles compared to larger nozzles. The timing of the injection event relative to the ignition delay appears to be important. When injection ends after ignition (negative ignition dwell), the luminosity rise is severe, indicating strong soot luminosity. However, when the injection ends prior to ignition (positive ignition dwell), the luminosity rise is mild, indicating only chemiluminescence from high-temperature combustion (confirmed by other diagnostics). This concept is similar to that explained for the success of MK combustion [3]. With fixed injection pressure, smaller nozzles tend to produce soot because of the required longer injection duration. Figure 6 shows that a solution to remove soot formation is to use both a small nozzle and higher injection pressure, thereby shortening the injection duration for a given injected mass.

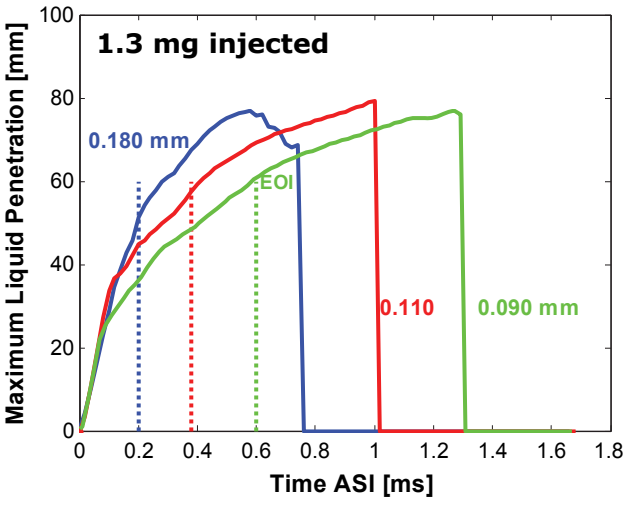

FIGURE 5. Transient Liquid Penetration for Various Nozzle Sizes, each with 1.3 mg Total Injected Mass (Thermodynamic conditions and fuel are the same as Figure 4.)

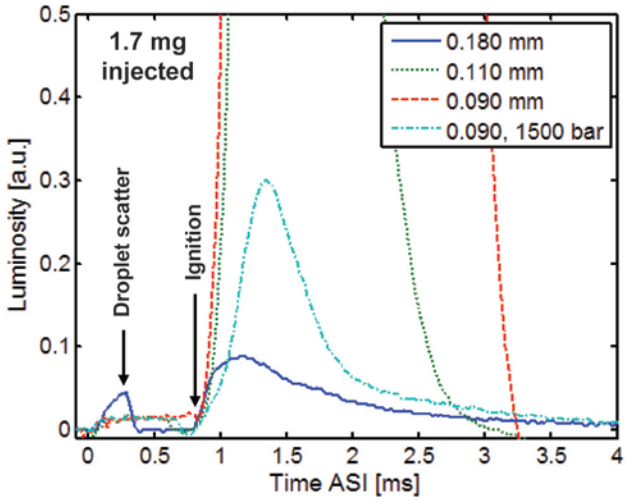

FIGURE 6. Luminosity Rise (Chemiluminescence and/or Soot Formation) for Various Nozzle Sizes, each with 1.7 mg Total Injected Mass (LTC ambient conditions: 900 K, 60 bar, 15% O_2. Injector conditions: #2 diesel; T_{fl} = 373 K; DP_{inj} = 110 MPa unless otherwise specified.)

Conclusions

The effects of injector variables such as nozzle size, injection pressure, injection duration, and number of injections on liquid phase penetration and combustion were investigated this year. Liquid-phase transients were investigated at conditions typical of early-injection LTC engines. Shortening the injection duration and applying multiple injections limits the liquid penetration to be much less than that of a steady-state spray. Results also show that variation in nozzle size and injection pressure while maintaining the same injection mass produces the same maximum liquid penetration. In addition, small nozzles actually form more soot than larger nozzles when the injection duration is adjusted such that the mass injected is constant.

References

1. Engine Combustion Network, http://www.ca.sandia.gov/ECN.

2. Siebers, D.L., "Liquid-Phase Fuel Penetration in Diesel Sprays," SAE Paper 980809, 1998.

3. Kimura, S., Aoki, O., Kitahura, Y., Aiyoshizawa, E., "Ultra-Clean Combustion Technology Combining a Low-Temperature and Premixed Combustion Concept for Meeting Future Emissions Standards," SAE Paper 2001-01-0200, 2001.

FY 2007 Publications/Presentations

1. Musculus, M.P.B, Lachaux, T., Pickett, L.M., and Idicheria, C.A. "End-of-Injection Over-Mixing and Unburned Hydrocarbon Emissions in Low-Temperature-Combustion Diesel Engines," SAE paper 2007-01-0907.

2. Idicheria, C.A. and Pickett, L.M. "Quantitative Mixing Measurements in a Vaporizing Diesel Spray by Rayleigh Imaging," SAE paper 2007-01-0647.

3. Pickett, L.M. and Idicheria, C.A. "Effects of Ambient Temperature and Density on Soot Formation under High-EGR Conditions," THIESEL 2006.

4. Idicheria, C.A. and Pickett, L.M. "Formaldehyde Visualization Near Lift-Off Location in a Diesel Jet," SAE Powertrain and Fluid Systems Conference, SAE 2006-01-3434.

Special Recognitions & Awards/Patents Issued

1. 2006 SAE Russell S. Springer Award to Cherian Idicheria for best technical paper by author less than 36 years of age. (SAE 2006-01-3434).

II.A.5 Achieving High Efficiency Clean Combustion (HECC) in Diesel Engines

Robert M. Wagner (Primary Contact),
Kukwon Cho, Manbae Han, C. Scott Sluder
Oak Ridge National Laboratory (ORNL)
2360 Cherahala Boulevard
Knoxville, TN 37932

DOE Technology Development Manager:
Gurpreet Singh

Objectives

- Increase speed-load operation range in HECC modes for improved emissions and efficiency.
- Investigate mixed-source exhaust gas recirculation (EGR) methods for improved control of dilution composition and temperature.
- Develop computer simulations for improved guidance for, and interpretation of, experiments.
- Commission modern light-duty diesel engine which is representative of state-of-the-art engine technology.

Accomplishments

- Demonstrated increase in speed-load range for HECC operation of a light-duty diesel engine.
- Characterized mixed-source EGR for controlling intake temperature and, correspondingly, emissions and efficiency.
- Explored relationship between brake specific fuel consumption (BSFC) and combustion noise for HECC operation.
- Commissioned and mapped modern light-duty diesel engine.

Future Directions

- Explore advanced combustion operation on a General Motors (GM) 1.9-L engine including efficiency, emissions, noise, and stability with a high-pressure loop (HPL) EGR system.
- Characterize effect of intake mixture temperature and composition on advanced combustion operation.
- Investigate acoustic and vibration energy transmission paths for diagnostics and control of conventional combustion and advanced combustion modes.

Introduction

Advanced combustion modes such as premixed charge compression ignition have shown promise as potential paths for meeting 2010 and beyond efficiency and emissions goals. ORNL, as well as others, have shown success in achieving reduced emissions and acceptable efficiency using high charge dilution for a somewhat limited speed-load range. This activity builds on many years of HECC experience at ORNL, including the demonstration of HECC operation in a multi-cylinder engine, characterization of cylinder-to-cylinder stability issues, detailed speciation of hydrocarbons in HECC modes, description of the effect of particulate matter (PM) precursors on engine-out emissions, and the demonstration of transitions to, from, and within HECC modes. The primary objective of this study is to investigate potential near-term technologies for expanding the usable speed-load range and to evaluate the potential benefits and limitations of these technologies for achieving HECC in light-duty diesel engines.

For further clarification, the term HECC was first introduced in the FreedomCAR Advanced Combustion and Emissions Control Tech Team and Diesel Cross-Cut Team in 2003. The intent was to convey the objectives of advanced combustion research in a fresh, all-encompassing name in a time when low-temperature combustion (LTC), premixed charge compression ignition (PCCI), homogeneous charge compression ignition (HCCI), modulated kinetics (MK), and many more acronyms were in use, but conveyed nothing about the advantages and were aligned with certain companies. DOE adopted HECC as the subject of a large request for proposals in 2004. ORNL adopted the term in 2004.

Approach

Significant progress in expanding the useful speed-load range and robustness of HECC operation will require an improved understanding of near- and long-term enabling technologies (e.g., EGR composition, injector design, etc.) on multi-cylinder engine efficiency, stability, and emissions. A combination of thermodynamic and detailed exhaust chemistry information will be used to improve the understanding of and issues related to achieving HECC operation, which is expected to contribute to more efficient and cleaner diesel engine operation. This information will be considered in other ORNL light-duty diesel engine activities as well as shared with other institutions for the

development and validation of improved combustion models and aftertreatment systems.

HECC operation is being investigated at ORNL on a modified Mercedes-Benz (MB) 1.7-L and GM 1.9-L common rail four-cylinder diesel engines. These engines are equipped with microprocessor-based dSpace control systems which permit unconstrained access to engine hardware including the integration of custom control algorithms. The GM engine also has an engine control unit donated by GM which allows for the monitoring and manipulation of the base engine calibration.

The MB engine also has a low-pressure loop (LPL) EGR system which is used in coordination with the original equipment HPL EGR system to achieve mixed-source EGR as shown in Figure 1. The potential of mixed-source EGR is explored using LPL EGR as a "base" for dilution rather than as a sole source. HPL EGR provides the "trim" for controlling mixture temperature and has the potential for enabling more precise control of dilution set points. The mixed-source approach is also useful for conditions when LPL EGR does not provide sufficient dilution for achieving HECC operation. Additional dilution is achieved with the HPL EGR system, mitigating the need for throttling or a LPL EGR pump.

Results

Four speed-load conditions which were originally defined by an industry working group to be representative of light-duty diesel engine operation were selected for use in this study. While this approach does not take into account cold-start or other transient phenomena, the metric has been successfully used by others for comparison purposes and to demonstrate potential improvements from one technology to another.

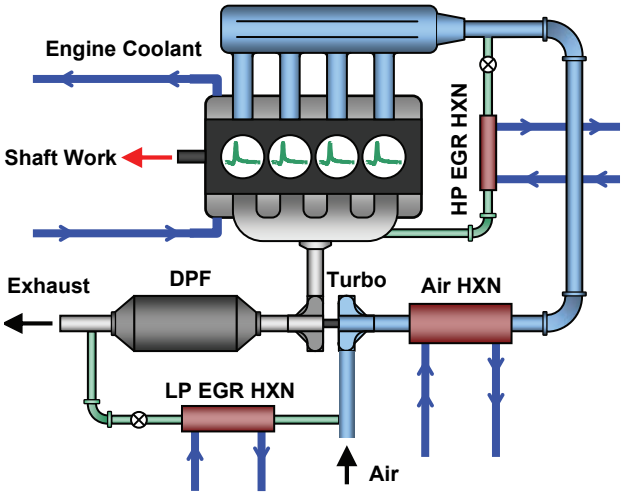

FIGURE 1. Schematic of Mixed-Source EGR System Showing HPL and LPL EGR Loops

TABLE 1. Representative Light-Duty Modal Conditions for Drive-Cycle Emissions Estimation

Mode	Speed / Load	Weight Factor	Description
1	1,500 rpm / 1.0 bar	400	Catalyst transition temperature
2	1,500 rpm / 2.6 bar	600	Low speed cruise
3	2,000 rpm / 2.0 bar	200	Low speed cruise with slight acceleration
4	2,300 rpm / 4.2 bar	200	Moderate acceleration

The four modes used in this study are summarized in Table 1. ORNL is also working with the Advanced Combustion & Emissions Control Technical Team to propose a new set of operating conditions for use in characterizing efficiency and emissions improvements from advanced engine technologies. A well-defined set of operating conditions would allow improved comparisons across the DOE light-duty diesel activities.

Experiments were performed on a MB 1.7-L diesel engine using HPL, LPL, and mixed-source (combination of HPL and LPL) EGR to achieve HECC operation for the modal conditions in Table 1. The recipe used for HECC in these experiments is a PCCI approach which makes use of high dilution, high fuel injection pressure, and proper combustion phasing to achieve efficient LTC operation. An example comparison of the heat release profiles for conventional and HECC operation is shown in Figure 2 for 1,500 rpm, 2.6 bar brake mean effective pressure (BMEP). The heat release profile for HECC operation is consistent with more premixed combustion as compared to conventional operation. This strategy may also lead to higher combustion noise levels as shown in Figure 3 for the 1,500 rpm, 2.6 bar BMEP condition. A significant increase in combustion noise was observed for HECC operation to achieve BSFC values similar to those for conventional operation.

The mixed-source EGR approach allows for the control of the intake air-EGR mixture temperature independent of overall dilution level. As an example, the relationship between PM and NOx is shown in Figure 4 for several EGR scenarios and engine conditions of 2,300 rpm, 4.2 bar BMEP. Shown are conventional combustion results for the original equipment EGR rate, HECC operation with HPL EGR, and HECC operation with mixed-source EGR where intake mixture temperature is held constant at 50°C. Intake mixture temperature was held constant by adjusting the ratio of LPL and HPL EGR and overall dilution. Although not shown, this trend was also observed for 1,500 rpm, 2.6 bar BMEP modal condition. The existence of this NOx-PM relationship within the HECC regime may have important implications for matching emissions (*i.e.*, the combustion process) to aftertreatment. Mixed-source EGR is a reasonable method for achieving the

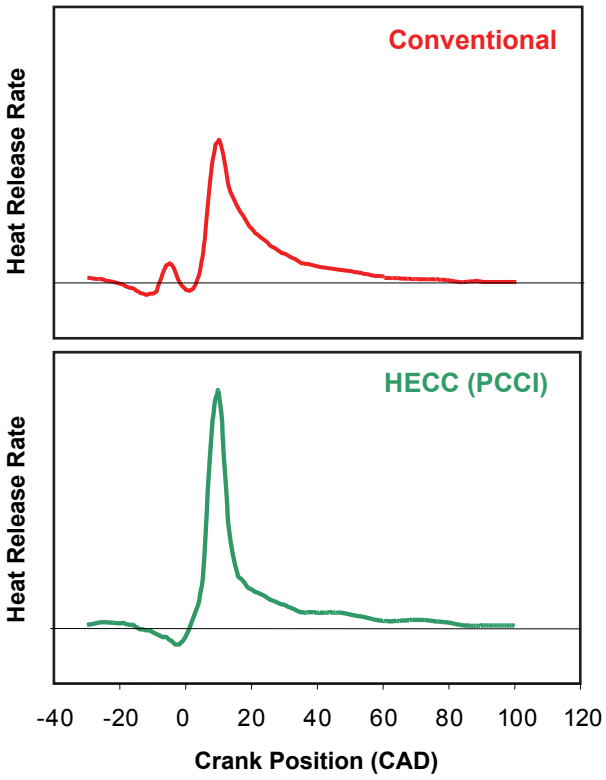

FIGURE 2. Example Heat Release Profiles for Conventional and HECC Operation at 1,500 RPM, 2.6 bar BMEP

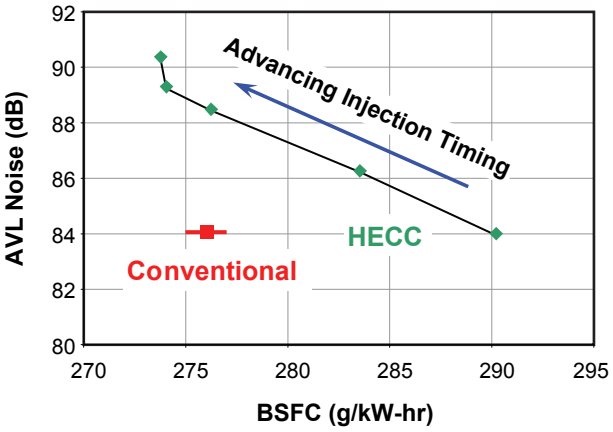

FIGURE 3. Combustion Noise and BSFC Relationship for Conventional and HECC Operation at 1,500 RPM, 2.6 bar BMEP

necessary precise control of dilution in real-world applications to take advantage of this NOx-PM relationship. Light hydrocarbon (HC) species and aldehyde compounds were also measured for the mixed-source EGR experiments and are shown in Figure 5. The results indicate an increase in methane, alkenes, and aldehyde compounds accompany a reduction in NOx emissions. This is consistent with a decrease in overall combustion temperature due to higher dilution of the

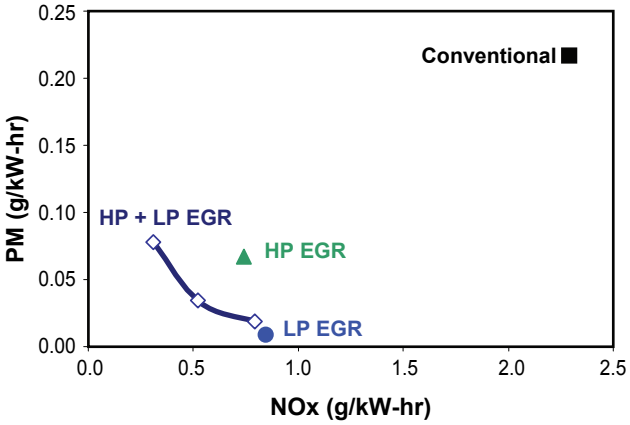

FIGURE 4. Comparison of NOx and PM Emissions with Intake Mixture Temperature Maintained Constant at ~50°C for HECC Operation at 2,300 RPM, 4.2 bar BMEP

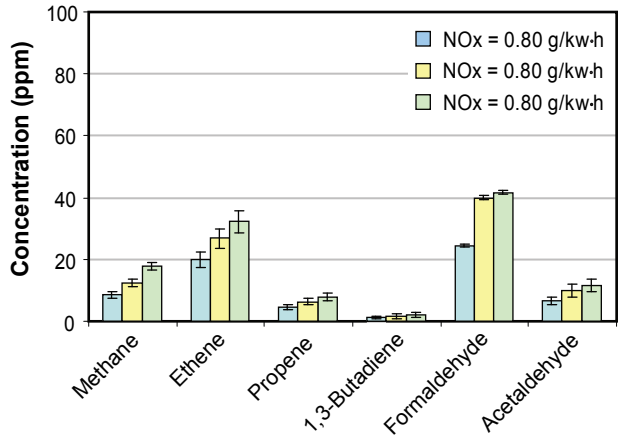

FIGURE 5. Light HC Species and Aldehyde Compounds with Intake Temperature Maintained Constant at ~50°C for HECC Operation at 2,300 RPM, 4.2 bar BMEP

combustion charge. A similar trend was observed for the 1,500 rpm, 2.6 bar BMEP condition.

Mixed source EGR was also used to investigate the effect of intake mixture temperature on PM emissions while maintaining a constant NOx emissions level. An example of this is shown in Figure 6 for the 2,300 rpm, 4.2 bar BMEP condition. An analysis of the accompanying heat release data indicates the reduction in PM with decreasing intake mixture temperature is most likely the result of a longer ignition delay and correspondingly a larger premixed burn fraction. Light HC species and aldehyde compounds are summarized in Figure 7 for theses experiments. An increase in these compounds was observed for decreasing intake mixture temperature. The higher concentrations at lower intake temperatures are most likely the result of lower bulk cylinder temperature which results in a larger quenching

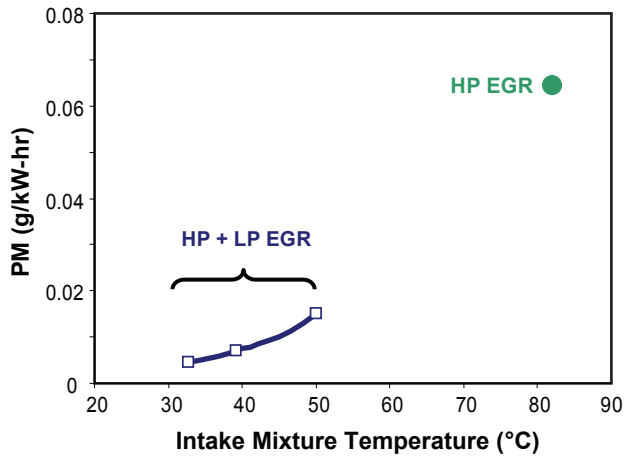

FIGURE 6. PM Emissions as a Function of Intake Mixture Temperature for Constant Engine-Out NOx of ~77 ppm for HECC Operation at 2,300 rpm, 4.2 bar BMEP

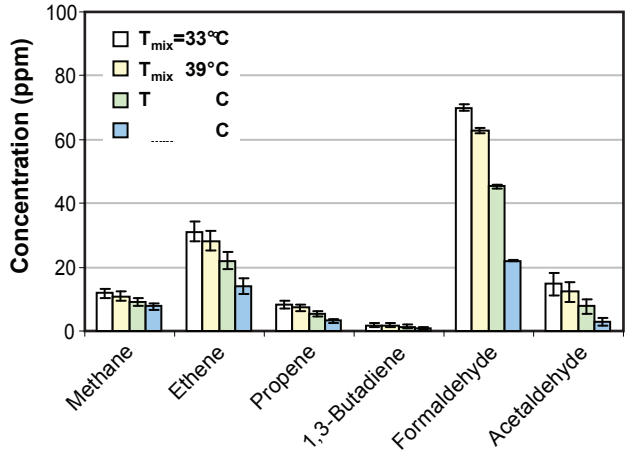

FIGURE 7. Light HC species and aldehyde compounds as a function of intake mixture temperature for constant engine-out NOx of ~77 ppm for HECC Operation at 2,300 RPM, 4.2 bar BMEP

volume. A similar trend was observed for the 1,500 rpm, 2.6 bar BMEP condition.

The mixed-source EGR HECC data summarized in the previous discussion does not always adhere to the strict definition of HECC used by ORNL. The LPL EGR method often has a BSFC penalty which is mostly dominated by the increase in backpressure (and corresponding increase in pumping losses) associated with the catalyzed diesel particulate filter (cDPF). The cDPF was not regenerated between each experiment and therefore the exhaust backpressure on the engine was not constant across the experimental matrix. The effect on BSFC is discussed in more detail in an upcoming SAE paper which has been submitted for the 2008 SAE Congress.

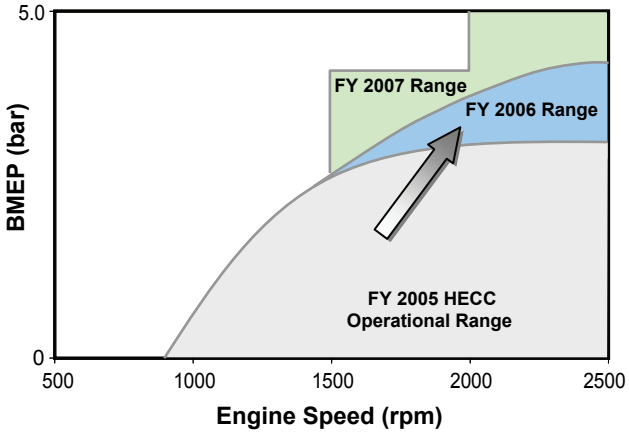

FIGURE 8. Speed-Load Range Expansion of HECC Operation Accomplished with Improved Control of Intake Mixture Temperature

Expansion of the speed-load range for HECC operation is important for reducing aftertreatment requirements and ultimately increasing the overall engine system efficiency. To this end, an effort was undertaken to investigate expansion of the HECC operational range with increased heat rejection of the HPL EGR system. This allowed for an extension of the upper range of the HECC operating envelope which is shown in Figure 8. BSFC values for the HECC conditions represented in this figure are similar to those observed for the original equipment factory conditions.

Due to the concise nature of this report, we were not able to discuss all of the research performed during this activity in FY 2007. Please see the publications/ presentations list for more information.

Conclusions

This activity has provided new information for expanding the usable speed-load range of advanced combustion operation and to better understanding the potential benefits and limitations of mixed-source EGR for achieving HECC in light-duty diesel engines. Specific observations are as follows:

- Characterized relationship between combustion noise level and BSFC for HECC operation. Increases in noise level make efficient operation a challenge in LTC modes.
- Improved cooling (*i.e.*, heat rejection) of the HPL EGR systems allows for an incremental improvement in expanding the HECC speed-load operational range.
- Mixed-source EGR has the potential for precise control of intake mixture temperature and dilution for more robust HECC operation and improved matching with aftertreatment systems.

- A GM 1.9-L engine with a flexible control system was commissioned at ORNL and will be the primary research platform for subsequent HECC research. This engine geometry is being used at Sandia National Laboratories (optical single-cylinder engine), Lawrence Livermore National Laboratory (modeling), and the University of Wisconsin (metal single- and multi-cylinder engines) and has resulted in improved collaboration in DOE funded activities in support of meeting FreedomCAR efficiency and emissions milestones.

FY 2007 Publications/Presentations

1. *Submitted*. K. Cho, M. Han, R. M. Wagner, C. S. Sluder, " Mixed-Source EGR for Enabling High Efficiency Clean Combustion Modes in a Light-Duty Diesel Engine", 2008 SAE Congress & Exposition (Detroit, MI; April 2008).

2. R. M. Wagner et al., "Update on ORNL efficiency and advanced combustion activities for LD diesel engines", 2007 AEC Working Group Meeting at USCAR (Southfield, MI; September 2007).

3. R. M. Wagner et al., "Modeling and Experiments to Achieve High-Efficiency Clean Combustion (HECC) in LD Diesel Engines", Advanced Combustion & Emissions Control Technical Team meeting (Southfield, MI; July 2007).

4. R. M. Wagner et al., "Modeling and Experiments to Achieve High-Efficiency Clean Combustion (HECC) in LD Diesel Engines", 2007 Department of Energy (DOE) Advanced Combustion Engines Merit Review (Washington, D.C.; June 2007).

5. C. S. Sluder, R. M. Wagner, "An Estimate of Diesel High-Efficiency Clean Combustion Impacts on FTP-75 Aftertreatment Requirements", SAE 2006-01-3311 (Toronto, Ontario, Canada; October 2006).

Special Recognitions & Awards/Patents Issued

1. FreedomCAR Technical Highlight in 2007.

2. J. B. Green, C. S. Daw, R. M. Wagner, "Combustion Diagnostic for Active Engine Feedback Control"; United States patent number 7,277,790 B1.

II.A.6 Large Eddy Simulation Applied to Low-Temperature and Hydrogen Engine Combustion Research

Joseph C. Oefelein
Sandia National Laboratories
7011 East Avenue, Mail Stop 9051
Livermore, CA 94550

DOE Technology Development Manager:
Gurpreet Singh

Objectives

- Combine unique state-of-the-art simulation capability based on the large eddy simulation (LES) technique with Advanced Engine Combustion R&D activities.
- Perform companion simulations that directly complement optical engine experiments being conducted at the Combustion Research Facility (CRF).
- Focus initially on optical hydrogen-fueled internal combustion (IC)-engine experiment and systematically extend to low-temperature combustion (LTC) applications.

Approach

- Adhere to strict algorithmic and implementation requirements for LES with emphasis placed on accuracy and application of science-based subgrid-scale models.
- Focus on state-of-the-art engine systems and geometries with emphasis placed on establishing an enhanced understanding of turbulence-chemistry interactions.
- Provide scientific foundation for advanced model development with emphasis placed on local, unsteady, intricately coupled in-cylinder processes, i.e.,
  - Flame structure, stability and effects of stratification,
  - Local extinction, re-ignition and auto-ignition, and
  - Pollutant emissions and soot formation.

Accomplishments

- Completed infrastructure and preprocessor modifications to make calculations routine.
  - Computational Combustion and Chemistry Laboratory for IC-engine research installed, tested and operational (256 processor Beowulf cluster).
  - Commercial grid generation capability established (ANSYS ICEM) and interfaced with the CRF LES code.
  - Implementation of tension-splines designed and tested to provide an efficient mesh movement capability in full IC-engine geometries (ports, valves, piston).
- Performed systematic model validation of two fundamental combustion models in collaboration with the DOE Office of Science (see Barlow et al., www.ca.sandia.gov/tnf).
  - Stochastic Reconstruction Model ("science-based").
  - Tabulated Linear Eddy Model ("engineering-based").
- Continued sequence of calculations focused on CRF optical hydrogen internal combustion engine (H_2-ICE) in collaboration with C. White and S. Kaiser (see related annual report).
  - Moved to treatment of direct-injection processes (several prerequisite tasks required to achieve this goal).
  - Initiated studies focused on H_2-injector pattern optimization (Collaboration with Ghandhi et al., University of Wisconsin).
- Systematically extended effort toward treatment of LTC engine processes.
  - Simulation of the effect of spatial fuel distribution using the Linear Eddy Model.
  - LES of direct injection processes for diesel and LTC engine applications (see Pickett et al., www.ca.sandia.gov/ecn).

Future Directions

- Continue high-fidelity simulations of the optical H_2-ICE.
  - Direct-injection with new head, match experimental activities.
  - Validation through comparison of measured, modeled results.
    - Chemiluminescence imaging and particle image velocimetry (PIV)
    - Planar laser induced fluorescence (PLIF)

  - Joint analysis of data extracted from validated simulations.
    - Enhance basic understanding
    - Improve engineering models
    - H_2-injector pattern optimization
- Systematically extend to homogeneous charge compression ignition (HCCI) engine experiments.
  - Perform detailed studies of LTC processes.
  - Work toward treatment of complex hydrocarbon processes.
- Continue leveraging between DOE Office of Science (OS) and Energy Efficiency and Renewable Energy (EERE) activities.
  - Detailed validation, analysis of key combustion phenomena.
  - Access to high-performance "leadership-class" computers.

Introduction

The objective of this research is to combine a unique high-fidelity simulation capability based on the LES technique with the Advanced Engine Combustion R&D activities at Sandia National Laboratories. The goal is to perform a series of benchmark simulations that identically match the geometry and operating conditions of select optical engine experiments. The investment in time and resources will provide two significant benefits. After systematic validation of key processes using available experimental data, quantitative information can be extracted from the simulations that are not otherwise available. This information will provide: 1) a detailed and complementary description of intricately coupled processes not measurable by experimental diagnostics, and 2) the information required to understand and develop improved predictive models. The combination of detailed experiments, complementary simulations, and the joint analysis of data will provide the basic science foundation required to systematically address the targeted research areas identified for Clean and Efficient Combustion of 21st Century Transportation Fuels. The approach is directly aligned with a recent workshop on the topic organized by the DOE OS.

To establish a scientific foundation for technology breakthroughs in transportation fuel utilization, the DOE Office of Basic Energy Sciences (BES) convened a workshop entitled "*Basic Research Needs for Clean and Efficient Combustion of 21st Century Transportation Fuels*" from October 30 to November 1, 2006 (www.sc.doe.gov/bes/reports/files/CTF_rpt.pdf). Execution of the workshop involved advance coordination with the DOE Office of EERE, FreedomCAR and Vehicle Technologies (FCVT) program, which manages applied research and development of transportation technologies. Results provide the collective output from over 80 leading scientists and engineers representing academia, industry, and national laboratories in the United States and Europe. Panels were convened to identify priority research directions in the area of novel combustion for new engine technologies, utilization challenges of alternative fuels in these systems, crosscutting science themes and gaps in our understanding of combustion processes related to 21st century fuels. Panel leads distilled the collective output to produce eight distinct targeted research areas required to advance the single overarching grand challenge of developing "*a validated, predictive, multiscale, combustion modeling capability to optimize the design and operation of evolving fuels in advanced engines for transportation applications*." This project targets the research issues identified for multiscale simulation and modeling of IC-engine processes.

Approach

As part of the *Reacting Flow Research* and *Advanced Engine Combustion* programs at the CRF, we have developed a high-fidelity, massively-parallel simulation framework that is capable of performing both direct numerical simulation (DNS) and LES of reacting flows in complex geometries. Two complementary projects have been established. The first is funded under the DOE OS, BES program, and focuses on LES of turbulence-chemistry interactions in reacting multiphase flows. The second is funded under the DOE Office of EERE, FCVT program, and focuses on the application of LES to low-temperature and hydrogen engine combustion research. Objectives and milestones for both projects are aimed at establishing high-fidelity computational benchmarks that match the geometry and operating conditions of key target experiments using a single unified theoretical-numerical framework. The projects are complementary in that the OS-BES activity provides the basic science foundation for detailed model development and the EERE-FCVT activity provides the applied component for advanced engine research.

The approach involves four key components: 1) application of unique software capabilities and computational resources, 2) implementation of a sophisticated set of subgrid-scale models that are consistent with the DNS technique in the limit as the grid cut-off is refined toward smaller scales, 3) rigorous validation of models using high-fidelity data acquired from the carefully selected target experiments, and 4) detailed characterization of complex turbulent combustion processes through combined-analysis of experimental and numerical data. Once validated against experiments, the high-fidelity simulations offer a wealth of information that cannot be measured directly. They provide a detailed description of

intricately-coupled processes, information required to improve and/or develop advanced control strategies, and the composite data required for development of advanced engineering models that provide the fast turn-around times required by industry designers.

Results

In addition to providing a comprehensive multiscale modeling framework based on LES, we have established direct collaborations and quantitative coupling with two of the "flagship" experimental efforts at the CRF. A scientific foundation for advanced development of subgrid-scale models for LES has been established in collaboration with Barlow et al. as a direct extension of the International Workshop on Measurement and Computation of Turbulent Nonpremixed Flames (i.e., the "TNF Workshop," www.ca.sandia.gov/TNF). Similarly, we have established funded collaborative research activities that focus on key optical engine experiments (as described in the following) and the Engine Combustion Network (i.e., ECN, as established by Pickett, www.ca.sandia.gov/ECN). The ECN has analogous objectives to those of the TNF workshop. The novelty our LES approach is that it provides direct one-to-one correspondence between measured and modeled results at conditions unattainable using DNS by providing detailed simulations that incorporate the fully coupled dynamic behavior of a given configuration in the full experimental or device-scale geometry without canonical approximations. As part of our long-term operating plan under the Advanced Engine Combustion program, needs and milestones in three critical areas have been established: 1) to continue a progression of LES studies focused on the CRF optically accessible H_2-ICE, 2) to establish a parallel task focused on HCCI engines, and 3) to begin a series of supporting studies focused on the development and validation of multiphase combustion models with emphasis placed on direct-injection processes. Following are three examples of recent progress.

LES of the CRF Optically Accessible Hydrogen-Fueled IC-Engine: Objectives related to this milestone are to perform benchmark simulations of the CRF optically accessible H_2-ICE shown in Figure 1a. Our primary goal is to provide a detailed understanding regarding optimal injection strategies and the three-dimensional characteristics of in-cylinder combustion processes. A series of staging studies in FY 2006 and FY 2007 have established our baseline capability for performing the simulations. The time-dependent grid has been designed and optimized, preliminary validation of the combustion models has been established, and initial comparisons with available experimental data have been performed. We have now advanced to the treatment of direct-injection (DI) processes, which is the operational mode of choice for development of a highly efficient engine cycle using hydrogen as the fuel. The LES calculations currently in progress will provide the most resolved high-fidelity results of in-cylinder combustion processes to-date. Our analysis is focused on multidimensional turbulence-chemistry interactions and related cycle-to-cycle variations. The simulations are coordinated with the experimental campaign at the CRF, which has similar goals using advanced imaging techniques in the optical engine but is limited to two-dimensional planes. Results from these calculations will provide a clear understanding of the power density limitations associated with hydrogen-fueled engine cycles, maximum fuel efficiency, NOx emissions, turbulent mixing characteristics, and the effects of mixture stratification as a function of local processes over full engine cycles.

LES of Direct Injection Processes for Hydrogen and Low-Temperature Combustion Applications: As a subset of the task outlined above, we have established an initial benchmark series of simulations aimed at understanding high Reynolds number, high-pressure, direct-injection processes for hydrogen and low-temperature engine applications (see Figure 1b). High-fidelity representations of direct injection processes in IC-engines are an essential component toward the development a validated predictive modeling capability. Direct injection of hydrogen at high-pressure conditions, for example, has emerged as a promising option for improving fuel economy and emissions in H_2-ICEs. Gaseous injection technology, however, is relatively new and there is only limited information on optimal configurations. Similarly, direct-injection of liquid fuels for low-temperature engine applications such as HCCI has many advantages, but detailed time-accurate models are still lacking. To address these issues, we have initiated a series of benchmark calculations that identically match key experimental efforts. Data from these experiments are being used for validation. Figure 1b shows an example result from LES compared to the shadowgraph data of Petersen and Ghandhi (University of Wisconsin). This represents the initial starting point to study a series high-pressure gas injectors designed for use in H_2-ICEs. We will also focus on issues related to liquid jet breakup using the case studies provided by Pickett et al. (www.ca.sandia.gov/ECN).

LES of In-Cylinder Homogeneous-Charge Compression-Ignition Engine Processes: The potential benefits of HCCI engine cycles and key technical barriers have been well established. Ignition timing must be controlled over a wide range of speeds and loads. The rate of heat release due to combustion must be limited to allow high-load operation. Smooth operation through rapid transients must be maintained. A robust cold-start capability must be developed. Finally, hydrocarbon and carbon monoxide emissions standards must be met. Overcoming these barriers requires an improved understanding of in-cylinder HCCI processes

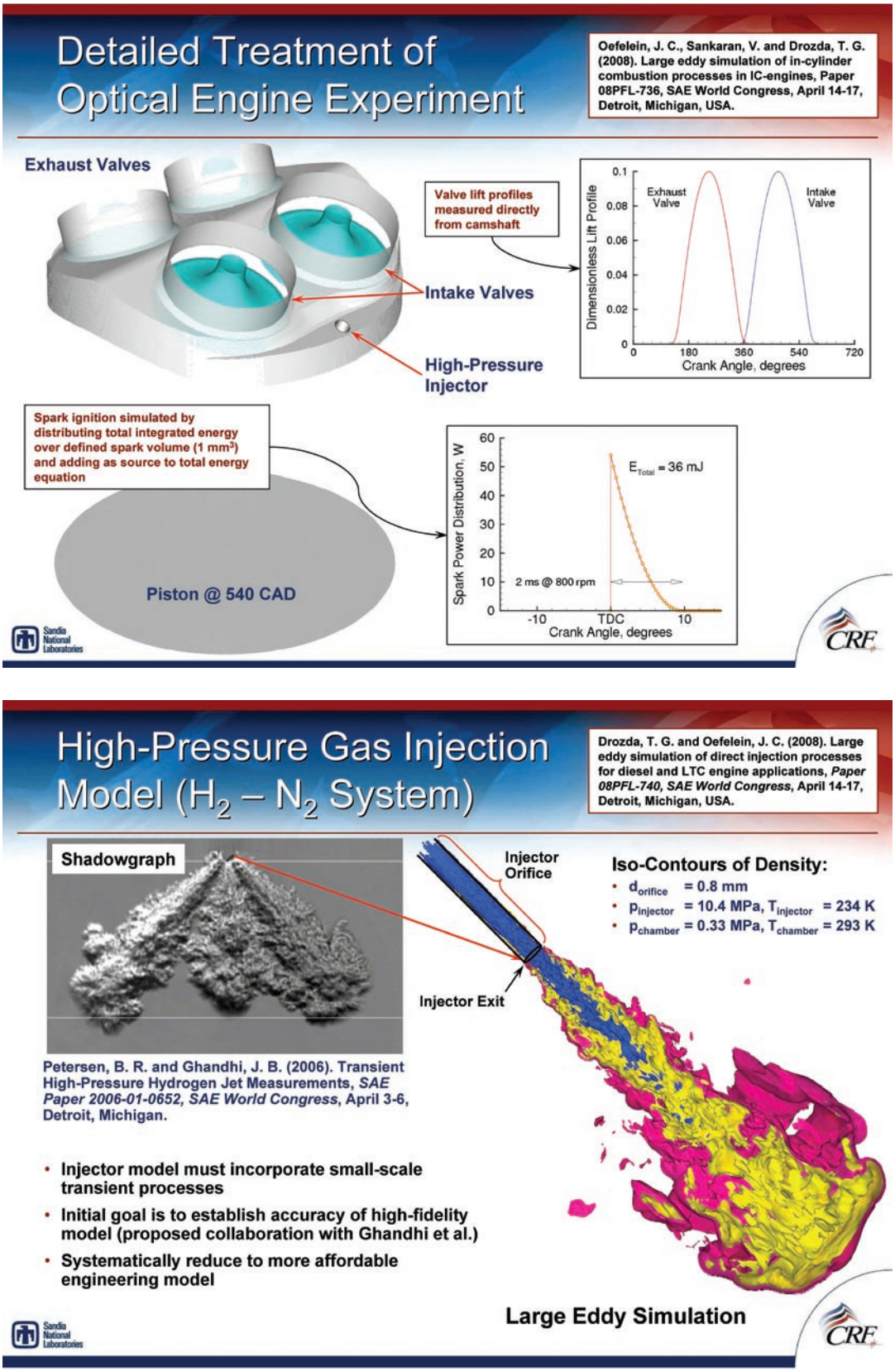

FIGURE 1. Images (top) show the LES grid surface topology and related details for calculations of the CRF optically accessible hydrogen-fueled IC-engine. Images (bottom) show the corresponding high-pressure injector dynamics simulated in this engine, with results compared to the shadowgraph data of Peterson and Ghandhi (University of Wisconsin).

combined with an understanding of how the coupled effect of these processes can be favorably altered using appropriate control mechanisms. Using the same approach as that described above for the H_2-ICE, we have begun a series of LES calculations that complement ongoing HCCI engine research. Initial emphasis has been placed on the optically accessible research engine developed at the CRF. Research conducted by Steeper et al. (see FY 2007 Publications) has provided an initial baseline for implementation of our combustion models using n-heptane as the fuel.

Conclusions

Future work will be focused both on hydrogen fuel injector pattern optimization and on the critical needs and challenges associated with the use of hydrogen as a fuel. These needs include obtaining a clearer understanding of power density limitations, maximum fuel efficiency, in-cylinder NOx formation, turbulent mixing characteristics, turbulence-chemistry interactions, and the effects of mixture stratification as a function of local in-cylinder processes over full engine cycles. Information from the simulations, combined with detailed laser-based experiments at well-defined target conditions, will provide the science-base needed by engine companies to develop fuel efficient, low-emissions H_2-ICEs. Through interdisciplinary leveraging with other projects, we will continually perform assessments of the base model and select chemical kinetics mechanisms to: 1) verify that the chemical mechanisms selected for the IC-engine work are capable of representing important phenomena such as ignition and extinction, and 2) build a validated level of confidence in the overall accuracy of the coupled LES model framework.

FY 2007 Publications/Presentations

1. J. C. Oefelein, V. Sankaran and T. G. Drozda (2008). Large eddy simulation of in-cylinder combustion processes in IC-engines, *paper 08PFL-736, SAE World Congress*, April 14–17, Detroit, MI.

2. T. G. Drozda and J. C. Oefelein (2008). Large eddy simulation of direct injection processes for diesel and LTC engine applications, *paper 08PFL-740, SAE World Congress*, April 14–17, Detroit, MI.

3. T. G. Drozda, G. Wang, V. Sankaran, J. R. Mayo, J. C. Oefelein and R. S. Barlow (2007). Scalar filtered mass density functions in nonpremixed turbulent jet flames, *Submitted to Combustion and Flame*.

4. R. R. Steeper, V. Sankaran, J. C. Oefelein and R. P. Hessel (2007). Simulation of the effect of spatial fuel distribution using a linear eddy model, *paper 07FFL-186, SAE Powertrain & Fluid Systems Conference and Exhibition*, October 29-November 1, Chicago, IL.

5. P. K. Tucker, S. Menon, C. L. Merkle, J. C. Oefelein and V. Yang (2007). An approach to improved credibility of CFD simulations for rocket injector design, *paper 2007-5572, 43rd AIAA/ASME/SAE/ASEE Joint Propulsion Conference & Exhibit*, July 8-11, Cincinnati, OH.

6. T. G. Drozda, G. Wang, V. Sankaran, J. R. Mayo, J. C. Oefelein and R. S. Barlow (2007). Scalar filtered mass density functions in nonpremixed turbulent jet flames, *Proceedings of the 5th US Joint Meeting of the Combustion Institute*, March 25-28, San Diego, CA.

7. V. Sankaran and J. C. Oefelein (2007). Advanced preconditioning strategies for chemically reacting flows, *Paper 2007-1432, 45th AIAA Aerospace Sciences Meeting & Exhibit*, January 8-11, Reno, NV.

8. T. C. Williams, R. W. Schefer, J. C. Oefelein and C. R. Shaddix (2007). Idealized gas turbine combustor for performance research and validation of large eddy simulations, *Review of Scientific Instruments*, 78(035114): 1-9.

9. J. C. Oefelein, V. Sankaran and T. G. Drozda (2006). Large eddy simulation of swirling particle-laden flow in a model axisymmetric combustor, *Proceedings of the Combustion Institute*, 31: 2291-2299.

10. J. C. Oefelein (2006). Large Eddy Simulation of mixing and combustion for direct-injection operation. *European Commission HyICE Program: Optimization of a hydrogen powered internal combustion engine*, Project 506604, Chapter D4.3.G: 1-18.

11. J. C. Oefelein, T. G. Drozda and V. Sankaran (2006). Large Eddy Simulation of Turbulence-Chemistry Interactions in Reacting Flows: The Role of High-Performance Computing and Advanced Experimental Diagnostics, *Journal of Physics*, 46: 16-27.

12. J. C. Oefelein (2006). Large eddy simulation of turbulent combustion processes in propulsion and power systems. *Progress in Aerospace Sciences*, 42: 2-37.

Presentations at Conferences and Project Meetings

1. BES 27th Annual Combustion Research Meeting, Wintergreen, VA, Jun. 06.

2. SciDAC 2006, Denver CO, Jun. 06.

3. 42nd AIAA/ASME/SAE/ASEE Joint Propulsion Conference, Sacramento, CA, Jul. 06.

4. 8th TNF Workshop, Heidelberg, Germany, Aug. 06.

5. 31st International Symposium on Combustion, Heidelberg, Germany, Aug. 06.

6. Penguin Computing Advisory Board Meeting, San Francisco CA, Sep. 06.

7. AFOSR Contractors Meeting, Annapolis, MD, Sep. 06.

8. AFRL Rocket Modeling Workshop, Annapolis, MD, Sep. 06.

9. CRF Advisory Board, Livermore, CA, Nov. 06.

10. 45th AIAA Aerospace Sciences Meeting, Reno NV, Jan. 07.

11. Advanced Engine Combustion and HCCI Working Group Meeting, Livermore, CA, Feb. 07.

12. CRF Diagnostics and Reacting Flow Peer Review, Livermore, CA, Mar. 07.

13. SERDP Project Meeting on Predicting the Effects of Fuel Composition and Flame Structure on Soot Generation in Turbulent Nonpremixed Flames, San Diego, CA, Mar. 07.

14. 5th US Joint Sections Meeting of the Combustion Institute, San Diego, CA, Mar. 07.

15. Multi-Agency Workshop on Next Steps in Development of a Cyber Infrastructure for Combustion, San Diego, CA, Mar. 07.

16. Simulation and Modeling at the Exascale for Energy, Ecological Sustainability and Global Security, 1st Town Hall Meeting, LBL, Apr. 07.

17. DOE Merit Review of Advanced Combustion, Emissions & Fuels Research, Washington, D.C., Jun. 06.

II.A.7 Detailed Modeling of Low Temperature Combustion and Multi-Cylinder HCCI Engine Control

Salvador Aceves (Primary Contact),
Daniel Flowers, Jonas Edman,
Nick Killingsworth, Francisco Espinosa-Loza,
Lee Davisson, Robert Dibble, Randy Hessel,
Aristotelis Babajimopoulos
Lawrence Livermore National Laboratory
7000 East Ave. L-644
Livermore, CA 94550

DOE Technology Development Manager:
Gurpreet Singh

Subcontractors:
- University of California, Berkeley, CA
- University of Wisconsin, Madison, WI

Objectives

- Obtain low emissions, high efficiency operation of homogeneous charge compression ignition (HCCI), premixed charge compression ignition (PCCI), and other low-temperature clean combustion regimes.
- Advance our analysis techniques to learn the fundamentals of HCCI and PCCI combustion and to make accurate predictions of combustion and emissions.
- Conduct experiments to determine strategies to control multi-cylinder HCCI engines.

Accomplishments

- Developed methodologies for experimental measurement of 40 hydrocarbon species in HCCI engine exhaust.
- Demonstrated high fidelity modeling of the Sandia HCCI engine (John Dec), including unprecedented prediction of 40 measured intermediate hydrocarbon species.
- Demonstrated innovative control strategies and applied them to the Caterpillar 3406 experimental HCCI engine, demonstrating optimum engine performance and fast transient response.

Future Directions

- *Validate KIVA3V-MZ-MPI against experimental data under partially stratified conditions*: we are working with engine researchers at Sandia Livermore (John Dec and Dick Steeper) to conduct validations of our code at PCCI conditions.
- *Use KIVA3V-MZ-MPI as a predictive tool for engine geometry and fuel injection optimization:* a well-validated KIVA3V-MZ-MPI code should be applicable for improving and optimizing engine characteristics in HCCI or PCCI engines.
- *Analyze spark-assisted HCCI experiments:* we are working with engine researchers at Oak Ridge National Laboratory (Robert Wagner) for analyzing spark ignition (SI)-HCCI transition experiments at high exhaust gas recirculation conditions.

Introduction

Modeling low-temperature, high efficiency engine concepts such as PCCI requires a balanced approach that captures both fluid motion as well as low- and high-temperature fuel oxidation. A fully integrated computational fluid dynamics (CFD) and chemistry scheme (i.e. detailed chemical kinetics solved in every cell of the CFD grid) would be the ideal PCCI modeling approach, but is computationally very expensive. As a result, modeling assumptions are required to develop tools that are computationally efficient, yet maintain an acceptable degree of accuracy. Multi-zone models have been previously shown by the authors to capture HCCI processes with enough fidelity to make accurate predictions. We have been testing methodologies for multi-zone analysis of PCCI combustion that show promise for delivering accurate results within a reasonable computational time. We are also developing new tools of analysis that apply to different aspects of HCCI/PCCI operation.

Approach

Our approach is to collaborate with national laboratories and universities conducting experimental work as a part of DOE's Advanced Combustion in Engines (ACE) Program. Our role in these collaborations is to provide analytical support that complements the very high quality experimental work being conducted at other locations. Although most collaboration to date is HCCI/PCCI centric due to the great importance of these combustion modes, we are working on extending our work to other areas of interest to the DOE ACE Program, such as low-temperature combustion and hydrogen engines. We have also

performed key experiments described in this report: exhaust speciation and advanced engine control.

Results

Engine experiments are typically limited to measurement of pressure and emissions of nitrogen oxide, carbon monoxide, and hydrocarbons. Hydrocarbon emissions are typically reported as "total," even though instruments (i.e., flame ionization detectors) do not detect, or only partially detect, oxygenated hydrocarbons.

Recently we teamed up with John Dec from Sandia Livermore to conduct very careful HCCI experiments at low- to mid-loads [1]. In addition to the typical engine measurements, we determined the exhaust composition by measuring the concentration of 40 hydrocarbon species in the exhaust.

Detailed measurement of exhaust composition is a complex process that starts with the collection of exhaust gases in Tedlar® bags that have previously been prepared by three successive evacuations and purgings with dry nitrogen. Two separate bag samples were collected for each operating condition: one for the C1-C2 hydrocarbons, and the other for the remaining species. The C1-C2 hydrocarbons were analyzed by direct injection of exhaust gases into an Agilent 6890 gas chromatograph and detected with a flame ionization detector. Fixed gas standards were used for calibration. All other hydrocarbons and oxygenated hydrocarbons were analyzed using an HP5890/5972MSD gas chromatography mass spectrometry (GC/MS). A Tedlar® bag sample and a 25 ml gas-tight syringe were first heated in an oven to 60°C. A 25 ml sample was drawn into the syringe and subsequently injected directly into a heated glass tube purged with a 25 cc/min high purity helium flow. The helium swept the sample onto an adsorbent comprising a mixture of Carbopak B and carboxen (Supelco VOCARB 3000). After 20 minutes the trap was heated to 250°C and the adsorbed species were concentrated onto the head of the GC column using the helium flow. Compound separation was facilitated using a DB-502 capillary column heated from 35°C to 250°C at 5°C/min and held for 10 minutes. Injector temperature and detector temperature were held at 225°C and 250°C, respectively. Standards were prepared by injecting 1-5 microliters of authentic standards into a Tedlar® bag filled with dry nitrogen and analyzed using the same method. Formaldehyde and acetaldehyde are not properly detected by the GC/MS, and therefore separate samples were collected using a dinitrophenylhydrazine derivatizing solution. After careful sample preparation, aldehyde concentration was measured with a ThermoFinnigan Survey high performance liquid chromatograph.

Detailed measurement of hydrocarbon species in the exhaust of HCCI engines is important for the design of low-temperature oxidizing catalysts and for determining optimum strategies for low power or idle engine operation. In addition to their practical importance, speciation experiments represent a unique opportunity to put our HCCI models to the test. We are confident in the ability of our models to accurately characterize the combustion event. However, trying to predict exhaust composition down to the small hydrocarbon species is a challenge, because these species are intermediate products of combustion that are generated and then consumed as the fuel breaks apart in a chemical kinetic cascade that starts with fuel and (ideally) ends with carbon dioxide. Accurately predicting these small species requires a good characterization of both the formation as well as the destruction of these species in a transient temperature field continuously modified by chemical heat release and turbulent fluid mechanics.

We analyzed the Sandia exhaust speciation experiments with our multi-zone parallel version of the KIVA code (KIVA-MZ-MPI) [2]. We took on the difficult challenge of accurately predicting exhaust composition by making a very detailed mesh that includes cylinder features seldom modeled, such as the gasket crevice and the space behind the top ring (Figure 1). We took advantage of the careful engine measurements to determine appropriate initial conditions (pressure and temperature at intake valve

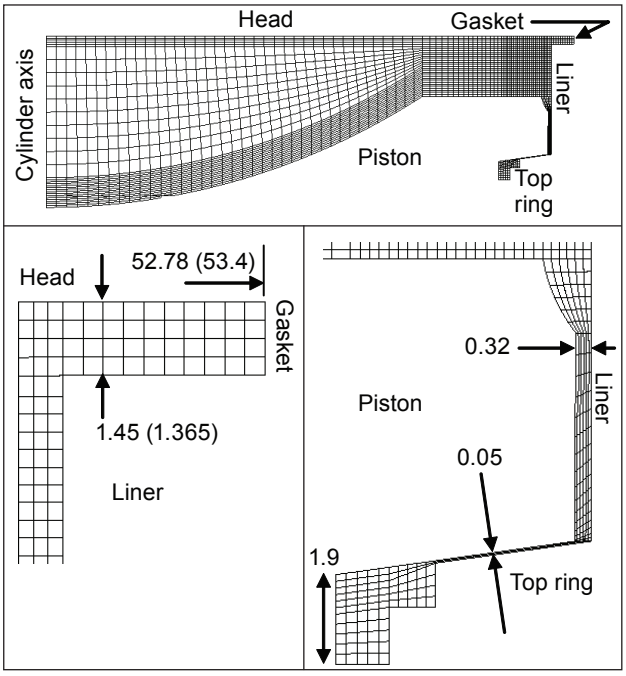

FIGURE 1. Top: Mesh of Computational Domain at Top Dead Center; Left: Head Gasket Volume; Right: Piston/Liner Crevice (Dimensions are mm)

closing) and boundary conditions (wall temperatures) as a function of equivalence ratio.

As expected, our model demonstrates good agreement with experimental pressure traces and heat release rates. In addition to this, we were also able to accurately calculate exhaust composition as a function of equivalence ratio. Figure 2 shows predicted and measured values of the main hydrocarbon species.

This year we also demonstrated the application of advanced control technology for optimizing HCCI engine efficiency. These experiments were conducted in our Caterpillar 3406 engine previously converted to HCCI mode, and were recently reported in *Mechanical Engineering* magazine [3].

Engine operation is typically optimized with a mapping procedure. At each operating point, multiple spark timings (or fuel injection timings for a diesel engine) are tried. The optimal combustion timing is then determined from the mapping data. This procedure is time and labor intensive, because many engine runs are required for mapping the desired region of operation. The process is even more involved for HCCI engines that lack an ignition trigger and require tuning of intake temperature and pressure to achieve the desired combustion timing.

We applied an innovative method to speed up this process: extremum seeking, which is a non-model-based real-time optimization method that iteratively modifies the input of a system such that a desired performance metric reaches a local optimal value. Extremum seeking differs from conventional optimization methods; it performs a non-model based parameter search, which is independent of whether the system is linear or has significant nonlinearities.

For the engine application, extremum seeking determines the combustion timing that minimizes the HCCI engine's fuel consumption. Figure 3 shows that extremum seeking delays the combustion timing from 3 degrees to approximately 9 crank angle degrees after top dead center while simultaneously reducing fuel consumption by more than 10%.

Conclusions

- We have contributed to unprecedented characterization of HCCI engine performance by measuring concentration of 40 hydrocarbon species in the exhaust.
- We have applied our parallel multi-zone KIVA code (KIVA-MZ-MPI) to make accurate predictions of exhaust composition as a function of equivalence ratio.
- Experiments conducted on our Caterpillar 3406 HCCI engine demonstrated the applicability of advanced control methodologies for fast optimization of engine performance.

References

1. Dec, J.E., Davisson, M.L., Leif, R.N., Sjoberg, M., and Hwang, W., "Detailed HCCI Exhaust Speciation and the Sources of Hydrocarbon and Oxigenated Hydrocarbon Emissions," SAE Technical Paper Offer number 08PFL-770, submitted for the 2008 SAE congress.

2. Hessel, R.P., Foster, D.E., Aceves, S.M., Davisson, M.L., Espinosa-Loza, F., Flowers, D.L., Pitz, W.J., Dec, J.E., Sjoberg, M., and Babajimopoulos, A., "Modeling Iso-octane HCCI using CFD with Multi-zone Detailed Chemistry; Comparison to Detailed Speciation Data over a Range of Lean Equivalence Ratios," SAE technical paper offer no. 08PFL-878, submitted to the 2008 SAE Congress.

3. Flowers, D., Killingsworth, N., and Dibble, R., "In Pursuit of New Engine Dynamics," Mechanical Engineering, pp. 20-21, July 2007.

FY 2007 Publications/Presentations

1. Analysis of Homogeneous Charge Compression Ignition (HCCI) Engines for Cogeneration Applications, Salvador M. Aceves, Joel Martinez-Frias, Gordon M. Reistad, Proceedings of the ASME Advanced Energy Systems Division, 2004, Journal of Energy Resources Technology, Vol. 128, pp. 16-27, 2006.

2. Gaseous Fuel Injection Modeling using a Gaseous Sphere Injection Methodology, Randy P. Hessel, Salvador M. Aceves, Daniel L. Flowers, SAE Paper 2006-01-3298, 2006.

3. Fast Prediction of HCCI Combustion with an Artificial Neural Network Linked to a Fluid Mechanics Code, Salvador M. Aceves, Daniel L. Flowers, J.Y. Chen, Aristotelis Babajimopoulos, SAE Paper 2006-01-3298, 2006.

4. A Simple HCCI Engine Model for Control, Nick Killingsworth, Salvador Aceves, Daniel Flowers, Miroslav Krstic, Proceedings of the IEEE International Conference on Control Applications, Munich, Germany, 2006.

5. A Comparison on the Effect of Combustion Chamber Surface Area and In-Cylinder Turbulence on the Evolution of Gas Temperature Distribution from IVC to SOC: A Numerical and Fundamental Study, Randy P. Hessel, Salvador M. Aceves, Daniel L. Flowers, SAE Paper 2006-01-0869.

6. Effect of Charge Non-uniformity on Heat Release and Emissions in PCCI Engine Combustion, Daniel L. Flowers, Salvador M. Aceves, Aristotelis Babajimopoulos, SAE Paper 2006-01-1363, 2006.

7. Overview of Modeling Techniques and their application to HCCI/CAI Engines, Salvador M. Aceves, Daniel L. Flowers, Robert W. Dibble, Aristotelis Babajimopoulos, in HCCI and CAI Engines for the Automotive Industry, Edited by Hua Zhao, CRC Press, Woodhead Publishing Limited, Chapter 18, pp. 456-474, 2007.

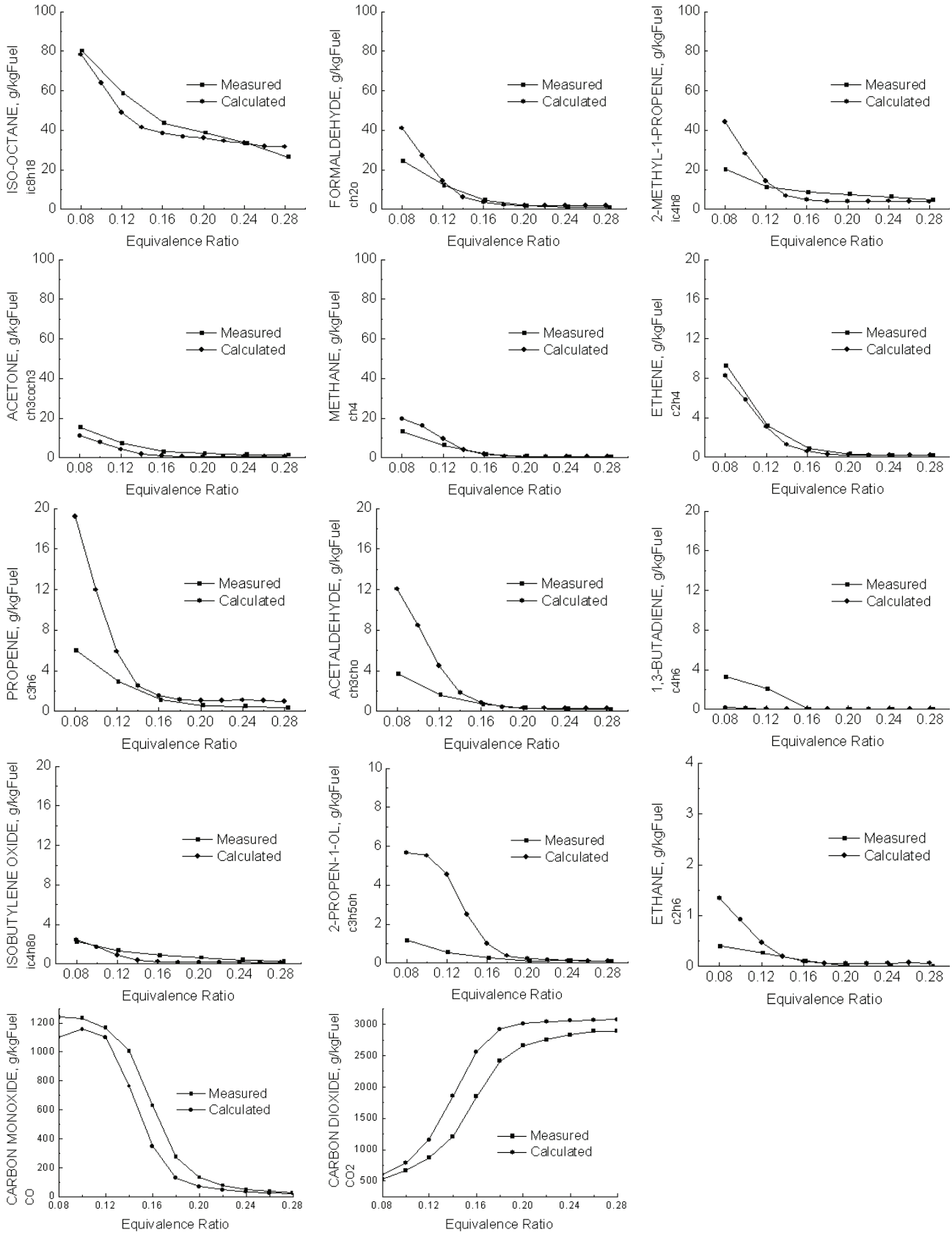

FIGURE 2. Measured and Calculated Species Concentrations as a Function of Equivalence Ratio for the Sandia HCCI Engine

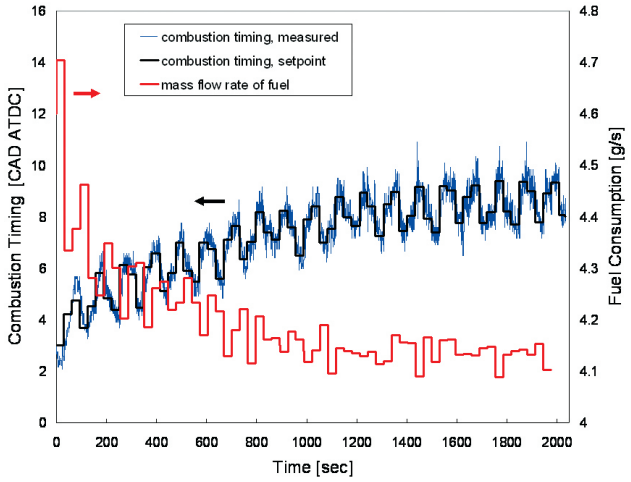

FIGURE 3. Use of extremum seeking for minimization of HCCI engine fuel consumption. Extremum seeking delays combustion timing from 3 degrees to 9 degrees after top dead center, reducing fuel consumption by more than 10%.

8. Improving Ethanol Life Cycle Energy Efficiency by Direct Utilization of Wet Ethanol in HCCI Engines, Joel Martinez-Frias, Salvador M. Aceves, Daniel L. Flowers, Paper IMECE2005-79432, Proceedings of the ASME International Mechanical Engineering Congress and Exhibition, 2005, Accepted for Publication, Journal of Energy Resources Technology.

9. Effect of Laser-induced Excitation of Oxygen on Ignition in HCCI Engines Analyzed by Numerical Simulations, Daniel L. Flowers, Salvador M. Aceves and Robert W. Dibble, Combustion Theory and Modelling, Vol. 11, No. 3, pp. 455-468, 2007.

10. Extremum Seeking Tuning of an Experimental HCCI Engine Combustion Timing Controller, Nick Killingsworth, Dan Flowers, Salvador Aceves, Miroslav Krstic, Proceedings of the American Control Conference, New York, NY, July 2007.

11. In Pursuit of New Engine Dynamics, Daniel Flowers, Nick Killingsworth and Robert Dibble, Mechanical Engineering, pp. 20-21, July 2007.

12. A Numerical Investigation into the Anomalous Slight NOx Increase when Burning Biodiesel: A New (Old) Theory, George A. Ban-Weiss, J.Y. Chen, Bruce A. Buchholz, Robert W. Dibble, Fuel Processing Technology, Vol. 88, pp. 659-667, 2007.

Special Recognitions & Awards/Patents Issued

1. Salvador M. Aceves invited to deliver a seminar at the SAE 2007 symposium on HCCI, September 2007, Lund, Sweden.

2. Daniel Flowers invited to deliver a seminar at the SAE 2007 symposium on HCCI, September 2007, Lund, Sweden.

II.A.8 HCCI and Stratified-Charge CI Engine Combustion Research

John E. Dec
Sandia National Laboratories
MS 9053, P.O. Box 969
Livermore, CA 94551-0969

DOE Technology Development Manager:
Gurpreet Singh

Objectives

Project Objective:

- Provide the fundamental understanding of homogeneous charge compression ignition (HCCI) combustion required to overcome the technical barriers to development of practical HCCI engines by industry.

FY 2007 Objectives:

- Investigate the effects of exhaust gas recirculation (EGR)/residuals and its constituents on combustion phasing for single- and two-stage-ignition fuels (*i.e.* gasoline-like and diesel-like fuels, respectively).
- Apply chemiluminescence spectroscopy and chemical-kinetic analysis to investigate how HCCI progresses through the autoignition/combustion event, for both one- and two-stage fuels.
- Investigate various techniques to improve fuel/air mixture formation for stratified HCCI at low loads to increase combustion efficiency.
- Support chemical-kinetics and computational fluid dynamics (CFD) modeling work at Lawrence Livermore National Laboratory (LLNL) to help develop improved kinetic mechanisms and advance the understanding of in-cylinder processes.

Accomplishments

- Determined the effects of EGR/residuals and its constituents on combustion phasing for single- and two-stage fuels.
- Showed how HCCI combustion progresses through various phases of autoignition, main combustion, and burnout using a combination of chemiluminescence spectroscopy and chemical-kinetic analysis.
- Investigated several fuel-stratification techniques to improve combustion efficiency at low loads, using a combination of metal-engine performance data and fuel planar laser induced fluorescence (PLIF) imaging.
  - Demonstrated 92.5% combustion efficiency at an idle fueling of $\phi = 0.12$.
- Initiated an improved, detailed exhaust-speciation study to determine the effects of changes in fueling rate, and fuel-stratification at low loads, on emissions (with LLNL).
- Supported chemical-kinetic and CFD modeling work at LLNL, and CFD modeling at the University of Wisconsin by providing data, analysis, and discussions for 1) improving primary reference fuel (PRF) kinetic mechanisms and 2) CFD/kinetic modeling of performance and emissions.

Future Directions

- Conduct an investigation of the potential of EGR/residuals for slowing the pressure-rise rate (PRR) at high loads to further extend the upper-load limit of HCCI.
  - Eliminate the combustion-phasing effects of EGR to correctly evaluate its effect on PRR.
- Investigate the development of thermal stratification and its distribution in the bulk gases during the latter-compression and early-expansion strokes using PLIF imaging.
- Complete detailed exhaust-speciation study over a range of fueling rates and for mixture stratification at low loads for iso-octane and gasoline (with LLNL).
- Determine the effects of ethanol and/or ethanol-gasoline blends on HCCI performance for well-mixed and mixture-stratified operation.
- Complete development and validation of an electro-hydraulic variable valve actuation system, and begin studies of techniques to control HCCI such as late intake valve closing and negative valve overlap.
- Work cooperatively with LLNL on CFD modeling to better understand the sources of HCCI emissions, and continue to support chemical-kinetic model development at LLNL.

Introduction

HCCI engines have significant efficiency and emissions advantages over conventional spark-ignition and diesel engines, respectively. However, several technical barriers must be addressed before it is practical

to implement HCCI combustion in production engines. As outlined under the accomplishment bullets above, studies have been conducted over the past year that provide new understanding related to overcoming three of these technical barriers: combustion-phasing control, fuel effects, and poor combustion efficiency at low loads. Addressing these respective barriers, our main studies for FY 2007 included: 1) the use of EGR to control combustion phasing over the load-speed map, 2) an improved understanding of the steps of HCCI autoignition and combustion for various fuels, and 3) techniques for improving combustion efficiency at low loads and reducing CO and HC emissions.

Approach

These studies were conducted in our dual-engine HCCI laboratory using a combination of experiments in both the all-metal and optically accessible HCCI research engines. This facility allows operation over a wide range of conditions, and can provide precise control of operating parameters such as combustion phasing, injection timing, intake temperature and pressure, and mass flow rates of supplied fuel and air. The laboratory is also equipped to meter N_2, CO_2 and H_2O vapor into the intake stream to simulate the addition of combustion products, *i.e.* EGR.

To study the effects of EGR and its constituents on combustion phasing, simulated EGR or its individual constituents were metered into the intake air, while engine performance and emission data were acquired using conventional cylinder-pressure and exhaust-emissions diagnostics. In addition, a cooled EGR loop was added to allow comparison of real and simulated EGR, as a method to determine the effects of trace species in the real EGR.

The investigation of the phases of HCCI autoignition and combustion for various fuels involved metal engine performance experiments followed by detailed studies of the combustion event in the optical engine. Calibrated chemiluminescence spectroscopy provided information on the key chemiluminescence species and the nature of the reactions. A chemical-kinetic analysis was also conducted to better understand the key reactions of each phase of autoignition and combustion, and the differences between single- and two-stage-ignition fuels.

Several fuel-stratification techniques were investigated to improve HCCI combustion efficiency at low loads. A combination of metal-engine performance data and PLIF imaging of the fuel distributions in the optical engine was used to determine the combustion efficiencies and to understand the reasons for the improvements or lack of improvements for the various techniques. As part of this investigation, a new PLIF image analysis technique was developed to account for the local cooling effect of fuel stratification, which can cause errors of up to 40% in the fuel concentration if no correction is applied.

In addition to these investigations, other efforts involved working cooperatively with external organizations. These efforts included: providing data to and working with both chemical-kinetic and CFD modeling groups at LLNL, CFD modelers at the University of Wisconsin, an analytical chemistry group at LLNL for detailed exhaust-species measurements, and continued interactions with the International Truck and Engine Co. on the development of a variable valve actuation system.

Results

EGR and high levels of retained residuals are widely used in HCCI engines to help control combustion phasing. However, the underlying causes are not well understood because exhaust gases can affect HCCI autoignition in multiple ways, and these effects vary with fuel-type. Therefore, an investigation was conducted into the effects of EGR and its constituents for representative single-stage-ignition fuels, iso-octane and gasoline, and two-stage-ignition fuels, PRF80 and PRF60 (80-20% and 60-40% blends of iso-octane and *n*-heptane, respectively) whose autoignition behavior is characteristic of diesel fuel. EGR addition was accomplished both by using real EGR gases and by simulating EGR with complete stoichiometric products (CSP): N_2, H_2O, and CO_2.

Figures 1a and 1b show the effects of CSP addition on the ignition timing for iso-octane and PRF80, respectively. Also shown are the individual CSP components and “dry CSP” which consists of only N_2 and CO_2, simulating complete water condensation. In these figures, the 10% burn point is used as a measure of the ignition point, and the amount of EGR gases added is shown in terms of the intake oxygen mole fraction. As can be seen, the ignition-retarding effect of CSP is similar for both fuels, but the effect of the individual components is substantially different for the two fuel-types. This occurs because these fuels have different sensitivities to the two main effects of EGR, which are a thermodynamic “cooling” effect on the compressed-gas temperature and changes to the autoignition chemistry.

For iso-octane, the effect on autoignition chemistry is limited to a rather weak sensitivity to the O_2 concentration. This is evident by the effect of N_2, which is thermodynamically almost the same as air, yet retards the autoignition slightly. However, this effect is weak, and the ignition timing of iso-octane is much more affected by the thermodynamic-cooling effect of the other CSP constituents. This effect results from the higher heat capacity of these constituents, which reduces

the compressed-gas temperature relative to that of air alone. CO_2 has the highest heat capacity followed by H_2O, then CSP, and finally dry CSP. Since the cooling effect of CO_2 is the largest, it causes the most timing retard for a given air displacement, with the timing retard caused by the other diluents following in the order of their specific-heat capacities. The behavior of gasoline (not shown) is similar to iso-octane.

In contrast, for PRF80, the effect of CSP addition is dominated by chemical effects. The strongest is the retarding effect of reduced O_2 concentration, as can be seen by comparing the slope of the N_2 curve with that of CSP. Another chemical effect for PRF80 is the autoignition enhancement by H_2O. The H_2O curve in Figure 1b falls right on top of the N_2 curve despite the thermodynamic cooling effect of H_2O (discussed above). This occurs because H_2O lowers the autoignition temperature for PRF80, almost perfectly counteracting the "cooling" effect of H_2O addition. This ignition-enhancing effect of H_2O explains why dry CSP causes more timing retard for PRF80 than does CSP. For iso-octane the opposite is observed. CO_2 addition adds thermodynamic cooling to the effect of reduced O_2 concentration, further increasing the timing retard. The effect of CSP addition with PRF60 (not shown) is similar to that of PRF80.

The effect of trace species in real EGR was examined by comparing the ignition-retarding effect of real EGR with that of CSP. The data showed real EGR advanced the combustion phasing relative to CSP for the single-stage-ignition fuels, iso-octane and gasoline, but to retarded it slightly for the two-stage fuel, PRF80. A complete discussion of this study can be found in Ref. [1].

A combined investigation in the metal and optical engines shows that the HCCI autoignition/combustion process occurs in three phases for single-stage-ignition fuels. Initially, a slow temperature rise above the compressed-gas temperature begins when the charge reaches 950–1050 K. This intermediate-temperature heat-release (ITHR) then progressively increases the charge temperature up to the thermal-runaway point, beyond which the temperature rises rapidly due to the high-temperature heat-release (HTHR) reactions. After the main combustion event, a weak burnout phase is observed. For two-stage ignition fuels, low-temperature heat-release (LTHR) or "cool-flame" reactions occur as an initial stage of ignition prior to reaching the ITHR phase. To better understand how the key reactions vary between these combustion phases, and why reaction rates vary with fuel type, spectra of the natural chemiluminescence emission were acquired in the optical engine for both iso-octane and PRF80. The example in Figure 2 shows that the emission spectrum varies significantly between the ITHR

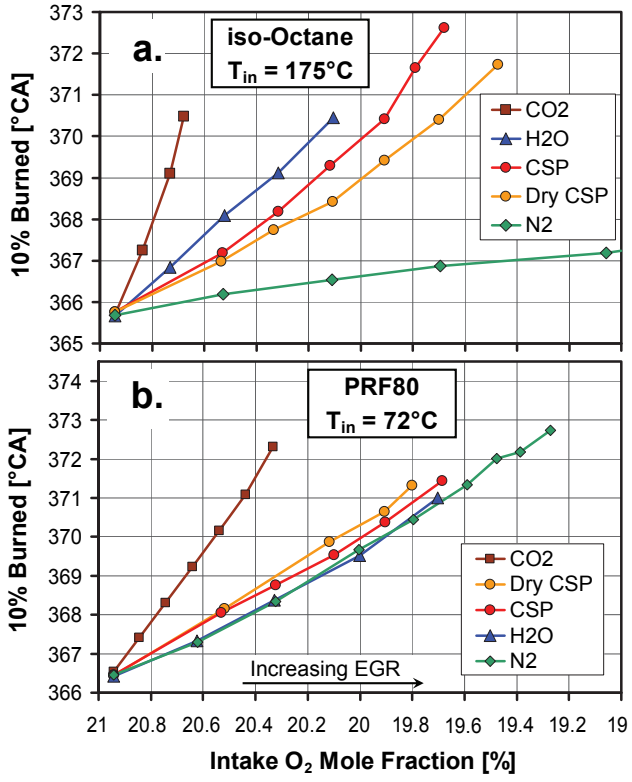

FIGURE 1. Combustion-Phasing (10% Burn Point) Retard with Diluent Addition for Iso-Octane (a) and PRF80 (b) (The amount of CSP or CSP constituent added is shown on the x-axis in terms of intake O_2 mole fraction, which decreases as diluent is added. Charge/fuel mass ratio = 37.8, corresponding to ϕ = 0.4 for no diluent.)

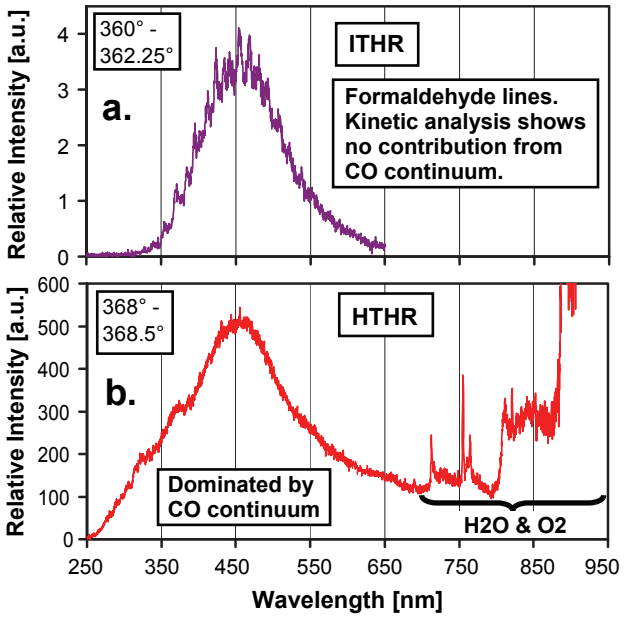

FIGURE 2. Chemiluminescence Spectra During the ITHR (a) and HTHR (b) Combustion Phases for Iso-Octane (The CO-continuum emission is from the $CO + O \rightarrow CO_2$ reaction.)

and HTHR phases, indicating significant differences in the key reactions. The ITHR phase is dominated by formaldehyde emission (note the regularly spaced formaldehyde lines in Figure 2a), while the main combustion is dominated emission from the CO-continuum with contributions from OH and HCO, as well as H_2O and O_2 emission to the red and infrared (Figure 2b). A full discussion of this study is given in Ref. [2].

Poor combustion efficiency at low loads, and the associated high emissions of CO and HC, is one of the significant challenges for practical HCCI engines. Previous work has shown that fuel-stratification can significantly improve low-load combustion efficiency by increasing the local combustion temperatures. However, the amount of allowable stratification is limited when the richest regions become sufficiently close to stoichiometric that NOx emissions exceed allowable levels. To improve this combustion-efficiency/NOx tradeoff, various mixture-formation techniques were investigated, including: using two different types of gasoline-direct injection (DI) fuel injectors (hollow-cone spray and 8-hole), varying the injection pressure, and varying the intake-air swirl. For each technique, the amount of stratification was increased by delaying the start of injection (SOI) from early in the intake stroke (well-mixed) until well up the compression stroke (highly stratified) at an idle fueling rate corresponding to $\phi = 0.12$.

Figure 3 summarizes the key findings. As can be seen, the combustion efficiency improves with increased stratification, but eventually the NOx emission rise above the allowable limit. For the base condition of the hollow-cone injector with 120 bar injection pressure, stratification improved the combustion efficiency from 64% for the well-mixed case to 89% at the NOx limit. Switching to the 8-hole injector provided the single largest improvement, increasing the NOx-limited combustion efficiency to 92%. Increasing the injection pressure to 170 bar gave a small additional improvement to 92.5%, which is approaching high-load HCCI combustion efficiencies.

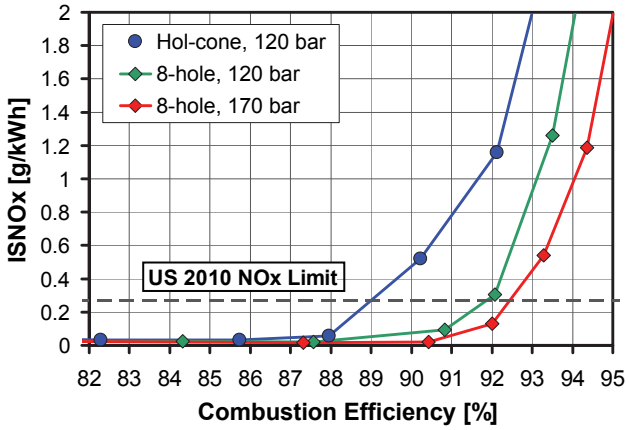

FIGURE 3. Combustion-Efficiency/NOx Tradeoff for Fuel Stratification at Low Loads ($\phi = 0.12$, Idle Fueling) for Iso-Octane (For each curve, the amount of stratification increases from left to right.)

To better understand the reasons for the observed changes in performance, and to gain insight into ways to further improve the mixture, a PLIF imaging investigation of the fuel distributions was also conducted. Figure 4 shows SOI sequences of ϕ-map images (derived from PLIF images) for the hollow-cone and 8-hole injectors. As can be seen, the amount of stratification increases for both injectors as SOI is delayed, resulting in higher local equivalence ratios. For each injector, the image outlined by the red box shows the fuel distribution corresponding to the data point just below the NOx limit in Figure 3. In agreement, these red-boxed images show maximum ϕ values of about 0.6, corresponding to combustion temperatures at which the onset of NOx formation would be expected. As indicated by the crank angles below each image, the NOx limit occurs at a later injection timing for the 8-hole injector (315° crank angle, CA) compared to the hollow-cone injector (300° CA). However, aligning the images sequences relative to the NOx limit shows that the changes in the ϕ distribution with increasing stratification are similar for the two injectors. Also, at the NOx limit, the fuel distribution pattern is similar, with no indication of multiple fuel pockets for the 8-hole injector as might have been expected. Based on these observations, the improved combustion-efficiency/NOx tradeoff with the 8-hole injector must result from fewer low-ϕ regions being present. Although the reason for this improvement is not fully understood, we believe that it is related to the faster mixing with the 8-hole injector, which allows a later SOI at the NOx limit. Considering all the techniques examined to improve the combustion-efficiency/NOx tradeoff, the data consistently showed that a later SOI at the NOx limit resulted in a higher combustion efficiency. We hypothesize that with a later SOI, there is less time for the in-cylinder flows and turbulence (*i.e.* mixing not produced by the injection process) to form overly lean regions by transporting fuel out of the main fuel pockets produced by the fuel-injection process. A complete discussion can be found in Ref. [3].

Conclusions

- EGR is very effective for suppressing the autoignition reactivity of both single- and two-stage ignition fuels, providing a means of controlling combustion phasing over the load-speed map.
- EGR retards the combustion phasing by both a thermodynamic "cooling" effect on the compressed-gas temperature and by changing the autoignition chemistry. For single-stage (gasoline-like) fuels,

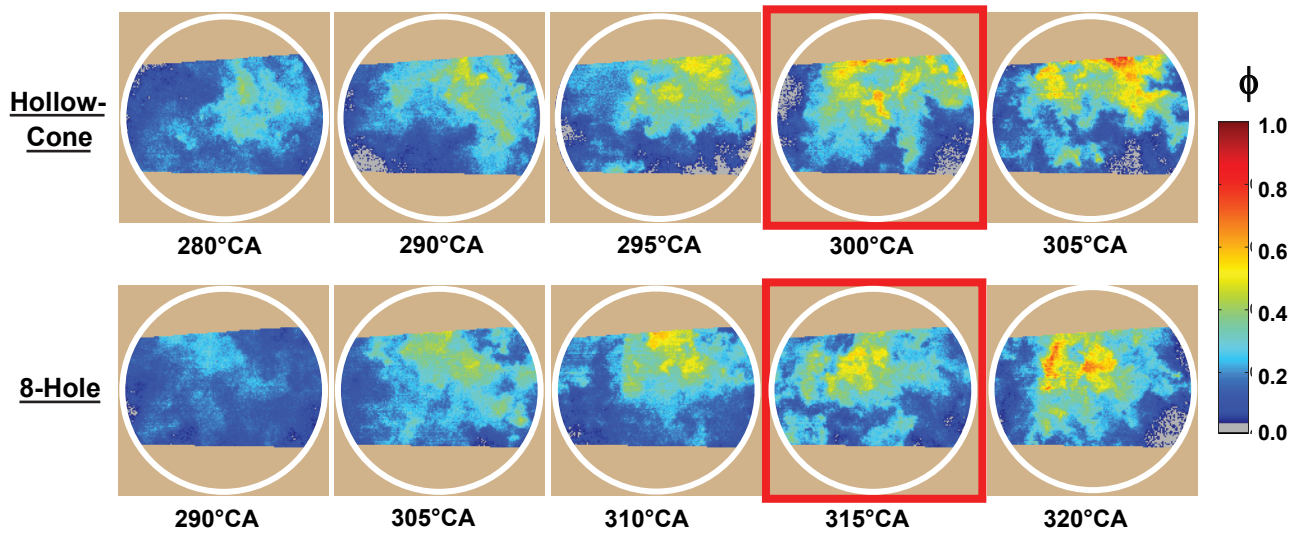

FIGURE 4. Equivalence-Ratio Image Sequences Showing the Changes in Fuel Stratification with Delayed Injection Timing for Both the Hollow-Cone and 8-Hole Injectors with 120 Bar Injection Pressure (The SOI is given below each image. All images were acquired at 365° CA [5° after top dead center].)

the thermodynamic effect is dominant, while for two-stage (diesel-like) fuels, the chemical effect dominates.

- Chemiluminescence-spectroscopy and chemical-kinetic analysis show that the HCCI autoignition/combustion process occurs in three or four phases for single- and two-stage fuels, respectively. Each phase has distinctly different key reactions. ITHR-phase reaction rates can vary significantly with fuel-type, and these differences are critical to differences in autoignition [2].
- Fuel stratification is very effective for increasing the combustion efficiency of HCCI at low-loads (and reducing CO and HC emissions). However, the amount of stratification allowable is limited by NOx emissions, resulting in a combustion-efficiency/NOx tradeoff.
- Compared to the base case of a hollow-cone injector with 120 bar injection pressure, switching to an 8-hole gasoline-DI injector and 170 bar injection pressure improved the combustion efficiency 3.5% at the NOx limit, for a combustion efficiency of 92.5% at an idle fueling of $\phi = 0.12$. This compares to a combustion efficiency of only 64% for well-mixed operation.
- PLIF imaging of fuel distributions, combined with metal-engine performance data, indicates that the improved combustion efficiency with the 8-hole injector is the result of less fuel in low-ϕ regions, for fuel stratification at the NOx limit.

References

1. Sjöberg, M., Dec, J. E., and Hwang, W., "Thermodynamic and Chemical Effects of EGR and Its Constituents on HCCI Autoignition," SAE paper 2007-01-0207, 2007.

2. Hwang, W., Dec, J. E. and Sjöberg, M., "Spectroscopic and Chemical-Kinetic Analysis of the Phases of HCCI Autoignition and Combustion for Single- and Two-Stage Ignition Fuels," submitted to *Combustion and Flame*, August 2007.

3. Hwang, W., Dec, J. E. and Sjöberg, M., "Fuel Stratification for Low-Load Combustion: Performance and Fuel-PLIF Measurements," SAE paper no. 2007-01-4130, 2007.

FY 2007 Publications/Presentations

1. Sjöberg, M. and Dec, J. E., "EGR and Intake Boost for Managing HCCI Low-Temperature Heat Release over Wide Ranges of Engine Speed," SAE paper 2007-01-0051, 2007 SAE Fuels and Emissions Conference.

2. Sjöberg, M., Dec, J. E., and Hwang, W., "Thermodynamic and Chemical Effects of EGR and Its Constituents on HCCI Autoignition," SAE paper 2007-01-0207, 2007 SAE Congress.

3. Hwang, W., Dec, J. E. and Sjöberg, M., "Spectroscopic and Chemical-Kinetic Analysis of the Phases of HCCI Autoignition and Combustion for Single- and Two-Stage Ignition Fuels," submitted to *Combustion and Flame*, August 2007.

4. Hessel, R., Foster, D., Aceves, S., Flowers, D., Pitz, W., Dec. J., Sjöberg, M., and Babajimopoulos, A., "Modeling HCCI using CFD and Detailed Chemistry with Experimental Validation and a Focus on CO Emissions,"

International Multi-Dimensional Engine Modeler's Meeting, Detroit, Michigan, April 2007.

5. Hwang, W., Dec, J. E., and Sjöberg, M., "Fuel Stratification for Low-Load HCCI Combustion: Performance and Fuel-PLIF Measurements," DOE Advanced Engine Combustion Working Group Meeting, February 2007.

6. Sjöberg, M. and Dec, J. E., "Comparing Late-cycle Autoignition Stability for Single- and Two-Stage Ignition Fuels in HCCI Engines," oral-only presentation at the 2007 SAE Congress.

7. Dec, J. E. "In-Cylinder Optical Diagnostics", AVL Technology Café presentation at the 2007 SAE Congress.

8. Hwang, W., Dec, J. E. and Sjöberg, M., "Spectroscopic Analysis of the Phases of HCCI Autoignition and Combustion for Single- and Two-Stage Ignition Fuels," 5th US Combustion Meeting, the Combustion Institute, San Diego, March 2007.

9. Musculus, M. P., Dec, J. E., and Lachaux, T. "Diesel Jet Mixing in Conventional and Low-Temperature Diesel Combustion," 10th International Conference on Present and Future Engines for Automobiles, Rhodes Island, Greece, May 2007.

10. Dec, J., Sjöberg, M, and Hwang, W., "The Effects of EGR and Its Constituents on the Autoignition of Single- and Two-Stage Fuels," 13th Diesel Engine-Efficiency and Emissions Research Conference (DEER 2007), August 2007.

11. Dec, J. E., Hwang, W., and Sjöberg, M., "Fuel Stratification to Improve Low-Load HCCI: Engine Performance and Fuel-PLIF Imaging," invited presentation, SAE HCCI Symposium, Lund, Sweden, September 2007.

12. Dec, J. E., "Advantages of Charge Stratification in HCCI Engines," plenary lecture, SAE/NA 8th International Conference on Engines for Automobiles, Capri, Italy, September 2007.

Special Recognitions & Awards/Patents

1. Plenary lecture (John Dec) at the SAE/NA 8th International Conference on Engines for Automobiles, Capri, Italy, September 2007.

2. Invited presentation (John Dec) at the SAE HCCI Symposium, Lund, Sweden, September 2006.

3. SAE Russell S. Springer Award (Magnus Sjöberg), presented at 2007 SAE Congress.

4. SAE Lloyd Withrow Distinguished Speaker Award (John Dec), presented at 2007 SAE Congress.

5. U.S. Patent number 7,128,046 B1, "Fuel Mixture Stratification as a Method for Improving Homogeneous Charge Compression Ignition Operation," Dec, J. E. and Sjöberg, M., issued October 31, 2006.

II.A.9 Automotive HCCI Combustion Research

Richard Steeper
Sandia National Laboratories, MS 9053
P.O. Box 969
Livermore, CA 94551-0969

DOE Technology Development Manager:
Gurpreet Singh

Objectives

This project comprises optical-engine investigations designed to enhance our understanding of in-cylinder processes in automotive-scale homogeneous charge compression ignition (HCCI) engines. Objectives for FY 2007 include:

- Establish the capability to operate in advanced HCCI operating modes, specifically recompression or negative-valve-overlap (NVO) mode.
- Continue our investigation of the correlation between fuel-air mixture preparation and combustion/emission processes in HCCI engines. Apply new turbulence-modeling tools to clarify the importance of *spatial* fuel-distribution statistics.
- Continue the development of laser-based temperature diagnostics at Stanford University, and conduct tests of the diagnostics in Sandia HCCI research engines.
- Continue development and application of collaborative HCCI-engine-simulation tools.

Accomplishments

- Installed NVO cams in the automotive HCCI engine. Conducted tests to establish the operating range of recompression operation and tested protocols to allow rapid and safe startup in the optical engine.
- Created a 1-D cycle-simulation model to aid the selection of stable NVO operating conditions.
- Adapted Sandia's linear-eddy model (LEM) to provide detailed, stochastic predictions of turbulent mixing in our HCCI engine. The model provided valuable insights into the effect of spatial fuel distribution on HCCI combustion and emissions.
- Continued development of multiple in-cylinder temperature diagnostics at Stanford University.
- Transported Stanford 2-laser diagnostic to Sandia and installed it in the automotive HCCI laboratory. Characterized performance of the diagnostic for simultaneous temperature/composition measurements in an operating engine. Established ±5% accuracy for temperature measurements during the compression stroke, with a sensitivity better than 10 K.
- Began tests of the planar laser-induced fluorescence (PLIF) diagnostic during fired recompression-HCCI operation.
- Continued development of HCCI simulation tools. The University of Wisconsin-Lawrence Livermore National Laboratory (UW-LLNL) model of the Sandia HCCI automotive engine (KIVA/Multi-zone model) achieved full-cycle simulation of homogeneous fired operation. The KIVA code was also coupled with the LEM to enable our spatial-fuel-distribution study.

Future Directions

- Complete operating-range tests of recompression-HCCI combustion.
- Investigate the use of alternative injection strategies, including injection during the recompression period, to accomplish advanced fuel-air mixing strategies. Apply PLIF diagnostic to characterize engine performance under these conditions.
- Examine spark-assisted HCCI operation to understand its potential role for widening the HCCI operating range.
- Test Stanford wavelength-modulation tunable diode laser (TDL) sensor and wavelength-ratioing laser-induced fluorescence (LIF) sensor in Sandia HCCI engines.
- Modify the automotive HCCI facility to enable more flexible valve timing, wider operating range, and multiple combustion modes.

Introduction

Major challenges to the implementation of HCCI combustion—including phasing control, operating-range extension, and emissions control—will require advanced, non-homogeneous, fuel-air mixing strategies. Alternative strategies such as retarded injection and variable valve timing can be used to modify local charge composition and temperatures, thereby affecting, and possibly controlling, ignition phasing, rate of heat release, combustion efficiency, and engine-out emissions. This project is focused on understanding the in-cylinder processes characteristic of automotive HCCI engine combustion. Optical engine experiments employ in-cylinder diagnostics to quantify mixture preparation,

ignition, combustion, and emission processes. Computational models help interpret the results and guide further research. The knowledge gained supports DOE's goal of facilitating the development of energy-efficient, low-emission engine combustion.

Approach

A variety of optical and mechanical diagnostics are applied to obtain information about HCCI in-cylinder processes. In-cylinder spray imaging allows assessment of spray evolution, penetration, and wall-wetting. LIF imaging produces vapor-fuel-distribution data, and statistics derived from the images quantify the state of mixing just prior to heat release. Chemiluminescence imaging provides information about combustion that can be related to the LIF fuel-distribution images. Finally, engine-out emission measurements help correlate mixture-preparation strategies with combustion/emission performance. Development of new diagnostics for in-cylinder temperature measurements, a critical need for HCCI research, continues at Stanford University, with testing taking place in Sandia's optical engines. Work on the KIVA simulation of our automotive HCCI engine continues at UW and LLNL, and the Sandia linear-eddy model adds important details of stochastic mixing. Technical exchanges with OEMs, national labs, and academia provide feedback and guidance for the research.

Results

NVO Operation

New cams were installed in the automotive HCCI engine this year to permit operation using recompression, or NVO, strategies. To accommodate these strategies, the cams provide a short lift duration of 145 crank angle degree (CAD), and can be timed for a range of NVO operation. When timed to set EVC = IVO (exhaust valve closing equal to intake valve opening), the operation approximates a conventional motored cycle as shown in Figure 1a. The short-duration valve-lift profile is responsible for a slight pressure rise (recompression) visible at top dead center (TDC) of the exhaust stroke. With the cams timed to set EVC = -90 and IVC = +90 CAD, an NVO of 180 CAD is achieved, producing the large recompression seen in Figure 1b during the exhaust and intake strokes. Plotted along with the experimental pressure traces in Figure 1 are model predictions from a GT Power model of our engine that we have developed. The model reproduces the data closely at all operating conditions, and is a useful tool for planning our experimental operating conditions.

Operating with large negative valve overlap is a challenge for optical engines, since typically such strategies require extended operation to reach steady-state. During this reporting period, we have begun to establish HCCI NVO stable operating regimes for the optical engine as well as strategies for rapid start-up. These strategies employ port injectors with gaseous fuels for warm-up and then transition into HCCI operation with direct-injected PRF90 fuel (primary reference fuel with 90 octane rating). Coupling NVO operation with LIF diagnostics is complicated by high exhaust gas recirculation (EGR) levels, and the possibility of fuel injection during both the compression and recompression strokes. We have successfully demonstrated the ability to make simultaneous temperature/composition measurements during NVO operation (see PLIF measurements in the following).

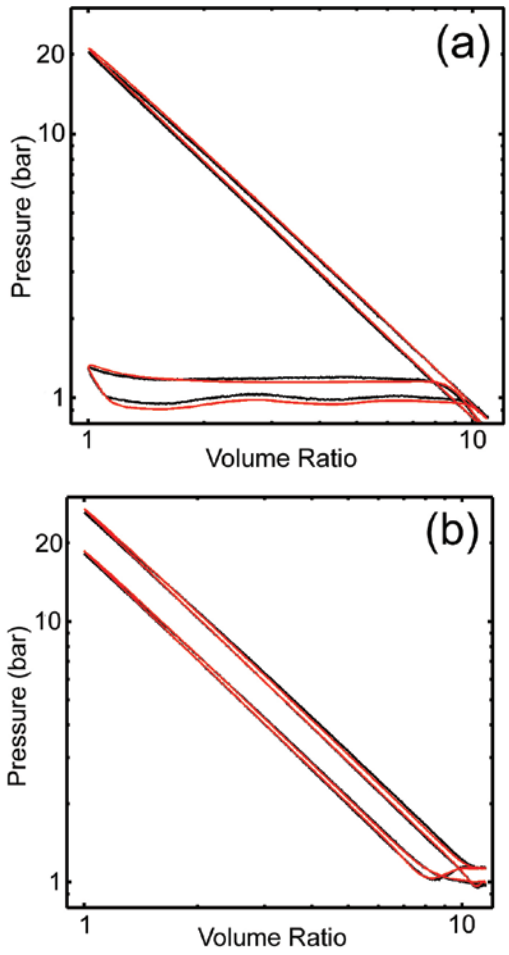

FIGURE 1. Measured and predicted motored engine pressure traces using NVO cams. Black curve = measured data; red curve = predictions from 1-D engine model. 1a: conventional cam timing. 1b: NVO timing with 180 CAD of negative overlap.

LEM Modeling

A primary project goal is quantifying the effect of mixture preparation on combustion. LIF measurements of fuel-air mixing provide mixture statistics at the time

of ignition, and in previous work we have demonstrated a correlation between LIF-based probability density function (PDF) statistics and engine-out emissions. But PDF statistics are a limited metric since spatial details of the fuel distribution are ignored. This issue was highlighted during an experimental comparison of two fuel injectors in our engine: the injectors produced similar fuel-distribution PDFs, but significantly different NOx emissions. Unlike the PDFs, spatial mixing statistics were distinct: the injector creating a coarser fuel distribution (fewer, larger fuel packets) produced more NOx. Since it is difficult to control mixing statistics experimentally, we have applied a novel combination of modeling tools this year to further examine the question: how do the spatial details of fuel-air mixing affect HCCI combustion?

Collaboration with the UW and LLNL produced a KIVA CFD model of our automotive HCCI engine as part of our project, and we have combined it with Sandia's LEM to capture the necessary turbulent mixing scales. The KIVA model is a full-cycle 3-D simulator with 150,000 grid cells; for computational efficiency, the cells are grouped into 100 zones of common temperature and composition during reaction computations. The 1-D LEM runs in series with the KIVA simulation, solving diffusion/reaction equations on a fine grid and simultaneously simulating turbulence by defining discrete eddy events that randomly rearrange fluid packets much like a physical eddy.

Since we are interested in the effect of fuel distribution on combustion, the LEM is run during the period of combustion (from -30 to +30 CAD after TDC). KIVA provides initial pressure and temperature values for the LEM, averaged over the core region of our engine (roughly corresponding to the measurement volume of our LIF diagnostic). In addition, spatially averaged turbulent kinetic energy and dissipation rate values predicted by KIVA are used at each time step to determine the location, timing, and intensity of the LEM eddy events. Finally, several hypothetical fuel distributions are defined to initialize the LEM simulation at -30 CAD. One such initial distribution, the Coarse distribution, is illustrated in Figure 2a. The LEM predicts the spatial and temporal evolution of temperature, fuel, and products as illustrated in Figure 2b, which is a snapshot of mixture profiles soon after the start of heat release. The visible random structure of the profiles is created by the LEM's turbulence mechanism, and it is an important feature that each cycle simulation produces unique results.

We have simulated initial spatial fuel distributions ranging from very fine to very coarse; Figure 3 presents predicted mean temperature histories for three of these cases, illustrating several insights gained from the work. The Fine distribution corresponding to the results in Figure 3a is similar to the Coarse distribution in Figure 2a, but with twice as many (narrower) fuel

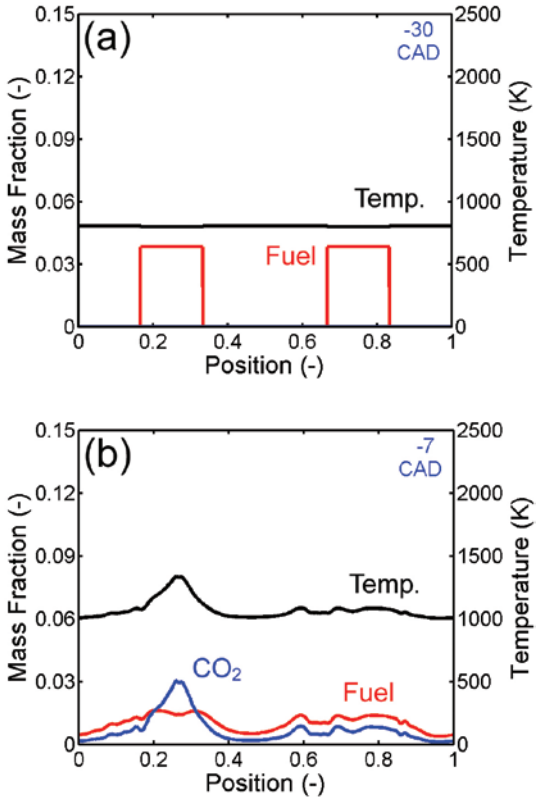

FIGURE 2. LEM predictions for the Coarse fuel distribution: composition and temperature profiles along the LEM's 1-D traverse of the engine core region. 2a: initial conditions at the start of the simulation. 2b: temperature, fuel, and CO_2 profiles soon after the start of heat release.

packets. The dotted line in Figure 3a is KIVA's predicted temperature history for homogeneous-charge operation. The dashed line is averaged temperature from an LEM run in which turbulence has been turned off for comparison purposes. The no-turbulence curve generally follows KIVA's predictions, although the low-temperature heat release (at -22 CAD) is not captured by the LEM's simplified kinetics model. In addition, the LEM main heat release is advanced due to the slight stratification of the Fine distribution. The red (solid) curve in Figure 3a represents LEM results with turbulence activated. There is little difference from the no-turbulence results, and we conclude that for the Fine case, diffusion alone (without turbulence) mixes the initial distribution nearly completely by the start of heat release.

Figures 3b and 3c present the same three curves for the Coarse and the Very Coarse fuel distributions. It is apparent that making fuel distributions more coarse (more stratified) monotonically advances the predicted combustion phasing. Perhaps the most significant results are two trends seen only in the Coarse case, Figure 3b. Here the turbulence (red) curve phasing is retarded with respect to the no-turbulence (dashed) curve, and its maximum rate of temperature rise is reduced as well. These trends are explained by the fact

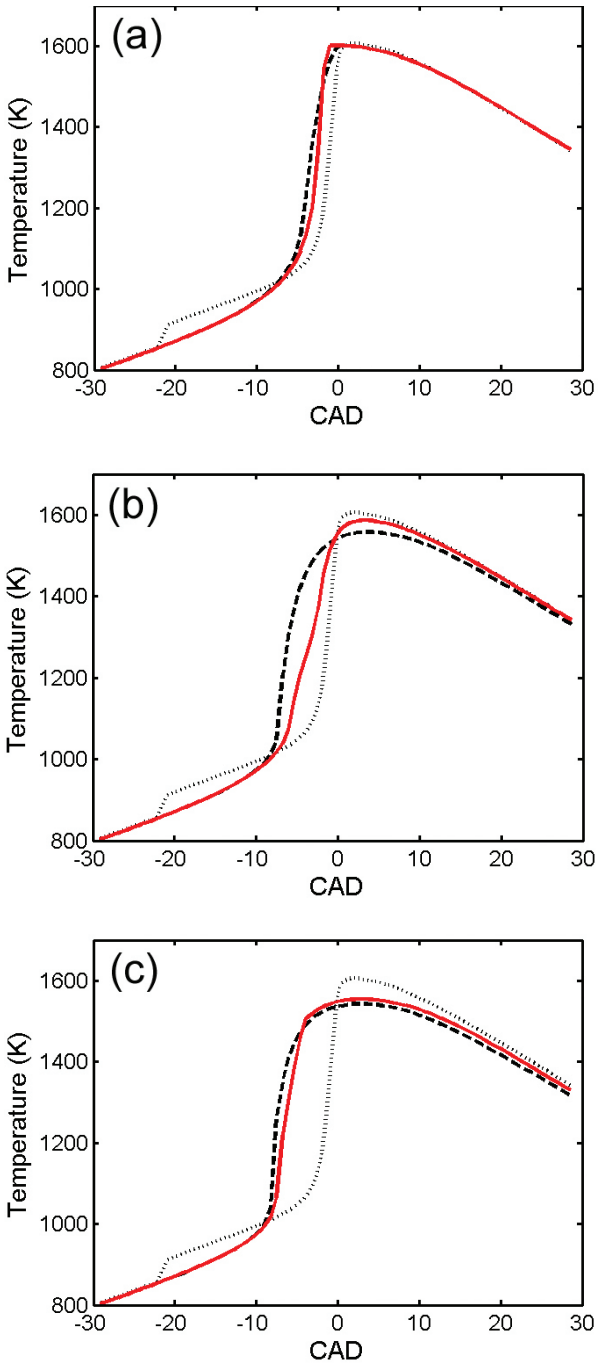

FIGURE 3. Model predictions of mean core-region temperatures: dotted lines = KIVA; dashed lines = LEM with no turbulence; solid red lines = LEM with turbulence. 3a: Fine fuel-distribution case; 3b: Coarse fuel-distribution case; 3c: Very Coarse fuel-distribution case.

that the turbulence integral length scale (estimated by KIVA) happens to match the Coarse fuel distribution length scale. In this case, and only this case, turbulence is effective in homogenizing the charge enough to delay heat release. In addition, the random turbulence mixes some fuel packets more than others, resulting in de-synchronized combustion that produces the more gradual heat release seen in the red curve of Figure 3b. Note that each realization of the LEM produces a unique temperature history: the resulting non-overlapping histories (not shown) allow an assessment of cyclic variation. Finally, the matching LEM temperature histories for the Very Coarse case, Figure 3c, indicate that diffusion and turbulence are ineffective in mixing fuel distributions that are as coarse as the Very Coarse case. We are optimistic that future embellishments, such as a more complex reaction mechanism and more realistic initial fuel distributions, will increase the utility of the LEM simulations.

PLIF Measurements

In collaboration with Sandia's HCCI engine program, Ron Hanson's group at Stanford University is developing in-cylinder temperature diagnostics. Both TDL absorption and LIF techniques have produced useful measurements in Sandia engines–this report highlights the successes of Stanford's two-laser PLIF diagnostic capable of simultaneous temperature and composition measurements. Excitation wavelengths of 277 and 308 nm (from two excimer lasers, with the output of one laser shifted in an H_2 Raman cell) were selected from seven candidate wavelengths to optimize temperature sensitivity when using the tracer 3-pentanone. A fast dual-frame camera records the fluorescence signal from each laser in rapid succession, and the ratio of the signals provides a 2-D image of in-cylinder temperature. Following temperature determination, simultaneous composition can be quantified using either of the fluorescence signals.

During this reporting period, we extensively tested the LIF diagnostic in the automotive HCCI optical engine. We began the tests with a homogeneous charge (both temperature and composition), measuring in-cylinder temperature in the core region of the engine during the compression stroke. Figure 4 compares these measurements with predictions based on isentropic compression and predictions from our GT-Power 1-D cycle simulation code. The LIF measurements are uniformly higher than the predictions, but remain within ±5% of those values over the entire range. Examination of the uniform temperature data allow us to estimate a sensitivity better than 10 K (one standard deviation).

Figure 5 presents measurements from a test in which a cool, unseeded nitrogen jet was injected into one intake port while hot, seeded air entered the other. This motored test simulates the addition of EGR in an engine, and the results in Figure 5 demonstrate the diagnostic's ability to capture simultaneous temperature and composition distributions. The simulated EGR is clearly concentrated on one side of the cylinder in Figure 5a, and Figure 5b shows a less distinct but complementary distribution of higher temperatures on the other side.

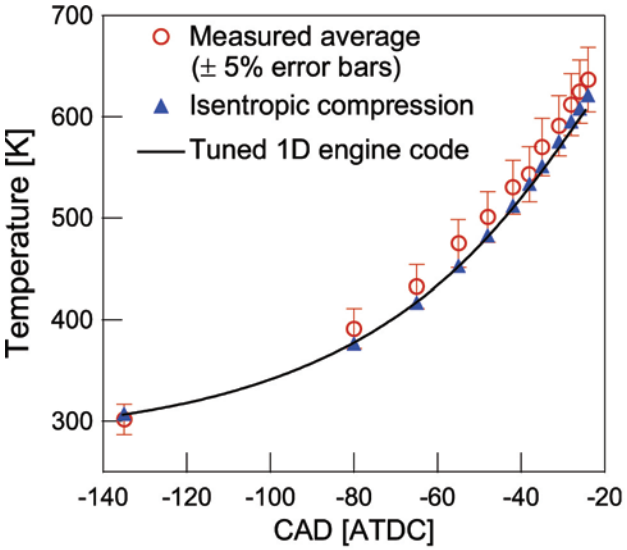

FIGURE 4. PLIF measurements of in-cylinder mean temperature during homogeneous motored operation. Red circles with error bars = PLIF measurements; blue triangles = predictions based on isentropic compression; line = predictions from 1-D cycle-simulation code.

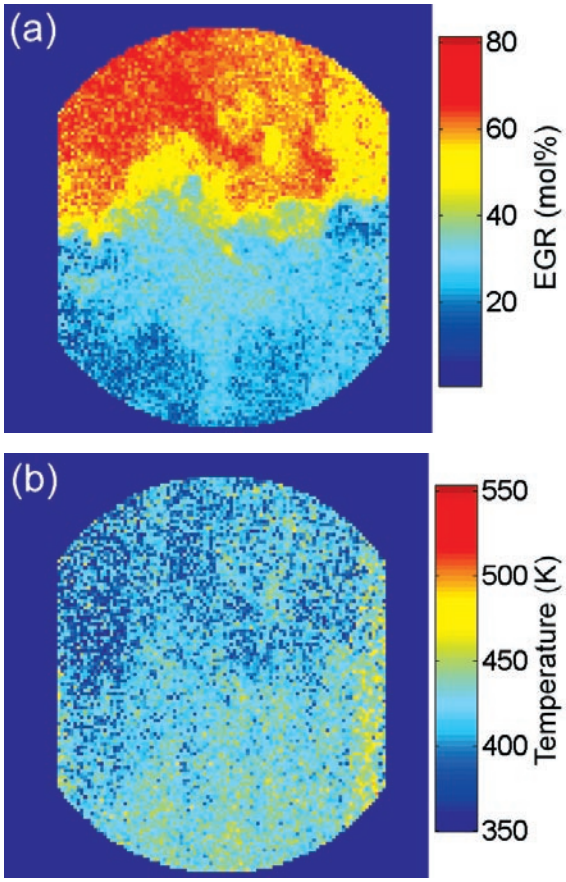

FIGURE 5. Single-cycle simultaneous composition/temperature images captured during motored operation with simulated EGR and temperature stratification. 5a: EGR mole fraction; 5b: temperature.

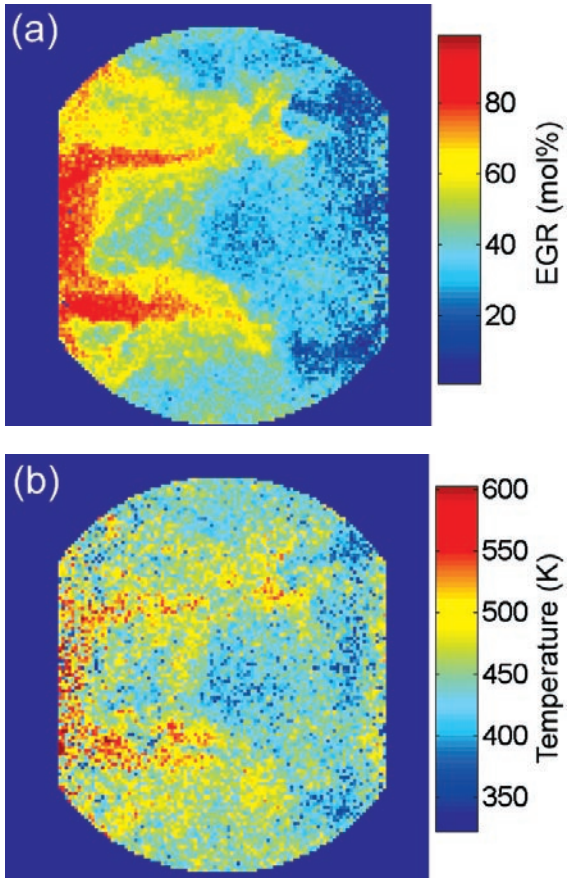

FIGURE 6. Single-cycle simultaneous composition/temperature images captured during fired operation with natural stratification. 6a: EGR mole fraction; 6b: temperature.

From these tests, we progressed to fired experiments, as illustrated in Figure 6. Figure 6a displays the distribution of retained residuals pushed to the exhaust (left) side of the cylinder soon after the opening of the intake valves (located on the right). The corresponding temperature distribution in Figure 6b shows that regions of high EGR concentration are hotter, as expected.

Conclusions

- New NVO cams installed in our optical HCCI engine enable fired operation with high-octane, automotive fuels.
- The LEM/KIVA modeling tool provides useful predictions relating mixture preparation to combustion performance. Simulation results predict that when the turbulence integral length scale matches the fuel-distribution length scale, turbulent mixing is most efficient and can influence phasing and heat-release rates during HCCI combustion. In such cases, cycle-to-cycle variation estimates (a unique feature of the LEM simulations) are predicted to be significant.

- Motored engine tests using Stanford's 2-laser LIF diagnostic indicate excellent temperature-measurement accuracy (±5%) and sensitivity (10 K). Further tests demonstrated an ability to characterize stratified-charge conditions (simultaneous temperature and composition) during fired operation. By seeding both the intake air and liquid fuel with 3-pentanone tracer, the technique successfully quantified in-cylinder residual-gas concentrations.

FY 2007 Publications/Presentations

1. Steeper, R. R., "Automotive HCCI Engine Research," Proc. of DOE Advanced Engine Combustion and Fuels Program Review, DOE/OFCVT Annual Report, 2006.

2. Steeper, R. R. and De Zilwa, S., "Improving the NO_X-CO_2 Trade-Off of an HCCI Engine Using a Multi-Hole Injector," SAE Paper 2007-01-0180, 2007.

3. Rothamer, D. A., Snyder, J., Hanson, R. K. and Steeper, R. R., "Optimized Two-Line Tracer PLIF Measurements of Temperature and Composition in an IC Engine," 2007 Fall Meeting, Sandia National Laboratories: Western States Section of the Combustion Institute, 2007.

4. Steeper, R. R., Sankaran, V., Oefelein, J. C., and Hessel, R. P., "Simulation of the Effect of Spatial Fuel Distribution Using a Linear-Eddy Model," SAE Paper 2007-01-4131, 2007.

5. Hessel, R. P., Foster, D. E., Aceves, S. M., Flowers, D. L., Pitz, W., and Steeper, R. R., "Pathline Analysis of Full-cycle Four-stroke HCCI Engine Combustion Using CFD and Multi-zone Modeling," SAE Paper 08PFL-853, 2007.

6. Rothamer, D. A., Snyder, J., Hanson, R. K., and Steeper, R. R., "Two-Wavelength PLIF Diagnostic for Temperature and Composition," SAE Paper 08PFL-726, 2007.

7. Steeper, R. R., "Modeling Study of the Effects of Spatial Fuel Distribution," DOE Advanced Combustion Engine Working Group Meeting, Sandia, February 2007.

8. Steeper, R. R., "Improving the NO_X-CO_2 Trade-Off of an HCCI Engine Using a Multi-Hole Injector," SAE World Congress, Detroit, April 2007.

9. Steeper, R. R., "Sandia Automotive HCCI Engine Project," DOE Advanced Combustion Engine Program Review, Washington, D.C., June 2007.

10. Steeper, R. R., "Simultaneous PLIF Temperature/Composition Measurements in an HCCI Engine," DOE AEC Working Group Meeting, USCAR, Detroit, October 2, 2007.

11. Steeper, R. R., "Simulation of the Effect of Spatial Fuel Distribution Using a Linear-Eddy Model," SAE Powertrain and Fluid Systems Conference, Chicago, October 31, 2007.

II.A.10 Spark-Assisted HCCI Combustion

Robert M. Wagner (Primary Contact),
K. Dean Edwards, C. Stuart Daw
Oak Ridge National Laboratory (ORNL)
2360 Cherahala Boulevard
Knoxville, TN 37932

DOE Technology Development Manager:
Gurpreet Singh

ORNL Project Manager: Johney B. Green, Jr.

Objectives

- Improved understanding of dynamic combustion instability in spark-assisted homogeneous charge compression ignition (SI-HCCI) transition.
- Make use of engine-based, dynamic combustion measurements to quantify effective global kinetic rates.
- Develop simplified cyclic combustion models for rapid simulation, diagnostics, and controls.

Accomplishments

- Established Cooperative Research and Development Agreement (CRADA) with Delphi Automotive Systems on "Control Strategies for HCCI Mixed-Mode Combustion."
- Developed data-based method to estimate global kinetic parameters from combustion measurements and form the basis of a low-order dynamic model to be used for prediction and control.
- Developed Wiebe-based combustion metric to be used for feedback control as well as improving model estimates of global kinetic parameters.

Future Directions

- Baseline and map SI-HCCI regions of operation on a multi-cylinder engine located at Delphi Automotive Systems.
- Perform detailed kinetics simulations of SI-HCCI transition to improved physical understanding of multiple combustion modes and inter-mode switching. Simulations will be performed in-house as well as in collaboration with Lawrence Livermore National Laboratory.
- Improve low-order combustion model for use in the development of fast diagnostics and control strategies.

Introduction

An improvement in the fuel efficiency of gasoline engines is necessary to realize a significant reduction in U.S. energy usage. HCCI in internal combustion engines is of considerable interest because of the potential reductions in flame temperature and nitrogen oxide (NOx) emissions as well as potential fuel economy improvements resulting from un-throttled operation, faster heat release, and reduced heat transfer losses. Unfortunately for many transportation applications, HCCI may not be possible or practical under the full range of speed and load conditions. Thus, the most important technical developments needed to achieve wide-spread HCCI utilization are expansion of the operational range and the ability to switch between HCCI and traditional propagating flame (e.g., spark ignition, SI) combustion as power and speed change. Several recent publications and presentations have begun to address the control issues but have not focused on the fundamental nature of the transition dynamics associated with switching from SI to HCCI combustion. The development of both combustion-mode switching and stabilization technologies requires that the fundamental nature of the transition be well understood, especially in the context of realistic engine conditions.

Delphi Automotive Systems and ORNL have established a CRADA on the control of advanced mixed-mode combustion for gasoline engines. ORNL has extensive experience in the analysis, interpretation, and control of dynamic engine phenomena, and Delphi has extensive knowledge and experience in powertrain components and subsystems. The partnership of these knowledge bases is critical to overcoming the barriers associated with the realistic implementation of HCCI and enabling clean, efficient operation in the next generation of transportation engines.

Approach

Significant progress in expanding the usefulness of advanced combustion modes of operation in gasoline engines will require an improved understanding of the potential of control methods to stabilize the transition between SI and HCCI combustion modes as well as to stabilize intermediate hybrid (mixed-combustion) modes which exhibit characteristics and benefits of SI and HCCI combustion. This improved understanding will be used to develop control strategies for improved utilization of hybrid combustion modes as well as for the development of physical models which will be useful

for linking global combustion characteristics with fuel chemistry.

A single-cylinder research engine is being used for a fundamental investigation of SI-HCCI combustion dynamics. The engine used in this study is a 0.5-L single-cylinder AVL research engine with an 11.34:1 compression ratio. The engine has two intake valves and one exhaust valve and is equipped with a full-authority hydraulic variable valve actuation system. Only a single intake valve was used in this study to promote swirl and mixing. The transition from SI to HCCI is achieved in this engine with high levels of exhaust gas retained in the cylinder through manipulation of the intake and exhaust valve events. All experiments were performed at stoichiometric fueling conditions and a range of speeds and loads.

A multi-cylinder research engine is being developed by Delphi Automotive Systems for use in this activity and is expected to be complete in early FY 2008. Specific tasks for this agreement include:

- Development and baseline of engine/management systems. The research platform under development is a 2.2-L four-cylinder engine equipped with direct-injection fuel delivery, production-realistic flexible valve train components, and an advanced high-speed controller.
- Model and control algorithm development for improved understanding of physics governing mixed-mode operation and for real-time, multi-cylinder prediction and control.
- Conventional SI, mixed-mode, and HCCI steady-state experiments to explore the operational range and potential benefits of mixed-mode operation.
- HCCI and SI transient experiments which will include maneuvering within the HCCI envelope as well as mode switching between SI, mixed-mode, and HCCI operation.

Results

One of the most widely used methods for achieving the preheat conditions required to initiate HCCI is retention of high levels of exhaust gas in the cylinder from one cycle to the next through manipulation of the intake and exhaust valve events. While effective, this internal exhaust gas recirculation (EGR) creates a strong coupling between successive cycles, and small variations in the thermal and chemical composition of the retained exhaust gas can lead to large variations in the combustion process. Recent results from our research have shown that, due to this highly variable combustion, the SI-HCCI mode transition is very unstable, with high torque variations, high unburned hydrocarbon emissions, and potential engine stall. Figure 1 illustrates the trend in engine stability and engine-out NOx emissions as internal EGR is increased to transition from SI to HCCI. The results reported here focus on observations from the transition region where combustion instability is highest but NOx emission levels are near HCCI levels. This interest is motivated by the recognition that it may be possible to limit variability in the transition region by applying the appropriate type of feedback control. The potential benefits would be to smooth the SI-HCCI transition and extend the window of steady-state operation with HCCI-like NOx emission levels.

A conceptual model of the SI-HCCI transition and intermediate mixed-mode combustion events has been developed based on experimental observations. Spark ignition combustion is dominant for low levels of EGR. As EGR is increased further, the inlet fuel-air mixture is diluted with exhaust and the SI flame speed decreases. In the transition region, combustion typically begins when the spark creates a reaction front that expands and propagates through the premixed charge. Energy is transferred from the reaction front to the unburned mixture which, if conditions are right, results in an

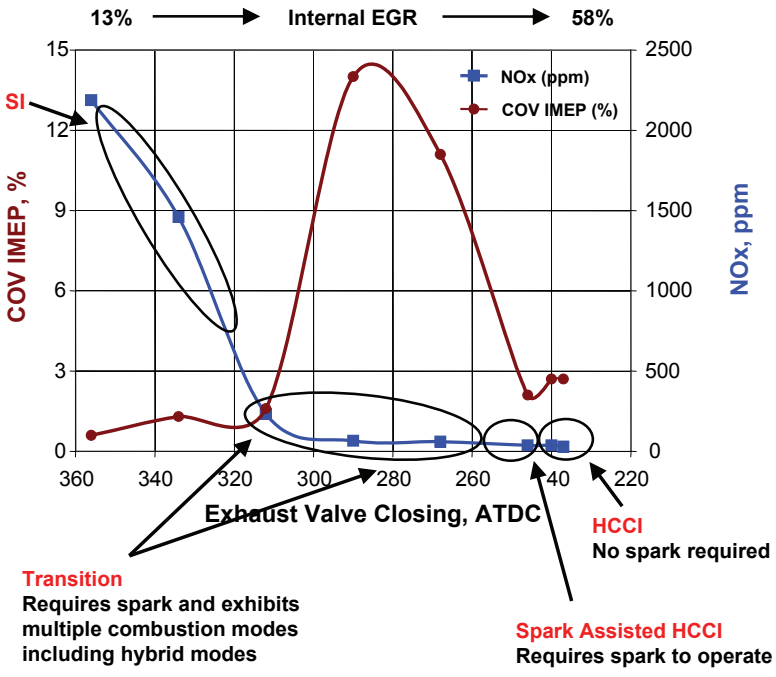

FIGURE 1. General combustion trends observed in the SI-HCCI transition experiments for 1,600 RPM, 3.4 BMEP. Internal EGR referenced in the figure was estimated using a full engine simulation code.

instantaneous, volumetric reaction over all (or some portion) of the remaining unburned charge. Thus, in the transition region, combustion occurs as a hybrid or mixed-mode event consisting of both propagating-flame and HCCI combustion during the same cycle (see Figure 2).

Analysis of experimental data indicates that the large combustion instabilities typical of the transition region arise from variations in the timing and relative strength of the secondary HCCI combustion process. These observations were used to develop a data-based combustion model for estimating global kinetic rate constants and ultimately a low-order empirical model of the combustion process. The global kinetic rate constants estimated from experimental data suggest that the HCCI combustion is actually switching between two different modes (or mechanisms) with different propensities to auto ignite. We hypothesize that the mode of combustion that occurs on a given cycle is determined by the presence or absence of sufficient concentration of partially oxidized fuel species that act as an enabler for HCCI combustion and accumulate in the cylinder through exhaust recirculation. As EGR is increased further, EGR heat becomes sufficient to stimulate HCCI, which preempts flame initiation (transition to HCCI is complete).

Characteristic post-top dead center (TDC) burn times (from estimates of global kinetic rate parameters) are shown in Figure 3 as a function of the unburned gas temperature at TDC. This figure clearly illustrates the distinct modes of HCCI combustion as was discussed previously. Of particular interest is the negative temperature effect (*i.e.*, where the burn rate decreases with increasing temperature) exhibited by both forms of HCCI. One of the observed HCCI modes appears to have a strong similarity to the predictions of fundamental kinetic mechanisms for HCCI such as the Pitsch mechanism for n-heptane shown in Figure 4. The similarity between the experimental results and the Pitsch mechanism suggests that at least part of the cycle-to-cycle combustion variations for our engine in the SI-HCCI transition involved n-heptane-like kinetics. Interestingly, we have not seen the level of negative temperature effect behavior observed in these experiments reported for indolene in other studies.

The experimental observations discussed above were used to develop a model of the hybrid combustion events, where combustion is divided into the initial propagating-flame event and the subsequent HCCI event. The strength and timing of the HCCI event is determined by the initial charge conditions and the amount of energy released during the initial reaction. An empirically derived switching rule is added to determine when combustion switches between the two modes. As shown in Figure 5, early attempts show promise in reproducing the dynamic behavior observed experimentally. The low-order model is able to predict the basic dynamic behavior observed in the experimental data and is expected to form a basis for future real-time control models and more detailed models for evaluating control algorithms.

A technique has also been developed that uses multiple Wiebe relations to estimate the timing and relative strengths of the two portions of the hybrid combustion event from experimental data. This

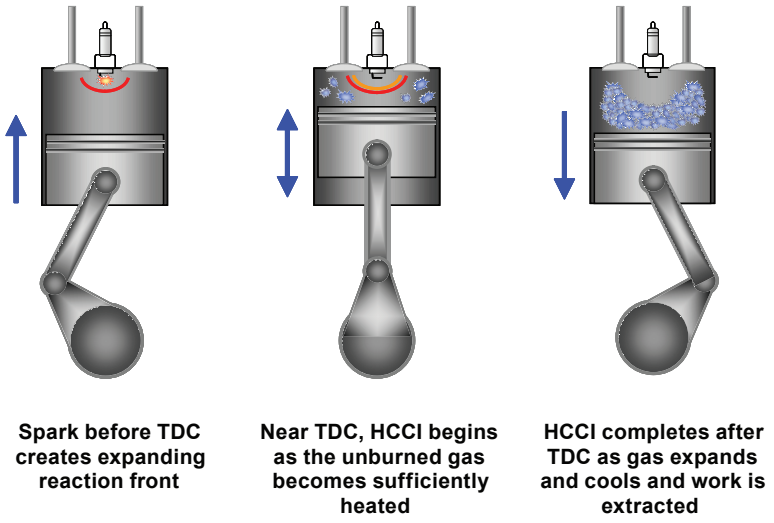

FIGURE 2. Illustration of the Possible Role of the Initial SI flame in SI-HCCI

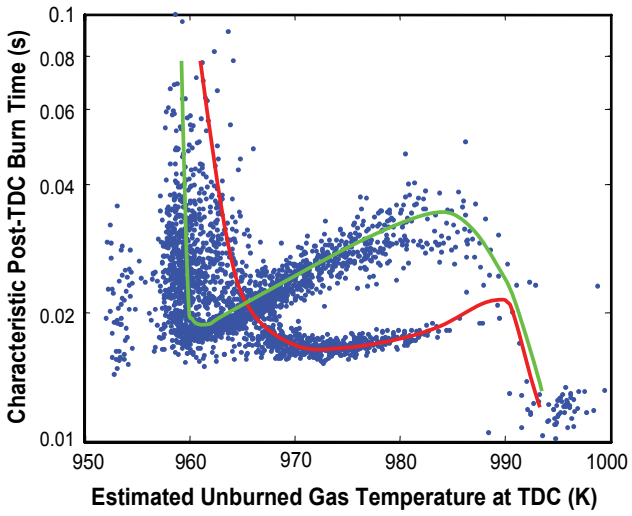

FIGURE 3. Characteristic Post-TDC Burn Time for SI-HCCI for $\phi = 1$ and EGR = 46%

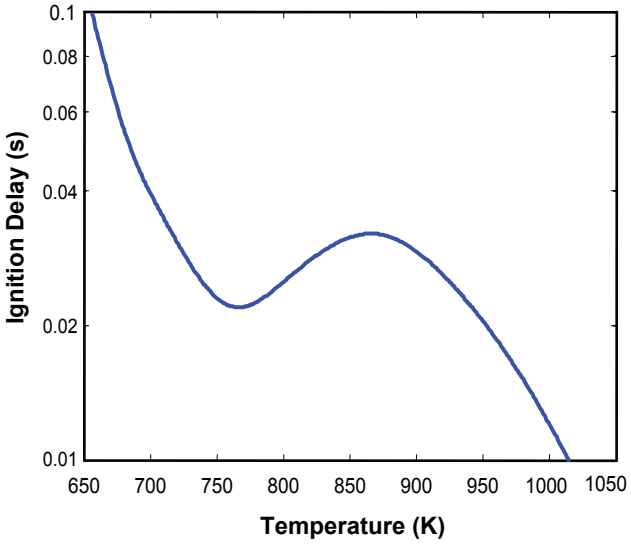

FIGURE 4. Ignition Delay for n-Heptane from Pitsch Mechanisms with $\phi = 0.4$, P = 8.2 atm, and intert/$O_2 = 5$

information will be useful in further refining our model and potentially as a combustion metric for feedback control. An example of the multiple-Wiebe analysis is shown in Figure 6. In this example, pure SI and pure HCCI combustion modes are best represented by a single Wiebe functions while the hybrid modes require two Wiebe functions for a reasonable fit. The selection of one or two Wiebe functions and correspondingly quality of the fit is based on a comparison of the sum of mean squared errors.

Conclusions

The results of this study indicate that global kinetic parameters may be estimated from sequential unstable cycle-resolved combustion measurements in the SI-HCCI transition. This information was then used to develop an empirical model capable of simulating the complex dynamics observed experimentally on a single-cylinder engine, providing new insight into the physics and chemistry of the transition dynamics. The next phase of this activity involves adapting these concepts to a multi-cylinder engine for the development and implementation of adaptive control strategies.

FY 2007 Publications/Presentations

1. R. M. Wagner, C. S. Daw, K. D. Edwards, J. B. Green Jr., "Global kinetics model for spark assisted HCCI," SAE HCCI Symposium 2007 (Lund, Sweden; September 2007). *Invited.*

2. K. D. Edwards, R. M. Wagner, C. S. Daw, J. B. Green Jr., "Ignition control for HCCI by spark augmentation and advanced controls", 2007 DOE National Laboratory Merit Review & Peer Evaluation (Washington, D.C.; June 2007).

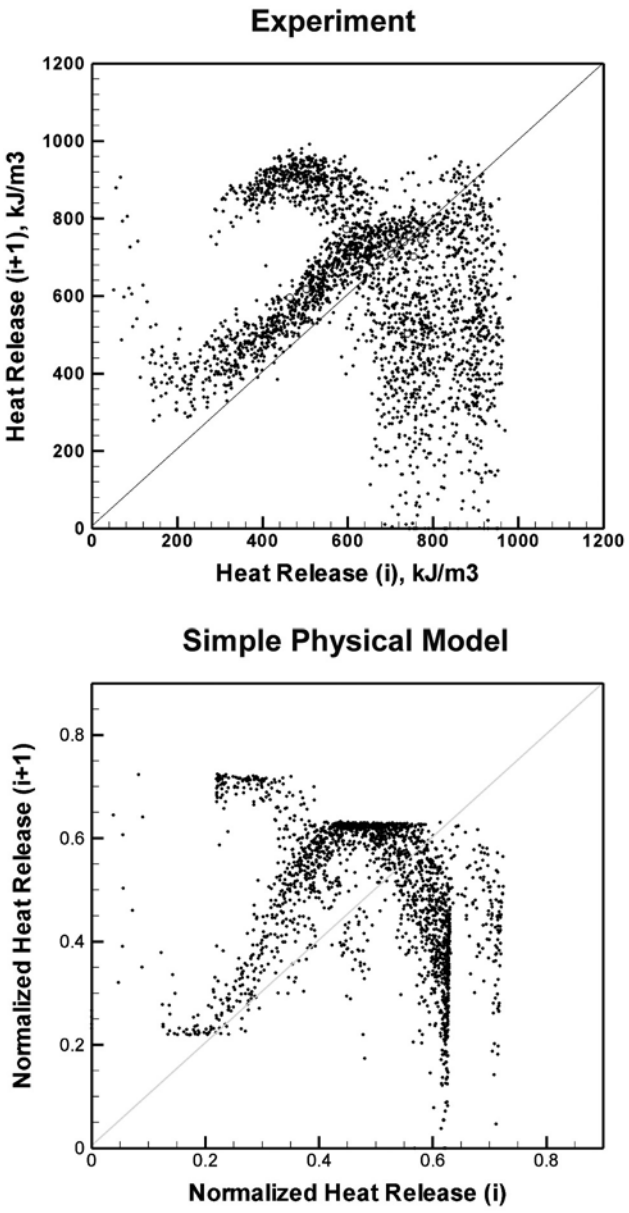

FIGURE 5. Comparison of Simple Physical Model and Experimental Observations of SI-HCCI

3. K. D. Edwards, R. M. Wagner, C. S. Daw, J. B. Green Jr., "Hybrid SI-HCCI combustion modes and the potential for control", Proceedings of the 5th U.S. National Combustion Meeting (San Diego, CA USA; March 2007).

4. C. S. Daw, K. D. Edwards, R. M. Wagner, J. B. Green Jr., "Modeling cyclic variability during the transition between SI combustion and HCCI", Proceedings of the 5th U.S. National Combustion Meeting (San Diego, CA USA; March 2007).

5. R. M. Wagner, K. D. Edwards, C. S. Daw, J. B. Green Jr., "Understanding the dynamic instability of the SI-HCCI transition and the potential for control", SAE HCCI Symposium (San Ramon, CA; September 2006). *Invited.*

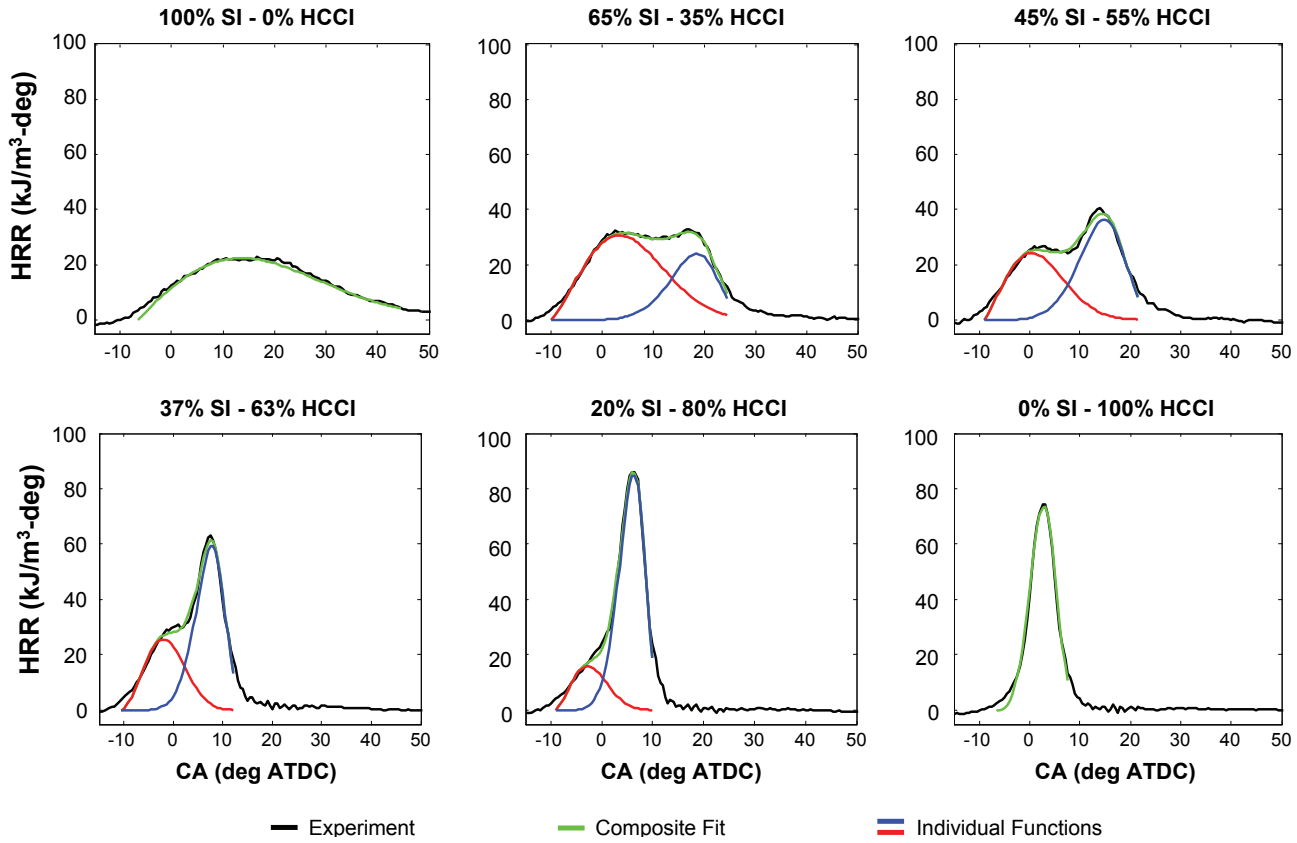

FIGURE 6. Examples of experimental heat release rate profiles and Wiebe function approximations for combustion cycles with various degrees of SI and HCCI as determined by a double Wiebe algorithm.

Special Recognitions & Awards/Patents Issued

1. "A method for diagnosing and controlling combustion instabilities in internal combustion engines operating in or transitioning to homogeneous charge compression ignition modes", IDEAS 05-156, patent pending.

2. Activity was recognized as a 2007 Science & Technology highlight for the Energy & Engineering Sciences directorate at ORNL.

II.A.11 KIVA-4 Development

David J. Torres
Los Alamos National Laboratory (LANL)
Theoretical Division, Group T-3, MS B216
Los Alamos, NM 87545

DOE Technology Development Manager:
Gurpreet Singh

Subcontractor:
Mario Trujillo
Applied Research Laboratory at Pennsylvania State University
State College, PA

Objectives

- Validate parallelization of KIVA-4 in realistic geometries
- Develop a parallel collocated version of KIVA-4
- Implement advanced combustion models in KIVA-4
- Develop converters to KIVA-4 from established mesh generation software
- Develop remapping capability in KIVA-4
- Reduce spray dependence on grid

Accomplishments

- The parallelization of KIVA-4 was tested in realistic geometries including 4-valve pentroof and 3-valve engine geometries.
- The collocated version of KIVA-4 was parallelized and run in parallel in a vertical valve engine geometry.
- The University of Wisconsin's chemistry and spray submodels were implemented in KIVA-4 and tested in a 2-D sector geometry.
- Reaction Design's chemistry package was interfaced with KIVA-4.
- Mesh converters to KIVA-4 format were developed for the TrueGrid and ICEM software programs.
- Remapping capability was demonstrated in a cylindrical tetrahedral mesh.
- Reduced spray dependence was achieved by using the grid overset method in KIVA-4.

Future Directions

- Continue validation of KIVA-4 in unstructured geometries and in parallel simulations of realistic engine geometries.
- Implement Lawrence Livermore's multi-zone combustion model [1] into KIVA-4.
- Develop the capability to perform turbulent calculations with the large eddy simulation (LES) turbulence model in KIVA-4.

Introduction

We have focused our efforts on parallelizing realistic geometries, developing a collocated version of KIVA-4, incorporating improved combustion and spray models, building interfaces with mesh generation software packages, developing remapping capability for KIVA-4 and reducing the spray dependence on the grid.

We previously had worked with relatively simple geometries in our parallel version of KIVA-4. In our recent work, we simulated two realistic engine geometries in parallel. These geometries include a 4-valve pentroof geometry and a 3-valve engine which has been studied experimentally by Dick Steeper at Sandia National Laboratory, Livermore.

We also developed a collocated version of KIVA-4 where the velocity is located at the cell-center along with the other field variables (pressure, temperature and density). This version is more appropriate for unstructured meshes that use a large percentage of tetrahedra or prisms. This version also has opened the door to more advanced meshes which include the grid overset technique in which two different meshes can be combined to model engine phenomena.

KIVA-4 inherited the combustion models of KIVA-3V which are Arrhenius type chemistry controlled combustion models. The University of Wisconsin Engine Research Center has had many years of experience with combustion models including mixing controlled models and ignition models which previous versions of KIVA-3V had not incorporated. We implemented the University of Wisconsin's combustion models into KIVA-4 to enhance the code and its applicability.

KIVA traditionally has accommodated large mesh movements with its snapper algorithm, where layers of cells become activated or deactivated during piston or valve movement. We have complemented KIVA's snapper routines with the capability of remapping fields to an entirely different mesh and continuing the engine simulation on the second mesh.

KIVA uses a grid generation program called K3PREP to construct its engine meshes. However, K3PREP can only generate structured meshes while KIVA-4 can accommodate unstructured meshes as well

as structured meshes. Mesh generation is a complex field in itself and we felt the best use of time would be spent developing interfaces from existing grid generation software. We have developed interfaces for ICEM (via its CHAD output format). Robert Rainsberger at TrueGrid developed a mesh output format for KIVA-4 with assistance from LANL. We have also run a simple mesh generated with the Cubit mesh generator with KIVA-4.

KIVA uses a set of Lagrangian particles that move through the computational mesh to model the liquid fuel spray. The computational mesh is used to model the gaseous phase. The Lagrangian particles experience a drag during their motion and momentum is transferred from the particles to the grid. The Lagrangian particles also collide and evaporate. Each of these processes is dependent on the resolution of the underlying grid. We have implemented the grid overset method in KIVA-4 which allows one to resolve the region around the spray without resolving the entire engine geometry, thus allowing one to calibrate sprays with a fine resolution.

Approach

We have focused our efforts on continued development of KIVA-4. Our approach is to develop KIVA-4 in areas that are most essential and will have the greatest impact. We believe that KIVA-4 would be adopted more readily and have more applicability if it could be complemented with a grid generator, could perform calculations of realistic geometries in parallel and could access advanced combustion and spray models.

Results

We present the results of parallel computations in a 4-valve engine shown in Figure 1. Table 1 shows the speed-up achieved with varying amounts of processors. One can see that four processors are being used effectively. Beyond four processors, the speed-up diminishes. The parallel performance tends to plateau for two reasons. First, the grid is relatively small using 38,392 cells. For comparison, we have achieved a speed-up of 10.21 in a cylinder with 430,000 cells with 14 processors in KIVA-4. Second, the mesh partitioning could be improved considering the fact that cells become deactivated when the piston moves up. Partitioning refers to how the mesh is subdivided among processors (or equivalently the way the computational load is divided among processors). We have implemented a means of repartitioning a mesh during the course of a simulation, thus providing a means of improving the parallel performance with larger amounts of processors. Figure 2 shows the 3-valve engine run in parallel. We were able to achieve a speed-up of 1.71 with 2 processors and 2.62 with 4 processors. In the 3-valve engine parallel computation, entire ports become deactivated during the course of the simulation which makes an effective single partitioning even more difficult.

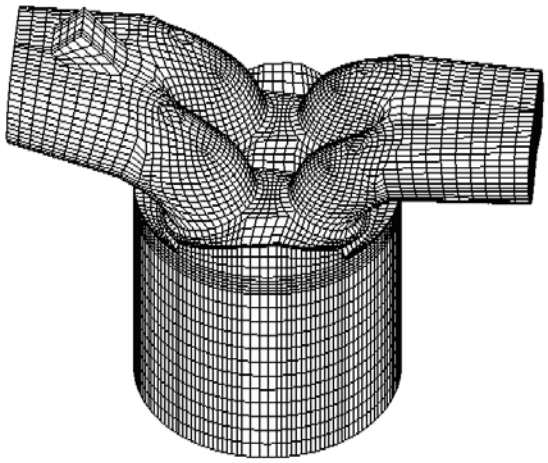

FIGURE 1. 4-Valve Pentroof Geometry Simulated in Parallel with KIVA-4

TABLE 1. Parallel Speed-Up with 4-Valve Engine

Number of Processors	Time (hours)	Speed-up
1	9.6	1.0
2	5.24	1.83
4	3.0	3.2
8	2.76	3.48
16	2.36	4.1

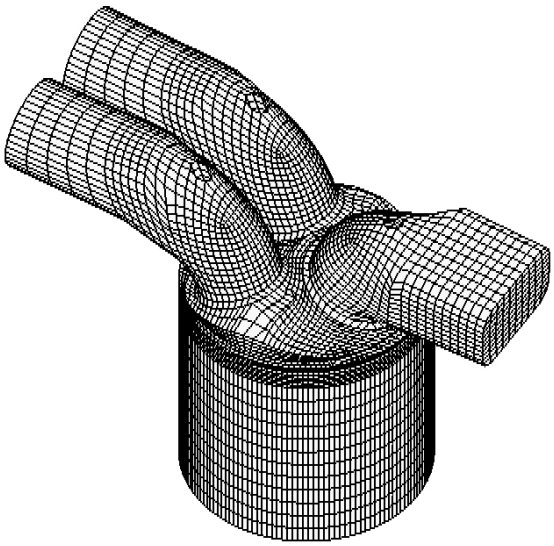

FIGURE 2. 3-Valve Geometry Run in Parallel with KIVA-4

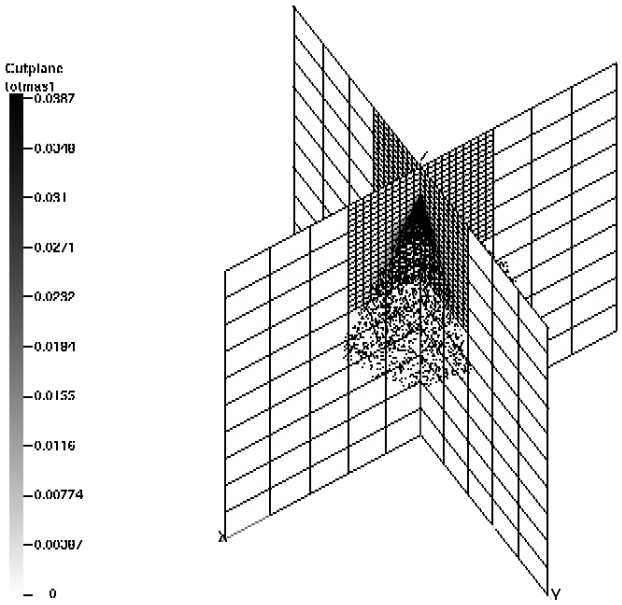

FIGURE 3. Use of Grid Overset Method to Resolve Spray

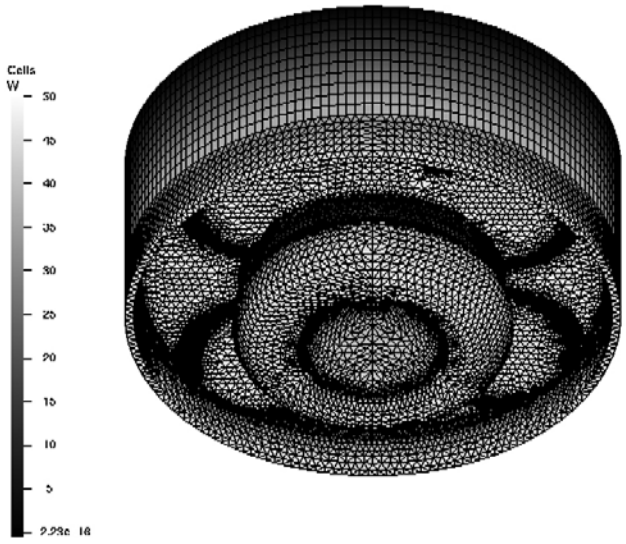

FIGURE 4. Vertical Velocity in Tetrahedral and Prism Mesh

Our repartitioning algorithm should prove effective in improving the 3-valve parallel efficiency.

Figure 3 shows a computation in a cylinder with the overset grid method where two grids are simultaneously used – one specifically for the spray and another for the engine geometry. Finer resolutions will improve the accuracy of the spray dynamics up to a point. We also hope to incorporate the collision improvements of Abani, et al. (2006) in the future to further decouple the spray dynamics from the underlying grid.

Figure 4 shows a mesh with tetrahedra and prisms that was simulated with KIVA-4. This mesh was created by Valmor de Almeida at Oak Ridge National Laboratory. We expect to use this strategy of using tetrahedra in the bowl and head region and prisms in the squish region for future simulations of engine meshes.

Conclusions

KIVA-4 has simulated realistic geometries in parallel. Advanced combustion models have been tested in KIVA-4. Grid converters have been developed to convert meshes to KIVA-4 format. Restart capability has been developed to remap fields from one mesh to another mesh and continue the KIVA-4 simulation on the second mesh. The grid overset method has been developed in KIVA-4 to reduce the dependence of the spray on the grid.

We would also like to acknowledge the help and suggestions of Qingluan Xue, Yuanhong Li and Song-Charng Kong of Iowa State University, Zheng Xu at Ford Motor Corporation and Valmor de Almeida at Oak Ridge National Laboratory.

References

1. A. Babajimopoulos, D.N. Assanis, D.L. Flowers, S.M. Aceves and R.P. Hessel, A Fully Coupled Computational Fluid Dynamics and Multi-zone Model with Detailed Chemical Kinetics for the Simulation of Premixed Charge Compression Ignition Engines, International Journal of Engine Research, 2005.

2. N. Abani, A. Munnannur and R. Reitz, Reduction of Numerical Parameter Dependencies in Diesel Spray Models, ILASS Americas, 19th Annual Conference of Liquid Atomization and Spray Systems, 2006.

FY 2007 Publications

1. D. J. Torres, Collocated KIVA-4, International Multidimensional Engine Modeling User's Group Meeting Proceedings at SAE Congress, April 2007.

2. Q. Xue, S.C. Kong, D.J. Torres, Z. Xu and J. Yi, DISI Spray Modeling using Local Mesh Refinement, submitted to Society of Automotive Engineers.

3. M. Fife, P. Miles, M. Bergin, R. Reitz and D.J. Torres, The Impact of a Non-Linear Turbulent Stress Relationship on Simulations of Flow and Combustion in an HSDI Diesel Engine, submitted to Society of Automotive Engineers.

FY 2007 Presentations

1. D. J. Torres, "KIVA-4 Development", Advanced Engine Combustion Working Group Meeting, Detroit, October 2007.

2. D. J. Torres, "KIVA Modeling to Support Diesel Combustion Research", DOE National Laboratory Advanced Combustion Engine R&D, Merit Review, Washington, D.C., June 2007.

3. D.J. Torres, "Collocated KIVA-4", International Multidimensional Engine Modeling User's Group Meeting, April 2007.

4. D.J. Torres, "KIVA-4 Development", Advanced Engine Combustion Working Group Meeting, Livermore, February 2007.

II.A.12 Chemical Kinetic Modeling of Combustion of Automotive Fuels

William J. Pitz (Primary Contact),
Charles K. Westbrook, Olivier Herbinet,
Emma J. Silke
Lawrence Livermore National Laboratory (LLNL)
P. O. Box 808, L-372
Livermore, CA 94551

DOE Technology Development Managers:
Gurpreet Singh and Kevin Stork

Objectives

- Develop detailed chemical kinetic reaction models for fuel components used in surrogate fuel models for diesel and homogeneous charge compression ignition (HCCI) engines.
- Develop surrogate fuel models to represent real fuels and model low temperature combustion strategies in HCCI and diesel engines that lead to low emissions and high efficiency.
- Characterize the role of fuel composition on low-temperature combustion modes of advanced engine combustion.

Accomplishments

- Developed a chemical kinetic model for n-hexadecane, a primary reference fuel for diesel fuel, and a realistic representation of n-alkanes in diesel fuels.
- Developed understanding of the chemical kinetics that control HCCI combustion under boosted conditions using LLNL surrogate fuel models and Sandia HCCI engine data.
- Developed a chemical kinetic model for methyl decanoate, a realistic component to represent methyl esters contained in biodiesel.

Future Directions

- Extend model capabilities to additional new classes of fuel components, including hepta-methyl-nonane which is a primary reference fuel for diesel fuel and represents iso-alkanes in diesel fuel.
- Further validate chemical kinetic model for n-hexadecane.
- Continue development of increasingly complex surrogate fuel mixtures to represent fuels for HCCI and diesel engines.
- Increase collaborations with programs outside LLNL dealing with automotive and heavy-duty truck fuel issues.

Introduction

Automotive hydrocarbon fuels consist of complex mixtures of hundreds or even thousands of different components. These components can be grouped into a number of structurally distinct classes, consisting of n-paraffins, branched paraffins, cyclic and branched cyclic paraffins, olefins, oxygenates, and aromatics. The fractional amounts of these mixtures are quite different in gasoline, diesel fuel and oil-sand derived fuels, which contributes to the very different combustion characteristics of each of these in different combustion systems.

To support large-scale computer simulations of each kind of engine, it is necessary to provide reliable chemical kinetic models for each of these fuel classes. However, few specific hydrocarbon components of some of these fuel classes have been modeled. For example, models for benzene and toluene have been developed, although models for few if any larger aromatic compounds such as naphthalene or styrene currently exist. Similarly, detailed models for small iso-paraffins such as iso-octane have been developed, but detailed models do not yet exist for the much larger versions such as heptamethylnonane, characteristic of diesel fuels. Current approaches to this problem are to construct a detailed model, containing one or more representatives of each class of components to serve as a surrogate mixture. In order for such a surrogate mixture model to be useful, each component must have a well-tested detailed kinetic model that can be included. This high-level approach can create realistic substitutes for gasoline or diesel fuel that reproduce experimental behavior of the practical real fuels, but these substitutes, or surrogates, will also then be reproducible in both experiments and modeling studies. Detailed kinetic models for groups of fuels can then be simplified as needed for inclusion in multidimensional computational fluid dynamic (CFD) models or used in full detail for purely kinetic modeling.

Approach

Chemical kinetic modeling has been developed uniquely at LLNL to investigate combustion of hydrocarbon fuels in practical combustion systems such as diesel and HCCI engines. The basic approach is to

integrate chemical rate equations for chemical systems of interest, within boundary conditions related to the specific system of importance. This approach has been used extensively for diesel and HCCI engine combustion, providing better understanding of low temperature combustion strategies, ignition, soot production, and NOx emissions from these engines in fundamental chemical terms.

The underlying concept for diesel engines is that ignition takes place at very fuel-rich conditions, producing a mixture of chemical species concentrations that are high in those species such as acetylene, ethene, propene and others which are well known to lead to soot production. Some changes in combustion conditions reduce the post-ignition levels of these soot precursors and reduce soot production, while other changes lead to increased soot emissions. The LLNL program computes this rich ignition using kinetic modeling, leading to predictions of the effect such changes might have on soot production and emissions.

Ignition under HCCI engine conditions is closely related to that in diesel engines, since both are initiated by compression ignition of the fuel/air mixtures. In very fuel-lean HCCI ignition, the premixing of fuel and air in the gaseous state results in no soot and extremely low NOx production. Kinetic modeling has proven to be exceedingly valuable in predicting not only the time of ignition in HCCI engines, but also the duration of burn and the emissions of unburned hydrocarbons, CO, NOx and soot.

Results

During the last year we completed chemical mechanisms for important components to include in surrogate models for diesel and bio-derived fuels. These components are n-hexadecane and methyl-decanoate (Figure 1). First, an n-hexadecane mechanism was developed to represent n-alkanes in diesel fuel. n-Hexadecane is a primary reference fuel for diesel fuel and is an important component to include in a diesel surrogate fuel model as recommended by the diesel research community [1]. Assembling a mechanism for n-hexadecane is very ambitious since it requires the inclusion of thousands of chemical species and reactions. The thermodynamic properties of each species and the rate constant of each reaction must be estimated. These estimations are performed by group additivity for the thermodynamic parameters and by established rules for the reaction rates [2]. The reaction mechanism addresses low temperature chemistry that is essential for simulation of low-temperature combustion in diesel engines. Low-temperature combustion strategies can lead to low soot and NOx emissions in diesel engines. The mechanism includes the reactions to address the oxidation and pyrolysis of n-alkanes from n-propane to n-hexadecane. It is built in a modular fashion so that users can easily pare down the mechanism from the full mechanism of 2,116 species and 8,130 reactions for n-hexadecane to a smaller mechanism of 940 species and 3,878 reactions for n-decane. Comparisons of computed results for n-decane and experimental data are shown in Figures 2 and 3. Figure 2 shows ignition delay times for n-decane and n-heptane from the chemical kinetics model and measured in a shock tube. The initial conditions for the ignition delay times are stoichiometric fuel/air mixtures, 13.5 bar and 670 K-1,350 K, conditions that are highly relevant to diesel and HCCI engines. The n-decane and n-heptane chemical kinetic models are able to reproduce the measured behavior over the entire temperature range including the critical region (700-800 K) important for low-temperature combustion. In Figure 3, results of the model are compared to measurements in a jet-stirred reactor [3]. These experiments were performed for stoichiometric mixtures of n-decane in O_2/N_2 at 10 atm and 750-1,100 K which are also conditions that are highly relevant to those in diesel and HCCI engines. The n-decane chemical kinetic model performed quite well, mimicking the experimental behavior for

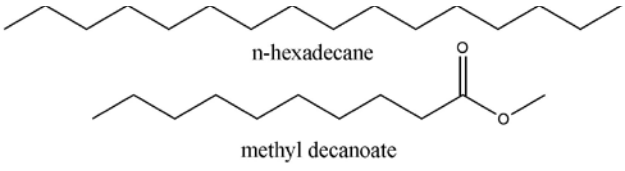

FIGURE 1. Molecular Structure of n-Hexadecane and Methyl-Decanoate

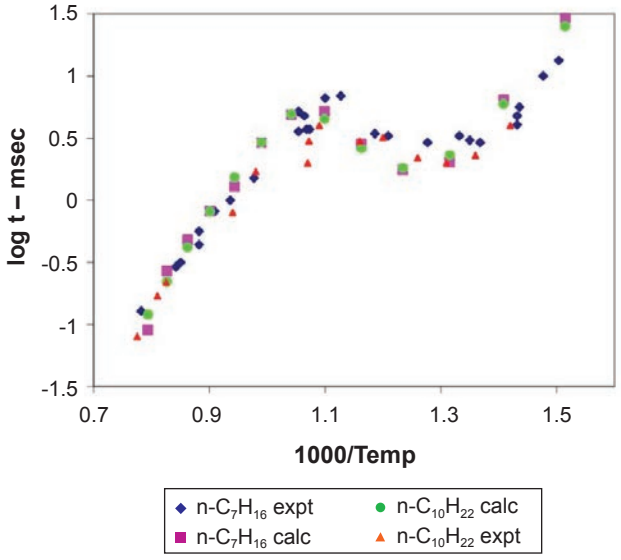

FIGURE 2. Shock tube ignition delay times for n-heptane and n-decane, all at 13.5 bar pressure and stoichiometric fuel/air. Experiments are from Ciezki and Adomeit [9] and Pfahl et al. [10]. n-Heptane computed results from ref [2].

the intermediate species concentrations as a function of reactor temperature. These results show that the evolution of species as the reaction proceeds from fuel/O_2/N_2 to products is being properly reproduced by the model at engine-like conditions. This chemical kinetic model is now available to the DOE supported Advanced Engine Combustion and HCCI University Working Groups for use in modeling engine combustion.

The second new fuel that was added as a surrogate fuel model was methyl decanoate (Figure 1). It is a large molecular weight methyl ester species to represent biodiesel fuel. Again, mapping out the reaction paths, estimating the thermodynamic properties for the needed species, and estimating the reaction rates was a very ambitious project. The thermodynamic property of each species needs to be estimated by group additivity and the reaction rate constants acquired from reaction rate rules. The reaction mechanism consists of 3,034 species and 8,580 reactions. The chemical kinetic model was validated by comparison to high pressure experiments in a jet stirred reactor at 800-1,040 K and 10 atm (Figure 4). These conditions are relevant to diesel and HCCI engine conditions. The agreement between the biodiesel surrogate (methyl decanoate) and the rapeseed derived methyl esters is very good. The biodiesel surrogate correctly simulates the early formation of CO_2 that is observed in the oxidation of esters. This early formation of CO_2 "wastes" some of the oxygen in the fuel that would otherwise help to reduce soot under diesel conditions [4]. Next the methyldecanoate model was used to simulate experiments in a single-cylinder engine [5] (Figure 5). The model was able to simulate the early formation of CO_2 in the engine and the evolution of intermediate products (CO and aldehydes). This chemical kinetic model represents a new capability to model biodiesel combustion in engines.

Finally, we investigated the behavior of an HCCI engine with increasing boost pressure and its effect on combustion phasing. Increasing the boost pressure is an important way to increase the load range for a HCCI engine. As boost pressure is increased and the intake temperature decreased, the combustion phasing is uniquely affected due to the onset of low temperature chemistry [6,7]. For reactive fuels such as gasoline, PRF80, and methylcyclohexane, the intake temperature must be reduced significantly to maintain combustion phasing at top dead center (TDC) as the intake pressure is increased [6]. This is due to the increased reactivity from the onset of low temperature chemistry at high intake pressure and low intake temperature.

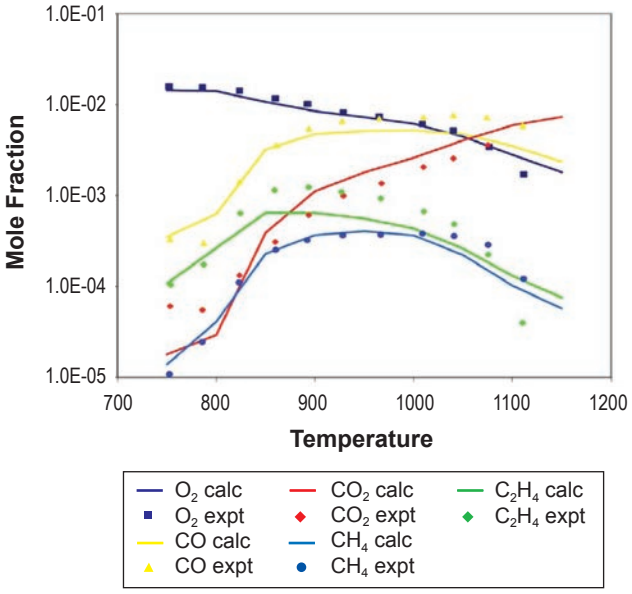

FIGURE 3. Chemical species concentrations in a jet stirred reactor for stoichiometric n-decane/O_2/N_2 mixtures at 10 atm and a residence time of 0.5 sec. n-Decane inlet mole fraction is 1,000 PPM. Lines represent computed values, symbols are experimental results [3].

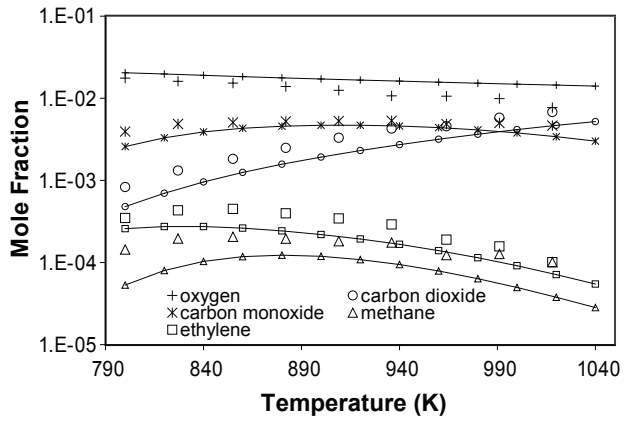

FIGURE 4. Comparison of the methyl decanoate model with rapeseed oil methyl ester experiments in a jet stirred reactor (P = 10 atm, equivalence ratio = 0.5, residence time = 1 s) [11].

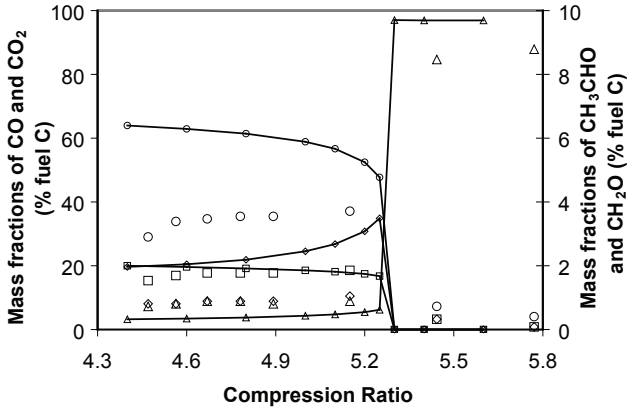

FIGURE 5. Comparison of methyl decanoate simulations in a CFR engine with experiments. Mass fractions of CO (◊), CO_2 (Δ), CH_2O (O) and CH_3CHO (□) at an equivalence ratio of 0.25. Open symbols correspond to experiments [5] and lines to simulations.

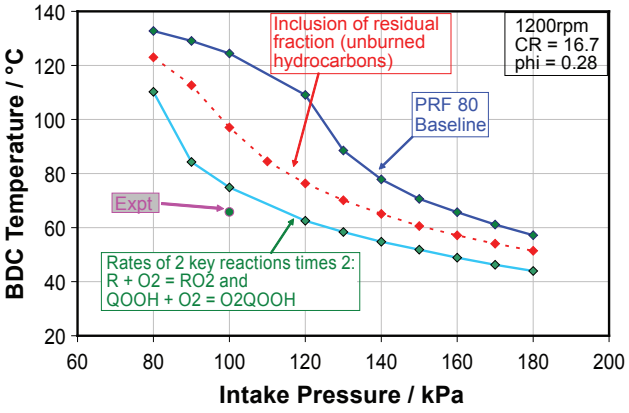

FIGURE 6. Bottom-dead-center (BDC) temperature required to maintain top-dead-center phasing in an HCCI engine. The model used is the LLNL primary reference fuel (PRF) model for gasoline. The fuel is PRF80 and the equivalence ratio is 0.28. The blue curve is for the baseline simulation. The red curve is when residuals left over from the previous cycle are included. The turquoise curve is when the rate constants of two key reaction rates are increased. The pink point is an experimental point take in an HCCI engine at Sandia National Laboratories [8].

In our recently submitted paper [7], we tested the ability of LLNL chemical kinetics models for gasoline, cyclohexane and PRF80 to simulate this behavior with increased boost pressure. We found that the inclusion of residual fractions from the previous cycle was critically important in these calculations because it sensitizes the next cycle so that reaction begins at an earlier time. We also found that the behavior was highly sensitive to two key reactions that lead to low temperature reactions,

$$R + O_2 = RO_2$$

$$QOOH + O_2 = O_2QOOH$$

(where R is a fuel molecule with one H atom removed and Q is a hydrocarbon structure representing the fuel with two H-atoms removed). Figure 6 shows the bottom dead center (BDC) temperature required to maintain TDC combustion phasing as the intake pressure is increased. The figure shows a baseline calculation with the LLNL chemical kinetic model for PRF80 and then the effect of including residual fraction in these calculations. The one experimental point available from Sjöberg and Dec's HCCI engine at Sandia [8] is also shown. The inclusion of residual fraction results in a better comparison to the experiment. Additionally, increasing the rate constants of the key reactions above improves the agreement with experiment and shows the importance of these reactions in controlling HCCI behavior with increased boost pressure.

Conclusions

Kinetic modeling provides a unique tool to analyze combustion properties of diesel, HCCI and spark-ignition engines. A kinetic model can be very cost-effective as an alternative to extended experimental analyses and as guidance for more efficient experimentation, and computations can also provide a fundamental explanation of the reasons for the observed results. LLNL kinetic models are providing this valuable capability for engine research at many university and industrial facilities in the United States and are an essential tool in engine research.

References

1. J. T. Farrell, N. P. Cernansky, F. L. Dryer, D. G. Friend, C. A. Hergart, C. K. Law, R. McDavid, C. J. Mueller and H. Pitsch, Development of an experimental database and kinetic models for surrogate diesel fuels, *SAE Paper 2007-01-0201, 2007 SAE World Congress*, Detroit, MI, 2007.

2. H. J. Curran, P. Gaffuri, W. J. Pitz and C. K. Westbrook, *Combust. Flame* 114 (1-2) (1998) 149-177.

3. P. Dagaut, *Physical Chemistry Chemical Physics* 4 (11) (2002) 2079-2094.

4. C. J. Mueller, W. J. Pitz, L. M. Pickett, G. C. Martin, D. L. Siebers and C. K. Westbrook, *Effects of Oxygenates on Soot Processes in DI Diesel Engines: Experiments and Numerical Simulations*, SAE 2003-01-1791, 2003 Arch T. Colwell Merit Award Paper, (2003).

5. J. P. Szybist, A. L. Boehman, D. C. Haworth and H. Koga, *Combust. Flame* 149 (1-2) (2007) 112-128.

6. C. V. Naik, P. W.J., M. Sjöberg, D. J.E., C. Orme J., H.J., S. J.M. and C. K. Westbrook, Detailed Chemical Kinetic Modeling of Surrogate Fuels for Gasoline and Application to an HCCI Engine, *2005 Joint Meeting of the U.S. Sections of The Combustion Institute*, 2005.

7. E. J. Silke, W. J. Pitz, C. K. Westbrook, M. Sjöberg and J. E. Dec, Understanding the Chemical Effects of Increased Boost Pressure under HCCI Conditions, *2008 SAE World Congress*, Detroit, MI, submitted, 2008.

8. M. Sjöberg and J. E. Dec, *Combined Effects of Fuel-type and Engine Speed on Intake Temperature Requirements and Completeness of Bulk-gas Reactions for HCCI Combustion*, SAE Paper 2003-01-3173, (2003).

9. H. K. Ciezki and G. Admeit, *Combust. Flame* 93 (1993) 421-433.

10. U. Pfahl, K. Fieweger and G. Adomeit, *Proc. Combust. Inst.* 26 (1996) 781-789.

11. P. Dagaut, S. Gaïl and M. Sahasrabudhe, *Proc. Combust. Inst.* 31 (2) (2007) 2955-2961.

FY 2007 Publications

1. Westbrook, C. K., Pitz, W. J., Herbinet, O., Silke, E. J. and Curran, H. J., "A Detailed Chemical Kinetic Reaction Mechanism for n-Alkane Hydrocarbons from n-Octane to n-Hexadecane," Fall Meeting Western States Section of the Combustion Institute, Livermore, CA, 2007.

2. Silke, E. J., Pitz, W. J. Westbrook, C. K., Sjöberg, M., Dec, J. E., "Understanding the Chemical Effects of Increased Boost Pressure under HCCI Conditions", 2008 SAE World Congress, Detroit, MI, submitted, 2007.

3. Herbinet, O., Pitz, W. J. and Westbrook, C. K., "Detailed Chemical Kinetic Oxidation Mechanism for a Biodiesel Surrogate," Fall Meeting of the Western States Section of the Combustion Institute, Livermore, CA, 2007.

4. Herbinet, O., Pitz, W. J. and Westbrook, C. K., "Detailed Chemical Kinetic Oxidation Mechanism for a Biodiesel Surrogate," Combustion and Flame (2007), submitted.

5. Pitz, W. J., Cernansky, N. P., Dryer, F. L., Egolfopoulos, F. N., Farrell, J. T., Friend, D. G., and Pitsch, H., "Development of an Experimental Database and Chemical Kinetic Models for Surrogate Gasoline Fuels", 2007 SAE World Congress, Detroit, MI.

6. Silke, E. J., Pitz, W. J., Westbrook, C. K. and Ribaucour, M. "Detailed Chemical Kinetic Modeling of Cyclohexane Oxidation", Journal of Physical Chemistry A, 111 (19) 3761 -3775, 2007.

7. C. K. Westbrook, W. J. Pitz and H. J. Curran, in:H. Zhao, (Eds), HCCI and CAI Engines for the Automotive Industry, Woodhead Publishing, Cambridge, UK, 2007.

8. R. P. Hessel, D. E. Foster, S. M. Aceves, M. L. Davisson, F. Espinosa-Loza, D. L. Flowers, W. J. Pitz, J. E. Dec, M. Sjöberg and A. Babajimopoulos, "Modeling Iso-octane HCCI using CFD with Multi-Zone Detailed Chemistry; Comparison to Detailed Speciation Data over a Range of Lean Equivalence Ratios", 2008 SAE World Congress, Detroit, MI, 2008, submitted.

9. Hessel, R., Foster, D., Aceves, S., Flowers, D., Pitz, B., Dec, J., Sjöberg, M. and Babajimopoulos, A., "Modeling HCCI Using CFD and Detailed Chemistry with Experimental Validation and a Focus on CO Emissions," 2007 International Multidimensional Engine Modeling User's Group Meeting, 2007.

10. Sakai, Y., Ozawa, H., Ogura, T., Miyoshi, A., Koshi, M. and Pitz, W. J., "Effects of Toluene Addition to the Primary Reference Fuel at High Temperature," SAE Commercial Vehicle Engineering Congress & Exhibition, Chicago, IL, 2007.

11. Sakai, Y., Inamura, T., Ogura, T., Koshi, M. and Pitz, W. J., "Detailed Kinetic Modeling of Toluene Combustion over a Wide Range of Temperature and Pressure," 2007 JSAE/SAE International Fuels and Lubricants Meeting, Kyoto TERRSA, Japan, 2007, SAE paper 2007-01-1885.

12. W. J. Pitz, C. V. Naik, T. Ní Mhaoldúin, C. K. Westbrook, H. J. Curran, J. P. Orme, and J. M. Simmie, "Modeling and Experimental Investigation of Methylcyclohexane Ignition in a Rapid Compression Machine", Proceedings of the Combustion Institute, Volume 31, 2007.

13. Metcalfe, W. K., Pitz, W. J., Curran, H. J., Simmie, J. M., and Westbrook, C. K. "The Development of a Detailed Chemical Kinetic Mechanism for Diisobutylene and Comparison to Shock Tube Ignition Times", Proceedings of the Combustion Institute, Volume 31, 2007.

14. Saylam, A., Ribaucour, M., Pitz, W. J., and Minetti, R., "Reduction of Large Detailed Chemical Kinetic Mechanisms for Autoignition Using Joint Analyses of Reaction Rates and Sensitivities", International Journal of Chemical Kinetics, 2007.

FY 2007 Presentations

1. Westbrook, C. K., Pitz, W. J., Herbinet, O., Silke, E. J. and Curran, H. J., "A Detailed Chemical Kinetic Reaction Mechanism for n-Alkane Hydrocarbons from n-Octane to n-Hexadecane," Fall Meeting Western States Section of the Combustion Institute, Livermore, CA, 2007.

2. Herbinet, O., Pitz, W. J. and Westbrook, C. K., "Detailed Chemical Kinetic Oxidation Mechanism for a Biodiesel Surrogate," Fall Meeting of the Western States Section of the Combustion Institute, Livermore, CA, 2007.

3. C. K. Westbrook, W. J. Pitz, O. Herbinet, and E. Silke, "Chemical Kinetics Modeling of Large n-Alkanes up to n-Hexadecane", Advanced Engine Combustion Working Group Meeting, Southfield, MI, October, 2007.

4. O. Herbinet, "Chemical Kinetics Modeling of a Biodiesel Surrogate", Advanced Engine Combustion Working Group Meeting, Southfield, MI, October, 2007.

5. W. J. Pitz, et al. "Development of an Experimental Database and Chemical Kinetic Models for Surrogate Gasoline Fuels", 2007 World Congress, Society of Automotive Engineers, Detroit, MI, April, 2007.

6. W. J. Pitz, "Development and Application of Chemical Kinetic Models for HCCI/Diesel Engines", Advanced Engine Combustion Working Group Meeting, Sandia, Livermore, February, 2007.

7. E. Silke, W. J. Pitz, C. K. Westbrook, M. Ribaucour, "Detailed chemical kinetic modeling of cyclohexane oxidation", 5th U.S. Combustion Meeting, San Diego, March, 2007.

8. E. J. Silke, J. Würmel, M.S. O'Conaire, J.M. Simmie, H.J. Curran, "The effect of diluent gases in the shock tube and rapid compression machine", 5th U.S. Combustion Meeting, San Diego, March, 2007.

9. W. J. Pitz, "Developing Chemistry Models for 21st Century Fuels", Department of Mechanical Engineering Seminar Series, University of Iowa, Iowa City, IA, October, 2006.

II.A.13 Achieving and Demonstrating FreedomCAR Engine Efficiency Goals

Robert M. Wagner (Primary Contact),
K. Dean Edwards, Thomas E. Briggs, Jr.
Oak Ridge National Laboratory (ORNL)
2360 Cherahala Boulevard
Knoxville, TN 37932

DOE Technology Development Manager:
Gurpreet Singh

Objectives

- Achieve and demonstrate peak brake thermal efficiency (BTE) of 42% in FY 2007 and 45% in FY 2010 with associated emissions levels as specified in the Office of FreedomCAR Research and Development Plan.
- Provide valuable insight into the development, implementation, and demonstration of technologies for improved BTE.

Accomplishments

- Achieved and demonstrated 2007 FreedomCAR goal of 42% peak BTE on two light-duty diesel engines.
- Completed installation of modern engine platform donated to ORNL by General Motors (GM).
- Developed thermodynamic analysis methods for use with engine simulation codes as well as experimental data to evaluate potential opportunities for waste heat recovery (WHR).
- Demonstrated potential of advanced combustion operation for achieving Tier 2 Bin 5 emissions regulations.
- Improved interactions with other national laboratories, universities, and industry through the Advanced Engine Combustion (AEC) working group, Cross-Cut Lean Exhaust Emissions Reduction Simulations (CLEERS) working group, and other forums.

Future Directions

- Characterize thermodynamic availability of engine system components (*e.g.*, exhaust gas recirculation [EGR] system, exhaust system, etc.) over the speed-load range of the engine.
- Evaluate potential efficiency benefits of bottoming cycle for WHR from the EGR system, exhaust system, etc.
- Investigate low-temperature combustion (LTC) approaches on the GM 1.9-L engine for reducing aftertreatment needs and improving overall system efficiency.
- Develop model of the GM 1.9-L and auxiliary systems for evaluating potential efficiency benefits of advanced technologies including variable valve actuation.

Introduction

Modern light-duty diesel engines have peak BTEs in the range 38-40% for high-load operation and considerably lower efficiencies for part-load operation. The FreedomCAR roadmap has established several goals over the next several years with a 45% peak efficiency being demonstrated in 2010, while meeting the Tier 2, Bin 5 emissions levels. The objective of this project is not to develop all the necessary technology to meet the efficiency and emissions goals but to serve as a focus for the integration of technologies into a multi-cylinder engine platform and to provide a means of identifying pathways for improved engine efficiency.

Approach

This activity makes use of knowledge discovery from internal ORNL activities, other national laboratories, universities, and industry. Internal activities include those focused on advanced combustion operation, aftertreatment, fuels, and novel or unconventional approaches to stretch efficiency. Significant external contributions occur through regular interactions with the AEC working group administered by Sandia National Laboratories and the CLEERS working group administered by ORNL.

Significant improvements in efficiency require new insight into understanding loss mechanisms as well as identifying efficiency opportunities. A Second Law of Thermodynamics perspective is being used toward this purpose and to provide guidance on developing and evaluating a path for meeting 2010 as well as intermediate milestones.

The following methodology will be used in this activity:

1. Establish baseline for modern light-duty diesel engine.
2. Acquire and/or develop models to characterize loss mechanisms.
3. Conceive methods to mitigate losses.

4. Evaluate methods (paths) with system models.
5. Integrate technologies and methods into engine experiments to characterize effects on BTE and emissions.

Technologies for improving efficiency and emissions in light-duty diesel engines are being investigated at ORNL on a highly modified Mercedes-Benz (MB) 1.7-L common rail four-cylinder diesel engine and a GM 1.9-L common rail four-cylinder diesel engine. These engines are equipped with microprocessor-based dSpace control systems which permit unconstrained access to engine hardware including the integration of custom control algorithms. The GM engine also has an electronic control unit donated by GM which allows for the monitoring and manipulation of the base engine calibration.

Results

A peak brake thermal efficiency of 42% was demonstrated on a GM 1.9-L engine satisfying a Joule milestone in Vehicle Technologies. The engine was donated by GM and is equipped with state-of-the-art features including a versatile microprocessor-based control system, variable geometry turbocharging, and common-rail fuel injection capable of multiple injections. Integrated control of the turbocharger and fuel injection phasing were critical to reaching this level of engine efficiency. This efficiency milestone was also achieved intermittently on a modified 1999 MB 1.7-L diesel engine. Efficiency results are shown in Figure 1 with comparisons to measured original equipment manufacturer (OEM) peak BTE.

A 1.9-L GM engine was commissioned at ORNL in FY 2007 and will eventually be the primary engine platform for this activity. A preliminary mapping of the performance and emissions characteristics of the engine at 36 speed-load combinations was performed to satisfy an interim FY 2007 milestone. BTE as a function of speed and load is shown in Figure 2. A peak BTE of approximately 40% was initially observed on this engine, which was considerably lower than the 42% expected based on the open literature and discussions with GM. The reduced peak BTE is most likely due to a non-optimized calibration for lower cetane U.S. diesel fuel and/or the engine not being sufficiently broken-in. A more detailed map (~120 speed-load combinations) is scheduled to be performed in FY 2008. The more detailed map will be used for calibrating a full engine model as well as for estimating thermodynamic availability and the potential of WHR across the speed-load range.

Meeting 2010 and interim BTE milestones will require some form of energy recovery from the engine system. Potential sources of recoverable energy are summarized in Figure 3. WHR in light-duty diesel engines has not been significantly explored due to the light-load operation common to this engine platform where engine temperatures are low. With LTC (or high dilution) combustion modes being implemented more and more to reduce emissions, a significant amount of heat rejection is necessary in the EGR system. This increased heat rejection is an opportunity for low-load WHR where pre-turbo exhaust/EGR temperatures are high. The implementation of WHR with modern advanced engines will require the consideration of numerous issues:

- Source, quality, and recovery method of energy.
- Integration with other technologies such as LTC operation, turbo-compounding, variable valve actuation, aftertreatment, etc.

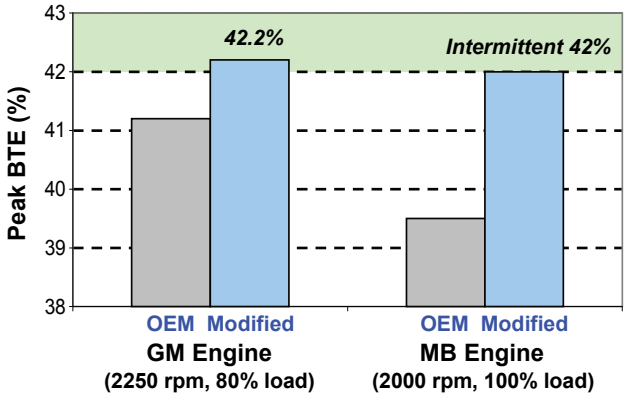

FIGURE 1. Maximum BTE Achieved on GM and MB Light-Duty Diesel Engines (Also shown for reference is the peak BTE of the OEM calibrations.)

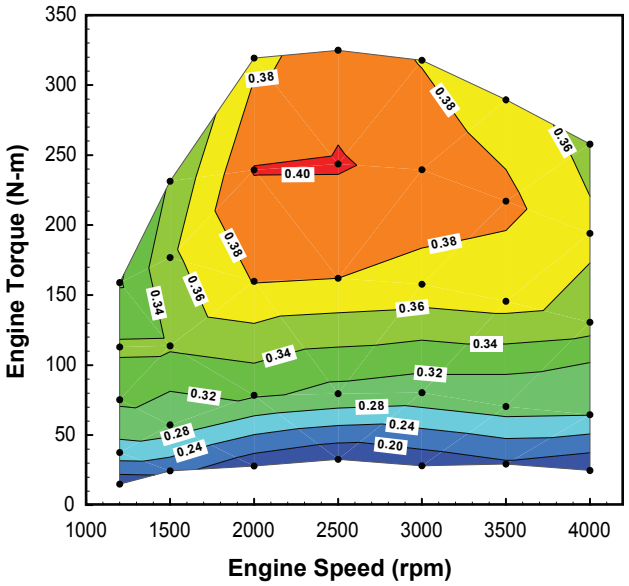

FIGURE 2. Preliminary Performance Mapping of GM 1.9-L Light-Duty Diesel Engine with 2007 Ultra-Low Sulfur Diesel Fuel

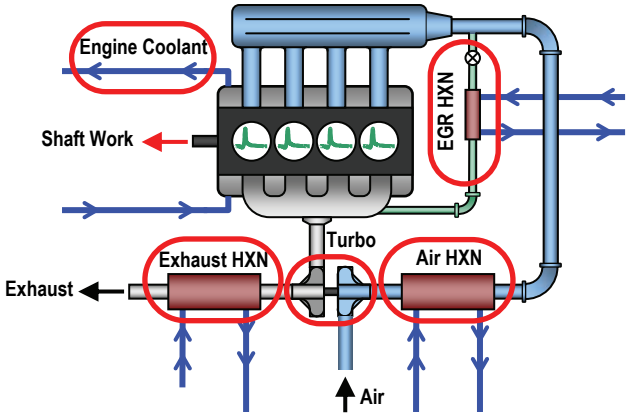

FIGURE 3. Schematic of Engine System with Potential Sources for Recovery of Waste Energy

- Potential benefits across the speed-load range of engine.
- Reintroduction of recovered energy to engine system.

A thermodynamic Second Law perspective is important for managing these issues as well as evaluating efficiency opportunities and providing guidance on developing and evaluating a plan for meeting 2010 as well as intermediate milestones. Analysis routines have been developed for use with WAVE™ and GT Power™ engine simulation codes for identifying availability and loss mechanisms for individual components. An example of a Second Law characterization of the MB engine simulation at 2,000 rpm, 100% load is shown in Figure 4 (a) with no insulation on exhaust manifold and (b) with insulation on exhaust manifold. This analysis is useful for evaluating the potential of different strategies (experiment and simulation) on the availability of unused energy from engine system components. For example in Figure 4, adding insulation from to the exhaust manifold results in an increase from 10% to 14% availability in the exhaust stream. As mentioned above, this perspective will also be critical in the thermal management of complicated engine-systems, which may include a combination of technologies competing for the same thermal resources.

Advanced combustion strategies were used as the primary method of achieving reduced emissions and were focused on the MB 1.7-L for FY 2007. Four speed-load conditions and weighting factors were used to estimate the magnitude of drive cycle emissions for advanced combustion operation. ORNL is working with the Advanced Combustion & Emissions Controls Technical Team to re-evaluate these modal conditions for estimating drive-cycle emissions and to suggest a new set of conditions if appropriate. The composite emissions estimates for high-efficiency, clean combustion (HECC) operation are shown in Figure 5 and compared to U.S.

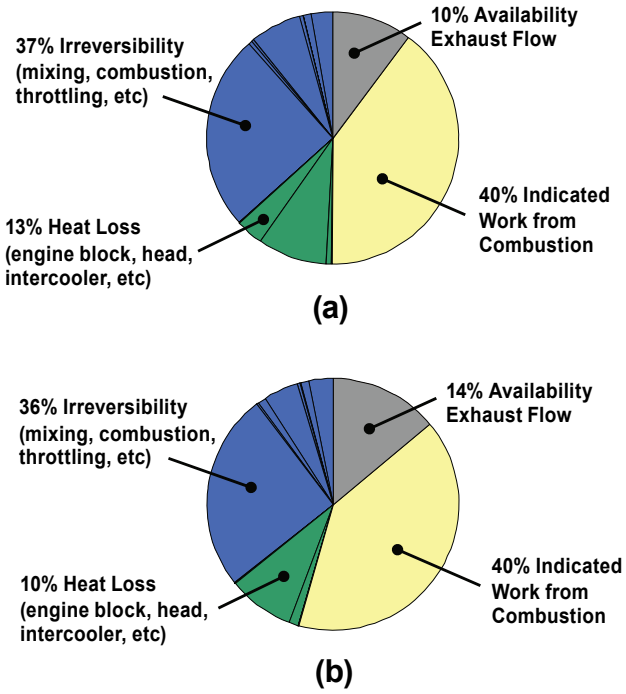

FIGURE 4. Example of Second Law Characterization of Fuel Energy for MB Engine Simulation at 2,000 RPM and 100% Load with (a) No Insulation on Exhaust Manifold and (b) Insulation on Exhaust Manifold

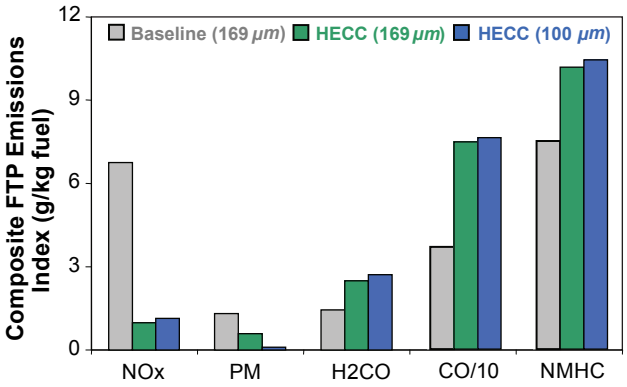

FIGURE 5. Composite Emissions Indices Based on Steady-State Modal Conditions Representative of the FTP Drive-Cycle

Tier 2 Bin 5 regulatory standards in Table 1. Recall that these emissions estimates are based on steady-state data from a fully warm engine and do not include important effects associated with cold-start and transient load-speed operation. Examination of Table 1 indicates some form of aftertreatment will most likely still be required for the form of HECC used in this activity. While significant in-cylinder NOx reduction was achieved and dramatically reduces the NOx aftertreatment requirement, HC and CO emissions were increased in the process, resulting in the need for increased aftertreatment oxidation as compared to conventional

operation. Also note that a diesel particulate filter was used in the low-pressure EGR system and is necessary to meet the engine-out HECC emissions values shown in Table 1. In the future, simultaneous improvements in efficiency and emissions will most likely involve a combination of advanced combustion operation working synergistically with the appropriate aftertreatment technologies. The reader is encouraged to reference the publications/presentations list for more information.

TABLE 1. U.S. Tier 2 Bin 5 Emissions Standards, HECC FTP Drive-Cycle Emissions Estimates, and Required Aftertreatment Effectiveness Estimates

Pollutant	Tier 2 Bin 5 g/mi	HECC g/mi	Required Aftertreatment Efficiency
NOx	0.07	0.075	7%
NMHC	0.09	0.694	87%
CO	4.2	5.08	17%
H_2CO	0.018	0.181	90%
PM	0.01	0.007	Required for low-pressure EGR

A long range path is being developed at ORNL through thermodynamic analysis as described above and experiments/modeling in LTC, waste heat utilization, and thermal management. A summary of technologies and status are summarized below:

- **Advanced Combustion.** Continued leveraging with existing ORNL activity on light-duty diesel HECC as well as other DOE sponsored activities at national laboratories, universities, and industry.
- **Waste Heat Recovery.** Continued development and implementation of WHR systems for recovering energy from the EGR cooler, air charge cooler, and post-turbocharger exhaust system.
- **Turbo-Compounding.** In discussion with Woodward and BorgWarner to evaluate hydraulically or mechanically coupled turbo-compounding concept for light-duty diesel engines.
- **Variable Valve Actuation.** Potential of this approach for improved efficiency is being evaluated with simulation models. Implementation would most likely be cam phase system developed by Delphi.
- **Friction Reducers.** Multiple projects recently proposed at ORNL and elsewhere to evaluate coatings for advanced combustion and novel lubricants including ionic fluids.

Conclusions

This activity has shown progress toward the development, implementation, and demonstration of technologies for improved BTE. Specific accomplishments are as follows:

- The 2007 FreedomCAR goal of 42% peak BTE was demonstrated on a 2005 GM 1.9-L and a modified 1999 MB 1.7-L light-duty diesel engines. Enablers for meeting this milestone on both engines included variable geometry turbochargers, revised fuel injection parameters, and control of air temperature.
- A GM 1.9-L engine with flexible control systems was commissioned at ORNL. This engine geometry is being used at Sandia National Laboratories (optical single-cylinder engine), Lawrence Livermore National Laboratory (modeling), and the University of Wisconsin (metal single-cylinder and multi-cylinder engines) and has resulted in improved collaboration in DOE funded activities in support of meeting FreedcomCAR efficiency and emissions milestones.
- Improved thermodynamic analysis methods were developed for use with engine simulation codes as well as experimental data.
- The potential of advanced combustion strategies for achieving Tier 2 Bin 5 emission levels was investigated on the MB 1.7-L engine.

FY 2007 Publications/Presentations

1. R. M. Wagner et al., "Update on ORNL efficiency and advanced combustion activities for LD diesel engines", 2007 AEC Working Group Meeting at USCAR (Southfield, MI; September 2007).

2. K. D. Edwards et al., "Identification of Potential Efficiency Opportunities in Internal Combustion Engines Using a Detailed Thermodynamic Analysis of Engine Simulation Results", 2007 AEC Working Group Meeting at USCAR (Southfield, MI; September 2007).

3. K. D. Edwards et al., "Identification of Potential Efficiency Opportunities in Internal Combustion Engines Using a Detailed Thermodynamic Analysis of Engine Simulation Results", Diesel Cross-Cut Team meeting (Southfield, MI; July 2007).

4. R. M. Wagner et al., "Modeling and Experiments to Achieve High-Efficiency Clean Combustion (HECC) in LD Diesel Engines", Advanced Combustion & Emissions Control Technical Team meeting (Southfield, MI; July 2007).

5. K. D. Edwards, R. M. Wagner, S. P. Huff, R. L. Graves, "A Thermodynamic Analysis of WAVE Engine Models for Identifying Potential Opportunities for Improving Efficiency in Internal Combustion Engines", 2007 Ricardo Software North American Users Conference (Plymouth, MI; June 2007). *Invited*.

6. R. M. Wagner et al., "Modeling and Experiments to Achieve High-Efficiency Clean Combustion (HECC) in LD Diesel Engines", 2007 Department of Energy (DOE) Advanced Combustion Engines Merit Review (Washington, D.C.; June 2007).

7. C. Scott Sluder, R. M. Wagner, "An Estimate of Diesel High-Efficiency Clean Combustion Impacts on FTP-75 After-treatment Needs", 2006 Powertrain & Fluid Systems Conference (Toronto, Ontario Canada; October 2006).

Special Recognitions & Awards/Patents Issued

1. DOE EERE Weekly Report.

2. ACEC Technical Team summary to USCAR Board of Directors.

3. ACEC Technical Team highlight.

4. FreedomCAR Technical Highlight in 2007.

II.A.14 Hydrogen Free Piston Engine

Peter Van Blarigan
Sandia National Laboratories
PO Box 969, MS 9661
Livermore, CA 94551-0969

DOE Technology Development Manager:
Gurpreet Singh

Objectives

- Optimize and quantify the efficiency of the linear alternator and associated control circuitry when utilized in a plug-in hybrid battery charger application.
- Design opposed piston research experiment.
- In collaboration with General Motors (GM) and the University of Michigan, assess the performance of a free piston generator as the auxiliary power unit (APU) in a series hybrid vehicle.
- Improve the efficiency of small output (30 kW) reciprocating generators by at least 20%, along with reduced emissions.

Approach

- Utilize Flux2D (electromagnetic analysis software), Mathematica-based model, and MATLAB/Simulink to optimize the Sandia-designed linear alternator for a battery charging application.
- Use PSpice to analyze and understand the voltage/current relationships.
- Recruit Ph.D. student and post-doc to replace moving-on students.
- Design the research experiment utilizing SolidWorks/COSMOS and experience base available from Sandia's Combustion Research Facility.
- Utilize homogeneous charge compression ignition combustion of lean mixtures to achieve the 20% efficiency improvement and emissions reductions via low-temperature combustion.

Accomplishments

- Developed linear alternator/multi-level converter configuration calculated to exceed 30 kW power output charging a battery at greater than 95% conversion efficiency.
- Hired Nan Jiang as a post-doc (University of Minnesota) and Jerry Fuschetto as a Ph.D. student (University of Michigan).
- Determined with collaborators that the opposed piston concept is preferred for hybrid vehicle applications due to its capability to operate independently of other units (due to self balance).
- Developed opposed piston research experiment design.

Future Directions

- Fabricate and construct a two-stroke cycle, opposed piston research experiment utilizing optimized coupling of Magnequench linear alternators as a proof-of-concept tool.
- Optimize the battery charging application for higher power-to-weight ratio.
- Operate the research experiment fueled by hydrogen to measure indicated efficiency in a continuous operation regime.
- Demonstrate flexibility and multi-fuel capability by operating on alternative fuels at various operating conditions (compression ratios, equivalence ratios).

Introduction

As fuel efficiency of the typical American automobile becomes more important due to hydrocarbon fuel cost and availability issues, powertrain improvements will require smaller output engines combined with hybrid technologies to improve efficiency. In particular, the plug-in hybrid concept will require an electrical generator of approximately 30 kW output. Unfortunately, current crankshaft spark-ignition internal combustion engines with optimized power outputs of 30 kW have indicated thermal efficiencies of less than 32%.

The free piston generator of this project has a projected fuel-to-electricity conversion efficiency of 50% at 30 kW output. The project has progressed by conducting idealized combustion experiments, designing and procuring the linear alternators required for control and power conversion, and conducting computational fluid dynamics design of the inlet/exhaust processes. The design has evolved into a dynamically balanced configuration suitable for seamless incorporation into an automotive application. The ultimate goal is to combine the developed components into a research prototype for demonstration of performance. Figure 1 shows the improvement based on single cycle experiments.

Approach

By investigating the parameters unique to free piston generators (linear alternator, opposed piston coupling, uniflow port scavenging) as separate entities, each piece can be used at its optimum design point. More importantly, upon assembly of a research prototype for performance demonstration (the goal of this project), understanding of the pieces in the device will allow proper contribution of each component to the combined performance of the assembly.

This year, our research activities concentrated on utilizing and optimizing numerical codes and waveform aids, modeling the linear alternator/electrical power management system for a battery charging application (plug-in hybrid), and designing the opposed piston experiment intended to quantify the indicated efficiency of a hydrogen-fueled APU. Our collaborators (GM and the University of Michigan) have concentrated on a ground-up hybrid vehicle model to optimize the size and configuration of the free piston APU.

Results

The most important result of the past year is the modeling result of the battery charging application required for hybrid vehicle optimization (particularly plug-in hybrid). Figure 2 shows the output energy per coil per cycle as a function of battery state of charge. The plot shows that the linear alternator is able to operate at full output power and charge the battery at this rate over a broad range of battery state of charge, essentially from fully discharged to fully charged.

The electrical configuration utilized is a multi-level converter approach. In this implementation each alternator coil (21 coils in our design) is matched to a single battery unit optimized in size to match the coil output. Figure 3 displays an individual coil/battery circuit. The solid state switches in the center (rectifier) are controlled to rectify the alternating, variable frequency output of the linear alternator, charging the battery shown in the center of the circuit. The solid state switches on the right (converter) side are controlled to assemble a sinusoidal output approximation, where each of seven batteries is added to form a single phase of a three phase output (there are three each of seven

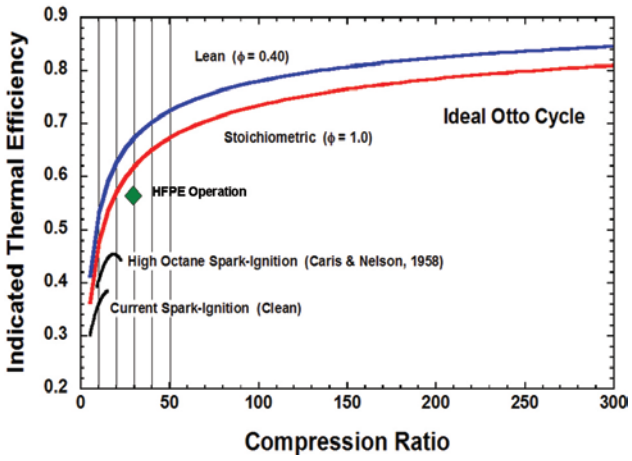

FIGURE 1. Indicated Efficiency as a Function of Compression Ratio – Ideal and Actual

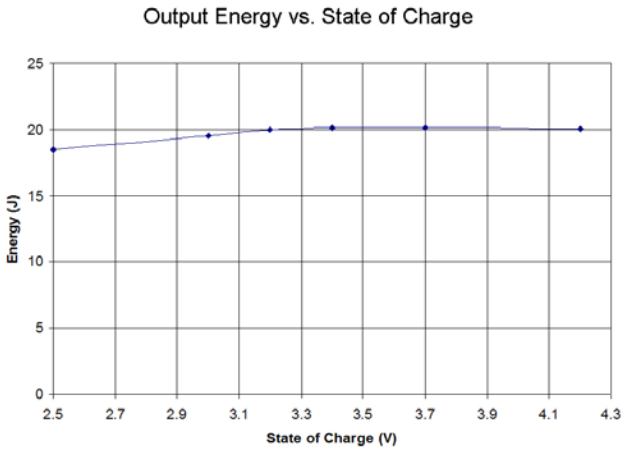

FIGURE 2. Output Energy per Coil per Cycle as a Function of Battery Cell State of Charge

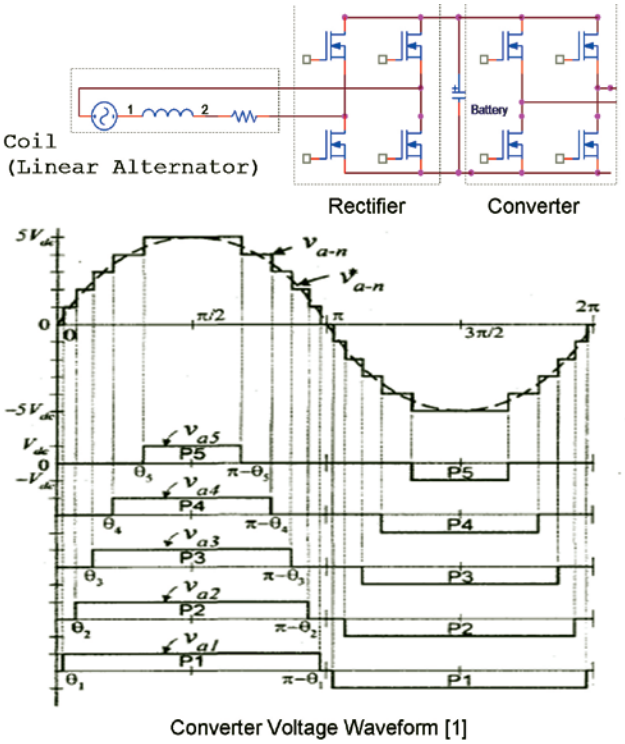

FIGURE 3. Electrical Circuit of Individual Coil/Rectifier/Battery/Converter and Converter Output Voltage Waveform

battery phases). This output waveform construction is shown at the bottom of Figure 3.

This configuration has three significant attributes. First, the charging operation is independent of the motor driving application, yet all batteries can be maintained at the desired state of charge by varying how much of each individual battery output is utilized in constructing the approximate sine wave motor driving waveform. Second, the controlled switches have losses of less than 1% of the output power, far less than diodes. Third, individual battery voltage can be maintained in the 50 V range, not posing any significant personnel hazard in a maintenance or accident scenario. Tolbert et al [1] has more details on multi-level converters.

Another significant effort involved modifying the Sandia-designed linear alternator for higher efficiency. Figure 4 shows the linear alternator mechanical-to-electrical output efficiency as a function of stator weight. Note that a rather small increase in weight results in a significant efficiency increase, with 95% achievable at small cost.

The final electrical optimization is shown in Figure 5. Power output per coil per stroke is shown for four various switching/capacitance combinations. The synchronous rectifier scheme controls the switches to behave like diodes and is the starting point. It can be seen that modifying the switching parameters can improve the power out by 15%, but adding a snubber/switch/capacitor can increase the output by 70%. Ron Moses, our former Los Alamos National Laboratory collaborator now retired, has developed the snubber concept.

Figure 6 shows the SolidWorks model of the opposed piston experiment. We will soon begin procuring the parts to assemble the device. We are working closely with C. Lee Cook Corporation, a builder of high pressure compressors and the supplier of piston rings for the optical engines in Sandia's Combustion Research Facility. We plan on using Cook as the prime supplier of the cylinders and pistons.

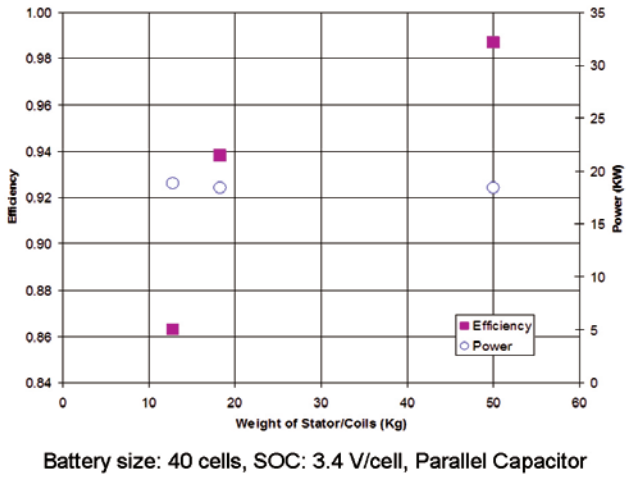

FIGURE 4. Power Output and Conversion Efficiency as a Function of Stator Weight

Conclusions

- The free piston/linear alternator generator is capable of charging a battery in a series/plug-in hybrid powertrain configuration at high efficiency (95%) and over a wide state of battery charge.
- Power output from the linear alternator can be significantly increased (70%) by application of snubber capacitors and computer controlled switches.
- Opposed piston design continues to have attractive features for prototype and for hybrid vehicles where low power output is often required.
- Prototype fabrication and characterization are on track to begin this fiscal year.

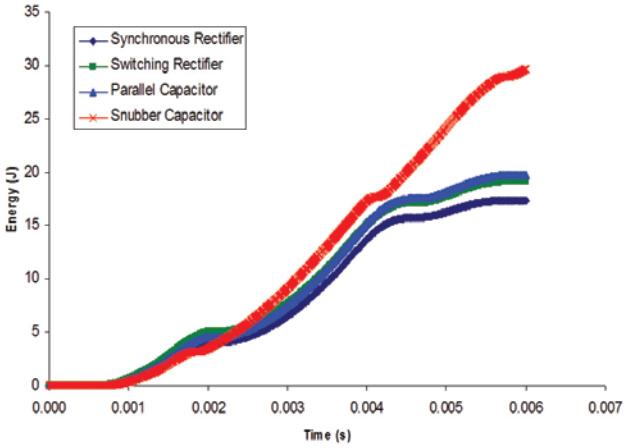

FIGURE 5. Energy Output per Coil per Cycle for Various Rectification Approaches

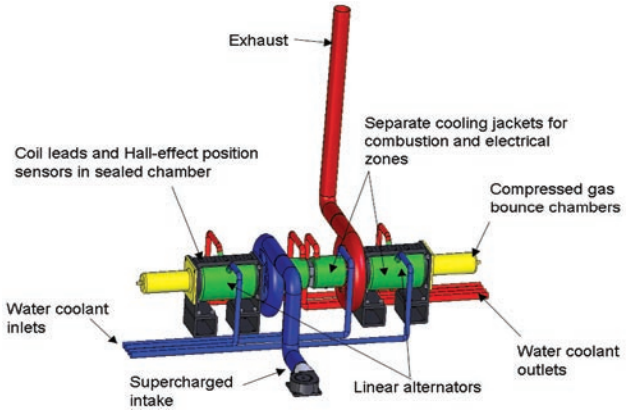

FIGURE 6. Solid Model of Opposed Piston Experiment

References

1. Tolbert et al, "Multilevel Inverters for Electrical Vehicle Application", WPET '98, Dearborn, Michigan, October 22–23, 1998, pp. 79-84.

II.A.15 Optimization of Direct Injection Hydrogen Combustion Engine Performance using an Endoscopic Technique

Thomas Wallner
Argonne National Laboratory
9700 S. Cass Avenue
Argonne, IL 60439

DOE Technology Development Manager:
Gurpreet Singh

Objectives

- Quantify the efficiency and emissions behavior of a hydrogen-powered combustion engine with particular focus on direct injection operation.
- Optimize the hydrogen combustion engine through improved injection strategies, multiple injection and injector nozzle designs.
- Demonstrate the potential of advanced diagnostic tools (endoscope imaging and spectroscopy) for optimization of hydrogen engine operation.

Accomplishments

- Characterized the influence of injection timing on engine efficiency and emissions in direct injection operation.
- Determined that nozzle design significantly influences brake thermal efficiency and emissions (2% increase in brake thermal efficiency and 47% decrease in nitrogen oxide [NOx] emissions at low engine load with changed nozzle design).
- Captured images of a multiple injection strategy.
- Performed and refined spectroscopic gas temperature measurements.
- Installed new cylinder head with central and side injector locations – specific injector nozzles designed and manufactured for either location.
- Expanded existing collaboration with Ford, BMW and the European HyICE consortium.

Future Directions

- Expand engine testing to include central direct injection in addition to current side injection location (new cylinder head provided by Ford Motor Company).
- Evaluate newly designed injector nozzles for performance and emissions benefits.
- Analyze the potential of water injection.
- Conduct test runs at higher engine speed conditions to evaluate the high-flow performance of the improved injectors.
- Evaluate hydrogen direct injection in a multi-cylinder engine (separate project proposal for FY 2008).

Introduction

In order to achieve the targets for hydrogen engines set by the U.S. Department of Energy (DOE) – a brake thermal efficiency of 45% and NOx emissions below 0.07 g/mi – while maintaining the same power density as comparable gasoline engines, researchers need to investigate advanced mixture formation and combustion strategies for hydrogen internal combustion engines. Hydrogen direct injection is a very promising approach to meeting DOE targets; however, there are several challenges to be overcome in order to establish this technology as a viable pathway toward a sustainable hydrogen infrastructure.

Approach

This research project at Argonne National Laboratory has been funded to evaluate hydrogen combustion strategies in a research engine and apply advanced diagnostics to identify areas for further improvement.

This report describes the use of endoscopic imaging as a diagnostic tool that allows further insight into the processes that occur during hydrogen combustion. It also addresses recent progress in the development of advanced direct-injected hydrogen internal combustion engine concepts.

The hydrogen combustion behavior in a single-cylinder research engine is characterized and an analysis of the results of hydrogen direct-injection operation is performed. In addition to conventional combustion analysis, which employs pressure traces and derived information (e.g., rate of heat release) as well as emissions measurement, the combustion characterization is performed by using an ultraviolet (UV)-transmitting endoscope in combination with an intensified charge-coupled device (ICCD) camera. By using this technique, we were able to obtain a two-dimensional optical signature of hydrogen combustion, even at high engine speeds and loads. Analysis of the optical information allowed us to draw conclusions

about the mixture homogeneity and possible stratification effects for different injection strategies.

Results

For the results shown, the injector was located on the intake side of the combustion chamber between the intake valves. Because of the 4-valve configuration with split intake ports, there is sufficient space available to accommodate the injector, as well as the hydrogen supply to the injector.

Influence of Injection Timing on Mixture Distribution and Emissions Behavior

Injection timing during hydrogen direct-injection operation has a crucial influence on the mixture distribution and, therefore, on the combustion characteristics. With early injection (shortly after intake valve closing) the injected fuel has sufficient time to mix with the air inside the combustion chamber and form an almost-homogenous mixture. With late injection, only limited time for mixing is available, resulting in a stratified charge at spark timing. This basic trend has also been shown by three-dimensional computational fluid dynamics (CFD) simulation tools [1].

The impact of this trend on NOx emissions is highly dependent on the engine load i.e. overall fuel/air equivalence ratio (Figure 1). At low engine loads (low ϕ) and unthrottled operation, early injection results in extremely low NO_x emissions because the mixture at ignition timing is very likely to be homogeneous. Thus, the lean homogeneous mixture burns without forming NOx emissions. Late injection at low loads, on the other hand, results in a stratified mixture with hydrogen-rich zones, as well as zones with very lean mixtures – or even pure air. Although the overall mixture is still lean, the combustion of rich zones causes a significant increase in NOx emissions. At high engine loads (high ϕ), this trend appears to be inverted. Early injection results in homogeneous mixtures that approach stoichiometry and produce high NOx emissions. Late injection is expected to result in stratification, with zones that are even richer than stoichiometric, along with lean zones. This kind of stratification avoids the NOx critical air/fuel ratio regime of $\phi \sim 0.75$ and thereby reduces overall NO_x emissions.

The above-described trends can be seen in analyzing the cylinder pressure and rate of heat release (ROHR) traces shown in Figure 2. The black lines represent early injection (start of injection [SOI] = 120° crank angle before top dead center [CA BTDC])and the grey lines represent late injection (SOI = 60°CA BTDC) at medium engine load (wide-open throttle, fuel/air equivalence ratio of $\phi \sim 0.47$, indicated mean effective pressure (IMEP) of ~6 bar. The rather homogenous mixture resulting from early injection (black line) requires an earlier spark timing (11°CA BTDC) than the late injection (6°CA BTDC) to achieve optimal combustion phasing. The overall lean and homogenous mixture with early injection also results in distinctively longer combustion duration (~35°CA) than the stratified case with late injection (~25°CA). Although the rate of pressure increase is higher with the stratified mixture than in the homogenous case, the peak pressures are almost identical, due to the earlier spark timing with early injection.

Influence of Injector Nozzle Geometry on Mixture Distribution, Emissions Behavior and Efficiency

The lean-burn capabilities of hydrogen are superior to those of any other fuel. The theoretical flammability limits of hydrogen in air are in a range of $0.09 < \phi < 2.0$ (gasoline: $0.7 < \phi < 2.5$) [2]. Although these wide flammability limits allow for homogenous unthrottled

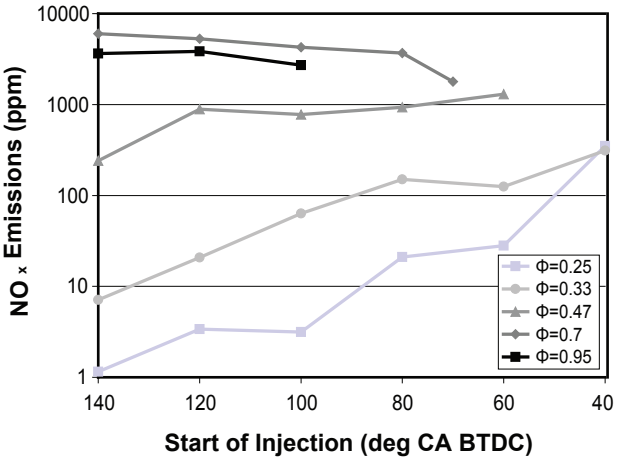

FIGURE 1. Influence of Injection Timing And Engine Load (Fuel/Air Equivalence Ratio) on NOx Emissions

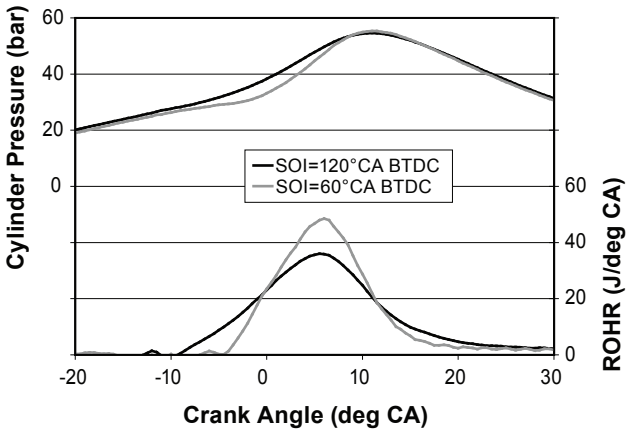

FIGURE 2. Comparison of Pressure Traces and Heat Release Rate with Variation of SOI at Medium Load

operation even under idling conditions, in many cases, more efficient engine operation can be realized with stratification.

Two different injector configurations were tested in an attempt to evaluate the influence of nozzle configuration on mixture stratification (Figure 3). The baseline nozzle was a 13-hole nozzle with one central hole and 12 surrounding holes staggered at an angle of 60°. The included injection angle was also 60°. With a hole diameter of ~0.38 mm, the total injector hole area was 1.5 mm^2. The second nozzle was a 5-hole nozzle with central hole and four surrounding holes. The included injection angle was 100°. The total injector hole area was held constant (1.5 mm^2), resulting in an individual hole diameter of ~0.62 mm. Because of the constant total injector hole area, the injection durations for the different nozzles at the same load are comparable. The larger hole diameter of the 5-hole nozzle theoretically results in a higher penetration depth of the individual jets [3] – the larger cone angle on the other hand is supposed to reduce the penetration depth as a result of increased wall interactions.

Different nozzle designs in hydrogen direct injection influence this stratification and, therefore, the engine performance at low engine load (IMEP~2 bar), as shown in Figure 4. The engine was operated at 2,000 RPM at wide-open throttle with an overall air/fuel ratio of ϕ~0.25. The start of injection was set to 40°CA BTDC with spark timing at 5°CA BTDC. The resulting torque is about 3 Nm. Although the amount of unburned hydrogen is significantly higher with the 5-hole nozzle (more than 4,000 ppm versus 1,000 ppm with the 13-hole nozzle), the brake thermal efficiency with the 5-hole nozzle is significantly better.

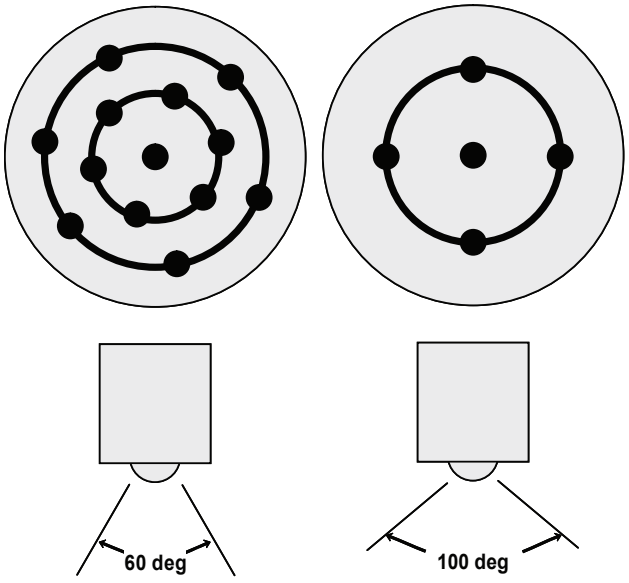

FIGURE 3. Schematics of Direct-Injection Nozzle Configurations

The low absolute levels of brake thermal efficiency are attributable to the low engine load and the high friction losses of the single-cylinder research engine. In addition to the efficiency advantage, the 5-hole nozzle also offers a significant reduction in NOx emissions.

To correlate the trends shown in Figure 4 to the stratification effects caused by the different nozzles, we measured the OH* chemiluminescence intensity during combustion. Figure 5 shows the OH* intensity for low engine load at a speed of 2,000 RPM. Figure 5a shows the results for the 13-hole nozzle with an injection angle of 100°; Figure 5b shows the intensity distribution for the 5-hole nozzle with a 60° injection angle. Injection and ignition parameters are identical to those in Figure 4 – a start of injection of 40°CA BTDC and a spark timing of 5°CA BTDC.

The first two frames for the 13-hole injector show the spark discharge; the third frame (top dead center) already shows a slight increase in the size of the area with high OH* intensities, which indicates the beginning of combustion. The area of high intensities increases in size within the next few frames. At 8°CA ATDC, an almost-symmetrical zone of high intensities close to the top of the combustion chamber has developed. This zone further expands in size in the subsequent frames, whereas the peak intensities already begin to decrease. Although the fuel/air equivalence ratio is very lean (ϕ~0.25) OH* chemiluminescence intensity signals can be detected during combustion. This is only possible because of the mixture stratification caused by the late injection. Early injection, resulting in an almost homogeneous mixture distribution, would result in very low (almost undetectable) OH* intensities.

Figure 5b shows the OH* intensities for the 5-hole nozzle with a much wider injection angle. Unlike for the 13-hole nozzle, there are no detectable OH* intensities besides the spark discharge with the 5-hole nozzle during the first six frames (the high intensity

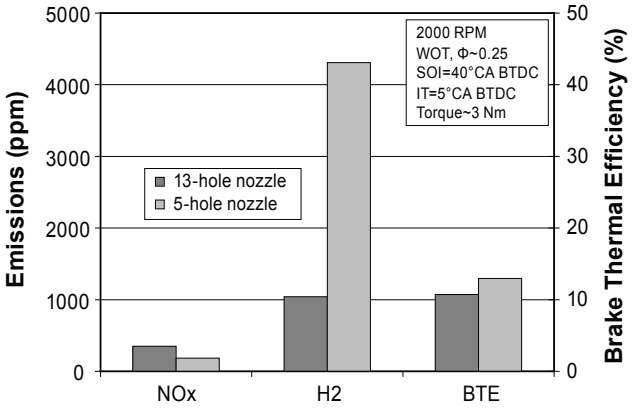

FIGURE 4. Influence of Nozzle Design on Efficiency and Emissions at Low Engine Load

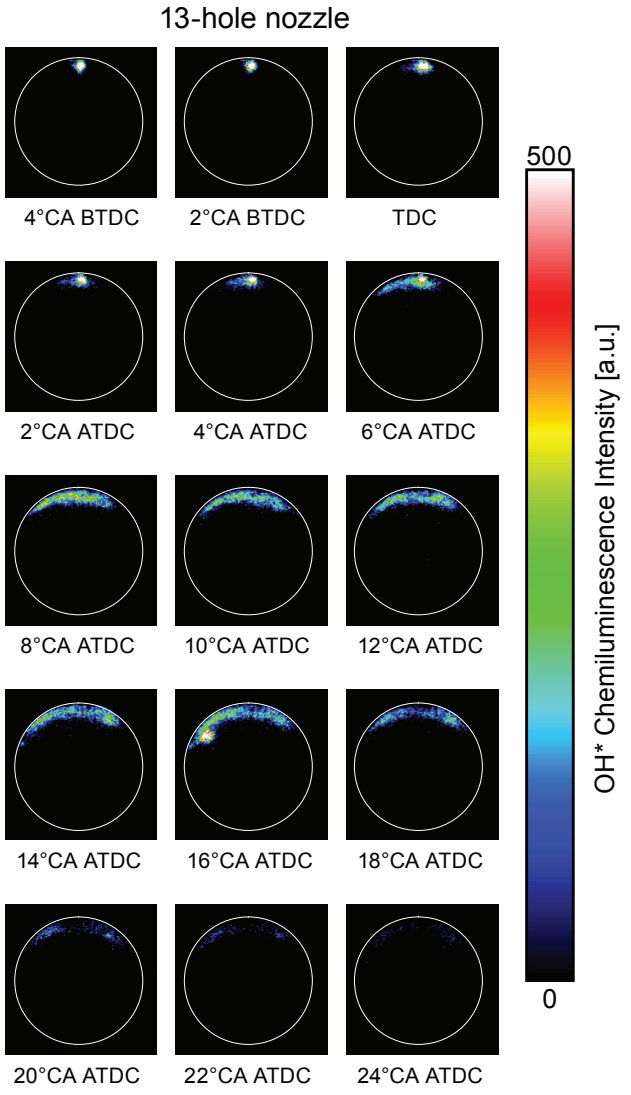

FIGURE 5A. Influence of Nozzle Geometry on Local Combustion Intensity at Low Engine Load – 13-Hole Nozzle

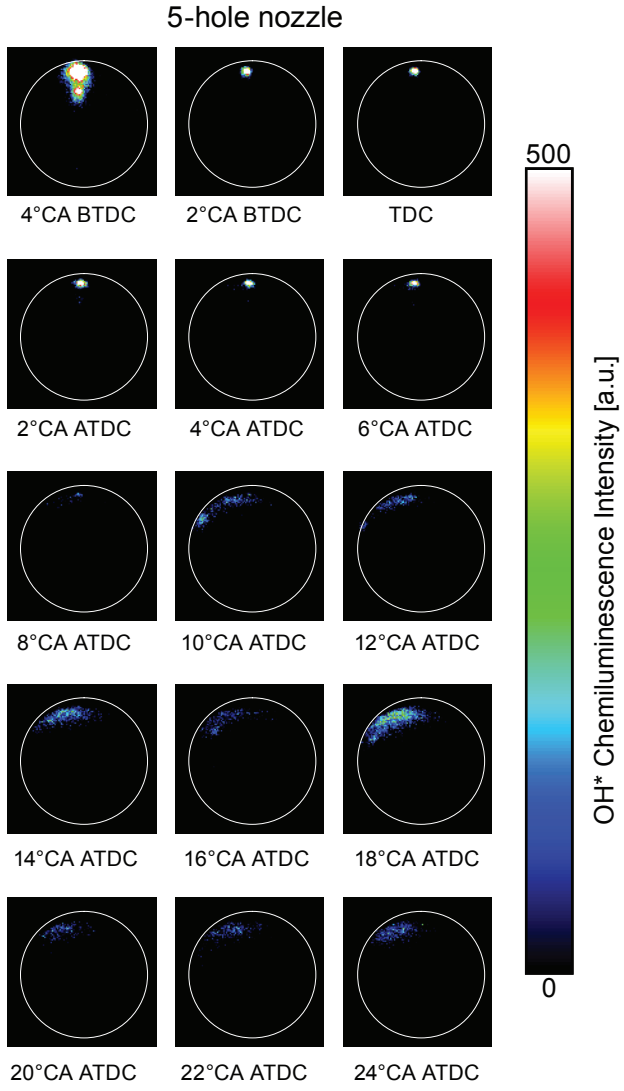

FIGURE 5B. Influence of Nozzle Geometry on Local Combustion Intensity at Low Engine Load – 5-Hole Nozzle

in frame 1 is a reflection of the spark discharge on the piston). Starting from frame 7 (8°CA ATDC), a zone of low (but detectable) OH* intensities start to form at the intake side of the combustion chamber (right side in the chemiluminescence results). The peak intensities occur at 18°CA ATDC, but the maximum intensities are significantly lower than with the 13-hole nozzle.

The intensity distribution for the 5-hole nozzle with high OH* intensities on the intake side (close to the fuel injector) is very likely attributable to the fact that the wider injection angle (100°) causes the injection jet to hit the combustion chamber walls and piston. In the case of the 13-hole nozzle with the 60° injection angle, the hydrogen jets are more likely to penetrate the combustion chamber.

The lower peak intensities also correspond with the lower NOx emissions, as shown in Figure 4. The lower intensities indicate leaner hydrogen air mixtures, which result in a lower local combustion temperature and thus in lower NOx emissions. The opposite can be said about the hydrogen emissions. Flame speed is highly dependent on local fuel/air equivalence ratio with high combustion velocities in rich zones [4]. An overall lean mixture with local rich zones is more likely to cause less unburned hydrogen than an overall lean homogenous mixture. Thus, the significant increase in unburned hydrogen with the 5-hole nozzle seen in Figure 4 is caused by the reduced stratification.

Overall, the general trends observed in the global emission results agree with the mixture distribution derived from the OH* chemiluminescence images.

Conclusions

- Injection parameters, such as injection timing and injector nozzle design, have a significant influence on the performance of a direct-injected hydrogen internal combustion engine.
- Imaging by using endoscopic access to the combustion chamber is a helpful tool to understanding the processes and mechanisms that influence emissions and efficiency behavior.
- By changing the nozzle design from a 13-hole nozzle with a 60° injection angle to a 5-hole nozzle with a 100° injection angle, we can significantly reduce NOx formation with late injection, while maintaining high brake thermal efficiency.
- Advanced nozzle designs as well as changes in injector location will be crucial steps toward reaching the challenging goals for hydrogen engines set by DOE.

References

1. Kovac, K., A. Wimmer, M. Hallmannsegger, and A. Obieglo, "*Mixture Formation and Combustion in a Hydrogen Engine – A Challenge for the Numerical Simulation*" International Congress, Engine Combustion Processes – Current Problems and Modern Techniques, Munich, Germany, 2005.

2. Pischinger, R., M. Klell, and T. Sams, *Thermodynamics of Internal Combustion Engines,* 2002.

3. Kovac, K., *Optimization of the Mixture Formation of a Hydrogen Direct-Injection Engine*, Dissertation, Graz University of Technology, Graz, Austria, 2005.

4. Wallner, T., *Development of Combustion Concepts for a Hydrogen-Powered Internal Combustion Engine*, Dissertation, Graz University of Technology, Graz, Austria, 2004.

FY 2007 Publications/Presentations

1. Wallner, T.; Ciatti, S.; Bihari, B.; Lohse-Busch, H.: "Research Update: Hydrogen Engine Research at Argonne National Laboratory." Progress Review at Ford Motor Company, Dearborn, USA, 2007.

2. Wallner, T.; Ciatti, S.; Bihari, B.: "Direct Injection Hydrogen Fueled Engine Research at Argonne." Presentation at DOE Semi Mega Merit Review. Washington, D.C., USA, 2007.

3. Wallner, T.; Ciatti, S.; Bihari, B.: "Assessment of combustion behavior in a direct-injected hydrogen internal combustion engine using an endoscope as well as in-cylinder temperature measurement." SAE World Congress, Detroit, USA, 2007.

4. Wallner, T.; Lohse-Busch, H.: "Research update: Hydrogen Projects at Argonne National Laboratory." Hydrogen Internal Combustion Engine Symposium, Los Angeles, USA, 2007.

5. Ciatti, S.; Bihari, B.; Wallner, T.: "Establishing Combustion Temperature in a Hydrogen Fueled Engine Using Spectroscopic Measurements." Journal of Automobile Engineering, 2007.

6. Ciatti, S.; Wallner, T.; Bihari, B.: "Progress in Hydrogen Fueled Engine Research at Argonne." Progress Review at Ford Motor Company, Dearborn, USA, 2006.

7. Wallner, T.: "Overview of American and European Hydrogen Research Activities." International Conference on Safety in Transportation, Benevento, Italy, 2006.

8. Wallner, T.: Ciatti, S.; Bihari, B.; Stockhausen, B.; Boyer, B.: "Endoscopic investigations in a Hydrogen Internal Combustion Engine." 1st International Symposium on Hydrogen Internal Combustion Engines, Graz, Austria, 2006.

9. Wallner, T.; Lohse-Busch, H.: "Light Duty Hydrogen Engine Application Research at ANL." Bridging the Technology – Hydrogen Internal Combustion Engines Conference, San Diego, USA, 2006.

II.A.16 Quantitative Measurements of Mixture Formation in a Direct-Injection Hydrogen ICE

Sebastian A. Kaiser (Primary Contact),
Christopher M. White*
Sandia National Laboratories
P.O. Box 969, MS 9053
Livermore, CA 94551
*University of New Hampshire

DOE Technology Development Manager:
Gurpreet Singh

Objectives

The H_2ICE (hydrogen internal combustion engine) project aims to provide the science base for the development of high-efficiency hydrogen-fueled vehicle engines. The technical focus is on direct-injection strategies, using laser-based in-cylinder measurements closely tied to advanced numerical simulations (performed by J. Oefelein at Sandia, see "Large Eddy Simulation Applied to Low-Temperature and Hydrogen Engine Combustion Research"). Specifically, at this point the goals of the project are to:

- Quantify the influence of injection strategies on pre-combustion in-cylinder mixing of fuel and air,
- Provide data for and collaborate in large eddy simulation (LES) validation,
- Investigate influence of charge stratification on the combustion event and NOx formation, and
- Complement metal-engine R&D at Ford and partially-optical engine research at Argonne National Laboratory (ANL).

Accomplishments

- Quantitative, instantaneous two-dimensional images of equivalence ratio and corresponding high-quality velocity measurements were made during the compression stroke with and without direct hydrogen injection.
- Analysis of the velocity field revealed that the observed substantial fuel stratification for late injection is favored by a relatively stable counter-flow situation created by jet-wall interaction.
- Velocity and fuel distribution measurements are initial building blocks of a database for the validation of companion large-eddy simulations by J. Oefelein at Sandia.

Future Directions

- Measure velocity field in the vertical (axial) plane during the intake stroke to validate pre-injection accuracy of the companion simulation.
- Implement *simultaneous* two-dimensional measurements of velocity/equivalence ratio.
- Install new engine head, supplied by Ford R&D, featuring central injection and central ignition. Engine geometry will then be identical to that of collaborating labs at Ford and ANL.
- Install emissions bench (already purchased, NOx and O_2).
- Use OH-planar laser-induced fluorescence (PLIF) to quantitatively investigate the influence of mixture formation on combustion.

Introduction

H_2ICE development efforts are focused to achieve an advanced hydrogen engine with peak brake thermal efficiency (BTE) greater than 45%, near-zero emissions, and a power density that exceeds gasoline engines. With respect to these efforts, the direct-injection (DI) H_2ICE is one of the most attractive H_2ICE options [1]. With DI, the power density can be approximately 115% that of the identical engine operated on gasoline. In addition, the problems of preignition associated with port fuel injection can be mitigated. Lastly, in-cylinder injection offers multiple degrees of freedom available for controlling emissions and optimizing engine performance and efficiency.

The challenge with DI-H_2ICE operation is that in-cylinder injection affords only a short time for hydrogen-air mixing, especially when start of injection (SOI) is retarded with respect to intake valve closing (IVC) to reduce the compression work of the engine and to mitigate preignition. Since mixture distribution at the onset of combustion is critical to engine performance, efficiency, and emissions, a fundamental understanding of the in-cylinder mixture formation processes is necessary to optimize DI-H_2ICE operation. Correct prediction of mixture formation before the onset of combustion is also of great importance for any engine simulation. The experimental results will therefore provide a benchmark test for the computational efforts of J. Oefelein.

Approach

In the optically accessible DI-H_2ICE, separate two-dimensional, quantitative measurements of equivalence ratio and velocity were made. Different post-IVC injection timings and a case corresponding to port fuelling were investigated at a global equivalence ratio of $\phi = 0.55$, intake pressure = 0.5 bar, an engine speed of 1,200 RPM, and an injector pressure of 25 bar. Equivalence ratio was measured using PLIF of acetone seeded in small amounts into the hydrogen fuel. Velocity was measured using particle image velocimetry (PIV) while seeding silicon oxide particles into the intake plenum. Both sets of experiments were performed with non-fired engine operation, since the pre-combustion charge movement and air/fuel mixing were of primary interest here. Results shown are for image acquisition at 32° crank-angle before top dead center (TDC), the latest position in the compression stroke for which both high-quality PLIF and PIV results could be obtained. The imaging plane is parallel to the flat top of the piston, as shown in the experimental schematic of Figure 1. Three different injection timings were investigated: "early" injection (starting just after IVC), "late" injection (with the injection extending just past the crank-angle at which imaging was performed), and "intermediate" (starting well after IVC, ending well before data acquisition). For reference, a near-homogeneous mixture was created by injecting during the intake stroke.

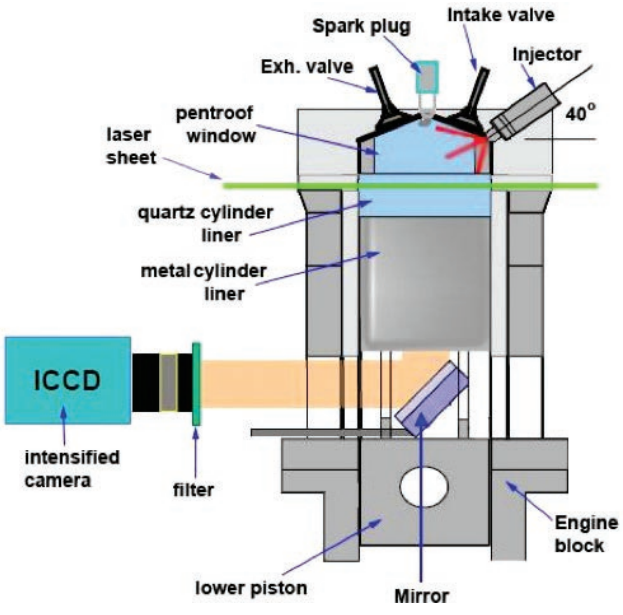

FIGURE 1. Optical Engine Experimental Set-Up

Results

PLIF measurements were reduced to equivalence-ratio images through a combination of calibration measurements with a homogenous mixture and a local temperature correction based on adiabatic mixing [2,3]. Currently, the PLIF-measurement precision is limited by the amount of acetone (the fluorescent tracer) that can be added to the high-pressure hydrogen in the gas cylinder supplying our laboratory with hydrogen. Because the vapor pressure of acetone is low compared to the cylinder pressure (200 bar), only about 0.5 % (by volume) can used before condensation occurs. To overcome this problem, a heated high-pressure compatible seeder has been built. The slightly increased temperature and the seeder's location in the lower-pressure part of the fuel supply system (at injector pressure, 25–100 bar) should allow us to achieve any practically useful acetone concentration. The new system is being tested now.

PIV measurements in engines are challenging because the necessary seed tends to accumulate on the optical surfaces (cylinder liner, piston window) and interfere with the measurement. Careful selection of seed particles, seeding system, and operating procedures enabled us to measure the instantaneous velocity field with high resolution. This will be important for a quantitative comparison with LES results. As opposed to KIVA-type simulations, LES can provide detailed, instantaneous realizations of the turbulent flow-field, demanding an at least equal level of detail from validation experiments. Although the bulk of the initial investigations this fiscal year involved non-fired, pre-combustion conditions, we did verify that high-quality velocity measurements could also be taken during and after combustion. Many previous flow studies have used oil droplets for seeding, thereby limiting the applicability to the low-temperature part of the engine cycle. The ability to measure two-dimensional velocity distributions throughout the entire cycle will be the basis of some of the future work (see above), including validation of the corresponding simulation during the expansion stroke.

Figure 2 shows the results of fuel and velocity measurements in a plane parallel to the piston, covering the central 65 mm of the 92 mm bore. Early injection (SOI/end of injection at -112°/-62° CA) results in a nearly homogenous fuel distribution. However, comparing the corresponding velocity field to that of the non-fuelled case we can see that the charge motion has been altered drastically by the injection event. The velocity magnitudes have greatly increased. The plots show that well-defined large-scale flow structures (i.e., turbulent vortices) are a common occurrence. At this crank angle, early injection timing in the mean yields a central, counter-rotating vortex pair that transports fluid from near the cylinder wall to the central region of the

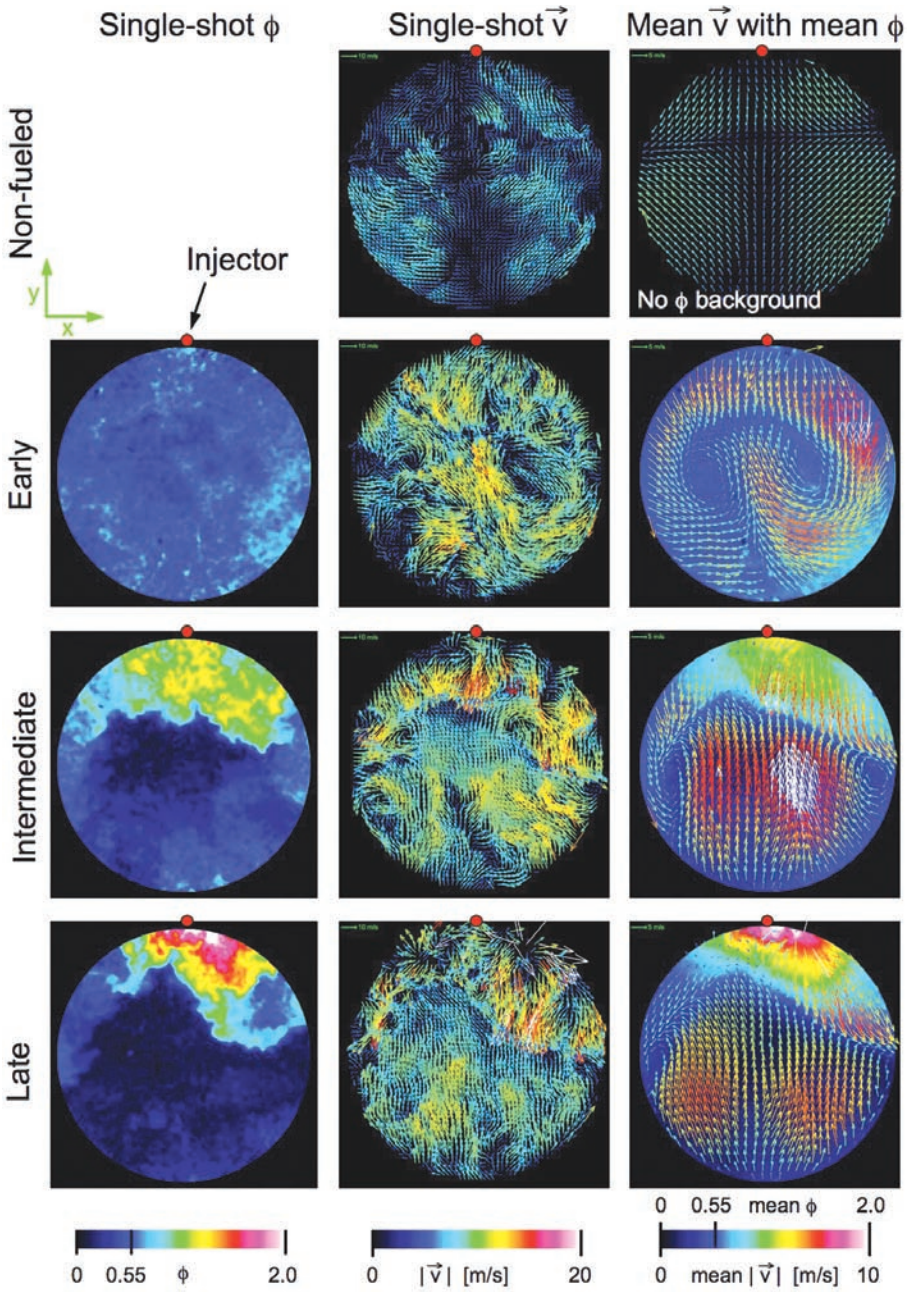

FIGURE 2. Equivalence ratio and velocity for different injection timings: a single instantaneous equivalence-ratio field (left column), a single instantaneous velocity field (center column), and the mean velocity field with the mean equivalence ratio as background (right column). Note that the vector color scale for the mean velocity is different from that for the single shots. For the non-fueled condition ($\phi = 0$), the background of the mean velocity vector plot is chosen uniformly black.

measurement plane. The PLIF images for early injection indicate that the flow is effective in mixing the hydrogen with air.

The fuel-distribution images show that intermediate and late injection produce progressively more inhomogeneous mixtures. This is to be expected due to the shorter time for mixing, but the velocity plots reveal one mechanism which in particular could be responsible for preventing effective mixing until late in the compression stroke: in the measurement plane, the injection has created a counter-flow situation, with a stable, strong bulk flow towards the injector separated by a sharp front from the turbulent, fuel-rich flow originating from the injector. The overlay of the PIV and PLIF means (right column) shows that on average

the two regions and the dividing "turbulent front" are spatially exactly collocated in vector and scalar field.

Motivated by this strong correlation, it is conjectured that the observed flow fields for both the intermediate and late injection timings result from jet and wall interactions that redirect the flow from those jets that are directed along the pent roof vertically back down towards the injector. In the y-z plane, the schematic sketch in Figure 3 shows this idea. Additionally, the injector geometry and the "inverted V" shape of the turbulent front suggest that those jets that issue to the sides, i.e., towards the cylinder liner, could supply additional momentum to the "upward" (positive y direction) flow after wrapping around the cylinder. As a result, the flow in the visible part of the measurement plane is effectively a counter flow that inhibits further jet penetration. The net result of these two effects would be high hydrogen concentration near the injector, consistent with the PLIF images. This scenario, although tentative at this point, suggests that the injector tip geometry, injector location, and injection timing are critical parameters with respect to in-cylinder mixing. Correspondingly, engine simulations would have to accurately capture the injection-induced flow to be able to make valid predictions for the ensuing combustion. Clearly, in this context the measurements presented here can only be considered preliminary and will have to be expanded for the purpose of understanding mixture preparation and in order to provide meaningful simulation validation.

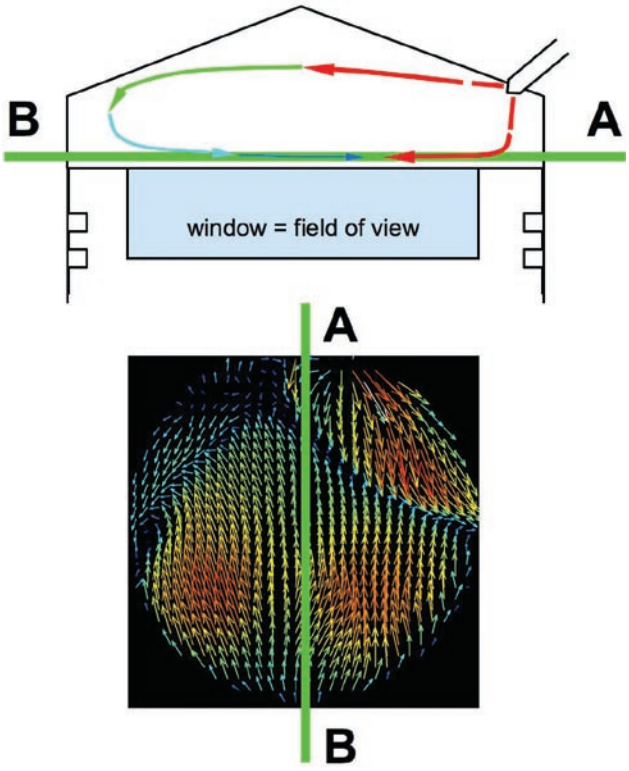

FIGURE 3. Conceptual Sketch of the Opposed-Flow Situation Created by the Wall/Jet Geometry

FY 2007 Publication 1 expands on the above observations and quantifies the global fuel distribution in form of probability density functions. Line-of-sight measurements of chemiluminescence from the excited hydroxyl radical (OH*) for the same series of injection timings, but after ignition, are reported in Publication 2. These qualitative measurements, which indicate the local equivalence ratio during the early burn, are in agreement with the non-fired fuel-imaging data described above. Additional velocity measurements investigating the flow-field throughout the compression cycle with and without injection have been made. A detailed evaluation is in progress and will be the basis for extensive validation of the hydrogen-jet sub-model being developed within the corresponding numerical effort.

Conclusions

- In the optically accessible DI-H_2ICE, high-quality measurements of the velocity field were possible for motored and fired conditions.
- In the same plane, quantitative images of equivalence ratio could be obtained. Accuracy and precision were reasonable and are being improved further.
- Direct hydrogen injection fundamentally alters the in-cylinder flow field.
- For the given side-injecting six-hole injector, three different post-IVC injection timings were investigated. At a point in the compression stroke shortly before the time of ignition, early injection produced a nearly homogeneous mixture, while intermediate and late injection resulted in significant stratification.
- Analysis of the velocity plots showed that the injection event creates a counter-flow situation, which inhibits mixing until breaking up into a vortex pair later in the cycle.
- Although the current injector geometry and location are not ideal for late-injection strategies from an engine-development point of view, the scalar and velocity data will be very useful for the validation of numerical simulations.

References

1. C.M. White, R.R. Steeper, A.E. Lutz, The hydrogen-fueled internal combustion engine: A technical review, Int. J Hydrogen Energy 31:1292-1305, 2006.

2. C.A. Idicheria, L.M. Picket, Quantitative Mixing Measurements in a Vaporizing Diesel Spray by Rayleigh Imaging, SAE Paper 2007-01-0647, 2007.

3. W. Hwang, J.E. Dec, M. Sjöberg, Fuel stratification for low-load HCCI combustion: performance & fuel-PLIF measurements, SAE Paper 2007-01-4130, 2007.

FY 2007 Publications/Presentations

1. S.A. Kaiser, C.M. White, PIV and PLIF to Evaluate Mixture Formation in a Direct-Injection Hydrogen-Fuelled Engine, paper 08PFL-743, submitted for SAE World Congress, April 14-17, 2008, Detroit, MI.

2. C.M. White, A Qualitative Evaluation of Mixture Formation in a Direct-Injection, Hydrogen-Fuelled Engine, SAE Paper 2007-01-1467, 2007.

3. C.M. White, OH* chemiluminescence measurements in a direct injection hydrogen-fuelled internal combustion engine, Int. J. Engine Res. 8:185-204, 2007.

4. C.M. White, H_2ICE Emissions and Near-ZEV Performance, presented at WestStart-FTA Hydrogen Internal Combustion Engines Symposium, Universal City, California, February 13, 2007.

5. C.M. White, *Advanced Hydrogen-Fueled Engines: Potential and Challenges*, presented at the ERC Symposium on Fuels for Future Internal Combustion Engines, University of Wisconsin, Madison, WI, June 6, 2007.

6. S.A. Kaiser, C.M. White, J.C. Oefelein, D.L. Siebers, Sandia Hydrogen Combustion Research: Simulation and Experiment, presented at the Ford/National Labs H_2ICE Meeting, Ford Research and Innovation Center, Dearborn, MI, July 18, 2007.

7. S.A. Kaiser, C.M. White, J.C. Oefelein, D.L. Siebers, Sandia Hydrogen Combustion Research: Simulation and Experiment, presented at the International Energy Agency Task Leaders Meeting, Gembloux, Belgium, September 2007.

II.A.17 Enabling High Efficiency Clean Combustion in Diesel Engines

Donald W. Stanton, Ph.D.
Cummins Inc.
1900 McKinley Ave.
Columbus, IN 47201

DOE Technology Development Manager:
Roland Gravel

NETL Project Manager: Carl Morande

Subcontractors:
- Oak Ridge National Laboratory
- BP Global Fuels Technology

Objectives

1. To design and develop advanced engine architectures capable of achieving U.S. Environmental Protection Agency (EPA) 2010 emission requirements while improving the brake thermal efficiency by 10% compared to current baseline engines.
2. To design and develop components and subsystems (fuel systems, air handling, controls, etc) to enable construction and development of multi-cylinder engines.
3. To specify fuel properties conducive to improvements in emissions, reliability and fuel efficiency for engines using high-efficiency clean combustion (HECC) technologies. Demonstrate a viable approach to reducing petroleum imports by at least 5% via renewable fuel sources. Demonstrate the technology is compatible with B20 (biodiesel) to enable reduction of petroleum imports by at least 5%.
4. To further improve the brake thermal efficiency of the engine as integrated into the vehicle. To demonstrate robustness and commercial viability of the HECC engine technology.

Accomplishments

- U.S. EPA 2010 steady-state oxides of nitrogen (NOx) emissions compliance achieved on the 15L ISX engine without NOx aftertreatment and 7% improvement in brake thermal efficiency against the 10% project objective.
- A 0.4 g/bh-hr NOx emissions level has been demonstrated on the 15L ISX for the U.S. EPA transient Federal Test Procedure (FTP) cycle with an improvement of 7% in brake thermal efficiency against the 10% project objective.
- U.S. EPA 2010 steady-state and transient NOx emissions compliance has been achieved without NOx aftertreatment for the 6.7L ISB engine while exceeding the 10% improvement in brake thermal efficiency project target.
- Analysis and design of additional subsystem technology for the 15L ISX have been completed to enable full U.S. EPA NOx emissions without NOx aftertreatment while achieving the target 10% improvement in brake thermal efficiency.
- Analysis and design of additional subsystem technology for the 6.7L ISB have been completed to enable additional 5% improvement in brake thermal efficiency.
- The design and procurement of a new generation of Cummins XPI high pressure common rail fuel system has been completed.
- Advanced turbomachinery has been designed and procured to provide fast transient response that is expected to allow engine-out transient NOx emissions compliance with acceptable particulate matter for the 15L ISX engine.
- A new exhaust gas recirculation (EGR) cooling system has been designed and tested that provides 3% to 4% fuel economy improvement on the 15L ISX and 6.7L ISB engines.
- A new analysis tool was created that can be used to simulate the engine system (air handling, EGR system, combustion, etc.), aftertreatment (diesel oxidation catalyst and diesel particulate filter), sensors, and controls algorithms over transient duty cycles.
- New model-based air handling and combustion control algorithms have been created for the 15L and 6.7L engine applications.
- HECC engine technology developed as part of this project has been shown to be robust for fuel economy and emissions with variations in diesel fuel properties representative of commercially available fuels in the marketplace. However, fuel sensing technology is required to maximize the fuel economy benefit for the HECC technology enabling changes in the engine controls strategy.
- The fuel economy benefits associated with the HECC engine technology developed can not be maintained when using biofuels at constant NOx emissions. However, a reduction of 20% to 40% in particulate matter can be achieved with the use of biofuels.
- The impact of biodiesel blends on NOx emissions have been explored extensively for a wide variety of engine technology and engine duty cycles.

Future Directions

- Multi-cylinder engine testing of advanced turbomachinery (electronic boosting, 2-stage turbocharging, and supercharging).
- Multi-cylinder engine testing of advanced EGR cooling system (EGR pump, 2-stage cooling, variable displacement pumps, etc.).
- Evaluation of variable valve actuation (VVA) including cylinder deactivation.
- Evaluation of piezo, common rail, fuel systems at high injection pressures.
- Development of combustion control using cylinder pressure sensor and VVA.
- Completion of calibration development of the 15L ISX and 6.7L ISB engines with advanced subsystem technology identified during the exploratory development phase of the program.
- Fuel economy and emissions robustness evaluation of HECC engine architectures operating on a wide variety of biofuels (soy, rapeseed, palm, mustard, and coconut).
- Evaluation of real and virtual fuel sensing technology for HECC engine architectures.
- The impact of biofuels on diesel particulate filters will be explored.
- Development of on-board diagnostics associated with the implementation of the new HECC subsystem technology to function properly during in-use.

Introduction

Cummins Inc. is engaged in developing and demonstrating advanced diesel engine technologies to significantly improve the engine thermal efficiency while meeting U.S. EPA 2010 emissions. The essence of this effort is focused on HECC in the form of low-temperature, highly premixed combustion in combination with lifted flame diffusion controlled combustion. Reduced equivalence ratio, premix charge in combination with high EGR dilution has resulted in low engine-out emission levels while maintaining high expansion ratios for excellent thermal efficiency. The various embodiments of this technology require developments in component technologies such as fuel injection equipment, air handling, EGR cooling, combustion, and controls. Cummins is committed to demonstrating commercially viable solutions which meet these goals.

In addition to the engine technologies, Cummins is evaluating the impact of diesel fuel variation on the thermal efficiency, emissions, and combustion robustness of the HECC technology. Biofuels are also being evaluated as part of the fuels study to determine if the thermal efficiency improvements and emissions compliance can be maintained.

Approach

Cummins' approach to these objectives continues to emphasize an analysis-led design process in nearly all aspects of the research. An emphasis is placed on modeling and simulation results to lead the way to feasible solutions.

Three areas of emphasis that lead to substantial improvements in engine thermal efficiency are the minimization or elimination of the engine aftertreatment, the maximization of the closed cycle efficiency, and the reduction of the open cycle losses and engine parasitics. Engine system solutions to address the three areas of emphasis include air handling schemes, control system approaches, EGR cooling strategies, and fuel system combinations. Based on analysis and limited engine testing, subsystem component technologies are identified for further development. Cummins is uniquely positioned to develop the required component technologies via the Cummins Component Business unit. A variety of laboratory tests are conducted to verify performance and to tune system functions. Model predictions are verified and models are refined as necessary. Often, different portions of the system are pre-tested independently to quantify their behavior and their data are analyzed in a model-based simulation before combined hardware testing is conducted. Concurrent to laboratory testing and tuning, a vehicle system demonstration is planned and prepared. Once satisfactory test cell system performance is verified, the vehicle demonstration is conducted.

Data, experience, and information gained throughout the research exercise will be applied wherever possible to the final commercial products. Cummins intends to continue to hone its technical skill and ability through this research while providing satisfactory results for our customers. Cummins continues to follow this cost-effective, analysis-led approach both in research agreements with the Department of Energy as well as in its commercial product development. Cummins feels this common approach to research effectively shares risks and results.

Results

During FY 2007, all Phase 2 milestone and deliverables have been met for the Cummins HECC project with the successful close-out of the Phase 2 work. The Phase 2 portion of the project focused on exploratory development of subsystems and related component technologies as depicted in Figure 1.

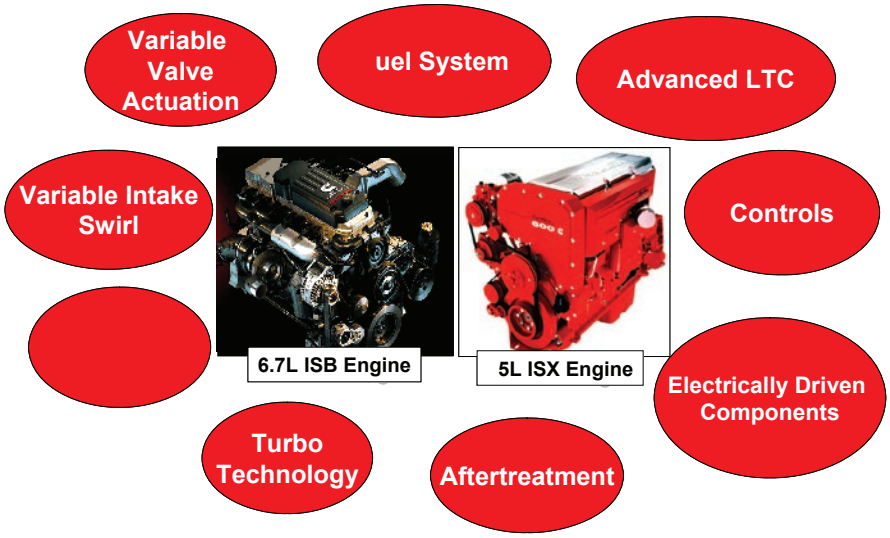

FIGURE 1. Cummins Component Business Technologies for High Efficiency, Clean Combustion

- A considerable amount of effort was concentrated on demonstrating significant fuel economy improvement on the 6.7L ISB engine used in light-duty engine applications in addition to the 15L ISX heavy-duty engine. The combustion strategy employed to achieve high efficiency is illustrated in Figure 2. The mixed mode combustion strategy relies on extending the early premixed charge, compression ignition (PCCI) combustion mode to encompass as much of the engine operating range as possible while implementing lifted flame diffusion controlled combustion for the remainder of the higher load operating range.

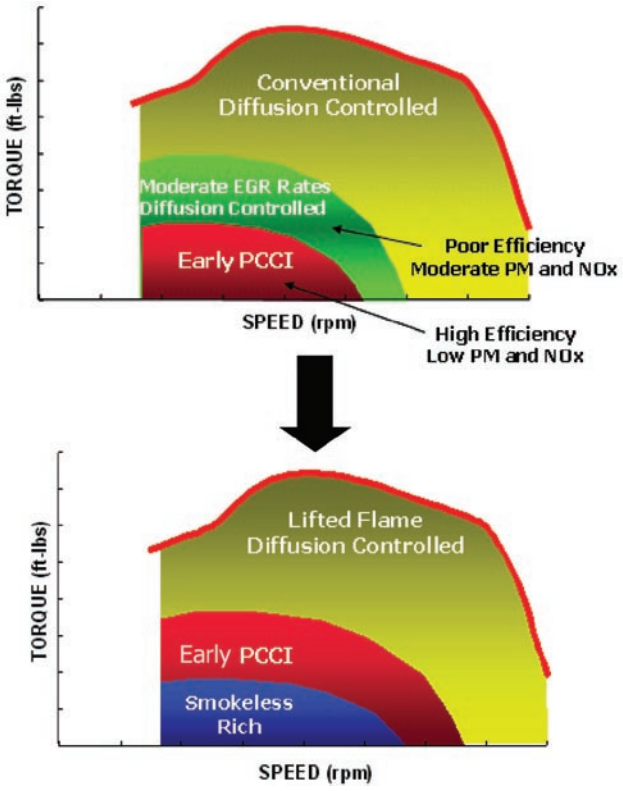

FIGURE 2. Mixed Mode Combustion Strategy for High Efficiency, Clean Combustion

- The fuel economy improvement targets have been exceeded for the ISB engine with low temperature, PCCI combustion technology that has demonstrated 2010 emissions capability (see Figure 3). An average of 12% fuel economy improvement has been realized. This is a significant accomplishment for the project. Additional engine technology has been explored during Phase 2 that is expected to provide an additional 5% fuel economy improvement that will be demonstrated in Phase 3 Multi-Cylinder System Integration portion of the project.
- Important fuel economy improvements have been achieved for the 15L ISX heavy-duty engine. The majority of the collaborative effort during Phase 2 has been concentrated on realizing high pressure injection, mixed-mode combustion. The specific engine technology explored in Phase 2 has demonstrated the ability to achieve steady-state emissions targets for 2010 assuming the availability of particulate filter aftertreatment. Transient emission results have been demonstrated, but are still above the target (approximately 0.4 g/bhp-hr NOx). Equivalent fuel economy improvement to baseline is 7% relative to a 10% project goal (including aftertreatment fuel penalty) as shown in Figure 4. It is anticipated that full engine-out transient emission targets will be difficult to achieve and further technology development will be necessary. Additional technology development in Phase 2 has been focused on advanced air handling systems to provide air on demand during transient engine

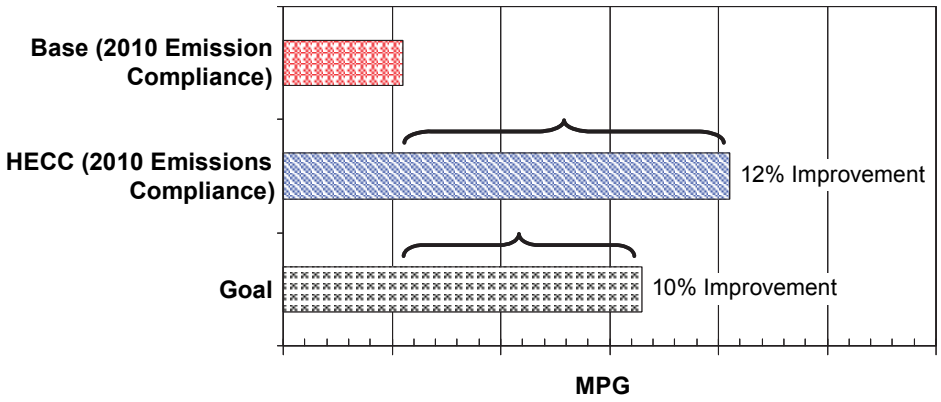

FIGURE 3. Fuel Economy Improvement of the HECC Engine Architecture for the 6.7L ISB Engine for Light-Duty Applications

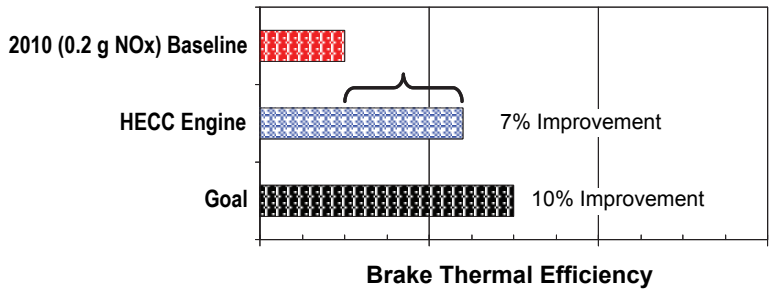

FIGURE 4. Thermal Efficiency Improvement for the 15L ISX Engine

operation. The advanced air handling systems include 2-stage turbocharging, electronic turbo, and supercharging. Other technology development explored in Phase 2 includes VVA, high frequency fuel injection, and EGR pumps. These technologies will enable full transient emissions compliance while meeting the project fuel economy target.

- The collaborative fuels study by Oak Ridge National Laboratory, Cummins and BP remained on plan during Phase 2 with the completion of the diesel fuels portion of the project. The fuel parameters selected for initial evaluation include cetane, aromatics, T10, and T90 distillation temperatures. Analysis of the ISB single-cylinder engine data collected at Cummins for the diesel fuels has been completed. The following conclusions have been formulated:
- Engine calibration parameters have the most significant impact on PCCI combustion compared to fuel properties.
- Lower cetane number fuels provided the best emissions and fuel economy results for PCCI combustion.
- Expected issues with PCCI combustion robustness at off-nominal engine operation such as cold ambient conditions with the expected variation in commercially viable ultra-low sulfur diesel fuel:
  - Unburned hydrocarbon and carbon monoxide emissions.
  - Diesel oxidation catalyst can be used to make PCCI emissions robustness possible.
  - Fuel economy deterioration expected.
  - Closed-loop combustion control is needed to offset fuel economy impact.

Conclusions

- During FY 2007, all Phase 2 milestone and deliverables have been met for the Cummins HECC project with the successful close-out of the Phase 2 work. Accomplishments include:
- U.S. EPA 2010 steady-state NOx emissions compliance achieved on the 15L ISX engine without NOx aftertreatment and 7% improvement in brake thermal efficiency against the 10% project objective.
- A 0.4 g/bh-hr NOx emissions level has been demonstrated on the 15L ISX for the U.S. EPA FTP cycle with an improvement of 7% in brake thermal efficiency against the 10% project objective.
- U.S. EPA 2010 steady-state and transient NOx emissions compliance has been achieved without NOx aftertreatment for the 6.7L ISB engine while exceeding the 10% improvement in brake thermal efficiency project target.

- Analysis and design of additional subsystem technology for the 15L ISX have been completed to enable full U.S. EPA NOx emissions without NOx aftertreatment while achieving the target 10% improvement in brake thermal efficiency.
- Analysis and design of additional subsystem technology for the 6.7L ISB have been completed to enable additional 5% improvement in brake thermal efficiency.
- The design and procurement of a new generation of Cummins XPI high pressure common rail fuel system has been completed.
- Advanced turbomachinery has been designed and procured to provide fast transient response that is expected to allow engine-out transient NOx emissions compliance with acceptable particulate matter for the 15L ISX engine.
- A new EGR cooling system has been designed and tested that provides 3% to 4% fuel economy improvement on the 15L ISX and 6.7L ISB engines.
- A new analysis tool was created that can be used to simulate the engine system (air handling, EGR system, combustion, etc.), aftertreatment (diesel oxidation catalyst and diesel particulate filter), sensors, and controls algorithms over transient duty cycles.
- New model-based air handling and combustion control algorithms have been created for the 15L and 6.7L engine applications.
- HECC engine technology developed as part of this project has been shown to be robust for fuel economy and emissions with variations in diesel fuel properties representative of commercially available fuels in the marketplace. However, fuel sensing technology is required to maximize the fuel economy benefit for the HECC technology enabling changes in the engine controls strategy.
- The fuel economy benefits associated with the HECC engine technology developed can not be maintained when using biofuels at constant NOx emissions. However, a reduction of 20% to 40% in particulate matter can be achieved with the use of biofuels.
- The impact of biodiesel blends on NOx emissions have been explored extensively for a wide variety of engine technology and engine duty cycles.

FY 2007 Publications/Presentations

1. "Enabling Technology for High Efficiency, Clean Combustion", Semi-Mega Merit Review presentation, Donald Stanton, 2007.

2. "Integration of Diesel Engine Technology to Meet US EPA 2010 Emissions with Improved Thermal Efficiency," DEER Conference, Donald Stanton, 2007.

3. "Effect of a 20% Blend of Methyl Ester Biodiesel on NOx Production," SAE 2008-01-0078, Stanton et. al, 2008.

4. Cummins Inc. Monthly and Quarterly Reports as submitted to the Department of Energy.

II.A.18 High Efficiency Clean Combustion (HECC) Advanced Combustion Report

David Milam
Caterpillar, Inc.
PO Box 1875
Peoria, IL 61656-1875

DOE Technology Development Manager:
Roland Gravel

NETL Project Manager: Ralph Nine

Subcontractors:
- ExxonMobil, Paulsboro, NJ
- Sandia National Laboratories, Livermore, CA
- IAV Automotive, Detroit, MI
- eServ, Peoria, IL

Objectives

Overall objective is to develop clean combustion technologies that achieve the highest possible brake thermal efficiencies. The approach Caterpillar and its partners are using is a form of homogeneous charge compression ignition (HCCI). The Phase 2 effort is divided into seven areas with the following objectives:

Sandia Optical Experiments: Utilize state-of-the-art optical diagnostics at Sandia National Laboratories to image the HCCI combustion process to gain a fundamental understanding of the mixing and combustion process.

Advanced Fuel System Concept Identification and Selection: Develop state-of-the-art fuel injection technologies to enhance the mixing and combustion process for HCCI.

Fuel Property Effects: Collaborate with ExxonMobil to understand the effects of fuel property changes on fuel/air mixing, combustion, emissions and thermal efficiency in HCCI engines.

Cooling System and Heat Rejection Analysis: Develop technologies to mitigate the air and water heat rejection increases associated with HCCI.

Advanced Controls Algorithm Development: Develop required sensors and advanced controls techniques to successfully achieve transient operation on multi-cylinder HCCI engines.

Combustion CFD Model Development Activities: Develop and validate combustion computational fluid dynamics (CFD) modeling tools so they are fully predictive and can be used to provide fundamental understanding of the mixing and combustion processes, design hardware and limit the required testing.

Combustion Development for Advanced Multi-cylinder HCCI Engines: Develop and demonstrate the advanced multi-cylinder engine technologies necessary to achieve the overall project objective.

Accomplishments

- Phase 2 optical diagnostic experiments complete.
- Single-cylinder engine fuels testing on low-cetane diesel boiling-range fuels completed.
- Prototype fuel injection system developed and tested on single-cylinder engine demonstrating ultra-low NOx and smoke emissions.
- Advanced multi-cylinder engine with compression ratio flexibility developed and tested demonstrating benefits for emissions, efficiency and controls.

Future Directions

- Continue optical engine tests to further develop fundamental understanding of low-temperature combustion.
- Improvements to further advanced fuel system capability and demonstration of benefits.
- Additional fuels effects testing to discern fuel property effects.
- Refine and validate improved CFD sub-models.
- Refinement of control strategies and implement on advanced multi-cylinder engines.
- Investigation of mixed mode combustion to utilize part-load HCCI with other low-temperature combustion for higher operating modes.

Introduction

Maintaining and improving fuel efficiency while meeting future emissions levels in the diesel on-road and off-road environments is an extremely difficult challenge but is necessary to maintain the level of customer value demanded by the end-users of compression ignition engines. Caterpillar® is currently engaged with several partners to address this challenge using advanced low-temperature combustion. This project provides a fundamental understanding of the in-cylinder fuel/air mixing and combustion process through advanced

optical diagnostics and CFD. We are also actively developing new fuel injection, controls, heat rejection reduction and engine technologies to enable this clean, efficient combustion. We are exploring the impact of different fuel types to understand the robustness of this combustion process to fuel variability. Successful completion of this project will provide Caterpillar and DOE with a clear understanding of the technology hurdles that must be overcome to increase the thermal efficiency and reduce emissions on future compression ignition engines.

Approach

In Task 1, we conducted fundamental optical diagnostic tests at Sandia National Laboratories on the single-cylinder optical research engine (SCORE) which is a derivative of a Caterpillar 3171 single-cylinder test engine to better understand the fuel/air mixing and combustion/emissions process in an advanced HCCI engine. The engine was prepared for evaluation of the Caterpillar HCCI method. This preparation included installation of a simulated exhaust gas recirculation (EGR) system, installation of exhaust emissions measurement equipment, modification of the fuel injection hardware, and reconfiguring the base engine hardware to match the Caterpillar metal engine hardware. A baseline operating condition was established to match the metal engine data. A suite of optical techniques was then used to characterize the fuel-air mixing and combustion process for this baseline condition.

A research prototype fuel injection system was developed and validated on a fuel systems bench in Task 2. This piezo-based research common rail fuel system is capable of multiple fuel injections and >250 MPa injection pressure.

Applied research in the area of fuels effects is the subject of Task 3. This work builds upon the collaboration between Caterpillar and ExxonMobil to better understand fuel property effects on HCCI combustion. Prior to shipment of any fuels, standard fuel property tests and detailed chemical characterization of each fuel were performed by ExxonMobil. These fuels were evaluated for performance in Caterpillar metal engines.

The cooling requirements for the HCCI engine are higher than normal combustion, and the heat rejection from such a system is a significant challenge to deal with in “real world” applications. Task 4 included a comprehensive modeling effort that was initiated to understand and identify alternatives to mitigate this risk. Conventional and alternative heat exchanger designs for combustion gas intercoolers and charge air inter/after coolers were evaluated including gas-to-coolant, gas-to-air, separate circuit and primary surface heat exchangers.

Advanced controls work was completed on a multi-cylinder engine in Task 5. This work included developing cylinder pressure-based feedback control architecture, utilizing intake valve actuation to balance individual cylinders and using advanced strategies to limit pressure rise rate and improve transient accelerations. Advanced hardware for cylinder pressure data processing in real-time was developed and tested.

Task 6 involved model development activities to enhance current predictive capabilities in cycle simulation and 3D combustion simulation tools. This task included the development and validation of reduced kinetic mechanisms for use in these combustion simulation calculations to model ignition, combustion, and pollutant formation. The optical diagnostic results from Task 1 were to be used to validate and tune the models of the combustion process to enable future HCCI combustion development in a virtual environment. The goal is to accurately simulate all of the important processes in HCCI combustion. In particular, the goal is to represent the spray droplet size and spatial distribution, the fuel vapor distribution, wall film thickness and location, combustion, and emissions formation accurately as they occur in a diesel engine. With a more complete model of the HCCI process, modeling activities then focused on refinement of piston bowl and spray geometries to minimize hardware procurement.

An advanced multi-cylinder HCCI engine was also developed and tested in Task 7. This engine has full variable compression ratio flexibility as well as variable valve timing flexibility. It has been used to demonstrate the performance, emissions and controls benefits such an engine can potentially offer.

Results

Task 1- Sandia Optical Engine Experiments: Many upgrades to the laboratory were completed in the first full year of the project. During this year, the SCORE head utilized in the HECC work was fitted with sealed valve guides to reduce the amount of lube oil entering the cylinder in order to bring the SCORE smoke levels closer in line with those observed in the single-cylinder test engine (3401 single-cylinder test engine) at Caterpillar. Cycle-integrated natural luminosity (CINL) imaging at 1,200 rpm, 300 kPa, 400 kPa, and 500 kPa conditions was completed to verify the sealed valve guide design. These images were collected and compared to the images in last year’s report. The CINL images do not show the bright spots indicative of lube oil combustion as previously noted.

Shortly after work on this project commenced, it became evident that a peak cylinder pressure (PCP) capability of 20 MPa would be necessary to study high-load operating conditions of interest. This amounts to

nearly doubling the PCP capability of the optical engine. Thus, all the combustion chamber components require re-evaluation for safe operation at 20 MPa PCP. Work continues on this task.

A new set of nozzles was delivered to Sandia in May 2007. This set of nozzles was matched to the flow rate of the nozzle used in the first two years of the HECC collaboration. Emissions and performance data as well as high-speed camera spray visualization, and natural luminosity images were collected with diesel fuel in the SCORE. Sweeps of load, injection timing, injection pressure, EGR level, boost and equivalence ratio were collected. Apparent heat release rate, spatially-integrated natural luminosity, and emissions data were collected. In-cylinder natural luminosity movies were collected using a Phantom V7.3, 14-bit, high-speed camera. Two camera views were utilized to provide the best possible spatial information about the bright soot luminosity. The first camera view is in through a cylinder-wall window. The second view is up through the piston window utilizing the Bowditch piston extension of the SCORE engine.

Figure 1 shows the injection spray visualizations with diesel fuel. From the image, fuel interaction with the piston bowl can be observed in the second and third rows of images. Figure 2 shows selected frames from the cylinder window view high-speed natural-luminosity movie. From Figure 2 it is clear that the soot luminosity begins with many small dots spread throughout the height of the piston bowl near top-dead-center (TDC), and then rapidly shifts to the bottom surface of the piston bowl where the intensity greatly increases. These results along with the spray visualizations substantiate the claim of diesel fuel jets impinging on the surface of the piston bowl are a significant factor in soot emissions.

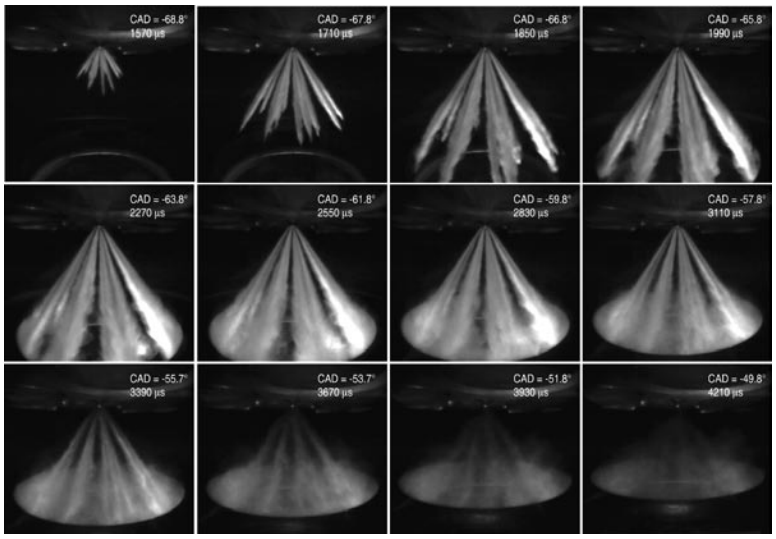

FIGURE 1. Injection spray visualization images acquired illustrating liquid fuel interaction with the piston bowl.

Task 2 - Advanced Fuel System Concept Identification and Selection: An advanced common rail fuel system was developed to enable low emissions and high efficiency combustion. The first version (Phase 1) features the ability to perform pilot injections of less than 5 mm^3 at rail pressures greater than 250 MPa with dwell between injections of less than 200 microseconds. The Phase 1, piezo-actuated injector has been fully characterized on the single-cylinder test engine. Several discrete tests have been successfully completed, which have demonstrated the benefits of the high injection pressure, and the multiple injection strategies, facilitated by this advanced injector. During this year, the work focused on HCCI combustion development utilizing the injection pressure and multiple injection capabilities of the advanced piezo injector design. As a baseline, single-shot HCCI combustion was studied over a range of injection pressures and timings while holding phasing, intake manifold pressure, intake temperature, and load constant. This baseline data provides insight into the fundamental injection parameters that affect HCCI combustion. The second set of experiments focused on multiple injection strategies to reduce the amount of EGR required for phasing and heat release of HCCI by increasing the mixture homogeneity through earlier injection timings. The results are shown in Figures 3 and 4 and indicate the effectiveness of advanced injection strategies. In addition, some simple spray modeling and spray visualization was performed to provide insight into the engine out emissions.

Task 3 - Fuel Property Effects on Emissions and Combustion Phasing: Significant progress was made towards understanding the effects of fuel properties on the operability and emissions of a heavy-duty engine performing under HCCI conditions. Five fuels in the diesel boiling range were prepared covering a wide range of fuel ignition quality and hydrocarbon composition. These fuels were developed using blend recipes with available fuels and fuel components. Fuel additives were included in each blend to ensure sufficient lubricity of engine components and fuel stability. After blending, all test fuels were subjected to a thorough analytical characterization, with particular emphasis on ignition quality, distillation/volatility, elemental composition (*e.g.,* sulfur content), and hydrocarbon composition, especially aromatics content. The ignition quality of the fuels was determined by both the cetane number, measured using ASTM method D613, and the derived cetane number (DCN), measured by the ignition quality tester using ASTM method D6890. The blended fuels covered a range of ignition quality from a DCN of 24.2 to 45.2.

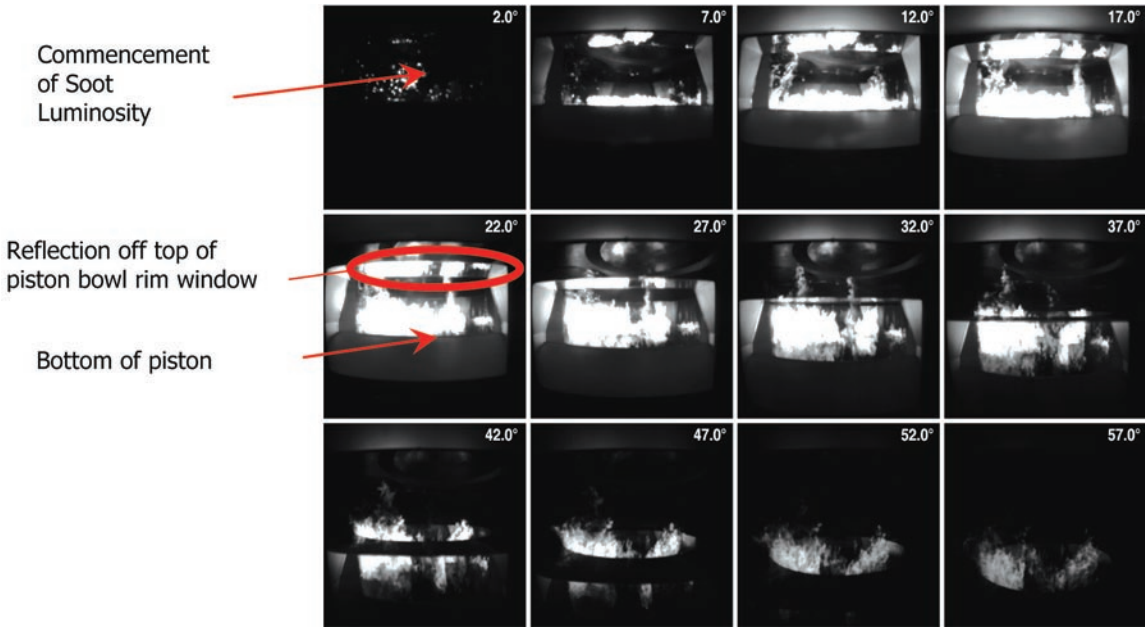

FIGURE 2. Natural luminosity images acquired illustrating liquid fuel impingement on the piston bowl as a significant factor for soot emissions.

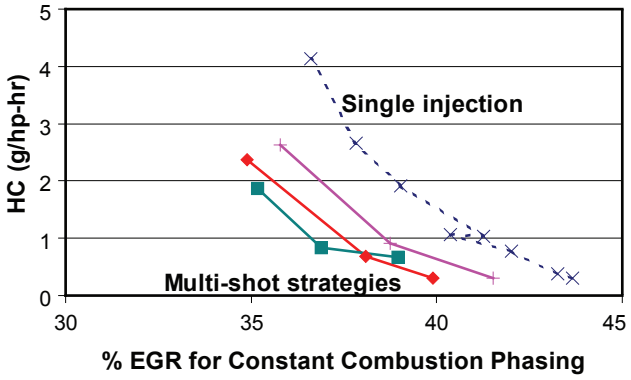

FIGURE 3. Multi-shot strategies using a Phase 1 advanced injector resulted in lower unburned hydrocarbon emissions.

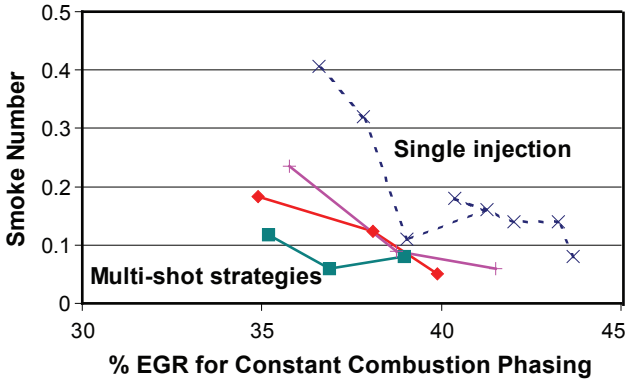

FIGURE 4. Multi-shot strategies using a Phase 1 advanced injector resulted in lower smoke emissions.

All five diesel boiling-range fuels were engine-tested in the Caterpillar 3401E single-cylinder oil test engine under HCCI conditions using a compression ratio of 14:1. This engine is rated at 62 kW at 1,800 rpm, and is equipped with a flexible air handling system, which includes intake boost temperature and pressure along with exhaust backpressure. The fuel injector is a Caterpillar hydraulically actuated electronically controlled unit injector, which allows for injection pressures up to 150 MPa.

In determining the minimum and maximum loads which could be achieved with each test fuel, several experimental limits were imposed based on the mechanical limitations of the engine, future emissions regulations, and heat rejection/packaging constraints. Figure 5 shows the operability results, which were attained as a function of the ignition quality of the fuel at an engine speed of 1,200 rpm. For the diesel fuel with a DCN of 45.2 (ignition quality representative of typical U.S. diesel fuel), a maximum load of nearly 1,000 kPa was achieved. However, the maximum load which could be attained generally increased as the ignition quality of the fuel decreased. The highest load was achieved for the fuel with the lowest DCN (24.2), which corresponds to an ignition quality well below that of conventional diesel fuel.

Differences in the hydrocarbon composition of the fuel were observed to have no significant effect on HCCI operability for the five fuels tested. The only fuel property, which was found to have a significant effect on operability, was the ignition quality of the fuel. In terms of emissions, fuel properties did not influence oxides of

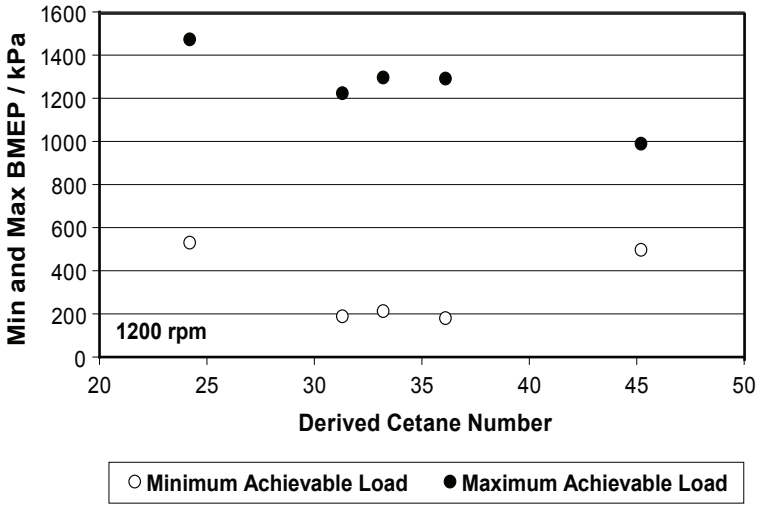

FIGURE 5. Engine Operating Range vs Derived Cetane Number (CR=14)

nitrogen (NOx), hydrocarbon (HC), or carbon monoxide emissions; however, a fuel with a lower aromatics content did show some modest benefit in reducing particulate matter emissions at high loads, compared to a fuel with a substantially higher aromatics content.

Task 4 - Cooling System and Heat Rejection Analysis: The goal of this work is to mitigate the increase in jacket water heat rejection (JWHR) with advanced combustion strategies in the cylinder liner and head by developing a process utilizing analytical tools which accurately predict heat transfer inside the engine. Once prediction capability is achieved, the cooling circuit passages can be designed to minimize heat transfer, while still maintaining structural life of the engine due to thermal cycling. The end-user benefit due to reduced heat rejection is a smaller frontal area cooling system and/or reduced fuel burned for cooling fan parasitic power. The premise is that the current structural development process utilizes coolant flow to keep the hottest areas of the engine (top land of liner and valve bridges) below material property design limits, and to achieve a desired structural life with combined assembly stresses plus thermal stress gradients. All excess jacket water (JW) pump flow is forced through the block and liner, resulting in overcooling of much of the iron and absorbing more JW heat than is necessary. Reduction in JWHR comes through reducing velocities of coolant in overcooled areas; hence the term "Precision Cooling". Success is only achieved by the integration of engine performance, JW coolant flow, and core engine cooling - including the prediction of boiling and structural analyses.

The method for developing predictive analysis tools for precision cooling JWHR has been to make the analytical prediction on a well defined baseline engine (Caterpillar C15) as well as its external cooling system, run appropriate tests, and then correlate/tune the analysis models to match test results. This preliminary step has been completed. Once this capability is achieved, then design changes to the coolant passages of the engine can be made analytically with design iterations, possibly with optimization software, to minimize JWHR. The impact on structural life will also be predicted and compared with a baseline prediction. The reduction in heat load benefit can then be quantified by modeling in terms of external cooling system fan parasitic fuel consumption or a reduction in frontal area.

Task 5 - Advanced Controls Algorithm Development: A rapid prototyping system was developed for controls development using Matlab/Simulink software for model building and code generation. The rapid-prototyping hardware consists of an xPC™ target box equipped with CAN™ cards and a Caterpillar-designed programmable field programmable gate array (FPGA) card enabling processing of speed-timing pulses from the crank/cam targets and generation of the output pulses needed for the various engine sub-systems such as fuel injection. In order to implement the control models into this real time engine controller, a fast and reliable data acquisition system that can capture crank angle based in-cylinder pressure values for combustion-timing feedback is required. The first device used to accomplish high-speed sampling of in-cylinder pressure sensors was based on FPGA chips. The former data acquisition system had robustness issues resulting in an occasional dropped data point or a corrupted crank angle measurement. Moreover, it was limited in its functionality. Its only purpose was to transfer the pressure measurements to the xPC™, which then performed all of the required calculations for desirable parameters (maximum pressure, crank-angle for maximum pressure, maximum pressure rise rate, and crank-angle for maximum pressure rise rate). In the new, microcontroller-based data acquisition (DAQ) system, all such calculations are performed within and only the desired parameters are passed to the real-time controller (xPC™) ensuring significant reduction in overhead on the real-time controller.

Experimental results for in-cylinder pressure are obtained from a single-cylinder engine running in HCCI combustion mode at different engine speeds. The new DAQ system results are benchmarked against the AVL™ Indimeter results obtained simultaneously. The microcontroller results show excellent match with the AVL™ results. Performing statistical analysis on the 100 cycles averaged maximum pressure rise rate values, as acquired by both AVL™ and the microcontroller-based

DAQ system, it is observed that the microcontroller-based DAQ has significantly less errors. Hence it is concluded that the microcontroller-based DAQ system is sophisticated enough to perform fast and robust pressure data sample and at the same time perform calculations on the acquired pressure data to determine parameters of interest (maximum rate of pressure rise and its crank angle).

The DAQ system is then coupled with the xPC™-based feedback controller to control combustion phasing at a desired crank angle while other control factors (like injection timing, etc.) are varied. One such experimental result is shown in Figure 6. Excellent control of combustion phasing is obtained at the desired combustion-phasing angle of 1 crank angle degree before TDC while the fuel injection timing is varied. In the next phase development of a similar DAQ system for a multi-cylinder (up to six cylinders) engine is planned. Initial hardware layout and communication protocols are selected. Software development efforts are underway. Once the software development is complete, validation using engine test data is planned.

Demonstration of transient operation of an HCCI engine has been completed. Five different control inputs are identified that can affect the transient operation of the HCCI engine. These are compression ratio (CR), intake valve actuation (IVA, for the purpose of this report it is the crank angle at which intake valve is closed), EGR, fuel injection pressure and end of injection angle. All of these parameters can be controlled in real time using our existing control architecture.

In order to best model the system, models must be developed that account for multiple inputs and non-linear behavior. Artificial neural networks have been chosen as one option to provide the level of accuracy and computational efficiency required. A neural networks-based approach requires collecting a diverse set of output data (emissions and performance) for a widely varying range of input parameters. Hence, a map-based approach is followed to accommodate different sets of input maps for a widely varying range of input parameters. A key requirement in successfully capturing the system response in a data-driven approach (like neural network based modeling) is to collect output data for almost all possible input parameters combinations. Since it is not realistically possible to exploit all possible input combinations, a large number of maps were generated to accommodate sufficient combinations of input parameters. Transient operations of a multi-cylinder HCCI engine within two points in the engine operation, with different control maps, are realized. These transients provide understanding of the effects of different control parameters on performance parameters during transients. This understanding helped in developing better maps for control parameters, which allowed improving engine performance during transients. The input-output data recorded during these transients are also utilized to develop the neural network based model for the engine. This model is used to perform multi-variable optimization on different input parameters and can be instrumental in developing optimum transient control strategies for HCCI engines.

Task 6 - Combustion CFD Model Development Activities: Significant improvements in the areas of liquid to gas momentum exchange, wall film treatment, and chemical kinetics have been made to the in-house CFD-code, CAT3D. This has made it possible to apply the tool to gain a deeper understanding of the physical processes underlying HCCI combustion. Simulations of the Caterpillar metal and Sandia optical engines have provided valuable insights into the mixing and combustion processes. The CFD tool has been used to design combustion systems (piston bowls and spray angles) for the single and multi-cylinder engines.

Task 7 – Combustion Development for Advanced Multi-cylinder HCCI Engines: A new variable compression ratio (VCR) engine was built and tested. The operational limits of the VCR HCCI engine were examined at two different engine loads. Specifically, the engine was run at numerous combinations of compression ratio, EGR fraction and IVA that yielded a combustion phasing of 2 degrees after TDC. Intake temperature and fuel injection timing, which are the other two parameters that can affect combustion phasing in this particular engine, were held constant for those tests. Tests were conducted at operating conditions as seen in Figure 7. In general,

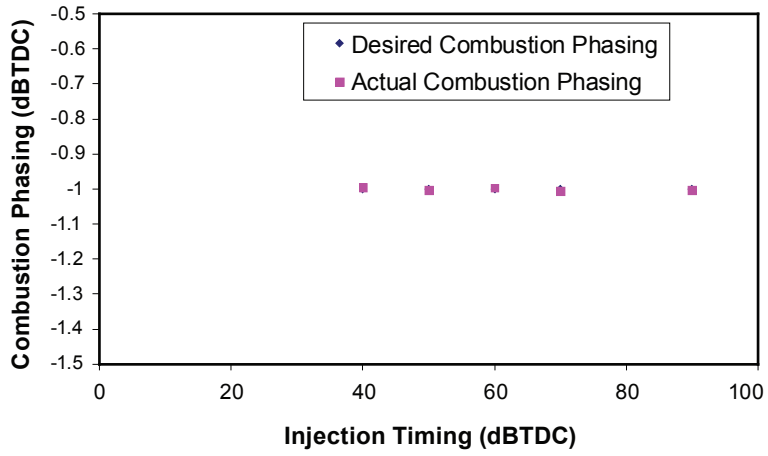

FIGURE 6. Utilizing the microcontroller-based DAQ system and real time engine controller, the combustion phasing is controlled at desired combustion phasing while injection timing is varied.

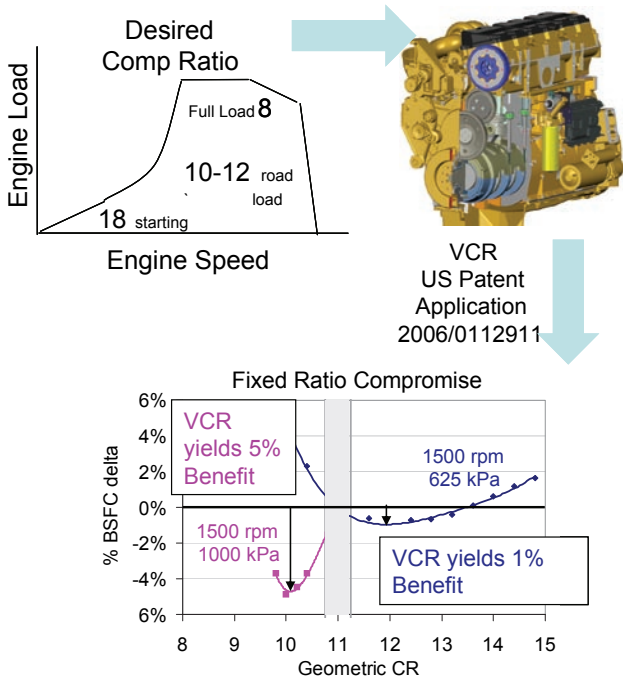

FIGURE 7. Utilizing the VCR engine, the compression ratio for each operating point can be optimized.

the range of IVA, EGR and CR settings over which the engine could run with a near-TDC combustion phasing was limited by either pressure rise rates, combustion retard, air-fuel ratio, NOx emissions or VCR mechanism limitations. The first sweeps were for three different combustion phasings from a baseline operation of fixed compression ratio, EGR fraction and IVA setting, which represented the best fuel consumption point at B25. The first sweep of combustion phasing was obtained by varying IVA from its baseline value while holding compression ratio and EGR constant. The second sweep was obtained by varying the compression ratio from its nominal setting while holding IVA and EGR constant, while the third sweep was obtained by varying EGR from its nominal setting while holding IVA and compression ratio constant. This set of data explored the effects of combustion phasing and highlighted the differences between the various methods by which the desired combustion phasing can be achieved. The second set of data consists of several EGR sweeps, each at a different combustion phasing value. This new data set illustrated how the limits of engine operation change for different values of combustion phasing. An understanding of this is required to get the complete picture of the interaction between CR, EGR, IVA and combustion phasing. To further support increased understanding of these fundamental trade-offs, the same approach was used on additional single-cylinder test engine work.

Conclusions

Significant progress was demonstrated on all tasks. See Accomplishments:

- Phase 2 optical diagnostic experiments complete.
- Single-cylinder engine fuels testing on low-cetane diesel boiling-range fuels completed.
- Prototype fuel injection system developed and tested on single-cylinder engine demonstrating ultra-low NOx and smoke emissions.
- Advanced multi-cylinder engine with compression ratio flexibility developed and tested demonstrating benefits for emissions, efficiency and controls.

FY 2007 Publications/Presentations

1. Q1, Q2, Q3, Q4 Quarterly reports
2. Presentation at 2007 DOE Merit Review
3. Presentation at 2007 DOE DEER Conference

Special Recognitions & Awards/Patents Issued

1. Ignition Timing Control with Fast and Slow Control Loops (IVP and EGR).
2. Mixed High and Low Pressure EGR in HCCI Engine.
3. Strategy for Extending the HCCI Operation Range using Low Cetane Number Diesel Fuel and Cylinder Deactivation.
4. Recipe for High Load HCCI Operation.
5. Caterpillar, Power Balancing Cylinders in HCCI Engine.

II.A.19 Low-Temperature Combustion Demonstrator for High Efficiency Clean Combustion

William de Ojeda, PhD, P.E. (Primary Contact), Philip Zoldak, MASc.
International Truck and Engine Corporation
10400 W. North Avenue
Melrose Park, IL 60160

DOE Technology Development Manager: Kenneth Howden

NETL Project Manager: Samuel Taylor

Subcontractors:
- Lawrence Livermore National Laboratory, Livermore, CA
- ConocoPhillips, Portland, OR
- University of California, Berkeley, CA
- FEV, Auburn Hills, MI

Objectives

- Demonstrate engine performance with conventional power density (12.6 bar brake mean effective pressure [BMEP].
- Demonstrate ability of engine operation over transient emission cycles.
- Attain compatibility with exhaust aftertreatment devices.
- Achieve U.S. 2010 engine-out emissions without aftertreatment.
- Achieve competitive efficiency over conventional combustion.

Accomplishments

The present Phase III of the demonstrator project involves steady-state testing of a redesigned International 6.4L V8 engine with technology to support low-temperature combustion (LTC). Phase I consisted of a design phase involving combustion and engine cycle simulations to select the necessary hardware to run LTC to the power density of 12.6 bar BMEP. Phase II consisted of exploratory development of LTC with the base hardware while the hardware designed in Phase II was being procured. The fuel used is standard diesel fuel.

The key technologies implemented and function tested on the engine to date consists of:

- A custom charge air cooler (CAC) and intake heater bypass system,
- Multi-hole multi-row injector nozzles for better atomization and mixture,
- A range of compression ratio pistons,
- Improved flow cylinder head,
- Two-stage, dual-variable nozzle turbine (VNT) turbocharger system,
- Two parallel exhaust gas recirculation (EGR) coolers,
- Stand alone processor, programmed to schedule multiple injection pulses, control the EGR, VNT and CAC/bypass, with crank-angle-based data acquisition for cylinder pressure, and
- Combustion diagnostics and feedback control over start of combustion and torque on each cylinder.

Technologies being procured for future engine builds include:

- A variable valve actuation (VVA) system.
- A variable compression ratio (VCR) system.

Engine testing results include:

- Demonstrated LTC combustion up to 1,500 RPM and 6 bar BMEP, with plans to extend to the full range in the remaining portion of Phase III. Oxides of nitrogen (NOx) levels are limited to below 0.2 g/bhp-hr with soot levels below 2 mg/mm^3. Fuel efficiencies are comparable to 'conventional' operation.
- Critical to operating at LTC conditions are the integration of injection timing with high EGR levels and sufficient air-to-fuel ratios (AFRs). The engine controller plays a decisive role to maintain combustion phasing and avoiding misfire.

Future Directions

- Complete the engine builds and benchmark the attributes of the VCR and VVA prototypes.
- Conduct KIVA3V combustion simulation to further optimize combustion hardware.
- Continue to conduct steady-state testing to optimize combustion hardware for U.S. 2010 HD emission regulations. Special emphasis will be in fuel economy.
- Develop a prototype engine control unit to handle in-cylinder combustion diagnostics and feedback.

Introduction

LTC offers a new method of diesel combustion with the potential to reduce engine-out NOx and particulate matter (PM) emissions to levels that will meet the 2010 limits without the use of aftertreatment devices [1]. The benefits of LTC have been documented in the literature [2,3,4]: the capability to lower NOx emissions due to low combustion temperatures and improved fuel economy and lower soot emissions due to lean mixtures.

A challenge to LTC is the increased unburned hydrocarbon (HC) emissions from long mixing times due to local equivalence ratios (ϕ) below the lean combustion limit [5], from locally rich regions due to over fueling or injector dribble, and from decreasing in-cylinder temperatures as the piston moves away from top-dead-center. A second challenge for the application of LTC is the controllability of the ignition timing [6]. This is particularly challenging as a diesel mixture tends to ignite at relatively low temperatures and too abruptly.

Extending the operating region to high loads may require the introduction of VVA to adjust the effective compression ratio or preferably by VCR to adjust the geometric ratio.

Approach

Implementation of LTC will be integrated into the production engine using the following approach:

- Phase I (completed) consisted of applied research, determining engine boundary conditions, combustion system design and simulation.
- Phase II (completed) consisted of exploratory development, engine hardware procurement, engine subsystem prove out, control system hardware procurement, controls software development.
- Phase III (in progress) consists of advanced development, steady-state testing of engine, combustion hardware development, fueling strategy development, and further controls system development.
- Phase IV consists of transient testing and production engine control unit development.

Results

The engine is designed to run LTC combustion with equivalence ratios 0.3 to 0.4 with 50% EGR. The engine will allow a maximum torque of 670 Nm (12.6 bar BMEP) at 2,000 RPM. Figure 1 shows the engine schematic.

Unique to this project are injector drivers capable to tune current slope (mA/µs) and opening and closing voltage supplied to the piezo stack. A variety of multi-hole, multi-row nozzles were bench tested and

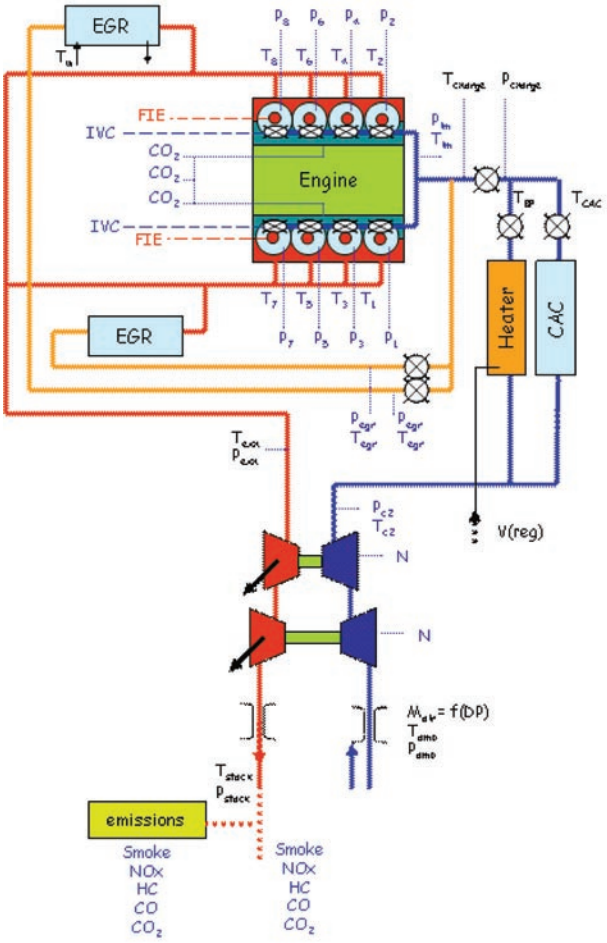

FIGURE 1. Test Engine Schematic

classified for their potential merits. Also unique, is that the controller optimizes the relative contribution of each turbocharger stage and coordinates the activity of the EGR valves. The rapid prototype system features cylinder pressure feedback control. Parts for the VVA system are being procured and are illustrated in Figure 2. Phase 3 of the project will yield two multicylinder V8 VCR prototype engines.

Test results to date have demonstrated LTC at 50% load or 6 bar BMEP. Operating at LTC involves flowing high EGR ratios, where combustion robustness depends on delivering sufficient AFR. Here the engine controller plays a decisive role to maintain combustion phasing and avoid misfire.

Figure 3 and 4 illustrate two LTC conditions at 1,500 RPM, 6 bar BMEP. The EGR rates are same, at 50%. In both cases, the controller is highly responsible for adjusting the injection timing to maintain the CA50 at 5° after top dead center. Despite good control over CA50, Figure 3 shows the combustion system at the edge of stability. The instability appears in cylinders 1 and 2, noticeably different from cylinder 3 through 8.

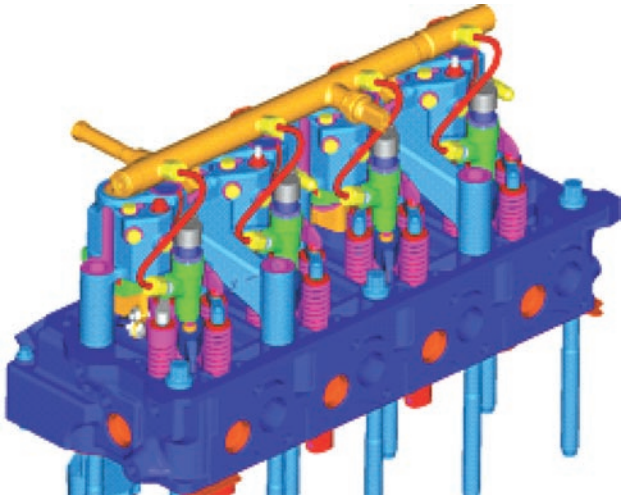

FIGURE 2. VVA Set-Up

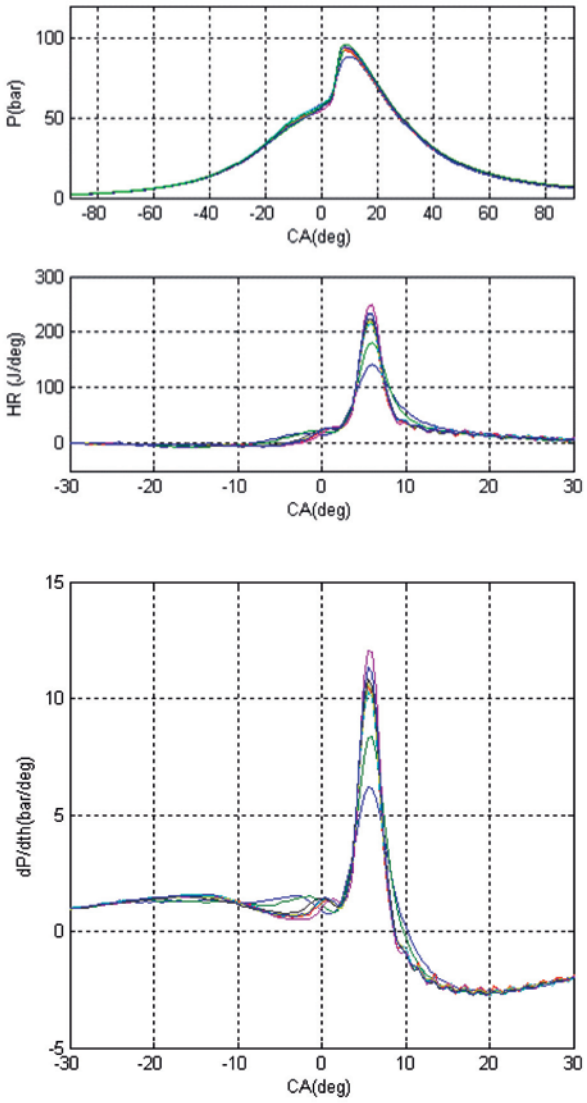

FIGURE 3. LTC at 1,500 RPM, 6 bar BMEP

Cylinders 1 and 2 display heat release traces (and dP/dtheta) characteristic of low oxygen concentrations (or higher EGR) with a stronger onset of a cool flame reaction. Figure 4 shows these cylinders becoming stable with increasing the boost and AFR. This issue illustrates the challenges of providing adequate EGR distribution in a real production-like application and the compensation techniques that may be implemented.

Figure 5 shows the performance and emissions corresponding to the speed and load above for varying engine configurations. Each subsequent hardware upgrade is capable of providing higher EGR rates. For the third configuration, corresponding to the above figures, demonstrates LTC conditions with 0.17 gNOx/bhp and 0.01 g/bhp-hr.

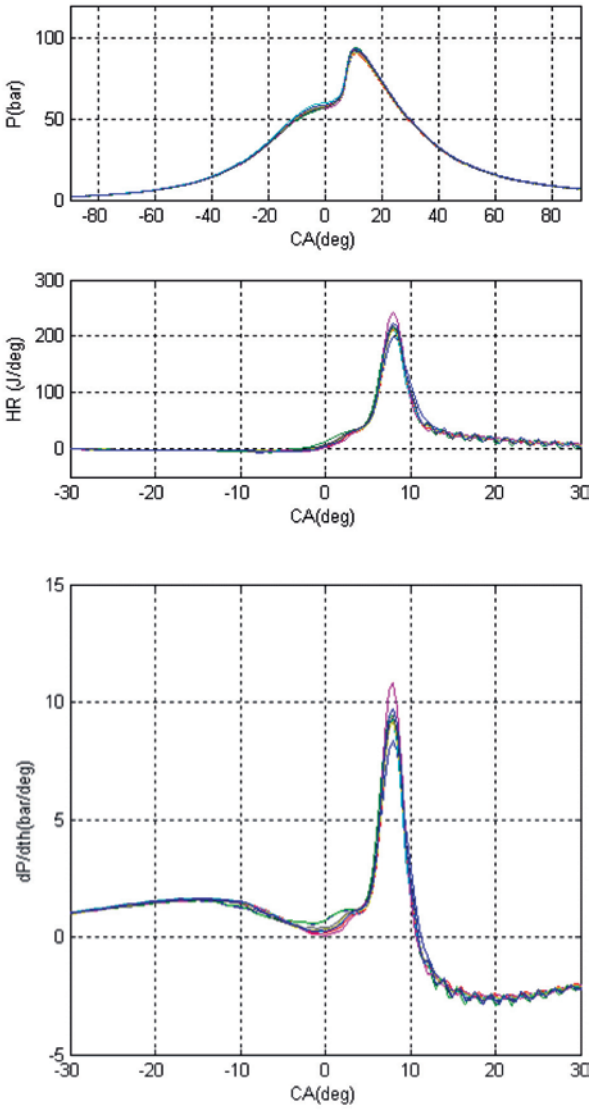

FIGURE 4. LTC at 1,500 RPM, 6 bar BMEP with AFR Adjustment

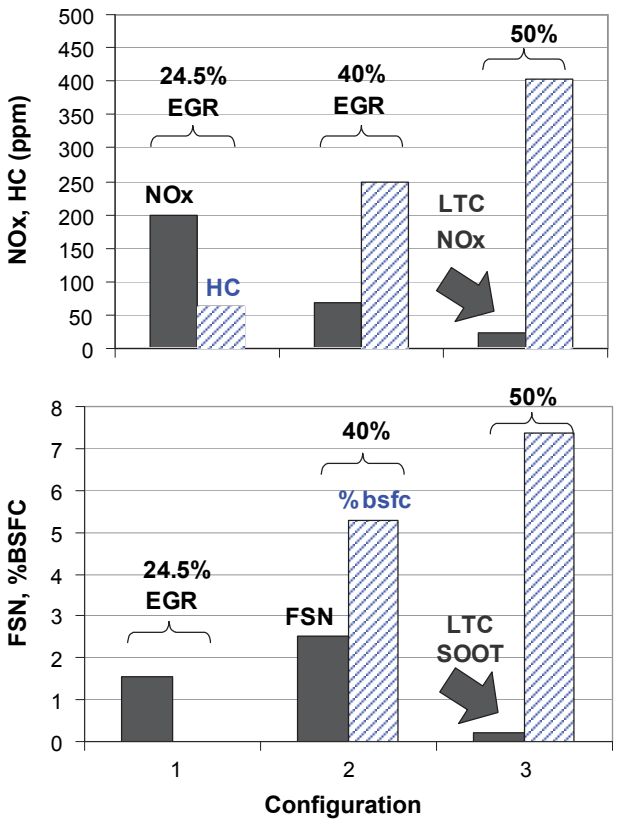

FIGURE 5. LTC NOx, Soot and Impact to BSFC (% Penalty), HC at 1,500 RPM, 6 bar BMEP

Conclusions

- To date, LTC-like emissions results were obtained up to 1,500 RPM and 6 bar BMEP, with plans to extend in the near future to 12.6 bar. NOx and soot levels were limited to 0.2 g/bhp-hr and 2 mg/mm^3, respectively.
- Integration of injection timing control with AFR is decisive to maintain combustion phasing and avoid misfire. Future work on either to detect or foresee misfire, and subsequent corrective action, will be critical to maintain combustion robustness.
- The present capability is owed to an optimum matching of engine hardware. The complete the engine build is still underway, however, with the design and procurement of the VCR and VVA prototypes.

References

1. Gui, Xinqun, "Project Narrative – Low Temperature Combustion Demonstrator for High Efficiency Clean combustion," International Truck and Engine Corporation, August 9, 2004.

2. Hasegawa, R., Yanagihara, H., "HCCI combustion in a DI Diesel Engine," SAE 2003-01-0745.

3. Takeda, Y., Kellchi, N., "Approaches to Solve Problems of Premixed Lean Diesel Combustion," SAE 1999-01-0183.

4. Akagawa, H., Miyamoto, T., Harada, A., Sasaki, S., Shimazaki, N., Hashizume, T., Tsujimura, K, "Approaches to Solve Problems of the Premixed Lean Diesel Combustion," SAE 1999-01-0183.

5. Musculus, M., Lachaux, T., Ticket, L.M., "End-of-Injection over-mixing and unburned hydrocarbon emissions in Low-Temperature-Combustion Diesel Engines," SAE 2007-01-0907.

6. P.L. Kelly-Zion, J.E. Dec, "A Computational Study of the Effect of Fuel Type on Ignition Time in Homogenous Charge Compression Ignition Engines", Proc. of the Combust. Inst., Vol. 28, pp. 1187-1194, 2000.

FY 2007 Publications/Presentations

1. de Ojeda, W., Zoldak, P., Espinosa, R., Kumar, R., "Development of a Fuel Injection Strategy for Diesel LTC", submitted to the 2008 SAE World Congress, Detroit.

2. de Ojeda, W., Zoldak, P., Espinosa, R., Kumar, R., Cornelius, D., "Multicylinder Diesel Engine Design for HCCI operation", Diesel Engine Development, DEER 2006, August 20-24, Detroit, Michigan.

II.A.20 21st Century Locomotive Technology 2007 Annual Report: Advanced Fuel Injection

Roy Primus (Primary Contact), Florian Pintgen, Jennifer Topinka, and Anthony Dean
GE Global Research
One Research Circle
Niskayuna, NY 12309

DOE Technology Development Manager: John Fairbanks

NETL Project Manager: Christopher Johnson

GE Project Manager: Lembit Salasoo

Objective

Develop and demonstrate an advanced fuel injection system to minimize fuel consumption, while meeting Tier 2 emissions levels.

Approach

- Use General Electric (GE) Global Research's locomotive single-cylinder engine as the experimental test facility.
- Determine baseline engine performance using current production unit pump system.
- Optimize engine performance with advanced high-pressure common rail (HPCR) fuel injection system.
- Investigate the hardware space (injector parameters, nozzle geometry, bowl shape) and fuel injection command sequence to determine most advantageous fuel injection strategy.
- Develop transfer functions and models, which guide and allow down-selecting the combinations of hardware and injection commands for various engine loads.

Accomplishments

- Installed new diagnostics tools. These include an opacity meter and an engine exhaust particle sizer (EEPS) for particulate matter (PM). In addition, an in-cylinder combustion visualization spray and flame characterization system was installed.
- Completed study to examine the effect of the following parameters on engine performance:
  - total nozzle flow,
  - number of nozzles holes,
  - spray cone angle,
  - needle seat diameter,
  - injector needle lift and fall rate,
  - piston crown geometry (two geometries studied), and
  - fuel sulfur level.
- Engine performance is evaluated by specific fuel consumption (SFC), nitrogen oxides (NOx) emissions, and PM emissions.
- Explored pilot injection experimental space (dwell and duration) at both medium and high load conditions for selected rail pressures and documented effect on engine performance.
- Quantify PM benefits for post injections and their effect on SFC-NOx tradeoff.

Future Directions

- Continue to optimize the performance by leveraging the obtained knowledge on hardware change trade-offs and injection command sequences.
- Validate the combination of down-selected hardware and injection sequences.
- Expand validation efforts to include all load conditions, allowing for a duty cycle entitlement estimation.
- Further optimize our multiple injection strategy. This includes combinations of pilot and post injections and multiple pilot and multiple post injections.

Introduction

GE's 21st Century Locomotive Program has the objective to develop freight locomotive engine technology and locomotive system technologies, which maximize the fuel efficiency while meeting Tier 2 freight locomotive emissions. The Tier 2 regulations have been in effect since 2005 in the U.S. GE's response to the Tier 2 emission regulations was to develop a completely new locomotive. In order to achieve future regulations like Tier 3 and Tier 4, GE is looking ahead, and developing new technologies and engine concepts. Existing technologies allow to a certain degree for reduction of emissions at a cost of increased fuel consumption. Compliance with tighter NOx and PM regulations while achieving a fuel consumption benefit requires new technologies; this is the objective of GE's project.

The following report summarizes GE's efforts over the past year, October 2006 to September 2007. During that time, GE focused on the development of an advanced fuel injection system and demonstrated and quantified the benefits of this system over the existing technology currently used.

Objective and Approach

The objective is to develop and demonstrate an advanced fuel injection system to minimize fuel consumption, while meeting Tier 2 emissions levels.

Fuel injection has a significant impact on a diesel engines' performance as it governs key parameters as atomization, penetration, fuel rate and ultimately mixing. A HPCR injection system was used to achieve performance and emissions improvements over the production unit pump system (UPS). The maximum injection pressure of the HPCR is above 1,800 bar. Multiple post and pilot injection commands allow for a flexible injection rate over the combustion cycle. The experimental facility being used for the studies is the locomotive single cylinder engine at the GE Global Research Center.

In a first step, geometrical fuel injector parameters such as number of holes, nozzle flow cone angle, have been studied over a wide range. This study resulted in a down-selected set of nozzle geometries to be tested with multiple injection strategies. While the focus in those studies was on part-load (Notch 4) and full-load (Notch 8), a wide range of injection pressures was covered. In a second step, designed experiments have been executed in order to explore and optimize the multiple injection strategy. In order to validate and quantify the benefits of the HPCR system, a baseline was established on the single-cylinder engine using the UPS system.

Accomplishments and Results

In the following section the main accomplishments are described in more detail. They are organized in five groups: a) diagnostics, b) nozzle geometry and injector configuration, c) multiple injections, and d) fuel type.

Diagnostics

An optically accessible engine head was installed on the single-cylinder engine test bed at the end of 2006. This allowed for combustion event visualization via a high-speed camera. The engine head also allows for illumination of the cylinder and studies on fuel spray and mixing. The modified engine head is also equipped with thermocouples to record the metal temperatures at eight locations, including the hottest regions of the combustion chamber. The metal temperatures were used to monitor bulk gas temperature due to various fuel injection strategies and changes. Furthermore, an EEPS was purchased and installed. The EEPS system allows for real-time analysis of particle size distribution.

Nozzle Geometry and Injector Configuration

The following key parameters defining the nozzle geometry have been studied: total nozzle flow, number of holes, spray cone angle, needle seat diameter and sac volume. Furthermore, by using various orifice plates the injector configuration was changed. Combinations of nozzle geometry and needle lift profiles were systematically studied and their impact on engine performance evaluated.

The nozzle flow area was changed over a range of approximately 20% of the baseline flow rate. The rates of needle velocity in the opening and closing where unchanged. Other parameters, including number of holes and spray angle, were held constant in the first set of designed experiments, in order to isolate the effect of total flow. To understand possible interaction between nozzle parameters, in later experiments, multiple parameters have been changed simultaneously. The study was carried out for a range of injection pressures. While the results indicated a fairly monotonic trend of PM as a function of nozzle flow area, the effect on fuel consumption was found to be more complex.

Nozzle flow, number of holes and hole diameter are dependent variables, from which only two can be chosen independently. In our nozzle geometry study we changed flow and number of holes independently. The number of nozzle holes was varied by up to four. The PM emissions level was strongly dependent on the number of holes. The effect of number of holes was notably stronger than the effect of injection pressure in the range tested. The SFC seemed to be less affected by the number of holes and more a function of the fuel injection pressure. The dependence of PM emissions on fuel injection pressure was found to be fundamentally different for different number of holes.

In order to explore the effect of spray cone angle on engine performance study the cone angle changed over a range of approximately 4% of the baseline nozzle. In the range studied, the trends for PM and SFC were found to be opposite. Changing the cone angle monotonically led to a benefit in fuel consumption while the PM emissions increased and vice versa.

Needle seat diameter and orifice plate flow have a strong effect on the needle lift profile. The needle seat diameter was increased by up to 12.5% compared to the baseline nozzle while the orifice plate flow was changed by up to a factor of two. A study was performed to investigate four different combinations of seat diameter and orifice plate flow. The choices were made to achieve four distinct needle lift and fall rates for the test matrix. The choice of seat diameter seems to affect the

PM emissions only for low injection pressures. The fuel consumption is affected for all injection pressures, even though the effect is minor compared to the other nozzle parameters studied. For certain needle lift profiles fuel consumption benefits have been observed. The effects were stronger at part-load than at full-load.

We demonstrated that specific nozzle geometries (hole number and angle) could offer fuel consumption benefits at NOx-parity over our baseline nozzle with a very minor increase in PM emissions. The nozzle geometry study was based on single injection performance. The optimum nozzle selection process was based on the observed SFC benefits at Tier 2 NOx-emissions levels while meeting PM regulations. Among the geometries tested, the most favorable nozzle geometry at part-load was found to be different to the most favorable one at full-load. Also, performance results where strongly dependent on rail pressure. Therefore, the overall optimum nozzle geometry has to be determined on a duty cycle basis. The most favorable nozzles have been used as initial hardware configuration for the multiple injection studies, described in the next section.

Multiple Injection

Multiple injection strategies have been explored for both piston crown geometries. Piston crown geometries A and B vary mainly by their extent of re-entrant shape. In the third quarter of 2006 we had completed a screening study to efficiently explore the multiple injection design space using piston A. In the forth quarter of 2006, the injection strategy, which gave the best results for the old nozzle/orifice plate configuration, was repeated with a new injector configuration. The trends observed by changing between single injection and multiple injections were found to be fairly similar. This indicates that the performance shift between multiple injections and single injections is consistent, even with small fuel injector nozzle/orifice plate changes. Note that the performance shifts between single and multiple injections were not found to be transferable across piston bowl geometries. While certain multiple injection commands offered benefits using piston A, the performance shift was not observed with piston B.

Using piston B, we explored in detail single-pilot and single-post injection schemes. In order to find the optimum pilot injection strategy, we explored a wide range of pilot injection durations and dwell times. For post injections the injection duration and location was varied in a similar fashion as for the pilot injection. The studies were carried out for several rail pressure levels and a range of main injection advance angles. In order to understand to what extend the benefits observed for pilot and post injections are additive, selected cases of combinations therefore have been tested.

For selected cases, we showed that the addition of pilot injections provides a SFC benefit (at constant NOx level) over the single injection. The addition of pilot injections was found to have little impact on PM emissions. For single injections, the rail pressure was found to have a strong effect on SFC. For rail pressures levels leading to a higher SFC with a single injection, the SFC benefits observed for adding on a pilot injection where larger. At full-load, pilot injection strategies have shown an improvement for limited NOx levels over the UPS. At part-load, pilot injections improved the NOx-SFC tradeoff compared to the UPS over a wider range of NOx levels.

The addition of post injections allowed for significant reduction in PM. In selected cases at part-load a simultaneous benefit in SFC was observed. The relative PM reduction using post injection was approximately twice at part-load than at full-load. The post injection duration was found to have a strong impact on the engine performance at all loads tested. While larger fuel quantities in the post injection decreased the PM emissions further in our study, the NOx-SFC tradeoff turned unfavorable for prolonged post injection durations. For specific load conditions, the engine performance was found to be fairly insensitive to the location of the post injection. In order to achieve NOx parity with an additional post injection, the main injection timing had to be slightly advanced.

Fuel Type

Three different fuels with sulfur levels changing by more than a factor of 200 where tested. As expected, a linear dependence of PM emissions on fuel sulfur level was found. The quantitative results at hand now allow for a better comparison of the data taken on the single-cylinder engine to data taken on other engines run with different sulfur levels.

Conclusions and Future Work

Changes in nozzle geometry have been proven to allow for further engine performance benefits. Clear trends have been identified and quantified. For the range studied, the number of holes seemed to have the strongest effect on PM, followed by rail pressure and nozzle flow. Changing the spray cone angle was found to have monotonic but opposing trends for SFC and PM. In this case, a trade-off function between SFC and PM was identified. Multiple injection strategies have been shown to allow for additional fuel and emission benefits over the optimized nozzle geometry single injection results. Pilot injections have been successfully proven to reduce NOx emissions, especially at part-load. Post injections have been shown to give significant reduction in PM, without imposing a measurable SFC penalty. Additional diagnostics, like in-cylinder visualization of

the combustion event and particle size measurements in the engine exhaust, allow for further understanding and guidance of future engine developments. Future work is needed to optimize the combination of post and pilot injections for the most favorable hardware combination. Furthermore, we will expand the studies over the entire engine duty cycle.

II.A.21 Stretch Efficiency in Combustion Engines with Implications of New Combustion Regimes

Ron Graves (Primary Contact), Stuart Daw, Josh Pihl, Lou Qualls, Dean Edwards, Kalyana Chakravarthy
Oak Ridge National Laboratory (ORNL)
NTRC Site
2360 Cherahala Blvd.
Knoxville, TN 37932

DOE Technology Development Manager:
Kevin Stork

Objectives

- Analyze and define specific pathways to improve the energy conversion efficiency of internal combustion engines from nominally 40% to as high as 60%, with emphasis on opportunities afforded by new approaches to combustion.
- Establish proof of principle of the pathways to stretch efficiency.

Approach

- Use literature study to reevaluate prior work on improving engine efficiency.
- Exercise appropriate engine models to define the greatest opportunities for further advancement.
- Develop improvements to those models as needed to address the impact of new approaches to combustion.
- Conduct availability (exergy) analyses using the Second Law of Thermodynamics as well as the First Law to study where the large losses inherent in conventional and alternative combustion approaches lie.
- Design and conduct proof-of-principle experiments.

Accomplishments

- Designed and constructed a bench-top experimental apparatus for demonstrating low-irreversibility combustion based on the concept referred to as counterflow-preheat with near-equilibrium reaction (CPER).
- Continued exploring better ways for recuperating exhaust heat and utilizing compound cycles for extracting work.
- Continued exercising engine and combustion models to identify combustion modifications that would mitigate exergy losses.
- Continued collaborating with Texas A&M in analyzing case studies of the major exergy losses during diesel engine operation.

Future Directions

- Shakedown and experimentally demonstrate low-irreversibility combustion in the CPER bench-top apparatus.
- Continue analyses of data from CPER experiments to determine efficiency implications and appropriate ways to model exergy losses under different operating modes.
- Continue exploring better ways for recuperating exhaust heat and utilizing compound cycles for extracting work.
- Continue exercising engine and combustion models to identify combustion modifications that would mitigate exergy losses.

Introduction

The best approach for improving engine efficiency is to understand the causes of losses, then develop ways to mitigate them. Numerous studies over the past 30 years have quantified the thermodynamics of engines (see [1], for example). These studies have demonstrated that both the First and Second Laws of Thermodynamics must be taken into account in order to understand how efficiently energy is actually utilized. The First Law simply accounts for energy in any form, but the Second Law distinguishes the 'quality' of energy as it relates to producing useful work. For the latter, a thermodynamic property known as availability (or exergy) is tracked as energy is processed by the engine. Because availability directly relates fuel energy to motive work generation, it gives deeper insights into the loss mechanisms for transportation engines than simple energy balances.

In conventional engines the largest efficiency losses (approximately 20-25%) occur in the combustion process itself and are difficult to mitigate. Such losses are not due to unburned fuel, which is a relatively small loss, but they are instead due to the generation of thermodynamic entropy by unrestrained chemical reactions. The net effect is to divert some of the fuel energy into molecular motion and heat. This diverted energy becomes unavailable to produce useful work according to the Second Law of Thermodynamics. Simple energy balances, which reflect the First Law of

Thermodynamics, don't distinguish between available energy (energy that can produce work) and unavailable energy (energy that can only make heat). However, as we discuss below, it is theoretically possible to carry out our combustion reactions in a more restrained way that produces less entropy and preserves more of the original fuel energy for work.

Typically, processes that generate entropy are referred to as thermodynamically irreversible. Detailed analyses of the irreversibility of unrestrained combustion have shown that it comes mostly from 'internal heat transfer' between the products (exhaust gases) and reactants (fuel and air). Such heat transfer is inevitable in both pre-mixed and diffusion flames, where highly energetic product molecules are free to exchange energy with unreacted fuel and air [2]. Since these molecules have large energy (i.e., temperature) differences, considerable entropy is generated when they interact. In general, combustion irreversibility is mitigated if the reactions take place nearer chemical equilibrium. This requirement can be accomplished when the reactants are preheated reversibly (slowly, with small temperature gradients) such that they are brought closer to the temperature of the products [3].

Approach

We previously conducted analytical studies of the exergy losses in current internal combustion engines in collaboration with Professors Jerald Caton (Texas A&M University) and David Foster (University of Wisconsin). Based on these studies, we have identified the irreversibility of the combustion step as the largest single contributor to fuel exergy loss. In response, we have shifted our efforts to experimental evaluation of novel approaches to combustion that can reduce this inherent irreversibility. A common theme of all the novel approaches being considered is that they attempt to create conditions under which the combustion reactions occur closer to a state of chemical equilibrium.

The first novel combustion approach being investigated combines two fundamental concepts to achieve reaction conditions closer to equilibrium:

- Counterflow preheating of the inlet fuel and air with exhaust, and;
- Introduction of a reforming catalyst to stimulate reforming of the fuel as it is preheated.

These two concepts are specific implementations of more general concepts emerging from our previous analytical and literature investigations referred to as CPER [3] and thermo-chemical recuperation (TCR) [4].

A bench-top experimental apparatus is being constructed to allow direct comparisons between conventional atmospheric combustion of hydrocarbon fuels and atmospheric combustion based on CPER-TCR. Measurements from the bench-top combustor will be used to validate the theoretical predictions and also explore practical ways to maximize the benefits.

Results

The majority of the FY 2007 effort has focused on the design and construction of a bench-top experiment that can be used to demonstrate the feasibility of more reversible combustion based on CPER-TCR. The basic concept behind CPER-TCR is illustrated schematically in Figure 1, where more reversible combustion is achieved by preheating the inlet fuel and air in counterflow to the exhaust to reduce the average temperature difference associated with internal heat transfer. In addition, the reversibility of the fuel preheating is enhanced by catalytically promoting simultaneous reforming reactions which occur closer to chemical equilibrium than the fuel decomposition reactions occurring in the flame.

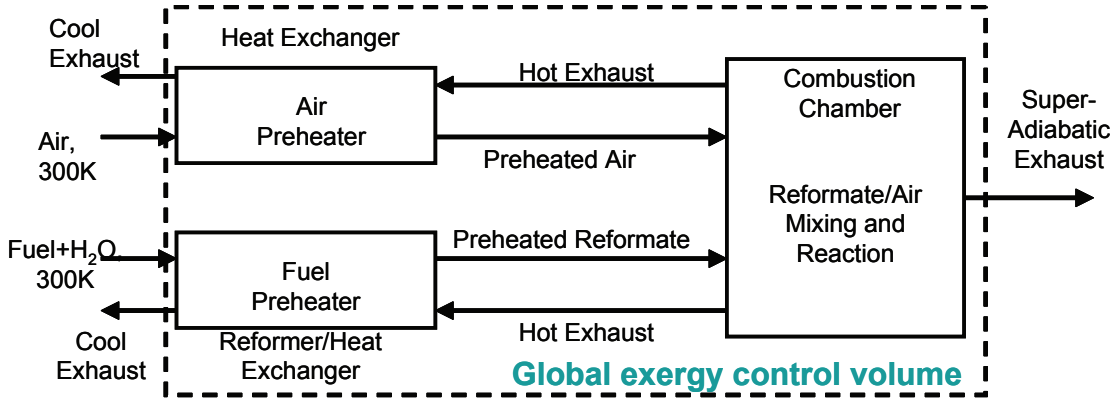

FIGURE 1. Conceptual schematic for restrained combustion by CPER and TCR. Fuel and air are preheated prior to combustion by counterflow heat transfer with exhaust. Additional exhaust exergy is retained in thermo-chemical form due to simultaneous reforming of the fuel.

Theoretical analyses suggest that as much as two-thirds of the fuel exergy normally lost during combustion can be retained through this type of process. For the experiment, all stages of preheating and combustion are designed to be carried out at nearly constant pressure. The two initial fuels being considered for shakedown experiments are methane and ethanol.

The experimental combustor is designed to burn fuels within an enclosed, insulated combustion chamber as schematically illustrated in Figure 2. Fuel and air can be delivered at constant flow into the chamber through vertical feed lines that pass through the upper plate of the combustion chamber, flow through counter-current heat exchangers, and finally into a small burner at the base of the upper plate assembly. The combustion exhaust gases exit from the top of the chamber through three separate vertical exhaust tubes as illustrated in the assembly photograph in Figure 3. One of the exhaust tubes vents directly from the combustion chamber into the atmosphere, while the other two discharge from the hot-side outlets of the fuel and air preheaters, respectively. Pressure regulators at the end of the exhaust lines control the rate of reaction products flowing through each exhaust outlet, permitting the degree of air and fuel preheating to be independently controlled.

Details of the air and fuel preheaters are illustrated in Figures 4 and 5, respectively. As noted in these figures, the fuel and air lines are introduced through the top plate via the corresponding exhaust vents. Fins and helical coils are used to enhance the counterflow heat transfer, and in addition, there is provision to include a reforming catalyst (either in pellet or monolithic form) on the cool side of the fuel preheater. The latter is intended to promote endothermic reforming reactions that recuperate additional exhaust heat in the form of thermo-chemical exergy, which is then returned to the combustor.

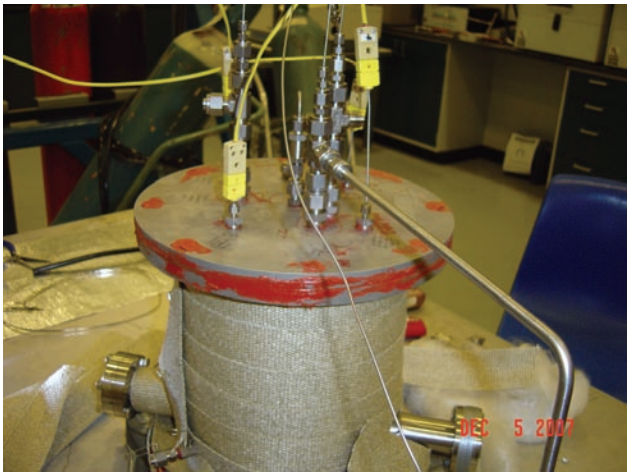

FIGURE 3. Photograph of the assembled experimental CPER-TCR combustor.

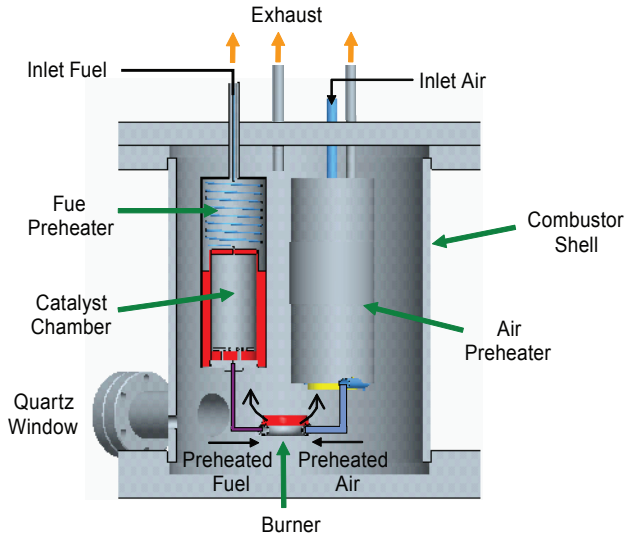

FIGURE 2. Schematic of the experimental CPER-TCR combustor. Incoming air and fuel are preheated by exhaust, and the fuel is partially reformed. Exhaust exits the top via three separate vents. Two quartz windows provide optical access.

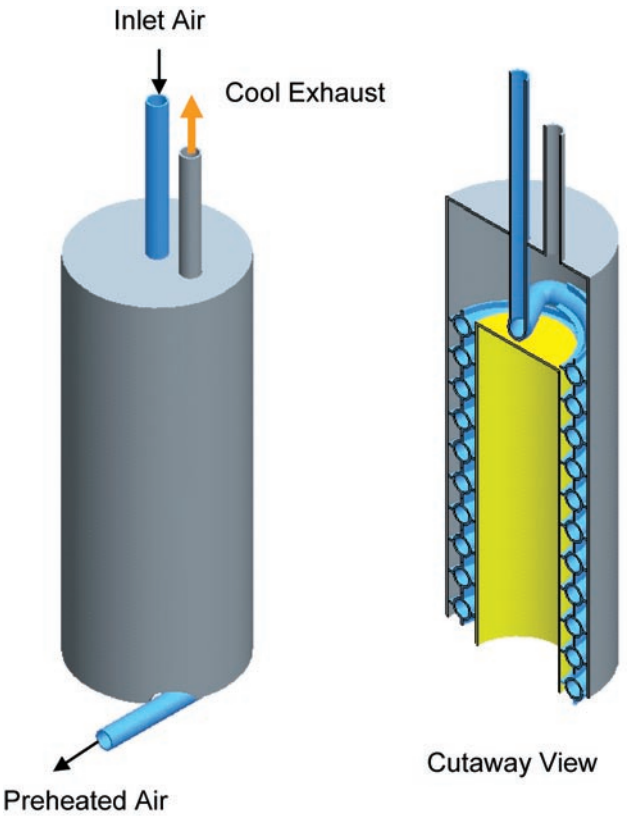

FIGURE 4. Schematic showing details of the air preheater. Heat is transferred from the hot exhaust in the surrounding manifold through the finned coil into the incoming air.

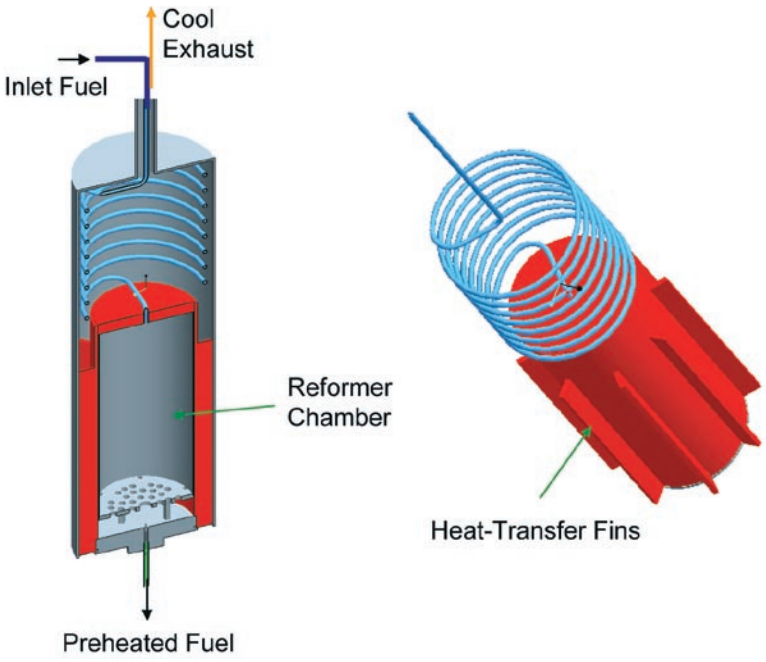

FIGURE 5. Schematic showing details of the fuel preheater. Heat is transferred from the hot exhaust in the surrounding manifold through the coiled tubing and canister into the fuel and refoming catalyst. The catalyst promotes endothermic reforming reactions that produce H_2 and CO from the raw fuel.

Details of the burner, which is located at the bottom of the combustion chamber, are still being resolved. It is expected that the burner will utilize some type of porous metal distributor (e.g., sintered metal) with a catalyst to stabilize the combustion at very lean conditions. While the irreversibility of lean combustion is known to be higher than for stoichiometric combustion, it is also recognized that the current materials of construction would be inadequate to sustain the temperatures involved in stoichiometric combustion. Since the current objective is to show the exergy advantage of the CPER-TCR configuration, it is sufficient to compare the combustor exergy performance at lean fueling conditions with and without preheating and reforming.

The fuel and air flows are controlled and measured by electronic control valves and flow transmitters, respectively. Water or steam can be added as needed to promote reforming reactions. The temperature of each stream (inlet and outlet) is monitored with thermocouples, and the composition of exhaust gas is monitored for unburned hydrocarbons and CO. The above measurements will be sufficient to develop global energy and exergy balances over the combustor at each steady-state operating condition.

Conclusions

An experimental bench-top CPER-TCR combustor has been constructed and is awaiting shakedown testing and demonstration of combustion with significantly reduced thermodynamic irreversibility. This combustor should provide the opportunity for the first experimental demonstration of a thermal combustion process that can retain a significant fraction of the exergy now destroyed in conventional combustors and combustion engines.

References

1. Primus, R. J., et al, An appraisal of advanced engine concepts using second Law analysis techniques SAE 841287, 1984.

2. Dunbar, W.R. and Lior, N., "Sources of Combustion Irreversibility," Combustion Science and Technology, 103, 41-61, 1994.

3. C. S. Daw, K. Chakravarthy, J.C. Conklin and R.L. Graves, "Minimizing destruction of thermodynamic availability in hydrogen combustion," International Journal of Hydrogen Energy, 31, 728, 2006.

4. Thermochemical Fuel Reformer Development Project: Higher Efficiency and Lower Emissions for Reciprocating Engines Used in Distributed Generation Applications. EPRI, Palo Alto, CA, California Energy Commission, Sacramento, CA: 2006. 1012774.

FY 2007 Publications/Presentations

1. Ron Graves, Stuart Daw, Josh Pihl, Lou Qualls, and Johney Green, Jr., "Stretch Efficiency Paths for Combustion Engines," U.S. DOE FCVT Program Merit Review, June 17–19, 2007.

II.A.22 Advancements in Engine Combustion Systems to Enable High-Efficiency Clean Combustion for Heavy-Duty Engines

Yury Kalish, Houshun Zhang (Primary Contact)
Detroit Diesel Corporation (DDC)
13400 Outer Drive, West
Detroit, MI 48239-4001

DOE Technology Development Manager:
Roland Gravel

NETL Project Manager: Carl Maronde

Objectives

Explore advancements in engine combustion systems to enable high-efficiency clean combustion (HECC) techniques to minimize cylinder-out emissions.

Accomplishments

- Successfully completed the first part of the Near-Zero Emissions at 50 Percent Thermal Efficiency (NZ-50) project. It demonstrated 50.2% thermal efficiency with integrated experimental and analytical technologies at Environmental Protection Agency (EPA) 2010 emissions levels at a single operating condition in a multi-cylinder engine configuration.
- Successfully launched the second part of the NZ-50 project in March of 2007, which focuses on high efficiency clean combustion.
- Identified an advanced fuel injection system with variable nozzle technology, genetic combustion optimization, and advanced control and calibration optimization as three key enabling technologies.
- Successfully completed project annual review with DOE in August, passing the first "Go/No-Go" decision point by developing a technical roadmap to achieve project objectives.
- Evaluated a new dual combustion mode concept using variable fuel nozzle technology. Analytically characterized the benefits of the dual combustion modes, demonstrating 12% improvement in brake specific fuel consumption (BSFC), 96% reduction in NOx, and 54% reduction in soot compared to the baseline engine at the A25 operating point. NOx and PM emissions are below the EPA 2010 emissions standard.
- Demonstrated and explored genetic combustion optimization and identified the best possible combinations of fuel injector hole size, numbers of holes, fuel spray angles, piston bowl geometry, injection timing, and swirl ratio.
- Developed and validated sophisticated advanced control logic through a large variety of offline simulations and optimizations. Down-selected a few calibration packages over hundreds of offline optimizations in a transient engine testing cell, achieving excellent trade-off between emissions and BSFC, thus saving significant time and resources.

Future Directions

- Procure advanced next generation fuel injection system including variable nozzles that can greatly enhance fuel injection flexibility.
- Develop a master plan on consolidation of fuel injection strategy and dual combustion modes to minimize cylinder-out emissions.
- Continue steady-state advanced combustion development. Implement genetic optimization recommendations for hardware procurement.
- Continue transient combustion and control development on a next generation of heavy-duty engine platform.

Introduction

Detroit Diesel Corporation is conducting the NZ-50 multi-year cooperative agreement. This project consists of two major parts. The first part started in 2000. This part emphasizes fuel economy in developing and integrating commercially viable, on-highway truck engine technology while demonstrating near zero emissions and 50% thermal efficiency. The first part of the project was successfully completed, demonstrating 50.2% thermal efficiency with integrated experimental and analytical technologies at EPA 2010 emissions regulation levels at a single operating condition in a multi-cylinder engine configuration [1]. The second part of the project started in March of 2007, focusing on engine combustion systems using HECC techniques to minimize cylinder-out emissions. Throughout the project, integrated analytical tool box with hardware experiments has been developed to define various most potential conceptual engine system technologies and component enhancements, and then tested. The key enabling technologies have been aggressively pursued, making significant progresses. This annual report will

primarily focus on the progress of the second part of the NZ-50 project.

Approach

Detroit Diesel Corporation has developed a proven concept and methodology of combining experimental and analytical tools to facilitate integrated engine, aftertreatment and vehicle development. It uses integrated analytical and experimental tools for subsystem component optimization encompassing advanced fuel injection, increased exhaust gas recirculation (EGR) cooling capacity and combustion process optimization. Model-based controls employing multiple input and output techniques enable efficient integration of the various subsystems and ensure optimal performance of each system within the total engine package. Project assessment and milestone achievement are based on the context of the total engine package with subsystem components that are capable of integration into a production feasible multi-cylinder engine product. This system approach benefits substantially from an integrated experimental and analytical approach to technology development. This results in a shortened developmental cycle, and substantial NOx-PM trade-off and fuel economy improvement in both engines and vehicles.

Moving to the second part of the project with the focus on HECC, the technical approach is tailored to key combustion enabling technologies in addition to the system approach mentioned above. One of the key enabling technologies is the fully flexible fuel injection system, which can facilitate different advanced combustion modes. Working with fuel injection suppliers, a highly flexible fuel injection system with variable nozzle technology is being developed, which results in an unprecedented technical road map. Displayed in Figure 1 is the technology map developed for this project. As can be seen in Figure 1, highly flexible fuel injection system can greatly simplify the combustion strategy into three combustion zones, which feature emerging dual mode combustion. Introduction of a generic combustion optimization technique in conjunction with advanced control technology that has been consistently developed can considerably enhance the project.

Results

Achievement of 50.2% thermal efficiency in the first part of the project required significant technology building blocks [1], which laid out a strong foundation for this current combustion focused project. Carrying this strong momentum with further identification of key enabling technologies, a new dual combustion strategy is emerging. This is done with an advanced fuel injection system in conjunction with highly flexible variable nozzle technology. This variable nozzle technology features a moving needle and nozzle body that can generate a micro-variable circular orifice (MVCO), which is equivalent to a 6~50 variable micro-hole nozzle. It can also generate a conical spray only or mixed-mode conical-multi-jet spray patterns to meet the needs of different engine operating conditions.

Use of an advanced three-dimensional computational program with sophisticated combustion and spray models was made to evaluate this dual mode combustion concept. Table 1 shows the simulated results for a low load point at the A25 operating point (25% load and A engine speed). As can be seen, with this dual combustion mode resulted from a high flexible variable nozzle with 12% improvement in BSFC, 96% reduction in NOx, and 54% reduction in soot are obtained, and NOx and soot emissions are below EPA 2010 emissions standards.

While focusing on analytical evaluation of the emerging dual mode combustion, two other key technical areas were also conducted in parallel. Genetic combustion optimization is one area, while advanced control and calibration optimization is another. Figure 2 shows the comparisons between traditional and genetic combustion optimization. The key difference between

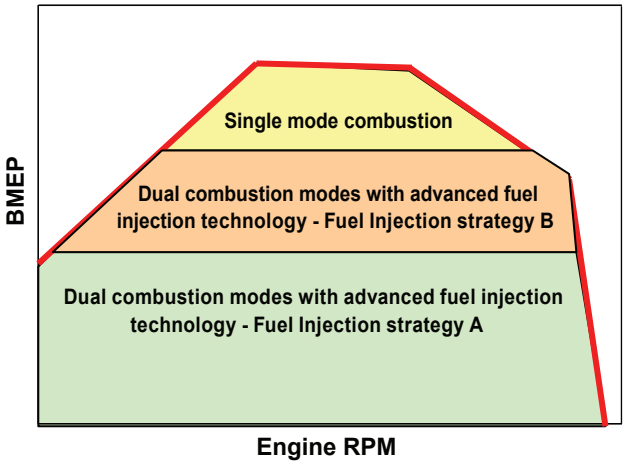

FIGURE 1. Strategy for Combustion Concepts Integration

TABLE 1. Emerging Dual Model Combustion with Variable Fuel Injection System

	Case	BSFC [g/kW·hr]	NOx [g/hp·hr]	Soot [mg/m³]	CO [g/hp·hr]	HC [g/hp·hr]
Baseline	Baseline	222	1.592	0.767	0.47	0.071
MVCO	MVCO (Dual Injection Mode)	195.2	0.07	0.349	0.473	0.189
	Improvement	12%	96%	54%	-1%	-166%

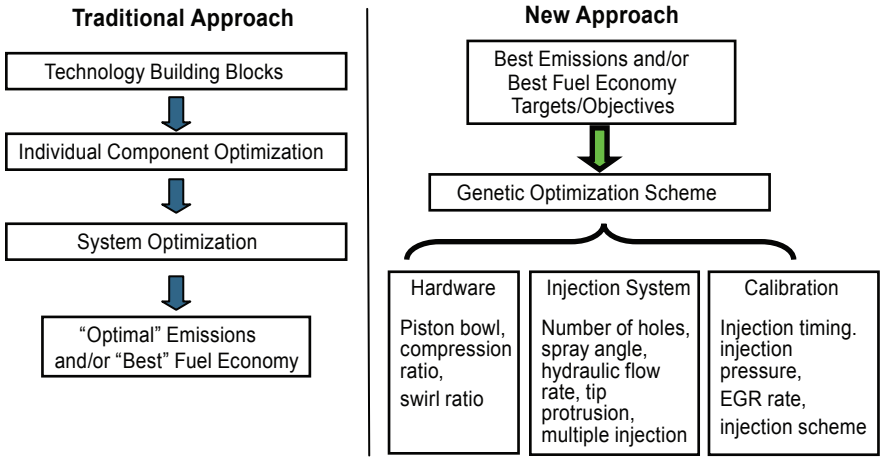

FIGURE 2. Innovative System Optimization Methodologies Emerging

these two approaches is that there is no guarantee for optimal results with the traditional approach since testing matrix is so large that it is virtually impossible to test all points. In contrast, the genetic optimization approach starts with top levels of objective definition, and then randomly selects testing matrix points, following well proven mathematical procedures to down-select optimal points. Figure 3 shows the genetic combustion optimization results at the A25 operating point. As can be seen, the pareto citizens that represent the optimal boundary among a large number of testing points are found, thus locating a trade-off between emissions and BSFC depending on applications.

Realizing that transient engine control is critical to proper torque response over the road, fuel economy and emissions, DDC continues spearheading development of next generation engine control techniques including model-based approaches, on-board setpoint adaptation and observer models. Experimental and simulation results help to quantify the benefits of nonlinear control techniques, both from a stability and response time standpoint. Displayed in Figure 4 is the trade-off between BSFC and NOx using advanced control logic to down-select a few optimal points through a large number of offline simulation points. More detailed descriptions of DDC's sophisticated control technology are available [2].

Conclusions

- Successfully completed the first part of the project with achievement of the March 2007 objective, demonstrating 50.2% thermal efficiency with integrated experimental and analytical technologies at EPA 2010 emissions regulation levels at a single operating condition in a multi-cylinder engine configuration.

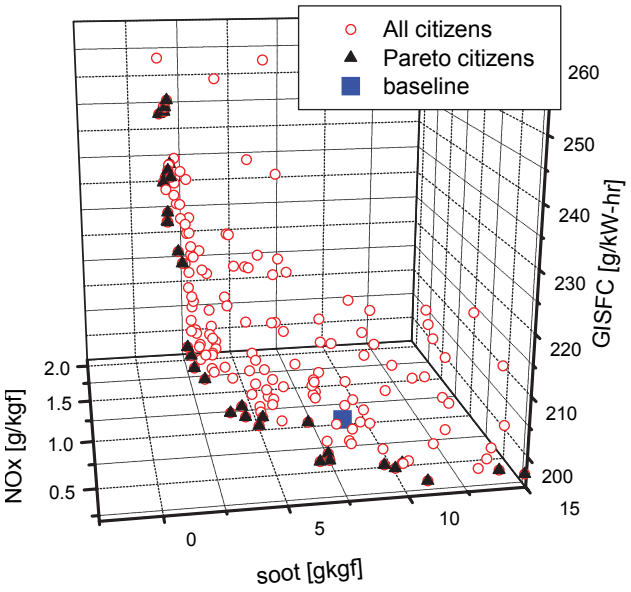

FIGURE 3. Genetic Combustion Optimization for A25

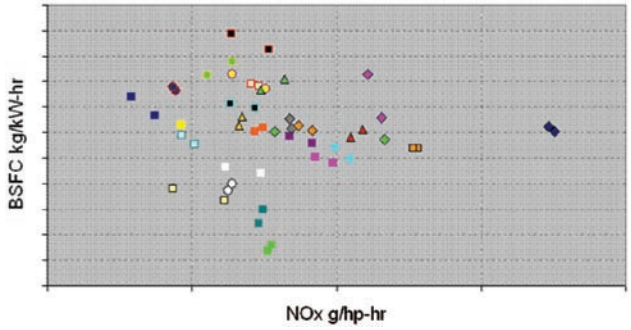

FIGURE 4. Advanced Control and Calibration Optimization
(Each point marker designates one calibration FTP set point.)

- Successfully launched the second part of the project in March of 2007, focusing on HECC.
- Identified variable nozzle technology, genetic combustion optimization, and advanced control and calibration optimization as key enabling technologies in achieving the project objectives.
- Analytically characterized dual-combustion modes with an advanced fuel injection system, demonstrating 12% improvement in BSFC, 96% reduction in NOx, and 54% reduction in soot compared to a baseline engine at the A25 operating point. The NOx and soot emissions are below EPA 2010 emission regulations.
- Explored genetic combustion optimization for combinations of fuel injector hole size, numbers of holes, fuel spray angles, piston bowl geometry, injection timing, and swirl ratio.
- Validated advanced control logic through a variety of offline optimizations. Considerably simplified the calibration process to obtain optimal calibration packages in transient engine testing cells, and excellent trade-off between emissions and BSFC were obtained.

References

1. Craig Savonen , Houshun Zhang, and Rakesh Aneja, "Heavy-Duty Engine Technology for High Thermal Efficiency at EPA 2010 Emissions Regulations", FY2006, Progress Report for Advanced Combustion Engine Research & Development, U.S. Department of Energy, December 2006.

2. Marc Allain, Craig Savonen, Yury Kalish, and Houshun Zhang, "Next Generation Diesel Engine Control," 13th Annual Diesel Engine-Efficiency and Emissions Research (DEER) Conference, Detroit, MI (Aug. 13–16, 2007).

FY 2007 Publications/Presentations

1. Guangsheng Zhu, Houshun Zhang, Yury Kalish, Rakesh Aneja, "Heavy-duty Engine Combustion Optimization for High Thermal Efficiency Targeting EPA 2010 Emissions," 13th Annual Diesel Engine-Efficiency and Emissions Research (DEER) Conference, Detroit, MI (Aug 13-16, 2007).

2. Marc Allain, Craig Savonen, Yury Kalish, and Houshun Zhang, "Next Generation Diesel Engine Control," 13th Annual Diesel Engine-Efficiency and Emissions Research (DEER) Conference, Detroit, MI (Aug 13-16, 2007).

3. Rakesh Aneja, Sathish Sankara Chinthamony, Min Sun, and Gunagsheng Zhu "Integrated Vehicle and Powertrain Technology for EPA 2010 and Beyond," 13th Annual Diesel Engine-Efficiency and Emissions Research (DEER) Conference, Detroit, MI (Aug 13-16, 2007).

4. Chris Atkinson, Marc Allain, Houshun Zhang, Yury Kalish, and Craig Savonen "Fuel Efficiency and Emissions Optimization of Heavy-Duty Diesel Engines using Model-Based Transient Calibration," 13th Annual Diesel Engine-Efficiency and Emissions Research (DEER) Conference, Detroit, MI (Aug 13-16, 2007).

Special Recognitions & Awards/Patents Issued

1. Marc Allain and Min Sun, "Method and System of Diesel Engine Setpoint Compensation for Transient Operation of a Heavy-Duty Diesel Engine", U.S. Patent No. 7,281,518, October 16, 2007.

2. Guangsheng Zhu and Houshun Zhang, "Invention of Squish-Induced Mixing-Intensified Low Emission Combustion (SIMILECOM)." Record of invention was submitted on August 16, 2007.

3. Jack Peckham, "Next-Generation Computer Controls Can Boost Diesel Fuel Efficiency without Compromising Emissions, Performance," Diesel Fuel News, Volume 11, issues 20, September, 2007.

II.A.23 Development of High Efficiency Clean Combustion Engine Designs for Spark-Ignition and Compression-Ignition Internal Combustion Engines

Kenneth Patton
GM Powertrain Advanced Engineering
895 Joslyn Avenue
Pontiac, MI 48340

DOE Technology Development Manager:
Kenneth C. Howden

NETL Project Manager: Carl P. Maronde

Subcontractors:
Sturman Industries, Woodland Park, CO

Objectives

- Develop and demonstrate prototype gasoline and diesel engine hardware which enables operation of homogeneous charge compression ignition (HCCI) combustion for improved fuel efficiency and emissions performance.
- Understand and reduce the risks and roadblocks associated with this new combustion system by designing and demonstrating hardware solutions.
- Demonstrate enabling system on a 2.0-2.4L inline four-cylinder (I4) gasoline engine in a mid-size car.
- Demonstrate fully flexible system on a 2.0-2.4L I4 gas engine in a mid-size car.
- Demonstrate simple variable valve actuation system on a 4.5L dual overhead camshaft (DOHC) V8 engine in a mid-size sport utility vehicle.
- Demonstrate fully flexible system on a single-cylinder diesel engine.
- Demonstrate fully flexible system on a 4.5L DOHC V8 engine in a mid-size sport utility vehicle.

Accomplishments

Gasoline Systems

- Functional performance of key components and subsystems that enable HCCI operation have been tested and documented.
- Enabling system (2-step valvetrain) concept has been built, tested, and continues development work:
  - Engine dynamometer testing ongoing.
  - Mule and demonstration vehicle builds assembled, basic functions demonstrated, limited amount of vehicle calibration work done.
- Fully-flexible system concept single valve test fixture has been built, and initial testing is underway with basic concept functions demonstrated.
- Fully-flexible multi-cylinder design effort continues with focus on part count, part complexity, packaging, assembly, service.

Diesel Systems

- Fully flexible variable valve actuation (VVA) system in use on single-cylinder engine.
- Late intake valve closing has been demonstrated to:
  - Increase premixed charge compression ignition (PCCI) load range, which gives fuel consumption improvement.
  - Reduce exhaust gas recirculation (EGR) requirement at Tier 2 Bin 5 oxides of nitrogen (NOx) level.
  - Reduce particulates.
  - Increase in boost pressure and hydrocarbon (HC) emissions.
- Demonstrated functionality of the cam phaser VVA system over required operating range on multi-cylinder engine.
- Discovered discrepancy between the GT-Power model predictions and actual test results that caused lower than expected air flow and EGR rates.

Future Directions

Gasoline Systems

- Continue development and calibration work on vehicles with enabling system.
- Continue work on fully-flexible system to understand part variation, dynamic range, and energy consumption.
- Continue to refine the fully-flexible system design for multi-cylinder engines, especially valve lift sensing from a function/cost/packaging standpoint.

Diesel Systems

- Investigate internal EGR benefits using fully flexible system.
- Investigate other efficiency improvements using VVA.
- Rectify turbo-machinery problems and procure a new high-pressure stage turbocharger that meets air flow and EGR requirements.
- Integrate VVA controls into electronic control unit for transient testing.

Introduction

The objective of the gasoline portion of this project is to demonstrate operation of gasoline HCCI engine designs using both an "enabling" valvetrain system and a fully-flexible valvetrain system. By executing design and development of hardware systems, the risks and roadblocks associated with gasoline HCCI engines will be better understood, and potential solutions may be identified. Reduction of risks and elimination of roadblocks are key aspects of understanding the cost-effectiveness and production feasibility of gasoline HCCI engine designs.

The objective of the diesel portion of this project is to demonstrate operation of diesel HCCI engines using both a simple and a fully-flexible valvetrain system design. The performance objectives are to improve fuel efficiency for diesel engines while meeting the Tier 2 Bin 5 emission specifications without needing NOx aftertreatment. The efficiency and cost effectiveness of the simple and the fully flexible VVA systems will be assessed based on their demonstrated performance.

Approach

The gasoline and diesel portions of this project include feasibility analysis, computer simulation work to guide concept selection and designs, overall engine design, engine component design and fabrication, subsystem bench testing, engine build and development testing, and vehicle build and development testing.

Results

Gasoline Systems

The focus of the gasoline hardware development is on generating designs that reduce costs, reduce technical risks, and demonstrate hardware systems. Two valvetrain variants are under development. The simpler system uses a 2-step valvetrain design that enables some level of HCCI operation, and its focus is on identifying cost-effective component solutions. The fully flexible concept uses an electro-hydraulic camless VVA system design that is less limited in terms of operating strategy, and its focus is on developing the VVA system and quantifying potential benefits. Other hardware systems to be evaluated as part of this hardware development include direct fuel injection and cylinder pressure sensing.

In order to design and develop engine systems that enable HCCI operation, an important intermediate step is to evaluate the functional performance of some key engine components and subsystems. This step is also important for the integration of the components into a well-balanced engine design which has the desired capabilities. The performance of the following key components and subsystems were tested: the 2-step oil control valve; the 2-step switching roller finger follower; the cam phaser; the cam phaser control system; and the cylinder pressure sensor. The results of these tests were documented in a project milestone report, and they strongly influenced the design and development of both the enabling and fully flexible VVA systems.

The enabling VVA system and the fully flexible VVA system provide the ability to deliver appropriate quantities of fuel at the appropriate times. They also have the ability to robustly measure cylinder pressure with mass production-viable sensing hardware under normal vehicle operating conditions. The enabling VVA system has the ability to deliver desired HCCI valve events with a low-friction, reliable 2-step switching valvetrain, which also provides the ability to mechanically switch from HCCI valve events to normal spark ignition valve events in a fast, robust, and predictable manner.

The fully flexible VVA system has several capabilities beyond those of the enabling VVA system. The drawing in Figure 1 shows the mechanism for electrically actuated cam phasing, which provides for a high range of authority and very fast response in HCCI mode. It has the ability to provide complete control of valve motion, including lift, timing, and closing velocity. It has the ability to meet system performance requirements under normal and extreme vehicle operating conditions, while reducing system energy consumption. It has the ability to meet basic packaging, assembly, and service requirements with mass-production-viable hardware. Finally, it has the ability to meet noise and vibration requirements.

In addition to the bench testing of most components, the enabling system has been incorporated into engines and vehicles where the testing and development has continued. Engine dynamometer

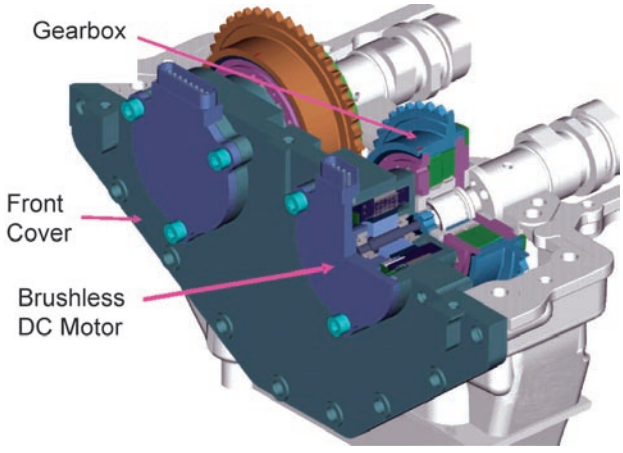

FIGURE 1. Mechanism for Electrically Actuated Cam Phasing

testing using this enabling system is ongoing. Mule and demonstration vehicles have been assembled, and they demonstrate basic functions by utilizing some limited vehicle calibration work.

For the fully flexible VVA system concept, a test fixture has been built as shown in Figure 2, and the basic concept functions have been demonstrated. Testing of this fixture and other aspects of the design are underway. The design for the fully-flexible multi-cylinder application continues with the focus on part count, part complexity, packaging, assembly, and service. However, more development work and testing must be performed to understand part variation, dynamic range, and energy consumption.

Diesel Systems

The single-cylinder diesel engine development has focused on testing a fully flexible electro-hydraulic VVA system. A schematic for this fully flexible system appears in Figure 3, which shows how the control system uses a servo valve to hydraulically control engine valve lift and duration. The benefit of this fully flexible VVA work is to improve our understanding of the upper bound efficiency potential of the diesel engine. This type of work is demonstrated in Figure 4, which shows how the system can adjust the intake valve closing (IVC) angle to control the effective compression ratio (CR).

Work on the multi-cylinder diesel engine has focused on the development of a production viable VVA system. In this system, a driveshaft within the cam is rotated to control intake valve timing. The benefit of testing this type of cam phaser system is to improve our understanding of the requirements and performance capabilities of a production viable VVA system. Both the single-cylinder and the multi-cylinder work are important for the development of technologies needed to achieve our goal of ultra-low engine-out NOx levels approaching Tier 2 Bin 5.

The fully flexible system on the single-cylinder engine has been used to investigate the potential benefits of various VVA strategies, such as late IVC. In theory, late IVC could increase the load range where PCCI occurs. Testing of late IVC has demonstrated the following:

- Increase in the PCCI load range, which produces fuel consumption improvement.
- Reduce EGR requirement at Tier 2 Bin 5 NOx level.
- Reduce particulates.
- Increase in boost pressure and hydrocarbon emissions.

For the multi-cylinder diesel application, the cam phaser VVA system demonstrated functionality over the required engine operating range. However, a discrepancy was found between the GT-Power model predictions and the actual multi-cylinder engine test results. As shown in Figure 5, this discrepancy caused lower than expected airflow and EGR rates. Further development will be required to resolve this air handling issue.

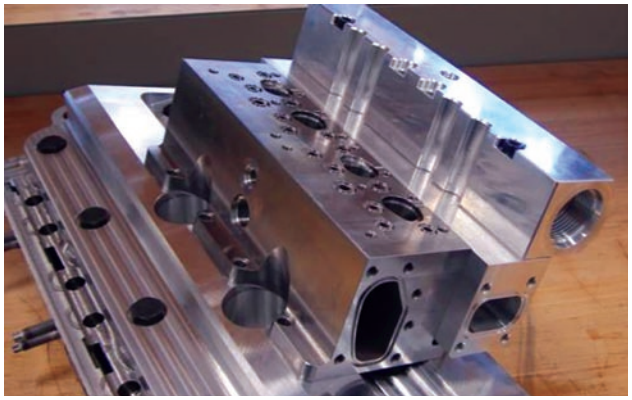

FIGURE 2. Test Fixture for Fully Flexible VVA Concept

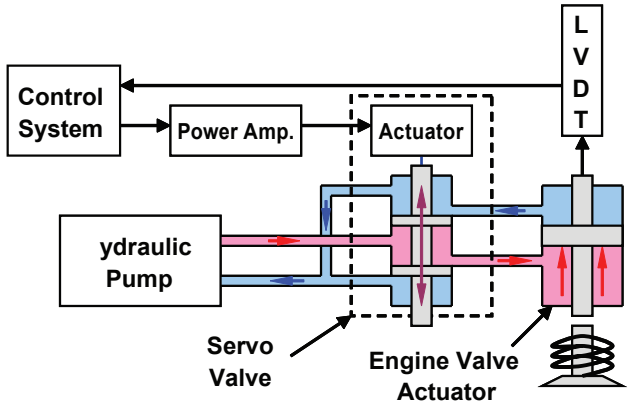

FIGURE 3. Schematic for Fully Flexible VVA System

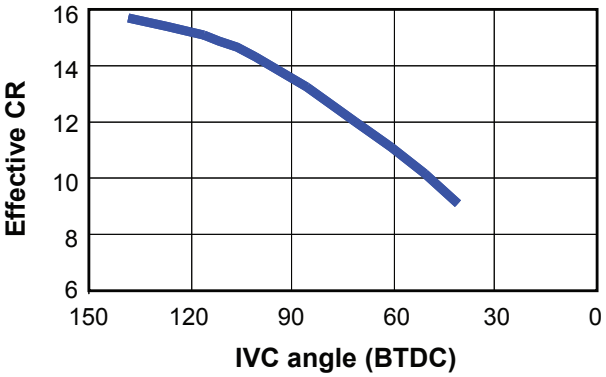

FIGURE 4. Impact of Late IVC to Reduce Effective CR

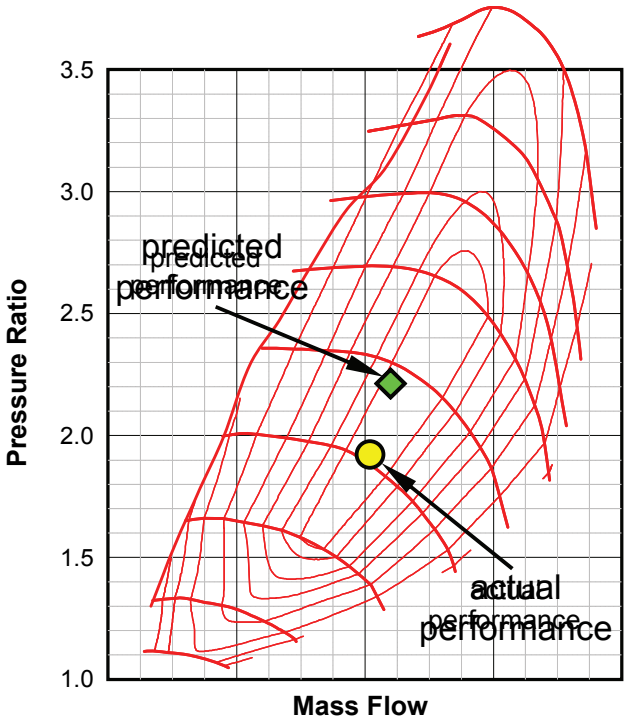

FIGURE 5. Difference between Predicted and Actual Performance of Cam Phaser System

Conclusions

Based on the successful demonstration of the "enabling" design on the gasoline HCCI engine in dynamometer testing and in vehicles, work on the enabling system should be continued. Based on the progress made on the fully-flexible design for the gasoline HCCI engine, the next steps of executing a multi-cylinder design should be taken.

For the diesel HCCI engine, significant progress has been made on both the simple and the fully-flexible designs. Both systems should continue to be developed, so that their potential performance, efficiency, and cost effectiveness can be properly assessed.

FY 2007 Publications/Presentations

Report at the DOE Merit Review – May 2007.

II. ADVANCED COMBUSTION AND EMISSION CONTROL RESEARCH FOR HIGH-EFFICIENCY ENGINES

B. Energy Efficient Emission Controls

II.B.1 Fundamental Studies of NOx Adsorber Materials

Do Heui Kim, Ja Hun Kwak,
Janos Szanyi, Xianqin Wang, and
Chuck Peden (Primary Contact)
Institute for Interfacial Catalysis
Pacific Northwest National Laboratory (PNNL)
P.O. Box 999, MS K8-93
Richland, WA 99352

DOE Technology Manager: Ken Howden

Objectives

- Develop a practically useful fundamental understanding of NOx adsorber technology operation.
- Focus on chemical reaction mechanisms correlated with catalyst material characterization.
- Actively participate in the CLEERS lean-NOx trap (LNT) subgroup. This latter activity now includes an additional 3-way collaboration between Oak Ridge National Laboratory (Stuart Daw and coworkers), Sandia National Laboratories-Livermore (Rich Larson), and PNNL.
- Transfer the developing fundamental understanding to industry via the CLEERS activity as well as periodic technical meetings with industry scientists and engineers.

Approach

- Utilize state-of-the-art catalyst characterization and testing facilities in the Institute for Interfacial Catalysis at PNNL, including:
  - Synchrotron temperature programmed X-ray diffraction (XRD): catalyst structural changes.
  - Transmission electron microscopy (TEM)/ energy dispersive X-ray (EDX) and scanning electron microscope (SEM) microscopies: catalyst morphological changes.
  - X-ray photoelectron spectroscopy: oxidation state and relative surface concentrations.
  - Fourier transform infrared (FTIR) and solid-state nuclear magnetic resonance (NMR) spectroscopies: catalyst reaction mechanisms.
  - Temperature programmed desorption (TPD)/ thermal gravimetric analysis (TGA): surface chemistry.
  - Lab Reactor: performance measurements, kinetics and mechanisms.
- Participate as an active member of the CLEERS subgroup on LNTs.

Accomplishments

- In prior work, the morphology of BaO/Al_2O_3 LNT materials was shown to be remarkably dynamic during NOx storage and reduction. A "monolayer" of $Ba(NO_3)_2$ forms on the alumina surface in addition to large "bulk" $Ba(NO_3)_2$ particles.
- These different morphologies were also found to display dramatically different behavior with respect to NOx removal temperature, formation of a deactivating high-temperature $BaAl_2O_4$ phase, and temperature requirements of desulfation.
- *In this past year, the effects of H_2O and CO_2 on these morphology changes were found to be profound under certain conditions.* While the effect of CO_2 is minimal (but results in $BaCO_3$ formation AFTER $Ba(NO_3)_2$ decomposition!), the presence of H_2O leads to a dramatic loss of the "monolayer" $Ba(NO_3)_2$ phase via formation of even larger particles of the "bulk" phase.
- Using a one-of-a-kind very high field NMR instrument at PNNL, the nucleation sites for Ba on the γ-alumina catalyst support material have been identified (discussed in the following).
- The chemical form and stability of barium carbonate species formed during stored NOx removal in the presence of CO_2 has been determined.
- Studies of the effects of water on the decomposition of the deactivating $BaAl_2O_4$ phase show how treatments may be devised to restore performance after deactivation.
- The relative performance of all alkaline earth oxide storage materials has been determined (discussed in the following).
- Numerous publications (nine), invited talks (six), and other presentations (11) have resulted from this project in the past year (see following list).

Future Directions

- Continue studies of CO_2 and H_2O effects on BaO morphology changes and NOx storage properties:
  - Ba-loading studies.
  - Are water-induced morphology changes reversible? If so, how?
- Detailed characterization (e.g., FTIR, TEM) of the roles (especially with respect to deactivation) and material properties of promoter species (such as ceria).

- Initial studies of interactions between multiple emission control devices (e.g., how to optimize LNT regeneration for NH_3 production if a downstream urea selective catalytic reduction catalyst system is present).

Introduction

One of the key challenges facing the catalysis community is the elimination of harmful gases emitted by internal combustion engines. In particular, the reduction of NOx from an exhaust gas mixture that contains an excess amount of oxygen is difficult. Traditional three-way catalysts do not work under lean conditions because the concentrations of the reductants (CO and hydrocarbons) are greatly reduced by their oxidation with O_2 on the noble metal components of these catalysts. Therefore, new approaches to NOx reduction have been considered in the last decade. In spite of all the efforts to develop new emission control technologies for lean NOx reduction, only limited applications have been achieved. One of the most promising technologies under consideration is the NOx adsorber catalyst (aka NOx storage/reduction [NSR] or LNT) method. This process is based on the ability of certain oxides, in particular alkaline and alkaline earth oxide materials, to store NOx under lean conditions and release it during rich (excess reductant) engine operation cycles. Since the original reports on this technology from Toyota in the mid `90s [1], the most extensively studied catalyst system continues to be based on barium oxide (BaO) supported a high surface area alumina (Al_2O_3) material [2].

Our project is aimed at developing a practically useful fundamental understanding of the operation of the LNT technology especially with respect to the optimum materials used in LNTs. As noted above in the summary Accomplishments section, we have made significant progress in a fairly wide-array of areas. For the purposes of this report, we briefly highlight progress in two areas: studies of i) the effect of Ba-loading and water on the formation and stability of $BaAl_2O_4$; and ii) the effects of water on BaO morphology and NOx uptake.

Experimental Details

Catalyst Preparation and Characterization

In a microcatalytic reactor system, LNT performance is evaluated in a fixed bed reactor operated under continuous lean-rich cycling. Rapid lean-rich switching is enabled just prior to the elevated temperature zone (furnace) where the LNT materials are contained in quartz tubing. After removing water, the effluent of the reactor can be analyzed by mass spectrometry and by a chemiluminescent NOx analyzer. For a typical baseline performance test, the sample is heated to a reaction temperature in flowing He, the feed switched to a 'lean-NOx' mixture containing oxygen and NO, as well as CO_2 and/or H_2O. After an extended period (15 minutes or more), multiple rich/lean cycles of one and four minute duration, respectively, are run and NOx removal performance is assessed after at least three of these are completed. In the LNT technology, the state of the system is constantly changing so that performance depends on when it is measured. Therefore, we obtain NOx removal efficiencies as "lean conversion (four minutes)", which measures NOx removal efficiencies for the first four minutes of the lean-period.

The BaO/Al_2O_3 LNT catalysts were prepared by the incipient wetness method, using an aqueous $Ba(NO_3)_2$ solution (Aldrich) and a γ-alumina support (200 m^2/g, Condea) to yield nominal two, eight and 20 wt% BaO-containing samples, dried at 125°C and then 'activated' via a calcination at 500°C in flowing dry air for two hours. State-of-the-art techniques such as solid-state NMR [3], XRD, XPS, TEM/EDS, FTIR, BET/pore size distribution, and temperature programmed desorption/reaction (TPD/TPRX), available at PNNL, were utilized to probe the changes in physicochemical properties of the catalyst samples. The time-resolved X-ray diffraction (TR-XRD) experiments were carried out at beam line X7B of the National Synchrotron Light Source (NSLS), at Brookhaven National Laboratory. The detailed experimental set-up and protocol have been discussed elsewhere [4,5].

Results

In prior years' reports, we have described studies that determined the cycle of morphology changes for BaO/Al_2O_3 NSR catalysts using synchrotron TPD, FTIR, TR-XRD, TEM and EDS. The results showed that large $Ba(NO_3)_2$ crystallites are formed on the alumina support material during its preparation by an incipient wetness method using an aqueous $Ba(NO_3)_2$ solution. A large fraction of the alumina surface remains Ba-free after this procedure. Upon thermal treatment, these large $Ba(NO_3)_2$ crystallites decompose to form nanosized BaO particles. In fact, we propose that a thin BaO film (monolayer) forms on the alumina support, and the BaO nanoparticles are located on top of this interfacial BaO layer. During room temperature NO_2 uptake, nanosized (<5 nm) $Ba(NO_3)_2$ particles form, and these particles are stable at room temperature. Heating the material to higher temperature (300°C) in the presence of NO_2 results in the formation of larger $Ba(NO_3)_2$ crystals (~15–30 nm). At still higher temperatures, as $Ba(NO_3)_2$ decomposes, the nano-sized BaO particles reform. These LNT material morphological changes during operation are summarized in Figure 1. We have also

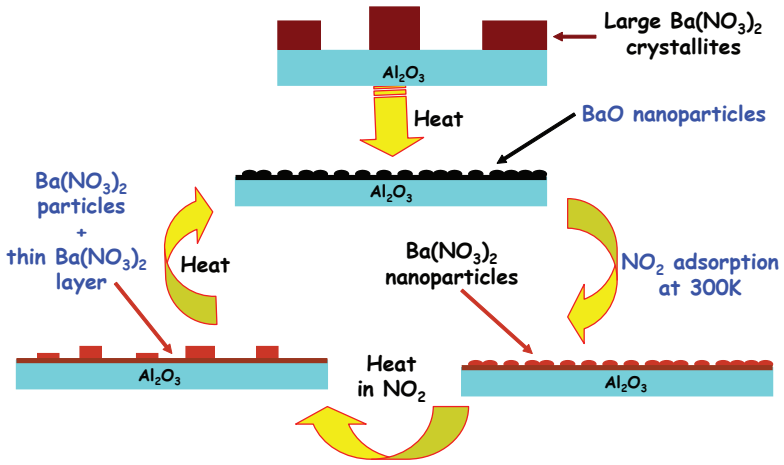

FIGURE 1. Schematics of the Cycle Of Morphology Changes Taking Place during NO_2 Uptake and Release on BaO/Al_2O_3 NOx Storage/Reduction Materials

previously described a number of important practical consequences of these cyclic morphology changes. In particular:

- From TPD experiments, the "monolayer" morphology is found to decompose at lower temperature in vacuum and in a reducing atmosphere than "bulk" nitrates [5,6];
- "Monolayer" Ba-phase is also easier to 'de-sulfate' [7];
- Formation of a high-temperature (deactivating?) $BaAl_2O_4$ phase requires BaO coverages above one monolayer [8]; and
- Morphology model at least partially explains relatively small use of Ba species (often <20%) in storing NOx during typical lean-rich cycling [9].

We have more recently studied the effects of water and/or CO_2 on these morphology changes (manuscripts in preparation).

In this year's report, we highlight two other aspects of our recent studies, the first of which is related to determining the Ba-phase morphologies on the surface of the γ-alumina support material.

Penta-Coordinated Al^{3+} Ions as Preferential Nucleation Sites for BaO on γ-Al_2O_3: an Ultra-High Magnetic Field ^{27}Al MAS NMR Study

In a recently published paper [3], we reported the first observation of preferential anchoring of an impregnated catalytic phase onto penta-coordinated Al^{3+} sites on the surface of γ-Al_2O_3. The interaction of barium oxide with a γ-alumina support was investigated by a high resolution solid state ^{27}Al magic angle spinning (MAS) NMR at an ultra-high magnetic field of 21.1T and at sample spinning rates of up to 23 kHz. Under these experimental conditions, a peak in the NMR spectrum at ~23 ppm with relatively low intensity, assigned to 5-coordinated Al^{3+} ions, is clearly distinguished from the two other peaks representing Al^{3+} ions in tetra-, and octahedral coordination. Figure 2 shows the high resolution solid state center band ^{27}Al MAS NMR spectrum of γ-alumina – to our knowledge, the highest resolution spectrum of this material obtained to date. The spectrum contains the well-known peaks at 0 (by definition here) and ~59 ppm, which are assigned to octa- and tetrahedral Al^{3+} ions, respectively. Interestingly, an additional clearly resolved peak at ~23 ppm with relatively low intensity was also observed when the sample was spun at 23 kHz, consistent with an assignment to penta-coordinated Al^{3+} ions [10]. Note, however, that this peak is not readily observable for typical γ-alumina samples in conventional low field (7.05T), low sample spinning rate (~5 kHz) MAS experiments [11], and is only poorly resolved at intermediate fields and spinning rates [12]. Importantly, spin-lattice ^{27}Al relaxation time measurements clearly show that the penta-coordinated Al^{3+} sites are located on the surface of the γ-alumina support.

BaO deposition onto this γ-alumina sample resulted in the loss of intensity of the 23 ppm peak. Figure 3 shows the 23 kHz center band ^{27}Al MAS NMR spectra obtained from γ-alumina samples loaded with BaO to

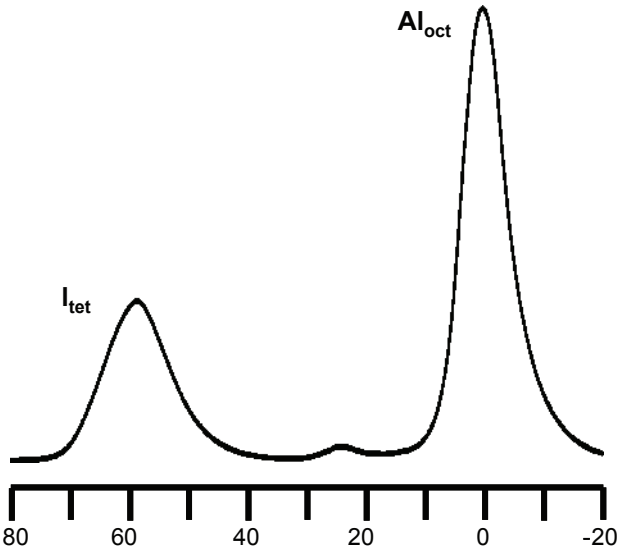

FIGURE 2. Solid State ^{27}Al MAS NMR Spectrum of γ-Alumina, Activated at 500°C for 2 hours, Collected at 21.1 T and a 23 kHz Spinning Rate

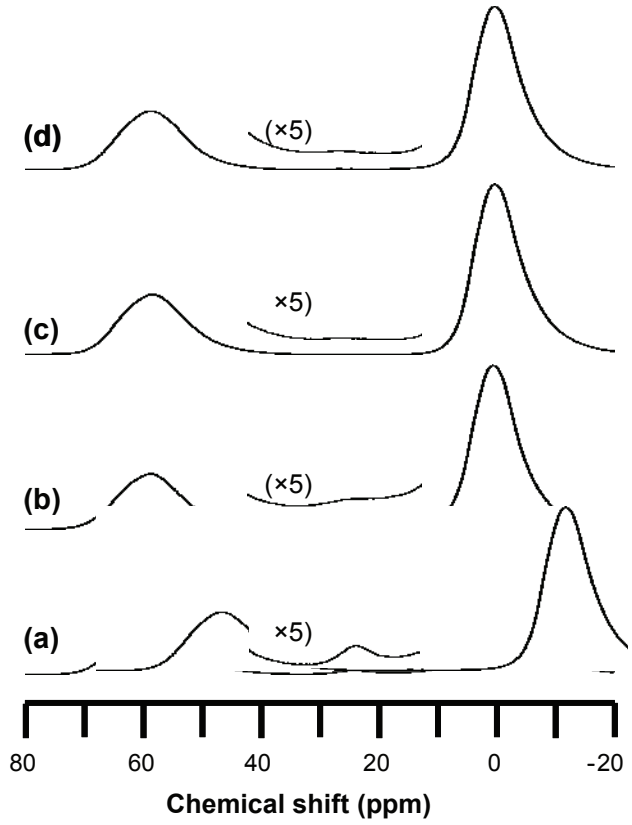

FIGURE 3. Solid State ^{27}Al MAS NMR Spectra, Collected at 21.1 T and 23 kHz Spinning Rate, as a Function of BaO loading: (a) γ-Al_2O_3; (b) 2%BaO/Al_2O_3; (c) 8%BaO/Al_2O_3; and (d) 20%BaO/Al_2O_3

varying levels via wet impregnation, and then activated at 500°C. Neither the peak positions nor the line shapes of the tetra- and the octahedral Al^{3+} ions changed as a function of barium loading. However, the intensity of the ~23 ppm peak decreased significantly for 2% BaO/Al_2O_3 relative to that of the BaO-free γ-alumina. Furthermore, there is essentially no intensity observed at 23 ppm for the eight and 20% BaO/Al_2O_3 samples. These results suggest that initially BaO preferentially occupied the penta-coordinated Al^{3+} sites during the impregnation and subsequent calcination (500°C) processes. The decrease, and eventual disappearance of the 23 ppm NMR peak upon BaO loading also strongly supports the assignment of this peak to Al^{3+} ions located on the surface of the alumina support, and not distributed homogeneously as crystalline defect sites in the bulk. Indeed, separate experiments (not shown) demonstrated that the intensity loss observed was linearly proportional to the amount of BaO deposited. Thus, the results of this study strongly suggest that, at least for BaO, these penta-coordinated Al^{3+} ions are the nucleation sites.

On the basis of the results reported here, the possibility that penta-coordinated Al^{3+} ions on the γ-Al_2O_3 surface generally serve as anchoring sites for catalytically important materials (possibly both oxides and metals) is intriguing. One of the main reasons that γ-Al_2O_3 is used so commonly as a catalyst support material is its ability to form and stabilize active centers (metal and metal oxide particles) with high dispersion. As noted above, our recent studies have shown that BaO, the active NOx storage phase in the LNT technology, initially anchors to these coordinatively unsaturated, pentahedral Al^{3+} sites. This is in excellent agreement with our previous observation that well dispersed BaO nano-particles formed upon the thermal decomposition of a $Ba(NO_3)_2$ precursor loaded onto the γ-Al_2O_3 surface [5]. However, the generality of this phenomenon is not established yet. As such, in our on-going research efforts we are studying the impregnation of other catalytically interesting metal and metal oxide particles onto γ-Al_2O_3 in order to determine whether these penta-coordinated Al^{3+} sites are the anchoring points (nucleation sites) for other catalytically active species. In particular, we are using both ultra-high field NMR and ultra-high resolution TEM, using the ACEM in the High Temperature Materials Laboratory at ORNL, to study Pt dispersion on γ-Al_2O_3. If this correlation holds for other active phase/γ-Al_2O_3 systems such as Pt/Al_2O_3, it could open up the possibility of systematically varying the number of penta-coordinated Al^{3+} sites, and thereby providing good control of dispersion of the catalytically active phase.

NOx uptake on Alkaline Earth Oxides (BaO, MgO, CaO and SrO) Supported on γ-Al_2O_3

NOx uptake experiments were performed on a series of alkaline earth oxide (AEO; *i.e.*, MgO, CaO, SrO, BaO) materials supported on γ-alumina [13]. TPD experiments were conducted on these catalysts in flowing He, revealing the presence of two kinds of nitrate species; i.e., bulk and surface nitrates. The ratio of these two types of nitrate species strongly depends on the nature of the alkaline earth oxide. For example, Figure 4 shows the results of TPD experiments conducted on each NO_2-saturated sample. Figure 4a displays the evolution of NO_2 as a function of temperature for each alkaline earth oxide. A generally systematic increase in the temperature of maximum NO_2 desorption rate can clearly be seen from the lowest temperature for MgO/γ-Al_2O_3 (~400°C), to the highest ones for SrO/ and BaO/ γ-Al_2O_3 (~440°C). (The smaller NO_2 desorption peak at low temperatures, around 120°C, has been attributed [8] to the desorption and decomposition of weakly held N_2O_3 species formed in the reaction of NO+NO_2, and adsorbed primarily on the Al_2O_3 support. This assignment has been confirmed by infrared spectroscopy.) The corresponding TPD profiles of NO evolution are shown in Figure 4b for each alkaline earth oxide. The temperature of maximum NO desorption rate for these materials fall into the very narrow range of 520-530°C. Significantly, the amount

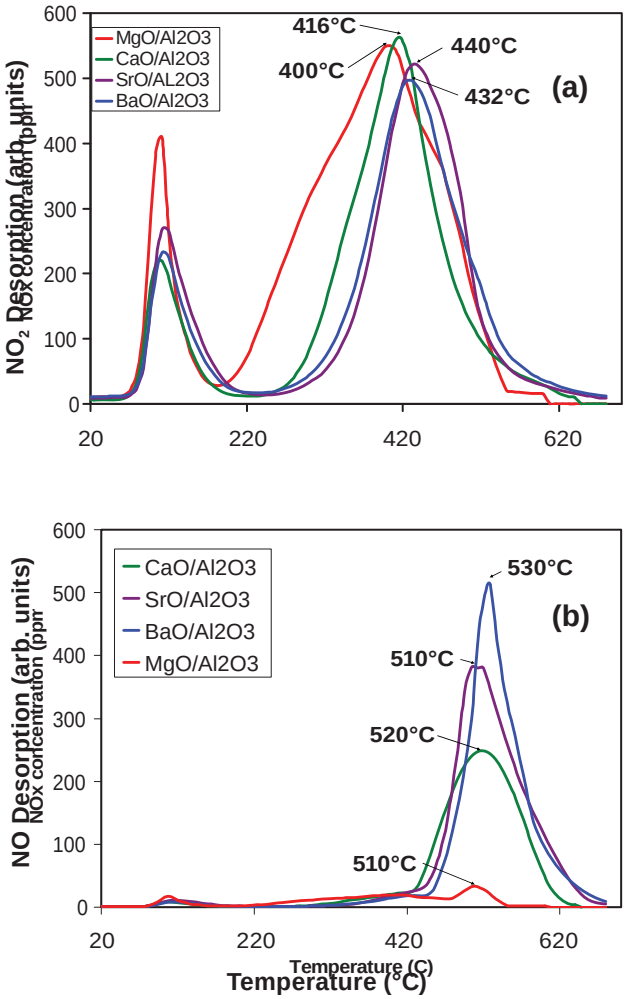

FIGURE 4. TPD Spectra from BaO-, SrO-, CaO- and MgO/γ-Al_2O_3 after NO_2 Saturation at 300 K (heating rate: 8°C/min): (a) NO_2 and (b) NO Desorption Curves

of NO released systematically decreases in the order of BaO > SrO > CaO > MgO. The amount of NO released for MgO/Al_2O_3 is very small (almost nonexistent), while that for the BaO/Al_2O_3 and SrO/Al_2O_3 systems are almost identical. Thus, the amount of bulk nitrate species increases with the basicity of the alkaline earth oxide. This conclusion was supported by the results of FTIR and ^{15}N solid-state NMR spectroscopic studies of NO_2 adsorption.

The effect of water on the NOx species formed in the exposure of the AEOs to NO_2 was also investigated. In agreement with our previous findings for the BaO/γ-Al_2O_3 system, an increase of the bulk nitrate species and the simultaneous decrease of the surface nitrate phase were observed for all of these materials. This is demonstrated in Figure 5 which shows FTIR spectra of NO_2 adsorbed on the various AEO catalysts before and after exposure to water. In the FTIR cell, the activated samples were first saturated with NO_2, the excess NOx was then evacuated and finally these NO_x/AEO/γ-Al_2O_3 samples were exposed to 1 Torr of H_2O, followed by evacuation at 300 K. The changes in the FTIR spectra can primarily be understood as decreases in the intensities of the surface nitrate-related infrared bands with corresponding increases in those due to bulk nitrates.

References

1. (a) Miyoshi, N.; Matsumoto, S.; Katoh, K.; Tanaka, T.; Harada, J.; Takahashi, N.; Yokota, K.; Sugiura, M.; Kasahara, K. SAE Paper 950809, 1995; (b) Miyoshi, N.; Matsumoto, S. Sci. Technol. Catal., 1998, 245.

2. Epling, W. S.; Campbell, L. E.; Yezerets, A.; Currier, N. W.; Parks, J. E. Catal. Rev.–Sci. Eng. 2004, 46, 163.

3. Kwak J.H.; Hu, J.Z. Kim, D.H.; Szanyi, J.; Peden, C.H.F. J. Catal. 2007, 251, 189-194.

4. Wang, X.; Hanson, J.C.; Frenkel, A.I.; Kim, J.-Y.; Rodriguez, J.A. J. Phys. Chem. B, 2004, 108, 13667.

5. Szanyi, J.; Kwak, J.H.; Hanson, J.C.; Wang, C.M.; Szailer, T.; Peden, C.H.F. J. Phys. Chem. B, 2005, 109, 7339.

6. Szailer, T.; Kwak, J.H.; Kim, D.H.; Hanson, J.; Peden, C.H.F.; Szanyi, J. J. Catal.. 2006, 239, 51.

7. Kim, D.H.; Szanyi, J.; Kwak, J.H.; Szailer, T.; Hanson, J.C.; Wang, C.M.; Peden, C.H.F. J. Phys. Chem. B, 2006, 110, 10441.

8. Szailer, T.; Kwak, J.H.; Kim, D.H.; Szanyi, J.; Wang, C.; Peden, C.H.F. Catal. Today, 2006, 114, 86.

9. Kwak, J.H.; Kim, D.H.; Szanyi, J.; Szailer, T.; Peden, C.H.F. Catal. Lett., 2006, 111, 119.

10. (a) F.R. Chen, J.G. Davis, J.J. Fripiat, J. Catal., 1992, 133, 263; (b) D. Coster, A.L. Blumenfeld, J.J. Fripiat, J. Phys. Chem., 1994, 98, 6201; (c) J.J. Fitzgerald, G. Piedra, S.F. Dec, M. Seger, G.E. Maciel, J. Am. Chem. Soc., 1997, 119, 7832.

11. (a) D.H. Kim, J.H. Kwak, J. Szanyi, S.D. Burton, C.H.F. Peden, App. Catal. B, 2007, 72, 234; (b) M.H. Lee, C.F. Cheng, V. Heine, J. Klinowski, Chem. Phys. Lett., 1997, 265, 673.

12. (a) A. Omegna, J.A. van Bokhoven, R. Prins, J. Phys. Chem. B, 2003, 107, 8854; (b) C. Pecharroman, I. Sobrados, J.E. Iglesias, T. Gonzalez-Carreno, J. Sanz, J. Phys. Chem. B, 1999, 103, 6160.

13. Verrier C, J Kwak, D Kim, CHF Peden, J Szanyi, Catal. Today, 2007, in press.

FY 2007 Presentations

INVITED

1. Peden, C.H.F. "Fundamental Studies of Catalytic NOx Vehicle Emission Control." Invited Presentations made by Chuck Peden at the following locations:

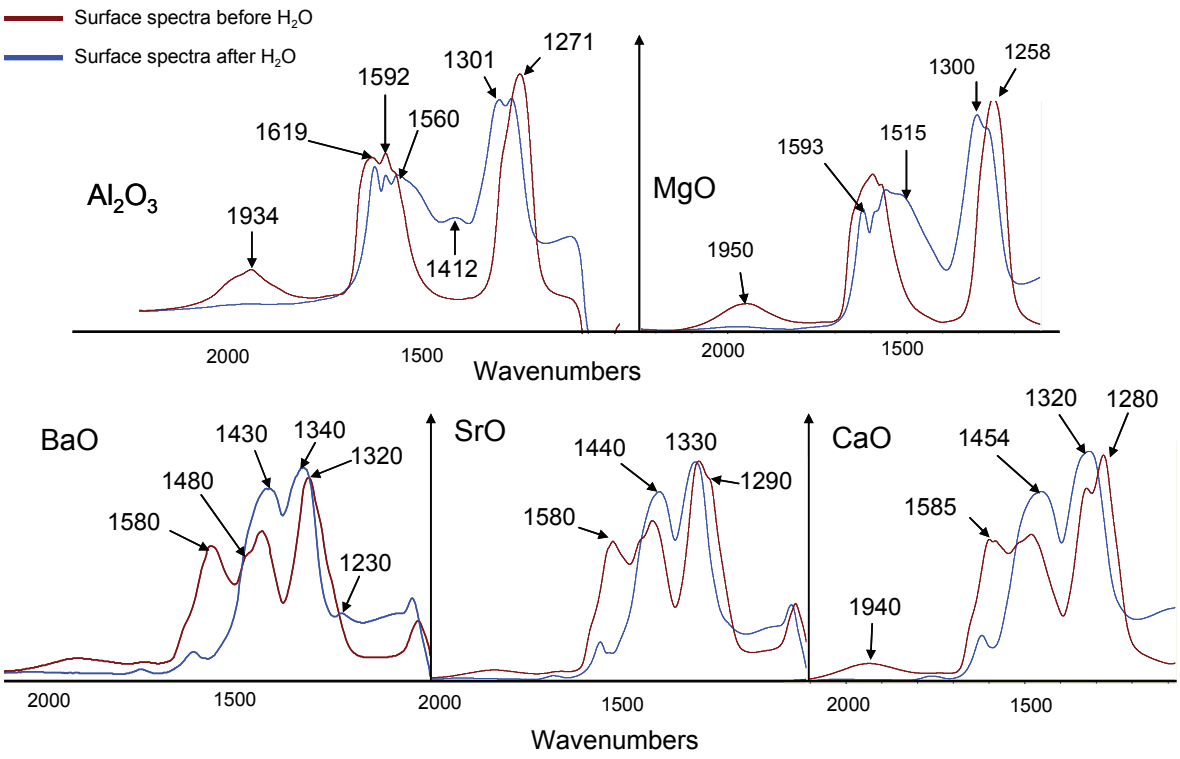

FIGURE 5. Infrared Spectra after NO_2 Adsorption and Evacuation (Brown Curves), Followed by Water Adsorption and Evacuation (Blue Curves) on BaO-, SrO-, CaO- and MgO/γ-Al_2O_3

- Dalian Institute of Chemical Physics, Dalian, China, December 11, 2007.
- Dalian University of Technology, Dalian, China, December 12, 2007.
- Tianjin University, Tianjin University, December 14, 2007.
- Texas A&M University, College Station, TX, January 29, 2007.

2. Peden, C.H.F; Ozensoy, E.; Yi, C.-W.; Szanyi, J. "Model Studies of BaO/Al2O3 NOx Storage Materials." Invited Presentation made by Chuck Peden at the 233rd American Chemical Society National Meeting, Chicago, IL on April 3, 2007.

3. Disselkamp, R.; Kim, D.-H.; Kwak, J.-H.; Szanyi, J.; Tonkyn, R.; Wang, X.; Peden, C.; Howden, K. "Fundamental Studies of NOx Adsorber Materials." Invited Presentation made by Chuck Peden at the 2007 Advanced Combustion Engine Peer Review Meeting, Washington, D.C. on June 18, 2007.

CONTRIBUTED

4. Kim D, J Kwak, J Szanyi, Y Chin, X Wang, JC Hanson, and CHF Peden. "The Various Roles of Water in the Pt-BaO/Al_2O_3 Lean NOx Trap Catalyst System." Presented by Do Heui Kim at the 2006 American Institute of Chemical Engineers (AIChE) Annual Meeting, San Fransisco, CA on November 13, 2006.

5. Peden CHF, D Kim, J Kwak, X Wang, T Szailer, WS Epling, JC Hanson, and J Szanyi. "LNT Morphology Changes with Lean/Rich Cycling." Presented by Chuck Peden at the 2006 American Institute of Chemical Engineers (AIChE) Annual Meeting, San Francisco, CA on November 14, 2006.

6. Peden CHF, D Kim, J Kwak, J Szanyi, Y Chin, X Wang, WS Epling, and JC Hanson. "The Various Roles of Water in the Pt-BaO/Al_2O_3 Lean NOx Trap Catalyst System." Presented by Chuck Peden at the APCAT 4 Conference, Singapore on December 8, 2006.

7. Peden CHF. "Fundamental Studies of NOx Adsorber Materials at PNNL." Presented by Chuck Peden at the 10th DOE CLEERS Workshop, Dearborn, MI on May 2, 2007.

8. Kwak J, D Kim, J Szanyi, and CHF Peden. "Solid State ^{27}Al NMR Study of BaO/Al_2O_3 Catalysts: $BaAl_2O_4$ Formation and Decomposition." Presented by Ja Hun Kwak at the 20th North American Meeting of the Catalysis Society, Houston, TX on June 18, 2007.

9. Verrier C, J Kwak, D Kim, CHF Peden, and J Szanyi. "NOx Storage over Alkaline Earth Oxides Supported on γ-Al_2O_3." Presented by Christelle Verrier at the 20th North American Meeting of the Catalysis Society, Houston, TX on June 18, 2007.

10. Szanyi J, J Kwak, D Kim, J Hanson, and CHF Peden. "The Effect of Water on the Adsorbed NOx species over BaO/Al_2O_3 NOx Storage Materials: A Combined FTIR and *In-Situ* Time-Resolved XRD study." Presented by Janos

Szanyi at 20th North American Meeting of the Catalysis Society, Houston, TX on June 21, 2007.

11. Szanyi J, J Kwak, D Kim, J Hanson, and CHF Peden. "The Effect of Water on the Adsorbed NOx species over BaO/Al_2O_3 NOx Storage Materials: A Combined FTIR and *In-Situ* Time-Resolved XRD study." Presented by Janos Szanyi at EUROPACAT 8, Turku, Finland on August 27, 2007.

FY 2007 Publications

1. Kwak J, D Kim, T Szailer, CHF Peden, and J Szanyi. 2006. "NOx Uptake Mechanism on $Pt/BaO/Al_2O_3$ Catalysts." *Catalysis Letters* **111**(3-4):119-126.

2. Disselkamp, R.; Kim, D.-H.; Kwak, J.-H.; Szanyi, J.; Tonkyn, R.; Wang, X.; Peden, C.; Howden, K. 2007. "Fundamental Studies of NOx Adsorber Materials." Combustion and Emission Control for Advanced CIDI Engines, FY2006 Progress Report, pp. 135-141.

3. Kim D, J Kwak, J Szanyi, SD Burton, and CHF Peden. 2007. "Water-induced Bulk $Ba(NO_3)_2$ Formation From NO_2 Exposed Thermally Aged BaO/Al_2O_3." *Applied Catalysis. B, Environmental* **72**(3-4):233-239.

4. Kwak J, J Hu, D Kim, J Szanyi, and CHF Peden. 2007. "Penta-coordinated Al^{3+} Ions as Preferential Nucleation Sites for BaO on γ-Al_2O_3: an Ultra-high Magnetic Field ^{27}Al MAS NMR Study." *Journal of Catalysis* **251**(2):189-194.

5. Szanyi J, J Kwak, RJ Chimentao, and CHF Peden. 2007. "The effect of H_2O on the adsorption of NO_2 on γ-Al_2O_3: an in situ FTIR/MS study." *Journal of Physical Chemistry C* **111**(6):2661-2669.

6. Szanyi J, J Kwak, D Kim, X Wang, J Hanson, RJ Chimentao, and CHF Peden. 2007. "Water-induced morphology changes in BaO/γ-Al_2O_3 NOx storage materials." *Chemical Communications* **2007**(9):984-986.

7. Szanyi J, J Kwak, D Kim, X Wang, RJ Chimentao, J Hanson, WS Epling, and CHF Peden. 2007. "Water-induced morphology changes in BaO/γ-Al_2O_3 NOx storage materials: an FTIR, TPD, and time-resolved synchrotron XRD study." *Journal of Physical Chemistry C* **111**(12):4678-4687.

8. Verrier C, J Kwak, D Kim, CHF Peden, and J Szanyi. 2007. "NOx uptake on alkaline earth oxides (BaO, MgO, CaO and SrO) supported on γ-Al_2O_3." *Catalysis Today*, in press.

9. Epling, W.S.; Peden, C.H.F.; Szanyi, J. 2008. "Carbonate Formation and Stability on a $Pt/BaO/Al_2O_3$ NOx Storage/Reduction Catalyst." *Journal of Physical Chemistry C*, submitted for publication.

II.B.2 Mechanisms of Sulfur Poisoning of NOx Adsorber Materials

Do Heui Kim, Xianqin Wang, George Muntean, Chuck Peden (Primary Contact)
Institute for Interfacial Catalysis
Pacific Northwest National Laboratory (PNNL)
P.O. Box 999, MS K8-93
Richland, WA 99354

DOE Technology Development Manager:
Ken Howden

CRADA Partners:
- Randy Stafford, John Stang, Alex Yezerets, Neal Currier - Cummins Inc., Columbus, IN
- Hai-Ying Chen, Howard Hess - Johnson Matthey, Wayne, PA

Objectives

- Develop and apply characterization tools to probe the chemical and physical properties of NOx adsorber catalyst materials for studies of deactivation due to sulfur poisoning and/or thermal aging. Utilize this information to develop mechanistic models that account for NOx adsorber performance degradation.
- Develop protocols and tools for failure analysis of field-aged materials.
- Provide input on new catalyst formulations; verify improved performance through materials characterizations, and laboratory and engine testing.

Accomplishments

Three major thrusts this year:

- Strong metal-support interactions (SMSIs) in Pt-BaO/Al_2O_3, and their effects on NOx storage. We observed:
  - A decrease in Pt accessibility for H_2 chemisorption with increasing reduction temperature without a corresponding change in Pt particle size, implying that BaO covers at least part of the Pt surface during reduction.
  - An increase in NOx storage capacity up to a reduction temperature of 500°C, strongly suggests that there is a promotional effect of this SMSI-like (Pt-BaO) interaction on NOx storage.
- Sequential high temperature reduction, low temperature hydrolysis for the regeneration of sulfated NOx trap catalysts.
  - Based on prior work, water promotes sulfur removal from deactivated lean-NOx trap (LNT) materials, although it can have a negative effect on Pt sintering, at least partially offsetting the benefits of desulfation on regenerating NOx storage activity.
  - We developed an approach that consists of two separate processes of high temperature reduction with H_2 followed by a low temperature hydrolysis step. As a result, Pt sintering is significantly inhibited and optimized NOx storage performance is achieved.
- The roles of Pt and BaO in the sulfation of Pt/BaO/Al_2O_3 LNT materials.
  - In last year's annual report, we described S X-ray absorption near-edge spectroscopy (XANES) and Pt X-ray absorption fine structure (XAFS) studies of the effect of initial barium morphology on the desulfation behavior of Pt-BaO/Al_2O_3 catalysts. In this last year, the same techniques were applied to elucidate the sulfation mechanism, and the roles of each catalyst component in the sulfation process for model LNT materials.
  - The results indicate that barium species have an ability to make sulfate species even without gaseous oxygen and Pt. In addition, even if aluminum sites are available, barium is preferentially sulfated to make barium sulfate.
  - We also find that Pt-O plays a crucial role in making sulfate until its pre-existing levels are consumed. If gaseous oxygen is present in the environment, such species can reform and continue to react with SO_2 to make additional sulfate species.

Four public presentations and four manuscripts have been cleared for release by the Cooperative Research and Development Agreement (CRADA) partners. One of the manuscripts has appeared in the National Synchrotron Light Source activity report as a highlight article.

Future Directions

- Further refine function-specific measures of 'aging':
  - More detailed studies to verify that techniques such as NO_2 temperature programmed desorption (TPD) and H_2 temperature programmed reaction (TPRX) are providing information content suggested by studies to date.

  - Some effort still to identify new approach to unravel some key unknowns (*e.g.*, role of precious metal/storage material 'contact').
- Validate most-suitable function-specific measures on samples incrementally 'aged' under realistic conditions.
- Apply developed techniques to the commercial fresh and "aged" samples in the monolith form:
  - Determine optimized regeneration conditions by using program-developed reaction protocol.
  - X-ray photoelectron spectroscopy (XPS), S XANES, time resolved (TR)-X-ray diffraction (XRD) studies to follow the changes of sulfur species with sulfation/desulfation.
  - Use technique capable of spatially resolving sulfur distributions, including scanning electron microscope energy dispersive (X-ray) spectroscopy and XPS, to follow changes in these distributions with sulfation/desulfation.
- Continue to improve mechanistic understanding of sulfur removal processes:
  - Investigate the role of Pt during desulfation.
  - Identify important desulfation intermediates.
  - Investigate the effects of sulfur concentration on Pt accessibility and barium phase changes.

Introduction

The NOx adsorber (also known as a LNT) technology is based upon the concept of storing NOx as nitrates over storage components, typically barium species, during a lean-burn operation cycle and then reducing the stored nitrates to N_2 during fuel-rich conditions over a precious metal catalyst [1]. This technology has been recognized as one of the most promising approaches for meeting stringent NOx emission standards for diesel vehicles within the Environmental Protection Agency's 2007/2010 mandated limits. However, problems arising from either or both thermal and SO_2 deactivation must be addressed to meet durability standards. Therefore, an understanding of these processes will be crucial for the development of the LNT technology.

This project is focused on the identification and the understanding of the important degradation mechanism(s) of the catalyst materials used in LNTs. 'Simple' and 'Enhanced Model' $Pt/BaO/Al_2O_3$ samples were investigated. In particular, the changes in physicochemical properties related to the reaction performances of these LNT materials, due to the effects of high temperature operation and sulfur poisoning, are the current focus of the work. By comparing results obtained on 'Simple Model' $Pt/BaO/Al_2O_3$ with 'Enhanced Model' materials, we try to understand the role of various additives on the deactivation processes. We now move on to the real commercial sample which is being used in a Dodge Ram truck with a Cummins diesel emission control system. However, the results about the 'commercial sample' will not be covered in this report. We further note here that while program progress for the entire year is summarized above in the "Accomplishments" section, we present in the following more detail about results obtained in this last year in three specific areas: i) SMSI in $Pt\text{-}BaO/Al_2O_3$ and their effects on NOx storage, ii) sequential high temperature reduction, low temperature hydrolysis for the regeneration of sulfated NOx trap catalysts, iii) the roles of Pt and BaO in the sulfation of $Pt/BaO/Al_2O_3$ LNT materials.

Approach

In a microcatalytic reactor system, LNT performance is evaluated in a fixed bed reactor operated under continuous lean-rich cycling. Rapid lean-rich switching is enabled just prior to the elevated temperature zone (furnace) where the LNT materials are contained in quartz tubing. After removing water, the effluent of the reactor can be analyzed by mass spectrometry and by a chemiluminescent NOx analyzer. For a typical baseline performance test, the sample is heated to a reaction temperature in flowing He, the feed switched to a 'lean-NOx' mixture containing oxygen and NO, as well as CO_2 and/or H_2O. After an extended period (15 minutes or more), multiple rich/lean cycles of 1 and 4 minute duration, respectively, are run and NOx removal performance is assessed after at least three of these are completed. In the LNT technology, the state of the system is constantly changing so that performance depends on when it is measured. Therefore, we obtain NOx removal efficiencies as "Lean conversion (30 minutes)", which measures NOx removal efficiencies for the first 30 minutes of the lean-period. In addition, material treatments such as SO_2 aging, and post mortem catalyst characterizations were conducted in the same test stand without exposing the catalyst sample to air. We have established a reaction protocol, which evaluates the performance of samples after various thermal aging and sulfation condition. In this way, we could identify optimum de-sulfation treatments to rejuvenate catalyst activities.

State-of-the-art catalyst characterization techniques such as XRD, XPS, transmission electron microscopy (TEM)/EDS, Brunauer, Emmett and Teller pore size distribution, and TPD/TPRX were utilized to probe the changes in physicochemical properties of the catalyst samples under deactivating conditions; *e.g.*, thermal aging and SO_2 treatment. Specifically, H_2 TPRX, Sulfur K-edge XANES and TR-XRD methods were used extensively to quantify the levels, speciation and phase

of sulfur on the model adsorber material (Al_2O_3, Pt/Al_2O_3, BaO/Al_2O_3 and Pt-BaO/Al_2O_3) as a function of desulfation process.

Results

SMSIs in Pt-BaO/Al_2O_3 and Their Effects on NOx Storage

H/Pt values determined from H_2 chemisorption measurements is a common way to measure the number and accessibility of active sites for many supported Pt catalysts. Figure 1 shows the H/Pt curve obtained as a function of reduction temperature for a Pt-BaO/Al_2O_3 catalyst. It shows that the H/Pt ratio decreases uniformly as a function of reduction temperature. Estimating Pt particle sizes based on this ratio, the results suggest that Pt particle sizes uniformly increased with increases in the reduction temperature, with an estimated Pt particle size of about 26 nm for the case of the sample after reduction at 800°C. However, the particle size from TEM images obtained from these samples is ~5-10 nm, suggesting that the actual Pt particle sizes were much smaller than those determined from the H_2 chemisorption method. Such an apparent discrepancy in the results from these two techniques strongly supports the existence of SMSI in the samples reduced at high temperature, especially above 500°C. In other words, the decrease in the H/Pt ratio actually arises from an encapsulation of Pt by a migrating BaO_x layer. We measured NOx uptakes of the Pt/Ba-Al_2O_3 catalysts after they were reduced at different temperatures. As shown in Figure 1, the results clearly show an increase in the NOx uptake up to a reduction temperature of 500°C, followed by a gradual decrease with further increases in the reduction temperatures. The decrease in NOx uptake after 500°C is attributed to a thermal aging effect.

Sequential High Temperature Reduction, Low Temperature Hydrolysis for the Regeneration of Sulfated NOx Trap Catalysts

Water is known to promote desulfation of LNT catalysts; however, it has also been shown to have a negative effect on catalytic performance via the promotion of Pt sintering. In addition, our group [2] has previously demonstrated that the NOx uptake efficiency is adversely affected by the growth of platinum particles arising from thermal aging. Hence, Pt sintering is detrimental to the performance of these LNT catalysts. Even more important is the irreversible nature of this deactivation process since the sintered Pt particles can not be re-dispersed. To explore ways to prevent such sintering, we designed a desulfation process in which H_2 and H_2O are separately introduced in two sequential steps as shown in Figure 2: desulfation with H_2 only at high temperatures (up to 800°C), followed by H_2O treatment at lower temperatures (maximum of 300°C). The first step transforms the sulfate species into sulfides and even desorbs some of the sulfur as H_2S, while minimizing the Pt sintering. In the second step, the thus formed BaS reacts with H_2O in a hydrolysis reaction to form BaO and additional H_2S. The second process is regarded as a key factor for promoting irreversible Pt sintering behavior. By using this sequential desulfation process, we can significantly decrease the levels of Pt sintering as shown in the TEM pictures of Figure 3, while the amount of sulfur removed from the sample is less than

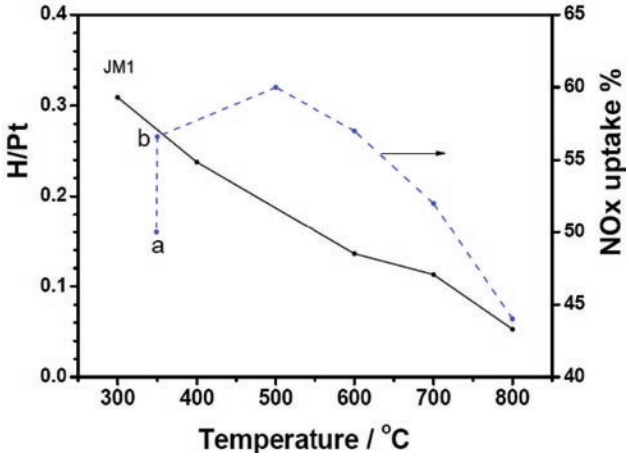

FIGURE 1. Comparison of a H/Pt curve with NOx Uptake as a Function of Reduction Temperature for a Pt-BaO/Al_2O_3 Sample

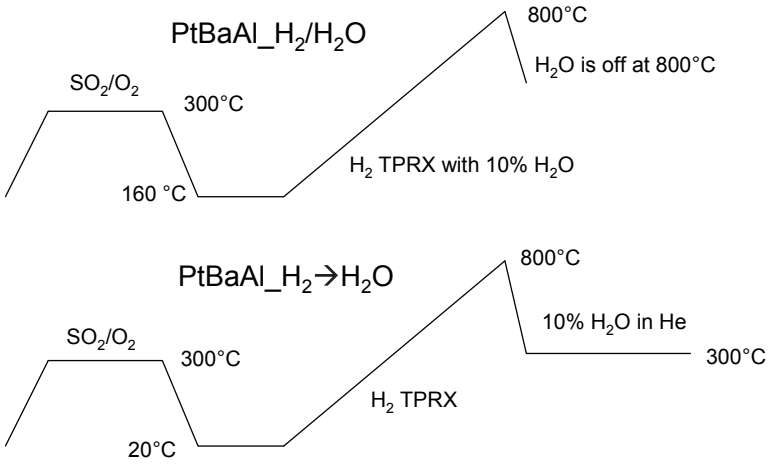

FIGURE 2. Two Regeneration Protocol Steps used to Desulfate Sulfated Pt-BaO(20)/Al_2O_3 Samples

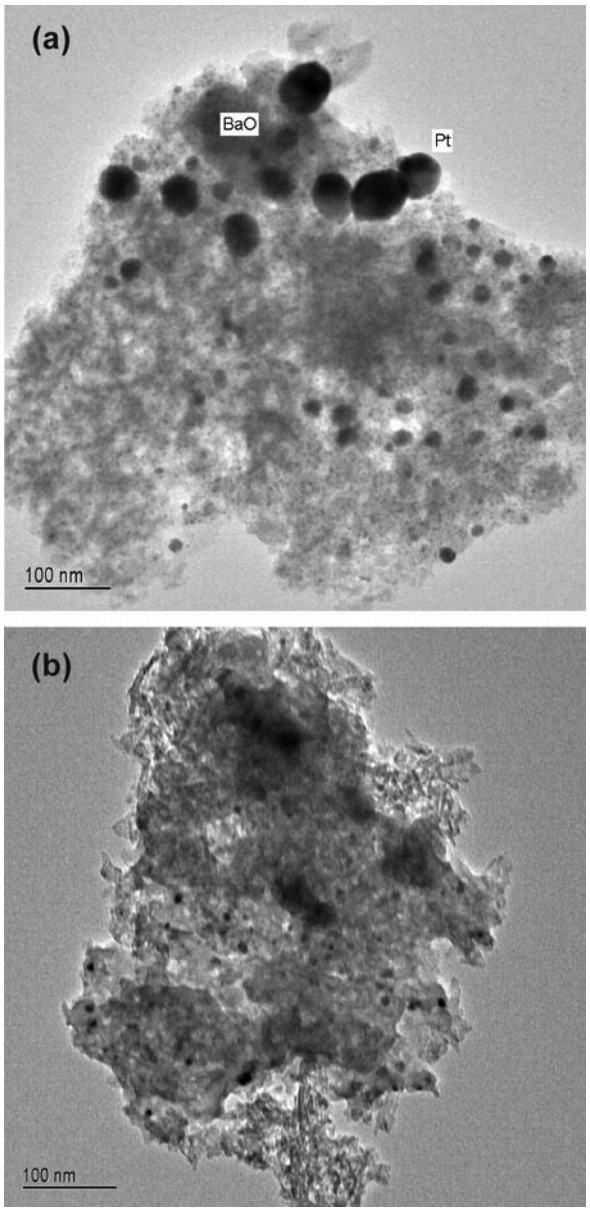

FIGURE 3. TEM Images of Samples of PtBaAl_H_2→H_2O (a) and PtBaAl_H_2/H_2O (b)

cooperative desulfation with H_2 and H_2O. The NOx uptake results showed similar NOx uptake performance for catalysts desulfated cooperatively with H_2 and H_2O or sequentially. Although the amount of H_2S desorbed during the cooperative desulfation process is larger than that of sequential one under the experimental conditions presented here, a modification of the two-step desulfation protocol may offer a means to improve the desulfation efficiency while maintaining the lack of Pt particle size growth. This can be achieved by optimizing the experimental conditions, in particular H_2O concentration and hydrolysis temperature.

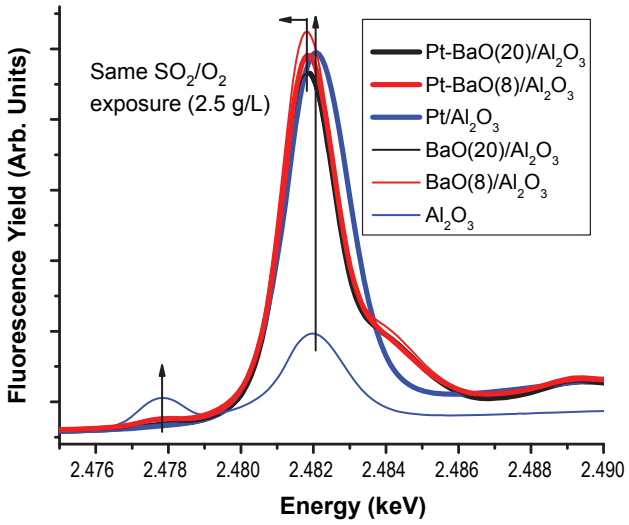

FIGURE 4. Sulfur K-edge XANES Spectra of Al_2O_3, Pt/Al_2O_3, BaO(8 or 20)/Al_2O_3 and Pt-BaO(8 or 20)/Al_2O_3, each Sample Having Been Given an Equivalent Sulfation Exposure of 2.5 g/L

The Roles of Pt and BaO in the Sulfation of Pt/BaO/Al_2O_3 LNT Materials

The roles of barium oxide and platinum during the sulfation of Pt-BaO/Al_2O_3 LNT catalysts were investigated by S K-edge XANES and Pt L_{III} XAFS. All of the samples studied (Al_2O_3, BaO/Al_2O_3, Pt/Al_2O_3 and Pt-BaO/Al_2O_3) were pre-sulfated prior to the X-ray absorption measurements.

Figure 4 compares the S XANES spectra obtained for Al_2O_3, BaO(8 or 20)/Al_2O_3 samples, in the presence and absence of Pt, after the same SO_2/O_2 sulfation processes. For the case of the Al_2O_3 support itself, two peaks are observed near 2,478 eV and 2,482 eV, which can be assigned to aluminum sulfites (SO_3^{2-}) and aluminum sulfates (SO_4^{2-}), respectively. The intensity of the white line at 2,482 eV for sulfated Al_2O_3 is much smaller than in samples containing Pt or BaO, implying that all SO_2 dosed was not fully adsorbed on Al_2O_3. The greater intensity for the Pt- and Ba-containing samples is consistent with the results of SO_2 breakthrough measurements indicating that all dosed SO_2 was adsorbed by Pt/Al_2O_3 and Pt-BaO(8 or 20)/Al_2O_3 up to sulfation levels of 2.5 g/L. Thus, both Pt and barium oxide play a critical role in promoting sulfation for the catalysts supported on alumina.

The 8 wt% and 20 wt% BaO on Al_2O_3 materials are estimated to correspond to 0.26 and 0.75 monolayer coverages of BaO on the alumina surface [3]. Therefore, significant areas of the alumina surface would still be available for SO_2 to adsorb to form aluminum sulfates. Despite this, the essentially identical peak shapes of the primary S XANES feature for the barium loaded samples, clearly showing that SO_2 preferentially

favors the formation of barium sulfates as long as barium remains available for this reaction. It can be summarized that barium oxide itself has the ability to directly form barium sulfate even in the absence of Pt and gas phase oxygen. In the platinum-containing samples, the presence of Pt-O species plays an important role in the formation of sulfate species. However, when oxygen is absent from the gas phase, the sulfation route that involves Pt-O is eliminated after the initially present Pt-O species are completely consumed.

Conclusions

PNNL and its CRADA partners from Cummins Inc. and Johnson Matthey are carrying out a project to study the mechanisms of deactivation of the materials proposed for use in LNTs arising from thermal aging and SO_2 poisoning. Results demonstrate that a strong metal support interaction between Pt and BaO was observed and resulted in a decrease in hydrogen uptake during chemisorption even though Pt particle sizes were not changing. By using a sequential desulfation process, *i.e.*, high temperature desulfation and low temperature hydrolysis, we can significantly decrease levels of Pt sintering. The NOx uptake results showed similar performance for catalysts desulfated cooperatively with H_2 and H_2O or sequentially. Combination of S XANES and Pt XAFS experiments allow us to elucidate sulfation mechanisms, and the roles in the sulfation processes of each component in the LNT catalyst. Overall, these studies are providing valuable information for overcoming critical durability issues in LNT catalysts.

References

1. Epling, W. S.; Campbell, L. E.; Yezerets, A.; Currier, N. W.; Parks, J. E. *Catal. Rev.–Sci. Eng.* 2004, 46, 163.

2. Kim, D.H.; Chin, Y.-H.; Muntean, G.; Yezeretz, A.; Currier, N.; Epling, W.; Chen, H.-Y.; Hess H.; Peden, C.H.F. *Industrial and Engineering Chemistry Research*, 2006, **45**, 4415.

3. Yi, C.-W.; Kwak, J. H.; Peden, C.H.F.; Wang, C.M.; Szanyi, J. *Journal of Physical Chemistry C*, 2007, **111**, 14942.

FY 2007 Publications/Presentations

1. Do Heui Kim, Ya-Huei Chin, George Muntean, Aleksey Yezeretz, Neal Currier, William Epling, Hai-Ying Chen, Howard Hess, and Charles Peden, "Relationship of Pt particle size with the NO_x storage performance over thermally aged $Pt/BaO/Al_2O_3$ lean NO_x trap catalysts", Industrial and Engineering Chemistry Research **45** (2006) 4415.

2. Do Heui Kim, Janos Szanyi, Ja Hun Kwak, Tamas Szailer, Jon C. Hanson, Chongmin Wang, and Charles H.F. Peden, "Sulfur K-edge XANES and TR-XRD studies of Pt-BaO/Al_2O_3 lean NOx trap catalysts: Effects of barium loading on desulfation", National Synchrotron Light Source Activity Report 2006, 2-36.

3. Do Heui Kim, Ya-Huei Chin, George Muntean, Aleksey Yezeretz, Neal Currier, William Epling, Hai-Ying Chen, Howard Hess, and Charles Peden, "Design of reaction protocol for de-coupling the desulfation and thermal aging effects during regeneration of Pt-BaO/Al_2O_3 lean NOx trap catalysts", Industrial and Engineering Chemistry Research **46** (2007) 2735.

4. Randy L. Vander Wal, Aleksey Yezerets, Neal W. Currier, Do Heui Kim, and Chongmin Wang, "HR-TEM Study of Diesel Soot Collected from Diesel Particulate Filters", Carbon **45** (2007) 70.

5. Do Heui Kim, Xianqin Wang, George Muntean, Charles Peden, Ken Howden, Randy Stafford, John Stang, Aleksey Yezerets, Neil Currier, Haiying Chen, Howard Hess, and Andrew Walker, "Mechanisms of Sulfur Poisoning of NOx Adsorber Materials", in Combustion and Emission Control for Advanced CIDI Engines: FY2006 Annual Progress Report, (2007) 142.

6. Do Heui Kim, Ja Hun Kwak, Xianqin Wang, Janos Szanyi, and Charles H.F. Peden, "Sequential high temperature reduction, low temperature hydrolysis for the regeneration of sulfated NO_x trap catalysts". Catalysis Today (2008) in press.

7. Do Heui Kim, Ja Hun Kwak, Xianqin Wang, Janos Szanyi, and Charles H.F. Peden, "The Roles of Pt and BaO in the Sulfation of $Pt/BaO/Al_2O_3$ Lean NOx Trap Materials: Sulfur K-Edge XANES and Pt L_{III} XAFS Studies", Journal of Physical Chemistry C, (2008) in press.

8. X. Wang, D.H. Kim, J.H. Kwak, C.M. Wang, J. Szanyi, and C.H.F. Peden, "Peculiar Changes in Pt Accessibility and Morphology for Pt/BaO-Al_2O_3 Lean NOx Trap Catalysts with Different Sulfation Levels", presentation at the AIChE Annual Meeting, San Francisco, CA, November 2006.

9. D.H. Kim, X. Wang, G.G. Muntean, C.H.F. Peden, N. Currier, R. Stafford, J. Stang, A. Yezerets, H.-Y. Chen, and H. Hess, "Mechanisms of Sulfur Poisoning of NOx Adsorber Materials", presentation at the DOE Advanced Combustion Engine and Emission Control Review, Washington, D.C., June 2007.

10. D.H. Kim, J.H. Kwak, J. Szanyi, X. Wang, J.C. Hanson, and C.H.F. Peden, "Barium loading effects on the Desulfation of $Pt/BaO/Al_2O_3$ Lean NOx Trap Catalysts: an *in situ* Sulfur XANES and TR-XRD Study", presentation at the 20th Meeting of the North American Catalysis Society, Houston, TX, June 2007.

II.B.3 Characterizing Lean-NOx Trap Regeneration and Desulfation

James Parks (Primary Contact), Shean Huff, Brian West, Mike Kass
Oak Ridge National Laboratory
2360 Cherahala Boulevard
Knoxville, TN 37932

DOE Technology Development Manager:
Kenneth Howden

Objectives

- Establish relationships between exhaust species and various lean-NOx trap (LNT) regeneration strategies.
- Characterize effectiveness of in-cylinder regeneration strategies.
- Develop stronger link between bench and full-scale system evaluations.
- Provide data through Cross-Cut Lean Exhaust Emissions Reduction Simulations (CLEERS) to improve models. Use models to guide engine research.

Accomplishments

- Analyzed model and commercial LNT catalysts on a full-scale engine system with in-cylinder regeneration techniques.
- Measured NH_3 emissions from LNTs and determined the effect of ceria on NH_3 control.
- Interacted with the CLEERS modeling community by presenting results in a CLEERS teleconference and the CLEERS workshop and by uploading data to the CLEERS web site database.

Future Directions

- Conduct experiments to analyze the potential benefit of NH_3 emissions from LNT catalysts for downstream selective catalytic reduction.
- Evaluate lower precious metal LNT catalysts to study possibilities for cost reduction (a key limitation to introduction of the technology).
- Examine LNT catalysts for lean gasoline engine applications.

Introduction

As part of the Department of Energy's strategy to reduce imported petroleum and enhance energy security, the Office of FreedomCAR and Vehicle Technologies has been researching enabling technologies for more efficient diesel engines. NOx emissions from diesel engines are very problematic and the U.S. Environmental Protection Agency (EPA) emissions regulations require ~90% reduction in NOx from light- and heavy-duty diesel engines in the 2004-2010 timeframe. One active research and development focus for lean-burn NOx control is in the area of LNT catalysts. LNT catalysts adsorb NOx very efficiently in the form of a nitrate during lean operation, but must be regenerated periodically by way of a momentary exposure to a fuel-rich environment. This rich excursion causes the NOx to desorb and then be converted by nobel metal catalysts to harmless N_2. The momentary fuel-rich environment in the exhaust occurs 2-4 seconds for every 30-90 seconds of normal lean operation (depending on operating conditions). The rich exhaust can be created by injecting excess fuel into the cylinder or exhaust, throttling the intake air, increasing the amount of exhaust gas recirculation (EGR), or through some combination of these strategies. The controls methodology for LNTs is very complex, and there is limited understanding of the how all of the competing factors can be optimized.

While LNTs are effective at adsorbing NOx, they also have a high affinity for sulfur. As such, sulfur from the fuel and possibly engine lubricant (as SO_2) can adsorb to NOx adsorbent sites (as sulfates). Similar to NOx regeneration, sulfur removal (desulfation) also requires rich operation, but for several minutes, at much higher temperatures. Desulfation intervals are much longer, on the order of hundreds or thousands of miles, but the conditions are more difficult to achieve and are potentially harmful to the catalyst function. Nonetheless, desulfation must be accomplished periodically to maintain effective NOx performance. There is much to be learned with regard to balancing all the factors in managing LNT NOx control performance, durability, and sulfur tolerance.

The objective of this project is to understand the complex chemistry that occurs during the regeneration processes for LNTs through experiments conducted on a full size engine-LNT catalyst system. Different strategies for introducing the excess fuel for regeneration can produce a wide variety of hydrocarbon and other species. Specific regeneration strategies were developed for this project by operating the engine with net rich air-to-fuel ratios; such "in-cylinder" techniques utilize throttling to reduce air flow and extra fuel injection

pulses during the combustion event to increase fueling. A primary focus of this work is to examine the effectiveness of various regeneration strategies in light of the species formed and the LNT formulation since the combined chemistry of the exhaust produced by the regeneration strategy and the chemistry of the LNT catalyst dictate performance.

Approach

A 1.7-L Mercedes Benz common rail engine and motoring dynamometer have been dedicated to this activity. The engine is equipped with an electronic engine control system that provides full-bypass of the original engine controller. The controller is capable of monitoring and controlling all the electronically controlled parameters associated with the engine (i.e., fuel injection timing/duration/number of injections, fuel rail pressure, turbo wastegate, electronic throttle, and electronic EGR). The experimental setup allows for full exhaust species characterization throughout the catalyst system. This includes the measurement of key reductants such as H_2, CO, and hydrocarbons as well as NOx and potential nitrogen-based byproducts like NH_3 at five locations within the LNT system. A full set of analyzers is applied to sample the various species; analysis techniques include: chemiluminescence for NOx, Fourier transform infrared spectroscopy for NH_3, magnetic sector mass spectrometry for H_2, non-dispersive infrared analysis for CO, and flame ionization detector analysis for hydrocarbons.

In the study presented here, three different LNT formulations were analyzed with in-cylinder regeneration strategies. The LNT formulations included a commercial LNT made by Umicore and two model LNTs that are of a more generic formulation. The active NOx adsorbing component for all of the LNTs was Ba, but the LNTs differed in Ba and CeO_2 (ceria) loadings. Ceria is an oxygen storage component commonly used in automotive catalysis. Table 1 contains a table that summarized the LNTs studied. Highlights from the study will be presented here; a detailed manuscript on the study has been submitted for the upcoming 2008 SAE Congress conference [1].

TABLE 1. LNT Formulations Studied

	Umicore	Low Ba	Med Ba
BaO	29 g/l	~11 g/l	~27 g/l
Al_2O_3	160 g/l	~137 g/l	~137 g/l
CeO_2	98 g/l	—	—

Results

The NOx conversion of all three LNTs was compared under different operating conditions. The lean-rich operating parameters were varied while the engine load and speed were held constant at 50 ft-lb and 1,500 rpm, respectively. LNT performance was characterized for 20-second and 60-second lean-rich periods each having a three second rich regeneration phase. Two types of in-cylinder regeneration techniques were used. The first technique referred to as the delayed and extended main (DEM) technique is initiated by slightly delaying the main injection pulse and extending its duration to enrich the air and fuel mixture; DEM results in high H_2 and CO reductants with lower amounts of hydrocarbons. The second technique referred to as the Post 80º (P80) technique is initiated by adding another fuel injection at 80º past top dead center in the combustion cycle; P80 generates relatively lower amounts of H_2 and CO and relatively higher amounts of hydrocarbons in comparison to the DEM technique. Specific details on the DEM and P80 regeneration strategies can be found in previous publications [2]. Figure 1 shows the NOx conversion for all three LNTs for the four different combinations of lean-rich period and regeneration strategy. Higher NOx conversions were obtained for the 20-second lean-rich periods as expected since less NOx is trapped by the catalysts per frequency of regeneration. Another trend consistent to all catalysts is that the DEM strategy leads to higher NOx conversion than the P80 strategy for all cases; this trend has been observed previously as is likely due to the greater concentration of the efficient CO and H_2 reductants for the DEM strategy [2]. Overall, the Umicore LNT gave the highest NOx conversion. The Medium Ba LNT was close to the Umicore LNT in performance, but the Low Ba LNT gave significantly poorer NOx conversion. So, NOx performance was

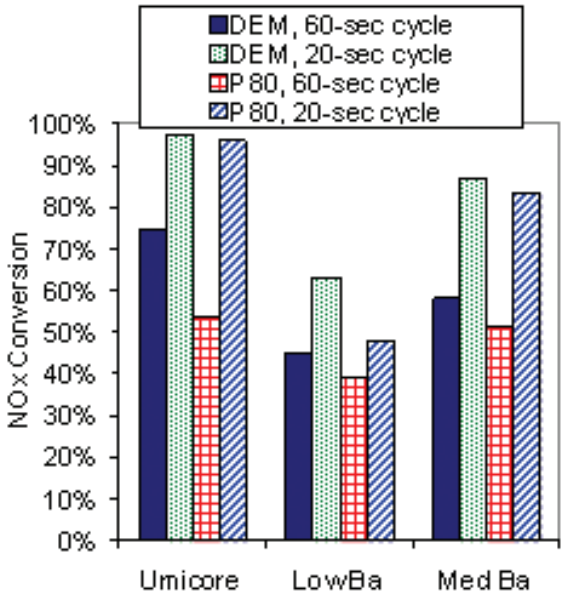

FIGURE 1. NOx Conversion for all Three LNTs for the Parameters Studied

closely associated with Ba load with higher Ba loadings giving greater NOx trapping capacity and improved NOx conversion performance.

In addition to the exhaust measurements made downstream of the LNT which resulted in the data shown in Table 1, exhaust measurements were made from points internal to the LNT to better understand the differences in chemistry occurring for the different LNT formulations. Figure 2 shows the cycle average NOx concentration for all three LNTs for the DEM 60-second cycle; exhaust samples were collected at engine-out (EO), at the LNT inlet (or AI, adsorber inlet), at the ¼ bed position of the LNT, at the ½ bed position of the LNT, at the ¾ bed position of the LNT, and at the tailpipe (TP) position. While the Medium Ba and Umicore LNTs have similar NOx levels at the TP position, the profile of NOx for these LNTs differs significantly. The Medium Ba LNT reduces NOx more effectively in the upstream half of the LNT, but the Umicore LNT reduces NOx more effectively in the downstream half of the LNT. These results indicate that the ceria content of the Umicore LNT may reduce regeneration effectiveness in the upstream half of the LNT since ceria consumes reductants as it is reduced. These internal chemical differences in the way the LNTs perform are important to understand in developing models for the LNTs and in optimizing performance for engine catalyst systems.

One important model parameter is the molar efficiency of the Ba storage component in the LNT. Every mole of Ba on the LNT is not capable of storing NOx; instead, the percentage of Ba moles that are active in storing NOx (the "molar efficiency") is dependent on the dispersion of the Ba material on the high surface area catalyst support material. The molar efficiencies for the Low and Medium Ba LNTs are shown in Figure 3. The lower Ba loading leads to higher Ba dispersion and higher molar efficiencies for NOx storage relative to the Medium Ba LNT case as expected. However, interestingly a similar trend in the molar efficiency as a function of catalyst position occurs. Thus, models that are effective in modeling one Ba load may also be effective in modeling other Ba loads since the mechanisms for NOx storage along the length of the LNT appear to be consistent for different Ba loads.

Internal NH_3 levels were also found to be quite different for the LNT formulations. Figure 4 shows cycle average NH_3 at different catalyst locations for the three LNT formulations for the DEM 60-second cycle. Although the Low Ba LNT gave the lowest NOx reduction efficiency, it had the highest N_2 selectivity and produced negligible amounts of NH_3. In contrast, the

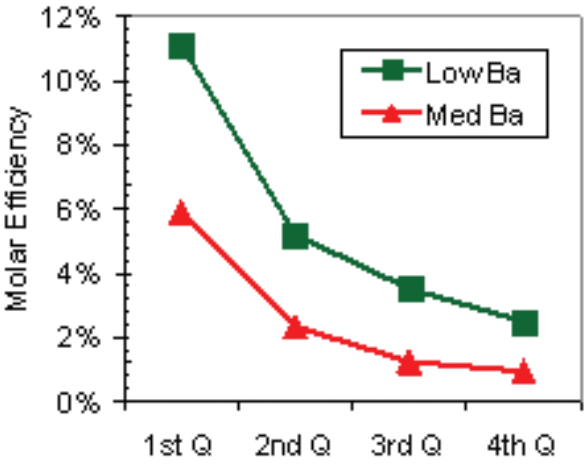

FIGURE 3. Molar Efficiency of the Ba Storage Component of the LNT for the Low and Medium Ba LNTs

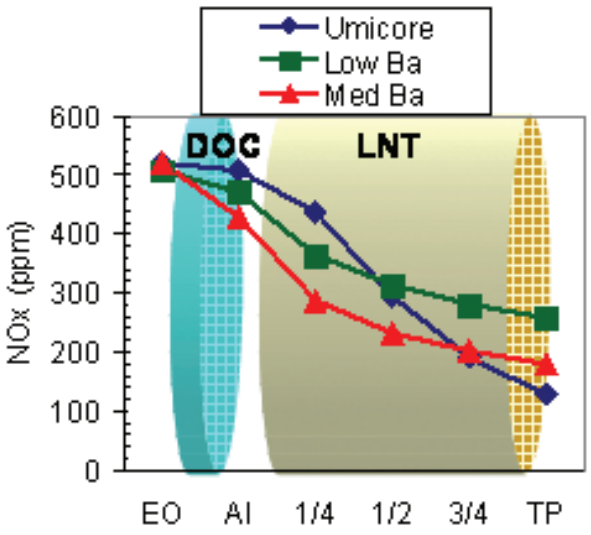

FIGURE 2. Cycle Average NOx Concentration vs. Position in the LNT System for the DEM 60-Second Cycle Condition

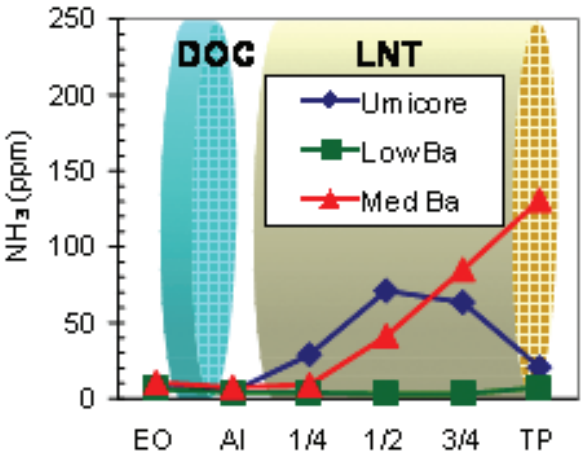

FIGURE 4. Cycle Average NH_3 Concentration vs. Position in the LNT System for the DEM 60-Second Cycle Condition

Medium Ba LNT produced a high amount of NH_3 which is consistent with bench reactor studies that have shown higher NH_3 production with higher Ba loadings [3]. Interestingly, the Umicore LNT produced NH_3 internally in the LNT but consumed the NH_3 in the downstream half of the LNT resulting in relatively low NH_3 emissions at the tailpipe. The downstream consumption of NH_3 is likely due the ceria content of the Umicore LNT. Understanding these NH_3 emissions are important since NH_3 can either (1) be an undesired emission if it exits the tailpipe or (2) be a useful reductant in hybrid systems were an LNT catalyst is combined with a selective catalytic reduction catalyst that reduces NOx with NH_3 catalytically.

Conclusions

- NOx conversion and NOx trapping increased with increasing Ba load.
- Reductant utilization is affected by LNT formulation.
  - The addition of ceria (Umicore LNT) alters the reductant utilization of the LNT and thereby alters the NOx storage as function of LNT position.
- Molar NOx trapping efficiency of the Ba storage component was greater for the Low Ba LNT as compared with the Medium Ba LNT, but trends of NOx sorption through the two LNTs were similar.
- N_2 selectivity decreased (NH_3 emissions increased) with Ba load for the Low vs. Medium Ba model LNTs.
- Although NH_3 was created in the commercial Umicore LNT, tailpipe NH_3 emissions were controlled at a lower level than the equivalent Ba loaded Medium Ba model LNT. The effect of ceria on NH_3 oxidation is the likely mechanism for the NH_3 control.

References

1. Jim Parks, Brian West, Matt Swartz, and Shean Huff, "Characterization of Lean NOx Trap Catalysts with In-Cylinder Regeneration Strategies", *submitted for the 2008 SAE Congress conference (under review)*.

2. Brian West, Shean Huff, James Parks, Sam Lewis, Jas-Soon Choi, William Partridge, and John Storey, "Assessing Reductant Chemistry During In-Cylinder Regeneration of Diesel Lean NOx Traps", *SAE Technical Paper Series* 2004-01-3023 (2004).

3. L. Castoldi, I. Nova, L. Lietti, and P. Forzatti, "Study of the effect of Ba loading for catalytic activity of Pt–Ba/Al_2O_3 model catalysts", *Catalysis Today* **96** (2004) pp. 43-52.

FY 2007 Publications/Presentations

1. Matt Swartz, Shean Huff, James Parks, and Brian West, "Intra-Catalyst Reductant Chemistry and NOx Conversion of Diesel Lean NOx Traps at Various Stages of Sulfur Loading", *SAE Technical Paper Series* 2006-01-3423 (2006).

2. Josh A. Pihl, James E. Parks II, C. Stuart Daw, and Thatcher W. Root, "Product Selectivity During Regeneration of Lean NOx Trap Catalysts", *SAE Technical Paper Series* 2006-01-3441 (2006) (*Selected for SAE 2006 Transactions*).

3. Jim Parks, Shean Huff, Matt Swartz, and Brian West, "Comparison of LNT Catalyst Performance with In-Cylinder Regeneration Techniques", *Presentation at the 10th DOE Cross-Cut Lean Exhaust Emissions Reduction Simulations (CLEERS) Workshop* in Dearborn, MI on May 1–3, 2007.

4. Jim Parks, Shean Huff, Mike Kass, and Brian West, "Lean NOx Trap Formulation Effect on Performance with In-Cylinder Regeneration Strategies", *Poster Presentation at the 13th Diesel Engine-Efficiency and Emissions Research (DEER) Conference* in Detroit, MI on August 13–16, 2007.

5. Jim Parks, Shean Huff, Mike Kass, and John Storey, "Characterization of In-Cylinder Techniques for Thermal Management of Diesel Aftertreatment", *SAE Technical Paper Series* 2007-01-3997 (2007).

6. Jim Parks, Brian West, Matt Swartz, and Shean Huff, "Characterization of Lean NOx Trap Catalysts with In-Cylinder Regeneration Strategies", *submitted for the 2008 SAE Congress conference (under review)*.

II.B.4 Development of Chemical Kinetics Models for Lean NOx Traps

Richard S. Larson
Sandia National Laboratories
MS 9409, P.O. Box 969
Livermore, CA 94551-0969

DOE Technology Development Manager:
Kenneth Howden

Collaborators:
Kalyana Chakravarthy, Josh A. Pihl, and C. Stuart Daw
Oak Ridge National Laboratory, Oak Ridge, TN

Objectives

- Identify a set of elementary (microkinetic) surface reactions that can account for the observed behavior of a lean NOx trap (LNT) during both the storage and regeneration phases of operation.
- Optimize the kinetic parameters associated with these reactions by matching model predictions with laboratory reactor data.
- Use the validated reaction mechanism to suggest improvements in the usage of existing LNT materials and to help in the development of a new generation of catalysts.

Accomplishments

- Completed construction and optimization of a thermodynamically consistent reaction mechanism for the precious metal sites on a benchmark LNT catalyst.
- Assembled tentative mechanisms for the NOx storage and oxygen storage sites on the catalyst and formulated the corresponding thermodynamic constraints.
- Using the combined reaction mechanism together with a Chemkin-based transient plug flow code and the Sandia APPSPACK optimization software, carried out a preliminary evaluation of the storage parameters by fitting simulations of full LNT cycles to experimental data from Oak Ridge National Laboratory (ORNL).

Future Directions

- Complete parameter optimization for the combined storage/regeneration mechanism, re-evaluating kinetic constants for the precious metal sites if necessary.
- Introduce reactions needed to describe sulfur poisoning and desulfation.
- Use the validated reaction mechanisms to investigate coupling between an LNT and other devices in the aftertreatment train.

Introduction

The increasingly strict constraints being placed on emissions from diesel and other lean-burn engines require the development of a new generation of aftertreatment technologies. LNTs represent one option for achieving the stated targets with regard to NOx emissions. In an LNT, NOx produced during normal lean engine operation is trapped and stored via adsorption on high-capacity catalytic sites, and periodically this stored NOx is released and reduced to harmless N_2 on precious metal sites by imposing rich conditions for a short time. While this qualitative description is widely accepted, a detailed quantitative understanding of the underlying chemistry is not yet available. Such knowledge is needed in order to use the LNT concept to best advantage, so it is the principal goal of this project to develop an elementary reaction mechanism that describes both phases of LNT operation.

Clearly, a comprehensive kinetics model with the ability to simulate an entire LNT cycle must account for the chemistry occurring on all kinds of catalytic sites: the metal oxide sites used to store NOx, additional oxide sites used (sometimes) for oxygen storage, and the precious metal sites involved primarily in the reduction of released NOx. While it is tempting to associate each of these kinds of sites with a particular phase of LNT operation, it must be remembered that the desorption of NOx from the storage sites is an integral part of the regeneration process, while oxidation of NO on the precious metal sites is thought to be a key part of the storage phase. Nevertheless, it is possible to design experiments that isolate a particular subset of the chemistry, and this has been used to facilitate model development in this project, as described below. The ultimate goal is to obtain a mechanism that can simulate LNT operation over a range of input NOx (NO and/or NO_2) compositions, a range of reductant (H_2 and/or CO) compositions, and a suitably wide range of temperatures.

Approach

The basic approach to mechanism development adopted here is to assemble a candidate set of elementary reactions, often with poorly known kinetic parameters, and then to optimize the parameters by fitting the results of reactor simulations to bench-scale experimental data provided by our collaborators at ORNL. This process requires two principal pieces of supporting software: a reactor code to simulate flow through a single monolith channel using the proposed reaction mechanism (expressed in Chemkin format), and an optimization code to carry out the fitting process on a massively parallel machine. For the former we have used either a steady-state or a transient Chemkin-based plug flow code, as appropriate, and for the latter we have adopted the Sandia APPSPACK code [1], which is ideally suited to this application.

As suggested above, we have found it helpful to split the mechanism development process into two parts. The first relies on a set of steady flow temperature ramp experiments conducted at ORNL. These were carried out with a variety of NOx/reductant and other related input mixtures, the aim being to minimize the possibility of NOx storage and thus to isolate the chemistry on the precious metal sites [2]. These experiments have been simulated with the steady-state Chemkin plug flow code and used to develop a submechanism for these metal sites alone. The second part of the process relies on a set of full cycle experiments using the same catalyst. The analysis in this case involves a complete mechanism with all three kinds of catalytic sites, together with a fully transient plug flow reactor code. At first the precious metal submechanism is fixed, and the storage submechanisms are optimized to provide the best overall fit to the cycle data. Then, if needed, all of the kinetic parameters can be allowed to vary as the complete mechanism is fit to both the cycle data and the temperature ramp data simultaneously.

A significant issue that must be addressed in all of the parameter estimation processes is that not all of the parameters can be varied independently if thermodynamic consistency is to be maintained. Thus, a number of well-defined relationships among the various parameters are enforced; this reduces the size of the optimization problem, but it greatly increases the programming complexity. In addition, all of the activation energies, whether varied independently or computed from thermodynamic constraints, are required for physical reasons to be non-negative. Fortunately, the resulting inequality constraints are easily handled by APPSPACK.

Results

The development of a submechanism for the precious metal sites on our benchmark LNT catalyst has been completed. While a great deal of the work involved in meeting this objective was carried out in FY 2006, a number of issues remained to be addressed this year. Foremost among these was the need to account for a puzzling experimental fact, namely that oxidation of NH_3 produces very significant amounts of N_2O, while reduction of N_2O (by either H_2 or CO) produces no measurable NH_3. Generally, an attempt to reconcile the mechanism with one of these observations tends to destroy its ability to match the other. Our solution to this was to introduce a third-order reaction that allows N_2O to be formed directly from surface fragments that would otherwise form the very stable N_2. While not a perfect solution, either on conceptual grounds or in terms of fitting the data, it seems at this point to be the best option available.

The submechanism ultimately adopted involves 10 gas-phase species, 13 surface species, and 28 surface reactions (all reversible). Thus, it is slightly larger than the preliminary version described last year. Among the reactions are 11 adsorptions, seven surface decompositions, and seven atom transfers. In addition, there are again two alternate pathways for hydrogen production from CO, namely the water-gas shift reaction and a two-step process involving an isocyanate intermediate. This submechanism is quite successful in reproducing the results of all 21 of the steady-state temperature ramp experiments conducted at ORNL. One of the more interesting cases is shown in Figures 1 and 2. These plots show, respectively, the experimental and simulated outlet gas concentrations for the case in which 200 ppm of NH_3 was fed to the reactor along with a large excess of O_2. Unlike the rest of the experiments, this one certainly did not involve reducing conditions,

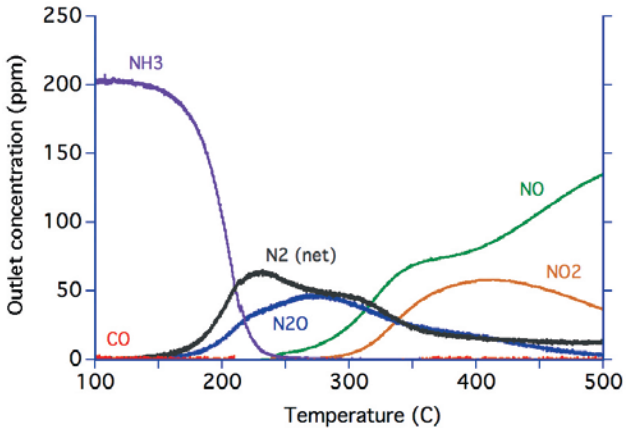

FIGURE 1. Experimental Outlet Concentrations for a Steady Flow Temperature Ramp Experiment with a Feed Stream Containing 200 ppm NH_3 and 10% O_2

so the assumption of no NOx storage can be questioned. However, this may not be a serious issue at steady-state, and the simulation results show that the model is quite capable of reproducing the data even for this unusual case. It remains to be seen whether the inclusion of storage reactions in the mechanism will have a significant effect on the simulated behavior.

Close examination of the computed results for the steady flow temperature ramps shows that the model admits multiple steady-state solutions for some of the cases over limited ranges of temperature. Specifically, multiplicity is found for all of the cases involving reduction of NO or NO_2 by CO. Not surprisingly, it can be shown that this phenomenon is due to the presence of the isocyanate pathway for water splitting by CO. Similar behavior is observed when a fully transient, rather than steady-state, plug flow code is used to simulate the pseudo-steady temperature ramps. An example of this is given in Figure 3, which shows results

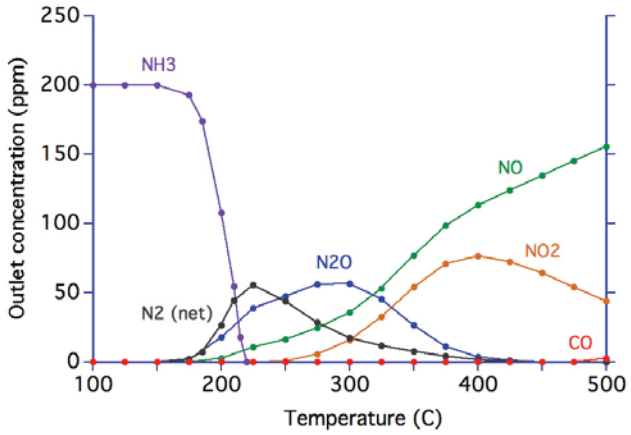

FIGURE 2. Simulated Outlet Concentrations for a Steady Flow Temperature Ramp Experiment with a Feed Stream Containing 200 ppm NH_3 and 10% O_2

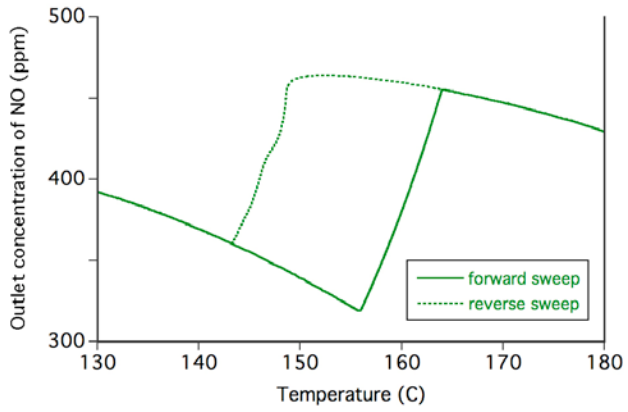

FIGURE 3. Fully Transient Simulations of Steady Flow Temperature Ramps for a Feed Stream Containing 500 ppm NO and 1250 ppm CO

for a feed stream containing NO and CO in a 1:2.5 ratio. The temperature is ramped both upward and downward through the given temperature range, and the previously observed steady-state multiplicity is manifested here as a pronounced hysteresis. While it is not clear that the catalyst would actually exhibit this behavior in practice, the possibility does exist, and certainly the capability of the model to produce unusual results of this kind should be kept in mind.

We have also made significant progress in constructing a complete mechanism involving all three of the catalytic surface phases of the LNT. As noted above, this involves adding to the so-called regeneration submechanism a set of reactions describing storage of both NOx and oxygen, each on its own type of site. The submechanism for the baria (NOx storage) phase involves five kinds of surface species, namely empty sites and adsorbed oxygen atoms, carbonates, nitrites, and nitrates. The first step in the proposed reaction scheme is the dissociative adsorption of oxygen. Reaction of gas-phase CO_2, NO, and NO_2 with the oxygenated sites yields surface carbonates, nitrites, and nitrates, respectively. Nitrites and nitrates can also be formed via displacement of carbonates by NO and NO_2, and nitrites can be oxidized to nitrates via reactions with adsorbed oxygen, carbonates, or gas-phase NO_2. Additional nitrite-forming reactions include direct adsorption of NO_2 on bare sites and spillover from adjacent precious metal sites. By contrast, the submechanism for the ceria (oxygen storage) phase is much simpler, consisting currently of just a single adsorption step.

As noted above, the kinetic parameters for the storage phases are evaluated by fitting transient plug flow simulations that use the complete mechanism to experimental data for complete LNT cycles. In the first round of optimization calculations, the parameters for the precious metal phase are held fixed. Because the surface site densities for all three phases are not known with any accuracy, they are also treated as adjustable parameters. However, they are first mathematically decoupled from the reaction rate terms (as opposed to the capacity terms) in the conservation equations, in much the same way that the activation energies are decoupled from the rate constants. This greatly facilitates the optimization process.

At this point, the model has been fitted simultaneously to data at three temperatures, namely 200°C, 300°C, and 400°C. The experimental [3] and simulated results at 400°C are shown in Figures 4 and 5, respectively. Given the relative crudeness of the storage models and the use of independently derived regeneration constants, the agreement is fairly encouraging. In particular, the slip of NO through the catalyst at the beginning of the regeneration period is reproduced nicely, although the subsequent production of NH_3 is somewhat overpredicted. It should be noted that, among other things, washcoat diffusional resistance

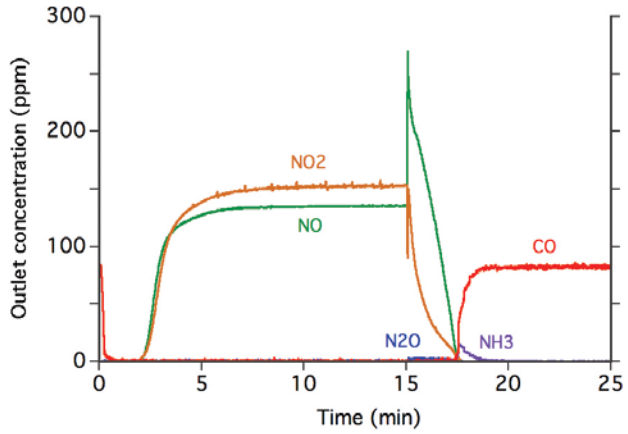

FIGURE 4. Experimental Outlet Concentrations for a Benchmark Long Storage/Regeneration Cycle at 400°C [3]

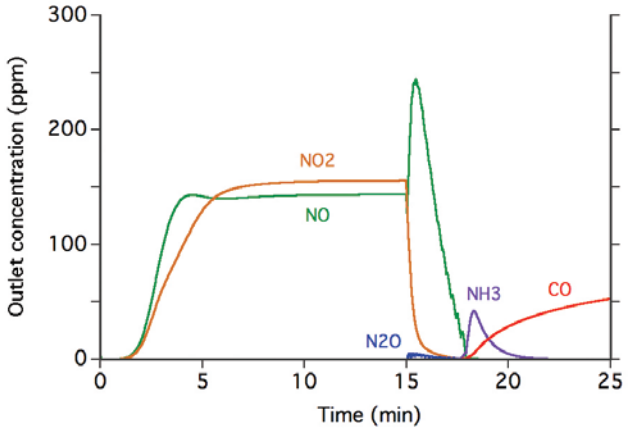

FIGURE 5. Simulated Outlet Concentrations for a Benchmark Long Storage/Regeneration Cycle at 400°C

has not yet been included in the model, so excellent agreement is not to be expected. The incorporation of such phenomena is to be considered in the near future.

Conclusions

- The steady-state behavior of an LNT under reducing conditions can be simulated quite well with an elementary reaction mechanism involving only the precious metal sites of the catalyst.
- Under certain conditions, simulations of LNT regeneration can exhibit multiple steady-state solutions and associated complex transient behavior.
- A reasonably successful storage/regeneration mechanism that incorporates the previously developed precious metal mechanism can be constructed, but further adjustment of the rate parameters will be beneficial.

References

1. J. D. Griffin, T. G. Kolda, and R. M. Lewis, Sandia National Laboratories Report SAND2006-4621, 2006.

2. J. A. Pihl, J. E. Parks, C. S. Daw, and T. W. Root, SAE 2006 Transactions Journal of Engines, 2006-01-3441 (2006).

3. J. A. Pihl, M.S. Thesis, University of Wisconsin–Madison, 2005.

FY 2007 Publications/Presentations

1. J. A. Pihl, R. S. Larson, V. K. Chakravarthy, and C. S. Daw, "Product Speciation during Regeneration of Lean NOx Traps," 2006 AIChE Annual Meeting, San Francisco, California, November 14, 2006.

2. R. S. Larson, V. K. Chakravarthy, J. A. Pihl, and C. S. Daw, "Mechanism Development for the Simulation of LNT Lean/Rich Cycling," Tenth CLEERS Workshop, Dearborn, Michigan, May 2, 2007.

3. R. S. Larson, J. A. Pihl, V. K. Chakravarthy, and C. S. Daw, "Micro-kinetic modeling of Lean NOx Trap regeneration chemistry," 20th North American Meeting of the North American Catalysis Society, Houston, Texas, June 21, 2007.

4. R. S. Larson, J. A. Pihl, V. K. Chakravarthy, T. J. Toops, and C. S. Daw, "Microkinetic Modeling of Lean NOx Trap Chemistry under Reducing Conditions," Catal. Today, submitted (2007).

II.B.5 Advanced Engine/Aftertreatment System Research and Development

Todd J. Toops (Primary Contact), Josh A. Pihl and Brian H. West
Oak Ridge National Laboratory (ORNL)
2360 Cherahala Boulevard
Knoxville, TN 37932

Cooperative Research and Development Agreement (CRADA) Partner:
International Truck and Engine Corporation,
Brad Adelman, Ed Derybowski, and Alan Karkkainen

DOE Technology Development Manager:
Ken Howden

Objectives

- Study effects of typical engine variation on a series of fully-formulated lean-NOx trap (LNT) catalysts in bench reactors; variants include temperature, space velocity, lean-rich cycle time and reductant.
- Identify factors limiting NOx conversion during low-temperature operation with CO and hydrocarbon (HC) reductants.

Accomplishments

- Evaluated engine-aged LNT samples in ORNL bench reactor.
- Determined reductant reactivity is the key parameter limiting low-temperature performance of the catalysts studied.
- Established trends in NOx conversion and product selectivity with temperature, space velocity, lean-rich cycle time, and reductant species.
- Provided input for calibration of operating strategies.

Future Directions

Refocus efforts on impacts of NH_3 storage on selective catalytic reduction catalyst performance, particularly at low temperatures and for aged catalysts.

Introduction

Both heavy- and light-duty emissions standards call for significant reductions in NOx emissions by 2009-2010. The LNT catalyst is a promising technology to help meet these stringent new NOx standards, but there are open issues that must be resolved prior to commercialization. Widening the operating temperature range of LNTs is one issue that must be resolved, particularly at the low-temperature end for heavy-duty applications. Another critical area where development is needed is sulfur poisoning and removal. The catalytic components degrade after a series of high-temperature desulfurizations. This degradation has a particularly significant impact on low-temperature operation. Prior work in this CRADA project has used engine experiments with full-scale LNT systems to quantify the activity of various hydrocarbon reductants and to study desulfurization strategies. Efforts during this year shifted to bench-scale experiments and focused on low-temperature LNT operation to better understand the fundamental limitations of the chemistry.

A second focus of the CRADA was to involve use of a unique camless engine prototype with infinitely variable valve timing. Limited resources and revised technical focus precluded activity with the camless engine.

Approach

Efforts during this year focused on developing a better understanding of the factors that limit the low-temperature performance of LNT catalysts. We relied on flow reactor experiments to enable better control over operating conditions than could be achieved in engine operation. Core samples (one inch diameter by three inches long) were cut from engine-aged LNTs and installed in a bench-scale flow reactor at ORNL. The experiments were designed to examine the effects of temperature, space velocity, lean/rich cycle duration, and reductant speciation on overall NOx conversion, reductant conversion, and product selectivity. The catalysts were held at constant temperature and exposed to a simulated exhaust gas stream that cycled rapidly between lean and rich conditions, as is typical for LNT operation. Measurements were performed once the catalyst had achieved pseudo-steady-state cycling (cycle-to-cycle variations in the catalyst effluent were negligible).

Results

Figure 1 illustrates that LNT performance is a strong function of temperature for the conditions used in this study. NOx conversion decreases rapidly below 250°C, with a particularly steep decline between 225 and 200°C. In this and all subsequent plots, space velocity is abbreviated SV, and SV1 < SV2 < SV3 < SV4. Space

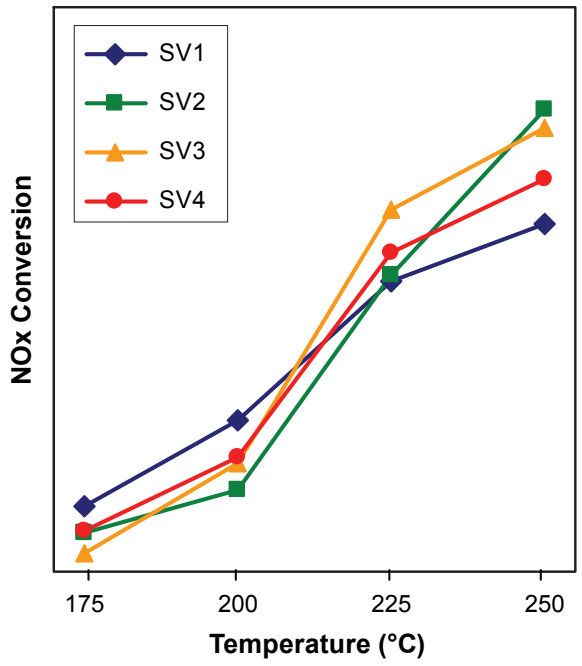

FIGURE 1. NOx Conversion as a Function of Temperature and Space Velocity for a Fully Formulated LNT with CO Reductant

velocity had a much smaller impact on overall NOx conversion than temperature, and the plot does not reveal any clear trends in NOx conversion with changes in space velocity.

Looking at the NOx breakthrough profiles (such as those for SV2 shown in Figure 2) yields additional insight regarding the factors limiting performance. Research on the NOx storage process has determined that oxidation of the NO in the exhaust stream to NO_2 is required to achieve high storage efficiencies. Low NO oxidation activity is often cited as a reason why LNT performance drops off at low temperatures [1]. However, looking at Figure 2, NO_2 can be observed at the catalyst outlet even at the lowest temperature. Thus, NO oxidation activity is not limiting the low-temperature LNT performance.

The flat breakthrough profile at 175°C indicates that essentially zero NOx is stored during the lean phase of the cycle. However, NOx storage capacity increases as temperature decreases, and NO_2 readily stores on LNT catalysts at temperatures as low as 25°C. The observed lack of NOx uptake when there should be significant storage capacity available implies that the catalyst has been saturated with NOx. Thus, the reduced NOx conversion at low temperatures is due to the inability of the reductant species (in this case CO) to regenerate the catalyst during the rich phase of the operating cycle.

The CO conversion trends illustrated in Figure 3 are consistent with limited reductant activity at low temperatures. The CO conversion is relatively high

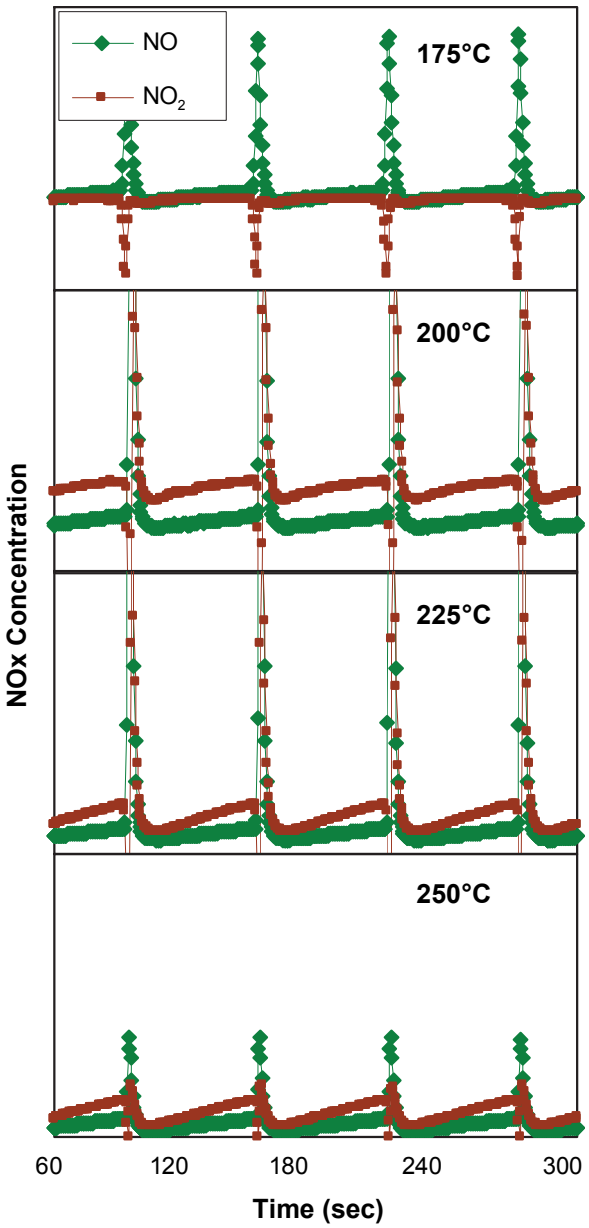

FIGURE 2. Catalyst Outlet NOx Concentrations During Pseudo-Steady-State Cycling at SV2

at 250°C, but drops substantially as the temperature is reduced. Unlike the NOx conversion results, there is a discernable trend with space velocity: lower space velocities lead to higher CO conversion. Interestingly, the CO conversion is higher than what would be expected from the amount of NOx reduced by the catalyst.

Product selectivity during the regeneration phase of the LNT operating cycle was also examined. Figure 4 shows the yield of each of the major nitrogen-atom-containing products for the cases shown in Figures 1 and 3. All cases showed a lack of selectivity to N_2.

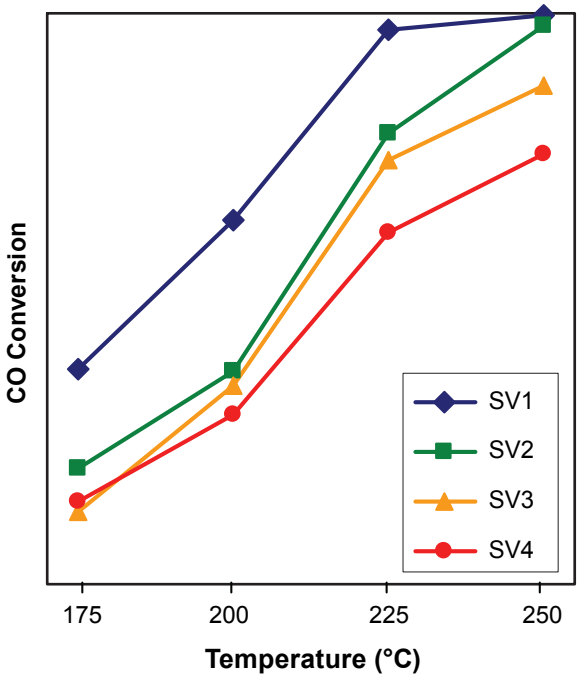

FIGURE 3. CO Conversion as a Function of Temperature and Space Velocity for a Fully Formulated LNT

This is consistent with regeneration product speciation experiments we have conducted previously that showed low temperatures tend to generate a mixture of N_2, N_2O, and NH_3. Formation of NH_3 increased at higher space velocities, while N_2O showed the opposite trend. A possible explanation for these trends can be found in the relative ratios of reductant delivered to NOx stored on the catalyst surface. Since the catalyst was approaching saturation for many of the operating conditions, the amount of NOx stored on the surface was the same regardless of space velocity. However, a higher space velocity results in a larger dose of reductant during the regeneration. The increased reductant will result in a higher ratio of reductant to stored NOx, which has been shown to generate more NH_3 [2]. Alternatively, the increased outlet concentration of NH_3 at higher space velocities could indicate that NH_3 is an intermediate in the regeneration reactions.

Experiments were also performed with propene (C_3H_6) rather than CO as the reductant. Figure 5 shows the NOx conversions at SV1 and SV2 for both C_3H_6 and CO. The performance with C_3H_6 is significantly lower than that achieved with CO for all but the lowest temperature. Considering our previous conclusion that reductant reactivity is limiting the performance for these conditions, it is not surprising that the less reactive C_3H_6 generates lower performance than CO. The corresponding hydrocarbon conversion for the C_3H_6 cases is shown in Figure 6. As expected, the C_3H_6 conversion is lower than the CO conversions shown

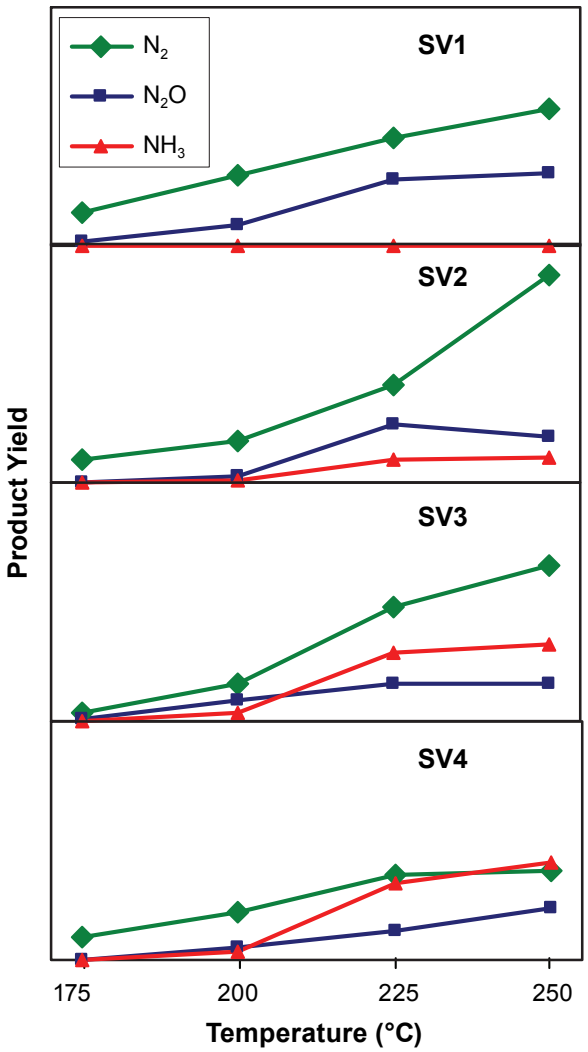

FIGURE 4. Product Yield as a Function of Temperature and Space Velocity for a Fully Formulated LNT with CO Reductant

in Figure 3, confirming the lower reactivity of the C_3H_6 reductant.

Improving the performance of these catalysts at low temperature will require increasing the activity of the reductant. Increasing the amount of H_2 in the reductant mixture could accomplish this goal. Strategies for increasing the H_2 concentration include altering the catalyst formulation to increase the water-gas shift and/or HC reforming activity, incorporating an upstream reformer catalyst, or changing engine operation to alter the exhaust chemistry.

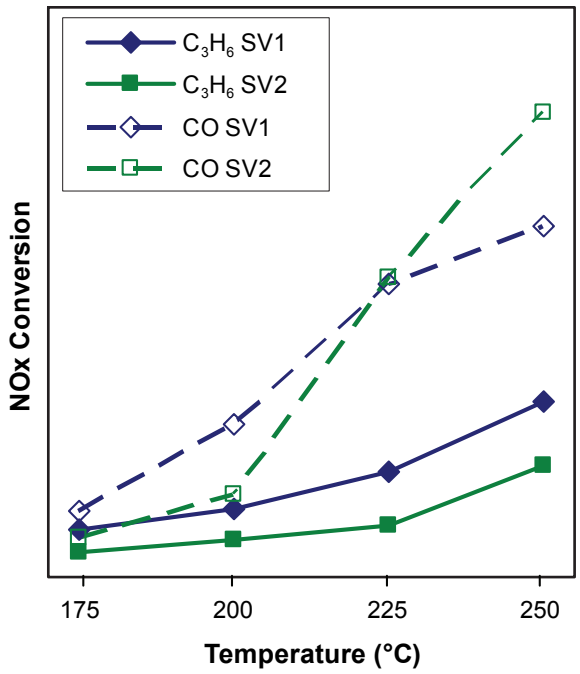

FIGURE 5. NOx Conversion as a Function of Temperature and Space Velocity for a Fully Formulated LNT with C_3H_6 reductant

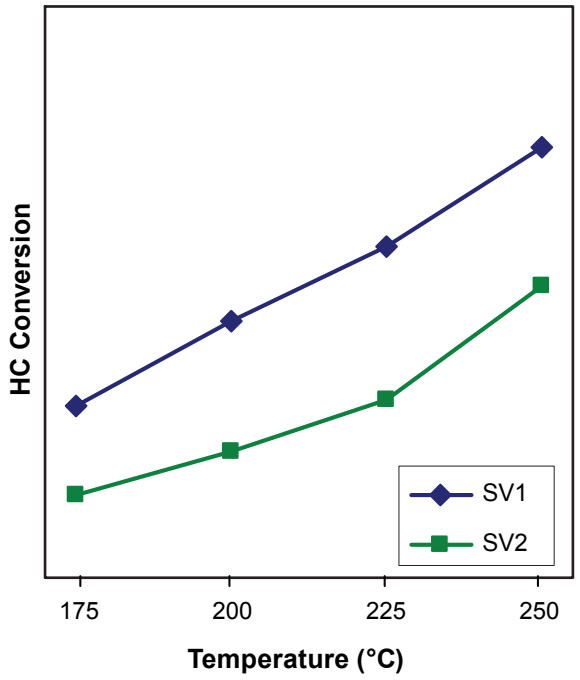

FIGURE 6. Hydrocarbon Conversion as a Function of Temperature and Space Velocity for a Fully Formulated LNT with C_3H_6 Reductant

Conclusions

A series of engine-aged LNT samples have been evaluated in ORNL bench reactors. The focus of the effort was to measure the low-temperature NOx conversion and product selectivity while using either CO or HC reductants. Specific conclusions include:

- LNT performance with CO reductant drops off rapidly below 250°C.
- The drop in performance at low temperatures is due to low reactivity of the reductant species and the associated inability to completely regenerate the catalyst.
- Outlet NH_3 concentrations increase at higher space velocities; N_2O formation shows the opposite trend.
- Propene is even less effective than CO at regenerating the LNT at low temperatures.

References

1. W.S. Epling, L.E. Campbell, A. Yezerets, N.W. Currier, J.E. Parks II, "Overview of the Fundamental Reactions and Degradation Mechanisms of NOx Storage/Reduction Catalysts," Catalysis Reviews 46, 163-245 (2004).

2. J.A. Pihl, J.E. Parks II, C.S. Daw, T.W. Root, "Product Selectivity During Regeneration of Lean NOx Trap Catalysts," SAE Transactions Journal of Engines, 2006-01-3441 (2006).

Presentations

1. B. West, T.J. Toops, J.A. Pihl, "ITEC CRADA-Advanced Engine/Aftertreatment System Research and Development", DOE-Advanced Combustion Engine Program Annual Merit Review, Crystal City, VA, May 2007.

II.B.6 Fundamental Sulfation/Desulfation Studies of Lean NOx Traps, DOE Pre-Competitive Catalyst Research

Todd J. Toops (Primary Contact) and
Josh A. Pihl
Oak Ridge National Laboratory
2360 Cherahala Blvd.
Knoxville, TN 37932

DOE Technology Development Manager:
Ken Howden

Objectives

- Provide a better understanding of the fundamental deactivation mechanisms that result during regeneration and desulfation of lean-NOx traps (LNTs).
  - Investigate ways to limit the impact of these mechanisms.
  - Guide models and help design desulfurization strategies that minimize fuel economy losses, sulfur inhibition of NOx activity, and the effects of thermal aging.

Approach

- Conduct pre-competitive LNT research.
  - Allows open dissemination of results and data.
- Study deactivation mechanism fundamentally.
- Evaluate deactivation from sulfur poisoning and de-sulfurization.
  - Use 15 ppm SO_2 to rapidly introduce sulfur.
  - Desulfurize under controlled temperature ramps with realistic exhaust constituents.
- Employ multiple analytical techniques to monitor activity and morphology effects.
  - Investigate surface species reactivity using diffuse reflectance infrared Fourier-transform spectroscopy (DRIFTS).
  - Monitor activity over typical operating range, 200-400°C.
  - Investigate morphological effects.

Accomplishments

- Presented recent efforts at the 20th North American Meeting (NAM), 2007 AIChE National Meeting, and DOE Advanced Combustion Engine (ACE) Merit Review.
- Submitted paper to Catalysis Today.
- Completed full sulfation study on model catalysts.
  - Study indicates temperature of sulfur exposure affects storage process but not desulfurization.
  - Presented at 20th NAM of the North American Catalysis Society and 2007 AIChE National Meeting.
- Completed full sulfation study on commercial LNT. Analysis in progress.
  - Abstract submitted for 2008 International Congress on Catalysis.

Future Directions

- Investigate fast desulfation to potentially drive off weakly bound sulfates before they convert to strongly bound sulfates.
- Determine sulfation/desulfation behavior of mixed model catalysts.
  - Investigate which phases preferentially adsorb/desorb sulfur first.
- Investigate effects of doping storage phase with other alkali/alkaline components to affect sulfate stability.

Introduction

Under future vehicle regulations, the efficiency of a diesel engine system will be correlated to the efficiency of the emissions aftertreatment system since a fuel penalty is sustained to achieve the emissions requirements. Computational modeling is an effective way to improve the efficiency of the emissions control systems, and basing the model on fundamental chemistry is critical for it to be transportable and broadly useful to industry; parametric-based models will not fill the need.

The complex heterogeneous nature of production catalyst washcoats critically obscures research of fundamental mechanisms. Model catalyst materials represent a subset of production materials, but allow isolation of individual fundamental processes. These processes include detailed mechanisms for desorption and poisoning, the existence and role of intermediate species, and NOx reduction details. Hence, this project has primarily employed model catalyst materials for experimental investigation of fundamental catalyst phenomena.

Approach

The emphasis of this project is to improve detailed understanding of mechanisms limiting catalyst performance. We work with catalyst-industry representatives to identify and investigate pre-competitive catalyst performance issues of broad relevance across the catalysis industry. Specific objectives are to improve the fundamental understanding of adsorption, reduction, and poisoning processes and their influence on catalyst morphology. The objectives of this project are consistent with those of the Diesel Cross-Cut Team regarding details of sulfur poisoning and catalyst morphology effects.

Having developed a base knowledge of the model catalysts, we have begun investigations on a commercial catalyst this year. A commercially available Umicore gasoline direct injection LNT catalyst, designated as the sample catalyst by the Cross-Cut Lean Exhaust Emissions Reduction Simulations (CLEERS) LNT focus group, has been implemented in sulfation studies in the microreactor and DRIFTS reactor. The information gained here will be used to complement efforts under the CLEERS kinetics efforts and Cummins Cooperative Research and Development Agreement.

Results

A sulfation study on a model LNT, $Pt/K/Al_2O_3$, shows the impact of sulfur on NOx stored during the lean phase (6.5 minutes with 300 ppm NO, 10% O_2, 5% CO_2 and 5% H_2O), unconverted NOx released during the rich phase (1 minute 0.56% CO, 0.34% H_2, 5% CO_2 and 5% H_2O), and overall NOx conversion. The NOx stored during the lean phase is the difference between the blank reactor NOx profile and the experimental NOx profile during the lean phase portion only. The unconverted NOx released is calculated from the NOx detected during the rich phase. Figure 1a shows that the NOx conversion during the first four hours of sulfation with 15 ppm SO_2 is not significantly impacted at any of the temperatures. After four hours, conversion decreases steadily, with the rate of deactivation increasing significantly with increasing temperature. Comparison to Figure 1b shows that the loss in conversion is directly related to the lean phase NOx storage at each temperature.

While the deactivation is generally linear and correlated to lean-phase storage for all temperatures, the impact of sulfation on the NOx profiles has a significant temperature variation. Figure 2a shows the complete lean and rich NOx profiles during sulfation at 300°C, and Figure 2b magnifies this profile at the lean to rich transition for the first three hours. It is clear in Figure 2b that the first portion of the NOx profile that is impacted is the NOx "puff" (or the unconverted

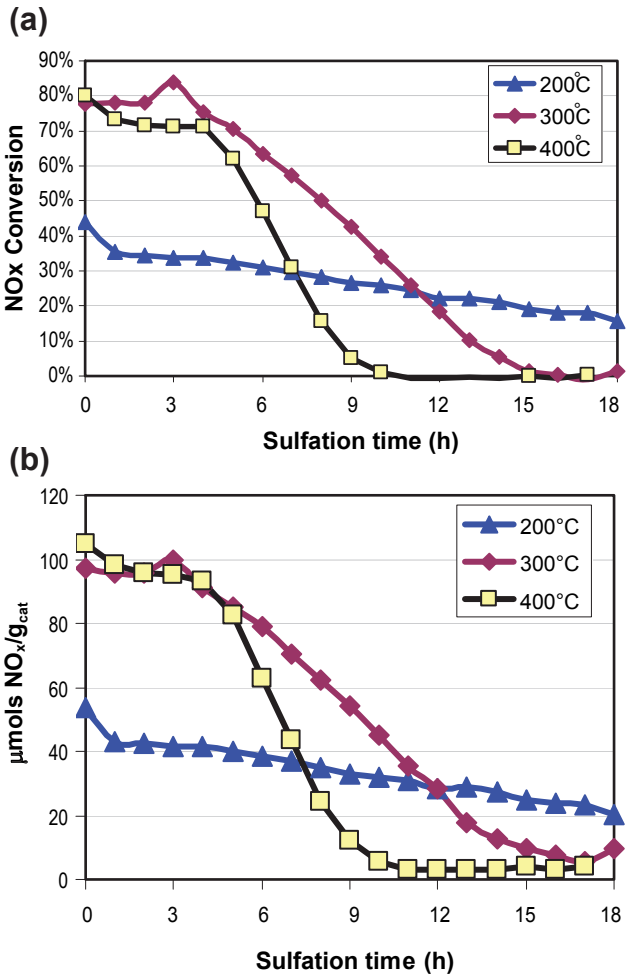

FIGURE 1. Model LNT ($Pt/K/Al_2O_3$): (a) NOx conversion and (b) lean phase NOx storage as a function of sulfation time at 200, 300 and 400°C.

NOx release during rich phase transition) directly after the switch from lean to rich. Based on a hypothesis proposed by several researchers [1-3], this observation suggests that the sulfur is initially poisoning storage sites in close proximity to the Pt and does not migrate away from these sites. Figure 3 shows the similar profiles for sulfation at 400°C. Here it is clear that the lean-phase storage is moderately decreasing during the first three hours while the NOx puff remains relatively constant. Working from the same hypothesis, it suggests that the sites near Pt are remaining free of sulfur; however, since the same processes that happen at 300°C will likely occur at 400°C, it suggests that sulfur is first adsorbing near Pt, but then is migrating away from the sites proximal to Pt.

At 200°C, it is difficult to study the sulfation route with this hypothesis since the release of NOx during the transition is significantly slow to not allow

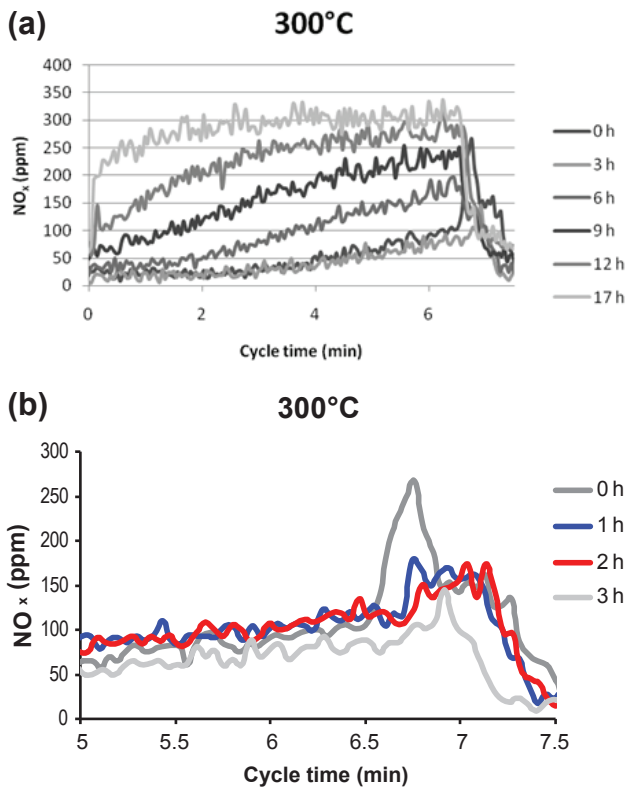

FIGURE 2. Model LNT ($Pt/K/Al_2O_3$): (a) Complete lean-rich NOx profiles at 300°C during sulfation. (b) Profiles during lean to rich transition shows the profiles experience reduction in the NOx puff first followed by decrease in lean phase storage.

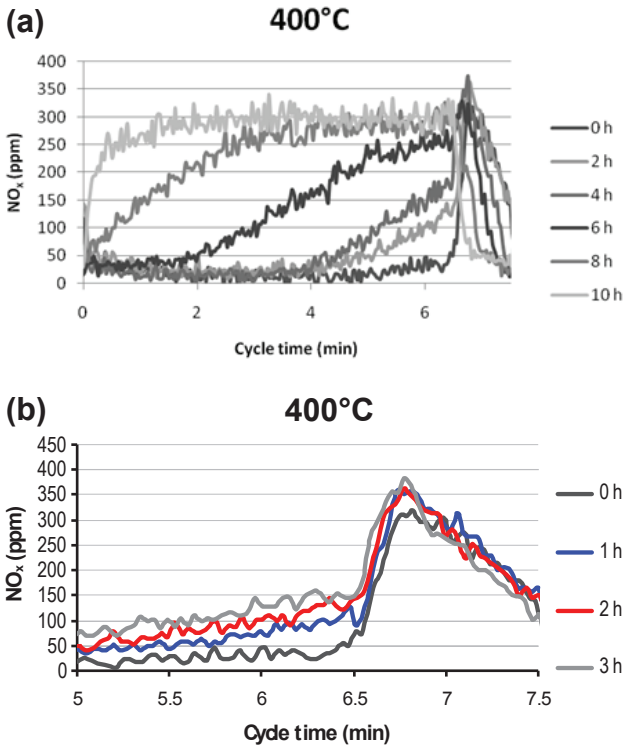

FIGURE 3. Model LNT ($Pt/K/Al_2O_3$): (a) Complete lean-rich NOx profiles at 400°C during sulfation. (b) Profiles during lean to rich transition shows the profiles experience reduction in NOx storage first followed by decrease in NOx puff.

a significant puff (Figure 4a). However, in performing the post sulfation performance sequence, i.e. evaluate performance while decreasing in temperature from 400°C to 300°C to 200°C, an interesting change was observed. Figure 4b shows the NOx profile at the end of sulfation at 200°C and compares it to the profile after heating to 400°C. There is a dramatic impact on the amount of NOx released during the lean to rich transition. To understand this impact it is necessary to draw on some results that were obtained using DRIFTS. We studied the same materials in the DRIFTS reactor and, following sulfation at each of the three temperatures, we heated the catalyst to 500°C while switching between lean and rich conditions. This similar approach showed that, even without the addition of SO_2 in the gas stream, the mild thermal treatment resulted in a loss of NOx capacity on the catalyst at 200°C. This effect is illustrated in Figure 4c, which shows the amount of NOx stored on the catalysts at the end of the lean phase for each sulfation temperature studied. The decrease in stored NOx is apparent at 200°C after heating to 500°C. This effect was minimal, or not observed, in the catalysts sulfated at 300 and 400°C. This observation shows that there must be sulfur stored on a non-potassium based site, i.e. alumina, and upon mild heating the sulfur is released and readsorbed on the potassium sites. To explain the increase in NOx released, it can be surmised that the desulfated alumina is then active for NOx storage. This low temperature NOx storage capacity of alumina has been reported in the past by many groups including our own [4-5]. Following the arguments that we have presented to this point it would follow that the sites being poisoned by sulfur and thus desulfated would be an alumina site proximal to Pt. This would then explain the observations for the profile with a large release of NOx at 200°C. The large release of NOx is observed in this case, rather than on the fresh catalyst, because 200°C is near the maximum temperature at which nitrates are stable on alumina. Therefore, the large release is observed here is analogous to the larger release that K displays at 400°C.

De-sulfurization was performed using a temperature programmed reaction (TPR) procedure with the rich conditions described above flowing continuously. This resulted in sulfur removal in the form of both SO_2 and H_2S for each sulfation temperature. The general shapes of the TPR curves are similar for each condition. The starting sulfation temperatures for each sulfur form as

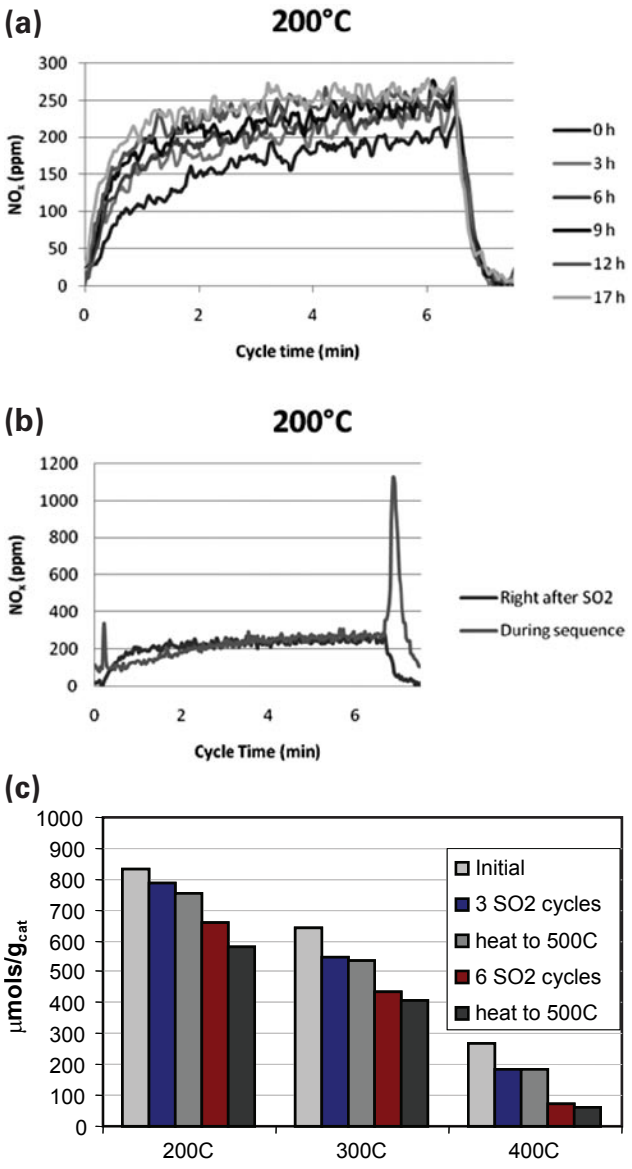

FIGURE 4. Model LNT ($Pt/K/Al_2O_3$): (a) Complete lean-rich NOx profiles at 200°C during sulfation. (b) NOx profiles at 200°C at the end of sulfation and after heating to 400°C then cooling to 200°C. (c) Quantified DRIFT spectra results showing that heating a sulfated catalyst from 200°C to 500°C in the absence of sulfur results in lost storage capacity; results not observed at 300 and 400°C.

well as the temperature of maximum release are listed in Table 1. This tabular comparison illustrates the similarities regardless of sulfation temperature. Further desulfated performance measurements also did not show a significant trend with respect to NOx conversion.

TABLE 1. Temperatures associated with the beginning of desulfation and the maximum sulfur release for sulfation temperatures of 200, 300, and 400°C on a model LNT ($Pt/K/Al_2O_3$).

T_S	200°C	300°C	400°C
De-S Start T			
H_2S	460°C	460°C	450°C
SO_2	460°C	400°C	470°C
De-S max T			
H_2S	690 + 750°C	750°C	735°C
SO_2	780°C	780°C	770°C

Additional efforts this year were focused on applying these techniques to Umicore's commercial catalyst. Figure 5 shows the progression of desulfation in the commercial catalyst is very similar to the general progression observed in the model $Pt/K/Al_2O_3$ LNT; specifically, the loss in activity is closely related to the amount of NOx stored during lean-phase operation (Figure 5b). Further analysis on this effort will be presented in the coming year.

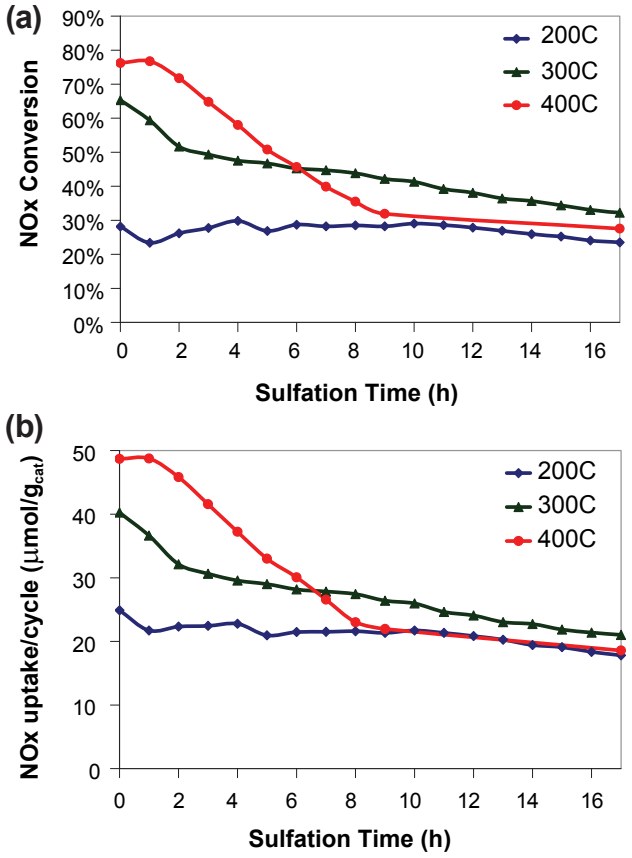

FIGURE 5. Commercial LNT (Umicore): (a) NOx conversion and (b) lean phase NOx storage as a function of sulfation time at 200, 300 and 400°C.

Conclusions

- Sulfation rate differs with temperature.
  - Rate of impact increases at higher temperatures.
  - NOx conversion closely linked to lean phase storage capacity.
- Sulfation routes are temperature dependent. Model catalyst results suggest:
  - Sulfur stored at 200°C migrates upon heating to 400°C.
  - At 300°C, SO_2 adsorbs near Pt before either diffusing to non-proximal sites or simply adsorbing on other sites.
  - At 400°C, if SO_2 adsorbs near Pt it quickly migrates to non-proximal sites.
- Sulfation temperature does not significantly impact de-sulfurization.
  - De-sulfurization temperature and form of sulfur release similar.
  - Sulfation temperature has minimal impact on recovery of NOx conversion activity.

References

1. W.S. Epling, L.E. Campbell, A. Yezerets, N.W. Currier, J.E. Parks, Catal. Rev. 46 (2004) 163.

2. I. Nova, L. Castoldi, L. Lietti, E. Tronconi and P. Forzatti, Catal. Today 75 (2002) 431.

3. I. Nova, L. Lietti, L. Castoldi, E. Tronconi and P. Forzatti, J. Catal., 239 (2006) 244.

4. L. Xu, G. Graham, R. McCabe, Catal. Lett. 115 (2007) 108.

5. T.J. Toops, D.B. Smith, W.S. Epling, J.E. Parks, W.P. Partridge, Appl. Catal. B 58 (2005) 255.

FY 2007 Publications/Presentations

1. J.A. Pihl, J.-S. Choi, V. Prikhodko, W.P. Partridge, K. Chakravarthy, Z. Gao, C.S. Daw, T.J. Toops, "CLEERS Coordination and Development of Catalyst Process Kinetic Data", DOE-Advanced Combustion Engine Program Annual Merit Review, Crystal City, VA, July 2007.

2. T.J. Toops, J.A. Pihl, "Sulfation and Desulfation Studies of Model Lean NOx Traps", 20th North American Catalysis Society Meeting, Houston, TX, June 2007.

3. T.J. Toops and J.A. Pihl, "Sulfation of Model K-based Lean NOx Trap while Cycling Between Lean and Rich Conditions", submitted to Catalysis Today, August 2007.

II.B.7 NOx Control and Measurement Technology for Heavy-Duty Diesel Engines

Bill Partridge[1] (Primary Contact),
Jae-Soon Choi[1], Jim Parks[1], Neal Currier[2],
Alex Yezerets[2], Mike Ruth[2], Shawn Whitacre[2]
[1]Oak Ridge National Laboratory
2360 Cherahala Blvd.
Knoxville, TN 37932
[2]Cummins, Inc.
Box 3005
Columbus, IN 47202-3005

DOE Technology Development Manager:
Ken Howden

Objectives

- Improve diesel engine-catalyst system efficiency through detailed characterization of chemistry and degradation mechanisms.
- Work with industrial partner to develop full-scale engine-catalyst systems to meet efficiency and emissions goals.

Accomplishments

- Demonstrated real-time on-engine measurements of oil dilution by fuel using a diagnostic developed under this cooperative research and development agreement (CRADA), and showed that results trend with more conventional but slower-feedback off-line measurements.
- Characterized impact of sulfation on the spatial nature of various lean-NOx (LNT) catalyst reactions, and used results to develop a conceptual model of LNT sulfation which explains integral catalyst performance.

Future Directions

- Quantify engine-system nonuniformities and mitigation strategies.
- Quantify selected LNT sulfation effects.
- Investigate selected nitrogen-selectivity issues related to LNT regeneration and hybrid catalyst systems.
- Develop and improve analytical techniques as necessary.

Introduction

Diesel engine technology has advanced significantly over the last decade. Modern diesels utilize advanced injector technology to enable multiple injections of fuel per combustion cycle. Precise control of injection timing allows optimization of efficiency and emissions. One application where the control of fuel injection offers a great advantage is the operation of the diesel engine in net-fuel-rich modes to regenerate LNT catalysts. The regeneration is necessary for catalyst operation which reduces engine-out NOx to regulated levels. During engine operation for catalyst management, extra fuel is injected into the cylinder, often in conjunction with throttling or higher exhaust gas recirculation rates to generate rich exhaust. The reductants present in the rich exhaust regenerate the catalyst, and specific parameters of the engine rich mode are adjusted to control both the overall magnitude and chemistry of the exhaust reductant mixture. However, extra fuel injection into the cylinder can lead to other issues of concern such as torque control, noise and vibration control, and oil dilution. CRADA work has addressed the potential problem of oil dilution that can occur when advanced in-cylinder fuel injection techniques are employed on a diesel engine. In some cases oil dilution can occur at levels that may impact engine durability.

The conventional method for quantifying oil dilution is based on gas chromatography (ASTM D 3524-04), and involves extractive sampling and off-line analysis. Using this methodology, a development engineer would design and run an engine test matrix, collect oil samples and send them out for analysis. The results from each measurement operation point would be received days later, correlated with the real-time performance data collected during the matrix run, and a new matrix designed. Thus, oil dilution analysis represents a significant delay in engine control development. Diagnostics that provide real-time on-engine assessment of oil dilution would significantly streamline the engine control development process. The CRADA has developed such a diagnostic, and evaluated it on a running engine and in parallel with conventional gas chromatographic (GC) methods.

Approach

Laser-induced fluorescence (LIF) spectroscopy is used to rapidly measure the fuel dilution of oil *in situ* on an operating engine. A fluorescent dye, commercially available and suitable for use in diesel fuel and oil systems, is added to the engine fuel. The LIF spectra

are monitored to detect the growth of the dye signal relative to the background oil fluorescence; fuel mass concentration is quantified based on a known sample set. The diagnostic is based on fiber optic probes for excitation light delivery and fluorescence collection; this allows flexibility of sampling location in the engine oil system, and could even be implemented in the cylinder-wall oil film where oil dilution is highest. A low cost 532-nm laser diode is used for excitation. Spectrally resolved fluorescence detection is effected via small fiber-coupled spectrometers. The diagnostic is portable.

The conventional approach for quantifying oil dilution requires off-line, and often off-site, analysis, and thus the oil-dilution data comes in at a significantly slower rate (days) compared to the other performance data. This forces a slow and iterative development process using conventional oil dilution diagnostics. The oil dilution diagnostic developed in the CRADA significantly shortens the engine-development time, by providing on-engine measurement and real-time feedback of the instantaneous oil dilution. This allows real-time tuning of the engine system to optimize the network of performance criteria; e.g., power, exhaust composition, durability, etc.

Results

The oil-dilution diagnostic has been demonstrated on a Mercedes 1.7-liter engine operated on a dynamometer. The timing of a late cycle fuel injection event was varied, as is typical of engine-managed reductant generation for catalyst management; such late-cycle injection often leads to oil dilution. In addition to real-time monitoring of oil dilution via the LIF-based diagnostic, oil samples were collected and analyzed using a modified ASTM method.

Figure 1 shows oil-dilution variations with and without (shaded region) post injection, and for various post-injection timings. The timing of the additional fuel injection for rich combustion operation was varied while holding the minimum air-to-fuel ratio during the rich event constant. The main injection pulse was kept constant, while the additional fuel was added at starting crank angles of 15º, 30º 45º, 60º, 75º, and 90º past top dead center. Results of the conventional GC analysis are also shown. It is apparent from both the LIF and GC methods that oil dilution increases with post injection. The LIF technique has greater precision and sensitivity than the GC technique which allows detection of smaller rates of dilution. Although the LIF- and GC-based dilution trends are similar, the magnitude of reported oil dilution differs by a factor of seven. The most likely explanation for the discrepancy is that the LIF technique is based on the dye which does not evaporate from the oil like fuel components. The LIF technique is most useful in applications where evaporation is of less significance; i.e., as a tool to measure dilution rates so that engineers can rapidly obtain feedback for controls development. Observations from this engine work leads to guidance for engineers to minimize fuel dilution during LNT regeneration strategy development, and is outlined in SAE paper 2007-01-4108 which describes the diagnostic and engine application [1].

Conclusions

- The LIF-based diagnostic provides fast feedback (ca. five min) of oil dilution significantly streamlining engine system development.
- The LIF-based oil-dilution diagnostic accurately trends with conventional off-line ASTM methodology.

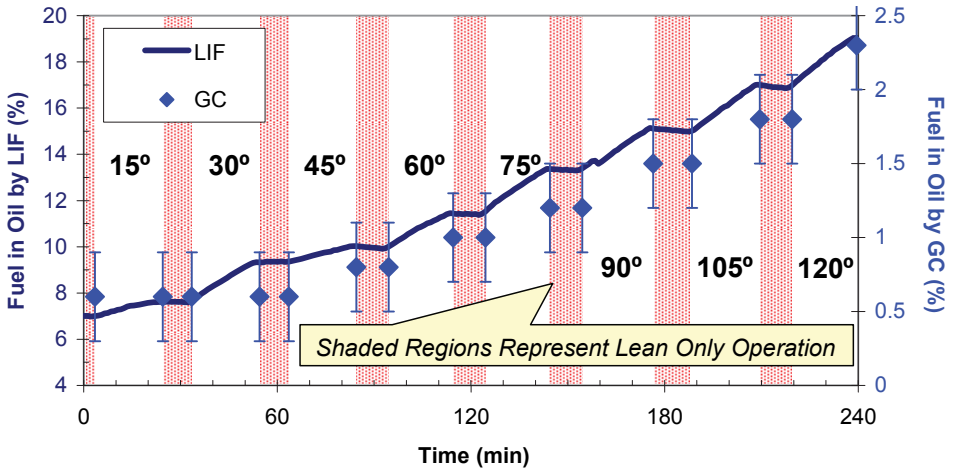

FIGURE 1. Comparison of LIF- and GC-based fuel in oil measurements. The shaded regions represent lean-only operation. Lean-rich cycling caused fuel dilution to occur during periods between the shaded regions.

- Optical probes for the oil-dilution diagnostic provide flexibility of sampling point within the engine system.
- A conceptual model of LNT sulfation effects which explains integral catalyst performance was developed based on detailed intra-LNT measurements.
- LNT sulfation produces a sulfated zone at the catalyst front where NOx storage and regeneration (NSR) reactions are inactive but oxygen storage capacity (OSC) reactions remain active but degraded.
- Sulfation impacts LNT NSR reactions in a plug-like manner and displaces the NSR zone down the catalyst axis.
- Sulfation has a more gradual impact on OSC reactions.
- As sulfation progresses, the NSR zone is continuously displaced down the catalyst axis, in turn shortening the OSC-only zone in the back of the catalyst downstream of the NSR zone; thus, the capacity to oxidize reductants such as hydrogen and ammonia slipping from the NSR region decreases with increasing sulfation, and reductant slip out of the catalyst can be expected.

References

1. Jim Parks, Bill Partridge and Shawn Whitacre "Rapid In Situ Measurement of Fuel Dilution of Oil in a Diesel Engine using Laser-Induced Fluorescence Spectroscopy," Society of Automotive Engineers Technical Paper 2007-01-4108, 2007.

FY 2007 Publications/Presentations

1. Jae-Soon Choi, William P. Partridge and C. Stuart Daw (2007). "Sulfur impact on NOx storage, oxygen storage and ammonia breakthrough during cyclic lean/rich operation of a commercial lean NOx trap," Applied Catalysis B: Environmental 77, 145–156; doi:10.1016/j.apcatb.2007.07.025.

2. Bill Partridge, Jae-Soon Choi, Stuart Daw "Distributed Impact of Sulfation on LNT Catalyst Reactions," 10th DOE Crosscut Workshop on Lean Emissions Reduction Simulation, University of Michigan, Dearborn, Michigan, May 2nd, 2007.

3. Jae-Soon Choi, Bill Partridge, Stuart Daw, "Assessing a Commercial Lean NOx Trap Performance via Spatiotemporal Species Profile Measurements: Sulfation & Its Impacts," North American Catalysis Society, 20th North American Meeting, Houston, Texas, June 22, 2007.

4. Jim Parks, Bill Partridge, and Shawn Whitacre, Rapid In Situ Measurement of Fuel Dilution of Oil in a Diesel Engine Using Laser-Induced Fluorescence Spectroscopy, presented at the SAE Powertrain and Fluid Systems Conference in Chicago, IL on October 29–31, 2007.

5. Jae-Soon Choi, William P. Partridge, Josh A. Pihl, C. Stuart Daw, "Sulfur Effects on Spatiotemporal Distribution of Reactions in a Commercial Lean NOx Trap," AIChE National Meeting, Salt Lake City, Utah, November 7, 2007.

Special Recognitions & Awards/Patents Issued

1. The unique value of this CRADA to Cummins' development program, and specifically to the successes related to the 2007 Dodge heavy duty pickup launch, was emphasized in a letter from Dr. John C. Wall, Cummins Vice President and Chief Technical Officer: "The knowledge and tools developed in our CRADA were critical to the R&D efforts that culminated in the release of the aftertreatment technology that meets the 2010 environmental standards in 2007."

2. Patent No. US7,211,793 B2; Date of Patent May 1, 2007; Neal W. Currier and Aleksey Yezerets, Cummins Inc., Mass spectrometry system and method.

II.B.8 Efficient Emissions Control for Multi-Mode Lean DI Engines

James Parks (Primary Contact), Brian H. West, Shean Huff, Mike Kass
Oak Ridge National Laboratory (ORNL)
2360 Cherahala Boulevard
Knoxville, TN 37932

DOE Technology Development Manager:
Ken Howden

Objectives

- Assess the relative merits of meeting emission regulations via catalytic aftertreatment or advanced combustion for engines capable of operating in multiple combustion modes ("multi-mode" engines).
- Determine the fuel efficiency of combinations of catalytic aftertreatment and advanced combustion modes.
- Characterize exhaust chemistry from advanced combustion and the resulting evolution of chemistry in catalysts for emissions control.

Accomplishments

Compared emissions and fuel efficiency for lean-NOx trap (LNT) catalysis with three combustion modes: no exhaust gas recirculation (EGR), production level EGR, and high efficiency clean combustion (HECC).

Future Directions

- Continue engine-based study to assess combination of LNT catalysis for HECC and traditional modes.
- Examine ability of catalysts to control increased carbon monoxide (CO) and hydrocarbon emissions from advanced combustion modes.

Introduction

New combustion regimes are being investigated as a means to increase the efficiency of, and to reduce the emissions from, diesel engines. The reduction of emissions during combustion is beneficial to the fuel efficiency of the system as a whole (engine plus emissions control system or "aftertreatment"). Specifically, lower engine-out NOx emissions can remove some burden from post-combustion emissions controls, and can thereby reduce the fuel penalty associated with NOx reduction. Although new combustion techniques have been developed that offer advantages for both engine fuel efficiency and emissions, often the techniques are not attainable over the entire range of load and speed required. Thus, engines seeking to implement the new combustion techniques often operate in a "multi-mode" fashion where, at certain loads, the engine is operated with advanced combustion techniques and, at other loads, the engine is operated with more traditional combustion. While modern control systems enable switching between the multiple modes of operation, the optimization of the system for fuel efficiency and emissions becomes more complex. One particular challenge is optimizing the size, cost, and complexity of the emissions control system. This project is aimed at understanding the complex issues of efficiency and emissions management for multi-mode engines with advanced emission control systems. Characterization of combustion exhaust chemistry and catalytic control are conducted to assist industry in the design of multi-mode engine and emission control systems.

Approach

This research has been conducted at ORNL in conjunction with ongoing engine studies. Two related projects at ORNL ("Measurement and Characterization of LNTs," and "Exploring Advanced Combustion Regimes for Efficiency and Emissions" in the Advanced Combustion Engines Program) are being leveraged with this activity. Experiments were performed on a Mercedes-Benz 4-cylinder, 1.7-liter diesel engine that has been significantly upgraded with advanced technologies (variable geometry turbocharger, high-throughput EGR, multi-injection control, etc.) to enable advanced combustion studies. The engine is operated on an engine dynamometer in ORNL's facility. All experiments were conducted at steady-state load and speed conditions which were chosen and weighted for estimating Federal Test Procedure (FTP) drive cycle emissions based on industry input.

LTC is a relatively new combustion mode that enables an order of magnitude reduction in NOx and particulate matter (PM) emissions through high levels of EGR. HECC is a new evolution of LTC that achieves extremely low NOx and PM emissions while maintaining low brake specific fuel consumption; HECC has comparable fuel efficiency to traditional modes [1]. HECC achieves good efficiency and emissions by coupling high levels of EGR with advanced injection timing. Although NOx and PM emissions are reduced in HECC, CO and hydrocarbon emissions increase. Formaldehyde emissions increase as well;

formaldehyde is classified as a mobile source air toxic by the Environmental Protection Agency. Thus, while the emissions control system does not need to reduce NOx and PM significantly during HECC, higher CO and hydrocarbon emission control is needed.

In FY 2006, experiments were conducted in an attempt to reduce NOx via hydrocarbon selective catalytic reduction (HC-SCR). This approach uses excess hydrocarbons emitted during HECC to control the smaller NOx emissions. Despite encouraging results with this approach on a bench-scale flow reactor with simulated exhaust, the results did not translate well to engine experiments, and the HC-SCR was not deemed efficient enough for practical use. This year (FY 2007) efforts shifted to LNT catalysis and focused on comparing fuel efficiencies of the combined engine and emissions control system for three combustion modes: no EGR, production-level EGR, and HECC. The LNT used for the study was provided by a member of the Manufacturers of Emission Control Association and has been used in other studies at ORNL.

Results

The engine was operated at 2.6 bar and 1,500 rpm which is point #2 of the engine set points shown in Figure 1; these load-speed points are representative of operation in the transient FTP driving cycle. With no exhaust emission control, engine-out NOx was reduced by the addition of EGR and by HECC. Figure 2 shows the reduction in NOx obtained by the production level EGR (17%) and HECC; results are shown relative to the 0% EGR case. As shown by Figure 2, HECC offers dramatic NOx reduction (96%) as compared with the significant but modest levels of NOx reduction obtained by traditional EGR levels (23%).

The effect of adding LNT emission control is shown in Figure 3; here the LNT was regenerated every 60 seconds with a 3-second duration of enrichment of exhaust at an air-to-fuel ratio of 13.5. For the 0% and 17% EGR cases, the LNT increased the NOx reduction efficiency significantly but not to desired levels. At the low exhaust temperatures associated with this load point, regeneration of the LNT is difficult and limits the performance in comparison to higher temperatures where >90% NOx reduction efficiencies can be achieved. HECC operation already reduced NOx by 96% relative to 0% EGR at the engine-out position, and the NOx reduction efficiency was actually reduced by the LNT to

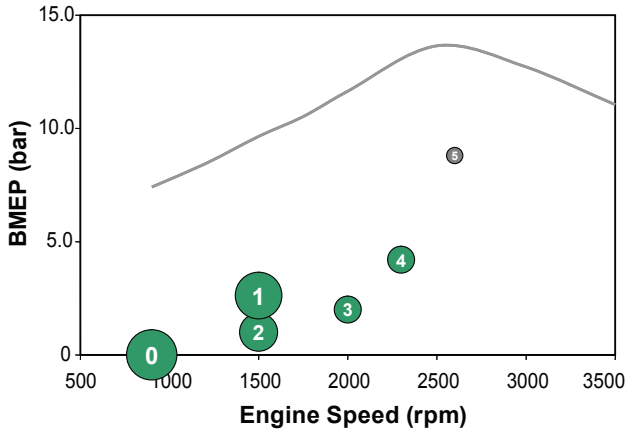

FIGURE 1. Steady-State Points for FTP Simulation on the Engine Load vs. Speed Map

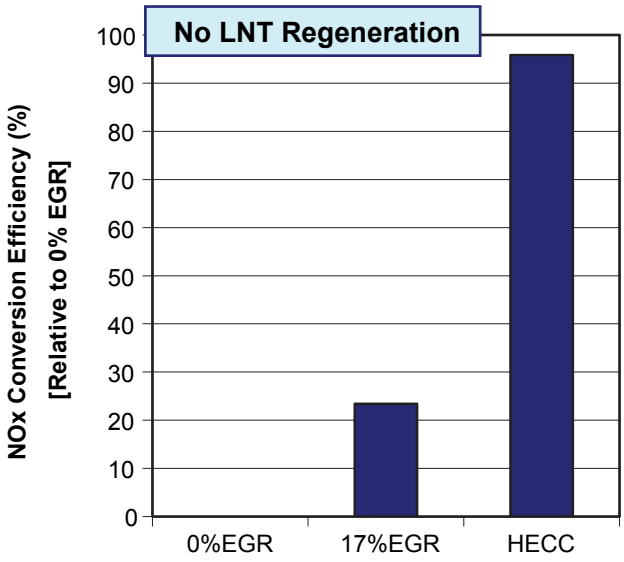

FIGURE 2. NOx Conversion Efficiency for Production EGR (17%) and HECC Relative to No EGR

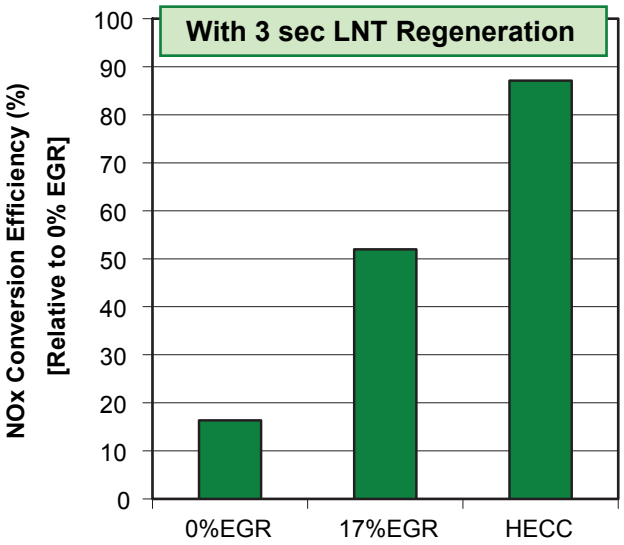

FIGURE 3. NOx Conversion Efficiency with LNT Emission Control at 3-Second Duration Regeneration for No EGR, Production EGR (17%) and HECC Relative to No EGR with No LNT Regeneration

87%. The increase in tailpipe NOx emissions was due to emissions of stored NOx on the LNT that occurred during the regeneration event. The reductants in the regeneration event create an exothermic reaction on the catalyst surfaces which can result in some NOx release.

The duration of the LNT regeneration enrichment was reduced to 1 second for the HECC case to further examine the effect of regeneration on NOx emissions during HECC operation; Figure 4 shows the result as compared with no regeneration and the 3 second duration regeneration. The 1 second duration did result in lower NOx emissions and gave 98% NOx reduction as compared to the 0% EGR base case. Thus, a correct amount of regeneration can enable the LNT to further reduce NOx emissions from the already extremely low NOx emissions of HECC operation. Here "correct amount" refers to the amount of reductant delivery to the LNT during regeneration. Larger amounts of reductant (produced during the 3-second duration regeneration) may reduce some stored NOx but can lead to NOx emission from the resulting exothermal desorption of NOx. Smaller amounts of reductant (the 1 second duration case) allow for NOx reduction and LNT regeneration while reducing the exotherm responsible for NOx desorption.

Overall, the advanced HECC mode is more fuel efficient at attaining NOx reduction at this load point. Fuel consumption for HECC is comparable to the 0% EGR case. However, adding LNT regeneration to the 0% and 17% EGR cases with a 3-second duration every 60 seconds entails a fuel penalty of 1%, and the resulting NOx reduction efficiency is much less than obtained with HECC. Thus, at low loads where LNT performance is limited by exhaust temperatures, HECC is favorable to traditional combustion coupled with LNT emission control. Results for higher loads may differ since HECC becomes more difficult but LNT regeneration becomes more efficient; future studies will investigate higher load points.

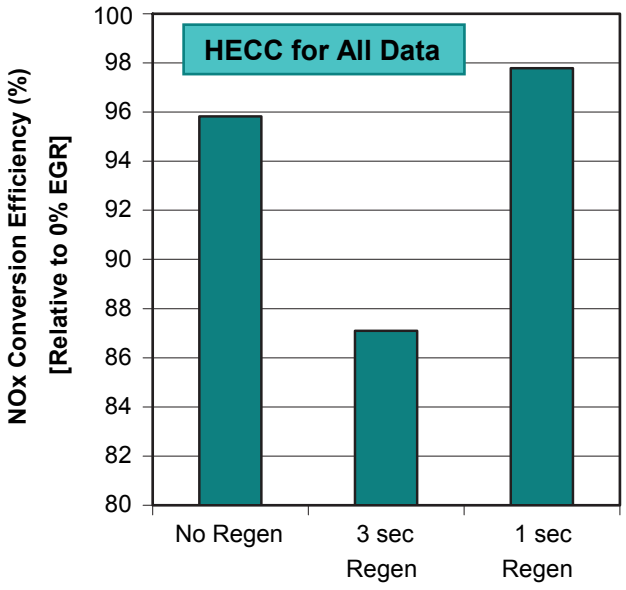

FIGURE 4. NOx Conversion Efficiency for HECC with No LNT Regeneration, 3-Second Duration Regeneration, and 1 Second Duration Regeneration (All Relative to No EGR with No LNT Regeneration)

Conclusions

- At the low load point studied (2.6 bar):
  - HECC enables a 96% reduction in NOx emissions as compared with traditional combustion with 0% EGR.
  - Low exhaust temperatures limited LNT performance by reducing regeneration efficiency.
  - Optimal combined NOx emissions and fuel efficiency are greater for HECC alone than for combined traditional combustion and LNT emission controls.
- Future studies will address higher load points where HECC becomes more difficult to control but LNT regeneration becomes more efficient.

References

1. C. Scott Sluder and Robert M. Wagner, "An Estimate of Diesel High-Efficiency Clean Combustion Impacts on FTP-75 Aftertreatment Requirements", *SAE Technical Paper Series* 2006-01-3311 (2006).

FY 2007 Publications/Presentations

1. Matt Swartz, Shean Huff, James Parks, and Brian West, "Intra-Catalyst Reductant Chemistry and NOx Conversion of Diesel Lean NOx Traps at Various Stages of Sulfur Loading", *SAE Technical Paper Series* 2006-01-3423 (2006).

2. Josh A. Pihl, James E. Parks II, C. Stuart Daw, and Thatcher W. Root, "Product Selectivity During Regeneration of Lean NOx Trap Catalysts", *SAE Technical Paper Series* 2006-01-3441 (2006) (*Selected for SAE 2006 Transactions*).

3. Jim Parks, Shean Huff, Matt Swartz, and Brian West, "Comparison of LNT Catalyst Performance with In-Cylinder Regeneration Techniques", *Presentation at the 10th DOE Cross-Cut Lean Exhaust Emissions Reduction Simulations (CLEERS) Workshop* in Dearborn, MI on May 1–3, 2007.

4. Jim Parks, Shean Huff, Mike Kass, and Brian West, "Lean NOx Trap Formulation Effect on Performance with In-Cylinder Regeneration Strategies", *Poster Presentation at the 13th Diesel Engine-Efficiency and Emissions Research (DEER) Conference* in Detroit, MI on August 13–16, 2007.

5. Jim Parks, Shean Huff, Mike Kass, and John Storey, "Characterization of In-Cylinder Techniques for Thermal Management of Diesel Aftertreatment", *SAE Technical Paper Series* 2007-01-3997 (2007).

6. Jim Parks, Brian West, Matt Swartz, and Shean Huff, "Characterization of Lean NOx Trap Catalysts with In-Cylinder Regeneration Strategies", *submitted for the 2008 SAE Congress conference (under review)*.

II.B.9 Cross-Cut Lean Exhaust Emissions Reduction Simulation (CLEERS): Administrative Support

Stuart Daw
Oak Ridge National Laboratory (ORNL)
National Transportation Research Center
2360 Cherahala Boulevard
Knoxville, TN 37932-6472

DOE Technology Development Manager:
Ken Howden

Key ORNL personnel involved in this activity are Stuart Daw, Vitaly Prikhodko, and Charles Finney.

Objectives

Coordinate the CLEERS activity for the Diesel Cross-Cut Team to accomplish the following:

- Promote development of improved computational tools for simulating realistic full-system performance of lean-burn engines and associated emissions controls.
- Promote development of performance models for emissions control components such as exhaust manifolds, catalytic reactors, and sensors.
- Provide consistent framework for sharing information about emissions control technologies.
- Help identify emissions control R&D needs and priorities.

Accomplishments

- Continued co-leading the CLEERS Planning Committee and facilitation of the Selective Catalytic Reduction (SCR), Lean-NOx Trap (LNT), and Diesel Particulate Filter (DPF) Focus Group teleconferences with strong domestic and international participation.
- Continued co-leading the LNT Focus Group and refinement of the standard LNT materials protocol.
- Identified key R&D priorities from CLEERS community, including coordination of R&D priorities survey with response from 14 DOE Diesel Cross-Cut Team companies and their partners in January, 2007.
- Provided regular update reports to the DOE Diesel Cross-Cut Team.
- Organized the 10th CLEERS workshop at University of Michigan, Dearborn on May 1-3, 2007.
- Maintained website functionalities, security, and data to facilitate web meetings and serve Focus Group interactions.

Future Directions

- Continue co-leading CLEERS planning committee.
- Continue co-leading the LNT Focus Group and support the DPF and SCR Focus Groups as needed.
- Continue providing standard reference LNT materials and data for Focus Group evaluation.
- Continue assisting in refinement of CLEERS technical priorities, especially in regard to the balance between LNT and urea-SCR R&D and synergies between these two technology areas.
- Organize the 11th CLEERS workshop in the spring of 2008.
- Continue maintenance and expansion of CLEERS web site.
- Continue providing regular update reports to the DOE Diesel Cross-Cut team.

Introduction

Improved catalytic emissions controls will be essential for utilizing high efficiency lean-burn engines without jeopardizing the attainment of much stricter U.S. Environmental Protection Agency emission standards scheduled to take effect in 2010. Simulation and modeling are recognized by the DOE Diesel Cross-Cut Team as essential capabilities needed to achieve this goal. In response to this need, the CLEERS activity was initiated to promote improved computational tools and data for simulating realistic full-system performance of lean-burn engines and the associated emissions control systems. Specific activities supported under CLEERS include:

- Public workshops on emissions control topics;
- Collaborative interactions among Cross-Cut Team members, emissions control suppliers, universities, and national labs under organized topical focus groups;
- Development of experimental data, analytical procedures, and computational tools for understanding performance and durability of catalytic materials;
- Establishment of consistent frameworks for sharing information about emissions control technologies;

- Recommendations to DOE and the DOE Cross-Cut Team regarding the most critical emissions control R&D needs and priorities.

ORNL is involved in two separate DOE-funded tasks supporting CLEERS:

- Overall administrative support; and
- Joint development of benchmark LNT kinetics with Sandia National Laboratories and Pacific Northwest National Laboratory.

Approach

In the administrative task, ORNL coordinates the CLEERS Planning Committee, the CLEERS Focus groups, CLEERS public workshops, and the CLEERS website (http://www. cleers.org). The specific activities involved include:

- Coordination of the CLEERS Planning Committee and the LNT Focus Group;
- Organization of the annual CLEERS public workshops;
- Maintenance of the CLEERS web site;
- Preparation and presentation of status reports to the Cross-Cut Team; and
- Response to requests and inquiries about CLEERS from the public.

Results

The 10th CLEERS workshop was held May 1–3, 2007 at the Dearborn campus of the University of Michigan. As with previous workshops, there were more than 100 registrants from emissions controls suppliers, universities (both foreign and domestic), software vendors, and consultants. The three traditional emissions control technology areas (LNTs, DPFs, and SCR) were highlighted as well as topics related to systems integration and component interactions. The technical program and presentations are available on the website (http://www. cleers.org) under the 10th workshop heading. Key observations coming from the workshop include:

- Integration of LNTs with NH_3-SCR continues to be a promising possibility.
- Kinetic mechanisms for LNT simulation continue to improve.
- Reliable public-domain kinetics for NH_3 storage and hydrocarbon poisoning are still lacking for urea-SCR modeling and simulation.
- Publicly available DPF soot oxidation kinetics continue to be inadequate for low-temperature combustion modes and with unconventional fuels (e.g., biodiesel).
- Integrated system performance (including combinations of diesel oxidation catalysts, SCR, LNTs, and DPFs) continues to increase in priority.

The LNT, SCR, and DPF Focus Groups have continued regular phone/web meetings throughout the year under the new single monthly meeting format adopted last year. So far this new format has worked well. R&D priorities identified by the CLEERS members were updated in an anonymous poll conducted in January 2007 by New West Technologies. Questionnaires developed by the CLEER Planning Committee were sent to 22 organizations (including heavy-duty and light-duty diesel and gasoline original equipment manufacturers, Tier 1 emissions control suppliers, and energy companies) and 64% responded. The results were summarized in a public presentation at the 2007 Diesel Engine Emissions Reduction (DEER) meeting (see Daw et al, 2007) and discussed at length with the Diesel Cross-Cut Team. Highlights from the poll include:

- Diesel respondents recommended that CLEERS-related R&D resources be allocated as: 31% SCR, 29% DPF, 25% integrated systems (IS), and 15% LNT.
- Lean gasoline respondents recommended that CLEERS-related R&D resources be allocated as: 60% LNT, 20% DPF, 16% IS, and 4% SCR.
- For both SCR and LNT technology areas, the top issues/concerns centered on poisoning, thermal aging, and development of improved kinetic mechanisms.

The above results are also summarized in Figure 1. Preliminary analyses of the poll results have been made by the CLEERS Planning Committee and focus group

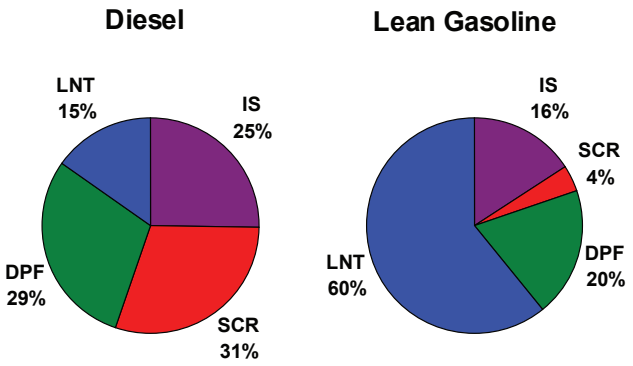

FIGURE 1. Summary of results from the 2007 anonymous poll of DOE Diesel Cross-Cut companies and their partners regarding emissions control R&D resource allocation preferences. Responses were separately averaged for diesel and gasoline responders according to technology area.

leaders to determine where there might be gaps in the current CLEERS-related research activities both in DOE and in industry. This analysis is expected to continue on the basis of a new poll planned for 2008.

Conclusions

CLEERS is playing an increasing role in coordinating emissions control R&D among the Cross-Cut Team members and their partners. The success of CLEERS is most noticeable in the broad industry, national lab, and university participation in the public workshops; the strong domestic and international participation in the monthly focus meetings; the heavy interest in the R&D priority survey among CLEERS community; and the large number of visits to the CLEERS web site.

FY 2007 Publications/Presentations

1. http://www.cleers.org

2. Stuart Daw, Michael Laughlin, and Richard Blint, "Aftertreatment Research Prioritization: A CLEERS Industrial Survey", Diesel Engine-Efficiency and Emissions Research (DEER) Conference, Detroit, MI, August 2007.

II.B.10 Cross-Cut Lean Exhaust Emissions Reduction Simulation (CLEERS): Joint Development of Benchmark Kinetics

Stuart Daw
Oak Ridge National Laboratory (ORNL)
National Transportation Research Center (NTRC)
2360 Cherahala Boulevard
Knoxville, TN 37932-6472

DOE Technology Development Manager:
Ken Howden

Key ORNL personnel involved in this activity are Stuart Daw, Kalyana Chakravarthy, Todd Toops, Jae-Soon Choi, Jim Parks, Josh Pihl, and Vitaly Prikhodko.

Objectives

Coordinate ORNL's collaboration with the Pacific Northwest National Laboratory (PNNL) and Sandia National Laboratories (SNL) in the development of kinetics information needed for aftertreatment component simulation through the following:

- Provide benchmark laboratory measurements of NOx reduction chemistry and reaction rates.
- Correlate laboratory measurements of lean-NOx trap (LNT) and selective catalytic reduction (SCR) materials with test-stand/vehicle studies in the NTRC facility.
- Develop and validate global chemistry and (low-order) models for LNT and SCR kinetics.

Accomplishments

- Continued refinement and validation of the LNT material characterization protocol in conjunction with the LNT Focus Group, SNL, and PNNL and collaborating suppliers.
- Initiated benchmarking of Umicore commercial reference LNT material for sulfation and desulfation characteristics.
- Continued in-depth study of the global kinetics of LNT regeneration, with specific emphasis on formation of byproduct N_2O and NH_3, effective fuel penalty, and potential coupling of LNT with SCR.
- Continued diffuse-reflectance infrared spectroscopy (DRIFTS) measurements of the fundamental mechanisms involved in S poisoning and desulfation of LNTs.

Future Directions

- Continue expansion of the ORNL bench-flow and micro-reactor capabilities.
- Continue development and demonstration of methods for utilizing LNT protocol data to generate global reaction kinetics and simulate device-scale performance.
- Continue characterization of Umicore LNT reference catalyst over a range of conditions relevant to both diesel and lean gasoline engine exhaust and transmit results to the LNT Focus Group as they become available.
- Update and post revised LNT kinetic models with input from SNL, literature, and ORNL experimental data as these become available.
- Continue identification of synergies between LNT NH_3 generation kinetics and NH_3-SCR as a potential alternative to urea-SCR NOx control.
- Coordinate bench reactor studies of the impact of sulfation and desulfation on LNT durability and kinetics.

Introduction

Improved catalytic emissions controls will be essential for utilizing high efficiency lean-burn engines without jeopardizing the attainment of much stricter U.S. Environmental Protection Agency emission standards scheduled to take effect in 2010. Simulation and modeling are recognized by the DOE Diesel Cross-Cut Team as essential capabilities needed to achieve this goal. In response to this need, the CLEERS activity was initiated to promote improved computational tools and data for simulating realistic full-system performance of lean-burn engines and the associated emissions control systems. Specific activities supported under CLEERS include:

- public workshops on emissions control topics;
- collaborative interactions among Cross-Cut Team members, emissions control suppliers, universities, and national labs under organized topical focus groups;
- development of experimental data, analytical procedures, and computational tools for understanding performance and durability of catalytic materials;

- establishment of consistent frameworks for sharing information about emissions control technologies; and
- recommendations to DOE and the DOE Cross-Cut Team regarding the most critical emissions control R&D needs and priorities.

ORNL is involved in two separate DOE-funded tasks supporting CLEERS:

- overall administrative support; and
- joint development of benchmark LNT kinetics with SNL and PNNL.

Approach

In the benchmark kinetics task, ORNL is collaborating with SNL and PNNL to produce kinetics information for predicting the performance of LNTs as individual devices and integrated with catalyzed particulate filters and ammonia-based SCR. The results of this work are discussed with the LNT, DPF, and SCR Focus groups prior to publication to provide technical review and guidance to the labs. Specific activities involved include:

- Regular direct interactions among ORNL, PNNL, and SNL;
- Experimental measurements of LNT chemistry and reaction rates using laboratory reactors and prototype devices installed on engine test stands and vehicles;
- Analysis and reconciliation of experimental data from different sources with predictions from computer simulations; and
- Publications in journals and presentations in public meetings and on the website.

Results

Studies of LNT kinetics have continued at a high pace as evidenced by the large number of publications and presentations. The reader is encouraged to consult the publications listed at the end of this report for additional details. Briefly, the focus has been on NOx reduction reactions, sulfur capture, and desulfation. The Umicore reference catalyst is of considerable interest because it is specifically intended for lean gasoline applications and because it is the only commercial LNT catalyst available to the CLEERS community with no restrictions on information about its formulation.

A complete set of reaction rate parameters for reducing conditions has been submitted to Catalysis Today for publication (see Larson et al., 2007). These thermodynamically consistent kinetics accurately predict ORNL observations of steady-state conversions of CO, H_2, NO, NO_2, and NH_3 for the Umicore catalyst over a wide range of species concentrations between 200 and 400°C. One interesting aspect of these kinetics is that they appear to predict the possibility of multiple steady-states. The next step is to link these kinetics to previously developed mechanisms for NOx capture in order to simulate the details of complete lean-rich cycles.

Studies of sulfation and desulfation kinetics have utilized the ORNL bench-flow reactor with its associated spatially resolved capillary inlet mass spectrometry (SpaciMS) capability (see Figure 1) and the DRIFTS micro-reactor. It has been found that sulfation proceeds in a sharp front beginning at the leading edge of the monolith and progressing downstream with time. Upstream of the front ceria continues to capture and release NOx, but Ba loses all NOx functionality. The oxygen storage capacity of the ceria is also degraded upstream of the front. Downstream of the sulfation front, NOx capture and release appear to proceed normally. This combined scenario is depicted schematically in Figure 2. One interesting impact of sulfation is to significantly increase NH_3 at the monolith exit.

Conclusions

Closely linked laboratory experiments and modeling have improved understanding of LNT kinetics. This understanding is leading to better simulation of NOx emissions controls in lean exhaust systems and identification of opportunities for reducing the fuel penalty and S poisoning currently limiting full implementation of LNT technology.

FY 2007 Publications/Presentations

1. W. P. Partridge, J.-S. Choi, "Intra-reactor measurements of transient species distributions", Presentation at the Instrumentation, Systems, and Automation Society 2006 Technical Conference, Houston, Texas, October 17–19, 2006.

2. J.A. Pihl, J.E. Parks II, T.J. Toops, C.S. Daw, T.W. Root, "Product Selectivity During Regeneration of Lean NOx Trap Catalysts," SAE 2006-01-3441.

3. R.S. Larson, K. Chakravarthy, J.A. Pihl, C.S. Daw, "Modeling of chemistry in lean NOx traps under reducing conditions," SAE 2006-01-3446.

4. V.Y. Prikhodko, "Effect of Length on the Performance of Lean NOx Traps," M.S. Thesis, University of Tennessee, Knoxville, Tennessee, May 2007.

5. V.Y. Prikhodko, J.-S. Choi, C.S. Daw, K. Nguyen, "Bench Studies of LNT Length Effects," Presentation at the 10th CLEERS Workshop, Dearborn, Michigan, May 1–3, 2007, http://www.cleers.org.

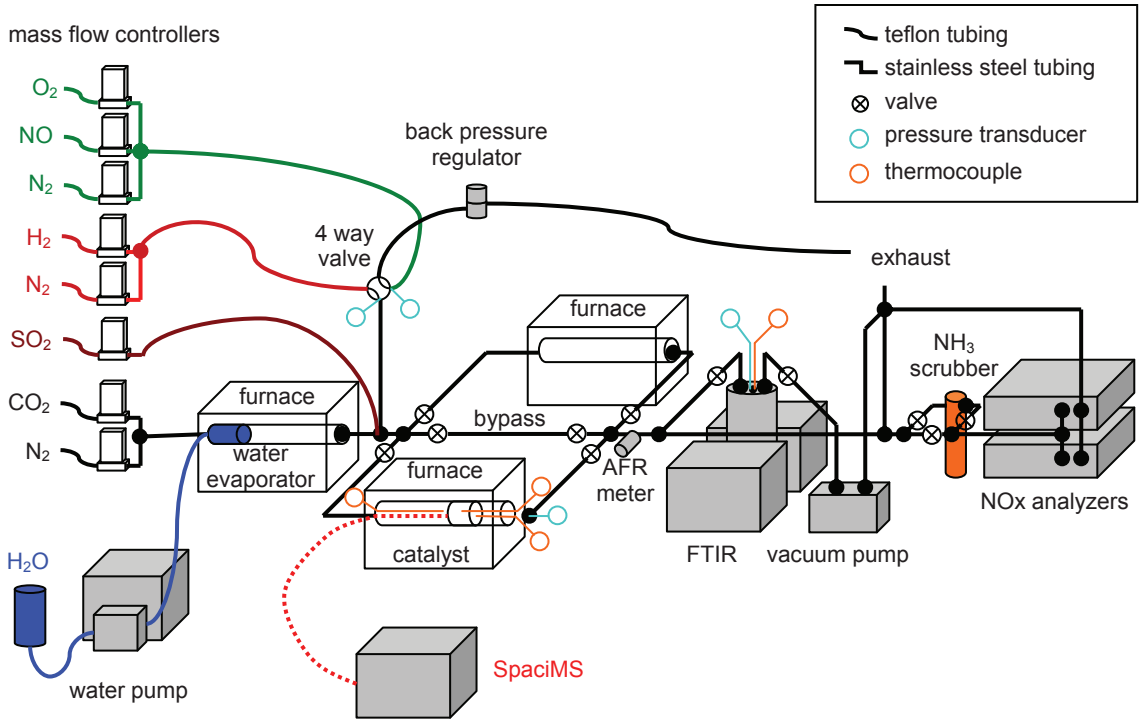

FIGURE 1. Schematic layout of the ORNL bench reactor used for sulfation and desulfation experiments. A SpaciMS capillary is installed for intra-monolith speciation.

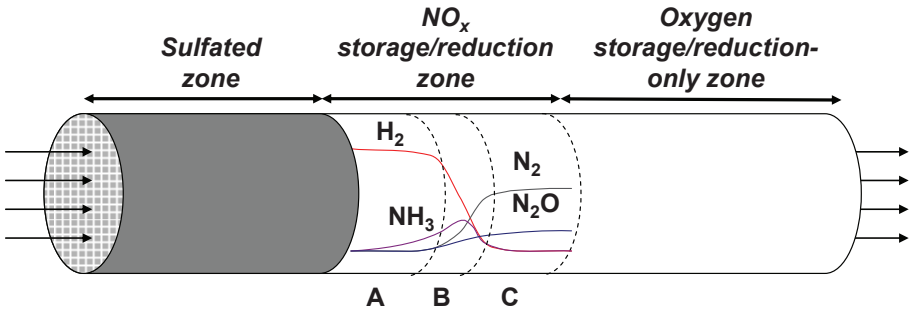

FIGURE 2. Conceptual diagram of the internal reactions occurring inside a partially sulfated LNT monolith. In the sulfated zone NOx capture and release have become deactivated, but some degree of oxygen storage and release is still present. Beyond the sulfation front, NOx capture, release and reduction still occur.

6. J.A. Pihl, C.S. Daw, T.J. Toops, "DRIFTS Investigation of Lean NOx Trap Regeneration," Presentation at the 10th CLEERS Workshop, Dearborn, MI, May 1–3, 2007, http://www.cleers.org.

7. W.P. Partridge, J.-S. Choi, C.S. Daw, "Distributed impact of sulfation on LNT catalyst reactions", Presentation at the 10th DOE Cross-Cut Workshop on Lean Emissions Reduction Simulation, Dearborn, Michigan, May 1-3, 2007, http://www.cleers.org.

8. B.G. Bunting, T.J. Toops, K. Nguyen, H. Kim, "Rapid Thermal Aging of Lean NOx Traps", Presentation at the 10th Cross-Cut Lean Exhaust Emissions Reduction Simulations (CLEERS) Workshop, Dearborn, Michigan, May 1–3, 2007, http://www.cleers.org.

9. J. Pihl, "CLEERS Coordination & Development of Catalyst Process Kinetic Data," Presentation at the FreedomCAR Combustion & Fuels Merit Review, June 18, 2007.

10. J.A. Pihl, R.S. Larson, V.K. Chakravarthy, C.S. Daw, "Micro-kinetic modeling of Lean NOx Trap regeneration chemistry," Presentation at the 20th North American Meeting of the North American Catalysis Society, Houston, TX, June 21, 2007.

11. T.J. Toops, J.A. Pihl, "Sulfation and Desulfation Studies of Model Lean NOx Traps," Presentation at the 20th North American Meeting of the North American Catalysis Society, Houston, TX, June 21, 2007.

12. T.J. Toops, B.G. Bunting, K. Nguyen, H. Kim, A.Gopinath, "Effect of Thermal Aging on Catalyst Morphology and Performance of Lean NOx Traps", Presentation at the 20th North American Catalysis Society Meeting, Houston, TX, June 17–22, 2007.

13. J.-S Choi, W.P. Partridge, C.S. Daw, "Assessing a commercial lean NOx trap performance via spatiotemporal species profile measurements", Presentation at the 20th North American Meeting of the North American Catalysis Society, Houston, Texas, June 17–22, 2007.

14. B.G. Bunting, T.J. Toops, A. Foster, N. Ottinger, K. Nguyen "Rapid Aging/Poisoning Protocols for Diesel Aftertreatment Devices: NOx Abatement Catalysts", Presentation at the Diesel Engine-Efficiency and Emissions Research (DEER) Conference, Detroit, MI, August 2007.

15. J.-S. Choi, W.P. Partridge, C.S. Daw, "Sulfur impact on NOx storage, oxygen storage and ammonia breakthrough during cyclic lean/rich operation of a commercial lean NOx trap", Applied Catalysis B: Environmental 77 (2007) 145.

16. Y. Ji, T.J. Toops, M. Crocker, "Effect of Ceria on the Storage and Regeneration Behavior of a Model Lean NOx Trap Catalyst", Catalysis Letters 119 (2007) 257.

17. T.J. Toops, B.G. Bunting, K. Nguyen, A. Gopinath, "Effect of Engine-Based Thermal Aging on Surface Morphology and Performance of Lean NOx Traps", Catalysis Today 123 (2007) 285.

18. J.-S. Choi, W.P. Partridge, J.A. Pihl, C.S. Daw, "Sulfur Effects on Spatiotemporal Distribution of Reactions in a Commercial Lean Nox Trap," Presentation at the AIChE National Meeting, Salt Lake City, UT, November 7, 2007.

19. T.J. Toops, J.A. Pihl, "Fundamental Investigations of Sulfation and Desulfation in Lean Nox Trap Catalysts," Presentation at the AIChE National Meeting, Salt Lake City, UT, November 7, 2007.

20. K. Nguyen, H. Kim, B.G. Bunting, T.J. Toops, C.S. Yoon, "Rapid Aging of Lean NOx Traps by High-Temperature Thermal Cycling", SAE-07-PFL-227 (2007).

21. R.S. Larson, J.A. Pihl, V.K. Chakravarthy, T.J. Toops, C.S. Daw, "Microkinetic Modeling of Lean NOx Trap Chemistry under Reducing Conditions," Catalysis Today (in press 2007).

22. T.J. Toops, J.A. Pihl, "Sulfation of K-based Lean NOx Trap while Cycling Between Lean and Rich Conditions: I. Microreactor Study," Catalysis Today (in press 2007).

23. Y. Ji, J.-S. Choi, T.J. Toops, M. Crocker, M. Naseric, "Influence of Ceria on the NOx Storage/Reduction Behavior of Lean NOx Trap Catalysts", Catalysis Today (in press 2007).

24. J.-S. Choi, W.P. Partridge, J.A. Pihl, C.S. Daw, "Sulfur and temperature effects on the spatial distribution of reactions inside a lean NOx trap and resulting changes in global performance," Catalysis Today (in press 2007).

II.B.11 Cross-Cut Lean Exhaust Emissions Reduction Simulations (CLEERS) Diesel Particulate Filter (DPF) Modeling

Mark Stewart (Primary Contact), George Muntean, Gary Maupin, Heather Dillon
Pacific Northwest National Laboratory (PNNL)
P.O. Box 999, MSIN: K7-15
Richland, WA 99354

DOE Technology Development Manager:
Ken Howden

Objectives

- Develop improved modeling capabilities for diesel particulate filtration:
  - Create improved models of the local properties of the soot filter, e.g. cake permeability, density, and morphology.
  - Develop improved sub-grid representations of the local soot oxidation reactions in diesel soot filters, e.g. oxidation mechanisms, detailed kinetics, and global rates.
- Coordinate and lead the CLEERS DPF sub-team activities:
  - Provide project updates to the industry sub-team, solicit feedback, and adjust work scope accordingly.
  - Lead technical discussions, invite distinguished speakers, and maintain an open dialogue on DPF modeling issues.

Accomplishments

- Added catalytic chemistry to micro-scale DPF models.
- Performed a number of simulation studies including:
  - Effect of particle size on soot deposit location, morphology, and properties.
  - Effect of platinum loading on total oxidation rate in a given pore geometry.
  - Effect of catalyst placement within the DPF wall on overall soot oxidation rate, NOx recycle, and final NO/NO_2 ratios.
- Carried out side-by-side loading and regeneration experiments with individual uncatalyzed and platinum-catalyzed DPF channels.
- Developed techniques for loading individual filter walls with aerosolized salt particles for fundamental filtration studies.
- Participated in monthly CLEERS teleconferences and coordinated the calls focused on DPF technology.

Future Directions

Activities carried out during FY 2007 conclude the original scope of work for this multi-year project. Now that sub-grid simulation tools have been developed which meet the original project requirements, follow-on research will focus on application of these tools and further development in targeted areas. Future activities will include:

- Research into the design and optimization of 4-way devices which address soot, hydrocarbons, CO, and NOx in a single unit.
- Exploration of issues surrounding nano-particulate emissions, including nano-particle detection, identification by size and composition, and prediction of nano-particle formation and behavior in after-treatment systems.
- Filtration and regeneration experiments and simulations to improve prediction of global reaction rates during active and passive regeneration and estimation of device state from sensor data.
- Study of catalyst washcoat placement, morphology, and composition; and effects on back-pressure and species transport during filter regeneration.

Introduction

The inherent fuel efficiency of diesel engines makes them an important part of any global strategy for near-term reduction of greenhouse gas emissions from vehicles. Emissions standards for new vehicles in the U.S., Asia, and Europe require filtration of potentially dangerous soot particles from the exhaust produced by currently available diesel engines. Removal of NOx from diesel exhaust will also be an important consideration as U.S. emission standards are tightened further. In addition to the increased production costs associated with the application of these combined after-treatment technologies, fuel efficiency penalties arise due to increased back-pressure and energy required for system regeneration. Optimization of these systems will require fundamental understanding of all governing mechanisms.

The way in which soot particles interact with substrate microstructures during filtration determines

removal efficiency and back-pressure. Overall back-pressure can also be minimized by prompt and efficient oxidation of soot trapped in the filter, which involves pore-scale transport of heat and active gaseous species such as NO_2. The project described in this report seeks to elucidate pore-scale mechanisms involved in DPF operation in order to promote more effective and reliable DPF devices with a minimum negative impact on fuel economy.

Approach

A computer model has been developed to predict the nature and location of soot deposits within porous filter substrates by simulating the flight and deposition of individual soot particles. The lattice-Boltzmann method is used to solve for the flow field of exhaust through the substrate microstructure as soot deposits form. Figure 1 depicts simulated soot deposits in a small section of a cordierite filter wall (exhaust flows downward through wall along the y axis). Simulations of various DPF substrates, including cordierite and silicon carbide, show how the substrate microstructures affect filtration performance. The micro-scale model also includes the transport of active gaseous species and chemical reactions associated with soot combustion and catalytic oxidation of NO to NO_2. Studies were conducted to examine the effect of substrate microstructure and catalyst location on net rates of soot oxidation.

Experimental methods have been developed to observe the loading and regeneration of external surfaces of individual channels cut from full DPF monoliths. Catalyzed and uncatayzed channels were loaded and regenerated side-by-side and monitored using visible and infrared cameras. Techniques have also been developed to measure fundamental parameters, such as filter wall permeability and channel flow resistance, which are necessary for accurate modeling of DPF performance at the device scale. Individual filter walls were loaded with aerosolized salt particles having a controlled size distribution. Unlike soot, many salts are easily distinguished from filter substrates using techniques such as energy dispersive X-ray spectroscopy (EDS). This may allow experimental characterization of aerosol penetration into filter walls, which has been difficult up to this point.

FIGURE 1. Predicted Soot Deposits in a Cordierite Filter Wall

Results

PNNL participates in CLEERS teleconferences, which occur at intervals of approximately one month, and coordinates the teleconferences which focus on DPF and selective catalytic reduction technology. Participants include original equipment manufacturers, universities, and other national laboratories. Representation by industry and academia has been consistently good, and presentations by various special speakers have sparked helpful and informative discussions on a variety of topics. One benefit of hosting the monthly meeting has been the opportunity to receive continual feedback on the direction of specific CLEERS research activities at PNNL.

Previously developed tools for simulation of DPF performance were applied in various ways over the course of FY 2007 to improve understanding of important phenomena. One example is a study of the effect of particle size on filtration behavior. Figure 2 illustrates the differences in soot deposit consistency and location which can arise as a result of varying particle sizes. Figure 3 shows the predicted relationship between particle size and initial filtration efficiency for a cordierite DPF substrate similar to Corning's Duratrap RC. Large particles are more readily removed from the exhaust by the mechanisms of interception and inertia,

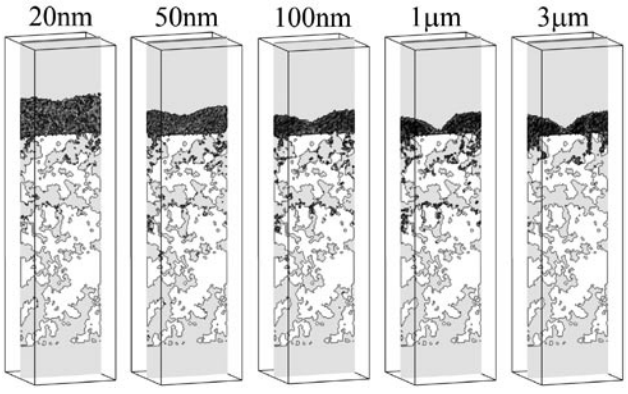

FIGURE 2. Effects of Particle Size on Deposit Location and Structure

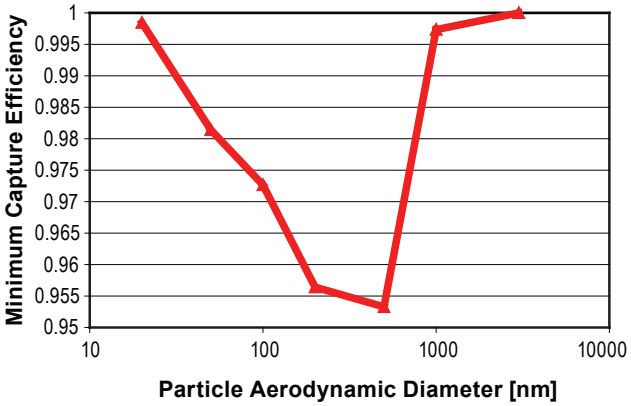

FIGURE 3. Relationship Between Particle Size and Initial Filtration Efficiency

while smaller particles are more readily removed by diffusion. This leads to a minimum efficiency at some intermediate particle size [1]. Predicted minimum removal efficiency for particle diameters lying between 100 nm and 1 µm agrees with experimental data for other types of aerosol filters [1] and other DPF substrates in particular [2].

A key addition to the micro-scale filtration model in FY 2007 was the inclusion of catalytic chemistry for conversion between NO and NO_2, which exist together in some ratio in engine-out exhaust. Soot can be oxidized by O_2 at high temperatures, but the reaction rate drops off rapidly as the temperature decreases. At moderate operating temperatures, the rate of oxidation by NO_2 (resulting in its conversion to NO) is many times faster than by O_2. Placing an oxidation catalyst upstream of the DPF can shift the NOx ratio toward NO_2 while also consuming hydrocarbons and carbon monoxide. Placing similar catalysts within the DPF itself, however, raises the possibility of a given molecule of NOx being used more than once for soot oxidation. How many times the average molecule can be 'recycled' and how this process might be affected by the substrate microstructure are key questions for DPF optimization.

To address these questions, the kinetic model for NOx oxidation presented by Mulla and associates [3] was implemented in the micro-scale simulation program. Soot oxidation kinetics were calculated using the model presented by Messerer and associates [4]. A number of catalyzed soot oxidation simulations were performed both with simple, idealized geometries and with pore geometries corresponding actual DPF substrates. One study examined the effect of catalyst placement on soot oxidation and NOx recycle. In flow-through catalytic devices (such as 3-way catalytic converters used with gasoline engines) most of the precious metal catalyst is typically placed on a base-metal washcoat layer on the substrate wall surface. This has also been the method employed in many catalyzed DPF prototypes. Advanced coating techniques may allow arbitrary placement of various catalysts within the porous substrate microstructure.

Figure 4 shows NO_2 concentration fields resulting from the placement of the same amount of platinum (equivalent to 120 g/ft^3 loading) either evenly throughout the filter wall (Figure 4a) or concentrated in the quarter of wall thickness closer to the upstream face (Figure 4b). It can be seen that the NO_2 concentration in the second case peaks within the porous wall, rather than at the down-stream face. This results in higher average NO_2 concentrations where more of the soot is located and overall soot oxidation rates roughly 30% higher than the case where platinum was distributed evenly throughout the wall. Placing the same amount of platinum in the top eighth of the substrate wall resulted in an overall oxidation rate approximately 39% higher than the uniformly distributed case. These results suggest that concentrating precious metal oxidation catalysts near the loaded surface results in higher soot oxidation rates. This is because the porous filter wall acts to some degree as a barrier to diffusion of active gaseous species generated downstream back to the loaded wall surface. This effect could actually be an advantage for multi-function catalytic systems designed to treat particulates, hydrocarbons, CO, and NOx in a single device, which may involve different catalyst systems on the upstream and downstream faces of a filter wall. In the case where Pt was distributed throughout the wall, the total soot oxidation rate was

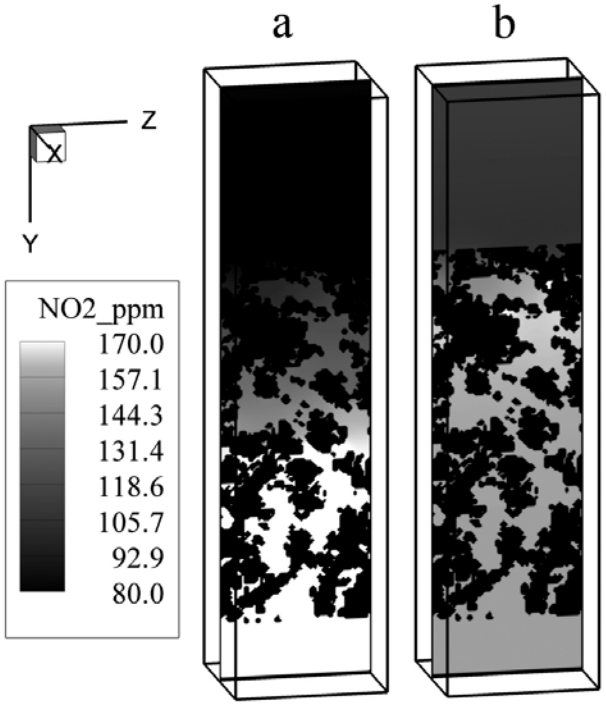

FIGURE 4. Effect of Catalyst Placement on NO_2 Concentration Profiles

nevertheless almost double that in an un-catalyzed wall under the same conditions. Soot oxidation rates were also enhanced at critical pore throats deep within the substrate. Since thick base-metal washcoats at the upstream filter wall surface tend to significantly increase the overall filter back-pressure, it is possible that advanced coating systems making use of more substrate surface area could still prove advantageous in some cases.

A number of experiments have been carried out to support modeling efforts and help provide fundamental understanding of filtration and regeneration mechanisms. Individual channels cut from Pt catalyzed and un-catalyzed DPFs were loaded on their exterior surfaces and regenerated side-by-side in the same exhaust stream. Observations with an infra-red camera showed slightly higher surface temperatures in the catalyzed sample, possibly indicating somewhat higher oxidation rates. The catalyst washcoat led to higher overall back-pressures under all conditions tested. However, at several engine loads, the differential pressure across the loaded catalyzed sample showed a marked downward trend, while that for the uncatalyzed sample held steady. This suggests a significant enhancement in the soot oxidation rate.

Individual filter walls were also cut from several types of DPF monoliths and mounted in a plastic manifold which allowed measurement of flow resistance at various gas velocities. The filter walls were then loaded with aerosolized salt particles. The salt particles are nearly spherical, lacking the complex, fractal structure which complicates fundamental filtration studies using soot particles. The size distribution of the salt particles may be manipulated to conduct parametric studies. Unlike soot, some salts are easily distinguished from filter substrates using EDS. Figure 5 shows an electron micrograph of a fractured filter wall which

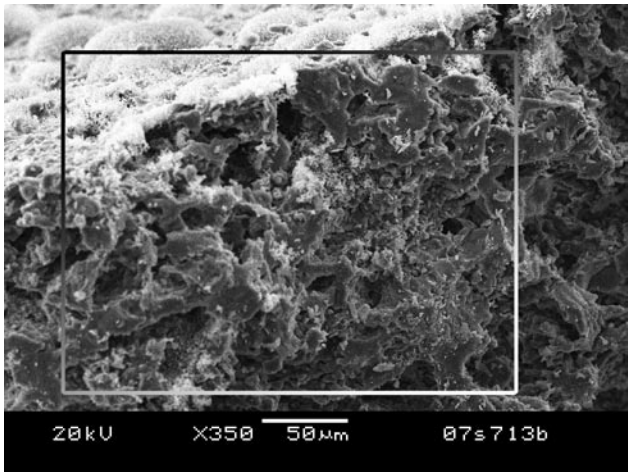

FIGURE 5. SEM Image of a Fractured Filter Wall Loaded with Ammonium Sulfate Particles

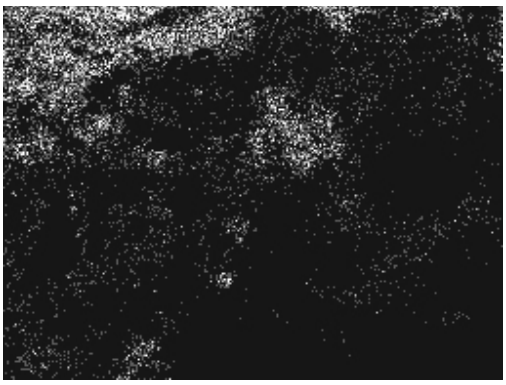

FIGURE 6. EDS Map of Sulfur in the Loaded Wall Cross-Section

has been loaded with ammonium sulfate particles. The loaded surface of the wall is visible in the upper left-hand corner. Figure 6 shows a corresponding EDS map of sulfur in the filter wall cross-section. This technique may allow quantitative measurement of aerosol penetration into the filter wall, which can then be directly compared to model predictions.

Conclusions

- Simulations demonstrate that particle size can have a dramatic effect on backpressure, filter efficiency, and the location and morphology of deposits.
- NOx oxidation catalysts have the greatest impact on soot oxidation when they are located close to the upstream filter wall face, where the majority of the soot is deposited.
- NOx oxidation catalysts distributed through the thickness of a DPF wall do, however, still enhance the overall regeneration rate, particularly increasing soot oxidation rates in critical pore throats deep within the substrate.
- Experiments demonstrate that Pt catalyzed substrates enhance the overall filter regeneration rate, but with only small observable increases in the soot surface temperature.
- Experiments with aerosolized salt particles hold promise for studying fundamental filtration mechanics, particularly the extent of particulate penetration into the filter wall.

References

1. Friedlander, S.K., *Smoke, dust, and haze : fundamentals of aerosol dynamics*. 2nd ed. Topics in chemical engineering. 2000, New York ; Oxford: Oxford University Press., 407 p.

2. Miyairi, Y., et al., *Diesel Particulate Filter (DPF) Trapping Efficiency Improvement Under No-Soot-Layer Conditions Obtained Through Pore Size Distribution Optimization.* SAE, 2006. **2006-01-1528**.

3. Mulla, S.S., et al., *Reaction of NO and O-2 to NO2 on Pt: Kinetics and catalyst deactivation.* Journal Of Catalysis, 2006. **241**(2): p. 389-399.

4. Messerer, A., R. Niessner, and U. Poschl, *Comprehensive kinetic characterization of the oxidation and gasification of model and real diesel soot by nitrogen oxides and oxygen under engine exhaust conditions: Measurement, Langmuir-Hinshelwood, and Arrhenius parameters.* Carbon, 2006. **44**(2): p. 307-324.

FY 2007 Publications/Presentations

1. Dillon, H.E., M.L. Stewart, G.D. Maupin, T.R. Gallant, C. Li, F. Mao, A. Pyzik and R. Ramanathan. 2007. *Optimizing the Advanced Ceramic Material for Diesel Particulate Filter Applications*. SAE WORLD CONGRESS, Detroit, MI. SAE 2007. **2007-01-1124**.

2. Dillon, H.E., G.D. Maupin, N.T. Saenz, S. Carlson and T.R. Gallant. 2007. *Visualization Techniques for Single Channel DPF Systems*. SAE WORLD CONGRESS, Detroit, MI. SAE 2007. **2007-01-1126**.

3. Male, J. 2007. *Path to 4-way Diesel Emissions Systems*. 10th DOE Crosscut Workshop on Lean Emissions Reduction Simulation, May 1st-3rd, 2007, Dearborn, MI.

4. Saenz, N., H.E. Dillon, S. Carlson and G.D. Maupin. *Advanced Metallographic Techniques Applied to Diesel Particulate Filters.* Microscopy Today, September 2007. **15**(5): p. 44.

5. Stewart, M.L. 2007. *Micro-Scale Simulations of Diesel Soot Oxidation*. 10th DOE Crosscut Workshop on Lean Emissions Reduction Simulation, May 1st–3rd, 2007, Dearborn, MI.

6. Stewart, M.L. 2007. *Micro-scale Simulation of Soot Filtration with ACM DPFs*. Dow Automotive Technical Center, May 3rd, 2007, Auburn Hills, MI.

Special Recognitions & Awards/Patents Issued

1. First Place Winner of the "DuBose-Crouse Award for Unique, Unusual and New Techniques in Microscopy"; 40th Annual IMS/ASM 2007 International Meeting, Fort Lauderdale, FL: Saenz, N., H.E. Dillon, S. Carlson and G.D. Maupin. *Advanced Meatallographic Techniques Applied to Diesel Particulate Filters.*

II.B.12 Innovative Emission Control Renewal

Eugene Gonze
General Motors Corporation
Powertrain Division
895 Joslyn Avenue
Pontiac, MI 48340-2920

DOE Technology Development Manager:
Ken Howden

NETL Project Manager: Aaron Yocum

Subcontractors:
HRL Laboratories, LLC – Malibu, CA
Michigan Technological University – Houghton, MI

Objectives

Develop a robust particulate matter (PM) regeneration technique that that allows low engine exhaust temperature regeneration while minimizing:

- Impact on engine operation
- Power consumption
- Incremental cost

Accomplishments

- An external heating technology has been developed that initiates low temperature diesel particulate filter (DPF) regeneration.
- This technology reduces the fuel required for an engine-initiated DPF regeneration as much as tenfold.
- A regeneration architecture and strategy has been developed.

Future Directions

This project was completed in 2007. Continued internal development is being considered. The issues which need further work are:

- Long-term system durability studies are needed.
- Further refinements of the external heater design are needed to optimize the system efficiency.
- Evaluation of DPF materials used with the external heating technology are needed to ensure DPF durability.

Introduction

Diesel and some lean-burn engines generate particulates that exceed regulated standards. However, the lean combustion cycles of these engines also increase overall fuel efficiency. Technologies such as particulate filters are aimed at enabling the use of lean-burn engines, while also ensuring that particulate emissions remain within acceptable limits. The volume of engine-out particulates is sufficiently large that these filters need periodic cleaning (regeneration) to maintain filtration efficiency and keep the device backpressure to a minimum. The commonly used approaches to initiate trap regeneration requires either engine exhaust temperatures of approximately 600+ °C or fuel injection into a diesel oxidation catalyst to reach soot oxidation temperature within the DPF. Both approaches carry a substantial fuel economy penalty for their use. The goal of this project was to develop a low-temperature, robust PM filter regeneration technology that minimizes impacts on fuel consumption and engine operation.

Approach

This project evaluated external heating technologies that could be used to initiate trap regeneration at low engine exhaust temperatures. Two of these technologies were evaluated at both laboratory and engine scales. Both were effective in initiating DPF regeneration. One was selected for additional development based on the lower overall energy consumption. Additional development included:

- Construction of full scale devices.
- Installation of the devices in vehicles for chassis dynamometer testing.
- Determination/evaluation of regeneration conditions with a minimum of added external energy.
- Development of a driving cycle regeneration strategy.

These tasks were all completed within this project.

Results

The externally heated DPF was installed on a fully instrumented vehicle with a complete aftertreatment system. The external heating and the vehicle operation were varied, refined and tested to:

- Develop a fuel efficient DPF regeneration technique.
- Develop a control strategy designed to maintain efficient regeneration under “real world” driving.

- Refine the external heater designs to minimize loads on vehicle.
- Integrate the heater to reduce thermal stress forces within the particulate filter.
- Develop a DPF regeneration strategy to minimize the impact on other exhaust aftertreatment devices.

This approach was successful in developing a low-temperature, externally heated regeneration technology that has a very low fuel economy penalty.

Figure 1 contains a plot of the rapid progress of the DPF regeneration enabled by the use of an external heat source.

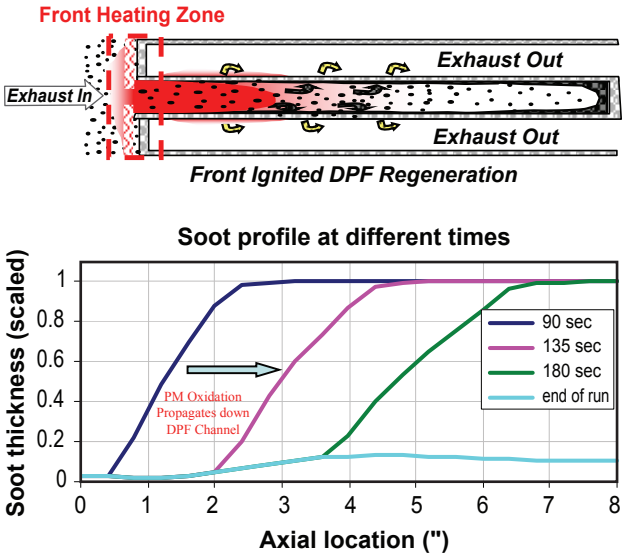

FIGURE 1. Rapid Progress of the DPF Regeneration Enabled by the Use of an External Heat Source

Conclusions

The project team developed a regeneration technique using the downselected external heating technology that provides effective filter regeneration (soot removal) with as much as a tenfold reduction in fuel consumption as compared to existing regeneration techniques currently in use on production vehicles. Major benefits of this technology also include:

- Low tailpipe temperature during the regeneration cycle.
- The ability to complete regeneration cycles in city and under other low-speed driving conditions.
- Regeneration times that are significantly lower than existing technologies. This fact provides the secondary benefit that regeneration has minimal impacts on other important exhaust aftertreatment technologies.

This project has developed a very promising technique for the regeneration of DPFs. The successful deployment of this technology has the potential to reduce the fuel consumed during regeneration cycles as much as tenfold over the prevailing existing approach. Additional work is underway that seeks to optimize the efficiency of the heating system used. Research aimed at expanding the operating range of the developed technique is also ongoing. Finally, research aimed at ensuring the reliability of DPF materials used in the application of this technique has also been initiated.

Special Recognitions & Awards/Patents Issued

The project has submitted over 40 invention disclosures related to this project. Numerous patent applications are in process.

II.B.13 Discovery of New NOx Reduction Catalysts for CIDI Engines Using Combinatorial Techniques

Richard J. Blint (Primary Contact, GM), Gerald Koermer (BASF Corporation, formerly Engelhard), George Fitzgerald (Accelrys, Inc.)
General Motors Corporation
Research and Development Center
Mail Code 480-106-185
30500 Mound Road
Warren, MI 48090-9055

DOE Technology Development Manager: Ken Howden

NETL Project Manager: Carl Maronde

Subcontractors:
BASF, Iselin, NJ
Accelrys, Inc, San Diego, CA

Objectives

- Develop new NOx selective catalytic reduction (SCR) catalysts that can operate in the lean exhaust of diesel or lean gasoline engines. These catalysts can:
  - Utilize the onboard fuel as the reductant (hydrocarbon selective catalytic reduction, HC-SCR).
  - Have oxides of nitrogen (NOx) conversion activities in excess of 80%.
  - Span the operating range (e.g.; temperature and flow rate) for these lean engines.
  - Have sufficient durability and resistance to poisoning to meet the 120,000-mile standard.

Accomplishments

- Tested over 8,000 materials for NOx reduction potential since the initiation of the project and testing of materials with simulated diesel fuel is the standard.
- Detailed engine testing has evaluated conversions over the Heavy-Duty Federal Test Procedure (HDFTP), Highway Fuel Economy Test (HWFET) and US06 test cycles, sulfur poisoning and fuel effects on coking.
- Phosphorus poisoning studies have been completed.
- Specific formulations for lean gasoline applications have been developed.

Future Directions

Project was completed at the end of the 2007 calendar year.

Introduction

This GM project was initiated 8/16/02. Its goal is to develop new NOx reduction catalysts for lean combustion systems such as both light- and heavy-duty diesels and for stratified charge gasoline engines. These new catalysts are needed to enable these engines to meet the Tier II NOx standards for the North American markets that are being phased in over the time period between 2007 and 2010.

Approach

HC-SCR is the technology that is the focus of development of the new catalytic materials. The approach is to use high throughput technology to develop the new materials (BASF), informatics to mine the data arising from the fast throughput experimentation (Accelrys and GM), classic reactor evaluation to determine the suitability of the new materials for automotive applications (GM) and engine dynamometer testing of full size catalysts.

Results

To date at BASF, over 8,000 new materials have been evaluated on the discovery system since the initiation of the project. Coatings and loadings from materials downselected from the discovery approach have been evaluated on the GM reactor for the effects of poisoning (sulfur and phosphorus poisoning), propensity to coke, thermal aging and potential control strategies. Additionally a wide range of engine dynamometer studies were completed to evaluate the potential of several of these catalysts for production applications.

This technology has been evaluated on the heavy-duty (greater than 18,000 pounds GVW) dynamometer certification cycles which include the HDFTP and the supplementary emissions test (SET). The aftertreatment configuration for this system is a diesel oxidation catalyst (DOC), followed by a fuel injector and then the HC-SCR catalyst. The heavy-duty certification requires NOx/CO/PM/NMHC = 0.2/15.5/0.01/0.14 (g/hp-hr). This is the only certification procedure for vehicles with gross vehicle weight greater than 14,000 pounds

and the engine exhaust is typically hotter for engine dynamometer certification than the chassis certifications. This work demonstrates some issues that will arise for the application of this technology to production drivetrains. The low volatility of diesel fuel makes it difficult to start dosing at temperatures much lower than 300ºC; consequently those initial portions of the test cycles before the exhaust temperature has reached 300ºC and idle conditions will not have reductant supplied to the HC-SCR catalyst. No rapid heat-up strategy was employed for this sequence of tests resulting in NOx conversions for the HDFTP of approximately 60%. For this particular engine, NOx conversions of 60% are not sufficient to reach the 2010 NOx emission standard. It is apparent from the HDFTP test cycles that much of the NOx emissions are arising from the early portions of the test before fuel dosing can be initiated. And so depending on the engine characteristics, a rapid heat-up strategy will most likely have to be employed to reach the emission standards. The SET certification test showed overall NOx conversions of about 65%. Idle (see Figure 1) had low conversions (on the order of 20%) because the exhaust gas temperatures were too low to dose. Four points of the SET test had NOx conversions in excess of 90%, five other points had conversions of 75% to 90% and the remaining three points were 45, 49 and 57% (A75, B100 and C100). Tuning of the engine operating conditions can increase the conversions at those SET points with low conversions. These results give indications of how this technology would perform on the emission standards for a 2010 heavy-duty diesel production application.

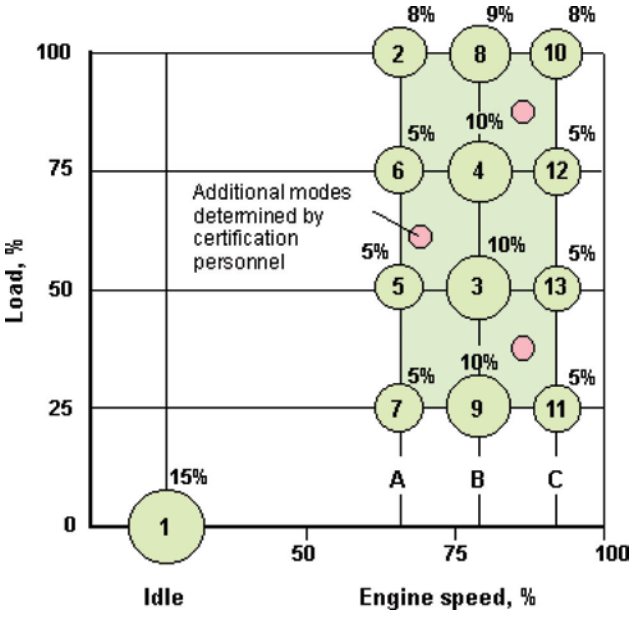

FIGURE 1. Description of the Steady-State Dynamometer Points for the SET Test for Heavy-Duty Diesel Certification

The durability requirement for 2010 production catalysts is 120,000 miles (light-duty) or 450,000 miles (heavy-duty). No long-term engine durability studies were included in this project; however, studies of poisoning and aging for the downselected catalysts were included. All catalysts were hydrothermally degreened at 650ºC for 16 hours before use. Phosphorous, sulfur and carbon are the common poisoning materials. Microprobe analysis of washcoat from an engine-tested full size catalyst piece shows accumulation of phosphorus on the top of the washcoat (Figures 2 and 3). This is a common finding and does not indicate excessive phosphorous poisoning. In addition, a systematic phosphorous loading and activity study was undertaken to provide a quantitative measure of phosphorous poisoning. This lab study also indicated that the catalyst was not especially sensitive to phosphorus poisoning. From this work and activity studies we conclude that phosphorous poisoning is not a major activity loss mechanism for these catalytic materials. Sulfur is found to cause a slow deactivation of the catalyst; however, the catalyst can be regenerated from that deactivation. The sulfur regeneration conditions are much less demanding than the common diesel particulate filter regeneration conditions. Hydrocarbon deactivation of these catalysts can be appreciable depending on temperature and exhaust gas composition. Figure 4 shows examples of very long exposure of the catalyst system to various hydrocarbons in diesel exhaust as a function temperature and exhaust. These exposure times are well in excess of any steady-state engine condition that is likely to be encountered. As can be seen, m-xylene is not a good reductant under most conditions. Long chain alkanes are typically good reductants, but do tend to slowly poison the catalyst surface at temperatures below 350ºC. At temperatures above 400ºC, most of the alkanes do not poison and typically regenerate. Ethanol appears to be a good reductant even at low temperature. In all cases the catalyst is easily regenerable from deactivation from these hydrocarbons.

Conclusions

The encouraging conversion results on the dyno test stand to a large degree have moved this project from new materials discovery for diesel NOx reduction into a product development phase. Much of the discovery work during the latter portions of FY 2006 was used to develop additives to address issues that could arise in applying this technology. Some of the discovery work has been applied to discovering active catalytic materials for lean gasoline NOx reduction.

Evaluation of the effects of sulfur poisoning, coking, phosphorous poisoning and thermal aging at this point do not seem to be a durability barrier for the use of these materials in automotive applications.

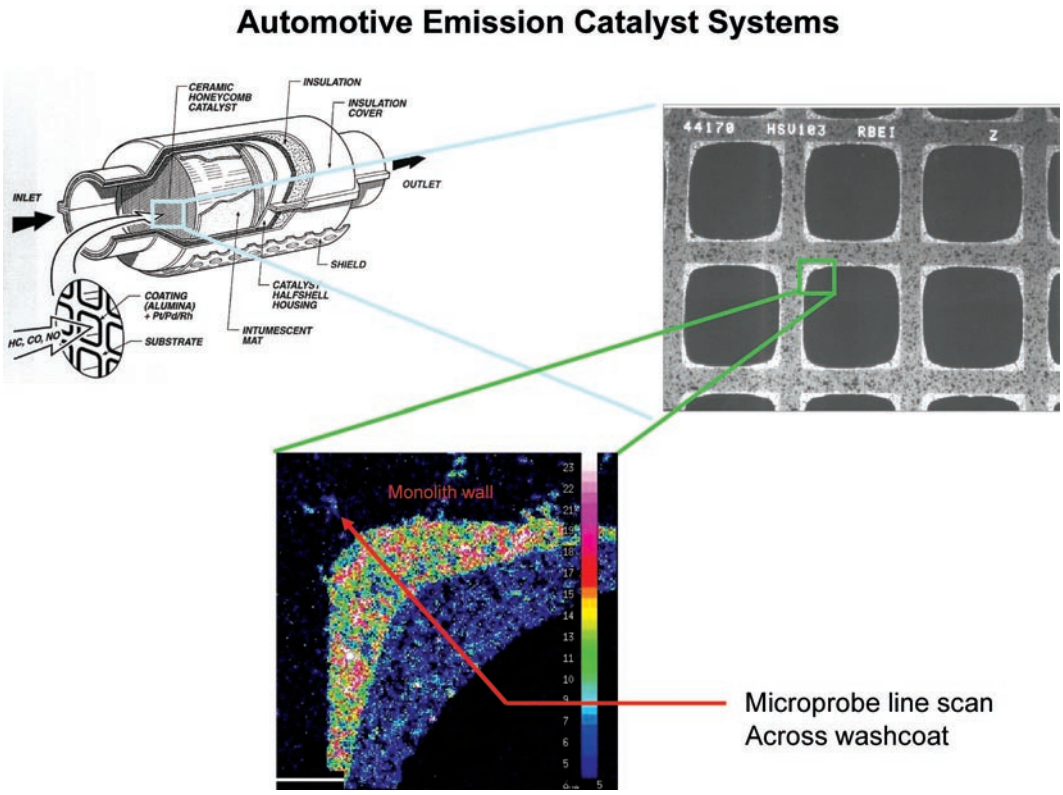

FIGURE 2. Schematic of the Monolith Area where Three Scans Across the Washcoat of an Engine-Tested Catalyst were Analyzed Using Electron Microprobe

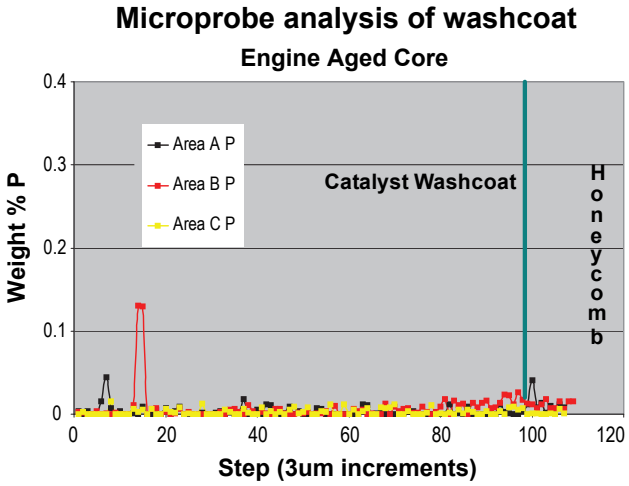

FIGURE 3. Materials Profiles of Phosphorous (P) as a Function of Linear Position for Scans Described in Figure 2

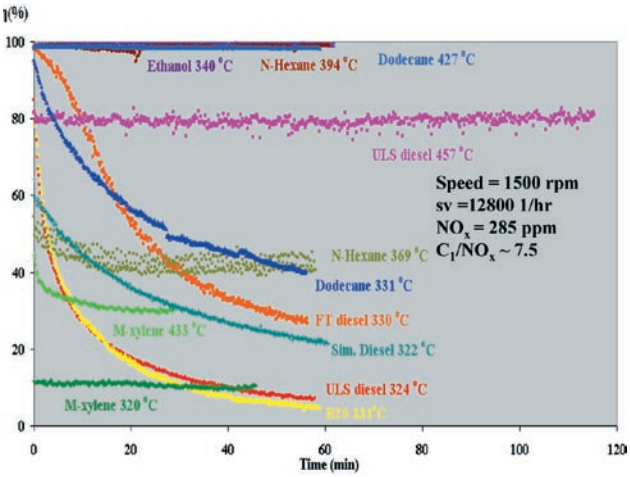

FIGURE 4. Description of NOx conversion (ή) as a function of time using a series of vaporized reductants. ULS indicates ultra-low sulfur fuel, B20 is a standard biodiesel fuel, FT indicates Fischer-Tropsch diesel fuel, and sim-diesel is the model mixture (67 vol.% n-dodecane, 33 vol.% m-xylene) used at GM.

This project is planned to complete in calendar 2007 so that refinements in the active catalytic materials will assist in developing the feasibility analysis planned for the end of the project.

FY 2007 Presentations

1. CLEERS workshop, May 1–3, 2007, Dearborn, MI.
2. DOE Peer review, June 18–19, 2007, Washington, DC.
3. Fall ACS meeting, August 19–23, 2007, Boston, MA.

II. ADVANCED COMBUSTION AND EMISSION CONTROL RESEARCH FOR HIGH-EFFICIENCY ENGINES

C. Critical Enabling Technologies

II.C.1 Variable Valve Actuation for Advanced Mode Diesel Combustion

Jeffrey Gutterman P.E.
Delphi Corporation
5500 West Henrietta Rd.
PO Box 20366
Rochester, NY 14602-0366

DOE Technology Development Manager:
Roland Gravel

NETL Project Manager: Jason Conley

Subcontractor:
Electricore Inc., Valencia, CA

Objectives

- Develop an optimal, cost-effective, variable valve actuation (VVA) system for advanced low-temperature diesel combustion processes.
- Design and model alternative mechanical approaches and down-select for optimum design.
- Build and demonstrate a mechanism capable of application on running engines.

Accomplishments

- Confirmation that a single cam design did not have the required control flexibility to meet requirements.
- Three dual cam design concepts were developed and modeled.
- A dual cam design was selected from concept designs and all dynamic analyses were completed.
- An original equipment manufacturer (OEM) confirmed that the proposed dual cam design is a cost-effective and production feasible design.
- Package size was reduced to require minimal change to OEM engine envelope.
- Advanced VVA math-based design process was introduced and design tools are now available for future modeling work.
- All of critical design analyses for high stress subcomponents including springs, bearings, gears and output rocker cam were completed.
- The mechanical actuator (cam phaser) development engineering work was completed and prints prepared.
- Cam phaser controller with proportional, integral, and derivative control capability built and tested.
- A single-cylinder device was built and installed on a free running lab engine.

Future Directions

- Recent continuously variable valve duration (CVVD) assembly finite element analysis (FEA) analysis results indicate the potential for output rocker cam pivot shaft deformation. Design enhancements will be integrated to improve stiffness and eliminate the variation.
- OEM engine in-cylinder air flow analysis using the Star-CD computational fluid dynamics (CFD) program is underway. Further analysis of the effect of the CVVD modified valve lift on air charge efficiency and swirl, will establish benefits of CVVD.
- Accelerated durability testing of mechanism.
- Dynamometer testing while monitoring exhaust emissions on running engines will verify benefits predicted by CFD modeling.

Introduction

Our objective is to develop and demonstrate an optimal cost-effective diesel VVA system for advanced, low-temperature combustion processes. Flexible control of the valve event is a significant enabler for advanced mode diesel combustion (AMDC). It is an essential factor in the control of the species and thermodynamic conditions for the combustion cycle. VVA is expected to enable expanding the operating load and speed range of AMDC. It is also a potential tool for enhancing the effectiveness of aftertreatment catalysts. Thus, viable VVA technology is expected to help in reducing the penalty in fuel consumption related to extremely low emission standards.

Delphi Corporation has major manufacturing and product development and applied R&D expertise in thee valvetrain area. Historical R&D experience included the development of fully variable electro-hydraulic valvetrain on research engines as well as several generations of mechanical VVA for gasoline systems. A new mechanism was taken from concept stage through design, modeling, build and bench testing on a single-cylinder engine test stand.

Approach

Working with an OEM was critical to determine the mechanism motion requirement and system specifications. To speed development, significant time was spent using advanced design tools and simulations before building the actual hardware. After modeling more than 200 variations of the mechanism it was determined that the single cam design did not have enough flexibility to satisfy three critical OEM requirements simultaneously, (maximum valve lift variation, intake valve opening timing and valve closing duration), and a new approach would be necessary.

Internal design reviews, including three with the OEM, resulted in a dual cam design that had the flexibility to meet all motion requirements. The second cam added complexity to the mechanism however the cost was offset by the simplification of the actuator subsystem.

Once the design was dynamically simulated and the FEA was completed, single-cylinder hardware was built and installed on a free-running engine test stand to verify predicted performance.

Results

Critical performance parameters were supplied by an OEM that had to be met before the mechanism could be applied to their engine. The previously detailed GEMS design was a single cam device that appeared to have the potential to meet all the requirements. However, after more than 200 design iterations it became apparent that it was not possible to simultaneously meet all three critical performance requirements. The OEM wanted the intake valve opening timing to remain constant while the intake valve closing was varied more than 60 crank degrees (30 cam degrees). Simultaneously, they wanted the maximum lift to vary no more than 0.5 mm over the same range. Figure 1 demonstrates a typical family of curves based upon the maximum and minimum limit valve lifts determined by the OEM.

Maximum valve lift varied by as much as 1 mm over the entire range of valve timing thus exceeding the OEM's requirement of less than 0.5 mm. Alternative design approaches were developed to insure that the base mechanism had no variation in maximum valve lift over the entire range.

Three design approaches were proposed and detailed as shown in Figure 2. Multiple design reviews were held and after evaluating the merits and demerits of each configuration, Design "A" was selected as the preferred approach (Figure 3). While a second cam was added, the mechanism allowed us to eliminate the electric motor actuator required for the GEMS mechanism. Figure 4 shows an isometric view of the Design "A" herein called CVVD.

Numerous design reviews were held with an OEM to integrate the design into their existing engine. The

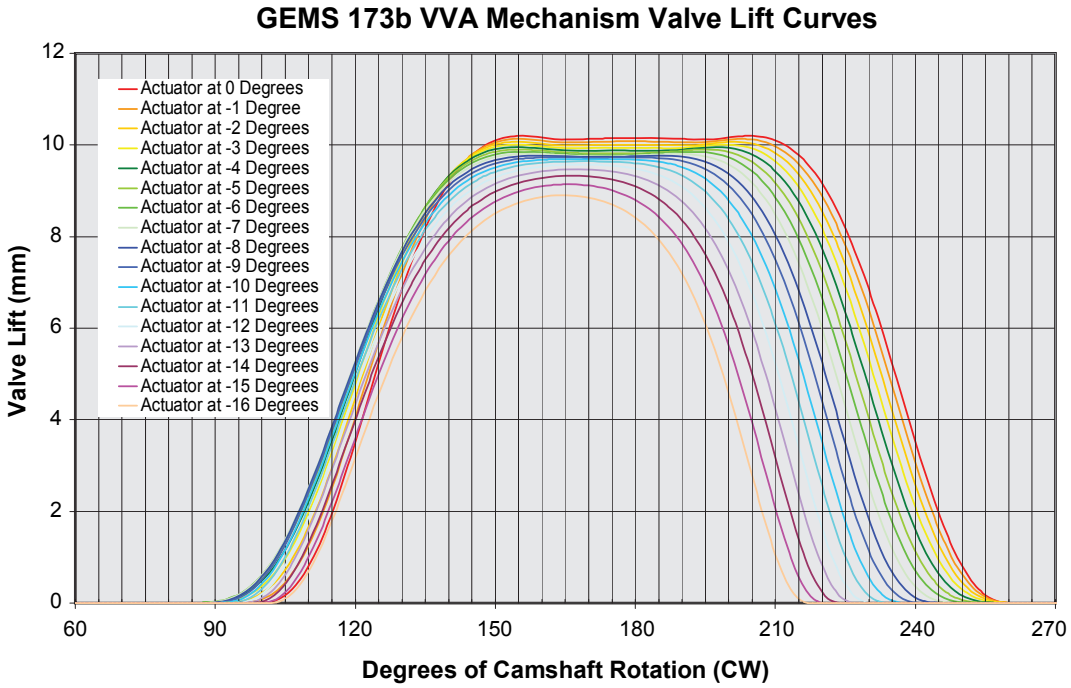

FIGURE 1. Typical Family of Lift Curves

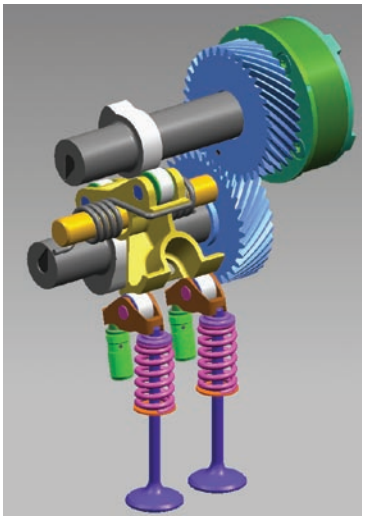

Design "A"

- Easy attachment of cam phaser
- Balanced rocker motion with easy roller bearing application

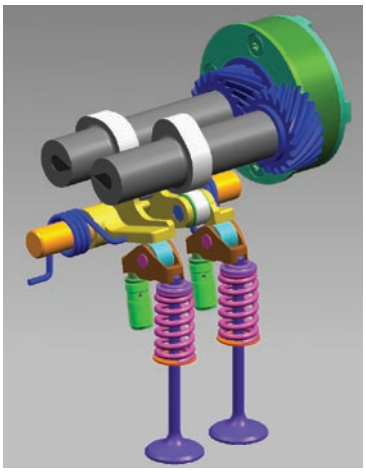

Design "B"

- Low packaging height
- Can avoid costly output cam grinding
- Concern about insufficient contact length on output cam

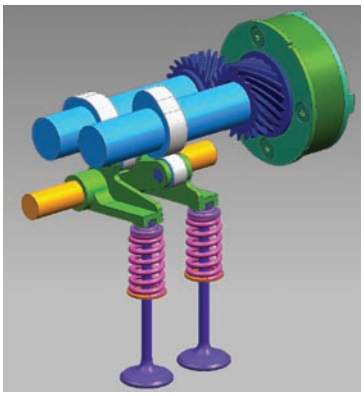

Design "C"

- Most cost effective design if OEM plans to re-design the cylinder head
- HEA can be added between rocker arm and valve stem

FIGURE 2. Representations of Three Design Approaches

CVVD was then integrated into the OEM's supplied cylinder head drawings.

FEA modeling with ABAQUS verified no areas of exceedingly high stress and suggested regions that could be further optimized for reduced weight and size. A typical run is shown in Figure 5.

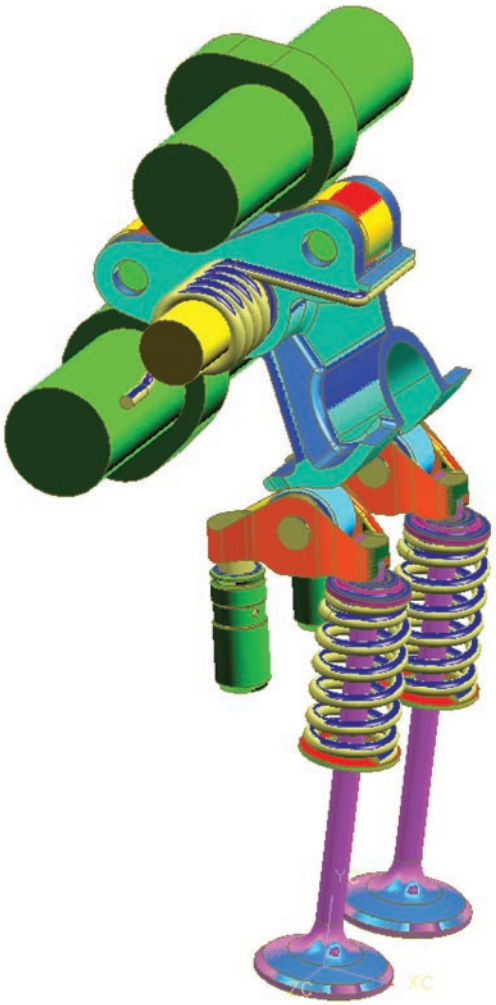

FIGURE 3. Selected Design "A" CVVD

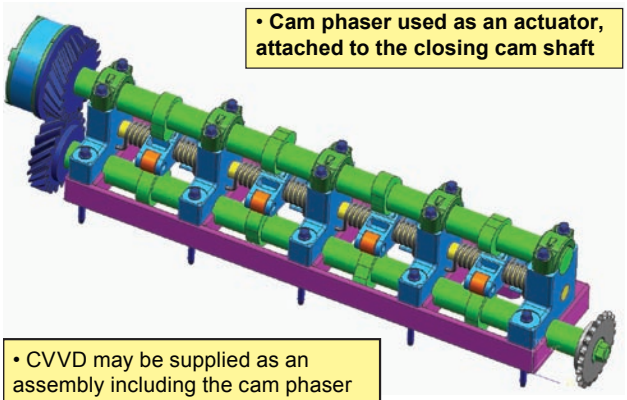

FIGURE 4. Isometric View of Valvetrain Carrier Assembly with CVVD

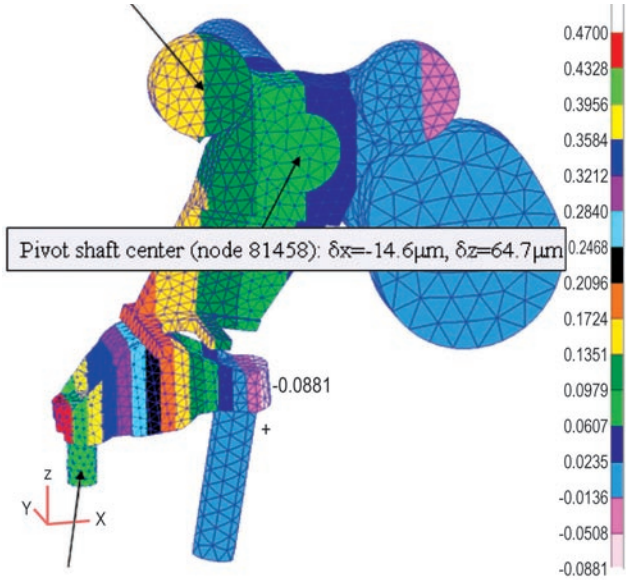

FIGURE 5. ABAQUS FEA Results for Pivot Shaft Deflection Parallel to the Valve (Z-Direction in the Figure)

ADAMS simulations were run on all configurations to assure that no dynamic forces exceeded the design parameters while operating at high engine speeds. A typical run is shown in Figure 6 indicating valve displacement, velocity, and accelerations at 3,000 engine RPM.

Once all modeling was completed the components were detailed and hardware built.

Hardware was then installed on the engine stand and is now in the process of full dynamic testing at varying speeds and loads utilizing a proven electro-hydraulic actuation system based upon current cam phasing technology now in production (Figure 7).

Conclusions

- All Phase I (Concept Selection) and Phase II (Design) objectives have been met.
- Math models were completed and evaluated before building test hardware to shorten the development process and produce an optimized design.
- Single-cylinder hardware was built and tested on a free-running engine and measured results matched the performance predicted by dynamic models.
- The selected design is suitable for engine application and affords the capabilities specified by the OEM.

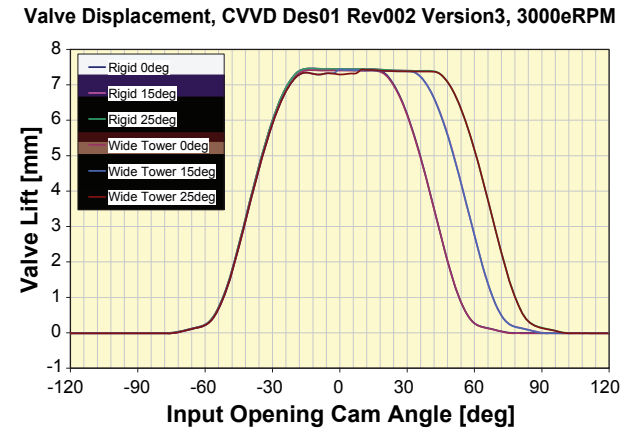

(a) Valve Lift, 3000eRPM

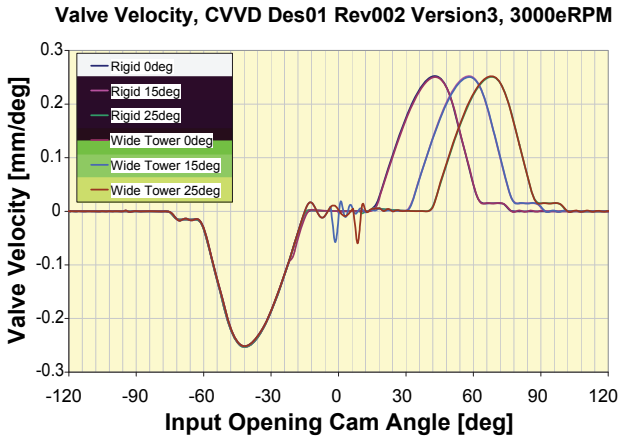

(b) Valve Velocity, 3000eRPM

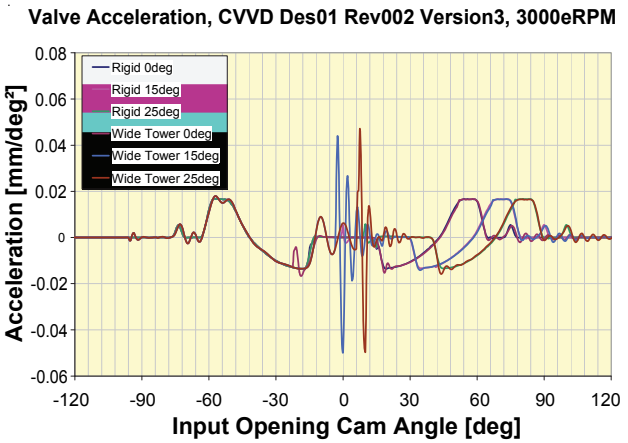

(c) Acceleration, 3000eRPM

FIGURE 6. ADAMS Valve Dynamics Modeling Indicating Displacements, Velocity And Acceleration for the Rigid Pivot Shaft

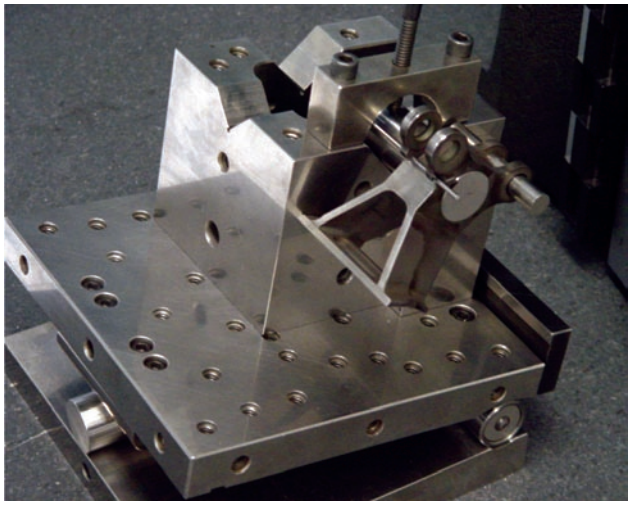

FIGURE 7. CVVD Undergoing Final Inspection

FY 2007 Publications/Presentations

1. DOE Semi-Mega Merit Review.
2. Four design reviews held with a domestic OEM.
3. Design reviews held with three overseas OEMs.

Special Recognitions & Awards/Patents Issued

Provisional Patents submitted:

1. System for Continuously Varying Engine Valve Duration.
2. Continuously Variable Valve Actuation System.
3. Electro-hydraulically actuated Variable Valve Duration System.

II.C.2 Variable Compression Ratio Engine

Charles Mendler
Envera LLC
7 Millside Lane
Mill Valley, CA 94941

DOE Technology Development Manager:
Roland Gravel

NETL Project Manager: Jason Conley

Objective

Phase I

- Design, build and bench-test a proof-of-concept variable compression ratio (VCR) actuator system.
- Optimize the actuator system where practical within the scope of Phase I funding.

Phase II

- Optimize the actuator hydro-mechanical design and its control system.
- Installation of existing VCR engine in test vehicle.
- Test the VCR actuator system in a test vehicle and demonstrate low-cost, fast-response and mass production practicality.

Accomplishments

- Hydraulic pressures in the actuator system were reduced by 86% through system optimization. The reduction in pressure significantly relaxes the demands that will be placed on the hydraulic system and enables cost to be reduced.
- A test rig was designed and built for evaluating actuator response. Test results indicate that compression ratio can be reduced from 18:1 to 8.5:1 in ~0.35 seconds, and increased from 8.5:1 to 18:1 in ~0.70 seconds. On average, 0.074 seconds is projected to elapse for each point increase in compression ratio.

Future Directions

- Optimize the hydro-mechanical system for improved performance and manufacturability.
- Installation of existing/optimized VCR engine in test vehicle.
- Test the VCR actuator system in a test vehicle and demonstrate low-cost, fast-response and mass production practicality.

VCR Overview

Prior analysis and hardware testing has shown that VCR engine technology can improve passenger car fuel economy by about 30% [1-7]. New analysis conducted by Envera indicates that VCR technology can provide substantively larger benefits for many light-duty trucks and sport utility vehicles. The analysis indicates that fuel economy improvements over 50% could be realized in the near term for a number of mass production light-duty vehicles.

For passenger cars, average on-road engine efficiency is significantly lower than peak engine efficiency. The efficiency of today's gasoline engines ranges from zero percent at idle up to about 35% at 40% of maximum power. Because the engine is operated most of the time at about only 10% of maximum power, actual on-road engine efficiency is only about 20%.

Efficiency can be significantly improved by using a smaller engine. Smaller engines provide better fuel economy because the engine is operating at its higher efficiency load conditions more of the time. The problem with reducing engine displacement is, of course, loss of power. Historically high mileage efficient cars have had poor acceleration. An effective method of regaining power is to use turbocharging. When turbocharging alone is used in gasoline engines, efficiency is poor at light power levels, largely canceling out the benefits of downsizing. VCR technology has two primary benefits. It provides higher efficiency at light power levels – unlike turbocharged engines that provide lower efficiency at light power levels. VCR also enables turbocharged engines to attain greater power levels. The engine can therefore be made smaller, while also providing added power – a sales plus for the car.

Envera is currently developing a VCR 4-cylinder engine. The 1.85 L engine is being designed to attain 300 horsepower (HP), or about 162 HP per liter (HP/L). The engine will attain about 38% efficiency at about 40 HP. Peak torque is expected to be about 300 ft-lb at 4,000 RPM.

The Envera 4-cylinder VCR engine has power and torque levels comparable to V8 engines currently available in a number of light-duty trucks such as the Ford F-150 pickup truck. The F-150 is one the highest sales volumes vehicles sold in North America, and is representational of many light-duty trucks sold in the United States. The vehicle is offered with a 4.6 L V-8

engine that produces 248 HP and 294 ft-lb torque. The engine is 2.5 times larger than the Envera VCR engine yet produces less power. The F-150 4.6 L engine has an efficiency of about 24% at 40 HP, which is significantly lower than the Envera VCR value of about 38% at 40 HP.

Efficiency gains are expected to be larger in light-duty trucks than in passenger cars because trucks in practice often have larger and lower performance engines. The benefit of downsizing is greater for many light-duty trucks because their engines tend to be over sized and under rated.

V-8 engines are popular and continue to be sold in high numbers based on consumer perceptions of image, durability, torque and power. Arguably, in each of those categories the VCR engine offers a more secure future commercial outlook. With respect to durability, the VCR engine has lower peak combustion pressure than diesel engines. There is no intrinsic reason that a VCR engine cannot match the durability and longevity of modern diesel engines. A 4-cylinder engine may not deliver the "tough" image that V-8 engines currently provide. Fleet operators of delivery vehicles, however, represent a very different type of customer. Companies seeking to attain cost savings and a greener image will be most interested in the fuel economy benefits provided by VCR. These same benefits will influence vehicle purchasing decisions for everyday people more and more as fuel prices rise.

Introduction

The current project effort is directed towards reducing VCR system cost and providing a fast actuator response. The technology has three main cost areas: the VCR mechanism; the actuator system for adjusting compression ratio; and the super or turbocharging hardware.

The Envera VCR mechanism comprises an eccentric carrier that holds the crankshaft of the engine. Pivoting of the eccentric carrier raises and lowers the crankshaft relative to the engine's cylinder head, and adjusts engine compression ratio. The Envera VCR eccentric carrier presently has a low cost.

A hydraulic actuator system is used to pivot the eccentric carrier. The current effort is directed towards reducing the cost of the actuator system and providing a fast actuator response. Another goal is to provide a durable compact VCR actuator design.

Envera anticipated that actuator response and cost would be optimized primarily through hydraulic control circuit system design and computer software. The results of Phase I have shown, however, that hydraulic cylinder sizing and mechanical design changes are of primary importance for attaining project and commercialization objectives. Specifically, hydro-mechanical design changes realized in Phase I have resulted in an 86% reduction in projected peak hydraulic system pressure. The lower pressure will enable a simpler more robust hydraulic control circuit system to be used. In consideration of the performance gains realized in Phase I of the initiative, work is currently focused on hydro-mechanical design, system hardware, and low-cost packaging within the crankcase. Figure 1 shows the preferred layout of the VCR system. The hydraulic cylinder is located vertically adjacent to engine cylinder bore three to provide a compact and stiff crankcase. Later in the project the optimized hardware will be procured and vehicle tested.

Approach

The current effort is directed towards the development of the actuator used for adjusting the pivot angle of the eccentric carrier. Development goals include low cost and a fast response. At the beginning of the project mechanical loading on the VCR eccentric carrier and hydraulic system were evaluated using:

ProEngineer Wildfire 2.0:	Part and mechanism assembly
MDO Extension:	Dynamic force analysis
GTPower:	Gas force on the piston (Prior data)
Origin 7.5:	Data conversion

Dynamic loads were modeled at five conditions, from 2,000 RPM 4 bar brake mean effective pressure (BMEP) to 6,000 RPM 12 bar BMEP. The 2,000 RPM

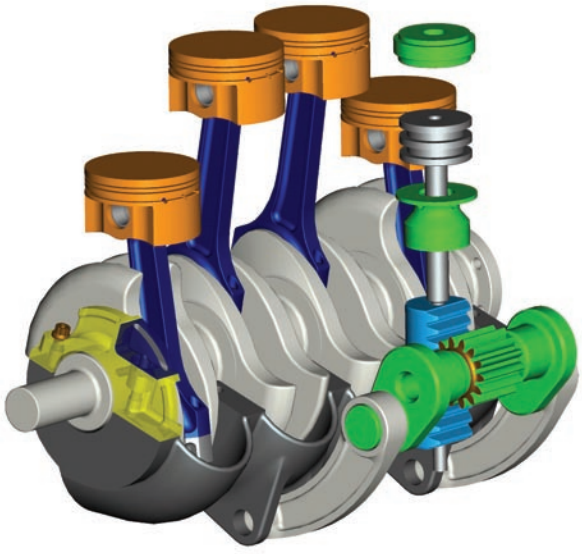

FIGURE 1. VCR actuator hardware, with hydraulic cylinder located vertically next to the 3rd engine cylinder. The hydraulic cylinder liner has been removed to show the double-acting hydraulic piston.

12 bar BMEP condition causes the highest loading on the hydraulic system of about 2,250 psi. In Phase I of the project Envera pursued reducing the size of the hydraulic pressure spikes through system optimization. Through this effort peak hydraulic pressures have now been reduced to an estimated 314 PSI, an 86 percent reduction in peak pressure. This reduction in peak pressure is a huge improvement.

In consideration of the performance gains realized through geometry optimization, work is currently focused on hydro-mechanical design, system hardware, and low-cost packaging within the crankcase. Design work is presently being done in ProEngineer Wildfire 3.0. Finite element analysis will be preformed on highly loaded components after geometrical design requirements for the VCR have been established. Later in the project the optimized hardware will be procured and vehicle tested.

Results

Hydraulic pressures in the actuator system were reduced by 86% through system optimization. The reduction in pressure significantly relaxes the demands that will be placed on the hydraulic system and enables cost to be reduced.

A test rig was designed and built for evaluating actuator response. Test results indicate that compression ratio can be reduced from 18:1 to 8.5:1 in ~0.35 seconds, and increased from 8.5:1 to 18:1 in ~0.70 seconds. On average 0.074 seconds is projected to elapse for each point increase in compression ratio.

Conclusion

- During Phase I of the project hydraulic pressures in the actuator system were reduced by 86% through system optimization. The reduction in pressure will significantly relax the demands placed on the hydraulic actuator system.
- Down-sized gasoline VCR engines having optimized combustion can provide very large fuel economy benefits, and attain low tailpipe emission levels using proven catalytic converter technology. The VCR engine can also be operated on alternative fuels such as ethanol derived from switch grass or other biomass feedstock.

References

1. Automotive Engineering International (SAAB), pages 54-57, SAE, April 2001.

2. Automotive Engineer (SAAB), page 36, December 2000.

3. Gravel, R., and Mendler, C.(DOE, ENVERA): Variable Compression Ration (VCR) Engine, OAAT Accomplishments, www.eere.energy.gov/vehiclesandfuels/pdfs/success/vcr3_29_01.pdf.

4. European Commission, Community Research, Variable Compression Ratio Technology for CO2 Reduction of Gasoline Engine Passenger Cars, europa.eu.int/comm/research/conferences/ 2002/pdf/presspacks/1-1-vcr_en.pdf.

5. Mendler, Charles (ENVERA): Variable Compression Ratio Engine, DOE FY 2003 Advanced Combustion Technologies Annual Report, US Department of Energy, 2003.

6. Mendler, Charles (ENVERA): Variable Compression Ratio Engine, DOE FY 2004 Advanced Combustion Technologies Annual Report, US Department of Energy, 2004.

7. Advanced Combustion and Emission Control Technical Roadmap for Light-Duty Powertrains, US Department of Energy, May 2006.

II.C.3 Development of Wide-Spectrum Voltammetric Sensors for Engine Exhaust NOx Measurement

Dr. Michael Vogt (Primary Contact),
Mr. Alton Reich, Dr. Marcus Ashford,
Ms. Amanda Lard
Streamline Automation, LLC
3100 Fresh Way SW
Huntsville, AL 35805

DOE Technology Development Manager:
Roland Gravel

NETL Project Manager: Aaron Yocum

Subcontractor:
University of Alabama, Tuscaloosa, AL

Objectives

- Fabricate and package voltammetric sensors to be suitable for engine exhaust testing.
- Operate the new sensors to provide nitrogen oxides (NOx) calibration data and results.
- Calibrate voltammetric sensor instrumentation with NOx results.
- Verify the operation of the instrumentation.

Accomplishments

- An all-new planar type voltammetric NOx gas sensor was designed, and all supplies for final fabrication were received.
- Existing monolithic cermet micro-arrays were modified with new solder-less leads for long-term high-temperature operation.
- A new rugged-ized stainless steel package was designed and prototyped.
- A new high-speed differencing voltammetry algorithm was engineered and employed for chemical characterization.
- Gas voltammetry was successfully applied to both commercial gas sensors (three) and to experimental gas micro-arrays (two).
- Unique electro-activity characterization was completed for NO, NO_2, CO_2, and NH_3 gases, all at typical automotive emissions concentrations. Characterization included identifying repeatable dissociation potentials for each gas, and defining broader voltammetric signatures in both low O_2 and high O_2 backgrounds.
- Multiple gas analysis from a single sensor was demonstrated (NO, NO_2, CO_2, and NH_3).
- Updates to the instrumentation design were completed, and a model for microcontroller deployment constructed.
- Collaboration relationships were established with Robert Bosch Corporation, to help construct the final sensors, and to evaluate the new NOx sensors for commercialization.

Future Directions

The immediate future work is to take the engineering lessons learned from the design of the new stainless steel package, and of high-temperature interconnects, and complete the final construction of the new planar-type NOx sensor. Robert Bosch Corporation has agreed to package these devices on a commercial assembly line, and provide the sensors for large-scale characterization in automotive test engine exhaust systems. During the next phase characterization, the differencing algorithm will be refined for real-time operation, and the identification and quantification portions of the signature processing will be integrated into that algorithm so that all processing is completed in real-time by an engine controller-type embedded computer.

Introduction

The drive to develop a NOx sensor is promoted by environmental factors - NOx gases cause problems such as smog and acid rain so many countries have passed laws to limit NOx emissions. Past R&D concluded that materials and forms of existing NOx sensors were not their failure - it was the limitations of the phenomenon and measurement technique each employed. A practical automotive NOx sensor, free of these limitations, can be successfully developed based upon gas voltammetry as its core technology. This can be done by:

- Adapting the latest thick-film voltammetric gas sensor design to a form-factor suitable for deployment in an automotive exhaust system, and
- Aerforming proof-of-principal characterization and testing on operating spark-ignition and compression-ignition engines.

Voltammetry involves sweeping an excitation potential between two electrodes and measuring the ionic current flowing through the electrolyte separating them (Figure 1). Chemicals present on the surface are forced to react, each at a potential characteristic for that chemical. The potential at which reactions occur indicates the species reacting, and the current reflects the concentration. For decades liquid voltammetry has been a standard trace element laboratory analysis technique for organics, inorganics, and metals. In the late 1980s Argonne National Laboratory was deeply involved in solid oxide fuel cell research. These fuel cells utilize solid electrolytes. The solid electrolytes complement the voltammetry and produce an NOx gas sensor that is compact, robust, and rugged. The sensing technique enables broad spectrum detection – multiple gases (O_2, NO, NO_2, N_2O) can be detected with the same sensor over a wide range of concentrations (Figure 2).

Approach

This Phase I investigation explored a new NOx sensor technology based upon a high-speed gas voltammetry measurement technique employed with both experimental and commercial solid electrolyte-type sensors. The measurement technique was applied successfully to previously-developed materialistically-tailored thick-film microarrays, and to three types of commercial gas (O_2 and CO_2) sensors that had similar lithography to the experimental sensors.

Results

Existing experimental micro-arrays were successfully modified to help design a new high-temperature package capable of sustained 600°C operation. The voltammetry measurement technique was successfully applied to three types of existing commercial sensors to demonstrate the chemical identification and quantification advantages of the measurement technique. The results show distinct sets of reaction dissociation potentials for each of the target component gases found in automotive and diesel truck exhaust (including NOx) and support the strategy of using one high-speed voltammetric analyzer-type sensor to produce concentration information for multiple gases, to an emissions control system (Figures 3 and 4).

A new rugged-ized version of the voltammetric micro-array has been designed. All parts have been received, but remains to be finally assembled for characterization.

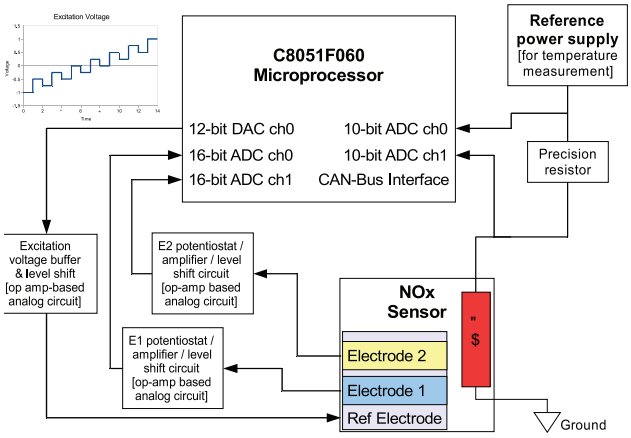

FIGURE 1. Voltammetric Multi-Gas NOx Sensor Block Diagram

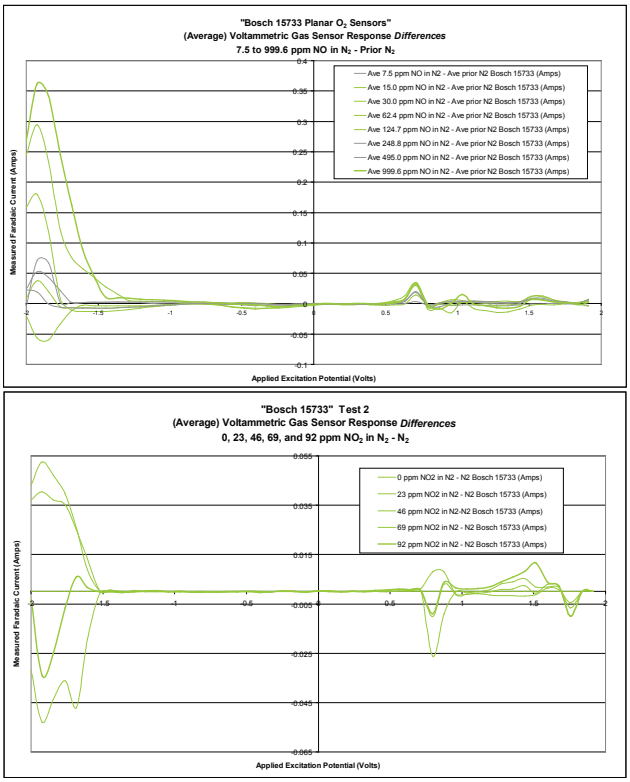

FIGURE 2. Bosch 15733 Dissociation Potentials for NO and for NO_2

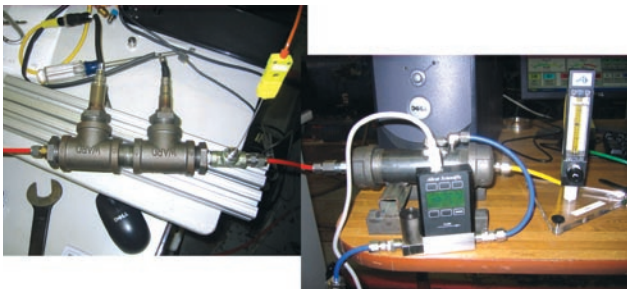

FIGURE 3. Sensor Testing at the University of Alabama

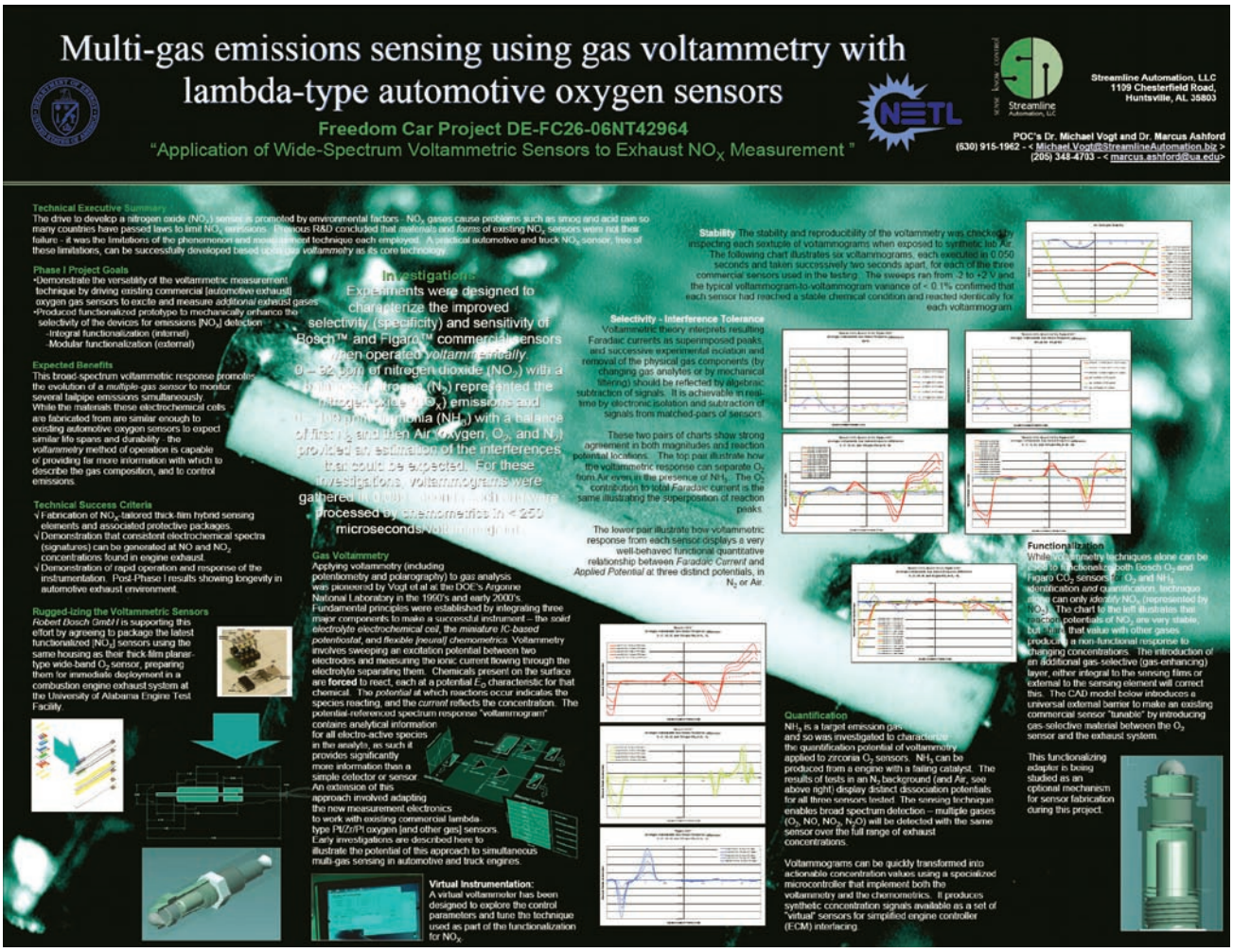

FIGURE 4. Voltammetric Multi-Gas NOx Sensor Poster

Conclusions

- Voltammetry does work with ceramic-metallic solid electrolyte electrochemical cell type sensors.
- Voltammetry does provide simultaneous multiple gas identification and concentration information, in real-time, across the concentrations desirable for engine emissions controls.

References

1. Vogt, M. C., E. L. Shoemaker, A.V. Fraioli, 1995, Electrocatalytic Cermet Gas Detector/Sensor, U.S. Patent #5,429,727 Issued July.

2. Shoemaker, E. L., M. C. Vogt, 1998, Improved O_2/CO_2 Gas Sensor, U.S. Patent #5,772,863 Issued July.

FY 2007 Publications/Presentations

1. Vogt, Michael C., M. Ashford, and A.J. Reich, *Multi-gas emissions sensing using gas voltammetry with lambda-type automotive oxygen sensors*, 2007, DOE FreedomCar Annual Presentation, June.

2. Vogt, Michael C., A.J. Reich, and M. Ashford, 2008, *Multi-gas emission detection using gas voltammetry with lambda-type automotive oxygen sensors* (being submitted soon to Sensors & Actuators: B).

Special Recognitions & Awards/Patents Issued

1. Provisional Patent filed – Voltammetry-Enhanced Multiple Gas Emissions Sensing, application number 60944156.

2. Provisional Patent filed – Aerodynamically-Efficient High-Performance Adapter for Exhaust Gas Sensors, application number 60944272.

3. Provisional Patent filed – Miniature Multi-Channel Potentiostat for Gas Voltammetry, application number 60950336.

4. Provisional Patent Application pending – Gas-Selective Filter for Automotive Exhaust Gas Sensors.

II.C4 Advanced Start of Combustion Sensor – Phase 1: Feasibility Demonstration

Chad Smutzer (Primary Contact),
Robert Wilson
TIAX LLC
15 Acorn Park
Cambridge, MA 02140

DOE Technology Development Manager:
Roland Gravel

NETL Project Manager: Samuel Taylor

Subcontractors:
- Wayne State University, Detroit, MI
- First tier automotive controls supplier (asked to remain anonymous)

Objectives

- Develop an accelerometer-based start of combustion (SOC) sensor which provides adequate SOC event capture to control a homogeneous charge compression ignition (HCCI) engine in a feedback loop.
- Ensure that the developed sensor system will meet cost, durability, and software efficiency (speed) targets.

Accomplishments

- Two engines of same model line/different serial number installed to verify engine-to-engine repeatability of the SOC sensor system (a potential drawback of accelerometer-based systems).
- Developed an array of algorithms to translate the accelerometer signal into the desired SOC value.
- A library of data has been generated relating engine cylinder pressure to accelerometer events, and the algorithms are being evaluated on the accelerometer data.

Future Directions

- Testing will continue to generate further data at more speed and load points, and this data will be tested in the algorithms.
- Low-temperature combustion is planned to evaluate the sensor for HCCI engine operation (current data has been measured in diesel mode).
- The sensor package will be tried on the second engine setup to determine the engine-to-engine repeatability of the algorithms.

Introduction

HCCI has elevated the need for SOC sensors. HCCI engines have been the exciting focus of engine research recently, primarily because HCCI offers higher thermal efficiency than the conventional spark ignition engines and significantly lower NOx and soot emissions than conventional compression ignition engines, and could be fuel neutral. HCCI has the potential to unify all the internal combustion engine technologies to achieve the high-efficiency low-emission goal. However, these advantages do not come easy. It is well known now that the problems encountered with HCCI combustion center on the difficulty of controlling the start of combustion. The emergence of a durable and effective SOC sensor will solve what is arguably the most critical challenge to the viability of HCCI engine platforms. The SOC sensor could be an enabler for a new breed of engines saving 15-20% of petroleum used in transportation, while meeting or exceeding 2010 emission targets.

Approach

The design phase of the project was initiated first, during which the algorithms are being conceptualized and the sensor configuration is being designed. In parallel to the conceptualization of the algorithms, the hardware test setups are being completed. To test the engine-to-engine repeatability of the sensor signals, two engines of different serial numbers but the same model were set up. Once the algorithms are conceptualized and implemented in software, the data from the engine set-ups will be fed into the algorithms to see if they successfully and robustly determine SOC. This process is designed to require some iteration, but following the tasks in the order shown will minimize the iterations and allow for the team to compensate should there be any surprises. Throughout all of these tasks, the team has guided the SOC sensor design effort toward what will be required for commercialization. The work flow was carefully designed to ensure the risk is minimal and that technical success probability is high, and iterations are included to counter any setbacks that may be encountered.

Results

A major portion of the work to date went to the set up of the hardware in the two separate engine test facilities. Due to a head start with hardware availability, Wayne State University was able to commission their engine test set-up prior to TIAX, thus the initial data generation was carried out at their test facility. After the Wayne State University testing is complete, the accelerometer package will be shipped to TIAX to repeat the data points. The hardware at each respective location is shown in Figure 1.

Since the effectiveness and robustness of the accelerometer-based sensor system depends on its ability to work across multiple engine blocks, installation of these two similar engines was a key accomplishment.

As mentioned in the Approach section, in parallel to the hardware installation, algorithms were developed to be able to take an accelerometer signal and derive the necessary information from it to determine the SOC. An example of one of the algorithms developed is shown in Figure 2.

As shown in Figure 2, the algorithm faithfully reconstructed the impulse event which caused the vibration of the cylinder block. This reconstruction is one element of the determination of SOC. The combustion event is essentially an impulse event which causes the cylinder block to vibrate. From this vibration, the algorithm can take the accelerometer signal and reconstruct the event which caused it. SOC, or the start of the event, may be readily determined from the reconstructed signal.

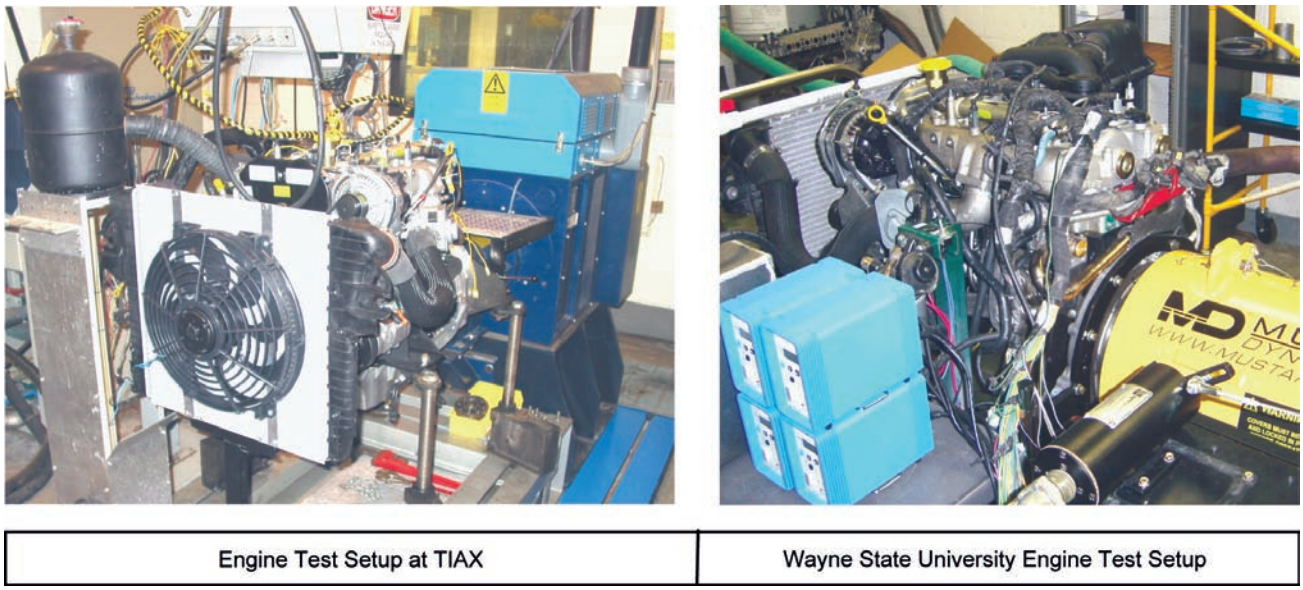

FIGURE 1. Photographs of the dual engine test setups (same engine model, different serial numbers) designed to test engine-to-engine repeatability of the sensor system.

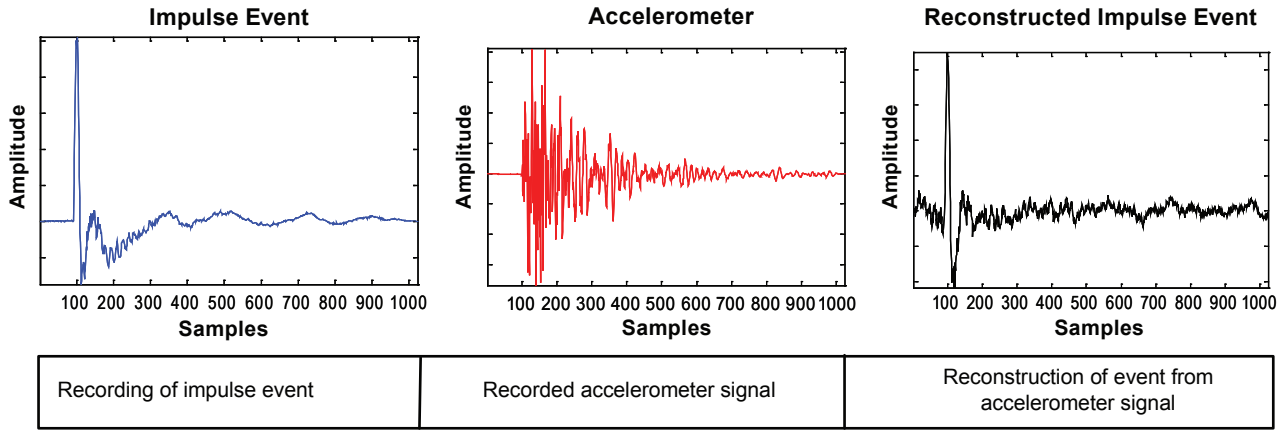

FIGURE 2. Graphical example of algorithm used to reconstruct an impulse event from an accelerometer mounted on the engine block.

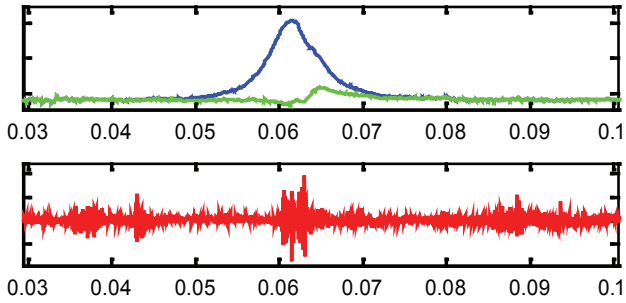

FIGURE 3. Pressure trace from the engine shown in parallel with accelerometer trace.

Application of this principle may be seen in a snapshot of the engine cylinder pressure data shown in Figure 3.

Here in Figure 3, the forcing function is the pressure rise of the cylinder due to combustion, the pressure shown in the top graph. In the lower graph is the accelerometer response to the combustion event. There is good correlation from the accelerometer trace to the combustion event. Using the algorithm exemplified in Figure 2, the SOC can readily be determined.

Conclusions

- Algorithms have been developed which show promise to be able to determine the SOC based upon an externally mounted accelerometer signal.
- Testing is ongoing to determine the engine to engine repeatability of these methods, with the hardware setups completed.
- Further testing (still ongoing at this time) will provide a range of speed and load points to ensure algorithm robustness.

FY 2007 Publications/Presentations

1. Smutzer, Chad A., and Robert Wilson. "Advanced Start of Combustion Sensor–Phase I: Feasibility Demonstration. FreedomCAR and Vehicle Technologies Merit Review and Peer Evaluation. June 18-19, 2007, Washington, D.C.

II.C.5 The Development of a Robust Accelerometer-Based Start of Combustion Sensing System

David Mumford (Primary Contact), Jim Huang
Westport Power, Inc.
1691 West 75th Avenue
Vancouver, BC V6P 6P2
Canada

DOE Technology Development Manager:
Roland Gravel

NETL Project Manager: Jason Conley

Objectives

Phase 1 (October 2006 to July 2007):

- Identify the critical parameters that influence engine-to-engine variation in the accelerometer sensor signal.
- Develop engine-to-engine compensation techniques, using data collected from two engine configurations.
- Verify on paper that the robustness compensation techniques will meet performance requirements.

Phase 2 (August 2007 to July 2008):

- Develop a charge amplifier for use with knock sensors, if required.
- Develop a sensor characterization method, and select the best sensor for the application based on sensor characterization tests.
- Further develop robustness compensation techniques to include the impact of sensor-to-sensor variations, using additional data collected from an engine with different sensor configurations.
- Verify on paper that the robustness compensation techniques will meet performance requirements.

Accomplishments

- Confirmed that the vertical acceleration of the main bearing caps (MBC) has the best correlation with the start of combustion timing.
- Developed an algorithm to obtain the timing for the start of combustion using accelerometers.
- The targeted start of combustion (SOC) error standard deviation is 0.5 crank angle degrees (CAD). The current results have largely exceeded this target for all the testing modes. The averaged engine-to-engine variation over all modes is 0.32 CAD with 98.9% confidence level.

Future Directions:

- Study sensor-to-sensor variation on the two Cummins ISB engines.
- Study the effectiveness of the current compensation methods in dealing with sensor-to-sensor variation.
- Investigate a charge amplifier for gain compensation.
- Further improve robustness using signals from non-adjacent bearing caps (higher degree of redundancy).

Introduction

The development of modern combustion systems increasingly relies on detailed knowledge of the combustion event. As the limits of combustion are approached, tight control of combustion leads to improved emissions and higher efficiencies, while retaining and even improving engine reliability and durability.

While developing a novel combustion technology, Westport found that there was no reliable cost-effective technology to monitor the combustion event. As a result, Westport began developing a solution based on commercially available knock sensors. Numerous other forms of combustion (high exhaust gas recirculation systems, homogeneous charge direct injection, etc) may also benefit from this work. Westport has previously proven this method on two different large compression ignition gas engines. The objective of the current work is to improve robustness of this technology; particularly, to identify and reduce the engine-to-engine and sensor-to-sensor variations.

Approach

The experimental study was carried out on two Cummins ISB 5.9L HPCR diesel engines. Accelerometer (knock sensor) data were collected for six of the 13 European Stationary Cycle (ESC) testing modes, which cover a wide range of engine load and speed conditions. Corresponding in-cylinder pressure data was also collected to determine the actual SOC and other combustion parameters.

This data was analyzed to develop a robust algorithm to reliably predict the SOC timing across the different engine modes. Initially this was assessed with two different engines to compare engine-to-engine

variation with the sensors. Current work is now focused on comparing different sensors and investigating the effect of charge amplification.

Results

The two Cummins engines were fully commissioned and baseline tests were conducted at the rated power and torque. A set of six Kistler 6607C1 water-cooled pressure transducers were used to measure the in-cylinder pressures. A Cummins CELL high speed data acquisition system was used to collect the pressure and knock sensor data generated during the engine testing.

For the current study, the accelerometers are mounted directly to the main bearing caps. Finite element analyses of the cap showed that the change in maximum stress due to drilling either a single hole or two holes into the cap was within the acceptable range with the desired safety factor.

Knock sensor and in-cylinder pressure data from the two engines were collected at six modes selected from the 13 ESC modes. For each mode, tests were conducted at nominal, advanced and retarded injection timing (Table 1). Motoring data were also collected for each mode at the nominal timing by intermittently cutting off the injection for a selected cylinder. A repeatability study was conducted on engine #1 to examine the effect on the knock sensor signal of remounting the sensor. Test points were also repeated for engine #2, except for remounting.

Data were also collected at all modes with a Ditran-302382 tri-axial research-grade accelerometer mounted on selected bearing caps. The data were used to compare with those from the knock sensors to improve the understanding of the sensor performance.

TABLE 1. Engine Test Modes

ESC Mode	%Load	Torque (Nm)	RPM	Power (BHP)	Start of Injection[1]
5	50	305	1885	109	a, n, r
6	75	457.5	1885	164	a, n, r
8	100	610	2292	266	a, n, r
9	25	152.5	2292	67	a, n, r
12	75	457.5	2698	235	a, n, r
13	50	305	2698	157	a, n, r

[1] Nominal (n), advanced (a) and retarded (r) timing

All firing data were averaged over 80 engine cycles. All motored data were averaged over 20 to 30 test cycles. Figure 1 shows an example of the heat release rate trace and the knock sensor signal. The knock sensor data show high frequency oscillations at the start of combustion, whereas previous studies with ISX engines show predominantly low-frequency signals. Analysis of the high-frequency signal established the reproducibility of a characteristic frequency between the two ISB engines. The high frequency signal and the low frequency signal were adopted as independent measures for determining SOC.

There are four main steps to the processing algorithm:

1. Pre-process the raw accelerometer data
2. Reconstruct the heat release rate
3. Extract SOC information from the accelerometer signals
4. Select the SOC timing with the highest confidence level

The rate of heat release curve in the current study has a unique double-peak feature. The complex shape of this curve together with the multiple-peak input signal from the knock sensor makes a general transfer function difficult to achieve. In particular, it is difficult to separate the accelerometer signal corresponding to the high-frequency components in the heat release rate from the noise.

The phase shift among different ignition timings was observed in the high-frequency, low-frequency and reconstructed data. A global and a local method were used to obtain the phase shift of SOC from the calibration signal. Both methods can provide an independent SOC estimate, and the results were crosschecked with each other to improve the reliability.

Timing swings were used at advanced, nominal, and slow combustion rates to test SOC detection at the widest expected range of heat release rates. The scatter

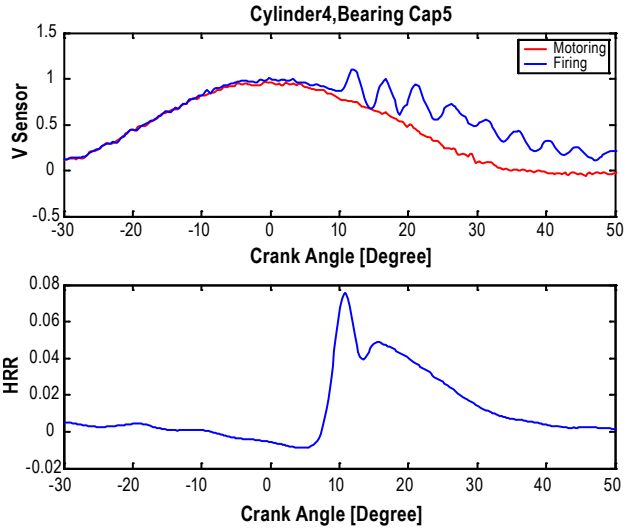

FIGURE 1. Comparison of Knock Sensor Signal with Heat Release Rate Data

of data tends to increase with delayed ignition. The signal to noise ratio was also found to be relatively low at high speed and low load conditions.

Figure 2 shows the total error (standard deviation) for individual modes. The total error is significantly lower than the 0.5 degree target for all modes. The total error averaged over all modes is 0.19 CAD.

Table 2 and Figure 3 show the engine-to-engine variability. For most modes, the variability is significantly less than 0.5 CAD. The average engine-to-engine variability with 98.9% confidence level (3σ) is 0.32, which meets the 0.5 degree target.

The cylinder-to-cylinder variation fits very well with the global correlation, which implies that cylinder to cylinder variation is very small with the current method.

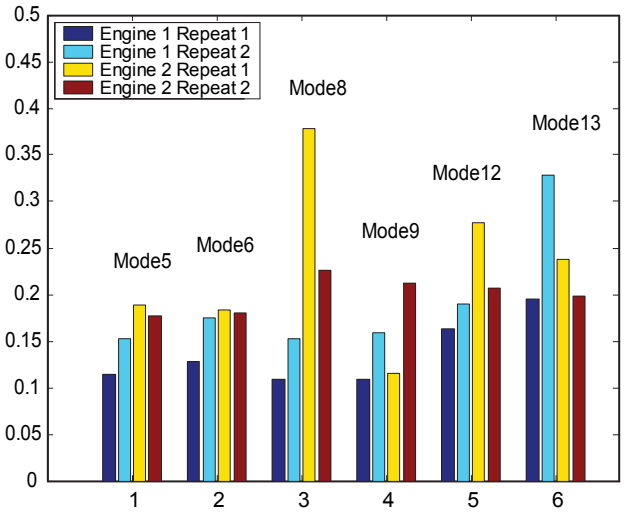

FIGURE 2. Total Error (1σ) at Different Modes

TABLE 2. Total Error and Engine-to-Engine Variation at Different Test Modes

ESC Mode	Speed (rpm)	Load (N.m)	Total Error (1σ) (CAD)	Engine-to-Engine Variation
5	1885	414	0.16	0.28
6	1885	620	0.17	0.29
8	2291	213	0.22	0.40
9	2291	812	0.15	0.20
12	2698	620	0.21	0.38
13	2698	414	0.23	0.36
Average			0.19	0.32

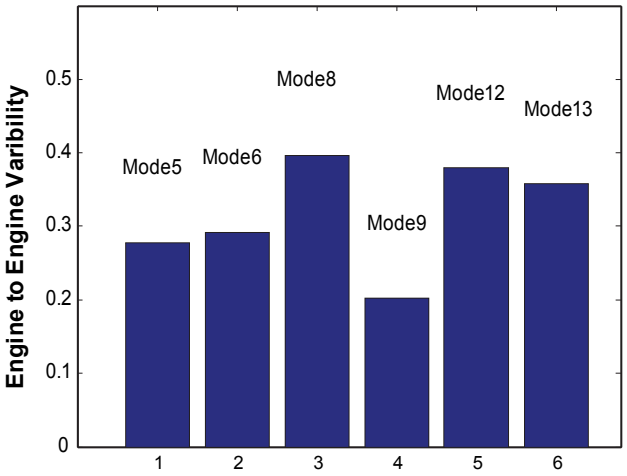

FIGURE 3. Engine-to-Engine Variation at Different Modes

Conclusions

- A new algorithm was successfully developed to obtain the timing for the start of combustion using accelerometer data.
- The targeted SOC error standard deviation is 0.5 CAD. The current results have largely exceeded this target for all the testing modes. The averaged engine-to-engine variation over all modes is 0.32 CAD with 98.9% confidence level.
- Late ignition has an adverse effect on the precision of the accelerometer results. Measurement error also tends to increase at high speed and low load conditions.
- The vertical acceleration of the main bearing caps has the best correlation with the start of combustion timing.

FY 2007 Publications/Presentations

1. DOE Quarterly reports filed for Oct-Dec 2006, Jan-Mar 2007, April to June 2007, and July to September 2007.

2. Presentation made to the DOE in July 2007.

Special Recognitions & Awards/Patents Issued

1. Patent application in progress for algorithm developed during this period.

II.C.6 Electrically Coupled Exhaust Energy Recovery System Using a Series Power Turbine Approach

Carl T. Vuk
John Deere Product Engineering Center
P.O. Box 8000
Waterloo, IA 50704

DOE Technology Development Manager:
John Fairbanks

NETL Project Manager: Ralph Nine

Subcontractor:
International Truck, Fort Wayne, IN

Objective

The overall objective of this project is to demonstrate the technical benefits of electrically-coupled turbo compounding. Specific objectives for 2007 included:

- Optimize system performance characteristics over operating envelope.
- Develop design of production viable hardware components.
- Demonstrate performance characteristics through vehicle testing.

Accomplishments

The overall project goal of a 10% improvement in fuel economy was successfully demonstrated over most of the operating speed range. Additional potential performance improvement was characterized. Technology was developed to exploit the flexibility of the electrical coupling to optimize system performance as a function of both engine speed and load.

Second generation components were designed. A smaller, higher performing turbo generator has been designed that exhibits considerable simplification. A series turbocharger system that provides improved performance and range was also successfully designed and modeled.

The Deere 8530 turbo compounded tractor was evaluated on the test track after developing suitable controls to handle normal vehicle transients. The International truck was also updated with a complete turbo compounding system.

Future Directions

Vehicle testing to better define actual operating fuel savings is the next step in the project. Emphasis will be primarily on the truck, since this application can have the greatest impact on national fuel usage.

Second generation hardware sized to match Tier 4 emissions regulations with interstage after-treatment has been designed. This hardware needs to be built and tested at Tier 4 conditions.

A systems approach to optimization has proven valuable in early work. Second generation hardware will have greater flexibility and hence more potential for optimization. Additional work is needed here for specific applications as well as broadening the scope of applications using common base hardware. Series turbochargers provide additional flexibility, but matching strategies with as much common hardware is desirable.

Commercialization potential needs to be defined. More detailed cost analysis and projections are required. Volume projections will be important here, so knowing the nature of the benefits over a range of applications will be required. With hybrid technology catching on in trucks, the economic justification becomes much easier.

Introduction

The objective of this project is to characterize fuel economy, power growth, and emissions benefits of electrically-coupled turbo compounding, an intelligent waste exhaust heat recovery technology. The rapid adoption of hybrid technology into trucks has the effect of promoting the technology in two ways. First, the widespread application of power electronics in heavy-duty applications will have a favorable impact on component costs required for turbo compounding. The second impact is related to the synergism of hybridization and electric turbo compounding. Hybrid vehicles bring considerable infrastructure that is required for turbo compounding. This effectively lowers the incremental cost of turbo compounding. Hybrid trucks have demonstrated significant fuel economy advantages in stop-and-go driving common to busses, delivery vehicles, and refuse haulers. The advantages in line haul applications are less clear. This is where electric turbo compounding is at its best. The combination of hybridization and turbo compounding is truly synergistic and together both technologies will advance.

Changes during the past year relative to CO_2 emissions have the potential to drive the technology. The Supreme Court's decision characterizing CO_2 as a regulated emission is significant. The proposal to increase Corporate Average Fuel Economy (CAFE) mileage targets and to also cover heavy-duty and off-road vehicles are also significant new drivers. Increasing fuel economy has direct benefits in lower operating cost, and in conservation, but now also impact CO_2 in direct proportion to the fuel economy improvement. Multiple technologies will no doubt be required to fully address these issues, but turbo compounding can clearly play an important role. This is new in 2007, and will help propel this technology into commercial vehicles.

Approach

Extensive dyno testing was completed in an effort to match turbo machinery hardware and optimize system performance over the operating envelope. The impact of Tier 4 after-treatment exhaust pressure restrictions were modeled and tested with several different architectures. Dyno testing was also used to help define transient system behavior prior to vehicle testing. Initial tractor testing was also completed on the test track to optimize dynamic system behavior and transient response characteristics.

Based on encouraging performance improvements, next generation system hardware architecture was defined, and design work initiated.

System hardware for the truck application was designed, built, and installed in an International 8600 truck. The truck will be used to determine the fuel economy benefits over a range of standard driving cycles.

Results

Typical output characteristics of a 50 kW electrically coupled turbo compounding system are shown in Figure 1 for a system matched to the Deere 9L Tier 3 engine. Fuel economy benefits are shown in Figure 2 in comparison to the baseline engine. Each point of the curve is matched for engine power and NOx emissions. The turbo compounding system puts out an additional 50 kW at rated conditions and provides a 10% improvement in fuel economy over the typical operating speed range. Significant additional fuel economy improvement potential is believed possible because hardware availability did not allow all components to be simultaneously optimized.

Next generation hardware will employ basically the same system architecture, but the turbocharger will be a series system rather than a single stage high pressure ratio machine. Surge margin of the single stage machine proved limited. The turbo generator will

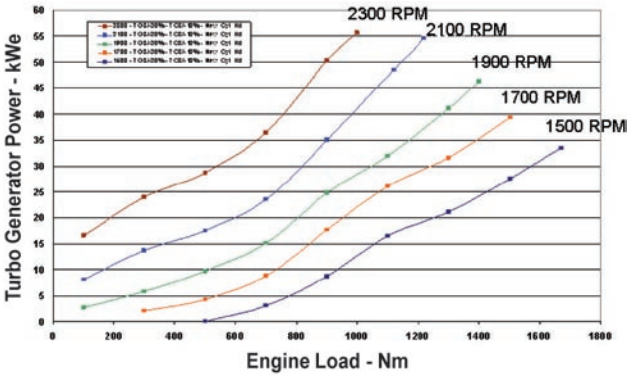

FIGURE 1. Typical System Output Characteristics

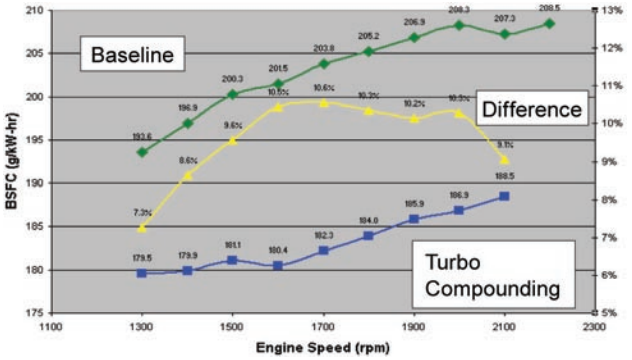

FIGURE 2. Fuel Economy Characteristics at 2100 RPM (Constant Engine Power and NOx Emissions w/50 kW Turbo Generator on a 280 kW Rated 9L Engine)

evolve to a smaller, higher speed machine. Voltages are also doubling in an effort to reduce costs, size, and losses. Analysis of the new design hardware predicts performance improvement. The hardware is expected to be closer to production viable, as more effort was put into manufacturing considerations in an automotive type environment. A comparison of Gen I and Gen II hardware is shown in Figure 3.

The electrically turbo compounded International truck (see Figure 4) is ready for programming and shakedown testing. The truck includes the Eaton hybrid transmission and the same engine used in the tractor and in dyno testing. Performance matching is different, given the lighter duty cycle, and more work is needed here to assure optimum fuel economy at light loads. The truck will be tested over a wide range to cycles to determine the benefits for each application.

Conclusions

Electric turbo compounding clearly works in providing significantly better fuel economy, lower emissions, and increased power density. The benefits are compatible with many other technologies, and are highly

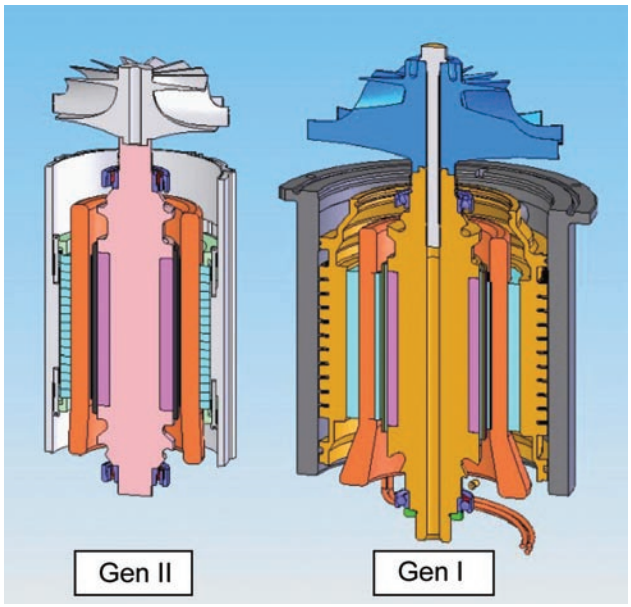

FIGURE 3. Turbo Generator Hardware Evolution

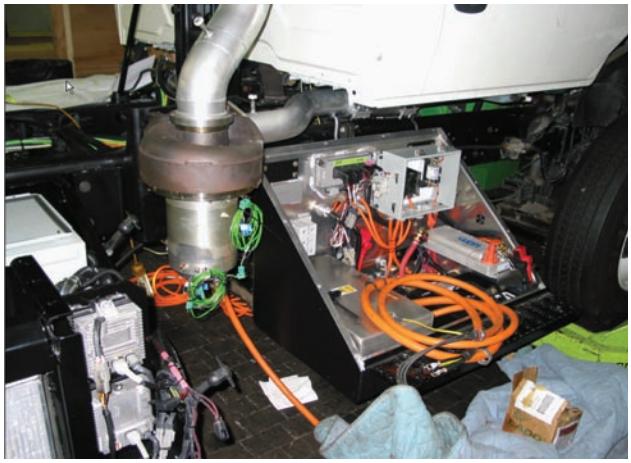

FIGURE 4. Electric Turbo Compounding System Hardware – International Truck Installation

synergistic with truck hybridization. The business case needs additional refinement, but looks very encouraging, particular when combined with hybrid technology. Additional potential performance benefits have been identified, but need to be confirmed through testing.

FY 2007 Publications/Presentations

1. Agricultural Machinery Conference, Cedar Rapids, IA, 9 May, 2007.

2. DEER Conference (Poster Session), Detroit, MI, 15 August, 2007.

3. WestStart – CALSTART, Technical Advisory Committee, Pasadena, CA, 12 September, 2007.

4. HTUF, Seattle, WA, 20 September, 2007.

Patent Applications

1. 17307 Turbo Generator Control with Variable Valve Actuation.

2. 18117 Circumferential Dual-Vane Turbine Inlet.

II.C.7 Exhaust Energy Recovery

Christopher R. Nelson
Cummins Inc.
1900 McKinley Ave.
Columbus, IN 47203

DOE Technology Development Manager:
Roland Gravel

NETL Project Manager: Ralph D. Nine

Objectives

- Improve engine fuel efficiency by 10% through the recovery of waste heat energy.
- Reduce the need for additional cooling capacity in Class 8 trucks.
- Provide conditioning (cooling) for combustion charge air.

Accomplishments

- Completed a system thermodynamic analysis across the engine's operating map to define the architecture of the waste heat recovery (WHR) system. The analysis results eliminated engine coolant and charge air as potential recovery sources and focused our efforts on waste energy recovery from recirculated exhaust gas (EGR) and the engine's main exhaust gas stream.
- Completed first generation component analysis and design for an on-engine system which will recover heat from the engine's EGR stream, thereby relieving the engine's jacket water system of this heat load and providing 6% fuel efficiency improvement (model-based results).
- Performed analysis to determine that an extra 2% efficiency improvement was possible by recovering waste heat energy from the engine's main exhaust gas stream when operating at off-peak design conditions.
- Established that with the presence of a 340 VDC electric bus on-engine, engine efficiency could be improved by an additional 2% through electric, load-driven accessories (water pump, brake air compressor, power steering pump, air conditioning system, etc.).
- Developed a dynamic engine and vehicle system model to predict the performance of the WHR system operating over a Class 8, linehaul vehicle duty cycle.

Future Directions

Continued effort is planned in the pursuit of an effective and efficient Organic Rankine Cycle (ORC) waste heat recovery system. The past activities have designed first-generation components which will be tested to verify model-based analysis and allow the development of an effective control system. Future work is focused on enhancing system performance and refining system architecture to be integrated into Cummins' future products. During 2008, we expect to:

- Proceed to laboratory-based, engine-integrated system testing with an EGR-only WHR system.
- Develop and tune the control system of the WHR system to provide optimum performance integrated with the engine and driveline systems.
- Acquire, incorporate and test components necessary for main exhaust stream energy recovery.
- Create specifications and initiate procurement of a second-generation hardware set appropriate for installation in-vehicle.

The ORC waste heat recovery concept introduces a significant number of new technologies into the engine system architectures which Cummins Inc. has traditionally pursued. Successful system integration for practical implementation will require that subsystem architectures be carefully reviewed for their effect on the overall engine, driveline, and vehicle.

Introduction

With the advent of low-NOx combustion techniques using cooled EGR, heat rejection has increased, driving cooling package space claims 'in vehicle' to their limits. A means to mitigate this increased heat rejection is desired to avoid extensive revisions to vehicle cooling packages. A solution which serves this purpose while providing operating efficiency benefits would be ideal.

The Rankine cycle is essentially a steam-turbine thermodynamic cycle wherein a working fluid (akin to water or steam) is heated to boiling and superheated (heated beyond boiling). Thereafter, the fluid is passed to an expansion device (in this case a turbine) where it releases its heating-induced energy and momentum to create mechanical work. This work is used to turn a generator which then provides additional power above what the diesel engine produces for the same amount of fuel burned. Using the Rankine cycle to extract energy (or to thereby provide cooling) from waste heat

streams serves to reduce the amount of heat which must be rejected while simultaneously providing extra power. Reducing heat rejection and minimizing cooling package size serves to provide vehicle manufacturers with continued opportunities to minimize vehicle frontal area, reducing aerodynamic drag, and improving fuel economy.

The Exhaust Energy Recovery project at Cummins Inc. was initiated by experiments conducted under the Heavy Duty Truck Engine project. During this testing, a Rankine cycle was employed in support of that project's high engine efficiency demonstration. In the current work, Rankine cycle heat recovery is being focused on the heavy duty diesel engine's EGR and main exhaust gas streams. Recovery of EGR heat will relieve the engine's cooling system of a significant portion of this waste heat energy. The EGR energy recovery system must necessarily be designed to capture the peak heat load from this waste energy stream. During off-peak operation, when excess heat rejection capacity exists in the EGR energy recovery system, additional energy may be recovered from the engine's main exhaust gas stream which will keep the Rankine Cycle system operating at its peak capability. This technique will maximize the benefit of the energy recovery system.

Approach

Cummins' approach to the project objectives emphasizes analysis-led-design in nearly all aspects of the research. An emphasis is placed on modeling and simulation results to lead the way into feasible solutions.

With the advent of cooled EGR-based combustion technology, the need to provide an effective cooling system for combustion charge conditioning has become vital. The additional cooling required for EGR and fresh charge air to thereby achieve low intake manifold temperatures (in pursuit of clean combustion) has driven an increase in vehicle cooling system performance.

A Rankine cycle extracting heat energy from the engine's EGR stream reduces the heat load on the engine system cooling package and simultaneously provides extra power from the engine system. The cycle's turbine-driven electric generator provides power which may be used for a number of different on-vehicle applications including:

- Traditional alternator load (alternator may be removed)
- Supplemental power to engine output (through the use of a driveline-coupled motor)
- More efficient parasitics in the form of coolant pumps, air compressors, etc.

To efficiently accommodate power from the Rankine cycle generator and to minimize its size, higher voltage than what is traditionally used on heavy-duty vehicles (12 VDC) is required. The recommended voltage level of approximately 340 VDC creates opportunities to use efficient and cost-effective power electronics developed for use in other industries (rectifiers, power conditioners, motor drives, etc.) and components and techniques common with hybrid electric vehicles. High-speed, permanent-magnet or switched-reluctance generators and motors are also compatible with this higher-voltage environment. This compatibility leads to further applications of these devices with subsequent efficiency benefits to the engine and vehicle.

Results

Research has been focused on identifying the most effective techniques and tools for Rankine cycle application to a heavy-duty diesel engine installed in a Class 8 tractor.

Simulation Analysis

A simple Recuperated Rankine Cycle is schematically presented in Figure 1. Saturated liquid working fluid (blue) comes from the system condenser and first passes through a recuperator which transfers energy left over after turbine energy extraction. The fluid then passes to the engine heat exchangers (charge air cooler and EGR cooler) where it reaches a superheated state. The superheated vapor is then passed through the turbine to generate electricity. The fluid then passes through the recuperator and then the condenser.

A performance analysis using R245fa as the working fluid in a Recuperated Rankine Cycle extracting energy only from EGR resulted in a maximum brake thermal efficiency improvement of 6% across the engine's steady-state operating map. Figure 2 presents data from a typical Class 8 vehicle operating across a Heavy Duty Corporate Composite (HDCC) duty cycle. Balloons represent the amount of fuel burned at various engine operating conditions and the amount of energy recovery power is indicated.

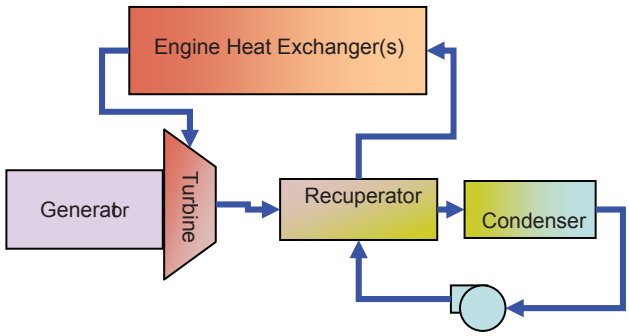

FIGURE 1. Simple Recuperated Rankine Cycle

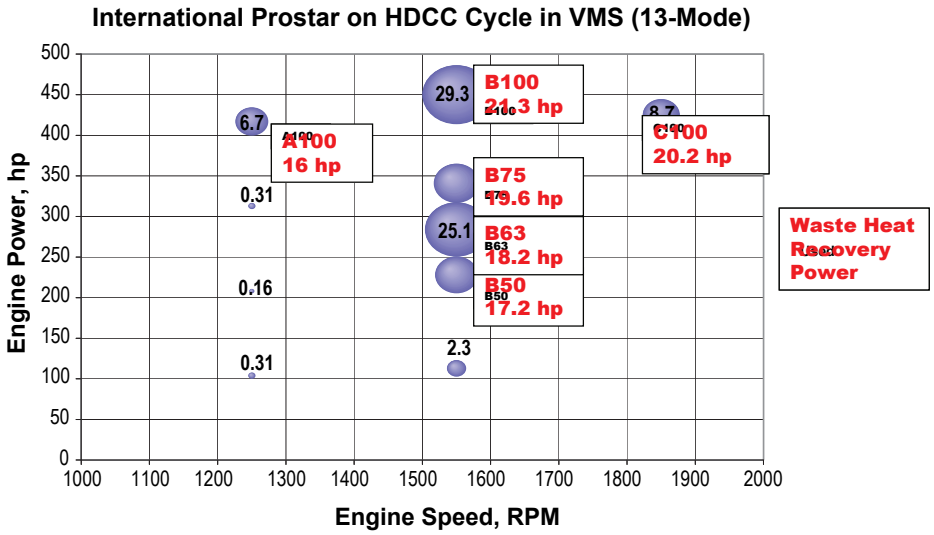

FIGURE 2. Additional Power Provided by the Cummins WHR system Across an Engine Operating Map

The additional recovered power is provided to the engine as high voltage (340 VDC) electricity which may be used to power engine and vehicle parasitics or to supplement the engine's brake power output through a driveline motor (incorporated into the engine's flywheel or elsewhere).

Hardware Design

During 2007, a significant effort was made to design and acquire a first-generation set of hardware in order to initiate laboratory-based testing. The primary focus of the hardware development has been on the EGR-only energy recovery concept. Figures 3 and 4 present a Cummins ISX engine incorporating EGR-only energy recovery hardware.

The WHR System will require that a separate, low-temperature cooling circuit be present on the engine/vehicle system to provide the lowest temperature coolant possible to the system's condenser. This low-temperature circuit will include a separate, electric water pump and radiator. The radiator will be incorporated into the vehicle's cooling package. Cooling package layout and analysis was performed during the year to establish that a practical system could be installed in a typical Class 8 tractor.

The system's driveline motor (flywheel motor generator in Figure 4) will combine the recovered electric power with the engine's brake power. Also, this device will provide the electric power necessary to run the vehicle and engine system when there is insufficient recoverable waste heat energy. The current alternator and belt drive is eliminated by this concept. The system has retained the traditional starter motor because the

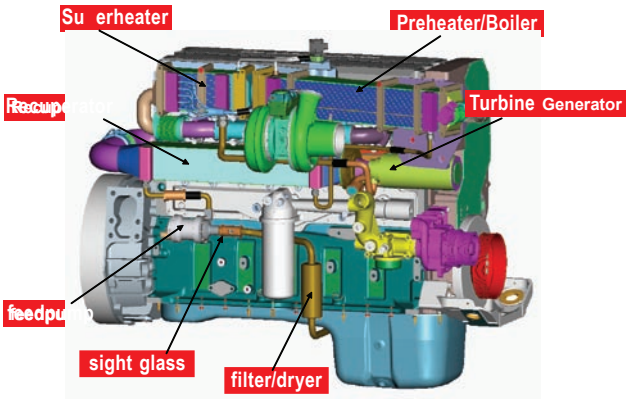

FIGURE 3. Cummins ISX Engine With EGR-Only WHR System Hardware

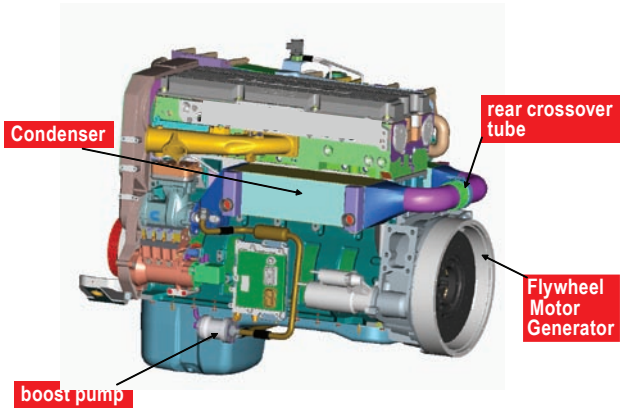

FIGURE 4. Cummins ISX Engine With EGR-Only WHR System Hardware

target duty cycle for this concept does not require a high level of engine off/on operation (as in a more traditional hybrid concept). Also, without the need to provide a high level of starting torque, the flywheel motor is designed as a more efficient motor at the engine's typical operating speeds.

Conclusions

Modeling and analysis performed to date, supported by the previous experiments with Rankine Cycle systems on the Heavy Duty Truck Engine project leads us to expect significant efficiency improvement from the heavy-duty diesel engine through the incorporation of this concept. The synergistic opportunities offered by the presence of additional electric power with subsequent efficiency gains and improved parasitic load characteristics indicate that this concept has significant potential to improve real, in-use fuel economy.

- The 10% efficiency improvement goal is technically feasible. The modeling effort has shown that across a driving cycle, recovery of waste energy from EGR and the main exhaust gas stream plus the incorporation of electric parasitics will reach this efficiency improvement target.
- First generation hardware will begin laboratory-based testing early in 2008. EGR-only energy recovery will be conducted first with exhaust gas energy recovery being pursued thereafter.
- Model validation and controls development for integrated engine and vehicle operation will be developed during laboratory testing.
- Vehicle-intent, second-generation hardware will be specified and designed based on validated model results and future engine architecture definitions.

FY 2007 Publications/Presentations

1. 2007 DEER Conference Presentation – "Exhaust Energy Recovery", poster presented by Christopher R. Nelson, August, 2007.

II.C.8 Very High Fuel Economy, Heavy Duty, Constant Speed, Truck Engine Optimized via Unique Energy Recovery Turbines and Facilitated by a High Efficiency Continuously Variable Drivetrain

Bahman Habibzadeh
Volvo Powertrain North America
13302 Pennsylvania Ave.
Hagerstown, MD 21742

DOE Technology Development Manager:
Roland Gravel

NETL Project Manager: Sam Taylor

Subcontractor:
Volvo Aero Corp., Malmo, Sweden

Objectives

- Increase engine efficiency by 10% while meeting U.S. 2010 emissions standards.
- Achieve efficiency increase by implementing turbocompounding and narrowing the engine operating speed range. Couple the engine to a continuously variable transmission (CVT) to enable narrow range or constant speed engine operation.
- Test the engine with turbocompounding, with and without a CVT over road cycles in a test cell to demonstrate system efficiency increase.

Accomplishments

- Through simulation, demonstrated an engine efficiency increase of 8.2% when operating over a road cycle and 10.5% during steady-state operation over the European Standard Cycle (ESC) at U.S. 2010 NOx levels (0.2 g/bhp-hr).
- Added investment for the CVT and energy recovery devices will be returned in less than 1.5 years assuming fuel prices of $2.50 per gallon.
- Net fuel efficiency gain when coupled to a CVT was estimated to be 5%.
- One compressor and two turbines (turbocharger and compound) were designed and tailored for the highly weighted engine operating points.
- Prototype of the high efficiency turbocharger was manufactured.

Future Directions

- Test compressor and turbines in special rigs.
- Build prototype of the high efficiency turbocompound device.
- Test turbocompound device along with turbocharger in special rigs in order to verify the theoretical performance.
- Begin baseline engine development with high efficiency turbocharger and turbocompound device.
- Demonstrate the engine and CVT system in a test cell to determine system efficiency.

Introduction

The heavy-duty trucking industry is very sensitive to fuel pricing. With new and more stringent emissions standards fuel economy will suffer as more energy is needed to drive the emissions control devices.

One way to increase the engine's efficiency is to recover some of the energy that is lost through the exhaust. A mechanical turbocompound device has the ability to direct some of that energy to increase the engine power output (see Figure 1). It is worth mentioning that a turbocompound engine reacts more positively to improved turbocharger efficiency than a conventional turbocharged engine. This project has taken an energy recovery approach along with operating

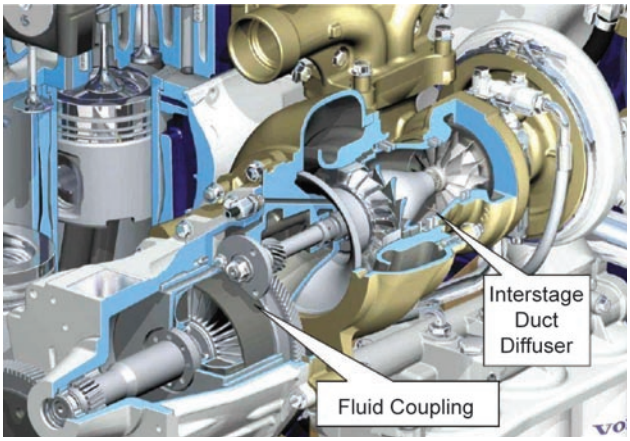

FIGURE 1. Schematic Close-Up of a Volvo D12 500 HP Engine Showing the Turbocharger, Interstage Duct Diffuser and Turbocompound Device

the engine in a different speed range than typical of today's engines. Narrowing the engine operating speed allows the designer to select the optimum speed where engine efficiency is highest. Conventional standard transmissions operate with gear steps too great to run the engine at a constant or narrow range but with the development of a CVT, narrow range operation is possible which will allow the engine to operate at peak efficiency over its entire operating range.

A narrow operating range leads to lower average engine speed which allows valve timing optimization and also use of a compressor with a vaned diffuser which has higher efficiency.

Approach

In order to achieve the efficiency, four techniques were combined: mechanical turbocompounding, high efficiency turbochargers, narrow range engine operation and optimized combustion and valve timings.

Detailed simulations were done based on a Volvo MD13 (485 HP/2600 Nm) engine to determine the benefit of reducing the engine speed and its impact on efficiency. The simulations guided the development of the narrow engine speed range approach and allowed the study of different operating ranges so the best one could be chosen. Simulations were also done to determine the best turbocharger and turbocompound device combination that would return the highest efficiency. Cost analyses were performed on the engine system including the CVT to determine the added cost and return on investment.

Based on the engine simulations, prototype turbocharger and turbocompound hardware had to be designed and manufactured. The prototype hardware will be installed onto a 13L Volvo engine for testing to compare simulation with actual results.

The final plan is to assemble the engine with the high efficiency turbocharger, turbocompound device, and CVT, and place in a test cell capable of running the same road cycles that were used during the simulation phase. The results of the testing will be compared to that determined through vehicle simulations.

Results

Previously Achieved

The simulation result showed:

- Fuel consumption reduction compared to the U.S. 2007 reference engine is 8.2 % when using the U.S. 2007 road cycle with weighting factors (flat 70%, rolling hills 25% and hilly 5%) and 10.5 % when using the ESC cycle, achieved by:
  - High efficiency turbocharger
  - High efficiency mechanical turbocompound device
  - Narrow range engine operation which allows optimized camshaft timings and combustion
- A narrow speed engine (1,000-1,300 rpm) is more efficient than constant speed - especially when the engine is not working in the full power range.
- The additional cost of the turbocharger, turbocompound device, and other modifications to the engine can be paid back in less than 15 months (assumed fuel price of $2.50 per gallon and the lowest recovered efficiency).

Recent Achievements

For the stress analysis (low-cycle fatigue), thermodynamic input in form of transient turbocharger speed, temperature, pressures etc. are required. In order to extract these data, a simplified truck operating cycle is defined for cold-starts, warm-starts and load/speed changes.

Both steady-state and high altitude (1,675 m/25°C) simulations have been performed for the MD13 TC engine with updated boundary conditions and turbo maps. The results are obtained by cycle optimization at "engine-out" conditions, i.e. NOx and soot emissions.

Turbocharger

The turbocharger, as seen in Figure 2, has a high performance compressor and radial turbine. The design speed is around 110,000 rpm. The turbine has a housing which is of the double entry type enabling each group of cylinders to feed 180° of the turbine's circumference.

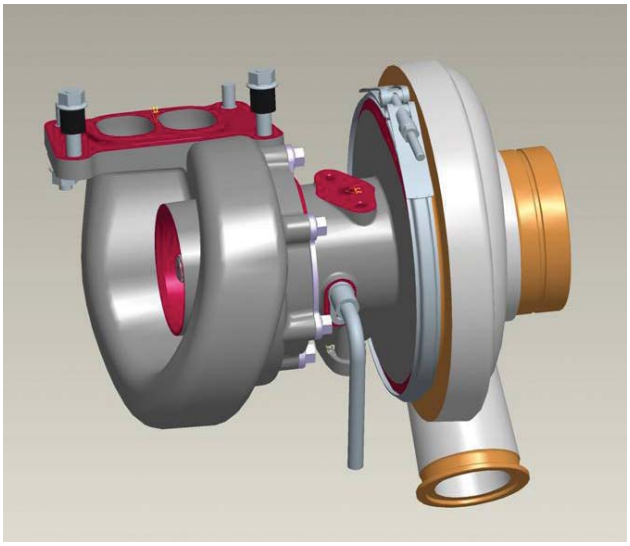

FIGURE 2. Computer Aided Design Drawing of the Turbocharger Unit

Compressor

The compressor has nine blades and nine splitters with an inlet hub diameter of 17 mm, inlet tip diameter of 54 mm and outlet diameter of 94 mm. Three diffusers will be tested (nominal, 1.5° opened and 1.5° closed). The compressor has no inducer shroud bleed as standard. In order to achieve a large operating range these considerations are taken:

- LSA diffuser
- Relatively low impeller blade number
- High backsweep angle
- High diffuser inlet to impeller exit radius ratio
- Low diffuser vane height

Turbine

The turbine has 11 blades and a stator with 18 blades. Considerations to achieve high efficiency are:

- Non-scalloped
- Relatively long axially
- Extensive computational fluid dynamics modeling for various running conditions
- Double entry turbine housing
- Fixed guide vanes

Turbocompound

As it is shown in Figure 3, the compound turbine is directly coupled to the crankshaft via fluid coupling, so it follows the speed of the engine normally operating between 1,000 and 1,300 rpm with a maximum allowed speed during engine braking of 1,900 rpm. This means that the turbine is relatively low stressed during the normal operation but highly stressed during engine braking.

Turbine

The power turbine is of the axial type and it has a stator. The turbine has an outside diameter of Ø118 mm and an inside diameter of Ø80 mm. The number of rotor blades is 23 and the number of stator blades is 17.

Fluid Coupling

A fluid coupling is needed to dampen the oscillations from the piston engine. The coupling is equal to the European Volvo D12 500 HP coupling except the gears, which are different due to new speeds and slightly changed center distance. The new design for the geartrain and interface to the rear transmission in the flywheel housing is done.

The turbocharger and the turbocompound units are located on a common axis which means the gas conduit between them is annular as it can be seen in Figure 4.

Summary

- The turbocharger and turbocompound device are aerodynamically designed and stress analyzed for various duty cycles.
- Layout of the turbocharger, turbocompound device, and other components such as the geartrain, flywheel housing, exhaust manifold, etc. are prepared.
- Compressor and turbine of the turbocharger are manufactured and are being tested.

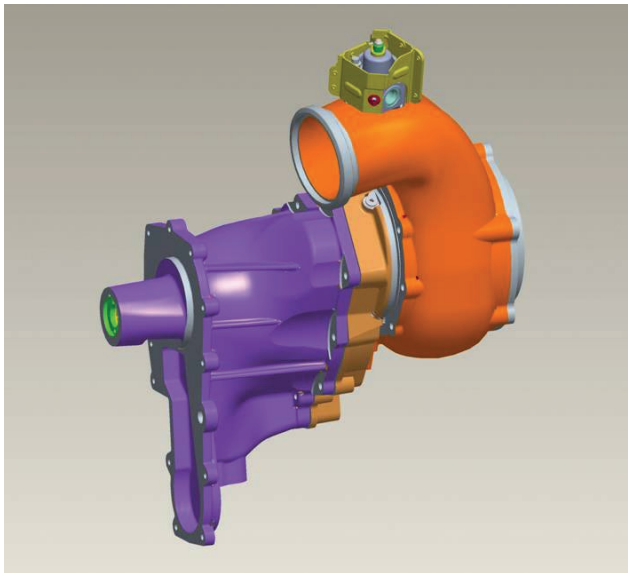

FIGURE 3. Computer Aided Design Drawing of the Turbocompound Unit

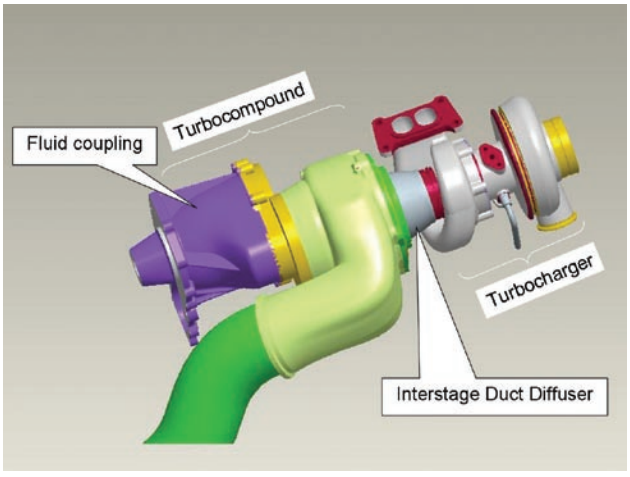

FIGURE 4. Computer Aided Design Drawing of the Turbocharger and Turbocompound Device Assembly Showing the Interstage Duct Diffuser and Fluid Coupling

- Base engine testing (ESC, Federal Test Procedure, road cycle) are done on a standard MD13 engine.
- Future plans
  - To test the compressor with a standard production turbocharger with three different diffusers.
  - To assemble and set instrumentation on the turbocharger and test in a hot-gas stand.
  - To manufacture and test the turbocompound unit.
  - To perform a functional test of the turbocharger and turbocompound device on an MD13 engine.

FY 2007 Publications/Presentations

1. Quarterly Reports DOE/NETL, Contract – DE-FC-05NT45421, 2006-2007.

2. FY2006 Report, DOE/NETL, Contract – DE-FC-05NT45421, 2006.

II.C.9 An Engine System Approach to Exhaust Waste Heat Recovery

David Patterson, Rich Kruiswyk
(Primary Contact)
Caterpillar Inc.
PO Box 1875
Mossville, IL 61552-1875

DOE Technology Development Manager:
John Fairbanks

NETL Project Manager: Ralph Nine

Subcontractors:
- Alipro, Peoria, IL
- ConceptsNREC, Oxon, UK
- eServ, Peoria, IL
- Turbo Solutions, Norwich, VT

Objectives

Overall Objective:

- Develop a new air management and exhaust energy recovery system that will demonstrate a 10% improvement in overall thermal efficiency with no emissions increase.
- Demonstrate resulting system and improvement benefits on a laboratory engine.

Phase II Objective:

- Validate approach to achieving project goal of 10% improvement in thermal efficiency via detailed component testing and analysis.

Accomplishments

- Designed, procured, and tested a novel nozzled/divided turbine stage, demonstrating a 5% improvement in turbine efficiency over standard production turbines.
- Designed, procured, and gas-stand tested a novel mixed-flow turbine stage, demonstrating the ability to shape the turbine efficiency characteristic to better match engine requirements.
- Designed, procured, and gas-stand tested a high efficiency compressor stage, demonstrating a 2-3% improvement in compressor efficiency over standard production compressors.
- Analyzed a Brayton bottoming cycle over the engine speed and load range. Engine thermal efficiency benefits of ~4% are predicted at full load; benefits of ~2.5% are predicted at half load.
- Completed aero designs for bottoming cycle turbomachinery components, with predicted efficiencies matching the requirements as determined by engine simulation.
- Completed preliminary design of a heat exchanger core for a bottoming cycle, with performance matching the requirements as determined by engine simulation.
- Conducted preliminary tests of an advanced turbocharger bearing design on a prototype turbocharger on the gas stand.

Future Directions

The Phase III objective is to carry out a mid-project demonstration of an improvement in thermal efficiency of 6-10% using prototype components. There will be two elements to this demonstration:

- An on-engine demonstration of a 4 to 4.5% improvement in thermal efficiency using advanced turbocharger technologies, intercooling, and insulated exhaust ports.
- A bench demonstration of the performance of the Brayton bottoming cycle components, worth another 3 to 4% improvement in thermal efficiency.

In addition, investigation of oil-less bearing technologies will continue. These technologies could simplify the remote mounting of the Brayton turbocharger. Development will continue on advanced turbine technologies. Investigation into transmission technologies for connecting the bottoming cycle to the engine will resume.

Introduction

Maintaining and improving fuel efficiency while meeting future emissions levels in the diesel on-road and off-road environments is an extremely difficult challenge. On today's heavy-duty diesel engines approximately 25% of the fuel energy leaves the exhaust stack as waste heat. Consequently, recovering energy from the diesel engine exhaust should pay significant dividends in improving diesel engine fuel efficiency. In this project Caterpillar is developing practical and production-viable solutions for improving waste heat recovery from heavy-duty diesel engines, with a goal of demonstrating a 10% improvement in thermal efficiency over today's production engines. Emphasis is placed on developing and incorporating cutting edge technologies

that meet demanding cost, packaging, and driveability requirements, and that are compatible with anticipated future aftertreatment needs. Technologies under investigation include high-efficiency turbochargers, compact high-efficiency heat exchangers, advanced bearing systems, and effective engine insulating components.

Approach

Achieving a 10% improvement in engine thermal efficiency via improved waste heat recovery is a very challenging goal. The Caterpillar team determined that achieving this goal with a practical and production-viable solution would require a system approach. This means developing technologies that will reduce all forms of exhaust energy loss, including: blowdown losses, aero machinery losses, fluid frictional losses, losses due to pulsating exhaust flow, heat transfer losses, and losses of energy out the exhaust stack. The team makes use of Caterpillar's advanced engine simulation and test capabilities to determine the performance targets of the individual components in the system. Detailed component design, analysis, and testing is then used to verify that the performance targets of each component in the system can be met. Consultation with outside technical experts is used to help push the envelope of component capabilities.

Results

The Caterpillar recipe for achieving a 10% improvement in engine thermal efficiency breaks down as follows: +4% from implementation of a bottoming cycle to recover stack waste heat, +3.7% from improving turbocharger efficiencies, +1.3% from intercooling the series turbocharging system, +0.5% from insulating the engine exhaust ports, and +0.5% from reducing exhaust piping flow losses. Progress in each of these areas is reported in the following:

Bottoming Cycle Development: A Brayton bottoming cycle was selected in Phase I of this project based on compatibility with future aftertreatment needs and system complexity. Detailed engine simulations over the speed and load range of a C15 on-highway heavy-duty truck engine were conducted to determine the performance capability of the system. Results of these simulations are shown in Figure 1. The results shown include the effects of the Brayton cycle along with the insulated exhaust ports and turbocharger intercooling, because the latter two building blocks have a strong effect on Brayton performance. As shown in the figure, the system is predicted to meet the target of +5.8% thermal efficiency at the peak torque design point. At half load, the predicted improvement is still an impressive +4%. These simulations are based on assumed efficiencies of the turbomachinery and

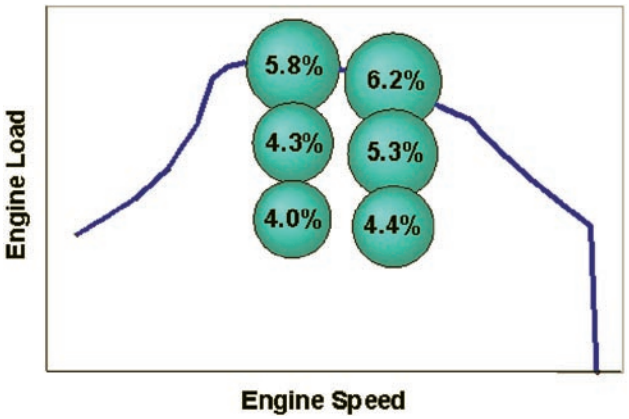

FIGURE 1. Brayton Cycle Simulation Results (Thermal Efficiency Benefit of Brayton Cycle + Port Insulation + Intercooling)

heat exchanger components, so the ability to design components to meet these efficiencies had to be verified.

For the Brayton turbocharger, aero designs of the turbine and compressor have been completed that meet the performance levels assumed in the engine simulations. Both designs are very similar to designs that have been used in prior research programs, and so confidence in the predicted efficiencies is high.

For the Brayton heat exchanger, the question is not whether a heat exchanger can be designed to meet the effectiveness and pressure drop requirements, but whether it can do so in a practical package size. Several advanced compact heat exchanger technologies are under investigation. A preliminary core design has been completed that meets the performance assumptions used in the simulation with a predicted core size of approximately 0.5 ft^3.

High Efficiency Turbomachinery: A novel high efficiency turbine with a nozzled/divided turbine housing was designed, procured, and tested on the Caterpillar gas-stand. Test results are shown in Figure 2. Turbine efficiency improvements of 4-6% over today's current production high-pressure (HP) turbine stage were measured. This should translate to an improvement of approximately 1% in engine thermal efficiency according to engine simulations.

A novel mixed-flow turbine was designed, procured, and tested on the Caterpillar gas-stand. Test results are shown in Figure 3. While peak efficiency levels fell short of the target, the goal of shaping the efficiency characteristic to better match on-engine requirements was achieved. Improvements to the efficiency levels in a Gen2 design are expected to result in engine thermal efficiency improvements between 0.5 and 1%.

An advanced high efficiency compressor stage was designed, procured, and tested on the Caterpillar gas-stand. A sample test result is shown in Figure 4. Compressor efficiency improvements of 2-3% were

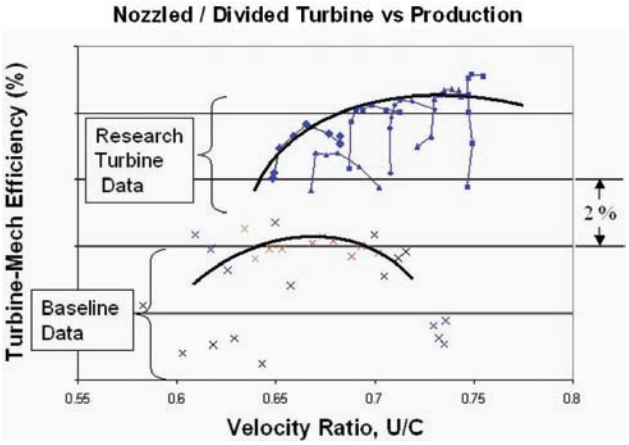

FIGURE 2. Radial-Nozzled-Divided Turbine Gas Stand Results

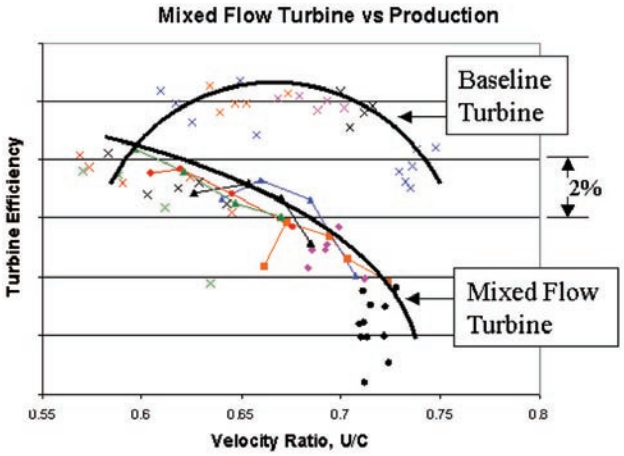

FIGURE 3. Mixed Flow Turbine Gas Stand Results

measured relative to today's production compressor stages. Duplicating this performance on both the HP and low-pressure (LP) compressors should translate to an engine thermal efficiency improvement of approximately 0.7% according to engine simulations.

Aero design work has been completed for an advanced LP axial turbine stage. The predicted turbine efficiency is approximately 6% higher than the current production LP turbine stage, and that performance should translate to an engine thermal efficiency improvement of 1% according to engine simulations. This stage is similar to axial stages Caterpillar has designed and tested for other research programs, and so confidence is high that the predicted performance will be achieved once hardware is procured and tested.

Intercooling: Engine simulation was used to evaluate the benefit of air-to-air intercooling to a series turbocharged truck engine, and a design point improvement of 1.3% in thermal efficiency is predicted. Preliminary design and analysis of an air-to-air intercooler stage that will package in an on-highway

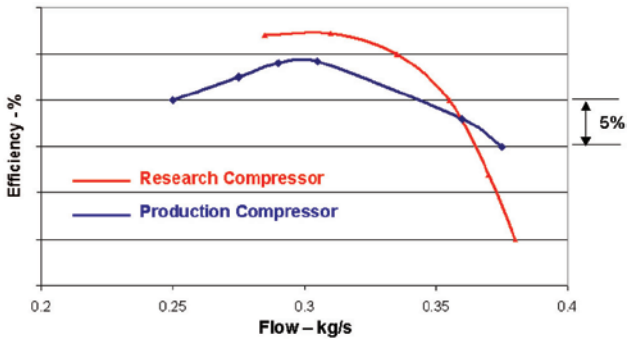

FIGURE 4. High Efficiency Compressor Gas Stand Results

truck chassis was conducted as part of Caterpillar's Heavy Truck Clean Diesel DOE project, and that work will be continued as this project advances.

Exhaust Port Insulation: Engine simulation was used to evaluate the benefit of exhaust port insulation to a series turbocharged truck engine, and a design point improvement of 0.5% is predicted.

Reduced Piping Flow Losses: During the Phase I recipe definition, it was estimated that a 0.5% thermal efficiency improvement could be achieved from reduction of flow losses in the piping system of the baseline series turbocharged truck engine. Since work in this phase was focused on component development, there are no results to date in this area.

Conclusions

The results of components tests, component design and analysis, and engine simulation has resulted in high confidence that the project goal of a 10% improvement in engine thermal efficiency can be achieved.
A predicted system-level benefit of 8.5% is solidly based on a combination of:

1. Components for which performance has been demonstrated via bench tests of prototype hardware.
2. Components for which performance has been predicted from design/analysis tools. In these cases confidence is bolstered by the similarity of these components to prototypes that have been demonstrated in hardware as part of prior research programs.

Additional technologies are under investigation and show promise for further improvements, thus leading to the conclusion that the 10% target can be met.

FY 2007 Publications/Presentations

1. Presented on 19 June 2007 at the U.S. DOE Semi-Mega Merit Review, Arlington, VA.

2. Presented on 15 August 2007 at the U.S. DOE Diesel Engine-Efficiency and Emissions Research (DEER) conference, Detroit, MI.

II.C.10 Demonstration of Air-Power-Assist (APA) Engine Technology for Clean Combustion and Direct Energy Recovery in Heavy-Duty Application

Dr. Hyungsuk Kang (Primary Contact),
Dr. Chun Tai
Volvo Powertrain North America
13302 Pennsylvania Avenue
Hagerstown, MD 21742

DOE Technology Development Manager:
Roland Gravel

NETL Project Manager: Samuel Taylor

Subcontractors:
- Sturman Industries, Woodland, CO
- University of California, Los Angeles, CA
- Dr. Paul Blumberg, Consultant, MI

Objectives

- Demonstrate APA engine technology that enables 15% fuel economy improvement for heavy-duty refuse truck application.

Accomplishments

- APA engine experimental setup was completed.
- APA engine functional testing was completed.
- Preliminary APA engine testing was completed.

Future Directions

- Analysis of test results with simulation results.
- Develop advanced hybrid engine control strategy.

Introduction

The concept of APA is to use the engine to convert braking energy into compressed air stored in an on-board tank. Later, during acceleration, the engine is powered by the stored compressed air with or without burning diesel fuel to get up to speed or until the compressed air is depleted. Once the vehicle has attained a cruising speed, the engine reverts back to a conventional diesel engine. The positive pumping work performed by compressed air during the intake stroke is added to the work performed by combustion gas during the gas expansion stroke. The additional work performed by the compressed air permits a reduction in the quantity of fuel needed to achieve the required engine power. In this way, the engine efficiency is increased, and the vehicle fuel economy is improved. The high boost pressure during engine acceleration helps reduce the emissions of particular matter. In addition, smaller quantities of fuel burned in each cylinder during each cycle lead to lower peak temperatures, which result in lower NOx emissions. The noise from the sudden exhaust gas blow-down process during engine braking is reduced by minimizing the pressure difference across the engine valves, and the reduced noise is further muffled by the air tank. This provides a solution to the noise issue that a conventional engine brake has. Therefore, regenerative compression braking can be utilized in the areas where conventional engine braking is prohibited due to its noise pollution. This facilitates greater usage of the engine brake, which in turn helps save fuel and reduces the frequency of brake service with its associated costs.

In summary, the APA engine absorbs the vehicle kinetic energy during braking, puts it into storage in the form of compressed air (air compressor [AC] mode), and reuses it to assist in subsequent vehicle acceleration (air motor [AM] mode).

The APA engine showed a 4-18% improvement in fuel economy over a wide range of driving cycles [1]. The amount of improvement depends on the cycle. The energy saving principle of this technology is similar to that of the electric hybrid technology, except that the high capital cost for an electric hybrid drive train is avoided.

Approach

A GT-Power™ engine simulation model was constructed to predict engine efficiency based on the second-law thermodynamic availability at various operating conditions and optimization of valve timing were achieved as well. The engine efficiency map generated by the engine simulation was then fed into a simplified vehicle model to predict fuel consumption of a refuse truck on a simple collection cycle and then proved a 4-18% fuel economy improvement over a wide range of driving cycles. Design and analysis work supporting the concept of retrofitting an existing hydraulic valve actuator (HVA) system with the modifications that are required to run the HVA system with APA functionality were completed. APA engine with HVA system was implemented to prove the concept of APA engine technology and preliminary APA engine testing was completed.

Results

Preliminary APA engine testing was completed in 2007. A Volvo MD11 (11L, 6-cylinder and 4 valves per cylinder) engine was used for the APA engine with HVA system. A general overview of the entire APA engine with air handling system is shown in Figure 1. In this view, one can see the exhaust three-way valves, compressor bypass valve system, an air tank and associated piping with HVA system.

Experimental Results

APA engine testing in AC mode was performed at 800 rpm and 5 bar air tank pressure by changing the exhaust valve opening (EVO) timing from 235° crank angle (CA) to 323° CA. A two-stroke engine mode is employed during AC mode. Figure 2 shows valve traces with changing EVO which can adjust exhaust valve duration time by using the flexible HVA system. Exhaust valve duration time and lift length are decreased with retarding EVO because the exhaust valves in AC mode run in ballistic trajectory, so their lift can't be controlled.

P-V diagrams for changing EVO are shown in Figure 3 at 5 bar air tank pressure and 800 rpm. Intake valve opening (IVO), intake valve closing (IVC) and exhaust valve closing (EVC) timing are constant at each case. When the exhaust valve is opened, in-cylinder pressure and air tank pressure are in equilibrium, however, the in-cylinder pressure increased by about 8.6 bar before opening the exhaust valve and then in-cylinder pressure decreased rapidly to equalize with air tank pressure after opening exhaust valve at EVO 323° CA.

Figure 4 shows negative torque (brake torque) in AC mode by changing EVO at each air tank pressure.

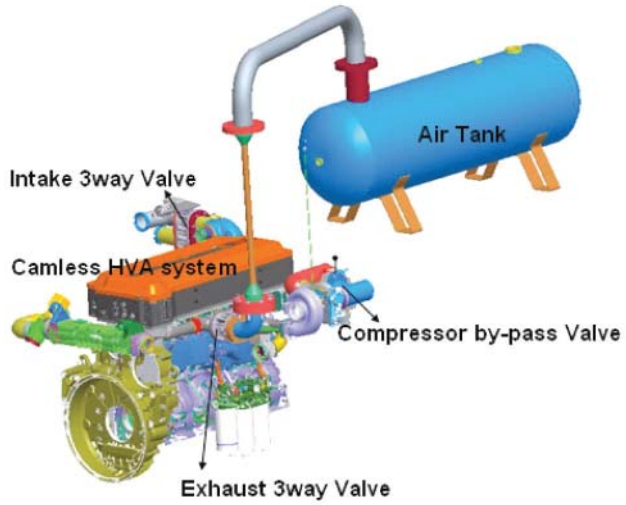

FIGURE 1. General View of the APA Air Handling System

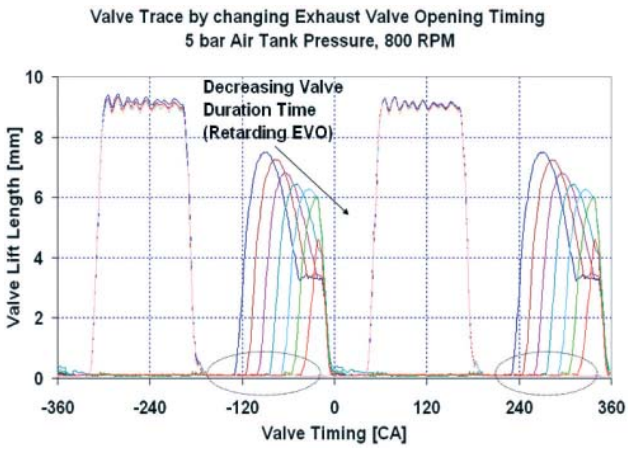

FIGURE 2. Valve Trace by Changing EVO at 5 Bar Air Tank Pressure, 800 RPM

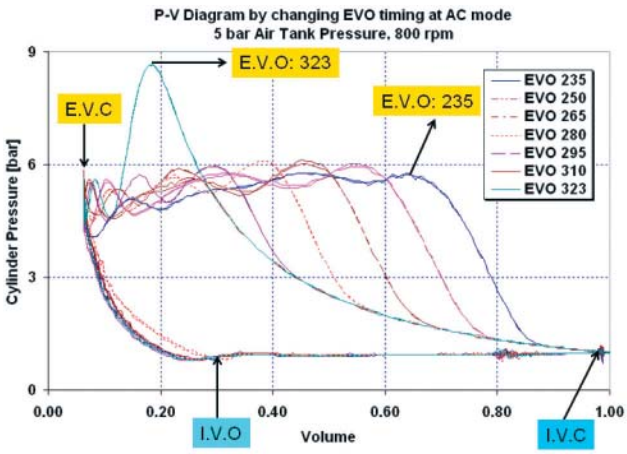

FIGURE 3. P-V Diagram by Changing EVO in AC Mode

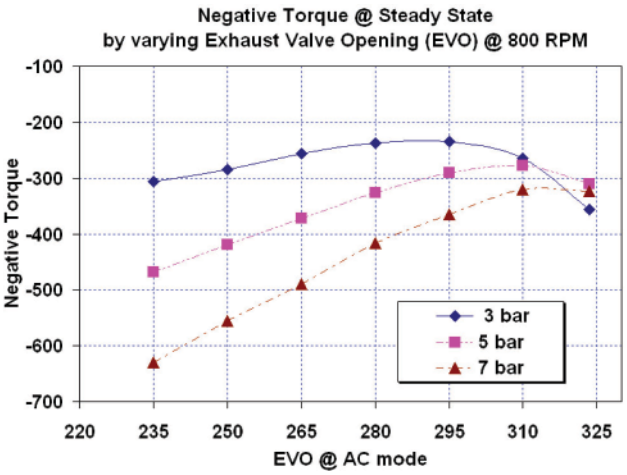

FIGURE 4. Negative Torque by Changing EVO at each Air Tank Pressure, 800 RPM

To keep constant air tank pressure, a pneumatically controlled relief valve was installed on the air tank. At each constant air tank pressure, there is a specific EVO timing which can generate a minimum negative torque. It means that a minimum engine braking energy requires achieving desired compressed air in the air tank at the specific EVO timing. Negative torque decreased with decreasing exhaust valve duration time and was optimum at EVO 310° CA for 5 and 7 bar air tank pressure.

Transient Testing from AC to AM mode

APA transient engine testing was conducted from AC to AM mode at constant speed with constant valve timing. Figure 5 shows an air tank pressure trace and engine brake torque from AC to AM at 800 RPM and fixed valve timing. When the air tank pressure reached about 10 bar during AC mode, the APA engine switched mode from AC to AM by changing valve timing and opening the intake three-way valve simultaneously. The compressed air in the air tank flowed from the exhaust side to the intake side while generating power without injecting fuel. Figure 6 shows engine brake torque from AC to AM mode by changing EVC in the AM mode. After switching to the AM mode, 10 bar air tank pressure could generate positive torque and the amount of positive torque depends on EVC in the AM mode.

Conclusions

The concept of APA engine technology was proved by experimental testing. APA engines can generate power without using fuel injection system based on these experimental tests.

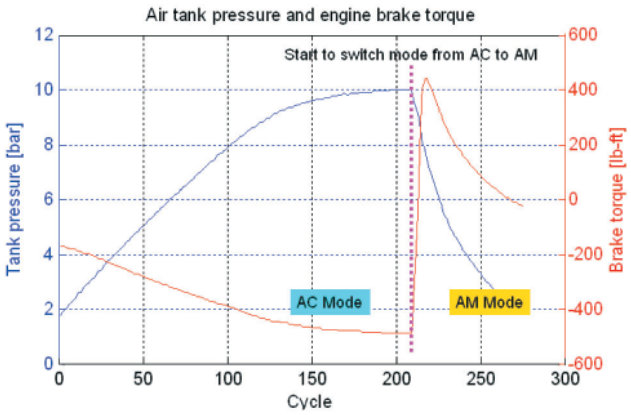

FIGURE 5. Air Tank Pressure and Torque from AC to AM Mode at 800 RPM, Fixed Valve Timing

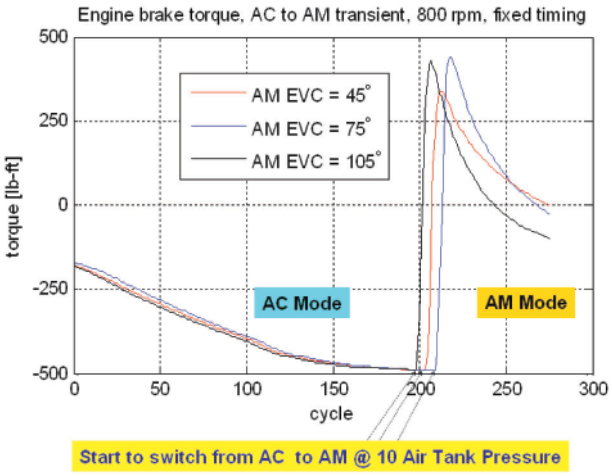

FIGURE 6. Torque from AC to AM Mode at 800 RPM by Changing EVC in AM Mode

References

1. Kang, H., "Demonstration of Air-Power-Assist Engine Technology for clean combustion and direct energy recovery in heavy duty application", Presentation, DEER Conference, Detroit, 2007.

FY 2007 Publications/Presentations

Publications

1. Kang, H. et al., "Demonstration of Air-Power-Assist Engine Technology for clean combustion and direct energy recovery in heavy duty application", Phase III Quarterly Reports, January, July and October 2007.

2. Kang, H. et al, "Demonstration of Air-Power-Assist Engine Technology for clean combustion and direct energy recovery in heavy duty application", SAE Technical Paper 08PFL-298 on processing.

Presentations

1. Kang, H., "APA project technical review", Local Internal Review Presentation, Hagerstown, MD. January and September 2007.

2. Tai, C., "APA project technical review" Presentation for DOE merit review, Washington, D.C. June, 2007.

3. Kang, H., "Demonstration of Air-Power-Assist Engine Technology for clean combustion and direct energy recovery in heavy duty application", Aug. 14th DEER Conference, Detroit, 2007.

4. Kang, H. et al., "APA project Phase III review meeting". Hagerstown, MD, Nov. 2007.

II. ADVANCED COMBUSTION AND EMISSION CONTROL RESEARCH FOR HIGH-EFFICIENCY ENGINES

D. Health Impacts

II.D.1 Health Effects from Advanced Combustion and Fuel Technologies

James Parks (Primary Contact), John Storey, Laura Kranendonk, Sam Lewis, Brian West
Oak Ridge National Laboratory
P.O. Box 2008, MS 6472
Oak Ridge, TN 37831-6472

DOE Technology Development Manager:
James J. Eberhardt

Objectives

- Understand potential impact of developing fuel, combustion, and aftertreatment technologies on air quality and, thereby, human health.
- Quantify mobile source air toxic emissions from advanced technologies.
- Link emissions measured in laboratory setting to air quality impact, and thereby, health impact.

Accomplishments

- Measured mobile source air toxics (MSATs) from European Saab Biopower vehicle that is optimized for performance with E85 fuel to provide information on the health impact of ethanol fuel introduction.
  - E85 increases cold-start ethanol emissions to levels of 48 mg/mile on the Federal Test Procedure (FTP) driving cycle.
  - E85 reduces gasoline-derived MSAT emissions by a factor of 10 as compared with gasoline fuel over the FTP and US06 driving cycles.
- Characterized mobile source air toxics from high efficiency clean combustion (HECC) on a diesel engine to determine any health impacts of advanced diesel combustion modes.
  - Formaldehyde emissions from HECC were a factor of two higher than the traditional diesel combustion emissions.
  - Acetaldehyde and acrolein emissions were also observed to increase significantly during HECC operation.

Future Directions

- Evaluate the impact of butanol fuel addition to ethanol-gasoline fuel mixtures on emissions.
- Determine the efficiency of catalytic aftertreatment for reduction of MSATs from HECC diesel operation.

Introduction

Scientists and engineers at national laboratories, universities, and industrial companies are developing energy efficient technologies for transportation, and the U.S. Department of Energy (DOE) is actively involved in this innovative research. However, care must be taken to insure that any new technology developed for transportation must not adversely directly impact human health or impact the health of the environment, which subsequently may impact human health. To address this need, DOE sponsors research studies on the potential health impacts of advanced technologies for transportation including advanced fuels, combustion techniques, and emissions controls (also known as “aftertreatment” or, more commonly, “catalytic converters”). DOE sponsored health impact research activities at Oak Ridge National Laboratory (ORNL) are presented in this report.

ORNL conducts research on advanced fuel, combustion and emissions control technologies at the National Transportation Research Center (a joint ORNL and University of Tennessee research center) in Knoxville, TN. As the research is being conducted on engine and chassis dynamometers, specific studies of the potential health impacts of the technologies are conducted by the ORNL team for DOE’s health impacts program. Results from two ORNL studies in FY 2007 are presented here. Both studies focused on measuring MSATs from advanced technologies; the technologies were (1) an ethanol fuel optimized vehicle and (2) an advanced diesel combustion technique that results in simultaneous reduction of NOx and particulate emissions called HECC.

Approach

MSATs from E85 Fueled Vehicle

A 2007 Saab 9-5 Biopower 2.0t vehicle was acquired by ORNL and DOE and evaluated for fuel efficiency performance on E85 and gasoline fuels [1]. The engine is optimized for performance with E85 fuel and in fact accelerates faster to 60 mph with E85 vs. gasoline fuel. CO emissions are lower with E85 fuel and the emissions overall are below U.S. EPA Tier 2, Bin 5 levels. MSAT

emissions were sampled and analyzed with a variety of techniques including Fourier transform infrared (FTIR) and gas and liquid chromatography via collection with 2,4-dinitorophenylhydorazine (DNPH) cartridges. The measurements were cycle averages for the FTP and US06 driving cycles; a photo of the vehicle on the chassis dynamometer is shown in Figure 1. In addition to MSAT emissions, ethanol, an unregulated species, was quantified.

MSATs from HECC Diesel Mode

A Mercedes 1.7-liter 4-cylinder diesel engine was operated at 1,500 rpm and 2.6 brake mean effective pressure (BMEP) on an engine dynamometer under production calibration conditions that are typical of traditional diesel combustion. The engine is shown in Figure 2. The load and speed chosen are representative of a universal moderate load condition for a light-duty vehicle. The engine was also operated at the same speed and load with the engine operating in HECC mode. The MSAT emissions from both the traditional and advanced HECC combustion modes were measured with FTIR and gas and liquid chromatography via collection with DNPH cartridges.

FIGURE 1. Saab 9-5 Biopower Vehicle on a Chassis Dynamometer

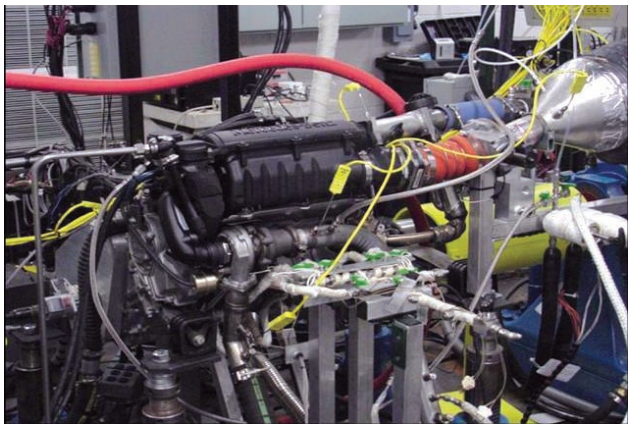

FIGURE 2. Diesel Engine Operated in HECC in ORNL's Engine Dynamometer Laboratory

Results

MSATs from E85 Fueled Vehicle

Ethanol emissions with E85 fuel operation were found only during the FTP driving cycle, but aldehyde emissions, typically associated with alcohol motor fuels, were higher than with gasoline operation, as shown in Figure 3. All of the FTP emissions essentially occurred in Bag 1 of the driving cycle, which indicates that the ethanol emissions were primarily due to cold operating conditions. Qualitative observation of the FTIR data indicated that the first thirty seconds of the Bag 1 portion was the source of both the ethanol and aldehyde emissions. The very low levels of aldehyde emissions during the US06 indicate that they are primarily associated with cold operation.

Although an increase was observed in ethanol emissions from E85 for cold conditions, E85 fuel demonstrated beneficial reduction of some MSAT species. Figure 4 shows select MSAT species emissions that are derived from gasoline fuel. The summation of these MSAT emissions decreased substantially for the E85 fuel relative to gasoline. The MSAT reduction occurred for both FTP and US06 driving cycles. Note that the US06 gasoline fuel results show higher levels of MSATs than the FTP gasoline fuel data due to the more aggressive driving cycle of the US06 test which results in more enrichment operation of the engine; enrichment

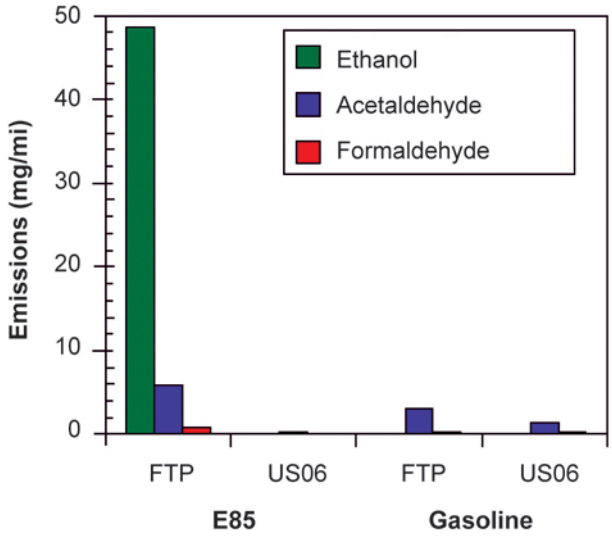

FIGURE 3. Ethanol and Aldehdye Emissions as a Function of Driving Cycle

leads to higher levels of unburned hydrocarbon emissions from the engine.

MSATs from HECC Diesel Mode

Diesel operation with the advanced HECC technique leads to a simultaneous reduction in NOx and particulate emissions without sacrificing fuel efficiency. At the 1,500 rpm, 2.6 BMEP operating condition used in this study, HECC operation resulted in a 90% reduction in NOx and a 70% reduction in smoke as compared with traditional diesel combustion. However, MSAT emissions for HECC were greater than with traditional diesel combustion. Figure 5 shows three common diesel MSAT emissions (formaldehyde, acetaldehyde, and acrolein) expressed in mass per time units for HECC and baseline (traditional combustion) conditions. Increases in the concentration of these species were even more significant due to the fact that lower exhaust flow results from HECC. Since emission regulations are mass-based as opposed to concentration-based, the emissions data here is reported as mass. The formaldehyde emissions were the highest and were almost double for HECC vs. the baseline. Although acetaldehyde and acrolein emissions were lower than formaldehyde, the increase in acetaldehyde and acrolein emissions relative to the baseline case were more dramatic. All the data reported here was obtained without emission control in the engine exhaust. Catalytic aftertreatment may be able to substantially reduce the increased MSAT emissions measured and will be the focus of future work.

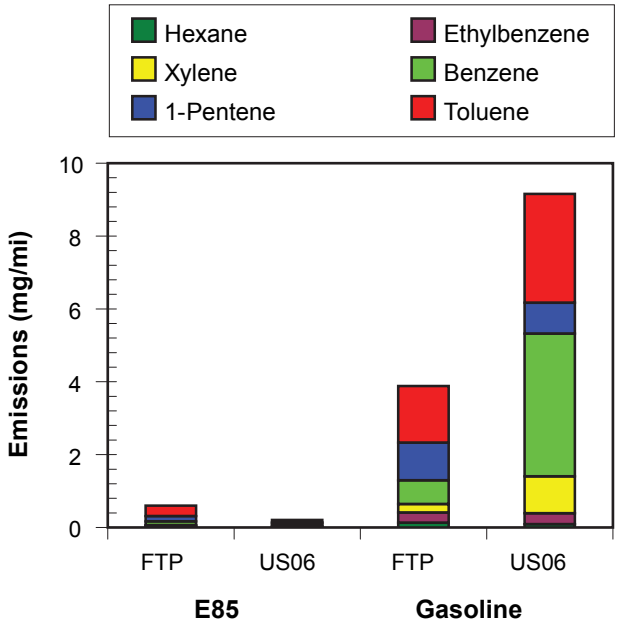

FIGURE 4. Gasoline-Derived MSAT Emissions as a Function of Driving Cycle and Fuel

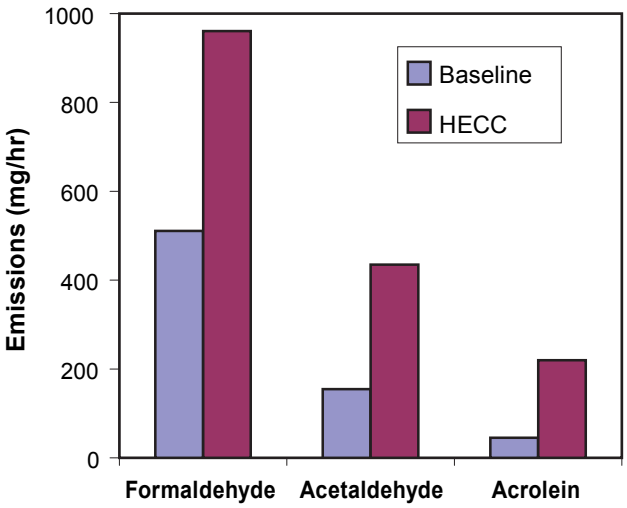

FIGURE 5. Formaldehyde, Acetaldehyde, and Acrolein emissions as a Function of Combustion Mode

Conclusions

- E85 Fueled Saab Biopower Vehicle:
  - E85 fuel decreases the amount of gasoline-derived MSATs by a factor of approximately 10 in comparison to gasoline fuel during FTP and US06 driving cycles.
  - Ethanol emissions increase dramatically for E85 in comparison to gasoline for the FTP driving cycle due to cold start emissions, but no increase in ethanol emissions were observed for the higher temperature US06 driving cycle.
- High Efficiency Clean Combustion:
  - In comparison to traditional diesel combustion, HECC operation results in lower NOx and particulate matter emissions; however, MSAT emissions from HECC were higher.
    - Formaldehyde emissions from HECC were almost a factor of two greater than from traditional combustion.
    - Acetaldehyde and acrolein emissions, while not as great as formaldehyde emissions, were observed at significantly higher quantities for HECC vs. traditional combustion.

References

1. Brian West, Alberto Lopez, Timothy Theiss, Ronald Graves, John Storey, Sam Lewis, "Fuel Economy and Emissions of the Ethanol-Optimized Saab 9-5 Biopower", *Society of Automotive Engineers Technical Paper Series* 2007-01-3994 (2007).

FY 2007 Publications/Presentations

1. Jim Parks, Sam Lewis, John Storey, Terry Miller, Joshua Fu, Boris Hromis, and Ralph McGill, "Mobile Source Air Toxics Measured at a Hot Spot of Diesel Truck Idling Emissions", *Presentation at the CRC Mobile Source Air Toxics Workshop* in Phoenix, AZ on October 24–25, 2006.

2. Terry Miller, Josh Fu, Boris Hromis, John Storey, and James Parks, "Diesel Truck Idling Emissions – Measurement at a PM2.5 Hot Spot", *Transportation Research Board,* Paper No. 07-3157 (2007).

3. James E. Parks, John M. E. Storey, Terry L. Miller, Joshua S. Fu, and Boris Hromis, "Diesel Truck Idling Emissions – Mobile Source Air Toxics Measured at a Hot Spot", *Transportation Research Board,* Paper No. 07-3158 (2007).

4. Douglas R. Lawson, John M. E. Storey, and James E. Parks II, "The OFCVT Health Impacts Program", *Poster Presentation at the 13th Diesel Engine-Efficiency and Emissions Research (DEER) Conference* in Detroit, MI on August 13-16, 2007.

5. Brian West, Alberto Lopez, Timothy Theiss, Ronald Graves, John Storey, Sam Lewis, "Fuel Economy and Emissions of the Ethanol-Optimized Saab 9-5 Biopower", *Society of Automotive Engineers Technical Paper Series* 2007-01-3994 (2007).

II.D.2 Collaborative Lubricating Oil Study on Emissions (CLOSE) Program

Dr. Douglas R. Lawson
National Renewable Energy Laboratory
1617 Cole Boulevard
Golden, CO 80401

DOE Technology Development Manager:
Dr. James J. Eberhardt

Subcontractors:
- Southwest Research Institute
  6220 Culebra Road
  San Antonio, TX 78228
- Desert Research Institute
  2215 Raggio Parkway
  Reno, NV 89512

Objective

The objective of this project is to quantify the role of engine lubricating oil on particulate matter (PM) emissions from in-use motor vehicles fueled with gasoline, 10% ethanol (E10), diesel, biodiesel, and compressed natural gas (CNG) while operating on fresh and used crankcase lubricants.

Accomplishments

- Established a Cooperative Research and Development Agreement (CRADA) between NREL and the South Coast Air Quality Management District (SCAQMD) and the California Air Resources Board (CARB) for program funding.
- Obtained funding from the Coordinating Research Council (sponsored by the automotive and petroleum industries) for program support.
- Obtained support from the American Chemistry Council Petroleum Additives Product Approval Protocol Task Group to provide new and aged engine lubricating oils for all vehicles that will be tested in the program.
- Increased scope of project to include medium-duty vehicles and E10 and biodiesel fuel testing as part of the overall project.
- Began testing of first vehicle in program in May 2007.

Future Directions

A variety of light-, medium-, and heavy-duty (LD, MD, HD) vehicles will be tested over different driving test cycles at room temperature (72°F) and cold temperature (20°F) on chassis dynamometers. The test matrix depicting the vehicles and test conditions is shown in Table 1.

TABLE 1. CLOSE Program Test Matrix

Test Temperature	72°F (nominal)				20°F			
Test Lubricant	Fresh		Aged		Fresh		Aged	
Vehicle / Sample Number	1	2	1	2	1	2	1	2
LD gasoline (normal PM emitter)	√	√	√	√	√	√	√	√
LD gasoline (high PM emitter)	√	√	√	√	√	√	√	√
LD E10 (normal PM emitter)	√	√	√	√	√	√	√	√
LD E10 (high PM emitter)	√	√	√	√	√	√	√	√
MD diesel (normal PM emitter)	√	√	√	√	√	√	√	√
MD diesel (high PM emitter)	√	√	√	√	√	√	√	√
MD biodiesel (normal PM emitter)	√	√	√	√	√	√	√	√
MD biodiesel (high PM emitter)	√	√	√	√	√	√	√	√
HD CNG (normal PM emitter)	√	√	√	√				
HD CNG (high PM emitter)	√	√	√	√				
HD diesel (normal PM emitter)	√	√	√	√				
HD diesel (high PM emitter)	√	√	√	√				

The engine lubricating oil used in the program is labeled with deuterated hexatriacontane ($C_{36}D_{74}$). This tracer, along with other naturally-occurring compounds found in lubricating oil, such as hopanes and steranes, will be used to quantify the relative contributions of PM formed from the fuels and the lubricants used in the vehicles that will be tested.

Normal and high-emitting vehicles representing gasoline, diesel, and CNG-powered vehicles will be tested. Lubricants used in each technology will be representative of those currently on the market, with both new and aged lubricants being tested in the program. The fuels used in the vehicles will be gasoline containing no ethanol, E10, CARB diesel, biodiesel, and CNG. Room temperature and cold temperature testing will be performed on all of the light- and medium-duty

vehicles. Cold temperature testing will not be conducted on the heavy-duty vehicles due to funding limitations.

The data collected throughout the study will be chemically analyzed with detailed speciation to quantify the relative importance of the fuel and lubricant to PM emissions from these vehicles under the variety of testing conditions specified in the study design.

Introduction

Recent air quality studies conducted in Denver, Phoenix, Washington D.C., and Office of FreedomCAR and Vehicle Technologies' (OFCVT) Gasoline/Diesel PM Split Study in Los Angeles have shown that PM from gasoline engines is a more significant contributor to ambient air quality than PM from diesel engines [1,2]. For example, data collected in Washington, D.C., over a ten-year period suggest that PM from gasoline exhaust is ten times more important to the emission inventory than diesel exhaust, as shown in Figure 1 [3].

OFCVT's Comparative Toxicity Studies have also shown that the toxicity from gasoline exhaust on a per-unit-mass basis is at least as toxic as that from diesel exhaust, and that high emitters' toxicity is even greater than that from normal emitters [4].

Because PM from both gasoline and diesel exhaust is so important to human health and ambient air quality, it is important to understand its source – whether it derives from the fuel, the lubricant, or both, and to understand the engine operating conditions that are responsible for PM emissions. That is the objective of the CLOSE Program.

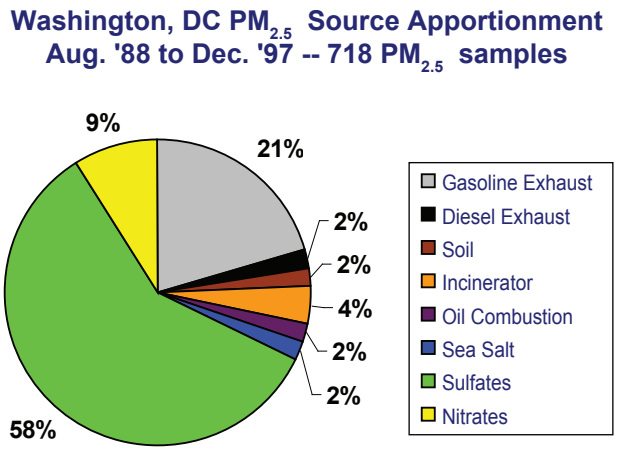

FIGURE 1. Source apportionment of $PM_{2.5}$ in the Washington, D.C. area. Samples were collected between 1988 and 1997.

Approach

The CLOSE Program will conduct extensive chemical and physical characterizations of PM emissions from vehicles fueled with gasoline, E10, diesel, biodiesel, and natural gas while operating on fresh and used crankcase lubricants in an effort to improve our current understanding of the impact of crankcase lubricant formulations on vehicle PM emissions. In-use light- and heavy-duty vehicles are being recruited, including both normal and high-PM emitters, and operated on chassis dynamometers at room temperature (72°F nominal) and 20°F. Gaseous (total hydrocarbons [THC], non-methane hydrocarbons [NMHC], carbon monoxide [CO], nitrogen oxides [NOx]) and real-time particle emissions are being measured, and PM and semivolatile organic compound (SVOC) samples are being collected for subsequent chemical analyses. Physical PM measurements will be conducted to obtain data on particle size, which will be investigated over the various driving conditions carried out on the dynamometers.

Results

At the time of this report, vehicle testing has begun on the light-duty normal emitter, which is a 2006 Chevy Impala having 37,000 miles on the odometer. Figure 2 shows the vehicle on the dynamometer, and Figure 3 shows the sampling ports and equipment used in the sampling tunnel.

FIGURE 2. Light-Duty Normal Emitter Tested in the CLOSE Program, a 2006 Chevrolet Impala

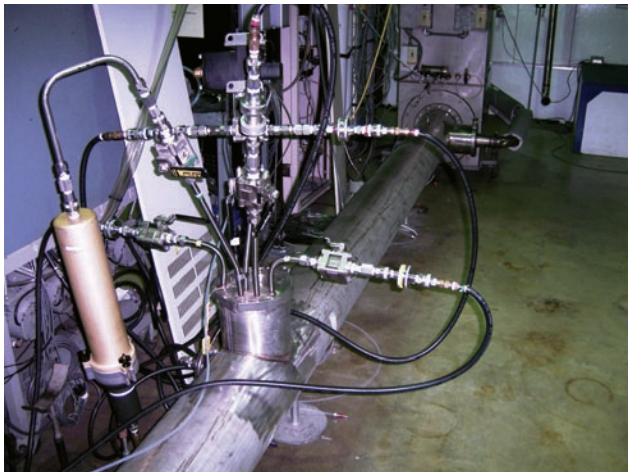

FIGURE 3. Sampling Probes Used to Collect Exhaust Emissions Samples from the Dilution Tunnel

Conclusions

Because this project has just started, there are no conclusions at the time of this report. The CLOSE Program will be completed by December 2008, so results will be available at that time.

References

1. Fujita, E.M., D.E. Campbell, W.P. Arnott, B. Zielinska, J.C. Chow. Evaluations of Source Apportionment Methods for Determining Contributions of Gasoline and Diesel Exhaust to Ambient Carbonaceous Aerosols, *J. Air & Waste Manage. Assoc.*, Vol. 57, pp. 721-740 (2007).

2. Lough, G.C. and J.J. Schauer. Sensitivity of Source Apportionment of Urban Particulate Matter to Uncertainty in Motor Vehicle Emissions Profiles, G.C. Lough and J.J. Schauer, *J. Air & Waste Manage. Assoc.*, Vol. 57, pp. 1200-1213 (2007).

3. Kim, E. and P. K. Hopke. Source Apportionment of Fine Particles in Washington, D.C., Utilizing Temperature-Resolved Carbon Fractions, *J. Air & Waste Manage. Assoc.*, Vol. 54, pp. 773-785 (2004).

4. McDonald, J.D., I. Eide, J.C. Seagrave, B. Zielinska, K. Whitney, D.R. Lawson, J.L. Mauderly. Relationship between Composition and Toxicity of Motor Vehicle Emission Samples, Environ. Health Persp., Vol. 112, pp. 1527-1538 (2004).

FY 2007 Publications/Presentations

1. "The Collaborative Lubricating Oil Study on Emissions (CLOSE) Project," presented at DEER 2007 Conference, Detroit, MI; August 15, 2007.

II.D.3 Health Impacts: Respiratory Response

Joe L. Mauderly
Lovelace Respiratory Research Institute
2425 Ridgecrest Dr. SE
Albuquerque, NM 87111

DOE Technology Development Manager:
James J. Eberhardt

NETL Project Manager: Ralph Nine

Objectives

- Compare health hazards of competing power technologies
- Determine the most biologically important components of emissions
- Evaluate health benefits of emission reduction technologies
- Evaluate emerging technologies for unanticipated health hazards

Approach

- Use animal and cell tests to characterize and quantify adverse health effects.
- Adapt, optimize, and validate biological test systems for emissions testing.
- Test whole and fractionated emissions from engines operated in the laboratory and vehicles operated elsewhere.
- Conduct detailed physical-chemical analysis of emissions and samples.
- Use physical-chemical fractionation and exposures to specific compounds to identify and confirm toxic components.
- Examine emerging technologies prior to commercialization.

Accomplishments

- Evaluated health effects of inhaled nanoparticles from new and used diesel crankcase oil and sulfate.
- Discovered that oil and sulfate nanoparticles had little lung toxicity, but altered responses of immune cells elsewhere in the body.
- Completed analysis of results from a comprehensive study of the effects of repeated inhalation exposure to laboratory-generated gasoline emissions.
- Discovered that inhaled nitrogen oxide and carbon monoxide can duplicate some effects of gasoline emissions on blood vessels outside the lung.

Future Directions

- This subproject of the Health Impacts activity will be completed in early FY 2008.
- Wrap-up will include examining effects of nanoparticles and emission gases at lower concentrations, and publishing results.
- Future effort in this area will focus on evaluating emerging technologies.

Introduction

This project is the biological evaluation subproject of the Health Impacts activity, and supports meeting DOE technical targets by: 1) placing in proper context the health hazards of engine emissions relative to other air quality hazards; 2) comparing the relative hazards of emissions from different fuel, engine, and emission reduction technologies; 3) determining the key toxic components among the hundreds of components of vehicle emissions; 4) demonstrating that reductions in emissions are paralleled by reductions in health hazards; and 5) evaluating emissions from emerging technologies to avoid unintended health consequences prior to commercialization. This project addresses potentially technology-limiting issues that are not addressed in other DOE or non-DOE programs. This project complements other Health Impacts subprojects that are characterizing emissions, determining the impacts of emissions on air quality, and conducting long-term health studies of 2007-2010-compliant diesel systems.

Approach

This project employs a four-tactic strategy to placing the health hazards of vehicle emissions in proper context, identifying the key toxic components, and evaluating new technologies. The first tactic involves laboratory evaluations of emission samples collected from vehicles and environments elsewhere. The second tactic involves animal studies of inhaled whole emissions, separated fractions of emissions, and specialized aerosols generated in the laboratory. Tissue oxidative stress, lung inflammation, cardiovascular effects, and immune responses are evaluated. The third tactic employs multivariate and univariate statistical analyses of data on composition vs. biological response

to identify components that cause adverse effects. The fourth tactic involves working with DOE managers and industry partners to identify advanced technologies having the greatest near-term commercialization potential, and using the above approaches to evaluate those technologies for unintended health consequences.

Work during the past year focused primarily on two issues pertaining to current technologies in order to clarify issues that must be addressed for emerging technologies: 1) the health importance of emission nanoparticles; and 2) the health effects of gases that comprise the non-particulate components of gasoline and diesel engine emissions. There has been considerable speculation about the health effects of so-called "nanoparticles" (under 50 nm diameter) from combustion and other sources. Questions have been raised about the importance of nanoparticles formed by condensation of vapors downstream of exhaust after-treatment devices. Such particles have always existed in engine emissions, but no technology has been available for separating them from other emissions for biological studies. A vaporization-condensation method was developed by this project last year to generate aerosols of nanoparticles from crankcase oil and sulfate, which are the primary sources of this material in contemporary emissions. This year, mice were exposed by inhalation to aerosols of new and used diesel engine lubrication oil and sulfate at a single high concentration to determine if measurable effects occur.

During the past few years, this project collaborated with other federal and non-federal partners (including several major large engine manufacturers and fuel providers) to conduct detailed studies directly comparing health effects of engine emissions to those of other pollution sources. Results finalized last year yielded the unexpected finding that blood vessels outside the lung were adversely affected by non-particulate components of gasoline emissions [3]. We hypothesized that nitrogen oxides and carbon monoxide might produce these effects through certain cellular chemical reactions, and might thus explain a portion of the known linkage between close proximity to traffic and cardiovascular effects in humans. This year, we exposed mice to these gases in pure form to determine whether these mechanisms were plausible.

Results

The detailed results of this project are communicated in numerous technical presentations and peer-reviewed scientific publications (FY 2007 products listed in Publications/Presentations, full listing available on request). Key recent results are summarized here.

For an initial exploration of the plausibility of hazard from emission nanoparticles, mice were exposed 6 hours/day for 7 days to aerosols of 20 nm oil and sulfate nanoparticles at 10^6 particles/cubic centimeter. Aerosols were formed by heating oil or dilute sulfuric acid, followed by carefully controlled condensation and dilution. We used new Shell Rotella-T® 15W-40 crankcase oil and the same oil from a normal change interval of a 2000 model Cummins 5.9L ISB engine using pre-2007 certification fuel and operated on repeated Environmental Protection Agency (EPA) heavy-duty certification cycles. Lung irritation was evaluated by analysis of lung surface fluid and histopathology. Earlier studies had revealed that the function of immune cells of the spleen was diminished by inhaled diesel emissions and wood smoke [1,2]. Cells (T and B lymphocytes) were therefore removed from spleens of nanoparticle-exposed mice and their ability to divide and produce antibody were measured.

The exposures to nanoparticles did not cause evidence of lung inflammation, either by histopathology or cell and biochemical markers in airway fluid. It is notable that exposure to this high concentration of the three aerosols did not cause inflammatory or irritant responses of the types considered sensitive indicators of the effects of whole emissions in human subjects. The only evidence that the lungs were exposed was an increase in tissue levels of hemeoxygenase-1, a general marker that is increased by many inhaled pollutants.

The exposure caused a mild suppression of the systemic (outside the lung) immune system. In a systemic immune response, lymphocytes in the spleen and other lymphoid tissues must divide to produce more cells, and must also produce antibodies to foreign materials. Two types of lymphocytes, T and B cells, were removed from the spleen and treated with materials that stimulate cell division and antibody production. In condensate-exposed animals, the cell division responses of both cell types were similarly reduced (Figure 1, showing only T cells). New and used oil caused similar modest reductions (approximately 20%), and sulfate caused a greater (nearly 40%) reduction. The three exposures also reduced the ability of cells to produce antibodies (Figure 2, showing only T cells). New and used oil caused reduced antibody formation approximately 60%, but sulfate reduced antibody production by over 70%.

These initial findings provide important new information. First, nanoparticles may present little, if any, hazard to the lung, but may have effects on the systemic immune system. Second, there was no difference between the responses to new and used diesel crankcase oil, suggesting that contaminants accumulating normally in diesel crankcase oil may not present an increasing hazard as they accumulate. Third, pure sulfate nanoparticles having quite different chemistry than oil caused the same effects, and actually caused greater immune suppression than the oil aerosols. Together with the concurrent finding in

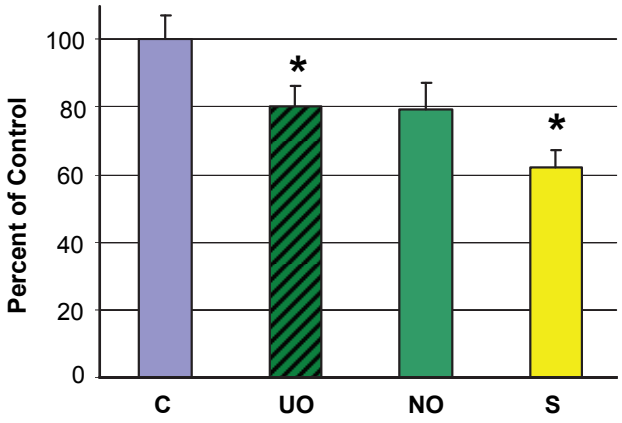

FIGURE 1. Response of Splenic T Lymphocytes to Stimulation to Divide (with Concanvalin-A) (Bars represent means ± standard error expressed as percentages of responses of sham-exposed mice. Asterisks indicate statistically significant responses. C = sham-exposed controls, UO = used oil, NO = new oil, S = sulfate.)

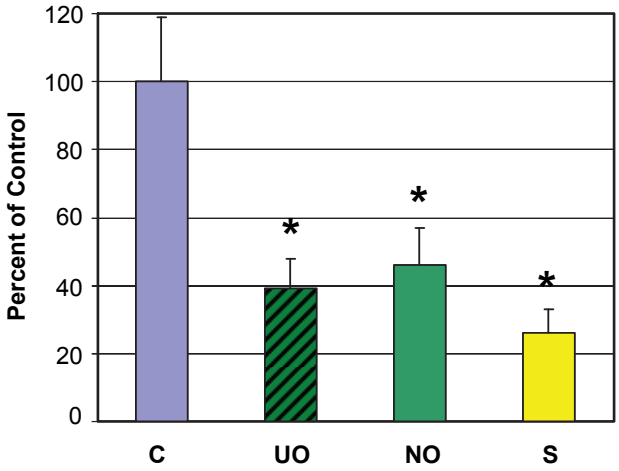

FIGURE 2. Response of Splenic T Lymphocytes to Stimulation to Produce Antibody to Foreign Protein (Sheep Red Blood Cells) (Bars represent means ± standard error expressed as percentages of responses of sham-exposed mice. Asterisks indicate statistically significant responses. C = sham-exposed controls, UO = used oil, NO = new oil, S = sulfate.)

another project that solid carbon nanoparticles cause very similar effects [4] and the earlier finding that whole diesel emissions and wood smoke exert similar systemic immune effects [1,2], these results suggest a general response to nanoparticles and pollution mixtures rather than a specific response to engine emissions. It will be important to follow up these first results with exposures to lower concentrations of emissions nanoparticles, to determine whether more broadly-relevant exposures cause measurable effects.

In the second study, mice were exposed 6 hours/day for 7 days to 17 ppm nitrogen oxide (NO), 0.2 or 2.0 ppm nitrogen dioxide (NO_2), 8 or 80 ppm carbon monoxide (CO), or the combination of 8 ppm NO_2 and 80 ppm CO. This study was an initial exploration of the plausibility that these gases might have caused the vascular effects observed in mice exposed to filtered gasoline emissions. The higher concentrations in this study mimicked those at the highest level of whole gasoline emissions in the previous work. Several indicators of oxidative stress and early stages of adverse tissue responses were measured in blood vessels near the heart.

As illustrated by the response of the indicator endothelin-1 in Figure 3, neither of the concentrations of NO_2 nor the lower concentration of CO caused changes in blood vessels. However, exposures to the high concentrations of CO and NO did cause significant responses. The lack of importance of NO_2 was reinforced by the finding that addition of NO_2 to the high concentration of CO did not increase the response. This same pattern was observed in the indicators

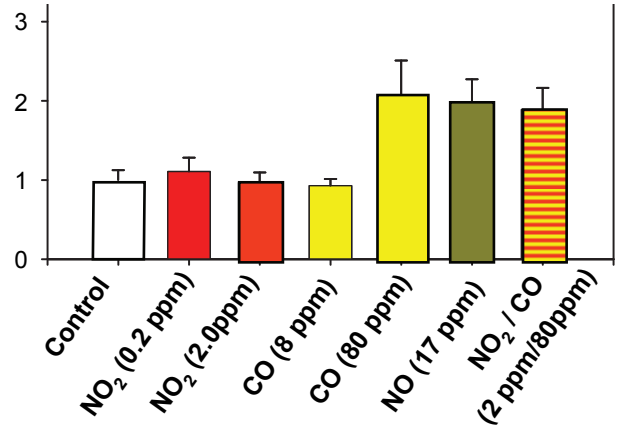

FIGURE 3. Levels of the Damage Indicator Endothelin-1 in Aorta near the Hearts of Mice Exposed to Gases (Bars represent means ± standard error of responses in comparison to sham-exposed controls [control response = 1]. Asterisks indicate statistically significant responses.)

hemeoxygenase-1 and matrix metalloproteinase-9. However, some other indicators of vascular response that were altered in the gasoline emission study were not altered by any of the single-gas exposures.

Although only a preliminary exploration, this study provided useful information. First, neither NO_2 nor CO at levels meeting current environmental standards caused measurable effects. The lack of effect of NO_2 is not surprising, because the reactivity of the gas would be expected to prevent any direct effect on tissues outside the lung. Second, the fact that high concentrations of both NO and CO did cause measurable effects suggests

that our hypotheses about the mechanisms of response to high levels of gasoline emissions are at least partially correct. Third, the fact that only some, but not all, of the markers of blood vessel effects were increased suggests that other non-particulate emissions, such as volatile organic compounds, also contributed to vascular responses at high concentrations of filtered gasoline emissions. Experimental logistics limited the number of exposures that could be included in this series; exposures to a lower concentration of NO and to a combination of NO and CO should be conducted. It will be important to determine whether more realistic exposures to NO present a hazard, and whether the effects of NO and CO are additive.

Conclusions

Emissions from all internal combustion motive power technologies evaluated to date are attended by potential adverse health impacts of some nature and at some exposure level. These effects need to be considered in the evaluation of emerging technologies. The new evidence indicates that attention to crankcase oil emissions is warranted, and emissions of organic and sulfate condensate nanoparticles should be minimized. The evidence also suggests that the non-particle components of emissions warrant continued attention. Fortunately, with few exceptions, significant effects are only observed at the highest exposure concentrations that might be encountered, and such exposures in a few occupational settings or traffic "hotspots" should be of shorter duration than the experimental exposures. Also fortunately, the fuel-trap-catalyst technologies required to meet 2010 on-road diesel emission standards should markedly reduce not only gases, but also vapors that could condense to form nanoparticles.

FY 2007 is the last year of funding for this project in its present form. Many, but not all, issues pertaining to the purpose of this project have been addressed. As noted above, a few additional exposures would be required to complete the recent work by determining whether effects occur at more widespread exposure levels. This will be accomplished as funding is available.

References

1. Burchiel, S.W., F.T. Lauer, J.D. McDonald, and M.D. Reed: Systemic Immunotoxicity in AJ Mice following 6-Month Whole Body Inhalation Exposure to Diesel Exhaust. *Toxicol. Appl. Pharmacol.* 196: 337-345, 2004.

2. Burchiel, S.W., F.T. Lauer, S.L. Dunaway, J. Zawadzki, J.D. McDonald, and M.D. Reed: Hardwood Smoke Alters Murine Splenic T Cell Responses to Mitogens Following a Six Month Whole Body Inhalation Exposure. *Toxicol. Appl. Pharmacol.* 202 (3): 229-236, 2005.

3. Lund, A.K., T.L. Knuckles, C.O. Akata, R. Shohet, J.D. McDonald, A. Gigliotti, JC. Seagrave, and M.J. Campen: Gasoline Exhaust Emissions Induce Vascular Remodeling Pathways Involved in Atherosclerosis. *Toxicol. Sci*. 95: 485-494, 2007.

4. Mitchell, L.A., J. Gao, R.V. Wal, A. Gigliotti, S.W. Burchiel, and J.D. McDonald: Pulmonary and Systemic Immune Response to Inhaled Multiwalled Carbon nanotubes. *Toxicol. Sci.* 100: 203-214, 2007.

FY 2007 Publications/Presentations

Publications

1. Braun, A., F.E. Huggins, A. Kubatova, S. Wirick, M.M. Maricq, B.S. Mun, J.D. McDonald, K.E. Kelly, N. Shah, and G.P. Huffman: Towards Distinguishing Wood Smoke and Diesel Exhaust Particulates in Ambient Particulate Matter. *Atmos. Environ*. (submitted).

2. Mauderly, J.L. and J.C. Chow: Health Effects of Organic Aerosols. *Inhal Toxicol*. (provisionally accepted – in revision).

3. Mauderly, J.L. and E. Garshick: Diesel Exhaust. Chapter 17 in: *Environmental Toxicants*, Lippmann, Ed., Wiley, New York (accepted and in press).

4. McDonald, J.D., M.D. Reed, M.J. Campen, E.G. Barrett, JC. Seagrave, and J.L. Mauderly: Health Effects of Inhaled Gasoline Engine Emissions. *Inhal. Toxicol.* 19(Suppl. 1): 107-116, 2007.

5. Lund, A.K., T.L. Knuckles, C.O. Akata, R. Shohet, J.D. McDonald, A. Gigliotti, JC. Seagrave, and M.J. Campen: Gasoline Exhaust Emissions Induce Vascular Remodeling Pathways Involved in Atherosclerosis. *Toxicol. Sci.* 95: 485-494, 2007.

6. Seagrave, JC., S. Dunaway, P. Hayden, J.D. McDonald, S. Stidley, and J.L. Mauderly: Responses of Differentiated Primary Human Lung Epithelial Cells to Exposure to Diesel Exhaust at an Air-Liquid Interface. *Exper. Lung Res.* 33:27-51, 2007.

Presentations

1. Mauderly, J.L.: Health Effects of Organic Aerosols, Introduction and Summary, Workshop on Health Effects of Organic Aerosols, EPRI, Palo Alto, CA, October 24–25, 2006.

2. Mauderly, J.L.: Disentangling Components Responsible for Health Effects of Complex Air Pollution Mixtures, Desert Research Institute, Reno, NV, November 21, 2006.

3. Mauderly, J.L.: Health Research Needs for Multi-Pollutant Air Quality Management. NARSTO Workshop on Multi-Pollutant Air Quality Management. Durham, NC, January 10, 2007.

4. Mauderly, J.L. et al.: Disentangling the Health Hazards of Complex Mixtures of Air Pollutants. Division of Occupational and Environmental Health Sciences, University of Texas School of Public Health, Houston, TX, February 16, 2007.

5. Seagrave, JC., M.J. Campen, S. Dunaway, G. Herbert, J.L. Mauderly, and J.D. McDonald. Exposure to Gasoline Engine Exhaust Causes Oxidative Stress in Rats. Society of Toxicology Annual Meeting, Charlotte, NC, March 2007.

6. McDonald, J.D., JC. Seagrave, L. Mitchell, A. Gigliotti, and J.L. Mauderly. Pulmonary Inflammatory and Systemic Immune Responses to Inhaled Oil Nanocondensates. Society of Toxicology Annual Meeting, Charlotte, NC, March 2007.

7. Lund, A.K., T. Knuckles, JC. Seagrave, C.O. Akata, J.D. McDonald, M.J. Campen: Exposure to Whole Gasoline Engine Emissions Results in Alterations of Molecular Pathways Involved in Progression of Atherosclerosis. Society of Toxicology Annual Meeting, Charlotte, NC, March 2007.

8. Reed, M.D., A. P. Gigliotti, and J.A. Berger: Gasoline Emissions Affect Clearance of Intratracheally Instilled *Pseudomonas aeruginosa*. Society of Toxicology Annual Meeting, Charlotte, NC, March 2007.

9. Mauderly. J.L.: Health Impacts of Diesel Emissions: An Update. Environment Canada, Ottawa, Canada, April 2007.

10. Mauderly, J.L.: ACES Phase 3: Chronic Inhalation Bioassay. Annual Meeting of the Health Effects Institute, Chicago, IL, April, 2007.

11. Barrett, E.G., M.D. Reed, J.D. McDonald, S. Shinnik, and M. Anaya: Effects of Gasoline Engine Emissions on Pre-Existing Allergic Airway Responses. Annual Conference of the American Thoracic Society International Conference, San Francisco, CA, May 2007.

12. Mauderly, J.L.: Health Impacts of Diesel Emissions: An Update. Committee on 21st Century Truck Program, National Research Council, National Academy of Sciences, Washington, D.C., May 2007.

13. Mauderly, J.L., M.J. Campen, J.D. McDonald, and JC. Seagrave: Components Responsible for the Health Effects of Engine Emissions. Diesel Engine Emissions Reduction Conference (DEER 2007), Detroit, MI, August 2007.

II.D.4 The Advanced Collaborative Emissions Study (ACES)

Dan Greenbaum (Primary Contact),
Robert O'Keefe, Jane Warren
Health Effects Institute (HEI)
Charlestown Navy Yard
120 Second Avenue
Boston, MA 02129

DOE Technology Development Manager:
James Eberhardt

NETL Project Manager: Ralph Nine

Subcontractor:
Coordinating Research Council (CRC), Alpharetta, GA

Objectives

- **Phase 1**: Extensive emissions characterization (at an existing emissions characterization facility) of four production-intent heavy duty diesel engine and control systems designed to meet 2007 standards for particulate matter (PM) and nitrogen oxides (NOx). One engine/aftertreatment system will be selected for health testing.
- **Phase 2**: Extensive emissions characterization of a group of production-intent engine and control systems meeting the 2010 standards (including more advanced NOx controls to meet the more stringent 2010 NOx standards).
- **Phase 3**: One selected 2007-compliant engine will be installed in a specially-designed emissions generation and animal exposure facility (Phase 3A) and used in chronic and shorter-term health effects studies to form the basis of the ACES safety assessment (Phases 3B and 3C). This will include periodic emissions characterization during both a core 24-month chronic bioassay of cancer endpoints in rats and shorter term biological screening assays in both rats and mice (Phase 3B) as well as emission characterization during a set of shorter animal exposures and biological screening using accepted toxicological tests after the end of the chronic bioassay (Phase 3C). (NOTE: Only the emissions characterization and shorter-term biological screening activities at the beginning and during Phase 3 are components of the DOE ACES contract.)

Accomplishments

General Oversight

- Held meetings with the ACES Oversight, Advisory and Steering Committees regarding finalization of emissions generation and characterization, health effects assessment, and cost savings options for Phase 3, and to finalize financial commitments (Fall 2006).
- Held a meeting with the ACES Oversight and Advisory Committees to discuss progress and technical issues (April 2007).
- Held meetings of the CRC ACES Panel at Southwest Research Institute (SwRI) to discuss technical issues pertaining to emissions characterization (Spring 2007).
- Communicated at meetings and conference calls with engine manufacturers, ACES Oversight, Advisory and Steering Committees, and selected members of the CRC ACES Panel to develop a plan for selection of one engine for use in Phase 3 (Spring and Summer 2007).
- Held a Panel meeting to discuss and review competitive proposals for biological screening studies submitted in response to Request for Applications (RFA) 06-2 (August 2007).

Phase 1

- Selected fuel and lubricant suppliers and arranged for delivery to both SwRI and Lovelace Respiratory Research Institute (LRRI) (October 2006).
- Finalized the contract with SwRI for Phase 1 emissions characterization (December 2006).
- Completed preparation of the engine testing facility at SwRI (February 2007).
- Received four test engines from the participating engine manufacturers at SwRI and agreed upon the order in which they would be tested (April 2007).
- Finalized and approved the 16-hour test day cycle developed by West Virginia University based on a combination of Federal Test Procedure (FTP) and California Air Resources Board (CARB) cycles for use in Phase 3 (June 2007).
- Finalized the emissions characterization protocol with the CRC ACES Panel and the investigators' team at SwRI and approved a revised program plan from SwRI (June 2007).
- Finalized the last remaining technical details concerning the emissions characterization protocol for Phase 1 and started emissions characterization

of the first 2007-compliant engine (engine A) at SwRI (July 2007).
- Completed emissions characterization of the first and second 2007-compliant engines (engines A and B) and finalized procedures for trap regeneration (September 2007).

Phase 3

- Selected LRRI to conduct Phase 3A and B, the core emissions characterization and chronic bioassay (Fall 2006).
- Finalized details of facility development, emissions characterization, and health effects assessment for Phase 3 with the LRRI principal investigator and the ACES HEI Oversight Committee, specifically regarding cost savings options (Fall 2006).
- Conducted a site visit to LRRI to discuss cost-saving options related to engine facility, dynamometer, and dilution systems with key experts on the HEI ACES Oversight and Advisory Committees and additional experts identified by CRC (December 2006).
- Extended the deadline for submission of proposals for biological screening under RFA 06-2 to May 24, 2007 to increase the potential of a large number of high quality applications for additional biological screening during Phase 3 and encouraged prospective applicants to contact the LRRI team to discuss technical and logistical issues (Spring 2007).
- Finalized remaining technical details of the chronic exposure bioassay and related biological screening studies in Phase 3 (May 2007).
- Agreed upon a revised budget with LRRI, completed the first round of contract negotiations, and began facility implementation (August 2007).
- Received five applications for shorter term biological screening studies during Phase 3B submitted under RFA 06-2 (May and June 2007).
- Reviewed the five applications to RFA 06-2 with an expert Review Panel and solicited revised applications (August 2007).
- Discussed with the four engine manufacturers and CRC the specifications of the facility implementation at LRRI in order to allow any of the 2007-compliant engines to be accommodated, if selected (August, September 2007).

Future Directions

Phase 1

- Complete emissions characterization of the third and fourth 2007-compliant engines (engines C and D) at SwRI (Fall 2007).
- Finalize the engine selection criteria described in the Initial Plan for Engine Selection with the ACES Oversight and Steering Committees (Fall 2007).
- Continue to work with LRRI, CRC, and the engine manufacturers to determine appropriate specifications for the LRRI engine facility (Fall 2007).
- Receive detailed the emissions characterization data for all four engines from SwRI and collaborating researchers at Desert Research Institute (Winter 2007).
- Adjust the engine selection criteria if warranted by the findings, as described in the Final Draft Initial Plan; agree upon a Final Plan for Engine Selection (Fall 2007).
- Select one engine for use in Phase 3; receive a duplicate engine and characterize its emissions at SwRI (Spring 2008).
- Ship the selected engine and its duplicate to LRRI for installation in their facility (Spring 2008).
- Receive a Phase 1 Final Report from SwRI (Summer 2008).

Phase 3

- Finalize the second stage of contract negotiations for conduct of the chronic bioassay and biological screening at LRRI (Winter 2007).
- Select contractors to conduct the biological screening study for Phase 3B (Fall 2007).
- Finalize protocols for biological screening with those contractors and the investigators' team at LRRI (Winter/Spring 2008).
- Complete facility implementation at LRRI (Spring 2008).
- Install the selected engine and store the duplicate engine (Spring/Summer 2008).
- Perform initial emissions characterization of the selected and duplicate engines at LRRI to ensure both engines perform in a similar fashion as when they were characterized at SwRI (Summer 2008).
- Start animal exposures for the chronic bioassay and biological screening studies (Fall 2008).

✧ ✧ ✧ ✧ ✧

Introduction

ACES is a cooperative, multi-party effort to characterize the emissions and assess the safety of advanced heavy-heavy duty diesel engine and aftertreatment systems and fuels designed to meet the 2007 and 2010 emissions standards for PM and NOx. The ACES program is being carried out by HEI and CRC. It is utilizing established emissions

characterization and toxicological test methods to assess the possible health effects of production-intent engine and control technology combinations that will be introduced into the market during the 2007-2010 time period. This is in direct response to calls in the U.S. Environmental Protection Agency Health Assessment Document for Diesel Engine Exhaust [1] for assessment and reconsideration of diesel emissions and health risk with the advent of new cleaner technologies.

The characterization of emissions from representative, production-intent advanced compression ignition (CI) engine systems will include comprehensive analyses of the gaseous and particulate material, especially those species that have been identified as having potential health significance. The core toxicological study will include detailed emissions characterization at its inception, and periodically throughout a two-year chronic inhalation bioassay in rats similar to the standard National Toxicology Program (NTP) bioassay. Other specific biological screening studies also will be undertaken in both rats and mice, to evaluate these engine systems with respect to carefully selected respiratory, immunologic, and genotoxic effects for which there are accepted toxicologic tests. It is anticipated that these emissions characterization and health effects studies will assess the safety of these advanced CI engine systems, will identify and assess any unforeseen changes in the emissions as a result of the technology changes, and will contribute to the development of a database to inform future assessments of these advanced engine and control systems.

Approach

Experimental work under ACES will be performed in three phases, as outlined in the Objectives. Detailed emissions characterization (Phases 1 and 2) will be performed by an existing engine laboratory (SwRI) that meets the U.S. Environmental Protection Agency specifications for 2007 and 2010 engine testing. In Phase 1, emissions from four 2007-compliant engine/control systems will be characterized. One engine will be selected for health testing in Phase 3. In Phase 2, emissions from four 2010-compliant engine/control systems will be characterized. In Phase 3, one selected 2007-compliant engine/control system will be installed in a specially designed emission generation facility connected to a health testing facility at LRRI to conduct a chronic inhalation bioassay in rats and shorter term biological screening in rats and mice. During the 2-year bioassay, emissions will be characterized at regular intervals throughout the testing.

The emissions characterization work will be overseen by CRC and its ACES Panel. The health effects assessment will be overseen by HEI and its ACES Oversight Committee. Set-up of the emission generation facility at the health effects testing facility (for Phase 3) and finalizing the protocols for periodic emission characterization throughout Phase 3 will be done with input from the team of investigators selected to conduct emissions characterization in Phase 1 and CRC.

Results

The emissions characterization in Phase 1 is well underway; at this time characterization of two of the four engine/aftertreatment combinations has been completed. Successful meetings were conducted with multiple stakeholders of ACES to discuss and agree upon technical issues for both Phases 1 and 3. Much progress was made this year in terms of developing and finalizing the test cycles and other technical procedures, including how to handle trap regeneration and crankcase emissions. Initial contract negotiations with the emissions characterization and health testing facility for conduct of Phase 3 were completed; facility implementation was started after various cost saving options were identified and agreed upon. A final draft of the Initial Plan for Engine Selection has been written and circulated and is expected to be finalized soon.

Conclusions

We have made substantial progress towards the implementation of the project: (1) emissions characterization in Phase 1 is well underway, and (2) facility implementation for Phase 3 has started and detailed experimental protocols will be finalized in the coming months. Furthermore, five additional teams of investigators have submitted proposals for supplementary biological screening studies to address important health endpoints; revised proposals will be reviewed and funding decisions made in the Fall of 2007.

References

1. U.S. Environmental Protection Agency, 2002. Health Assessment Document for Diesel Engine Exhaust. EPA/600/8-90/057F. U.S. Environmental Protection Agency, National Center for Environmental Assessment, Office of Research and Development, Washington, D.C.

FY 2007 Publications/Presentations

1. Poster Presentation at the CRC ON-Road Vehicle Emissions Workshop in San Diego, March 26-28 2007, "Status of the Advanced Collaborative Emissions Study (ACES)."

2. Poster Presentation at the HEI Annual Conference in Chicago IL, April 15-17 2007, "Status of the Advanced Collaborative Emissions Study (ACES)" (HEI Annual Conference 2007 Program Book, page 68).

3. Poster Presentation "Status of the Advanced Collaborative Emissions Study (ACES)" at the DOE Semi-Mega Merit Review Meeting, Crystal City, VA, June 18, 2007.

4. Poster Presentation at the Diesel Engine Emissions Reduction (DEER) meeting in Detroit MI, August 13–16 2007, P-23: "Status of the Advanced Collaborative Emissions Study (ACES)."

III. SOLID STATE ENERGY CONVERSION

III.1 Developing Thermoelectric Technology for Automotive Waste Heat Recovery

Jihui Yang (Primary Contact), T. Anderson, G. S. Nolas, C. Uher, D. T. Morelli, A. Wereszczak, and H. Wang
GM Research and Development Center
30500 Mound Road, MC 480-106-224
Warren, MI 48090

DOE Technology Development Manager: John W. Fairbanks

NETL Project Manager: Carl Maronde

Subcontractors:
- General Electric (GE), Niskayuna, NY
- University of South Florida, Tampa, FL
- University of Michigan, Ann Arbor, MI
- Michigan State University, East Lansing, MI
- Oak Ridge National Laboratory, Oak Ridge, TN

Objectives

- Provide a manufacturability and feasibility assessment of thermoelectric (TE) devices based on bulk and thin film materials, and provide a recommendation going forward.
- Optimization of the cost-effective bulk materials.
- Finalize material selections for exhaust and/or radiator heat recovery.
- Finalize design for exhaust and/or radiator waste heat recovery devices, with estimated performance.
- Identify volume capable and cost-effective manufacturing processes for TE modules.

Accomplishments

- We found that existing bulk TE materials in an exhaust generator can meet the minimum 350 W requirement; the exhaust TE waste heat recovery has higher, but not significantly higher, cost than the existing fuel economy improving technologies
- We found that low quality heat at the radiator makes recovering significant heat cost prohibitive using existing materials, and requires both TE figure of merit (ZT) enhancement and cost reduction.
- Finalized our material selections for exhaust TE waste heat recovery subsystem.
- Established thermal conductivity reduction mechanisms in multiple-filled skutterudites, and achieved record high ZT in double-filled skutterudites in the temperature range relevant to automotive TE exhaust waste heat recovery.

Future Directions

- Finalize TE waste heat recovery subsystem design.
- Provide initial production-ready TE modules for application-based testing.
- Start TE exhaust waste heat recovery subsystem prototype construction.
- Develop cost-effective TE materials and modules.

Introduction

In the past year, the project has been focused on several areas: feasibility of automotive TE waste heat recovery subsystem based on exhaust and radiator heat; design and performance estimates of the exhaust and radiator heat recovery subsystems; materials down-select; and the search for high performance and cost-effective TE materials and modules.

The discovery part of this project has demonstrated cost-effective skutterudite materials as potential material candidates. We have also achieved record ZT values in filled skutterudites in the temperature range relevant to automotive exhaust TE waste heat recovery. We have identified a method of enhancing ZT in clathrate compounds. We have also determined the correlation between lattice thermal conductivity and structural properties of antifluorite materials. High temperature mechanical property characterizations have been carried out for many materials chosen for module construction.

Approach

The overall approach we use to achieve the project goal is to combine science and engineering. Existing and newly developed materials are carefully selected by the materials research partners of the project and supplied to the system engineers at GE. Most of the material properties are also validated at Oak Ridge National Laboratory to avoid potential pitfalls. System engineers work closely with vehicle engineers at GM to ensure that accurate vehicle level information is used for developing subsystem models and designs. Subsystem output is then analyzed by GM for potential fuel economy gains.

Our project incorporates material, module, subsystem, and integration costs into the material selection criteria. Dollars/W has been chosen as the metric for balancing various materials, module and subsystem design, and vehicle integration options.

Results

Dual-Frequency Resonant Phonon Scattering in Multiple-Element-Filled Skutterudites

We have realized such behavior in a series of polycrystalline $Ba_xR_yCo_4Sb_{12}$ (R = La, Ce, and Sr) samples. Fe-doping on the Co site was intentionally avoided to isolate the influence of rattlers. The reduction of lattice thermal conductivity could lead to ZT enhancement, if x and y are optimized so as not to substantially degrade the electronic properties. Samples used for this study were fabricated by solid-state reaction and spark plasma sintering (SPS); the detailed procedures were described previously [1]. The nominal and actual compositions are listed in Table 1, along with some room temperature transport property data.

Figure 1 shows the temperature (*T*) dependence of total thermal conductivity (κ) for all samples and lattice thermal conductivity (κ_L) for selected samples, between 2 K and 310 K. The total thermal conductivity of all samples (Figure 1 (a)) is consistent with a large body of literature developed for filled skutterudites [2], with room temperature values between 2 W/m-K and 6 W/m-K and the peak values significantly lower than that of $CoSb_3$. For almost the entire temperature range studied, $Ba_{0.07}La_{0.04}Co_4Sb_{12.08}$ and $Ba_{0.12}Ce_{0.06}Co_4Sb_{12.08}$ have the lowest κ values, while samples with both Ba and Sr filling have lower κ values than those of Ba-only samples.

Our calculations show that the filler elements for filled skutterudites can be approximately categorized into three groups according to their resonant phonon frequencies: rare-earths, alkaline-earths, and alkalines (Table 2) [3]. The phonon resonant frequencies are comparable for filler elements with similar chemical nature; however, they are significantly different amongst various groups. This further suggests that multiple-filling using elements from different groups can be an effective method for additional κ_L reduction in filled skutterudites. Data shown in Figure 1 (b) clearly demonstrate that dual-filling of $CoSb_3$ with Ba and Ce, or Ba and La is much more effective than Ba and Sr in lowering κ_L. Our recent study using misch-metal (a rare earth alloy having the naturally occurring La, Ce, Pr, and Nd composition)

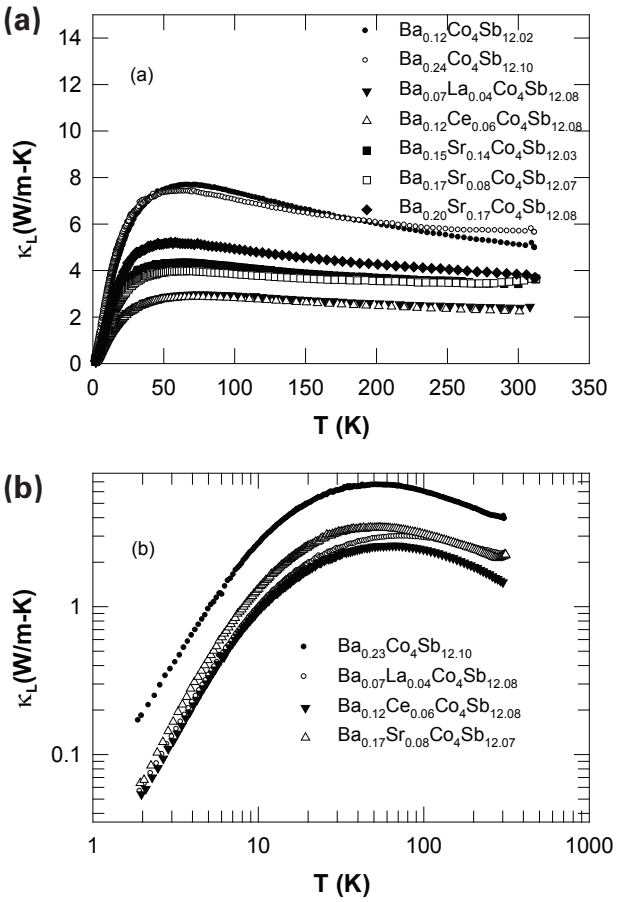

FIGURE 1. (a) Total thermal conductivity vs. temperature between 2 K and 310 K for $Ba_xR_yCo_4Sb_{12}$ (R = La, Ce, and Sr) samples, (b) Lattice thermal conductivity vs. temperature between 2 K and 310 K for selected samples.

TABLE 1. Nominal composition, actual composition (determined by electron probe micro-analyzer), and room temperature total thermal conductivity κ, lattice thermal conductivity κ_L, thermopower *S*, electrical resistivity ρ, power factor S^2/ρ, carrier concentration *n*, and thermoelectric figure of merit *ZT*.

Nominal composition	Actual composition	κ (W/m K)	κ_L (W/m K)	*S* (μV/K)	ρ (mΩ cm)	S^2/ρ (μW/cm K²)	*n* (10^{20} cm^{-3})	*ZT*
$Ba_{0.15}Co_4Sb_{12}$	$Ba_{0.12}Co_4Sb_{12.02}$	5.04	4.32	−120.46	1.03	14.09	2.19	0.08
$Ba_{0.25}Co_4Sb_{12}$	$Ba_{0.23}Co_4Sb_{12.10}$	5.63	3.92	−106.63	0.43	26.44	3.29	0.14
$Ba_{0.1}La_{0.05}Co_4Sb_{12}$	$Ba_{0.07}La_{0.04}Co_4Sb_{12.08}$	2.40	2.21	−119.47	4.10	3.48	2.12	0.04
$Ba_{0.15}Ce_{0.1}Co_4Sb_{12}$	$Ba_{0.12}Ce_{0.06}Co_4Sb_{12.08}$	2.24	1.46	−104.64	0.95	11.53	10.70	0.16
$Ba_{0.17}Sr_{0.15}Co_4Sb_{12}$	$Ba_{0.15}Sr_{0.14}Co_4Sb_{12.03}$	3.44	2.33	−79.51	0.85	7.43	11.50	0.06
$Ba_{0.20}Sr_{0.1}Co_4Sb_{12}$	$Ba_{0.17}Sr_{0.08}Co_4Sb_{12.07}$	3.54	2.18	−79.03	0.54	11.57	3.81	0.10
$Ba_{0.22}Sr_{0.2}Co_4Sb_{12}$	$Ba_{0.20}Sr_{0.17}Co_4Sb_{12.08}$	3.85	2.39	−72.38	0.50	10.48	14.40	0.08

as filler in $CoSb_3$-based skutterudites shows that κ_L of misch-metal-filled skutterudites is comparable to those single-rare-earth-filled skutterudites [4], further substantiating our conclusions.

Based on these result, the project has achieved record ZT values for skutterudite compounds in the range of automotive exhaust temperatures. We expect that the concept of reducing lattice thermal conductivity by dual-frequency resonant phonon scattering is also effective for other cage-structure compounds, such as clathrates.

Spark Plasma Sintering Process

TE materials can be produced by conventional ceramic processing techniques or from single crystal growth techniques. However, single crystals are limited by the size of the crystals, poor mechanical properties, and chemical heterogeneity. In the polycrystalline approach, dopants are incorporated into the alloy by melting the precursors and casting an ingot. The ingot is then crushed followed by consolidation by cold pressing, sintering, and low temperature anneal.

Our team has set in place a manufacturing process for processing various TE materials following the above general powder processing approach. GM and GE have in-house sintering capabilities of inert atmosphere sintering, hot pressing, hot isostatic pressing and SPS. Currently, our project is pursuing the SPS approach for sintering of its TE materials.

SPS has been used to successfully sinter many materials to greater than 99% theoretical density in a short time (<15 minutes) using the SPS unit (Figure 2). Fully dense n- and p-type disks with outer diameter of 15 mm were processed using the SPS with thickness ranging from 3 to 6 mm.

Diffusion barrier layers (thickness ~250 to 300 μm) were also successfully bonded by a one-step SPS process from particulate sources.

TABLE 2. Spring constant k and resonance frequency ω in the [111] and [100] directions of $R_{0.125}Co_4Sb_{12}$, where R = la, Ce, Eu, Yb, Ba, Sr, Na, and K.

		[111]		[100]	
R	Mass (10^{-26} kg)	*k* (N/m)	ω_0 (cm^{-1})	*k* (N/m)	ω_0 (cm^{-1})
La	23.07	36.10	66	37.42	68
Ce	23.27	23.72	54	25.18	55
Eu	25.34	30.16	58	31.37	59
Yb	28.74	18.04	42	18.88	43
Ba	22.81	69.60	93	70.85	94
Sr	14.55	41.62	90	42.56	91
Na	3.819	16.87	112	17.18	113
K	6.495	46.04	141	46.70	142

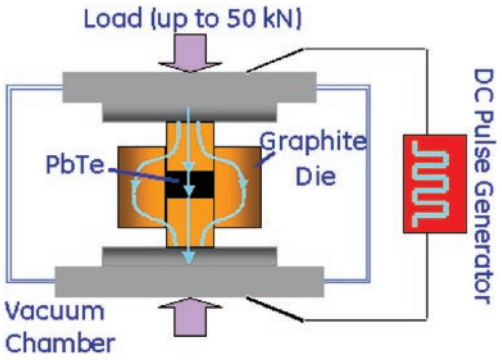

FIGURE 2. Schematic of the SPS Process and SPS Unit

Anticipated Output of TE Exhaust Waste Heat Subsystem over the FTP City Driving Cycle

Based on our TE module, heat exchanger, and subsystem design, we expect that the average electrical power output over the FTP city cycle of an exhaust waste recovery system would be higher than the 350 W minimum requirement. Figure 3 shows the output as a function of the exhaust mass flow and temperature using a specific candidate material.

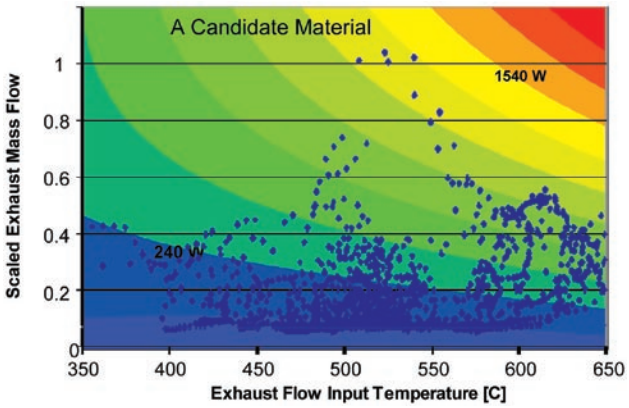

FIGURE 3. Anticipated Electrical Output of a TE Exhaust Waste Heat Recovery Subsystem over the FTP City Cycle

Conclusions

The project has made significant progress in the areas of feasibility of automotive TE waste heat recovery subsystems based on both exhaust and radiator heat; design and performance estimates of the exhaust and radiator heat recovery subsystems; materials down-select; and the search for high performance and cost-effective TE materials and modules. The next phase of our project will be focused on module and subsystem construction and testing.

References

1. L. D. Chen, X. F. Tang, T. Kawahara, J. S. Dyck, W. Chen, C. Uher, T. Goto, and T. Hirai, Proceedings of the 20th International Conference on Thermoelectrics (IEEE, Piscataway, NJ, 2001), p. 57.

2. C. Uher, in Recent Trends in Thermoelectric Materials Research I, Semiconductors and Semimetals, Vol. 69, edited by T. M. Tritt (Academic, San Diego, 2000), p. 139, and references therein.

3. J. Yang, G. P. Meisner, and L. Chen, Appl. Phys. Lett. **90**, 192111 (2007).

4. J. Yang, G. P. Meisner, C. J. Rawn, H. Wang, B. C. Chakoumakos, J. Martin, G. S. Nolas, B. L. Pedersen, and J. K. Stalick, J. Appl. Phys. **102**, 083702 (2007).

FY 2007 Publications/Presentations

1. J. Yang, W. Zhang, S. Q. Bai, Z. Mei, and L. D. Chen, "Dual-frequency resonant phonon scattering in $Ba_xR_yCo_4Sb_{12}$ (R=La, Ce, and Sr)", Appl. Phys. Lett. **90**, 192111, 2007.

2. J. Yang, G. P. Meisner, C. J. Rawn, H. Wang, B. C. Chakoumakos, J. Martin, G. S. Nolas, B. L. Pedersen, and J. K. Stalick, "Low temperature transport and structural properties of misch-metal-filled skutterudites", Journal of Applied Physics **102**, 083702 (2007).

3. J. Yang, invited, Department of Mechanical Engineering, University of Colorado at Boulder, Boulder, CO, March 2007: "Materials for High-efficiency Automobiles".

4. J. Yang, invited, United States Council for Automotive Research, Southfield, MI, May 2007: "Thermoelectric Technology for Automotive Waste Heat Recovery".

5. J. Yang, invited, GM Global Electrical Council Meeting, Warren, MI, June 2007: "Cost of Automotive Electric Power and Thermoelectric Waste Heat Recovery Program".

6. J. Yang, 26th International Conference on Thermoelectrics, Jeju, Korea, June, 2007: "Dual-frequency resonant phonon scattering in $Ba_xR_yCo_4Sb_{12}$ (R=La, Ce, and Sr)".

7. J. Yang, invited, Electronic Structure and Functionality of Thermoelectric Materials Workshop, Reykjavik, Iceland, July 2007: "Thermoelectric Waste Heat Recovery Based Efficient Automobiles".

8. J. Yang, invited, Electronic Structure and Functionality of Thermoelectric Materials Workshop, Reykjavik, Iceland, July 2007: "Properties of Novel Skutterudites".

9. J. Yang, 2007 Diesel Engine-Efficiency and Emissions Research (DEER) Conference, Detroit, MI, August 2007: "Developing Thermoelectric Technology for Automotive Waste Heat Recovery".

10. J. Yang, invited, Ceramics Division, National Institute of Standards and Technology, Gaithersburg, MD, October 2007: "Novel Materials for Thermoelectric Waste Heat Recovery Based Efficient Automobiles".

11. G. P. Meisner "Developing Thermoelectric Technology for Automotive Waste Heat Recovery", Direct Energy Conversion Review and Workshop, Vail, CO, August 20–23, 2007.

12. De Bock, P. and Novak, V., "An Efficiency Entitlement Study for Thermoelectric Generators," Proceedings of 2nd Energy Nanotechnology International Conference, ENIC2007-45040, Santa Clara, CA, September 5–7, 2007.

13. Anderson, T.A., De Bock, P., Jiang, J. and Nagarkar, K., "Development of a Thermoelectric Automotive Waste Heat Recovery Generator," Direct Energy Conversion Review and Workshop, Vail, CO, August 20–23, 2007.

14. Shi X., Zhou Z., Zhang W., Chen L. D., Yang J., and Uher C., "Solid Solubility of Ir and Rh at the Co Site of Skutterudites", *J. Appl., Phys.,* 101, 123525 (2007).

15. Shi X., Zhang W., Chen L. D., Yang J., and Uher C., "Theoretical Study of the Filling Fraction Limits for Impurities in $CoSb_3$", *Phys. Rev. B,* 75, 235208 (2007).

16. Shi X., Chen L. D., Bai S. Q., Huang X. Y., Zhao X. Y., Yao Q., and Uher C., "Influence of Fullerene Dispersion on High Temperature Thermoelectric Properties of $Ba_yCo_4Sb_{12}$-based Composites", *J. Appl. Phys.* (in press)

17. Shi X., Zhang W., Chen L. D., Yang J., and Uher C., "Ab Initio Study on the Filling Fraction Limits for Impurities in $CoSb_3$: II. Thermodynamic Analysis" (submitted to *Acta Mater.*).

18. Shi X., Kong H., Yang J., Salvador J. R., Wang H., and Uher C., "Low Thermal Conductivity and High Thermoelectric Figure of Merit in *n*-type $Ba_xYb_yCo_4Sb_{12}$ Double-Filled Skutterudites" (to be submitted to *Appl. Phys. Lett.*).

19. Uher C., Shi X., and Kong H., "Filled $Ir_xCo_{1-x}Sb_3$-based Skutterudite Solid Solutions", *Proceedings of the 26th International Conference on Thermoelectrics* (2007) (in press).

20. J H. Wang, W.D. Porter, Jihui Yang and G. Meisner, "High Temperature Thermoelectric Properties of Misch-metal-filled Skutterudites", submitted to Applied Physics Letter, September 2007.

21. H. Wang, "Thermal Conductivity and Figure of Merit of Bulk Thermoelectric Materials", Invited Talk at MS&T06: MS & T 2006 Cincinnati OH, Oct. 16–19, 2006.

22. H. Wang, J. Yang, W.D. Porter, and G.P. Meisner, "Thermoelectric Properties of Misch-metal-filled Skutterudites from 300K to 800K", International Conference of Thermoelectrics (ICT2007) Jeju Island, South Korea, June 4–7 2007.

23. H. Wang, "Thermoelectrics Power Generation: A Review of DOE Waste Heat Recovery Program at ORNL", invited talk at Material Science and Engineering Department, Seoul National University, Seoul, South Korea, June 11 2007.

24. H. Wang, J. Yang and G.S. Nolas, "Low Thermal Conductivity Bulk Thermoelectrics", Thermal Conductivity 29, June 25–27, Birmingham, AL, 2007.

25. Timothy P. Hogan, H. Wang, Chun-I Wu, Joseph Sootsman, Duck-Young Chung, Mercouri G. Kanatzidis, Edward Timm, Harold Schock, "Transport Properties of Bulk Nanostructured Thermoelectric Materials", invited talk, Thermal Conductivity 29, June 25–27, Birmingham, AL, 2007.

26. Jane Y. Howe, H. Wang, and Jihui Yang, " Structure of the Polycrystalline Thermoelectric Bulk Material AgPbmSbTe2+m", Microscopy and Microanalysis 2007 in Ft. Lauderdale, Florida, USA, August 5-9, pp. 852-853, 2007.

27. G.S. Nolas, D. Wang and M. Beekman, 'Transport properties of polycrystalline Mg2Si1-ySby', Phys. Rev. B (in press).

28. J. Martin, G.S. Nolas, H. Wang and J. Yang, 'Thermoelectric properties of silicon-germanium type I clathrates', J. Appl. Phys. (in press).

29. G.S. Nolas, D. Wang and X. Lin, 'Synthesis and low temperature transport properties of Mg2Ge1-ySby', Physica Status Solidi (Rapid Research Letter) 1, 223 (2007).

30. J. Martin, G.S. Nolas, W. Zhang and L. Chen 'PbTe nanocomposites synthesized from PbTe nanocrystals', Appl. Phys. Lett. 90, 222112 (2007).

31. D. Wang and G.S. Nolas, "Thermoelectric Properties of mix-crystals of Mg2E (E=Si, Ge)-Mg3Sb2", Proc. Adv. Elec. Ceramics 28(8), 185 (2007).

32. J. Martin, D. Wang and G.S. Nolas, "Synthesis and characterization of nanocrystalline chalcogenides" Proc. Adv. Elec. Ceramics 28(8), 221 (2007).

33. G.S. Nolas, given an Invited presentation to The International Conference on New Quantum Phenomena in Skutterudite and Related Systems (Skutterudite2007), Kobe, Japan, Sept 26 – 30, 2007 (due to scheduling conflicts, I was not able to attend this conference).

34. G.S. Nolas, 'Fundamental study of inorganic clathrates', Invited, Max Planck Institute for Chemical Physics of Solids, Dresden, Germany, August 7, 2007.

35. G.S. Nolas, 'Novel Materials for Energy Technology", Invited, University of Kentucky Physics Seminar, Lexington, KY, March 21, 2007.

36. G.S. Nolas, 'Overview and new directions in bulk materials research for thermoelectric power generation applications', Invited, Presented at the 31st International Cocoa Beach Conference & Exposition on Advanced Ceramics and Composites, Daytona, FL, January 21, 2007.

37. J. Martin, W. Zhang, L. Chen and G.S. Nolas, "Synthesis and Characterization of Nanocomposite Chalcogenides", presented at the American Physical Society, Denver, CO, March 7, 2007.

Special Recognitions & Awards/Patents Issued

1. J. Yang - The John M. Campbell Award (outstanding contributions to pure or applied science), GM R&D Center.

III.2 High-Efficiency Thermoelectric Waste Energy Recovery System for Passenger Vehicle Applications

J. LaGrandeur (Primary Contact), D. Crane
BSST LLC
5462 Irwindale Avenue
Irwindale, CA 91706

DOE Technology Development Manager:
John Fairbanks

NETL Project Manager: Aaron Yocum

Subcontractors:
- BMW, Palo Alto, CA
- Visteon, Van Buren Township, MI
- Marlow Inc., Dallas, TX

Objectives

The primary objective of 2007 is to operate the key subsystems of the waste heat recovery system (WHRS) in a bench test environment using a hot gas torch to simulate engine exhaust. Gas flow and temperature will be varied to simulate a variety of driving conditions. The key subsystems include the primary heat exchanger (PHX), thermoelectric (TE) generator module (TGM) and power conversion system (PCS). The test results will be finalized and used to update the computer simulation model. Predicted performance using the model will be compared to the test results and fuel efficiency gains will be predicted for the system operating in a variety of driving conditions. An architectural simplification will be evaluated to determine how commercialization may be accelerated without degrading fuel efficiency or other performance factors.

Key objectives for 2007 include:

1. Build and test of a low-temperature TGM incorporating BiTe TE material:
   - An initial 100 watt BiTe TGM
   - A full-scale (>500 watt) BiTe TGM
   - Operation and test of the TGM with Phase 2 PCS electronics
2. Build and test of a high-temperature TGM incorporating PbTe/TAGs/BiTe TE material:
   - An initial 100 watt Pb/TAGS/BiTe TGM
   - Operation and test of the 100 watt Pb/TAGS/BiTe TGM with Phase 2 PCS electronics
3. Evolution of the system model to predict transient performance conditions that are critical during engine start-up and city driving conditions where wide variations in exhaust gas mass flow are encountered.
4. Evaluation of a simplified system architecture to accelerate the commercialization and economic viability of the system.

Accomplishments

1. A fractional BiTe TGM has been built and tested that produced 130 watts of electric power.
2. A full-scale BiTe TGM was built and tested that produced over 500 watts of electric power.
3. A fractional high temperature TGM has been built using PbTe/TAGS that produced 20 watts electric power.
4. A fractional high temperature TGM has been built using PbTe/TAGS/BiTe that demonstrated 10% conversion efficiency.
5. The system model has been updated to predict transient performance and is being used to evaluate system performance over a variety of driving conditions including engine start-up.
6. A simplified architecture has been modeled and preliminary results are being evaluated.

Future Directions

Phase 3 activities are scheduled to conclude at the end of February 2008. In 2008 BSST will complete the build of a full-scale high temperature TGM and perform a bench test including the PHX and PCS subsystems.

Phase 4 activities include engine integration and test and are planned to begin early Q2 2008.

Introduction

BSST began work to develop a high efficiency TE waste energy recovery system for passenger vehicle applications in November 2004.

In Phase 1, the team created an initial system architecture shown in Figure 1, developed a system model to predict performance, and established system and subsystem design requirements. Phase 2 was completed in January 2007, in which key subsystem

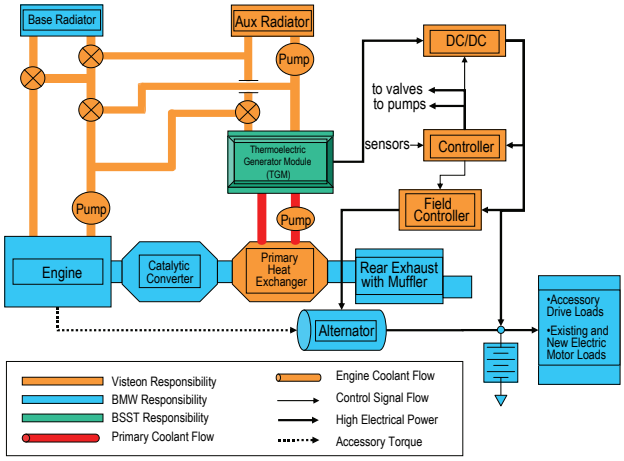

FIGURE 1. Initial System Architecture

components were built and tested and the system model updated to provide revised performance predictions.

Engine exhaust gas passes through the PHX where thermal energy is extracted and transferred to a gaseous working fluid (preliminarily designated as 75% He, 25% Xe). Wide variations in exhaust gas mass flow, which result in correspondingly wide variations in thermal flux, are managed by means of a pump which circulates the working fluid between the PHX and TGM's hot side. The use of this working fluid loop enables optimal usage of the TE material in the TGM as well as providing a dense, minimally sized hermetic enclosure for the TE material. Heat rejection from the cold side of the TGM can be facilitated by either the vehicle's powertrain cooling system or a supplemental cold-side cooling loop. TGM electrical power is linked to the vehicle electrical bus via a load matching DC/DC converter in the PCS. Fuel efficiency is increased by off-loading the vehicle alternator by use of power generated in the TGM.

Approach

A key element in BSST's approach to building TGMs for the WHRS is in the application of proprietary high density design and construction for joining TE materials to substrates. TE subassemblies based on traditional and BSST high density principles are shown in Figure 2.

TGMs will be built using the BSST configuration (with variation in the TE elements and geometry of the "Y" substrates) to better accommodate TE material compatibility, coefficient of thermal expansion mismatches and to significantly reduce the amount of TE material required.

An incremental approach is being followed in which low-temperature TGM subassemblies are built and tested prior to building high-temperature systems. This approach includes validation of TE material properties

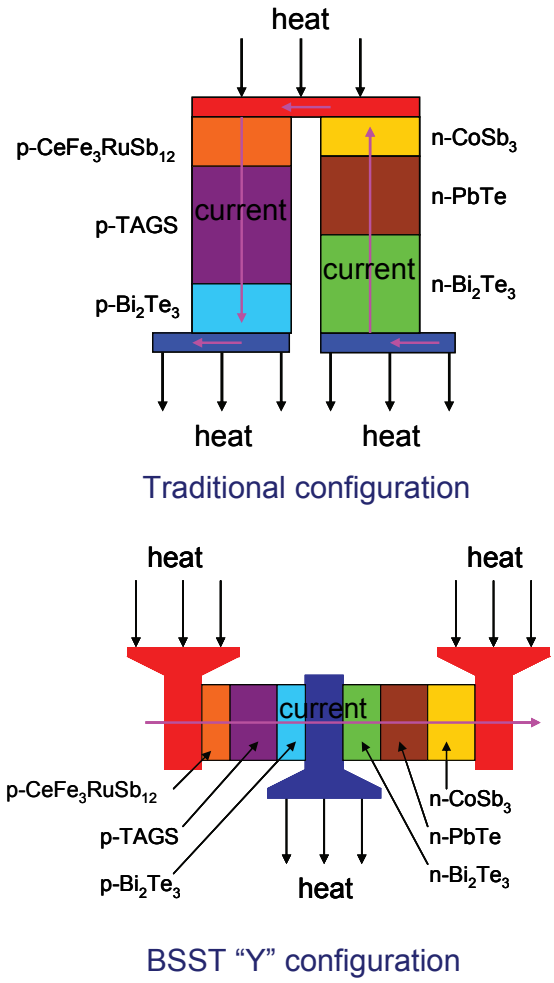

FIGURE 2. Traditional and BSST High Density TE Subassemblies

and performance models at the subassembly and subsequently at the full-scale level.

Results

Low-Temperature TGM Results

A low-temperature fractional TGM using BiTe TE material was modeled, built and tested. A TE subassembly of the BiTe TGM is shown in Figure 3 (heat exchangers not shown).

N and p type TE material was soldered to copper substrates which were placed in close contact with cold and hot heat exchangers. Current flows through the substrates and TE material as shown in Figure 3.

One partial layer of the fractional BiTe TGM is shown in Figure 4. BiTe subassemblies were arranged on a liquid heat exchanger through which hot oil flows. The hot heat exchanger is anodized aluminum to prevent electrical shorting of the subassemblies and thermal grease is used to promote heat transfer. A similar cold-

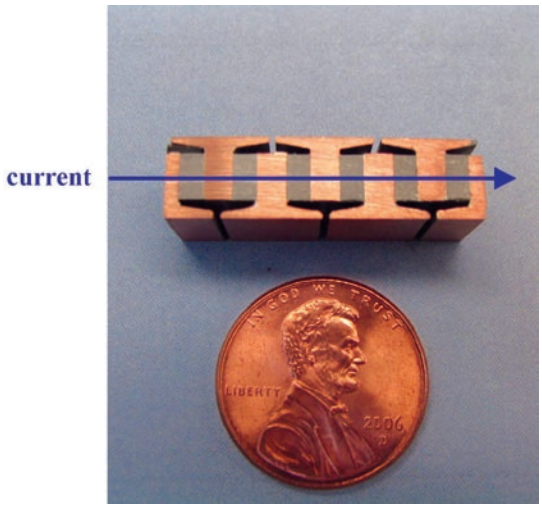

FIGURE 3. BiTe Subassembly

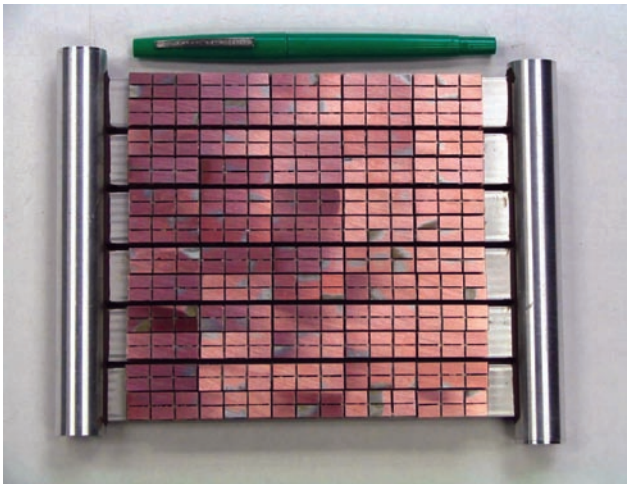

FIGURE 4. BiTe Fractional TGM

side heat exchanger (not shown) is set atop the BiTe subassemblies to complete the TGM. Another layer of BiTe subassemblies and additional cold heat exchanger is placed on the opposite side.

Test results for the fractional BiTe TGM operated over a range of cold- and hot-side temperatures are shown in Figure 5. As shown in the data, 130 watts of electric power was generated at a peak ΔT of 205°C.

Additional layers were then built and a full-scale BiTe TGM was assembled. Five hot and six cold heat exchangers were used in the full-scale TGM. The full-scale BiTe TGM is shown in Figure 6.

The full-scale BiTe TGM was operated over a range of cold and hot side temperatures. Data are shown in Figure 7 that depicts the performance of the full-scale BiTe TGM with the oil inlet temperature at 210°C and

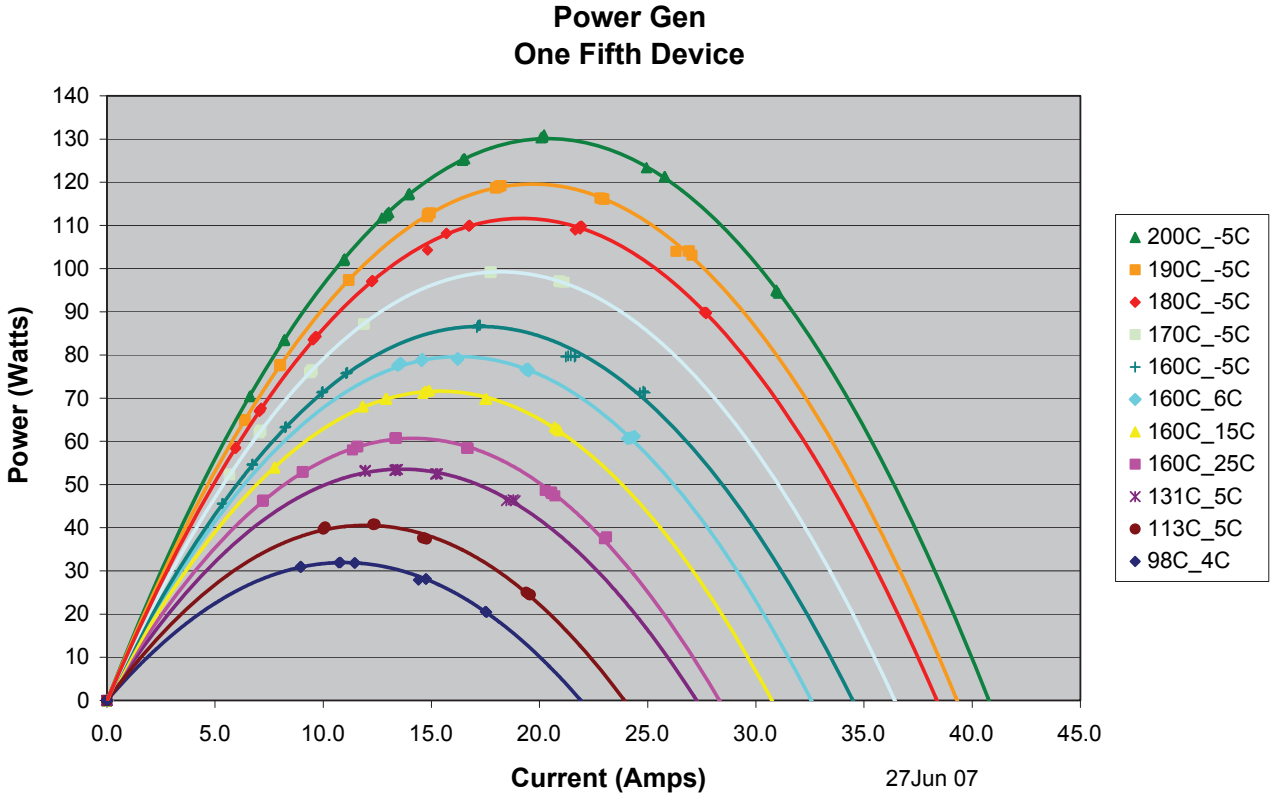

FIGURE 5. Fractional BiTe TGM Test Results

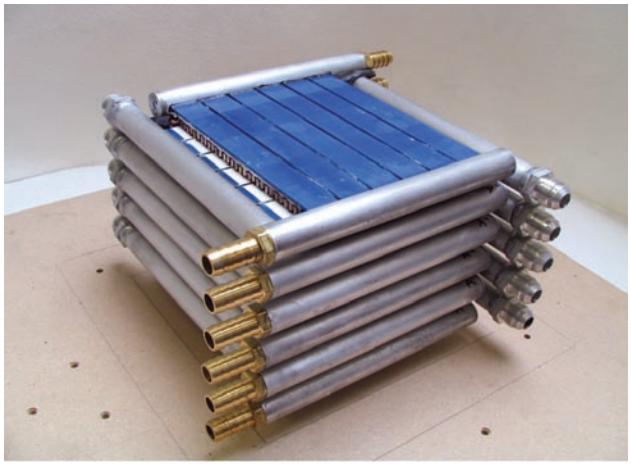

FIGURE 6. Full Scale BiTe TGM

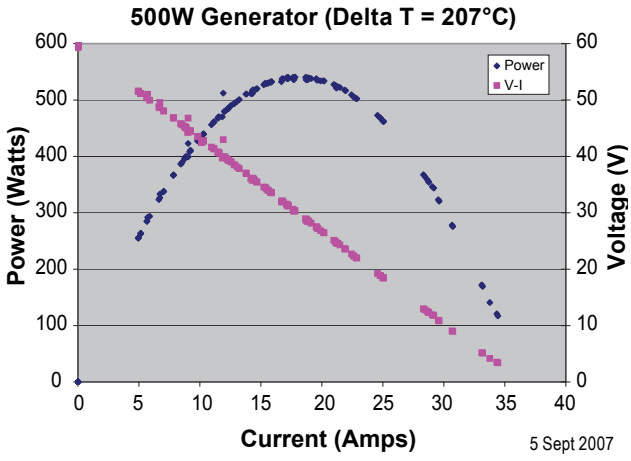

FIGURE 7. Full Scale BiTe TGM Test Results

the water inlet temperature at 2.5°C. For this condition ($\Delta T = 207°C$) over 500 watts of electric power was produced.

High-Temperature TGM Results

Fractional, 20 watt TGM

A fractional high temperature TGM was built using PbTe/TAGS TE material with cartridge heaters providing the thermal power. A portion of the fractional PbTe/TAGS TGM is shown in Figure 8 (cold side liquid heat exchangers not shown).

Three hot side TE subassemblies were built, each having eight total TE elements (four n-type PbTe and four p-type TAGS). The hot-side TE subassemblies were placed between cruciform shaped copper parts which were set between liquid heat exchangers through which a cold fluid was circulated.

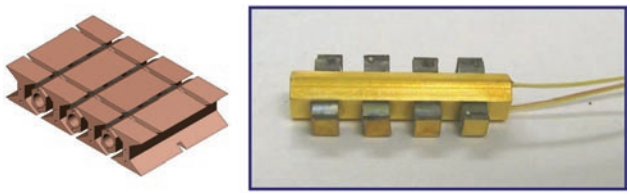

FIGURE 8. Fractional Pb/TSAGS TGM Isometric Drawing and Hot-Side Subassembly (Substrate with Interior Cartridge Heater and TE Elements)

Test results for the fractional PbTe/TAGS TGM are shown in Figure 9. Over 20 watts of electric power was generated for the test condition in which the average hot side temperature was 472°C and the cold side average temperature was 33°C.

Fractional, 10% efficient TGM

A 10% efficient fractional TGM was built and tested using PbTe and TAGS TE material segmented with BiTe. The design and construction of the fractional TGM was similar to the 20 watt PbTe/TAGS TGM, with the exception that BiTe material was joined to each n and p type PbTe and TAGS element, respectively and only one hot-side TE subassembly was used. A cartridge heater was used to generate thermal power which enabled precise measurement of power into the device.

The PbTe/BiTe and TAGS/BiTe segmented elements are shown in Figure 10.

A converter efficiency of 10% was measured when the device was operated with a hot-side temperature of 500°C and cold-side at 20°C. The calculation of efficiency was made inclusive of all electrical and thermal parasitic losses. Segmented couple TGM performance is shown in Figure 11.

System Modeling Status

The migration of the steady-state bumper-to-bumper system simulation model from the AVL Advisor platform to Gamma Technologies GT Cool was completed in early 2007. The steady-state system model was validated by comparing predicted and measured values of exhaust gas mass flow, temperature and fuel consumption for various driving conditions and found to show good agreement. Preliminary fuel efficiency predictions were made showing fuel efficiency improvement from 0% to over 8% based on driving conditions.

A transient system model was developed and is currently being evaluated. The transient vehicle model was coupled with a transient TEG model and provides a large variety of parameters for optimization, e.g. working fluid (exhaust or primary coolant such as He/Xe), heat exchanger design, TE leg design and other parameters.

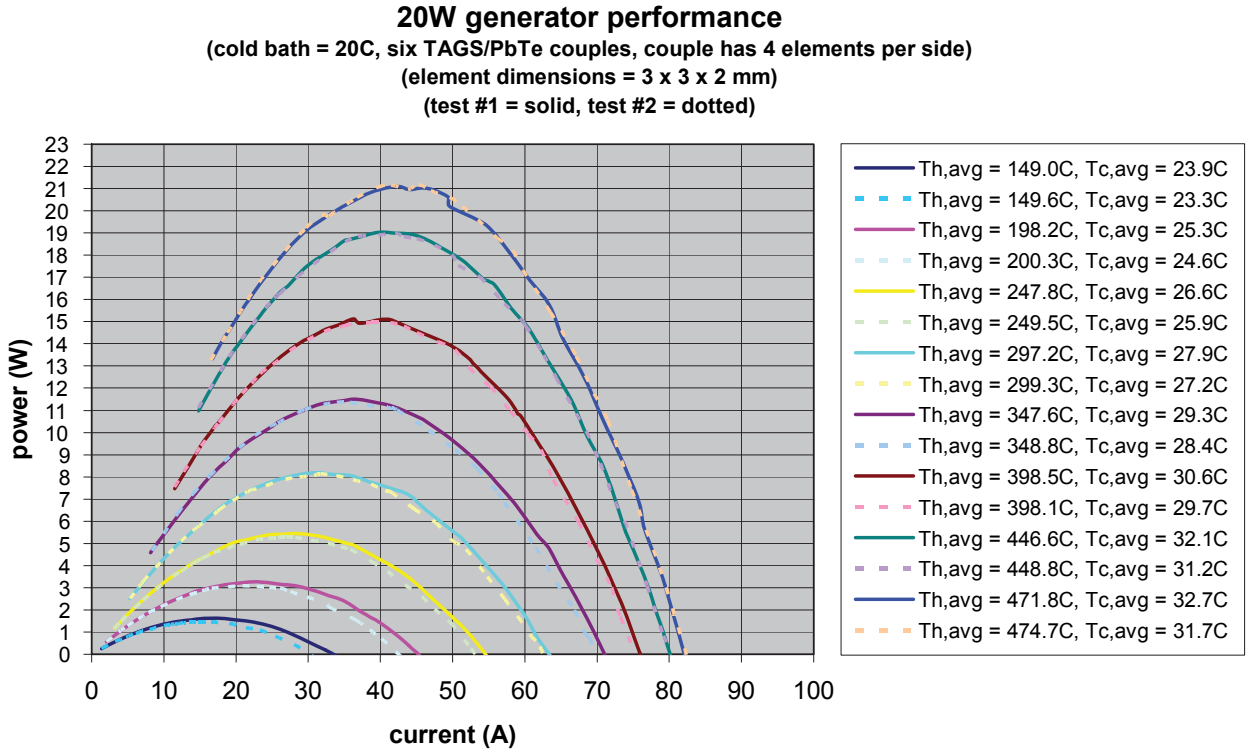

FIGURE 9. Fractional Pb/TSAGS TGM Test Results

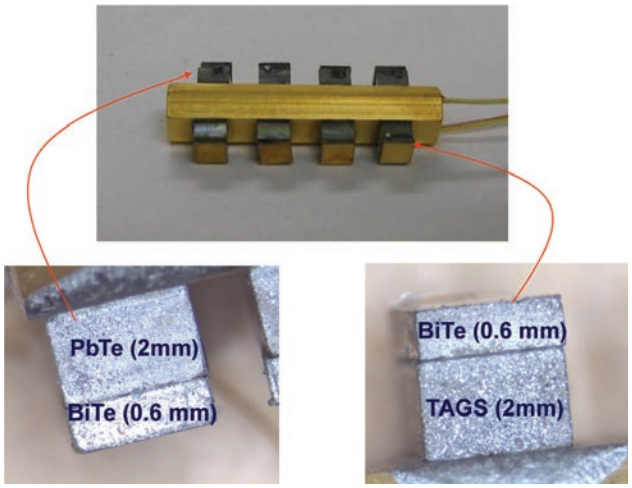

FIGURE 10. 10% Efficient Pb/TSAGS/BiTe Fractional TGM Hot Subassembly

The transient system model is being used to evaluate the performance of two system architectures. The initial system architecture, shown in Figure 1, features a secondary loop that moves exhaust gas heat to the TGM. A second architecture is simplified and does not feature the secondary loop, but does provide a means for managing the variation in exhaust gas flow to optimize TGM efficiency. These results are in review and will be provided in the near future.

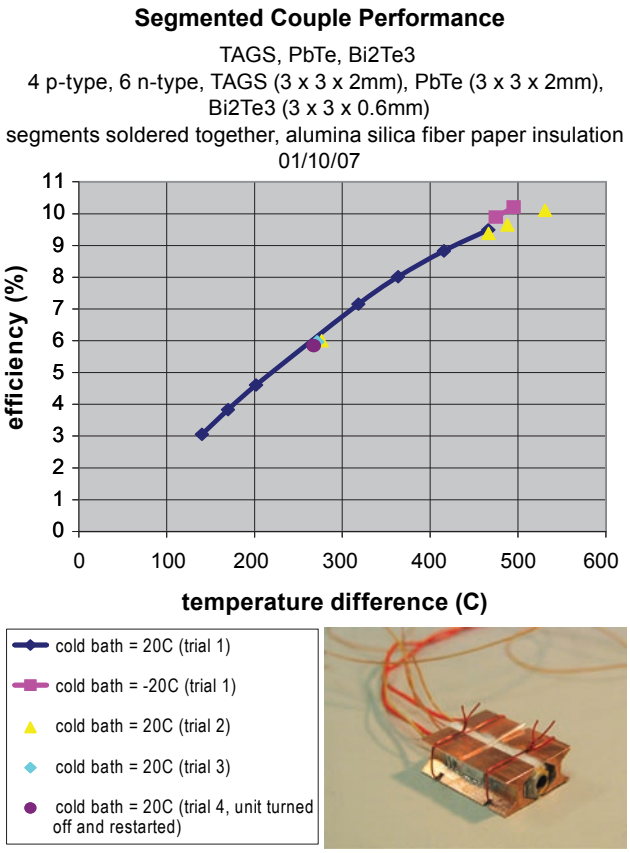

FIGURE 11. 10% Efficient Pb/TSAGS/BiTe Fractional TGM Test Results

Conclusions

BSST has effectively demonstrated the viability and performance of TGMs based on proprietary high density design and construction principles using low- and high-temperature TE materials.

The system performance model has been migrated from AVL ADVISOR to Gamma Technologies GT Cool. As a result, the model more closely reflects the baseline performance of the vehicle platform and therefore more accurately models the performance of the WHRS. In addition, the model has been updated to predict transient performance.

Future Directions

- Use of segmented elements to maximize ZT over the entire temperature range.
- Adjustment of segment thicknesses to combat TE material incompatibility within each element.
- Adjustment of element thicknesses to combat TE material incompatibility in the direction of flow.
- Use of alternative "Y" connector configurations to accommodate differing element thicknesses and to combat differing thermal expansion coefficients.
- Use of non-rigid joints to continue to combat thermal expansion mismatch.
- Use of advanced modeling and optimization concepts to maximize the benefits of the above mentioned design concepts.

FY 2007 Publications/Presentations

1. 2007 DEER Conference
2. 2007 DTEC Conference
3. 2007 Semi-Annual Mega Merit Review

III.3 Thermoelectric Conversion of Waste Heat to Electricity in an IC Engine Powered Vehicle

Harold Schock (Primary Contact),
Eldon Case, Adam Downey, Tim Hogan,
Mercouri Kanatzidis, James Novak, John Miller,
Fang Peng, Fei Ren, Ed Timm
Michigan State University (MSU)
East Lansing, MI 48864

DOE Technology Development Manager:
John Fairbanks

NETL Project Manager: Samuel Taylor

Subcontractors:
- Jeff Sakamoto, NASA Jet Propulsion Laboratory, Pasadena, CA
- Tom Shih, Iowa State University (ISU), Ames, IA
- Todd Sheridan, Cummins Engine Company, Columbus, IN
- Charles Cauchy, Tellurex, Traverse City, MI

Objectives – Phase II (approximately half of the effort has been completed)

- Using thermoelectric (TE) energy recovery from the exhaust system, determine material performance needed to produce a 10% improvements in brake specific fuel consumption for an over-the-road (OTR) truck operating under cruise conditions.
- Evaluate currently available TE materials to determine engineering developments required for their implementation in a thermoelectric generator (TEG) for an OTR truck, which can be demonstrated within five years.
- Determine requirements for a heat exchanger needed in this application.
- Determine power electronic and control requirements for this application.
- Assemble the equipment needed to conduct the necessary material synthesis, fabrication and hardware necessary for a scaled demonstration.
- Determine if Phase II results warrants a prototype engine. TEG final design in Phase III.

Accomplishments in Phase II

- Systems for material synthesis, powder processing, hot pressing, leg preparation, material mechanical and TE property characterization, and couple fabrication have been demonstrated at MSU. Systems are in place to produce a 40 W module in one week.
- Using the measured properties of known materials for the temperature range of operation we estimate that a segmented couple can provide a conversion efficiency of over 12%.
- The first batch of Skutterudite material has been synthesized at MSU.
- Advantages of power impedance load matching experiments were demonstrated.
- Analytical studies show potential improvement of up to 6.2% in fuel economy for a Class 8 OTR truck operating at cruise conditions using current materials.

Future Directions for Phase II

- Conduct design and analysis of the power conditioning system to optimize thermoelectric system performance, including fault remediation.
- Refine leg fabrication methods (e.g. wet milling/dry milling, hot pressing) for improving mechanical properties and microstructural characteristics.
- Refine fabrication techniques for scaleable couple/thermoelectric (TE) modules.
- Finalize analytical studies on the full engine system including coupling current simulations to the 3-D heat transfer studies to provide efficiency gains for the optimum TEG-engine configurations.
- Improve the thermoelectric figure of merit (ZT) by exploring several more promising thermoelectric material compositions with emphasis this period on PbTe systems, with S doping, as well as Skutterudite synthesis.
- Extensive mechanical, thermal cycling and thermoelectric property testing of segmented hot-pressed legs including Bi_2Te_3 and lead-antimony-silver-tellurium (LAST)/(T).
- Continue development of module fabrication methods.

Introduction

At peak efficiency, current diesel engines are capable of converting 40 percent of fuel energy to useful work. When a Class 8 diesel truck is loaded, the engine might deliver 300 kilowatts of power to drive the wheels, while at the same time, another 300-400 kilowatts of

energy goes out through the exhaust stack as wasted energy. This research project is attempting to find ways to capture that wasted energy and convert it to back into useful energy. A reasonable long-term goal would be to increase the diesel power plant efficiency to greater than 50%.

This unique project requires input from a number of researcher collaborators within the College of Engineering at MSU, as well as experts from outside of MSU. The aim of the research is to use a direct conversion device, fabricated out of TE materials, to recover waste heat from the exhaust of internal combustion engines and turn it into useful electricity. The team is working with TE materials that have already been developed and are assessing them to see if they can be implemented into a powertrain in a cost-effective manner. The team is also developing new high efficiency TE materials that will permit a 10% improvement in fuel economy of OTR Class 8 trucks. We expect that completion of the project through Phase 4 will result in a scaled demonstration of the internal combustion (IC) engine and TE energy recovery system.

Approach

This MSU led multidisciplinary research effort is to evaluate the entire system and identify the required processes needed to bring TE technology to a cost effective commercial product for OTR trucks. The Phase II analysis involves an exploratory analysis and feasibility study, which includes system design, new TE material synthesis, power electronics design, material thermoelectric and mechanical property characterization, heat exchanger design, TE material fabrication methods, module fabrication and evaluation of system performance. To date, about half of the Phase II effort has been completed.

Results

1. Property Characterization - Experimental Procedure

The elastic moduli measurements at Oak Ridge National Laboratory (ORNL) and at MSU were performed using resonant ultrasound spectroscopy (RUS) (Figure 1) to evaluate the elastic moduli both before and after thermal cycling.

The acoustic resonant spectrum induced in a mechanically driven specimen is a function of the elastic moduli, geometry, dimensions and mass density of the specimen.

It is important to note that this equation not only describes the thermal fatigue behavior of LAST, but Case *et al* [1], has shown that it also describes the strain versus # of cycles thermal fatigue behavior of a

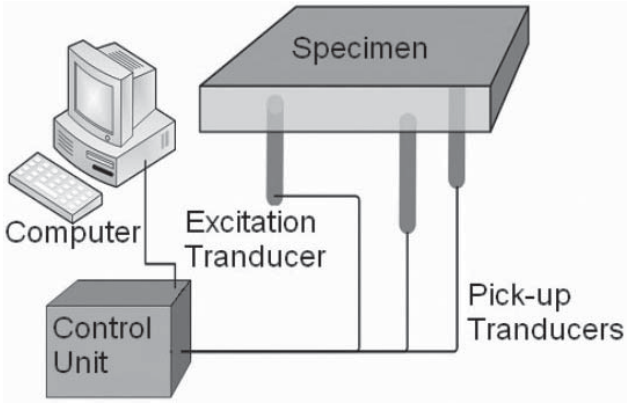

FIGURE 1. Resonant Ultrasound Spectroscopy Apparatus used for Young's Modulus Measurements

wide variety of brittle materials including unreinforced ceramics, whisker-, fiber- and platelet- reinforced ceramics, metal matrix composites, and polymeric composites.

Although much more thermal fatigue work needs to be done to characterize the evolution of thermal fatigue damage in LAST materials, this work shows that the evolution of thermal fatigue damage in LAST can be described in terms of the same equation describing thermal fatigue damage in a wide range of brittle materials, which aids our overall understanding of the damage process in LAST TE legs.

Additional thermal fatigue testing at both ORNL and MSU will involve a greater range of ΔT values and a greater number of thermal fatigue cycles. In addition to performing fatigue tests on individual legs, we will conduct thermal fatigue tests on unicouples. Also, we will work toward designing experiments that more closely approximate in-service thermal cycling conditions.

2. TEG Design Alternatives for Heat Transfer

The proposed efforts are as follows:

1. Design and analyze geometrical configurations needed for transferring heat from the high temperature exhaust gases to the hot side of the thermoelectric generator.
2. Design and analyze geometrical configurations needed for transferring heat from the cold side of the thermoelectric generator to ambient surroundings.
3. Design, analyze, and select method and working fluids necessary to perform intermediate heat transfer within the thermoelectric generator.

During this past quarter, a series of 3-D computational fluid dynamics (CFD) analyses were made to understand how heat transfer from the hot

gas to the TE legs could be increased, so that heat transfer rate and hence electric generation can be increased. Three design concepts were examined. The first design concept is to add advanced heat-transfer enhancement techniques on the hot-gas sidewall (e.g., inclined rounded ribs) to increase the heat transfer rate through the thermoelectric couples. The second design concept is to use heat-transfer enhancement techniques plus exposing the thermoelectric legs (with a protecting coating) to the hot gas in regions where the heat-transfer coefficient is the highest. The third design concept is a combination of design concepts one and two described above plus using the wall that separates the hot gas from the thermoelectric couples as a heat reservoir to store thermal energy.

The key findings from the CFD results generated are as follows:

1. Design concept 1 can be quite effective. Since the Biot number is quite low, the wall temperature is nearly constant across the wall and that temperature is higher when the heat transfer coefficient is higher. Thus, considerable heat can be transferred directly from the wall to the thermoelectric legs, provided that the contact resistance is not high and thermal stress issues can be resolved.
2. Design concept 2 can also be quite effective. Since the thermoelectric leg is in direct contact with the hot gas, the temperature on the surface of the thermoelectric leg in contact with the hot gas is the highest possible for a given heat-transfer coefficient. The advantage of this design concept is that it has the potential to minimize thermal stresses.
3. Design concept 3 can be highly effective when used with either design concept 1 or 2. If the maximum amount of heat that can be transferred to the wall that separates the hot gas and the thermoelectric couples is higher than the amount of heat that can be transferred from the wall to the thermoelectric couples and the Biot number of the wall is low, then the temperature in the wall will keep rising until is it reaches some maximum value close to the hot gas temperature. Thus, the wall behaves like a heat reservoir at nearly constant temperature (analogous to a flywheel) to transfer heat from the hot gas to the thermoelectric couple. The advantage of this approach is that the wall temperature can be very high even when the heat-transfer coefficient is low.

Efforts are still underway to quantify design concept 3, in order to better understand the maximum wall temperatures that can be achieved and the number of thermoelectric couples that can be packed per unit area.

3. Power Electronics - Demo and Test Results of the Power Electronics (PE) Circuit for Maximum Power Point Tracking

A heat exchanger capable of 100 W electrical power output has been developed in the last quarter and explained in a previous report. The installed 20 TE modules (G1-1.4-219-1.14) are grouped into two sets and each one is connected in series. Previous test results showed that those two sets of TEG modules can output electric power of 50.6 W and 48.4 W, respectively, if a resistive load of 40 ohms was applied.

Based on the understanding of TEG module characteristics, a PE circuit capable of 60 W was designed and fabricated in our lab to interface the TEG modules with real loads. The first set of the TEG modules were directly connected to a 50 W light bulb, and the second set was connected to a 50 W light bulb via the power electronics circuit. The light bulbs have variable and non-linear resistance, which is close to most real loads. Three thermal conditions were tested and the electrical output power vs. ΔT (T_{Hot}-T_{Cold}) curves were drawn in Figure 2. We found that TEG module set 2 (with PE interface circuit) can output as much as twice of the electric power of set 1 (directly connected to the light bulb) under same heat flux. Under the thermal condition of ΔT =150°C -31°C (T_{Hot}-T_{Cold}), TEG set 1 can only output electric power of 23 W, although it is capable of 50.6 W output. This is due to the heavily mismatched load impedance. However, the TEG set can still output electric power of 47 W, which is the maximum output power that can be provided from set 1. In summary, the PE circuit can extract the maximum electric power from the TE modules and feed it to loads regardless of TE module's heat flux and load impedance or conditions.

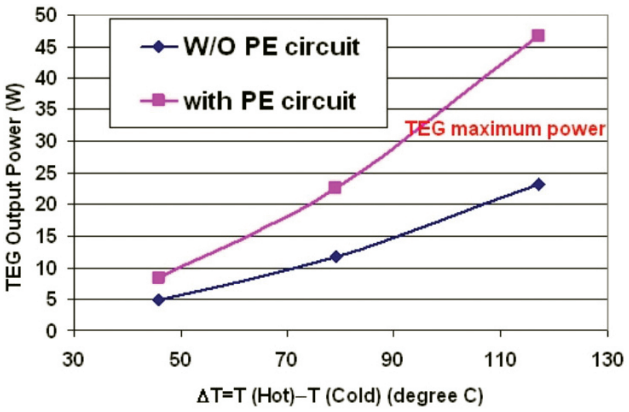

FIGURE 2. TEG Output - Electric Power vs. ΔT (T_{Hot}-T_{Cold})

4. Skutterudite Module Fabrication

Previous reports have described the results of our LAST synthesis efforts. Concurrently, an effort has been underway with the Jet Propulsion Laboratory (JPL) to fabricate Skutterudite thermoelectric modules. The primary focus is on fabricating and testing 40 W thermoelectric modules operating at greater that 12% thermal-to-electric conversion efficiency (Figure 3). The first generation modules will consist of n and p-type Skutterudite legs. The cold side of the module will share a common substrate where electrical contacts consist of copper pads patterned on an aluminum oxide substrate. The Skutterudite legs are pre-metallized (metallized during hot pressing). Bonding the cold side of the metallized legs is achieved with standard soldering techniques and leg alignment is achieved with precision graphite egg-crate tooling (designed and fabricated in house). The hot side metal interconnects are made using a brazing or diffusion bonding technique developed by Dr. Sakamoto, while at JPL. It is important to note that the hot side of the 40 W modules does not involve bonding the legs to a common hot side heat exchanger. Instead, the hot side interconnects are free-standing or free to expand and contract laterally/independently, thus significantly reducing shear stress on the legs and hot side metallization addition. The proposed design could enable the placement of the hot side interconnects/ heat collectors directly into the exhaust stream to gain access to the hottest exhaust gas temperatures. In this paradigm, thermal management is key, thus we propose the integration of aerogel-based thermal insulation (Figure 4). Because aerogel is a highly porous form (99% porous) of silica, it has extremely low thermal conductivity. In particular, pores within aerogel are nano to sub nano in scale, thus gas conduction in aerogel is lowest of any material.

5. Engine Thermoelectric System Modeling

The second phase of this study involves modeling of the full six-cylinder Cummins ISX engine with integrated TEG units and including the turbocharger, intercooler, and exhaust gas recirculation bypass systems. This is necessary to understand the balance of exhaust energy flow split between the TEG and the variable geometry turbocharger in order to meet the engine's power output demands. Figure 5 shows the new system model illustrating the interconnected on this engine. On the left side of the figure the cloud represents the intake air after the air cleaner which feeds into the compressor side of the turbocharger. Likewise, the cloud on the right side of the figure represents the outlet of an exhaust pipe connected to the outlet of the turbocharger turbine. Various alternatives for extracting energy using the TEG while increasing fuel economy and maintaining performance are being investigated.

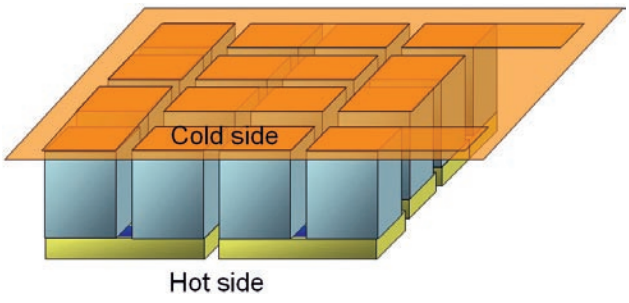

FIGURE 3. Free Standing Hot Shoe Module Design; Produces 40 W and Consists of 16 Skutterudite Legs 7mmx7mmx6mm Long

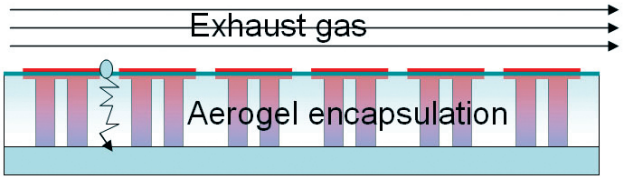

FIGURE 4. Aerogel-based thermal insulation could enable TE devices integrated directly in to the exhaust stream. Gas transport through the aerogel is significantly impeded by the highly-tortuous, nanoscale porosity, thus providing effective thermal insulation.

6. Summary

Completion of the Phase II effort will provide the following results:

- Preliminary TEG design will be completed using the most promising TE materials.
- Demonstrate the viability of a module which can produce between 20 and 40 W of power with a temperature difference of less than 800 K on the hot side and 300 K on the cold side.
- Accurately quantify the bulk mechanical properties for the LAST/tellurium material for use in the finite element analysis (FEA) studies of the thermoelectric generator.
- Complete selection of appropriate TE materials, metallization for segmented couples, voltage insulators and required sublimation suppression.
- Couple detailed Iowa State University heat transfer models to WAVE and FEA models of thermoelectric generator. Perform comparison of system efficiency for various options.
- Estimate potential TEG-engine performance gains using demonstrated materials with measured mechanical and thermoelectric properties.

Results to date suggest that using TEG technology, a 5% improvement in brake specific fuel consumption for an OTR truck is a reasonable 5 year goal - 10% improvement possible with advanced designs and new TE materials.

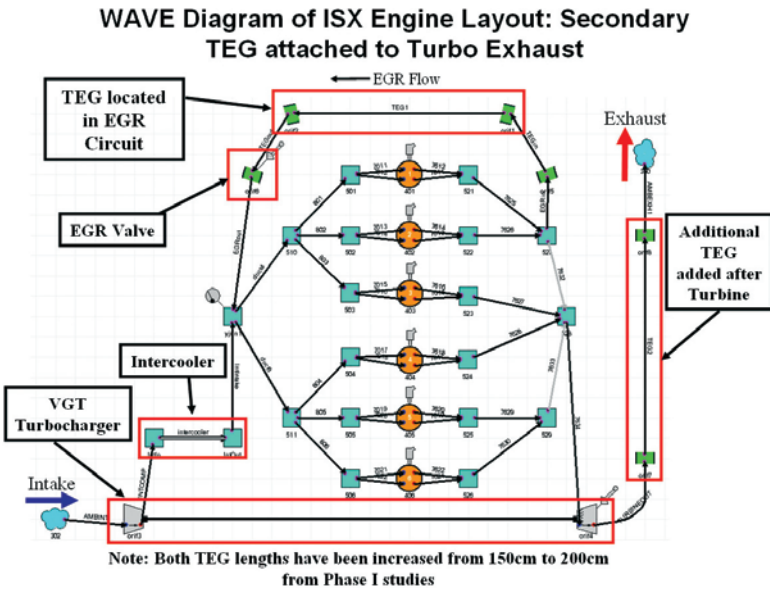

FIGURE 5. WAVE Diagram of Cummins ISX Engine Layout: Secondary TEG attached to Turbo Exhaust - Note: Both TEG lengths have been increased from 150 cm to 200 cm from Phase I studies.

References

1. E. D. Case, The Saturation of Thermomechanical Fatigue in Brittle Materials, Thermo-Mechanical Fatigue and Fracture, WIT Press, Southampton, UK, editor M. H. Alibadi, 2002, pp. 137 – 208.

FY 2007 Publications and Presentations

1. Characterization of Dry Milled LAST (Lead-Antimony-Silver-Tellurium) Thermoelectric Material, Pilchak, A., Ren, F., Case, E., Timm, E. and Schock, H., submitted to Philosophical Magazine, Spring 07.

2. Nanostructured Thermoelectric Materials and High Efficiency Power Generation Modules, Hogan, T., Downey, A., Short, J. et al., prepared spring 07.

3. The Young's Modulus and Poisson's Ratio of Lead-Telluride Based Thermoelectric Materials as a Function of Temperature, Ren, F., Case, E., Timm, E., Schock, H., Lara-Cuzio, E., Trejo, R., Lin, C.H., Kanatzidis, M., submitted to International Journal of Applied Ceramics Technology, Spring 07.

4. Hardness as a Function of Composition for N-Type LAST Thermoelectric Materials, F. Ren, E.D. Case, E.J. Timm, and H.J. Schock, Journal of Alloys and Compounds, (2007) doi:10.1016/jallcom.2007.01.086.

5. Young's Modulus as a Function of Composition of N-Type Lead-Antimony-Silver-Telluride (LAST) Thermoelectric Materials, F. Ren, E.D. Case, E.J. Timm, and H.J. Schock, submitted to Philosophical Magazine, Spring 07.

6. Weibull Analysis of the Biaxial Fracture Strength of a Cast P-Type LAST-T Thermoelectric Material, F. Ren, E.D. Case, E.J. Timm, M.D. Jacobs and H.J. Schock, Philosophical Magazine Letters, Vol. 86, No. 10, Oct. 2006, 673-682.

IV. UNIVERSITY RESEARCH

IV.1 Consortium on Low-Temperature Combustion for High-Efficiency, Ultra-Low Emission Engines

Dennis Assanis
University of Michigan (UM)
Mechanical Engineering
2045 W.E.Lay Auto. Lab.
1231 Beal Avenue
Ann Arbor, MI 48109-2133

DOE Technology Development Manager:
Gurpreet Singh

NETL Project Manager: Samuel Taylor

Subcontractors:
- Massachusetts Institute of Technology (MIT), Cambridge, MA
- Stanford University (SU), Stanford, CA
- University of California, Berkeley (UCB), Berkeley, CA

Objectives

- Investigate the fundamental processes that determine the practical boundaries of low-temperature combustion (LTC) engines.
- Develop methods to extend LTC boundaries to improve the fuel economy of homogeneous charge compression ignition (HCCI) engines fueled on gasoline and alternative blends, while operating with ultra low emissions.
- Investigate alternate fuels, ignition and after-treatment for premixed compression ignition (PCI) engines.

Accomplishments

- Multi-cylinder supercharged engine operation for high-load limit extension has been demonstrated using port fuel injection. Initial experiments up to 1.7 bar intake pressure have shown proportional load increases. Combustion control is provided by an intake air cooler/flow splitter arrangement.
- Single-cylinder experiments have achieved low-load extension by fuel injection during negative valve overlap (NVO). Further, varying the timing of the injection affects the combustion phasing and shows promise as a control tool.
- Different valve timing strategies for achieving HCCI have been explored using an engine simulation based on GT-Power® and enhanced with user-derived HCCI combustion and heat transfer models. Studies indicate that load limits are strongly affected by complex interactions between sensible residual gas heat, effective compression ratio associated with the particular valve strategy employed, and cycle-to-cycle feedback of residual gas.
- Spark assist has been shown to have an effect in stabilizing and controlling HCCI combustion under limit conditions. To investigate this effect, the interaction of a laminar flame and auto igniting gas has been modeled using HCT, a one dimensional transient reacting gas code. The results are consistent with the experimental findings, and by demonstrating the independence of the flame and autoignition process, point to relatively simple computational fluid dynamics (CFD) models of spark-assisted HCCI to be developed.
- Rapid compression ignition studies of several isomers of the biofuel component methyl-butanoate have been carried out. The results have been used to update a detailed kinetic model by Westbrook et al. at Lawrence Livermore National Laboratory (LLNL).
- An after-treatment model has been developed for PCI combustion products which successfully describes the performance of a production-type low-temperature diesel oxidation catalyst (DOC) under PCI and normal diesel operation.

Future Directions

- Carry out single- and multi-cylinder experimental investigations of upper and lower load combustion limits with supercharging/turbocharging and fast thermal management of intake temperature.
- Explore valve actuation and supercharging/turbocharging implementations with the GT-Power® system model and evaluate performance and fuel economy benefits.
- Develop model of spark-assisted HCCI and explore potential benefits of the technology from the point of view of control and range extension.
- Adapt after-treatment model to gasoline conditions and apply to HCCI system studies.

Introduction

LTC is a new technology for internal combustion engines which promises to provide improved fuel economy with low emissions. With this technology, the engine is operated lean and cool enough to drastically

reduce NOx emissions and reduce particulate matter. In addition, operating lean allows high compression ratios for gasoline and reduces particulate emissions in diesels. The overall effect is to increase fuel economy for gasoline applications by up to 25%, and in the case of diesel engines, provide the means of satisfying the new, more stringent emissions regulations.

Because LTC implies operation at temperatures near the limit of flame propagation, reliable combustion must be initiated by auto-ignition which requires successful management of the thermal history of the engine and the gas charge. In principle, this can be achieved with adequate thermal management; control and various methods have been suggested for accomplishing this. However, as shown in Figure 1, full use of LTC has been limited at both high and low loads and threatens to reduce the ultimate fuel economy benefit that can be achieved in a vehicle system. At low load there is not enough heat in the charge to keep combustion healthy, while at high load the combustion is too rapid and may damage the engine structure. The focus of this consortium is to investigate the limit phenomena and to propose methods of extending the limits.

Approach

Our research project, in its second year, combines experiments and modeling at four university research centers in order to acquire the knowledge and technology to develop methods to extend the load range of LTC engines. To accomplish this, both single-cylinder and multi-cylinder engine experiments are investigating direct fuel injection strategies, turbocharging/ supercharging, and fast thermal management as possible approaches. Other tasks concentrate on spark-assisted LTC, and possible roles of alternate fuels. Recognizing the role of emission constraints particularly in the context of transient vehicle operation, studies of after-treatment devices are underway with specific application to the LTC environment both for HCCI and for PCI systems.

An array of modeling tools are being developed and refined, and brought to bear on the specific limit problems of importance. These models cover a range of detail from system models for engines and after-treatment devices, through detailed and reduced chemical mechanisms, to fully coupled CFD/kinetic models. Our intent is to take advantage of the broad range of capabilities of the university partners and the collaborative relationships among them.

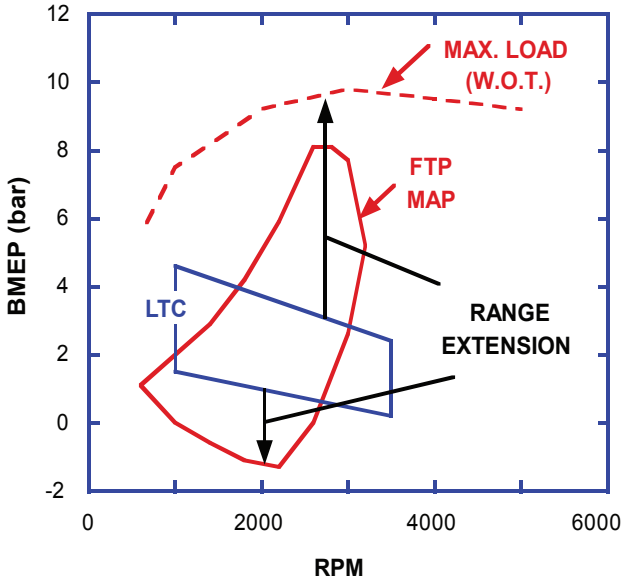

FIGURE 1. Performance map showing limited current achievable LTC range relative to a typical automotive range for maximum load over the FTP driving cycle.

Results

HCCI Results

Engine Experiments on HCCI Limit Extension - Experiments at UCB with a four-cylinder engine have shown supercharged operation up to manifold absolute pressure of 1.7 bar. Initial results from this study are shown in Figure 2 for both gasoline and ethanol fuel, where indicated mean effective pressure (IMEP) is shown as a function of 50% burned combustion phasing (CA50) varied by adjusting the intake temperature with an intake flow splitter arrangement. The expected increase in load with manifold pressure is observed along with the characteristic fall off in IMEP with retarded combustion phasing. These tests were carried out at a constant equivalence ratio of 0.3. Future work

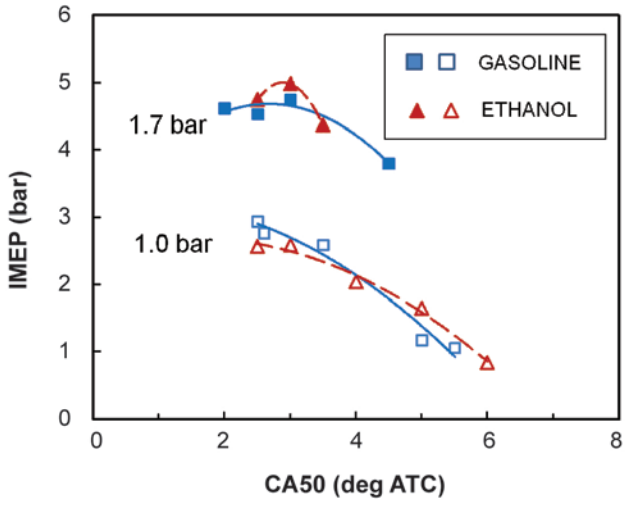

FIGURE 2. Experimental timing sweeps measured on the UCB four-cylinder supercharged HCCI engine showing increased IMEP at higher manifold pressure. Tests carried out for both gasoline and ethanol fuel at an equivalence ratio of 0.3.

will work towards higher equivalence ratios and load and will exercise the rapid thermal management flow system in real time.

Last year, experiments at Stanford University found that fuel injection during NVO has the potential to extend the low-load limit of HCCI operation to approximately 1 bar of net mean effective pressure (NMEP). The experiments were carried out on a variable valve actuation single-cylinder engine. It was found that when fuel is injected during this overlap period the ignition is advanced so that lower loads can be obtained. The mechanism for this enhancement is the partial release of energy due to pre-reaction of the injected fuel prior to the main intake and power stroke. This advances combustion and extends the lean limit. This year the studies have determined that the phasing of the injection is important and that earlier injection results in earlier combustion. The effect is greatest at low equivalence ratios where there is an abundance of excess oxygen to support the pre-reaction. It is hoped that these findings will lead to improved combustion control at light load.

A third test facility is now in operation at MIT. This approach uses a computer-controlled turbocharger emulator to simulate a multi-cylinder application on a single-cylinder engine. Experiments are just getting underway at that facility.

Modeling and Simulation Tools for HCCI - Last year we reported on a parametric study at UM of HCCI combustion carried out with a fully coupled CFD/kinetic model. Extensive data was gathered from over 400 simulations for variables such as engine speed, equivalence ratio, turbulence level, wall temperature, and piston shape. The focus was on understanding the combustion broadening effect of the in-cylinder temperature distribution caused by heat transfer from the cylinder walls.

This year the CFD-generated results were used to develop a correlation of combustion burn rates and combustion efficiency that we have applied to a system study of HCCI limit behavior. This novel correlation is unique in that it includes not only the effect of main operating variables such as ignition timing, RPM, and equivalence ratio on burn rate variables, but also includes the physically plausible finding that combustion efficiency is primarily a function of peak cylinder temperature. Ignition is described by a suitable auto-ignition integral developed earlier.

The combustion correlation was incorporated into a GT-Power®-based engine model and combines in a computationally efficient way, the chemically determined combustion limits, as well as the engine features which determine the thermodynamics. A knock model and a NOx model were also added to the engine system model to account for roughness and emission constraints.

The model has been used to explore the load limits of several valve timing strategies for internal exhaust gas recirculation. Figure 3 shows the limit behavior of two strategies for providing residual gas fraction control: the first employs recompression or negative valve overlap; the second uses rebreathing enabled by a second exhaust valve event, open during the normal intake stroke. The

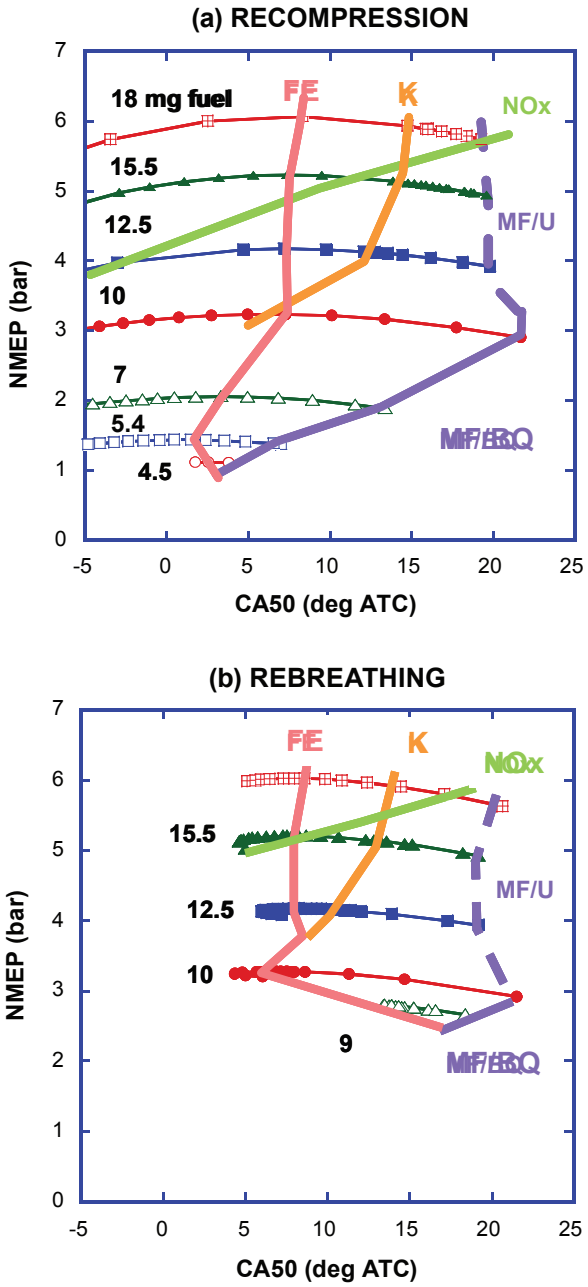

FIGURE 3. Calculated NMEP timing sweeps for two valve strategies: (a) recompression, and (b) rebreathing, for different fueling levels using UM combustion correlation. Constraints for fuel economy (FE), knock (K), NOx, misfire/unstable (MF/U), and misfire/bulk quench (MF/BQ) define the region of viable operation for each strategy.

figure shows NMEP phasing sweeps for a number of fueling levels at 2,000 rpm.

Superposed on the NMEP curves are a number of limit lines. The line labeled FE denotes the phasing for best fuel economy for the particular fueling employed. The knock and NOx constraint lines are labeled K and NOx, respectively. In general, these limit the maximum upper load achieved. At any given condition as the combustion is retarded, misfire eventually develops. At higher loads this appears first as unstable operation in which the cycles oscillate between strong and weak combustion. Eventually full misfire develops. This misfire unstable limit is denoted by the dashed line labeled MF/U. At low loads the unstable behavior does not appear before misfire and bulk quench occurs. This solid line is indicated by MF/BQ. Together these lines define the regions for viable HCCI operation, shown shaded.

Figure 3 shows that in this case, the upper limits are similar for the two strategies while the lower limits are much reduced for the rebreathing strategy due to the excessive heat losses sustained by the re-inducted exhaust gas which is in contact with the exhaust port and pipe walls. Based on studies of other valve strategies, these results are not general and are sensitive to the details of the valve strategy such as effective compression ratio, pumping work, and heat transfer. Currently, additional strategies are being evaluated.

As reported last year, optical engine experiments at UM have demonstrated the beneficial effects of spark assist in extending the low-load stability limit of HCCI. Under certain conditions a spark produces a turbulent flame structure which precedes and advances the general bulk autoignition of the rest of the charge. In order to better understand these processes, the unsteady, one-dimensional reacting flow code HCT was used to simulate the interaction between a laminar flame and the autoignition process. The simulations were conducted with a detailed 179 species, 996 reaction, kinetic mechanism for propane fuel obtained from LLNL. Conditions were chosen to match those in the optical engine experiments. Pressure was 15.5 bar, unburned temperature was 932 K, and equivalence ratio was 0.45. The simulation was carried out at constant pressure in order to focus on the diffusion effects rather than the well understood compression heating effects occurring due to the flame heat release in a constant volume situation.

The results are shown in Figure 4 where temperature profiles are shown as a function of the integrated mass coordinate with origin at an adiabatic wall on the left hand side. The flame moves in a steady fashion from right to left up to about 5 ms, when the first temperature rise is seen ahead of the flame due to autoignition. Combustion is complete by 5.7 ms. The flat temperature

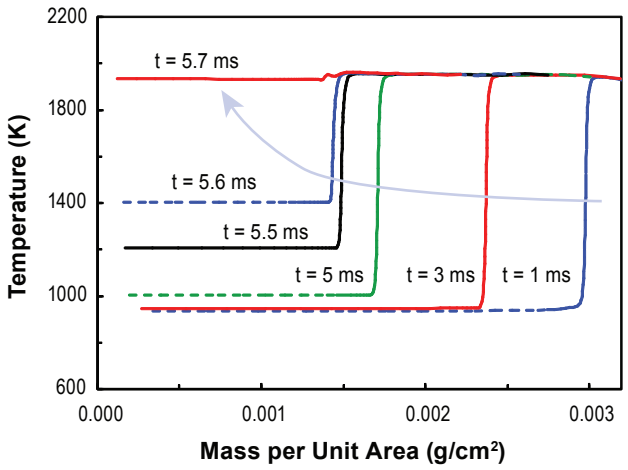

FIGURE 4. Simulation of a laminar flame moving leftward into constant pressure, auto-igniting gas using the HCT one-dimensional unsteady flame code. Temperature plotted vs. integrated mass coordinate. The autoignition process is relatively unaffected by the presence of the flame, while the flame can be seen to accelerate as the unburned temperature rises.

profiles ahead of the flame indicate that the flame travel has minimal effect on the autoignition event. However, the autoignition event appears to have an effect on the flame speed which approximately doubles between 3 and 5.5 ms from 60 to 120 cm/s due to the pre-reactions occurring upstream of the flame.

These findings mean that spark-assisted HCCI may be described by a combination of relatively independent autoignition and flame propagation processes, for which models exist. The next phase of modeling work will be aimed at adapting an existing Coherent Flamelet Model CFD code to include the appropriate interaction between flame and autoignition.

PCI Results

Kinetics and Alternate Fuels - During this year, the investigation of biofuel surrogate autoignition chemistry in the UM Rapid Compression Facility (RCF) has been expanded to include additional C5 esters, beyond work reported last year on methyl butanoate. These studies have quantified the effects of chemical structure on the ignition properties of isomers of methyl butanoate: butyl methanoate and ethyl propanoate. The ignition delay times of these ester/air mixtures were measured at moderate temperatures ~900-1,100 K and pressures (~10 atm) relevant to low-temperature combustion strategies. These data are the first of their kind to quantify the reactivity of these important reference compounds of oxygenated hydrocarbons at conditions important to advanced engine technologies. Figure 5 shows ignition delay results for the three esters along with data for isooctane.

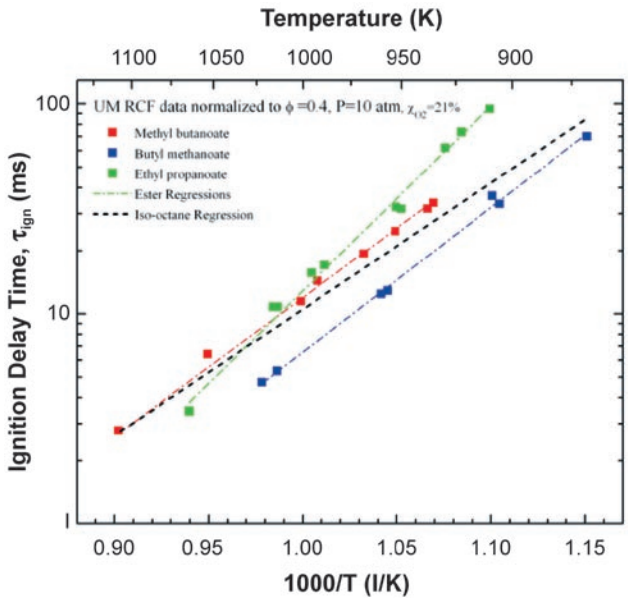

FIGURE 5. Ignition delay results for three esters: methyl butanoate, butyl methanoate, and ethyl propanoate, measured in the UM Rapid Compression Facility.

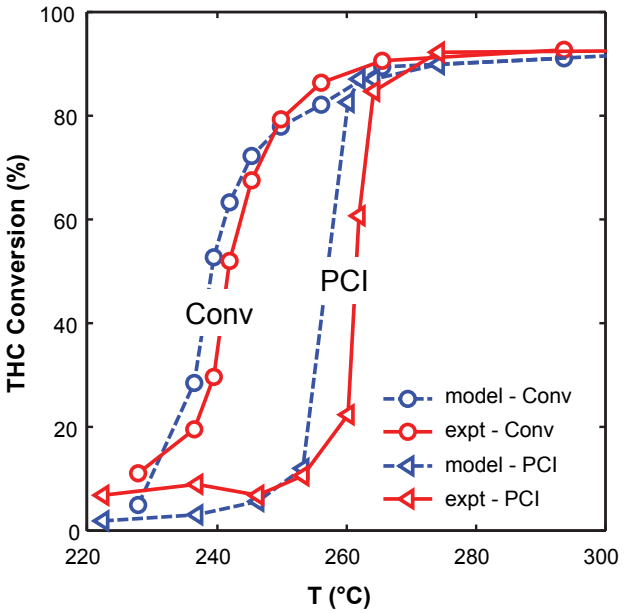

FIGURE 6. After-treatment model comparison with experimental THC light-off curves for conventional diesel (Conv) and for PCI conditions. Model successfully predicts the shift in light-off temperature for PCI exhaust conditions.

In a collaborative effort with Dr. Charles Westbrook and Dr. Bill Pitz of LLNL and Sandia National Labatories, the ester reaction mechanisms used to describe the chemistry of these compounds has been improved. The revised mechanism for methyl butanoate yields predicted ignition delay times in excellent agreement with the experimental data (improving the model results by nearly a factor of two). Next steps for the UM RCF studies include investigating the effects of blends of these ester compounds with reference gasoline and diesel compounds.

After-Treatment System Modeling - The goal of this task is to develop successful after-treatment models and system models for low-temperature applications in PCI. For this purpose a systematic methodology was developed to generate heterogeneous global reaction kinetics for hydrocarbons, CO, H_2 and NO under lean conditions and temperature ranges typically observed in oxidation catalysts. The methodology involves bench reactor tests, optimization of kinetic parameters, modifying and re-optimization of the rate expressions, and finally, validation by comparison with actual engine experimental light-off curves. So far the work has concentrated on diesel exhaust. The results for total hydrocarbon (THC) emissions are shown in Figure 6 for both PCI and conventional diesel operation. As seen in the figure, the model agrees well with the experimental data, and demonstrates the higher light-off temperatures required for PCI operation. This is due to the higher levels of concentration of CO and HC that this mode produces. Good agreement is also obtained with CO (not shown). The methodology, experimental set-up and optimization algorithms can very easily be extended to other catalytic converter systems, specifically to oxidation catalysts which are intended to be used in gasoline LTC aftertreatment.

Conclusions

- Multi-cylinder supercharged engine operation for high-load limit extension has been demonstrated using port fuel injection. Initial experiments up to 1.7 bar intake pressure have shown proportional load increases. Combustion control is provided by an intake air cooler/flow splitter arrangement.
- Low-load extension experiments on a single-cylinder engine have shown that varying the timing of the injection at low load affects the combustion phasing and shows promise as a control tool.
- Based on CFD/kinetic calculations a combustion correlation has been developed for use in engine system models. The correlation was incorporated into a GT-Power® engine model and used to explore different valve timing strategies for achieving HCCI. The results indicate that load limits are strongly affected by complex interactions between sensible residual gas heat, effective valve strategy compression ratio, and cycle-to-cycle feedback of residual gas.
- To investigate the mechanism of spark-assisted HCCI, the interaction of a laminar flame and auto-igniting gas has been modeled using HCT, a one dimensional transient reacting gas code. The results for typical HCCI conditions showed

at constant pressure that the laminar flame had little effect on the autoignition event ahead of the flame. The flame speed however increased steadily as the upstream gas temperature increased during autoignition. These findings will be used to develop CFD models of spark assisted HCCI.

- Rapid compression ignition studies of several isomers of the biofuel component methyl-butanoate have been carried out. The results have been used to update a detailed kinetic model by Westbrook et al. at LLNL.
- An after-treatment model has been developed for PCI combustion products which successfully describes the performance of a production-type low-temperature DOC under PCI and normal diesel operation.

FY 2007 Publications/Presentations

1. Andreae, M., Cheng, W. K., Kenney, T., Yang, J. (2007) "Effect of Air Temperature and Humidity on Gasoline HCCI Operating in the Negative-Valve-Overlap Mode," SAE Paper 2007-01-0221.

2. Andreae, M., Cheng, W. K., Kenney, T., Yang, J. (2007) "On HCCI Engine Knock," SAE Paper 2007-01-1858, SAE/JSAE Joint Powertrain and Fluid Systems Meeting, Kyoto, Japan, June, 2007.

3. Angelos, J.P., Andreae, M.M., Green, W.H., Cheng, W.K., Kenney, T., Xu, Y. (2007) "Effects of Variations in Market Gasoline Properties on HCCI Load Limits," SAE Paper 2007-01-1859, SAE/JSAE Joint Powertrain and Fluid Systems Meeting, Kyoto, Japan, June, 2007.

4. Babajimopoulos, A., Lavoie, G. A., and Assanis, D. N. (2007) ON THE ROLE OF TOP DEAD CENTER CONDITIONS IN THE COMBUSTION PHASING OF HOMOGENEOUS CHARGE COMPRESSION IGNITION ENGINES. *Combustion Science and Technology,* Vol. 179, No. 9, 2039 - 2063.

5. Bansal G. and Im H. G., (2007) Time Scales in Unsteady Premixed Flame Extinction with Composition Fluctuations, *Combustion and Flame*, v. 150, pp. 404-408.

6. Bansal G., Im H. G., and Lee S. R., (2007) Auto-ignition in Homogeneous Hydrogen/Air Mixture subjected to Unsteady Temperature Fluctuations, *2007 Fall Technical Meeting of Eastern States Section of Combustion Institute,* Charlottesville, VA, October 21–24, 2007.

7. Bansal G., Im H. G., and Lee S. R., (2008) Unsteady Scalar Dissipation Rate Effects on Nonpremixed *n*-Heptane Autoignition in Counterflow, *46th AIAA Aerospace Sciences Meeting and Exhibit,* Reno, NV, Jan. 7–10, 2008.

8. Bogin, G., Chen, J.Y., Dibble, R.W. (2007) "Numerical and Experimental Investigation of Ions in a Homogeneous Charge Compression Ignition Engine," Western States Section of the Combustion Institute, Fall 2007.

9. Guralp, O. A., et al. (2006) Characterizing the Effect of Combustion Chamber Deposits on a Gasoline HCCI Engine. SAE Paper No. 2006-01-3277.

10. Mack, J.H., Flowers, D.L., Aceves, S.M., Dibble, R.W. (2007) "Direct Use of Wet Ethanol in a Homogeneous Charge Compression Ignition (HCCI) Engine: Experimental and Numerical Results," Western States Section of the Combustion Institute, Fall 2007.

11. Sampara, Chaitanya S., Bissett, Edward J., and Chmielewski, Matthew (2007) "Global kinetics for platinum diesel oxidation catalysts" Accepted for publication in *Ind. Eng. Chem. Res*.

12. Sampara, Chaitanya S., Bissett, Edward J., and Chmielewski, Matthew (2007) "Global kinetics for a commercial diesel oxidation catalysts with two exhaust hydrocarbons" Submitted to *Ind. Eng. Chem. Res*.

13. Sampara, Chaitanya S., Bissett, Edward J., and Chmielewski, Matthew (2007) "Global Kinetics for a Commercial Diesel Oxidation Catalyst with Two Exhaust Hydrocarbons", Presented at the Diesel Engine – efficiency and Emissions Research (DEER) Conference, August 13–16, Detroit, MI

14. Sankaran, R., Im, H. G., and Hewson, J. C. (2007) ANALYTICAL MODEL FOR AUTO-IGNITION IN A THERMALLY STRATIFIED HCCI ENGINE. *Combustion Science and Technology,* Vol. 179, No. 9, 1963 - 1989.

15. Song, H. H., and Edwards, C. F.,(2008) "Optimization of Recompression Reaction for Low-Load Operation of Residual-Effected HCCI", SAE paper 08PFL-406, submitted

16. Walton, S. M., Perez, C., Wooldridge, M. S. (2007) "An Experimental Investigation of the Auto-Ignition Properties of Two C5 Esters: Methyl Butanoate and Butyl Methanoate," Technical Publication ASME IMECE2007-41944.

17. Zigler, B. T., Walton, S. M., Karwat, D. M., Assanis, Dimitris, Wooldridge, M. S., and Wooldridge, S. T., (2006), "A Multi-Axis Imaging Study of Spark-Assisted Homogeneous Charge Compression Ignition Phenomena in a Single-Cylinder Research Engine" Proceedings of ICEF2007, Paper No. ICEF2007-1762.

IV.2 Optimization of Low-Temperature Diesel Combustion

Profs. Rolf Reitz (Primary Contact), Pat Farrell, Dave Foster, Jaal Ghandhi, Scott Sanders, Chris Rutland
Engine Research Center (ERC)
University of Wisconsin-Madison
1500 Engineering Drive
Madison, WI 53706

DOE Technology Development Manager: Gurpreet Singh

NETL Project Manager: Samuel Taylor

Objectives

- Develop methods to optimize and control low-temperature combustion diesel technologies (LTC-D) that offers the potential of nearly eliminating engine nitrogen oxides (NOx) and particulate emissions at reduced cost over traditional methods by controlling pollutant emissions in-cylinder.
- Use single and multi-cylinder engine experiments and detailed modeling to study factors that influence combustion phasing, and particulate, nitric oxide (NO), unburned hydrocarbon (HC) and carbon monoxide (CO) emissions.
- Recommend improved combustion chamber geometries matched to injection sprays.
- Investigate role of fuel-air mixing, fuel characteristics, fuel spray/wall impingement and heat transfer on LTC-D engine control.
- Provide criteria for transition to other engine operation regimes (e.g., standard diesel and low-temperature combustion).

Approach

- Use fully-instrumented engines with prototype fuel injection systems and combustion sensors to map and define HCCI combustion regimes, and apply optimization techniques to discover low emission operation methodologies.
- Develop and apply modeling tools, including multi-dimensional codes (e.g., KIVA with state-of-the-art turbulent combustion and detailed and reduced chemistry models) to reveal combustion mechanisms.
- Use advanced fuel injection strategies, and manipulation of fuel characteristics to explore approaches to achieve optimal low temperature combustion operation.
- Use fast response diagnostics to formulate transient engine operation strategies during load and speed changes to extend LTC-D engine operating limits.

Accomplishments

- Combustion models and reaction mechanisms have been formulated and applied to analyze and optimize low emissions diesel engine operation.
- In-cylinder optical diagnostics have been developed for H_2O species, temperature and turbulence dissipation measurements for use in chemistry and turbulence model validation.
- A two-stage combustion strategy has been formulated and demonstrated with modeling and experiments to achieve 2010 emissions levels with low-temperature combustion operation.
- Engine experiments have revealed that relatively small diesel fuel composition modifications have a significant influence on low-temperature combustion and emissions.
- Advanced large eddy simulation (LES) turbulence models have been applied to reveal more detailed flow information than standard Reynolds averaged Navier Stokes (RANS) models.
- Analysis tools have been developed for development of engine control algorithms, and strategies for thermal and load changes and mode transitions have been explored.

Introduction

This project was initiated in response to a Department of Energy solicitation for research and development on homogeneous charge compression ignition (HCCI) diesel-fueled engines under the "FreedomCAR and Vehicle Technologies Program Solicitation for University Research and Graduate Automotive Technology Education Centers of Excellence." The program is in response to the fact that the engine industry is currently facing severe emissions mandates. Pollutant emissions from mobile sources are a major source of concern. For example, U.S. Environmental Protection Agency (EPA) mandates require emissions of particulate and NOx from heavy-duty diesel engine exhaust to drop at least 90 percent between 1998 and 2010. Effective analysis of the combustion process is required to guide the selection of technologies for future development since exhaust after-treatment solutions are not currently available that can meet the required emission reduction goals. The goal

of this project is to develop methods to optimize and control LTC-D technologies that offer the potential of nearly eliminating engine NOx and particulate emissions at reduced cost over traditional methods by controlling pollutant emissions in-cylinder. The work is divided into five tasks, featuring experimental and modeling components:

1. Fundamental understanding of LTC-D and advanced model development
2. Experimental investigation of LTC-D combustion control concepts
3. Application of models for optimization of LTC-D combustion and emissions
4. Impact of heat transfer and spray impingement on LTC-D combustion
5. Transient engine control with mixed-mode combustion

Outcomes from the research include providing guidelines to the engine and energy industries for achieving optimal low-temperature combustion operation, and low emissions engine design concepts will be proposed and evaluated.

Results

Task 1 - Fundamental Understanding of LTC-D and Advanced Model Development

Homogeneous or partially premixed charge compression ignition combustion is considered to be an attractive alternative to traditional internal combustion engine operation because of its extremely low levels of pollutant emissions. However, since the start-of-combustion timing is controlled by chemistry, kinetic models for diesel combustion are needed for engine analysis. The goal is to reduce available detailed chemistry mechanisms to a manageable size (ideally less than 60 species and 100 reactions) for use in multidimensional simulations. Validation of the mechanism predictions is being done by comparing measured and simulated in-cylinder gas compositions, under LTC conditions. Hyperspectral absorption spectroscopy is being explored for temperature and species concentration measurements. An H_2O gas thermometer has been developed that allows temperature measurements to be made in the engine at 3.5 kHz (1 crank angle degree at 600 rev/min) with an unprecedented 0.1% (2 K at 2,000 K) root mean square precision. Sample results are shown in Figure 1. In addition, a new methodology based on Fourier transform infrared spectroscopy has been implemented that will allow ready access to numerous species of interest including H_2O, CO_2, CO, C_2H_2, and CH_4. Additional information about the diagnostic tools is available at

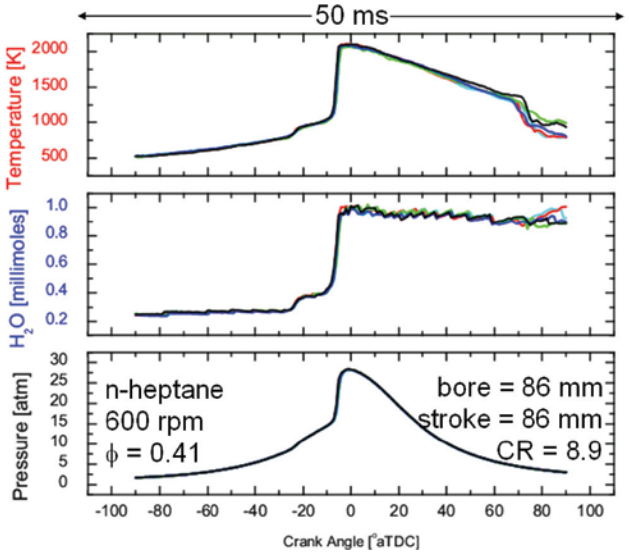

FIGURE 1. Temperature and H_2O content measured by hyperspectral H2O absorption spectroscopy for five consecutive engine cycles. The temperature precision exhibits an unprecedented precision of 0.1% (2 K at 2,000 K).

www.erc.wisc.edu (click on "optical diagnostics"), and a patent application has been made [1].

Methodologies for the reduction of kinetic mechanisms are being formulated. As an example, a detailed kinetic reaction mechanism for methyl butanoate (mb) with over 264 species and 1,219 reactions has been reduced and combined with a skeletal mechanism for n-heptane oxidation. The combined mechanism, ERC-bio, contains 55 species and 156 reactions and it has been validated against the detailed mechanism in constant volume simulations. A combined mb/n-heptane mechanism has been applied in KIVA/CHEMKIN engine simulations and compared to biodiesel-fueled engine experiments. The mechanism successfully predicted ignition timing in the simulated engine over a wide range of engine loads.

Task 2 – Experimental Investigation of LTC-D Combustion Control Concepts

An advanced two-stage or dual mode combustion strategy for simultaneous reductions of HC, CO, and NOx has been tested on the ERC's Caterpillar 3401 SCOTE heavy-duty diesel engine. In this case, a low pressure Bosch gasoline direct injection injector (10 MPa injection pressure) is used together with a high pressure Bosch common rail injector (150 MPa injection pressure), as depicted in Figure 2. The tests were conducted at a high-speed (1,737 rev/min), 57% load operation condition, with a maximum boost pressure of 238 kPa. The optimized pilot low-pressure start of injection (SOI) timing was –145° crank angle (CA) after top dead center (ATDC), and the main high-pressure

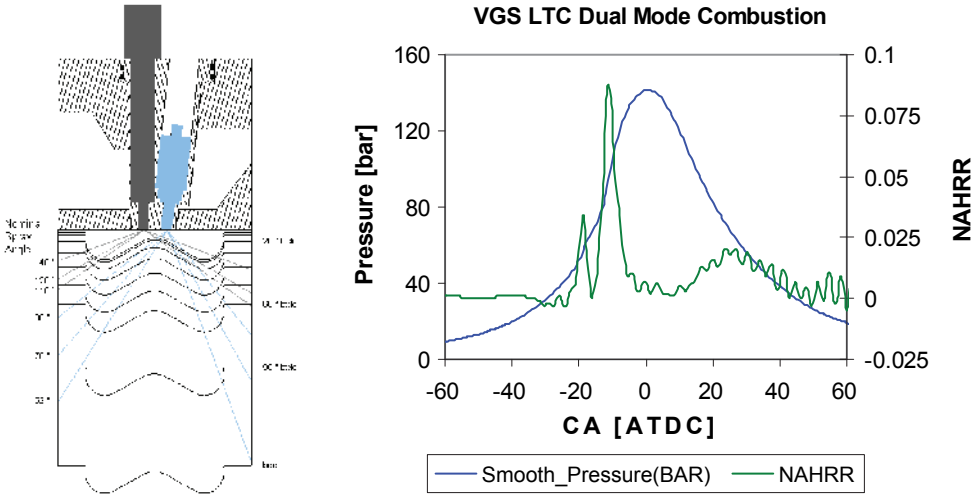

FIGURE 2. Variable Geometry Spray (VGS) Arrangement with High and Low Pressure Injectors (Left), and Two-Stage Combustion Results (Right).

SOI timing was 15° CA ATDC. Limited by mechanical constraints of the engine, fuel amount tests showed that 70% of the fuel should undergo premixed combustion from the early injection, while the remaining 30% participates in the late injection diffusion burn.

The low-pressure narrow cone angle injector geometry (six-hole 90° cone angle, 168 µm nozzle hole diameter) was found to reduce wall impingement significantly, as well as the associated HC and PM emissions that can result from premixed charge compression ignition (PCCI) fuel preparation with a traditional high pressure diesel injector. The two-stage combustion results produced HC emissions of 1.5 g/kW-hr, CO of 12 g/kW-hr, with NOx near the EPA mandate levels of 0.27 g/kW-hr. Late intake valve closure (IVC) of -85° CA ATDC combined with moderate exhaust gas recirculation rates (30%) adequately phased the premixed combustion event while limiting pressure rise rates, as shown in Figure 2. Ongoing experiments are concentrating on optimizing the injector geometries and fuel delivery characteristics to study their effect on spray targeting and PM emissions, and a patent application has been filed that describes the use of a single injector with low and high injection pressures for two-stage combustion [2,3].

The potential of achieving LTC-D operation with wide spray angle direct injection in a high-speed direct injection automotive diesel engine was also explored. In addition to studying spray and mixing parameters, the work explored whether the low-temperature combustion operating range can be expanded with modifications to fuel volatility and cetane number. The work is a collaborative effort between the ERC, GM Research and Development and BP. Tests have included a typical U.S. ultra-low sulfur diesel (ULSD) fuel supplied by BP, a narrow cut U.S. No.2 diesel from ExxonMobil, and European ECD-1 diesel fuel. A fuel test matrix which varies cetane number, volatility, and total aromatic content has been designed and several fuels have already been blended and delivered by BP. A high cetane number (Fuel E) has been tested at baseline conditions for comparison with the European and U.S. fuels, as shown in Figure 3. As can be seen in the heat release rate plots, differences in cetane number clearly affect ignition delay and combustion phasing, and CO emissions are significantly affected by relatively small differences in fuel composition.

Task 3 – Application of Detailed Models for Optimization of LTC-D Combustion and Emissions

Optimization tools have been used to recommend low-emission engine combustion chamber designs, including non-axi-symmetric piston bowls that could provide better matching with spray plume geometries for enhanced mixing. By coupling genetic algorithm with KIVA-CFD codes, and also utilizing automated grid generation technology, multi-objective optimizations with goals of low emissions and fuel economy have been achieved [4].

In addition, computations have been made using advanced turbulence models. The new KIVA-LES model has been used to study the effect of variable valve actuation on engine-out NOx emissions in the Caterpillar 3401 engine. The simulation results have been compared with experimental measurements [5] and standard KIVA-RANS results. The simulations were based on the experimental data where the original or 'stock' IVC timing of 217° ATDC is compared to late IVC timing of 275° ATDC. Combustion is simulated using detailed chemistry for n-heptane with the CHEMKIN solver [6]. NOx emissions are simulated by a reduced

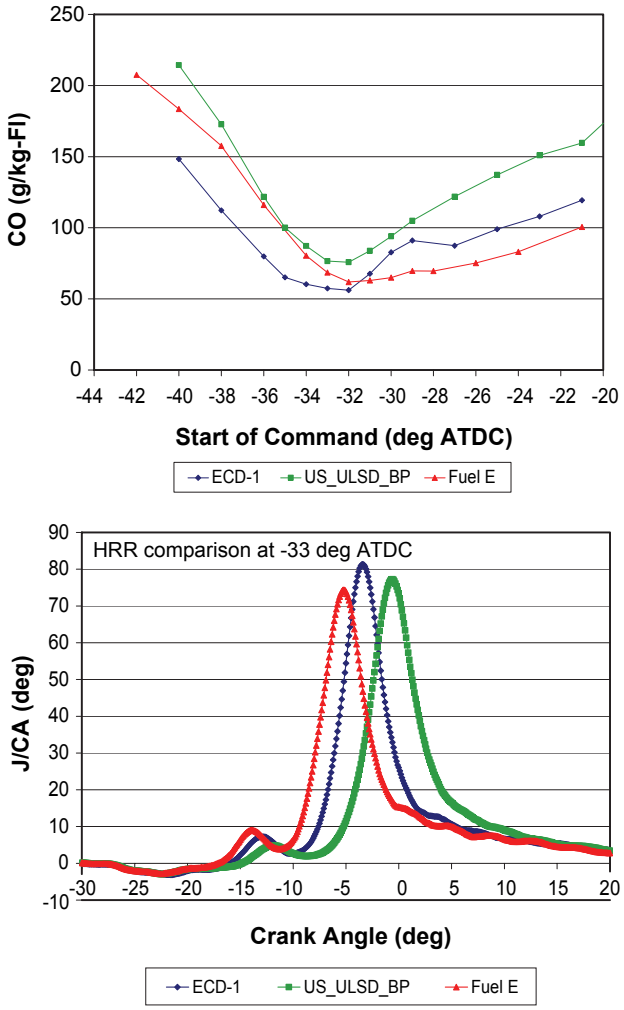

FIGURE 3. Measured engine-out CO emissions with European, U.S. and high cetane number (Fuel E=60 cetane number) fuels (top). Fuel effect on heat release rate (bottom).

mechanism with four additional species (N, NO, NO_2, N_2O) and nine reactions. In the engine experiments, NOx was reduced for the late IVC case. The LES results predicted this trend but did not show as large a reduction as seen in the experimental results. In contrast, the RANS results showed an increase, rather than a decrease in NOx for the late IVC case. Some of the change in NOx is due to different temperature distributions in the cylinder, as seen in Figure 4. In comparing the two IVC cases, the LES results show a smaller region of high temperature gases for the late IVC case while the RANS results show a larger region.

Task 4 – Impact of Heat Transfer and Spray Impingement on LTC-D Combustion

Coupled CFD and thermal analysis codes are being applied to consider heat transfer augmentation by fuel films from spray wall impingement and tested

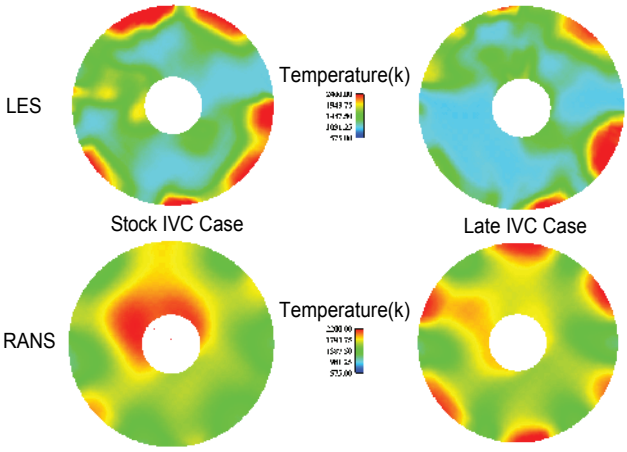

FIGURE 4. Comparison of LES and RANS In-Cylinder Temperature Contours for Stock and Late IVC Cases at CA = 357° ATDC

against experimental data. Wall films are predicted for early injection cases and this leads to increased NOx emissions due to locally high fuel concentrations. A radiation model based on the discrete ordinates method (DOM) is included in the study.

To validate the soot radiation submodel, comparisons of simulated results to experimental two-color thermometry data from a Sandia optical engine has been conducted. The soot radiation signal between the engine results and the KIVA-CHEMKIN-DOM predictions are being compared. In addition, a new surface grid generator has been developed for use with the wall film model that can be specified independently of the structured KIVA grid. This is needed because unphysical film accumulation has been observed at grid boundaries and this effect is mitigated with the new model. The model is being applied to compute the operation of the Caterpillar SCOTE engine for validation with experimental data. A linkage system has been developed to allow piston surface temperature and heat flux measurements during low temperature diesel combustion.

Task 5 – Transient Engine Control with Mixed-Mode Combustion

The objective of the research is to incorporate and evaluate LTC-D techniques developed as part of the other tasks into the multi-cylinder engine, operating under transient conditions. In addition to the transient operation we are exploring approaches to transition between normal and LTC operation. The engine experiments use the 4-cylinder GM 1.9L engine, and system level tools have been developed for modeling the engine. Single and multi-zone external cylinder models have been implemented in the most recent version of the commercial cycle simulation code GT-Power, together with incorporation of an improved heat transfer

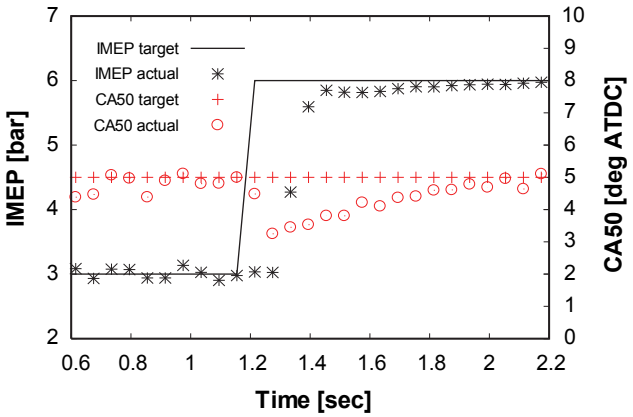

FIGURE 5. Load transient using 1.9L high-speed direct injection diesel engine model in GT-Power. Combustion phasing (indicated by CA50) is controlled using variable intake valve closing timing.

correlation, and application of transient load control strategies and simulation.

The single zone external cylinder model has been applied to explore early injection diesel HCCI operating conditions. The model allows exploration of engine transients spanning multiple cycles with reasonable computational times. The external cylinder models incorporate sub-models for vaporization, detailed chemistry calculations (CHEMKIN), heat transfer, and species conservation. No mixing effects are considered and the fuel droplets are dispersed as point sources. The research has shown that control of diesel HCCI operation can be accomplished by a range of actuators. Currently, two closed-loop controllers are used to actuate injected fuel quantity and IVC. In this way indicated mean effective pressure (IMEP) and CA50 are regulated to target values, as shown in Figure 5.

References

1. Sanders, S. T.,"Multiplexed-wavelength lasers based on dispersion mode-locking," UW WARF Patent Application P07171, 5/15/2007.

2. Sun, Y., and Reitz, R.D., "Adaptive Injection Strategy (AIS) for Diesel Engines," UW WARF Patent Application P07342US, May, 2007.

3. Sun, Y., Kokjohn, S., Weninger, E., and Reitz, R.D., "Adaptive Injection Strategies for Ultra-Low Emissions Diesel Engines," 13th Diesel Engine Emission Reduction Conference, Detroit, MI, August 24, 2006.

4. Shi, Y and Reitz, R. D., "Assessment of Optimization Methodologies to Study the Effects of Bowl Geometry, Spray Targeting and Swirl Ratio for a Heavy-Duty Diesel Engine Operated at High-load", SAE 08PFL-126.

5. Nevin, R.M. "PCCI Investigation Using Variable Intake Valve Closing in a Heavy Duty Diesel Engine," M.S. Thesis, University of Wisconsin–Madison, 2006.

6. Kong, S.C., Sun, Y. and Reitz, R.D. (2007), "Modeling Diesel Spray Flame Lift-Off, Sooting Tendency and NO_X Emissions with Phenomenological Soot Model," ASME Journal of Gas Turbines and Power, Vol. 129, pp. 245-251, 2007.

FY 2007 Publications/Presentations

1. UW DOE HCCI Working Group Presentation Meetings: February and October 2007.

2. Sun, Y., Kokjohn, S., Weninger, E., and Reitz, R.D., "Adaptive Injection Strategies for Ultra-Low Emissions Diesel Engines," 13th Diesel Engine Emission Reduction Conference, Detroit, MI, August 24, 2006.

3. Abani, N., and Reitz, R.D., "A Model to Predict Spray-tip Penetration for Time-varying Injection Profiles," Proceedings of ILASS Americas, 20th Annual Conference on Liquid Atomization and Spray Systems, Chicago, IL, May 16, 2007.

4. Sun, Y., and Reitz, R.D., "Modeling Low-Pressure Injections in Diesel HCCI Engines," Proceedings of ILASS Americas, 20th Annual Conference on Liquid Atomization and Spray Systems, Chicago, IL, May 16, 2007.

5. Park, S.W., Reitz, R.D., Modeling the effect of injector nozzle-hole layout on diesel engine fuel consumption and emissions, Submitted to ASME Journal of Gas Turbines and Power, 2007.

6. Park, S.W., Reitz, R.D., Optimization of fuel/air mixture formation for stoichiometric diesel combustion using a 2-spray-angle group-hole nozzle, Submitted Combust. Theory & Model, 2007.

7. Park, S.W., and Reitz, R.D., "Numerical Study on the Low Emission Window of Homogeneous Charge Compression Ignition Diesel Combustion" Combustion Science and Technology, Vol. 179:11, pp. 2279-2307, 2007.

7. Hu, B., Jhavar, R., Singh, S., Reitz, R.D., and Rutland, C.J., "Combustion Modeling of Diesel Combustion with Partially Premixed Conditions," SAE 2007-01-0163, 2007.

8. Nevin, R.M., Sun, Y., Gonzalez, M.A., and Reitz, R.D., "PCCI Investigation Using Variable Intake Valve Closing in Heavy Duty Diesel Engine," SAE 2007-01-0903, 2007.

9. Tamagna, D., Ra, Y., and Reitz, R.D., "Multidimensional Simulation of PCCI Combustion Using Gasoline/Dual-fuel Direct Injection and Detailed Chemical Kinetics," SAE 2007-01-0190, 2007.

10. Singh, S., Wickman, D., Stanton, D., Tan, Z., and Reitz, R.D., "Development and Validation of a hybrid, auto-ignition/flame-propagation model against engine experiments and flame lift off," SAE 2007-01-0171, 2007.

11. Genzale, C., Wickman, D., and Reitz, R.D., "A Computational Investigation into the Effects of Spray Targeting, Swirl Ratio and Bowl Geometry for Low-Temperature Combustion in a Heavy-Duty Diesel Engine" SAE 2007-01-0119, 2007.

12. Hagen, C.L. and Sanders, S.T., "Toward hyperspectral sensing in practical devices: measurements of fuel, H2O, and gas temperature in a metal HCCI engine," J. Near Infrared Spectroscopy, 2007.

13. Kraetschmer, T., Lan, C., and Sanders, S.T., "Custom multiwavelength frequency-division-multiplexed laser based on dispersion mode locking" IEEE Photo. Tech. Letters, in press, 2007.

14. Kranendonk, L.A., Caswell ,A.W. and Sanders, S.T.,"Robust Method for Calculating Temperature, Pressure and Absorber Mole Fraction from Broadband Spectra," Appl. Opt., 2007.

15. Hagen, C.L. and Sanders, S.T., "Investigation of Multi-species (H2O2 and H2O) Sensing and Thermometry in an HCCI Engine by Wavelength-Agile Absorption Spectroscopy," Measurement Sci. Tech., in press, 2007.

16. Opat, R., et al., "Investigation of Mixing and Temperature Effects on HC/CO Emissions for Highly Dilute Low Temperature Combustion in a Light Duty Diesel Engine," SAE paper 2007-01-0193, 2007.

IV.3 Low-Temperature Combustion with Thermo-Chemical Recuperation to Maximize In-Use Engine Efficiency

Nigel N. Clark (Primary Contact),
Francisco Posada, Clint Bedick
Center for Alternative Fuels, Engines & Emissions (CAFEE)
Department of Mechanical and Aerospace Engineering
West Virginia University
PO Box 6106
Morgantown, WV 26506-6106

DOE Technology Development Manager:
Gurpreet Singh

NETL Project Manager: Aaron Yocum

Subcontractors:
- Gas Technology Institute (GTI), Des Plaines, IL (John Pratapas, Lead Investigator)
- Atkinson LLC, Morgantown, WV (Christopher Atkinson, Lead Investigator)

Objectives

- To substantially improve (10% fuel use reduction) the efficiency of compression ignition engines for both light-duty and heavy-duty use while meeting or exceeding the ultra-low NOx emission requirements for the 2010 engine model year.
- To utilize alternative combustion modes, coupled with thermo-chemical reforming of fuel to recover exhaust waste heat, with an optimization of the mean effective pressure versus displacement tradeoff.
- To develop technology under this project that will enable engine prototype development by 2012.

Accomplishments

- Simple models for low-temperature combustion (LTC) and diesel engines were implemented to obtain the pressure and temperature data required for the evaluation of efficiency for each type of engine.
- Values of energy losses in the LTC engine were compared with energy losses of a diesel engine with half the displacement of the LTC engine. Energy losses assessed in this model include friction, auxiliaries and heat transfer.
- A model to evaluate the total cooling burden was developed and to assess the impact of the energy losses in the fan energy requirements, which is also powered by the engine.
- Model results showed that the total cooling burden on a LTC engine with higher displacement and lower power density was 15.6% lower than the diesel engine for the same amount of energy addition in the case of high load (43.57 mg fuel/cycle).
- A steam/fuel reforming bench was designed, built and tested by GTI. n-Heptane was employed as a surrogate fuel, in order to analyze the impact on H_2 and CO production due to changes in reforming temperature, fuel flow rate, steam/n-heptane mole ratio and heat addition to the reformer.
- Laboratory results, at a steam/carbon mole ratio less than 2:1, confirm that reforming reactions, in the temperature range of 550 K to 650 K, can produce 10-30% hydrogen (by volume, wet) in the product stream.

Future Directions

The project, based on the original objectives, included three phases, which included experimental verification of the "two fuels" approach to LTC, which provided for integration of a reformer with an engine, and which provided for system controls development. Although Phase 1 results suggest that the LTC/thermo-chemical recuperation (TCR) combination is attractive, DOE funding constraints have dictated a more austere project, directed at (1) modeling to demonstrate the "two fuels" approach benefits in managing in-cylinder combustion, (2) determination of the optimal use of pre- and post-turbocharger heat from a system perspective, (3) design of the integrated heat exchanger and reformer, and (4) addressing the complete system design and control through modeling.

Introduction

LTC is a broad concept that involves combustion systems where the in-cylinder temperature is kept below temperatures that promote substantial NOx and soot formation [1]. Although LTC combustion has emerged as an alternative to spark ignition and compression ignition direct injection (CIDI) combustion due to decrease in exhaust emissions and improvement in fuel economy, it is difficult to maintain LTC combustion over the entire operational engine load range. The control over ignition timing and the rate of heat release are the

primary parameters affected by the nature of this kind of combustion process. The control of LTC is the most challenging issue for commercial applications of LTC.

In general, two directions have been investigated to extend the operational range of LTC and provide the required control: modifying air/fuel mixture properties and modifying engine operation and design parameters [2]. The final purpose of each of these strategies is to modify the composition and/or temperature of the in-cylinder charge. The research presented in this report examines the feasibility of using TCR technologies to produce the secondary fuel stream in an on-board reforming reactor as a reformed product of the primary fuel in the tank. In parallel, an optimization of the mean effective pressure versus displacement tradeoff was studied to address the need for broad operating range in LTC operation.

Approach

It is proposed in this research to accept the mean effective pressure (MEP) values at which LTC has been shown to work successfully, and increasing cylinder displacement to reach the typical power output of a CIDI engine. Initial modeling was performed to determine the differences in MEP, heat loss, friction and auxiliary losses, and efficiency between a diesel CIDI engine and a LTC engine. The diesel CIDI cylinder basic geometry was taken from a Cummins B-series 5.9 liter engine and the LTC cylinder was modeled with double the displacement of the CIDI while keeping the same compression ratio. The results from LTC modeling were applied to TCR experimental results to determine the feasibility of combining the two systems to extend the operational range of LTC. Throughout initial modeling and experimental research, n-heptane was used as an alternative to diesel fuel, but future research and a final LTC/TCR system would implement diesel. This report presents results from LTC modeling and TCR experimental work in order to show that the overall system is feasible and has the potential to increase engine efficiency and extend the actual operational range of LTC engines.

Results

Comparison Between Diesel Engine and LTC Engine: Heat Transfer, Friction and Auxiliaries Losses

The authors have argued that the lower power density of LTC might be accepted by increasing displacement without altering the engine lower end design. A comparison was considered for an LTC engine with twice the displacement of the diesel engine, but approximately half of the indicated mean effective pressure (IMEP). In this way, the output of the engines could be similar. Therefore, the CIDI engine was modeled using a 0.98 liter displacement for one cylinder and the LTC engine was modeled at double (1.96 liter) this displacement. The bore and stroke were varied in two different ways to represent a 1.96 liter displacement engine. In the first case the face area of the piston was doubled and the stroke remained unchanged. In the second case the volume was doubled but the aspect ratio of the cylinder was kept the same (bore/stroke=1).

Typical pressure and temperature curves for the LTC and CIDI engines are shown in Figure 1. The peak pressure values obtained in the LTC model were higher than those obtained for the CIDI model, although the general trend showed a lower pressure for the LTC engine as should be expected from a higher cylinder face area. Intake temperatures for LTC were higher than those used for CIDI simulation due to auto-ignition requirements of the LTC case. It should be noticed that although the peak temperature in the LTC case was similar to the maximum temperature obtained in the CIDI case, the LTC peak temperature value was overshot with respect to typical experimental homogeneous charge compression ignition data and the general trend showed a lower cylinder temperature for the LTC case as expected from higher expansion ratios.

Heat Transfer Losses

The cumulative heat loss was compared for two different engines, a LTC engine and a CIDI engine, operating at the same amount of fuel per cycle. Two different load cases were applied: a low load of 21.89 mg of fuel per cycle and a high load of 43.57 mg of fuel per cycle. Figures 2a and 2b show the cumulative heat loss in both cases. At low load the total amount of heat loss was slightly higher (1.2%) for the CIDI engine because

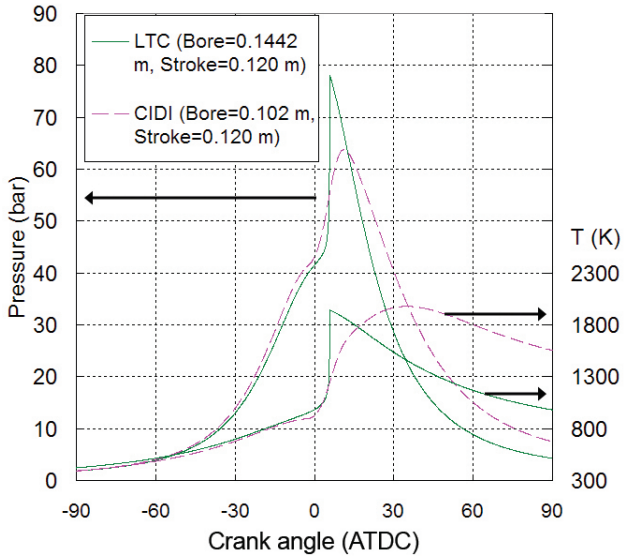

FIGURE 1. Pressure and Temperature Trends for LTC and CIDI at the Same Amount of Fuel Per Cycle (43.57 mg)

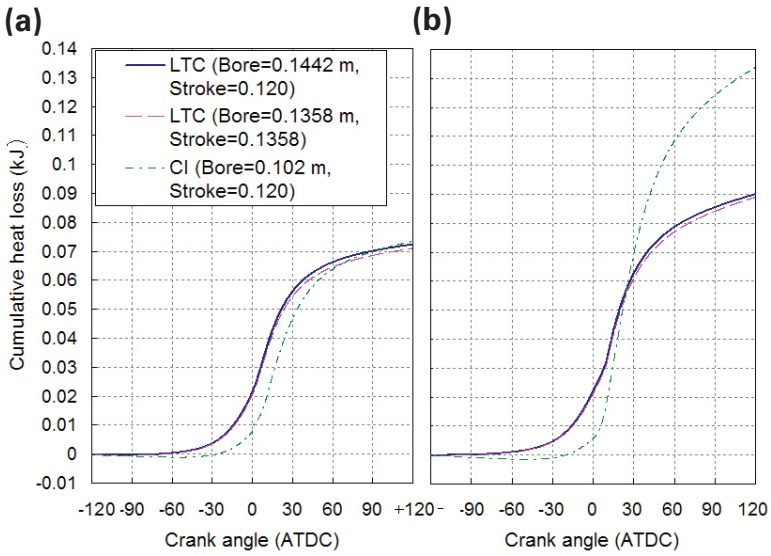

FIGURE 2. LTC and CIDI Cumulative Heat Transfer to Walls: (a) Low Load Case: 21.89 mg of Fuel per Cycle; (b) High Load Case: 43.57 mg of Fuel per Cycle

the larger surface area associated with the LTC engine compensates for the higher heat transfer produced by the CIDI combustion. At higher load, 43.57 mg of fuel per cycle, the results were more favorable for LTC with a heat loss 32.8% higher for the CIDI compared to the LTC engine.

Friction and Auxiliary Losses

The friction model, based on the work of Taraza et al. [3], produced results showing lower frictional losses for the LTC cases compared to the CIDI cases for a given amount of fuel. The piston-ring assembly in particular was most sensitive to changes in parameters, since the in-cylinder pressure largely determined the frictional losses for that section of the model. Figure 3 shows the piston-ring assembly (PRA) friction force for the two LTC and one CIDI bore/stroke combinations.

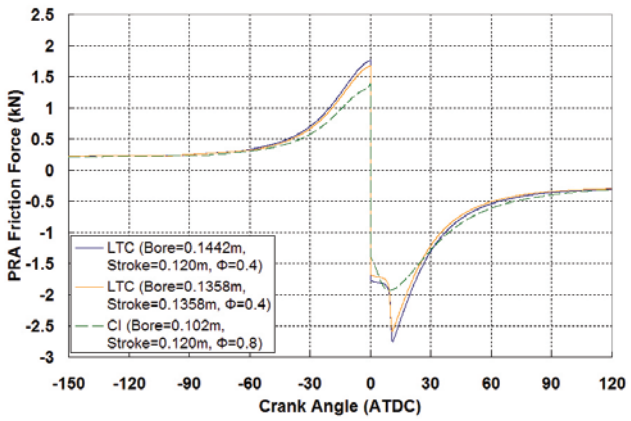

FIGURE 3. Piston-Ring Assembly Friction Force (43.57 mg of fuel)

The bearing model showed some differences, but the differences were small compared to that of the PRA. The rapid pressure increase of the LTC cases produced large bearing friction forces for a very short period of time. Despite this, the overall integrated friction work was lower for both LTC cases. The auxiliary losses were constant for all diesel CIDI and LTC cases since they were only dependant on physical engine parameters, engine speed, and instantaneous crank angle. Figure 4 shows the contribution of each friction component (PRA, bearings, valvetrain, auxiliaries) for the two LTC and one diesel CIDI bore/stroke combinations. The results are shown in terms of MEP, defined as total friction or auxiliary work done between the time when the intake valve closes and the exhaust valve opens divided by the total displacement volume of the cylinder.

In addition, Table 1 shows a complete summary of the friction results in terms of total friction energy lost and mechanical efficiency. By examining the total friction work done for a given amount of fuel and boost, it can be seen that the LTC case had lower friction work for both bore/stroke combinations.

Comparison Between Diesel Engine and LTC Engine: Total Cooling Burden

By increasing the volume of the cylinder, lower IMEP was achieved and the amount of work obtained was found to be similar compared with an engine working with the same amount of fuel in the cylinder. Lower power density generated lower friction losses as summarized in Table 1.

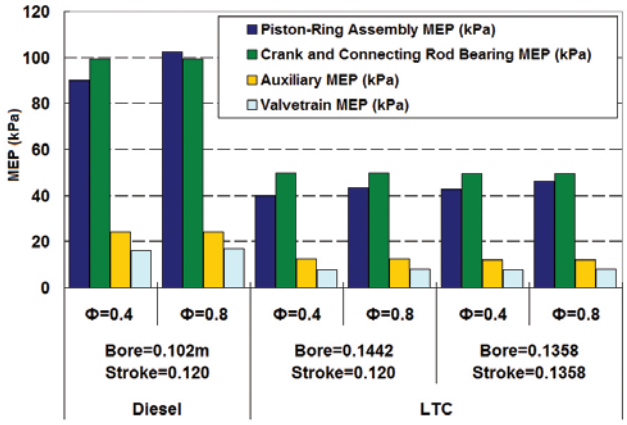

FIGURE 4. Friction MEP comparison

TABLE 1. Summary of Conditions, Friction Losses, Heat Transfer and Work During One Cycle

		CIDI		LTC			
Equivalence Ratio	---	0.4	0.8	0.2	0.4	0.2	0.4
Bore	m	0.102	0.102	0.144	0.144	0.136	0.136
Stroke	m	0.120	0.120	0.120	0.120	0.136	0.136
Fuel Per Cycle	mg	21.89	43.57	21.89	43.57	21.87	43.59
Displacement	liter	0.980		1.96		1.96	
Friction Energy Losses	kJ	0.225	0.238	0.214	0.222	0.220	0.228
Heat Transfer to Walls	kJ	0.074	0.134	0.072	0.090	0.071	0.089
Fan Load	kJ	0.0012	0.0026	0.0010	0.0014	0.0011	0.0015
Total Cooling Burden	kJ	0.300	0.374	0.287	0.313	0.292	0.318
Work Developed Per Cycle	kJ	0.492	0.836	0.509	0.896	0.517	0.886
Thermal Efficiency	---	0.509	0.434	0.526	0.465	0.534	0.460
Mechanical Effieciency	---	0.541	0.712	0.577	0.751	0.571	0.741

A comparative evaluation of the fan load showed that although the absolute values were not representative, the relative values were highly favorable for the LTC engine. At light loads the benefit was 14.3% and at higher loads the benefit was more substantial, reaching 44.23% when compared to the CIDI results. The total cooling burden values obtained for LTC were approximately the same at lower loads compared with the CIDI engine. At higher loads the benefit was more noticeable, with 15.5% lower cooling burden for the LTC compared to the CIDI engine. The amount of work produced per cycle showed a slightly benefit in the case of the LTC engine (double displacement) when it was compared at the same amount of fuel per cycle, which increases its thermal and mechanical efficiency respect to the CIDI engine. The calculated efficiency benefit of the LTC was more evident at higher loads where the actual experimental results are limited by knock phenomena.

n-Heptane Steam Reforming Experimental Results

A TCR system was developed by GTI for implementation on a LTC engine. Initial modeling of n-heptane steam reforming was performed by GTI using equilibrium reactions and HYSYS software. Validation of modeling results was performed based on typical exhaust flow and temperatures of the LTC engine. The reformer, presented in Figure 5, was tested in order to estimate the reforming rate and process efficiency for non-catalytic and catalyzed reforming.

Experimental data, including reformer gas composition and hydrogen yield, was produced for a range of reformer temperatures. In addition, a comparison to modeling results was performed to validate the model. Figure 6 shows the main components of the reformed fuel composition (measured wet) for a steam/carbon molar ratio of 2:1 with catalyst. There was up to 45% H_2 and 18% CO (by volume,

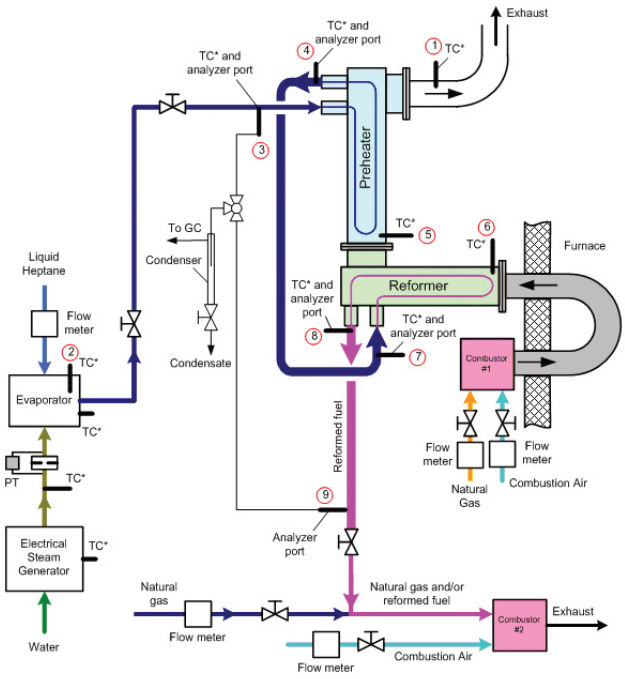

* TC – thermocouple; PT – pressure transmitter; GC – gas chromatograph

FIGURE 5. Experimental Setup for n-Heptane/Steam Reforming

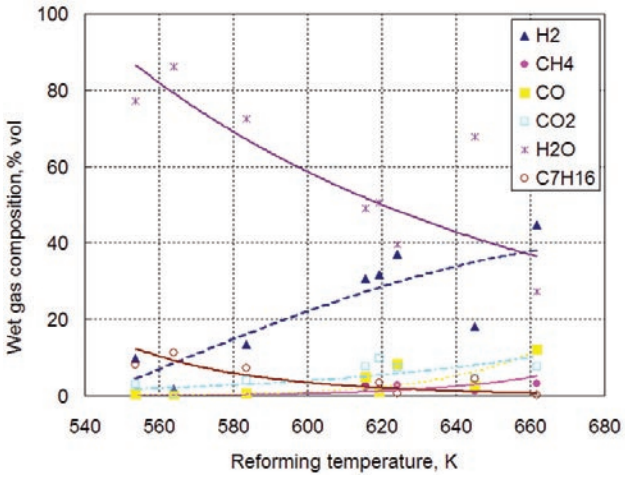

FIGURE 6. Reformed Gas Composition with Catalyst (Steam/Carbon Molar Ratio 2:1)

wet) in the reformed fuel at a relatively low reforming temperature (≈700 K)

To characterize the process efficiency for hydrogen production, hydrogen yield was estimated as the weight ratio of hydrogen produced to n-heptane fed into the reformer. The hydrogen yield varied from zero to near 20% almost linearly with the temperature varying from 570 K to 700 K. Inferior values of hydrogen yield were obtained without catalyst even when the reforming temperature was increased up to at 850 K. Process

completeness was used as a parameter to describe the reforming process, defined by actual conversion amount as a percentage of theoretical equilibrium conversion amounts. The experimental reformer could provide close to 100% process completeness at 690 K for catalytic reforming and 860 K for non-catalytic reforming. Approximately the same process completeness was achieved for catalytic and non-catalytic reforming at temperatures 550 K-650 K, suggesting that those temperatures are low for the catalyst.

Synergy Between LTC and TCR

The well known sensitivity of the LTC mode to temperature and charge composition has been proved with a simple two-step chemical kinetics model. The strong influence of intake temperature, equivalence ratio and exhaust gas recirculation on the ignition event shows that the LTC engine requires additional sources of control to obtain the desired benefits regarding emissions and thermal efficiency of this technology. Based on the results obtained from the LTC model, values of exhaust temperature were calculated to examine the operational range of the TCR system. The resulting values of exhaust temperatures based on a model of adiabatic expansion of ideal gas mixture (at 100 kPa) match the operational range where the catalyst is more effective and where the process completeness is higher than 60%. Moreover, the LTC mode has demonstrated good behavior in the low power requirement, range where TCR would not be required and where the available reforming temperature from exhaust gases was low and therefore low reforming process completeness was obtained. It should be noticed that the temperature of the gases obtained from the adiabatic expansion model may be higher than those obtained from a real prototype where heat transfer losses are involved in the process, but the exhaust area can be configured to minimize heat loss if the intent is to optimize waste heat recovery.

Conclusions

Modeling results demonstrated that the LTC engine with double the displacement of the CIDI engine shows a higher overall efficiency, with lower cooling burden and friction losses for a given amount of fuel per cycle when compared to CIDI diesel combustion.

1. Values of heat loss at different load conditions were evaluated for both the CIDI engine and the LTC engine and the results showed that the amount of heat transfer was significant at higher load. In this case the heat transfer at 43.57 mg of fuel per cycle was 32.8% higher for the CIDI engine than for the LTC engine.
2. Slight differences were found in the final value of friction losses for both the CIDI engine and the LTC engine operating at the same amount of energy input.
3. The total balance of cooling burden, including heat transfer and frictional losses was favorable for the proposed LTC engine at double displacement when it was compared to the diesel engine under the same energy input base.
4. Mechanical efficiencies at low load were similar between the CIDI and the LTC engine. At high load the calculated difference is 4.4% higher for the LTC engine.

Experimental results showed that TCR could produce a hydrogen-rich reformer fuel at various exhaust temperatures by steam reforming of liquid n-heptane.

1. For steam/n-heptane mole ratio of 15, complete n-heptane conversion was expected for temperatures slightly above 700 K.
2. Steam/n-heptane ratio could be optimized in order to maximize n-heptane conversion.
3. Appropriate catalysts should be selected for higher n-heptane conversion at low temperature.
4. Additionally, LTC modeling has proven that the LTC exhaust temperature was within the range of significant hydrogen production.

References

1. Kook S., Bae C., Miles P.C., Choi D., Pickett L.M., *"The Influence of Charge Dilution and Injection Timing on Low-Temperature Diesel Combustion and Emissions,"* SAE Paper 2005-01-3837, 2005.

2. Milovanovic N., and Chen R.., *"A review of experimental and simulation studies on controlled auto-ignition combustion,"* SAE Paper 2001-01-1890, 2001.

3. Taraza, D., Henein, N., Bryzik, W., *"Friction Losses in Multi-Cylinder Diesel Engines,"* SAE Paper 2000-01-0921, 2000.

FY 2007 Publications and Presentations

1. Posada F., Bedick C., Clark N., Kozlov A., Linck M., Boulanov D., Pratapas J., *"Low Temperat ure Combustion with Thermo-chemical Recuperation,"* SAE Paper 2007-01-4074, 2007.

2. Diesel Engine-Efficiency and Emissions Research (DEER) conference poster presentation: Enabling Low Temperature Combustion Trough Thermo Chemical Recuperation. Detroit, MI, 2007.

IV.4 Kinetic and Performance Studies of the Regeneration Phase of Model Pt/Ba/Rh NOx Traps for Design and Optimization

Michael P. Harold (Primary Contact) and Vemuri Balakotaiah
University of Houston
Department of Chemical and Biomolecular Engineering
S222 Engineering Building 1
Houston, TX 77204-4004

DOE Technology Development Manager: Ken Howden

NETL Project Manager: Aaron Yocum

Objectives

- Carry out studies of regeneration kinetics on lean NOx trap (LNT) catalysts.
- Evaluate and compare the effect of different reductants on LNT performance.
- Incorporate the kinetics findings and develop and analyze a first-principles based predictive LNT model for design and optimization.
- Test the new LNT designs in a heavy-duty diesel vehicle dynamometer facility.

Accomplishments

- Carried out a comprehensive experimental study of the steady-state behavior of the NO/H_2 and $NO/H_2/O_2$ reaction systems on model Pt and Pt/Ba monolith catalysts. Integral conversion and selectivity data were obtained over a range of temperatures, feed compositions, and catalyst loadings (Pt, BaO). The analytical system was upgraded to include a mass spectrometer, enabling the measurement of N_2 and H_2 in addition to the remaining species measured by Fourier transform infrared (FTIR) spectroscopy. The kinetics of several underlying chemistries was also studied, including NO reduction by ammonia, ammonia oxidation by O_2, and ammonia decomposition. These data are being used to develop a predictive microkinetic model. The anaerobic data will appear in a combined experimental-modeling paper in Applied Catalysis B. Environmental. The aerobic data are the basis for a second publication in the same journal.
- Carried out a comprehensive study of the performance of model Pt/Ba catalysts under simulated cycling with H_2 as the reductant. Detailed performance data on instantaneous and cycle-averaged product distributions were obtained. Several key findings were obtained of the transient product distribution. A series of varied-length experiments elucidated the role of ammonia as both a byproduct and reductant. A manuscript will be submitted to Applied Catalysis on this work.
- Carried out transient kinetics studies of model Pt catalysts with the temporal analysis of products (TAP) reactor. Sequential pulsing of NO and NO/H_2 pump/probe experiments on Pt catalysts revealed a complex dependence on temperature, pulse timing, and NO/H_2 feed ratio. The data helped to elucidate the mechanistic sequence describing the production of N_2, N_2O, and NH_3.
- Developed a mathematical model to simulate the NO decomposition and NO/H_2 reaction system in the TAP reactor. An algorithm has been developed to estimate kinetic parameters using this model.
- Developed a predictive microkinetic model for the NO/H_2 on Pt reaction system. A monolith reactor model incorporating the microkinetic model and transport processes predicted all of the main features of steady-state data over a wide range of temperature and feed composition.

Future Directions

During the third year of the project we will focus our efforts on the following activities (with more detailed plans to follow):

- Conduct bench-scale experiments on the role of Rh and CeO_2 on the performance of the LNT.
- Focus on the effect of Pt/Ba interfacial coupling through bench-scale and TAP reactor experiments that quantify the effect of Pt/Ba interfacial perimeter on the activity and product distribution.
- Carry out selected TAP experiments using monolith catalysts, enabling a direct comparison of bench-scale and TAP data.
- Estimate unknown kinetic parameters through simulation of TAP experiments with monolith catalysts.
- Extend the LNT modeling through continued upgrades of the microkinetics. Focus efforts on the simulation of transient data.
- Utilize the LNT model with the microkinetics to investigate different NOx trap operating strategies and designs.

Introduction

During the second year of the project we have made very good progress in integrating experimental and theoretical efforts spanning bench-scale reactor studies, TAP reactor studies, microkinetic modeling, and reactor modeling. Our efforts have focused on mechanistic studies in TAP reactor, bench-scale studies of NOx trap using synthetic feeds and model NOx storage and reduction (NSR) catalysts, and development of first-principles NOx trap reactor model comprising a microkinetic description of the storage and reduction chemistry. Our activities involved elucidating steady-state and transient studies of several underlying chemistries in the bench-scale and TAP reactors, in formulating a predictive microkinetic model, and incorporating the chemistry knowledge into monolith reactor models. The experiments to date have considered Pt, and Pt/Ba catalysts using H_2 as the reductant. A family of model catalysts has been provided to us during the past year by BASF Catalysts LLC; these contain additional components including Rh and CeO_2.

Approach

We utilize a combination of experimental and theoretical tools to advance the LNT technology. Fundamental kinetics studies are carried out of model Pt/Rh/Ba NSR powder and monolith catalysts with reductants H_2 and CO in the TAP reactor. The TAP reactor provides transient data under well-characterized conditions, enabling both the identification of key reaction pathways and estimation of the corresponding kinetic parameters. The performance of model NSR monolith catalysts are evaluated in a bench-scale NOx trap using synthetic exhaust, with attention placed on the effect of the pulse timing and composition on the instantaneous and cycle-averaged product distributions. From these measurements we formulate a mechanistic-based microkinetic model that incorporates a detailed understanding of the chemistry, and incorporate the kinetic model into a LNT model. The NOx trap model is used to determine its ability to simulate bench-scale data and ultimately to evaluate alternative LNT designs and operating strategies.

Results

During the second year we continued mechanistic studies of NO uptake (storage) and NO reduction by H_2 on Pt/Al_2O_3 and $Pt/Ba/Al_2O_3$ powder catalysts (provided by BASF Catalysts LLC). This work involves both TAP reactor experimental and modeling studies and is the doctoral thesis of one of the graduate students. Up to this point in the project we have primarily used the TAP experiments to elucidate certain features of the NO/H_2 transient uptake and catalytic chemistry. NO pulsing experiments provide information about the adsorption and decomposition while NO/H_2 pump-probe experiments provide detailed information about the reaction pathways to products N_2, N_2O, and NH_3. The principle effort involved the completion of NO/H_2 pump-probe experiments on the Pt and Pt/Ba catalysts over a range of temperature (150-350°C). This has been important for guiding our efforts in elucidating bench-scale reactor performance data and for constructing a microkinetic model.

We made considerable progress in forming a comprehensive database for steady-state and cyclic bench-scale monolith reactor experiments. This task is conducted by a doctoral student who is partially supported by DOE. We utilize a monolith reactor system comprising a simulated exhaust feed system, flow through reactor, and dedicated analytical system. During the last quarter we added a quadrupole mass spectrometer to the system to provide critical capability for measuring non-infrared active species including N_2 and H_2. Up to this point, both of these species were estimated by overall N and H balances, respectively. Coupled with the FTIR, this gives us the ability to conduct more detailed experiments.

Comprehensive steady-state experiments on the selective catalytic reduction of NO on a series of Pt, Pt/BaO, and BaO monolithic catalysts were carried out to evaluate the light-off, NOx conversion and product distribution features as a function of the feed composition, temperature and catalyst composition. The reaction between NO and H_2 produces a mixture containing N_2O, NH_3, and N_2, the composition of which is a function of the catalyst temperature and NO/H_2 ratio in the feed. NO strongly inhibits the reaction at low temperatures. NOx conversions were found to be complete at space velocities below 90,000 hr^{-1} and above 100°C for Pt loadings exceeding 1.27%. Particular attention focused on the production and consumption of ammonia, a problematic byproduct during NSR. NH_3 is a key product in O_2 deficient conditions typical of the rich pulse in NSR, while N_2 and N_2O are the main products at higher O_2 concentrations (lean conditions). NH_3 oxidation ignites on Pt catalysts at 180-200°C; in the ignited state a mixture of N_2, NO, NO_2 and N_2O is produced, the composition of which is sensitive to the NH_3/O_2 feed ratio and temperature. The decomposition of NH_3 is observed above 360°C and is inhibited by small amounts of H_2. Experiments involving a feed containing H_2, NH_3, and NO reveal that H_2 is a much more effective reductant. A comparison of the three catalysts reveals similar steady-state behavior between the Pt and Pt/BaO catalysts. The BaO catalyst exhibited a non-negligible but lower activity and a different product distribution than the Pt and Pt/BaO catalysts. The data are interpreted with a phenomenological

reaction network model. Complementary theoretical analyses elucidate selected kinetic trends and the effect of Pt loading.

The cyclic experiments complement the steady-state experiments in terms of elucidating the dependence of the time-averaged conversion and selectivities on catalyst temperature, feed composition, monolith length, and catalyst composition. We have completed an extensive set of cyclic tests under different conditions that provide critical information about instantaneous and cycle-averaged product distributions. The anaerobic environment brought about by reaction of the reductant with surface and gas phase oxygen leads to NH_3 formation. Testing with monoliths of different lengths clearly indicate that NH_3, once formed, reacts with stored NOx downstream in the monolith by standard ammonia-based selective catalytic reduction. The data are being analyzed currently to determine which reductant (H_2 or NH_3) produces more of the N_2.

During the past year we have also made good progress on microkinetic model development using our TAP and bench-scale data. To this end, we have completed a model that captures the main trends in the anaerobic NO + H_2 on Pt reaction system. We utilized selected experimental results of the reduction of NO by H_2 on Pt/Al_2O_3 and $Pt/BaO/Al_2O_3$ catalysts in the temperature range 30-500°C and H_2/NO feed ratio range of 0.9 to 2.5 (Figure 1). The microkinetic model captures the kinetics of NO reduction by H_2 on Pt/Al_2O_3. Kinetic parameters were estimated from literature data and thermodynamic constraints, and involved some tuning to predict the main trends in the data. The microkinetic model was combined with the short monolith flow model to simulate the conversions and selectivities corresponding to the experimental conditions. Both the model and the experiments show that N_2O formation is favored at low temperatures and low H_2/NO feed ratios, N_2 selectivity increases monotonically with temperature for H_2/NO feed ratios of 1.2 or less but goes through a maximum at intermediate temperatures (around 100°C) for H_2/NO feed ratios 1.5 or higher. Ammonia formation is favored for H_2/NO feed ratios of 1.5 or higher and intermediate temperatures (100 to 350°C) buts starts to decompose at a temperature of 400°C or higher. Finally, the microkinetic model was used to determine the surface coverages and explain the experimentally observed selectivities.

Conclusions

During the second year we have made very good progress towards the project objectives 1, 2 and 3. The third year efforts will be focused on kinetic studies using $Pt/Rh/CeO_2$ catalysts, further development of a comprehensive microkinetic model, and incorporation of the microkinetic model into a monolith model to simulate LNT performance as a means of better understanding the complex chemistry and transport interactions.

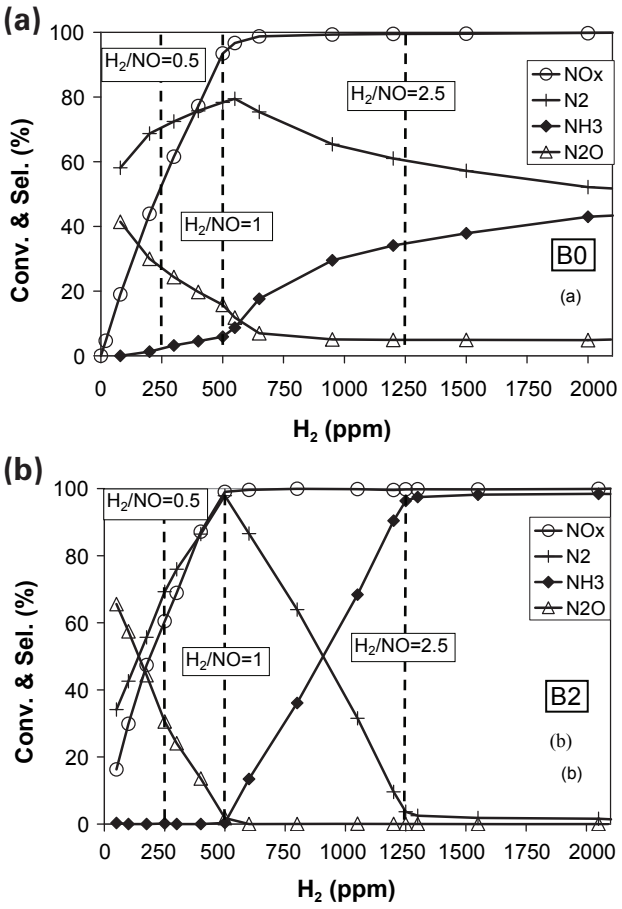

FIGURE 1. NOx conversion and N_2, NH_3, and N_2O selectivities during steady-state NO reduction by H_2 at 360°C (a) B0 (0%Pt,16.7%BaO); (b) B2 (1.27 wt%Pt,16.5%BaO); (500 ppm NO and varied H_2 concentrations.

FY 2007 Publications/Presentations

Refereed Journal Publications:

1. Medhekar, V., V. Balakotaiah, and M.P. Harold, "TAP Study of NOx Storage and Reduction on Pt/Al_2O_3 and $Pt/Ba/Al_2O_3$," Catalysis Today, **121**, 226-236 (2007).

2. Sharma, M., R.D. Clayton, M.P. Harold, and V. Balakotaiah, "Multiplicity in Lean NOx Traps," Chem. Engng. Sci., **62**, 5176-5181 (2007).

3. Xu, J., R.D. Clayton, V. Balakotaiah and M.P. Harold, "Experimental and Microkinetic Modeling of Steady-State NO Reduction by H_2 on $Pt/BaO/Al_2O_3$ Monolith Catalysts," Appl. Catal. B. Environmental, to appear (2007).

4. Clayton, R.D., M.P. Harold, and V. Balakotaiah, "Selective Catalytic Reduction of NO by H_2 in O_2 on $Pt/BaO/Al_2O_3$ Monolith NOx Storage Catalysts," Appl. Catal. B. Environmental, accepted with minor revisions (2007).

Conference Presentations: (during second year)

1. "Modeling and Experimental TAP Studies on the Kinetics of NOx Storage and Reduction over Pt/Al2O3 and $Pt/BaO/Al_2O_3$ Catalysts," presented at the AIChE National Meeting, San Francisco, CA, 11/06 (M. Harold,V. Medhekar and V. Balakotaiah).

2. "Steady State and Dynamic Studies of NOx Storage and Reduction with H2 on $Pt/BaO/Al_2O_3$ Monoliths," presented at the AIChE National Meeting, San Francisco, CA, 11/06 (R. Clayton, M. Harold, and V. Balakotaiah).

3. "Modeling of NOx Storage and Reduction in Catalytic Monolith Reactors," presented at the AIChE National Meeting, San Francisco, CA, 11/06 (J. Xu, M. Harold, and V. Balakotaiah).

4. "Ammonia Formation During Steady-State and Cyclic Operation of the NOx Trap with H_2 as the Reductant," Clayton, R., V. Balakotaiah, and M. Harold, NASCRE 2, Houston, TX, 2/07 (R. Clayton, M. Harold, and V. Balakotaiah).

5. "Determination of the Microkinetics of NOx Storage and Reduction on $Pt/BaO/Al_2O_3$ Catalysts Using TAP," NASCRE 2, Houston, TX, 2/07 (A. Kumar, V. Medhekar, V. Balakotaiah, and M. Harold).

6. "Ammonia and Nitrous Oxide Formation during NOx Storage and Reduction on Pt/Ba Monolith Catalysts," poster presented at North American Catalysis Society Conference, Houston, Texas, 6/07 (R.Clayton, M. Harold, and V. Balakotaiah).

7. "Microkinetic Model Development of NOx Storage and Reduction over $Pt/BaO/Al_2O_3$ Catalyst using Temporal Analysis of Product Reactor," poster presented at North American Catalysis Society Conference, Houston, Texas, 6/07 (A. Kumar, V. Medhekar, M. Harold and V. Balakotaiah).

IV.5 Investigation of Aging Mechanisms in Lean NOx Traps

Mark Crocker (Primary Contact), Yaying Ji, Vence Easterling
University of Kentucky Center for Applied Energy Research
2540 Research Park Drive
Lexington, KY 40511

DOE Technology Development Manager:
Ken Howden

NETL Project Manager: Aaron Yocum

Subcontractor:
Oak Ridge National Laboratory, Oak Ridge, TN

Partners:
- Ford Motor Co., Dearborn, MI (Bob McCabe)
- Umicore Autocat USA, Inc., Auburn Hills, MI (Owen Bailey)

Objectives

- Examine the effect of washcoat composition on lean NOx trap (LNT) catalyst aging characteristics. To this end, prepare model Pt/Rh/CeO_2(-ZrO_2)/BaO/Al_2O_3 catalysts with systematic variation of the main component concentrations.
- Study the physical and chemical properties of the model catalysts in the fresh state and after aging.
- Investigate transient phenomena in the fresh and aged catalysts during lean-rich cycling using spatially resolved capillary inlet mass spectrometry (SpaciMS).
- Investigate the kinetics and mechanism of desulfation in fresh and aged catalysts using chemical ionization mass spectrometry for the simultaneous analysis of evolved sulfur species.
- Correlate evolution of catalyst microstructure to NOx storage and reduction characteristics.

Accomplishments

- Bench reactor tests were performed on a series of model monolith catalysts, in which the concentrations of the four main active components, Pt, Rh, CeO_2 (or CeO_2-ZrO_2) and BaO were systematically varied. From the resulting data, catalyst activity-composition (and in some cases selectivity-composition) correlations were derived.
- An automated catalyst aging cycle has been implemented for the accelerated aging of model monolithic catalysts.
- SpaciMS was applied to the study of transient catalyst response in the model monolithic catalysts. Under lean-rich cycling conditions, ceria was found to exert significant effects on the intra-catalyst chemistry, as demonstrated by the analysis of rich phase intra-catalyst H_2 concentration profiles.
- Desulfation experiments were performed on the model monolith LNTs, revealing a dependence of desulfation efficiency on catalyst ceria content and precious metal loading.

Future Directions

- Complete accelerated aging of model monolithic catalysts (repeated sulfation/desulfation cycles).
- Characterize aged catalysts using standard physico-chemical techniques, in tandem with bench reactor tests, in order to correlate catalyst aging characteristics with washcoat composition.
- Perform *in situ* diffuse reflectance infrared fourier transform spectroscopy (DRIFTS) and on-line mass spectrometry measurements on model powder catalysts in order to gain improved insights into the chemistry of catalyst desulfation.

Introduction

LNTs represent a promising technology for the abatement of NOx under lean conditions. Although LNTs are starting to find commercial application, the issue of catalyst durability remains problematic. LNT susceptibility to sulfur poisoning is the single most important factor determining effective catalyst lifetime. The NOx storage element of the catalyst has a greater affinity for SO_3 than it does for NO_2, and the resulting sulfate is more stable than the stored nitrate. Although this sulfate can be removed from the catalyst by means of high temperature treatment under rich conditions, the required conditions give rise to deactivation mechanisms such as precious metal sintering, total surface area loss, and solid state reactions between the various oxides present. The principle objective of this project is to improve understanding of the mechanisms of LNT aging, and to understand the effect of washcoat composition on catalyst aging characteristics.

Approach

The approach utilized makes use of detailed characterization of model catalysts prior to and after aging, in tandem with measurement of catalyst

performance in NOx storage and reduction. In this manner, NOx storage and reduction characteristics can be correlated with the evolution of catalyst microstructure upon aging. The effect of washcoat composition on catalyst aging characteristics is studied by systematic variation of the concentration of the four main active components, Pt, Rh, CeO_2 (or CeO_2-ZrO_2) and BaO (supported on alumina). In addition to the use of standard physico-chemical analytical techniques for studying the fresh and aged model catalysts, use is made of advanced analytical tools for characterizing their NOx storage/reduction and sulfation/desulfation characteristics, such as SpaciMS and *in situ* DRIFTS.

Results

Composition-Activity Relationships in Model LNT Catalysts

The NOx storage and release properties of a series of fresh (de-greened) model monolith catalysts were assessed on a bench reactor under steady-state cycling conditions in the range 150-450°C. In order to illustrate the effect of ceria content on catalyst performance, results for four catalysts are compared in Figure 1, *viz.*: catalyst 30-0 (containing 30 g BaO and 0 g CeO_2 per liter of catalyst), 30-50 (30 g BaO/L and 50 g CeO_2/L), 30-100 (30 g BaO/L and 100 g CeO_2/L) and 30-100Z (containing 30 g BaO/L and 100 g CeO_2-ZrO_2/L, the latter corresponding to 70 mol% CeO_2 and 30 mol% ZrO_2). In all cases the BaO was present as 20 wt% BaO supported on alumina, while fixed Pt and Rh loadings were used (3.5 g/L and 0.7 g/L, respectively).

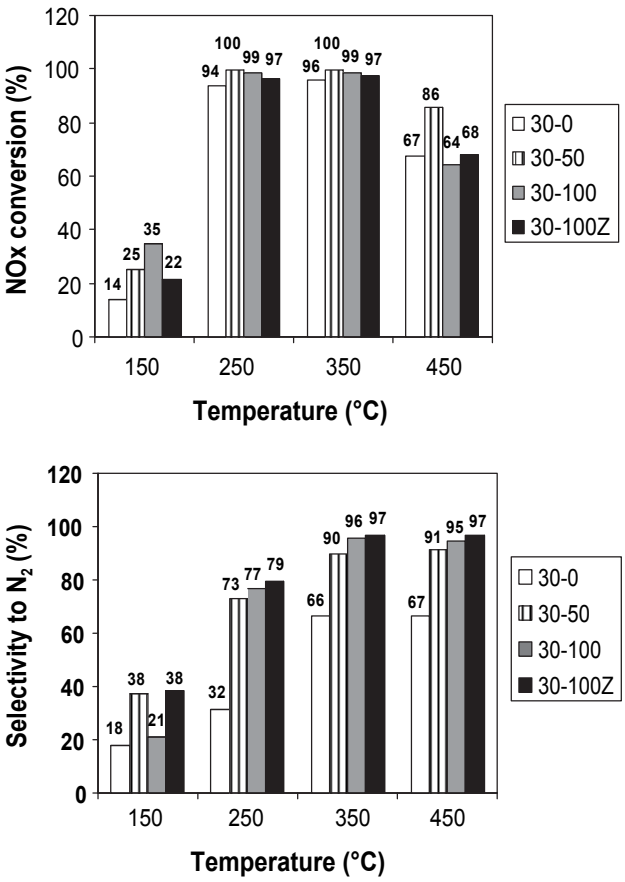

FIGURE 1. Cycle Averaged NOx Conversion (top) and Selectivity to N_2 (bottom) Conditions: lean (60 s): 300 ppm NOx 10% O_2, 5% CO_2, 5% H_2O; rich (5 s): 1.575% H_2, 2.625% CO, 5% CO_2, 5% H_2O, with N_2 as balance, GHSV = 30,000 h^{-1}

From the data collected, several trends emerge:

(i) Under the cycling conditions employed (60 s lean/ 5 s rich), NOx storage efficiency in the temperature range 150-350°C was improved upon addition of ceria to the base Pt/BaO/Al_2O_3 formulation. At 150°C each of the catalysts displayed lean phase NO_2 slip, indicating that NO oxidation was not rate limiting; rather, NOx storage at this temperature appears to be limited by the inability to remove nitrates and nitrites during the regeneration phase.

(ii) High rich-phase NOx slip was observed for all of the catalysts at 150°C, resulting from an imbalance in the rates of nitrate decomposition and NOx reduction. Although the ceria-containing catalysts showed increased NOx slip during the regeneration phase, the overall NOx conversion increased with ceria loading at 150°C. Further, the presence of ceria was found to be beneficial for NOx conversion across the temperature range 150-350°C.

(iii) N_2O was the major NOx reduction product at 150°C over all of the catalysts, although low NOx conversion levels limited the N_2O yield. At higher temperatures N_2 was the main product of NOx reduction, although NH_3 formation was also observed. Selectivity to NH_3 decreased with increasing ceria loading, which is rationalized on the basis that NH_3, formed as a primary reduction product [1], is consumed by reaction with stored oxygen (and residual stored NOx) as the reaction front propagates along the length of the catalyst.

In the next stage of this work, the monolith catalysts will be subjected to a program of accelerated aging, in order to enable catalyst aging characteristics to be correlated with washcoat composition. An automated bench reactor has been constructed for this purpose.

Effect of Ceria Loading on Intra-Catalyst H_2 Concentration during Rich Purging

Ceria has the ability to both catalyze the production of H_2 *in situ* via the water-gas shift reaction ($CO + H_2O \rightarrow H_2 + CO_2$), and contribute to the consumption of reductants via their reaction with stored oxygen. In order to better understand this apparent trade-off, we have studied the measurement of intra-catalyst hydrogen

concentrations during NOx reduction. Figure 2 shows the results obtained for catalysts 30-0, 30-100 and 30-100Z under steady-state NOx storage-reduction cycling at 350°C, the H_2 concentrations being measured at (i) the catalyst inlet ("In Cat"), (ii) one quarter of the way along the catalyst length ("0.25 Cat"), (iii) halfway along the catalyst length ("0.5 Cat"), and (iv) at the catalyst outlet ("Out Cat").

For catalyst 30-0, a slight increase in the H_2 concentration is observed along the length of the catalyst during rich phase operation, resulting from the water-gas shift reaction. In the case of 30-100, high concentrations of H_2 (up to 3%) are measured at the positions one-quarter and halfway into the catalyst (from the inlet), indicative of high water-gas shift activity. This can be attributed to the presence of the Pt/CeO_2 component, which is known to be a highly active catalyst for this reaction. However, the H_2 concentration measured at the catalyst outlet is very low (<0.5%), suggesting that the H_2 formed is subsequently consumed by reaction with oxygen stored in the rear of the catalyst. It can be inferred that towards the rear of the catalyst most of the CO in the feed gas has been consumed, such that the rate of H_2 production from the water-gas shift reaction no longer exceeds the rate of H_2 consumption. Fourier transform infrared data are consistent with this notion; as shown in Figure 3, for catalyst 30-50 the rich phase outlet CO concentration measured during lean-rich cycling does not exceed 0.1% (as compared to the inlet CO concentration of 2.625%), while that for catalyst 30-100 is even lower (maximum of 132 ppm).

For catalyst 30-100Z very different behavior is observed, resulting from the high oxygen storage capacity of the ceria-zirconia component. The H_2 concentration in the catalyst falls off rapidly from the inlet value (Figure 2), such that no H_2 is detected at the mid-point or in the rear of the catalyst. Coupled with this, the CO concentration measured at the catalyst outlet is found to be near zero for the duration of the rich purge (Figure 3), consistent with rapid depletion of the CO and H_2 reductants via reaction with stored oxygen. This result underscores the need to balance the oxygen storage capacity in LNT catalysts [2].

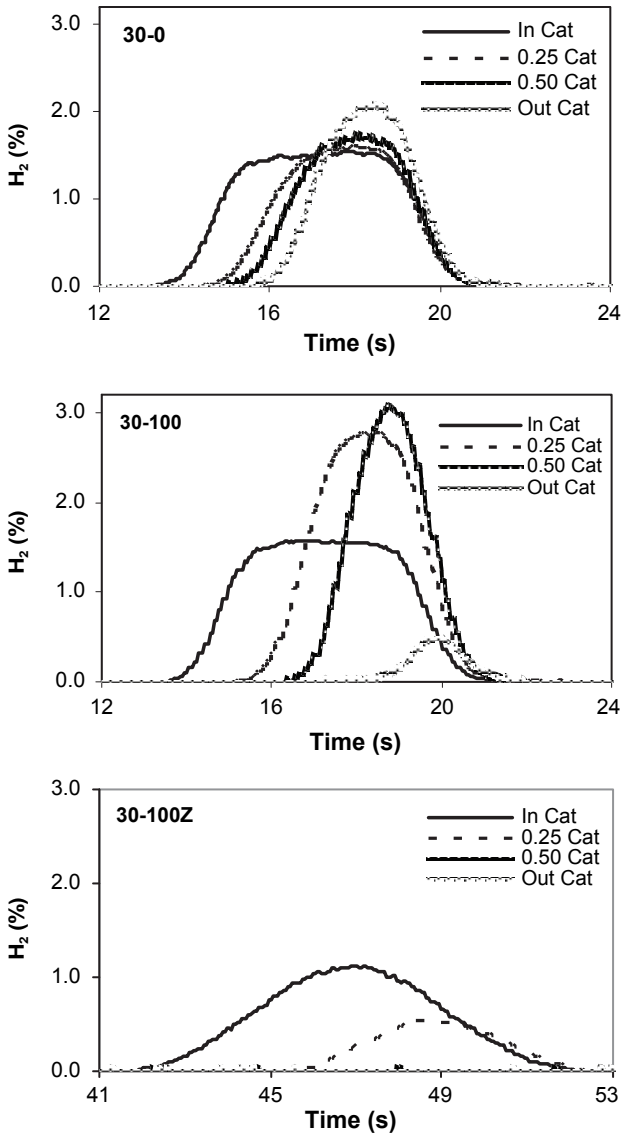

FIGURE 2. H_2 Concentration Profiles Measured along Catalyst Length During Rich Purge (T = 350°C)

Desulfation Studies

Given that LNT thermal degradation can in principle be minimized by the application of low desulfation temperatures, the relationship between catalyst composition and ease of sulfur removal during desulfation is of particular interest. To this end, experiments were performed using an on-line chemical ionization mass spectrometer to monitor the evolution of sulfur species during desulfation of the de-greened model monolith LNTs. Catalyst samples were first sulfated by exposure to lean gas containing SO_2 at 350°C for a fixed period (1 h); subsequently, desulfation was performed under constant rich conditions at different temperatures for 10 min. Shown in Figure 4 is the percent sulfur removed for selected catalysts during desulfation at 650, 675 and 700°C. Comparing the results for the series of catalysts varying in ceria loading, *viz*., 30-0, 30-50 and 30-100, it is apparent that at the relatively low desulfation temperatures of 650 and 675°C, the effectiveness of desulfation increases with the ceria loading of the catalyst. Also of note are the results obtained for catalysts Pt-50 and Pt-100; these contain the same BaO and CeO_2 loadings as catalyst 30-50 but contain half the Rh loading (10 g/ft^3 versus 20 g/ft^3) and either the same Pt loading (100 g/ft^3, hence the notation Pt-100) or half the loading (50 g/ft^3; hence the notation Pt-50). At 675°C the percent sulfur removed follows the order 30-50 > Pt-100 > Pt-50, suggesting that reducing

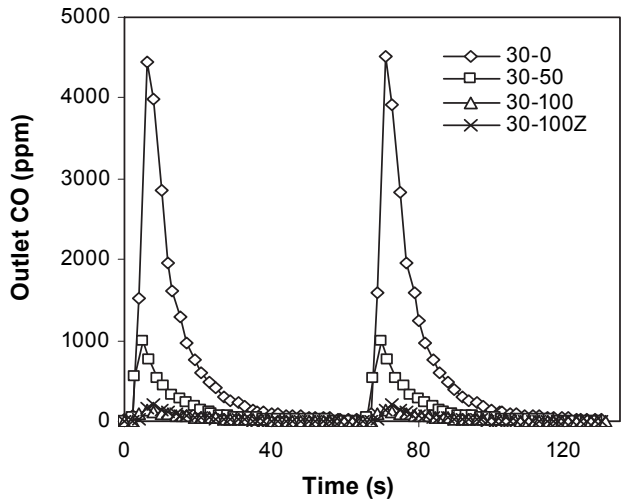

FIGURE 3. Outlet CO Concentration Measured During Rich Purge (T = 350°C).

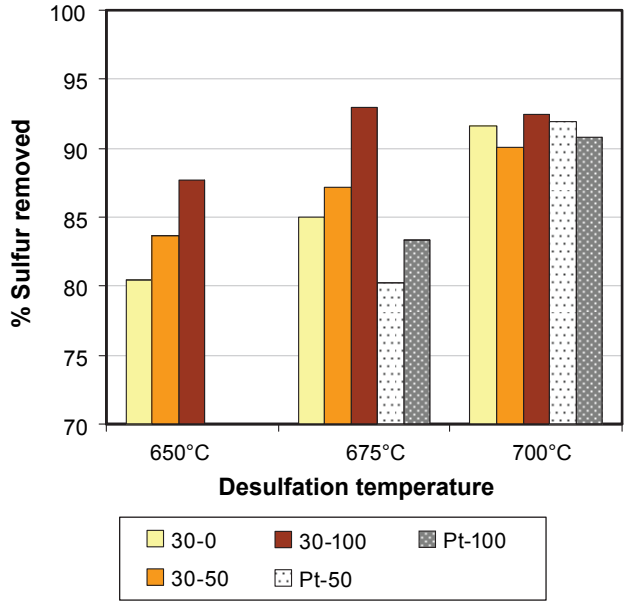

FIGURE 4. Percentage of Stored Sulfur Removed from Selected Catalysts during Desulfation

precious metal content adversely affects catalyst desulfation. This is consistent with the involvement of precious metal sites in the desulfation process. It can be hypothesized that, analogous to catalyst denitrification (i.e., rich phase regeneration), desulfation proceeds via the dissociative adsorption of H_2 on Pt and Rh sites, the resulting ad-H atoms spilling over onto the sulfated oxides present and inducing decomposition of the sulfate groups. Further studies are planned in order to investigate this hypothesis.

Conclusions

- Lean-rich cycling experiments performed on model monolith LNT catalysts have identified significant effects associated with the presence of ceria; these include increased NOx storage (particularly at low temperatures), resulting in improved NOx conversion levels, and superior selectivity to N_2 during reduction of stored NOx (at fixed reductant concentration).
- Transient response studies have shown that the introduction of ceria into LNT catalysts results in increased water-gas shift activity. However, the use of high OSC ceria-based oxides can result in rapid depletion of the CO and H_2 reductants along the length of the catalyst, due to reaction with stored oxygen. This finding underscores the need to balance the oxygen storage capacity in LNT catalysts.
- Bench reactor experiments have confirmed that the presence of ceria is beneficial for lowering the required desulfation temperature of barium-based LNT catalysts; the precious metal loading is also indicated to be of importance.

References

1. L. Cumaranatunge, S.S. Mulla, A. Yezerets, N.W. Currier, W.N. Delgass, F.H. Ribeiro, J. Catal. 246 (2007) 29.

2. J. Theis, J. Ura, C. Goralski Jr., H. Jen, E. Thanasiu, Y. Graves, A. Takami, H. Yamada, S. Miyoshi, Society of Automotive Engineers 2003-01-1160.

FY 2007 Publications/Presentations

1. Y. Ji, T.J. Toops, J.-S. Choi, M. Crocker, "The Effect of CeO_2 on the Performance of Lean NO_x Trap Catalysts", 10th Cross-Cut Lean Exhaust Emissions Reduction Simulation (CLEERS) Workshop, Dearborn, MI, May 1-3, 2007.

2. Y. Ji, T.J. Toops, J.-S. Choi, M. Crocker, "Investigation of Aging Mechanisms in Lean NO_x Trap Catalysts", 1st Annual DOE Semi-Mega Merit Review Meeting, Crystal City, VA, June 18-19, 2007.

3. Y. Ji, T.J. Toops, J.-S. Choi, M. Crocker, "Effect of CeO_2 on the Storage and Regeneration Behavior of Lean NO_x Traps", 20th North American Catalysis Society Meeting, Houston, TX, June 17-22, 2007, paper O-S4-41.

4. Y. Ji, T.J. Toops, J.-S. Choi, M. Crocker, "Composition-Activity Relationships in Lean NO_x Trap Catalysts", Europacat VIII, Turku, Finland, August 26-30, 2007, paper P14-9.

IV.6 Improved Engine Design Concepts Using the Second Law of Thermodynamics: Reducing Irreversibilities and Increasing Efficiencies

Jerald A. Caton
Texas A&M University
Department of Mechanical Engineering
TAMU 3123
College Station, TX 77843–3123

DOE Technology Development Manager:
Gurpreet Singh

NETL Project Manager:
John (Jason) Conley

Objectives

- Complete a study of the effects of compression ratio and expansion ratio on engine performance and second law parameters.
- Initiate studies of diesel engine operation – using experimental data for calibration.
- Upgrade the exhaust gas recirculation (EGR) sub-model to reflect combustion termination for high (>20%) levels of EGR for spark ignition (SI) engines.
- Complete studies of "reversible" combustion for a reciprocating device using Professor Keenan's concept.

Accomplishments

- The engine cycle simulation was used to determine the effects of compression ratio and expansion ratio on engine performance and second law performance. The results showed that increases of compression ratio beyond about 10:1 do not provide significant thermodynamic gains. The use of a greater expansion stroke compared to the compression stroke ("Atkinson cycle") was most effective for wide-open-throttle conditions. The use of a greater expansion stroke had modest effects on the second law parameters.
- The simulation was modified to be able to consider diesel engine operations. Preliminary results were obtained and compared to experimental results for a 1.7 liter, direct-injection, Isuzu engine.
- The EGR sub-model was improved to reflect the termination of combustion as EGR levels increase. The improved EGR sub-model was then used in a series of computations to complete a parametric study.
- An examination of hypothetical "reversible" combustion at high temperatures and pressures was completed. This concept was based on the proposal by Professor Keenan from the 1940s. The results indicate possible scenarios where the availability destruction can be zero by preselecting the reactant composition such that at the end of compression the species are in equilibrium. Although the availability is preserved, most of the availability remains in the exhaust gases and the engine efficiency is typically low.

Future Directions

- Continue to use the engine cycle simulation to study diesel engines.
- Initiate studies to examine novel engines such as the "iso-engine" (which uses an isothermal compression process).
- Complete the on-going study of EGR for SI engines.

Introduction

This work has been using comprehensive thermodynamic evaluations to better understand the details of engine operation with the goals of defining operating conditions and design parameters which provide the highest possible efficiencies with minimal emissions. The use of the second law of thermodynamics is central to this effort. The second law of thermodynamics provides a rich and significant insight concerning the proper use of energy and its conversion to mechanical shaft power. The second law allows this feature to be quantified using the thermodynamic property of availability (also known as exergy).

Traditionally, the first law has been used to provide basic understandings of engine operation, but the use of the second law of thermodynamics has not been as widely used. The work conducted as part of this project was directed to help provide a deeper understanding of these results. To date, this work has included a number of detailed studies which have included reciprocating engines, and simple (e.g., constant pressure or volume) systems. A number of fuels have been used in these evaluations. Examples of this work have included detailed examinations of the use of EGR for spark ignition engines, the use of oxygen enriched inlet gases,

comparisons of hydrogen and isooctane for the same engine, and the effects of compression ratio and greater expansion ratios (for the same compression ratio) on performance and second law parameters.

Approach

The main feature of this project is the use of a comprehensive engine cycle simulation which is based on consistent and rigorous thermodynamics, and includes new features such as the use of the second law of thermodynamics. The engine cycle simulation has been described in numerous previous publications [1-3]. In summary, this simulation is largely based on thermodynamic formulations, and is a complete representation of the four-stroke cycle including the intake, compression, combustion, expansion and exhaust processes. The simulation uses detailed thermodynamic gas properties including equilibrium composition for the burned gases. The cylinder heat transfer is based on a correlation from the literature, and the combustion process is based on a mass fraction burn relation.

Figure 1 is a schematic of the thermodynamic system for the simulation. For the combustion processes, three zones (each spatially homogeneous) are used. The three zones are: the unburned zone, the adiabatic core burned zone, and the boundary layer burned zone. The adiabatic core and boundary layer zones together comprise the burned zone. The use of an adiabatic core zone is critical for correct nitric oxide formation rates. The flow rates are determined from quasi-steady, one-dimensional flow equations, and the intake and exhaust manifolds are assumed to be infinite plenums containing gases at constant temperature and pressure.

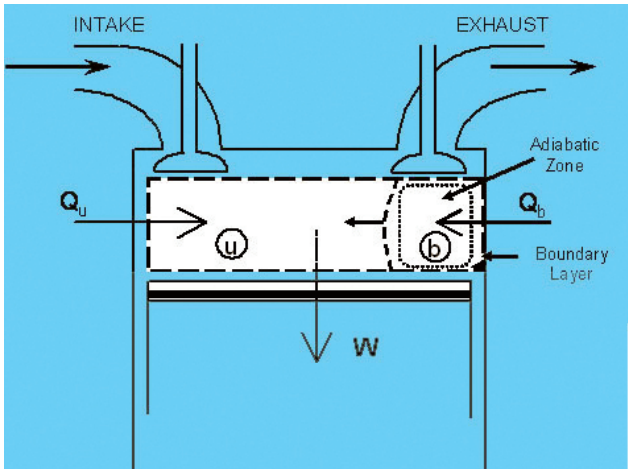

FIGURE 1. Schematic of the Engine Cylinder Depicting the Three Zones During Combustion

Results

A few of the results from the studies of the over-expanded (Atkinson cycle) engine will be reported here. Other results are available elsewhere. For this study, a conventional, automotive V-8, SI engine is used as the framework for this work [1-3]. The simulation has been modified for these studies to permit a longer expansion stroke than compression stroke. Details on the modifications are included in [3].

The first example of results for the Atkinson cycle is based on a compression ratio of 15 and an expansion ratio of 20. Figure 2 shows the instantaneous cylinder volume as a function of crank angle for this configuration, and for reference, also shows the cylinder volume for the conventional case where the compression ratio and expansion ratio are the same (and equal to 15). To the right of the figure is a schematic of the cylinder arrangement with the two stroke dimensions indicated. The cylinder volume decreases during the compression stroke from intake valve closing (IVC) to top dead center (TDC) at 0.0º crankangle (CA), then increases to a maximum volume during the expansion stroke from TDC to 180º after top dead center (ATDC). Although two expressions were used for the volume computation, the transition appears smooth on this scale.

Part Load: Figure 3 shows the computed brake thermal efficiency as functions of expansion ratio for three compression ratios (6, 10 and 15) for the base case part load engine conditions. For these computations, the brake mean effective pressure BMEP was constant (= 325 kPa) – so as the brake efficiency increased, the inlet pressure was reduced. For each compression ratio case, as the expansion ratio increases the thermal efficiency first increases, reaches a maximum, and then decreases. The expansion ratio for the highest efficiency appears to be equal to about the compression ratio plus three. The use of this expansion ratio provides a thermal efficiency increase of about 1% (e.g., from 24% to 25%). These results are examined more fully in the following.

To better understand the results of Figure 3, the intake and exhaust flow rates as functions of crank angle for the different cases were examined. The most significant difference is the lower flow rates during the blow-down portion of the exhaust flow for the over-expanded cases. This is because of the greater expansion which results in a lower cylinder pressure at the time of exhaust valve opening. This is compensated by the greater flow rates during the exhaust displacement phase of the exhaust process. This less effective exhaust process for the higher expansion ratios is one reason why the efficiency decreases for the higher expansion ratios. Another important reason for this decrease is the increase in the heat losses for the larger expansion ratios due to the increase in surface area.

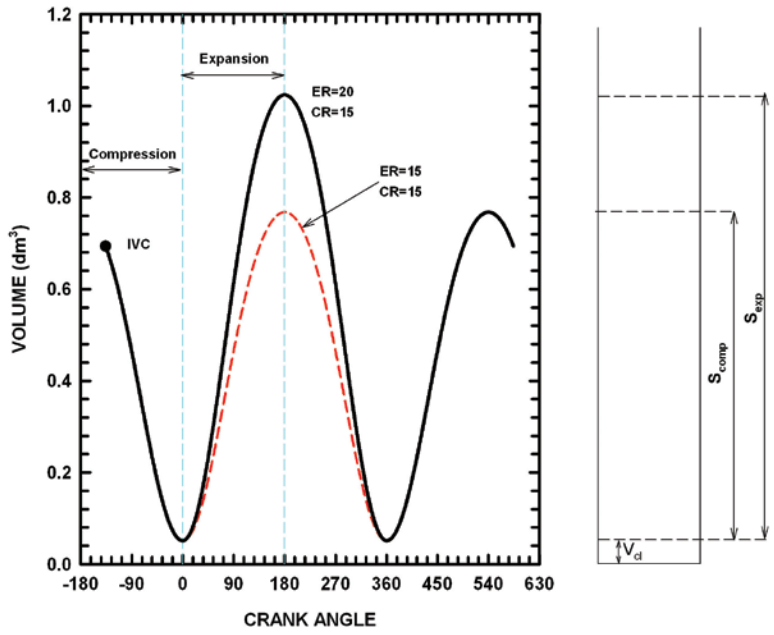

FIGURE 2. Cylinder Volume as a Function of Crank Angle for a Compression Ratio of 15 and for Expansion Ratios of 15 (dashed lines) and 20 (solid lines) (Schematic of engine cylinder shown on right side.)

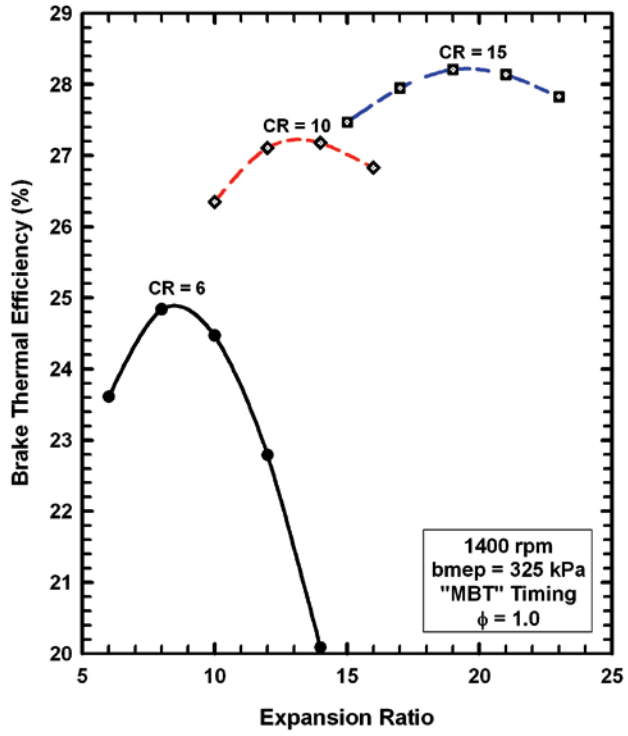

FIGURE 3. Brake Thermal Efficiency as Function of the Expansion Ratio for the Base Case for Three Compression Ratios

Finally, for these part load cases, the destruction of availability during the combustion process as a function of expansion ratio was examined. For the case with a compression ratio of 6, the percentage of availability destroyed was nearly constant, and ranged between 21.74% and 21.79% for expansion ratios between 6 and 14. One of the major reasons for this negligible difference is the modest changes of the combustion gas temperatures as the expansion ratio increased.

Full Load: In addition to the above results for a part load condition, results were obtained for the use of greater expansion ratios for the case of wide-open-throttle (WOT). Figure 4 shows the brake thermal efficiency as functions of the expansion ratio for three compression ratios (6, 10 and 15). For each compression ratio, the thermal efficiency first increases, reaches a maximum, and then decreases. The expansion ratio for the highest thermal efficiency is about 19, 29, and 44 for the compression ratios of 6, 10 and 15, respectively. The use of these expansion ratios resulted in an increase of the thermal efficiency of about 10%. For example, for a compression ratio of 6, the brake thermal efficiency increased from about 30% to slightly over 40% as the expansion ratio increases from 6 to about 19. Compared to the previous part load cases, the WOT cases result in much greater improvements with greater values of expansion ratios. Of course, these high expansion ratios are probably not practical, but they do illustrate the important potential thermodynamic gains. The following will discuss some aspects of these results.

Figure 5 shows the log of the cylinder pressure as a function of the log of the cylinder volume for the WOT case with the highest brake thermal efficiency (of the cases examined) which was for a compression ratio of 15 and an expansion ratio of 44 (solid line). For comparison, Figure 5 also shows (dashed line) the results for the WOT case for a compression ratio of 15 and an expansion ratio of 15 (standard engine configuration). The pressures during the compression stroke are the same for both configurations, but the pressures during the expansion are different, and of course, for the over-expanded configuration, the expansion proceeds to a much greater volume. The additional area within the pressure-volume diagram associated with the over-expanded configuration is indicative of the additional work (power) obtained with the greater expansion. The pressures for the exhaust stroke are generally higher for the over-expanded configuration, but the pressures during the intake stroke are nearly the same.

For completeness, Figure 6 shows that the availability destroyed due to combustion increases slightly (from about 20.2% to 21.0%) as the expansion

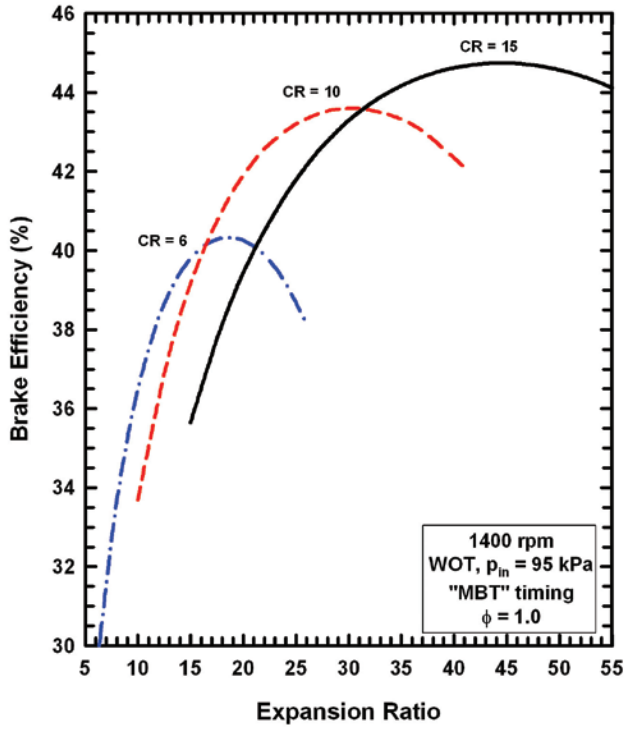

FIGURE 4. Brake Thermal Efficiency as a Function of Expansion Ratio for Compression Ratios of 6, 10 and 15 for an Engine Speed of 1400 RPM and an inlet manifold pressure of 95 kPa (WOT).

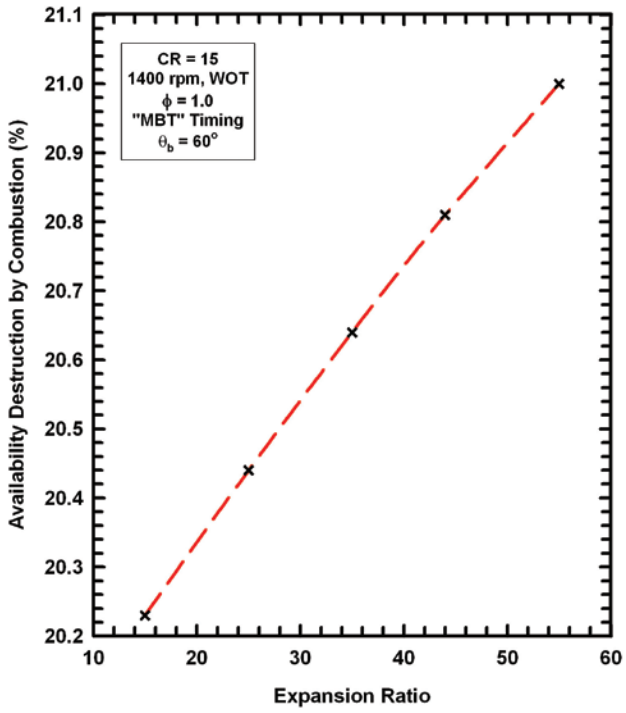

FIGURE 6. Availability Destruction Due to Combustion as a Function of the Expansion Ratio for a Compression Ratio of 15 for an Engine Speed of 1400 RPM and an Inlet Manifold Pressure of 95 kPa (WOT)

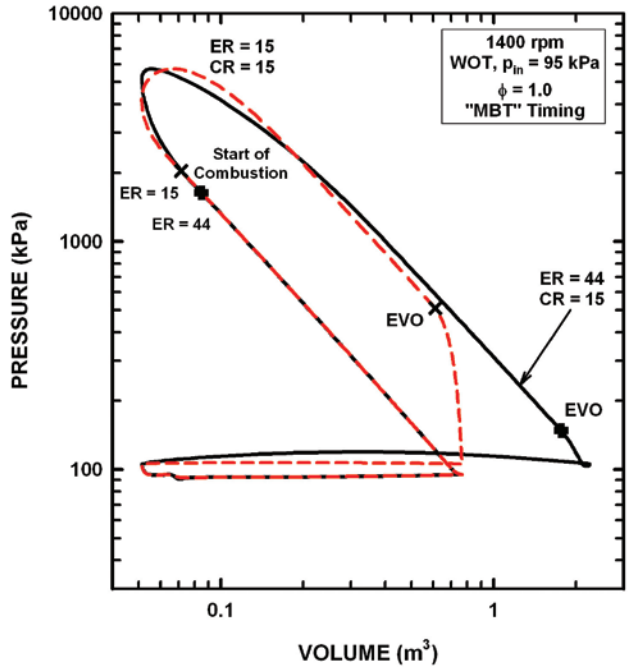

FIGURE 5. Log of Cylinder Pressure as a Function of Log of Cylinder Volume for a Compression Ratio of 15 and Expansion Ratios of 15 and 44 for an Engine Speed of 1400 RPM and an Inlet Manifold Pressure of 95 kPa (WOT)

ratio increases from 15 to 55 for a compression ratio of 15 for the WOT case. This slight increase is due to the lower combustion temperatures associated with the higher expansion cases. Since the work output increases for the higher expansion ratios, the gas temperatures decrease slightly which is a major cause of availability destruction during the combustion process.

One final consideration was the mechanical friction. For an over-expanded configuration, the mechanical friction would be expected to be higher due to the additional mechanism and the longer stroke. This can not be quantified without some knowledge of the specific design and experimental information.

Conclusions

- The study included expansion ratios up to four (4) times the compression ratio. For most cases, the thermal efficiency first increased as expansion ratio increased, then attained a maximum efficiency, and then decreased. The decrease in efficiency after the maximum value was shown to be due to increased heat losses, increased friction, and in-effective exhaust processes (due to the reduced cylinder pressure at the time of exhaust valve opening).

- For the part load cases, the higher expansion ratio provided only modest gains due to increased pumping losses associated with the constant load requirement.
- For the wide open throttle cases, however, the higher expansion ratios provided significant gains. For example, for a compression ratio of 10, expansion ratios of 10 and 30 provided brake thermal efficiencies of about 34% and 43%, respectively. Although the net thermodynamic gains are significant, large expansion ratios such as 30 may not be practical for most applications.
- For the wide open throttle cases, for a compression ratio of 15, the availability destroyed due to the combustion process increased slightly from about 20.2% to 21.0% as the expansion ratio increased from 15 to 55.

References

1. J. A. Caton, "Utilizing a Cycle Simulation to Examine the Use of EGR for a Spark-Ignition Engine Including the Second Law of Thermodynamics," in proceedings of the 2006 Fall Conference of the ASME Internal Combustion Engine Division, Sacramento, CA, 5–8 November 2006.

2. J. A. Caton, "First and Second Law Analyses of a Spark-Ignition Engine Using Either Isooctane or Hydrogen," in the proceedings of the 2006 Fall Conference of the ASME Internal Combustion Engine Division, Sacramento, CA, 5–8 November 2006.

3. J. A. Caton, "The Effects of Compression Ratio and Expansion Ratio on Engine Performance Including the Second Law of Thermodynamics: Results from a Cycle Simulation," accepted for the proceedings of the 2007 Fall Conference of the ASME Internal Combustion Engine Division, Charleston, SC, 14–17 October 2007.

FY 2007 Publications/Presentations

1. J. A. Caton, "Utilizing a Cycle Simulation to Examine the Use of EGR for a Spark-Ignition Engine Including the Second Law of Thermodynamics," in proceedings of the 2006 Fall Conference of the ASME Internal Combustion Engine Division, Sacramento, CA, 5–8 November 2006.

2. J. A. Caton, "First and Second Law Analyses of a Spark-Ignition Engine Using Either Isooctane or Hydrogen," in the proceedings of the 2006 Fall Conference of the ASME Internal Combustion Engine Division, Sacramento, CA, 5–8 November 2006.

3. J. A. Caton, "Improved Engine Design Concepts Using the Second Law of Thermodynamics: Reducing Irreversibilities and Increasing Efficiencies," poster presentation at the FreedomCAR Program Semi-Mega Review (SMMR), U. S. Department of Energy, Crystal City Marriott Hotel, Arlington, VA, 18–19 June 2007.

4. J. A. Caton, "The Effects of Compression Ratio and Expansion Ratio on Engine Performance Including the Second Law of Thermodynamics: Results from a Cycle Simulation," accepted for the proceedings of the 2007 Fall Conference of the ASME Internal Combustion Engine Division, Charleston, SC, 14–17 October 2007.

5. H. Sivadas and J. A. Caton, "Effects of Exhaust Gas Recirculation on the Availability Destroyed due to Combustion for a Range of Conditions and Fuels," accepted by the *International Journal of Energy Research*, October 2007.

IV.7 High-Compression-Ratio Atkinson-Cycle Engine Using Low-Pressure Direct Injection and Pneumatic-Electronic Valve Actuation Enabled by Ionization Current and Forward-Backward Mass Air Flow Sensor Feedback

Harold Schock (Primary Contact),
Farhad Jaberi, Ahmed Naguib and George Zhu
Michigan State University (MSU)
East Lansing, MI 48864

DOE Technology Development Manager:
Roland Gravel

NETL Project Manager: Samuel Taylor

Subcontractor:
Visteon (David Hung), Dearborn, MI

Objectives

- Demonstrate an advanced high efficiency controlled combustion (HECC) engine which includes a 15% improvement in fuel economy over the baseline 5.4L production engine.
- Demonstrate the benefits of advanced technology developed on this project including infinitely variable valve actuators (timing and lift), ionization flame detection for engine control, low pressure direct injection and a cycle resolved mass air flow sensor.

Accomplishments

- A fluidic rectifier with area ratio (AR) of 8, length (L) of 5 mm and extension of 5 mm was fabricated and integrated into a forward/backward mass air flow sensor (FBMAFS) prototype and was characterized in the unsteady air intake flow facility and tested with robust, automotive hotwires.
- High-speed visualization of fuel air mixing and in-cylinder flame distribution was achieved to reveal the spray distribution, flame propagation, and fuel impingement in the optical engine.
- A novel and affordable high fidelity mathematical/computational methodology has been developed for detailed simulation of realistic combustion systems employing an efficient two-phase Lagrangian-Eulerian-Lagrangian large eddy simulation (LES) with a two-phase probability density function-based sub-grid gas-liquid combustion model.
- Work is in progress to develop experimental data for controlled, well-defined flow conditions for model validation. Three test cases are considered, one with geometrical features very close to MSU's 3-valve engine. These cases are being simulated via our LES models.
- The development of our Opal-RT based prototype engine controller has been completed. It has been validated in both our engine hardware-in-the-loop (HIL) simulation and in engine dynamometer experiments.

Future Directions

- Correction of oscillation tracking deficiency in present automotive hotwire technology for improved frequency compensation methods through development of new, fast-response, yet robust sensor technology.
- Completion of LES model validation.
- Complete performance testing of the HECC engine.

Introduction

The goal of this project is to demonstrate an improvement in the fuel economy of light-duty vehicles by increasing the cycle efficiency of Otto cycle engines. Otto cycle engines have been shown to be of excellent value in cost per kilowatt, meet strict emission standards, and billions of dollars have been invested in the facilities to manufacture these engines and their associated components. Thus, technologies that offer improvements in current engines provide a good value proposition for both the consumer and the manufacturer. As mentioned prior, our goal is to demonstrate an advanced low pressure direct injected engine which has a 15% improvement in road-load fuel economy over a baseline 5.4L production engine.

Approach

There are four technologies that we have been investigating to meet the goals of this project. They include a low pressure direct injector which will increase volumetric efficiency and facilitate aggressive deceleration fuel cutoff. The second is an electronic-pneumatic valve actuator which will enable variable compression ratio control and valve deactivation. The third is a FBMAFS which allows for cycle-resolved measurement of the inducted fresh air charge so that fueling can be accurately maintained. Fourth, a

key aspect needed to achieve these engine efficiency improvements is the ability to detect information associated with combustion events and in this application we have focused on the ability to use a measure of the ionization current associated with these events. The technical highlights of these developments are discussed in the next section.

Results

Development of a FBMAFS

A custom experimental setup was constructed to conduct the transient response tests. In particular, the tests were conducted by placing a single fluidic rectifier in an air jet that was turned on/off using a rotating chopper. The rectifier was oriented relative to the flow such that it operated in the flow-suppression regime. The bottom plot in Figure 1 displays the chopper signal indicating the on/off jet flow state. The top plot in the same figure shows the associated hotwire output with (blue) and without (red) the nozzle/diffuser. The comparison of the "flat" portion of these response curves clearly shows the suppression of the velocity when the nozzle/diffuser is in place relative to the case when the hotwire is free. However, it appears that during the transient towards the steady-state, the fluidic rectifier response experiences some oscillations. This suggests that high-frequency oscillations may be inherent to the transient response of the fluidic rectifier. Further experiments are needed to clarify this issue further.

In-Cylinder Fuel Mixture Visualization and Fuel Impingement Analysis

Figure 2 shows the comparison of two fuel injector spray patterns on the fuel distribution and fuel impingement on the cylinder wall. For an existing configuration of injector mounting orientation and cylinder geometry in this engine, a wider spray angle directed the fuel towards the center of the cylinder

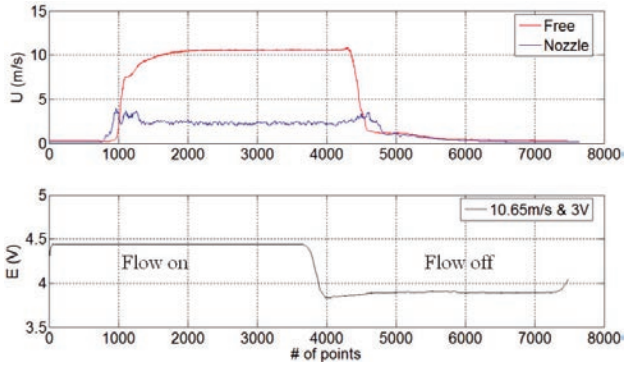

FIGURE 1. Sample Transient-Response Results: Hotwire Signals (Top) and Jet-Flow State (Bottom)

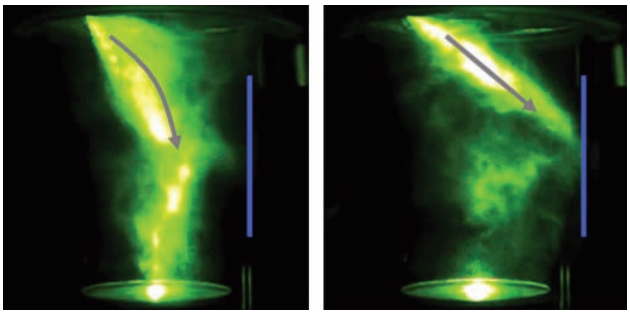

FIGURE 2. Fuel Distribution and Wall Impingement of Two Spray Injector Patterns (Left: 80° Spray Angle/10° Offset Angle; Right: 40° Spray Angle/0° Offset Angle)

to form a more homogeneous fuel distribution with less wall impingement. Image processing algorithms have been developed to measure the semi-quantitative information of the magnitude of fuel spray impingement on cylinder wall. A fuel impingement index on the cylinder wall was defined based upon the illumination intensity of the location (pixel) on the image near the cylinder wall. This index was used to track and analyze the extent of fuel impingement at each crank angle degree over the injection cycle. The sequence and the duration of the fuel impingement of different spray patterns were revealed. Based upon the optical engine visualization, fuel injector with special nozzle was optimized to further improve the fuel distribution in the cylinder.

Large Eddy Simulation of In-Cylinder Flow

Flow around a poppet valve - As a first test case, the LES ability to capture these fluid motions was tested by simulating the flow in a sudden expansion geometry with a fixed popper valve. The results confirm the generation of two large-scale vortical structures behind the valve. To make a quantitative comparison with the experimental data, the "mean" axial velocity and the root mean square (RMS) values of the axial velocity at 20 and 70 mm from cylinder head are calculated and are compared with the experimental data. The mean axial velocity is in good agreement with the experimental data. The RMS of axial velocity also compares reasonably well with the Laser Doppler Anemometry laboratory data. The differences can be partly attributed to the uncertainty in measurements and the averaging process. Good prediction of mean and RMS values of the axial velocity demonstrate the ability of our LES model in predicting the highly unsteady and turbulent flows that are similar to those observed in a realistic engine.

Simple engine with one intake/exhaust valve - As a second test case, the in-cylinder flow filed in a piston-cylinder assembly is simulated via LES. Here, we have simulated the flow in this idealized flow configuration

for further validation of the LES flow solver and sub-grid scale models. Because the piston and therefore the grids are moving, mean (time-averaged) velocity and RMS are obtained by averaging in the azimuthal direction over several cycles. Both the mean axial velocity and the RMS values are found to be in good agreement with the experimental data. These test cases have some geometrical and flow features of realistic engines and are simulated here to assess the capabilities of our LES flow solver and its moving mesh technique. It is clear that the LES method is indeed able to predict the flow in these configurations. This gives us enough confidence to apply the model to more complex and more realistic engines.

MSU's three-valve engine - Within the past several months, the computational fluid dynamics group have worked on the grid generation and large eddy simulation of nonreacting flows in realistic engine configuration with moving valves. To have a high quality grid for a moving piston, complex cylinder head and moving valves, a unique multi-block grid system was developed for MSU's 3-valve laboratory engine. The final grid system is made of 18 blocks. Like the previous case with flat cylinder head, simulations of the new case are started when the piston is at top dead center and free stream boundary condition is applied at the inlet section of the manifolds. Inside the cylinder, the velocity is initially zero and the thermodynamic variables are at standard atmospheric conditions. Examples of our LES model flow field predictions in the 3-valve engine are demonstrated in Figures 3 and 4.

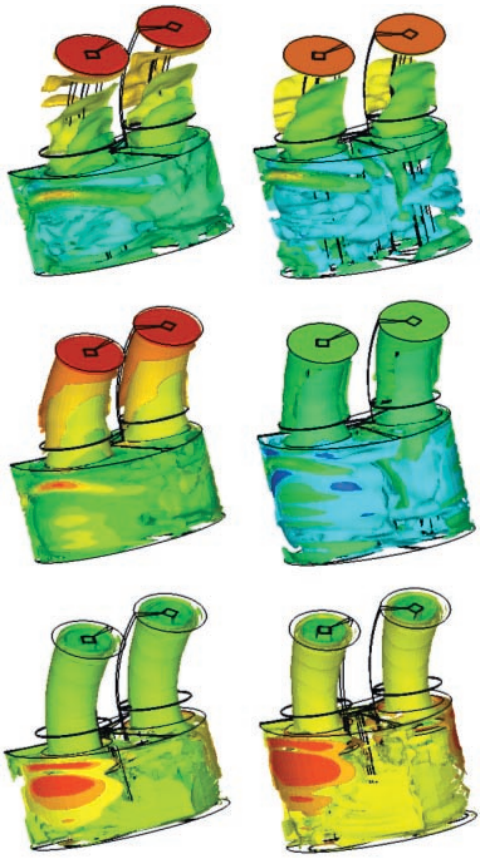

FIGURE 3. Isosurface Plots of Pressure (Top), Temperature (Middle) and Vorticity (Bottom) at 90° (Left) and 130° (Right) After Top Dead Center

Model Based Predictive Control of Electro-Pneumatic Exhaust Valve

Variable intake valve timing and lift can be used to optimize engine performance over a wide operating range, for instance, to reduce engine pumping losses, deactivate selected cylinder(s), and control flame speed by manipulating in-cylinder turbulence. Exhaust valve timing and lift control makes it possible to vary the amount of residual gas recirculation (RGR) and control valve overlap when combined with intake valve control. Variable valve timing and lift control is also a key technology for homogeneous charge compression ignition combustion control.

The electro-pneumatic valve actuator (EPVA) utilizes the supplied air pressure to actuate either the intake or exhaust valve by electronically controlling solenoids that control the motion of the actuator's piston. The EPVA system is able to provide either a multiple stepping or a continuously changing valve timing phase shift.

Unlike the intake valve, the exhaust valve opens against an in-cylinder pressure that varies as a function of the engine operational conditions with cycle-to-cycle combustion variations. This pressure disturbance slows down the valve actuator response and as a result, it increases the variation of valve opening delay. In fact, this disturbance makes it difficult to maintain repeatable valve opening timing and lift. As a result, unrepeatable valve lift affects the closing timing control which is critical for RGR control. Therefore, this work addresses exhaust valve lift control.

A mathematical in-cylinder pressure model at exhaust opening was developed and integrated with the exhaust valve model for control development. The thermodynamic data was obtained using WAVE^{TM} simulation. The WAVE^{TM} model was calibrated and validated using experimental in-cylinder pressure data. The mathematical in-cylinder pressure model is then used to develop the model-based predictive control scheme for exhaust valve lift. The controller consists of two parts: feedforward and closed-loop controls. The feedforward control is used to provide a nominal lift control based upon the predicted valve opening trajectory, while the closed-loop controller is used to minimize the mean control error. The closed-loop control strategy was developed and verified in simulation using the combined mathematical model of exhaust valve and in-cylinder pressure.

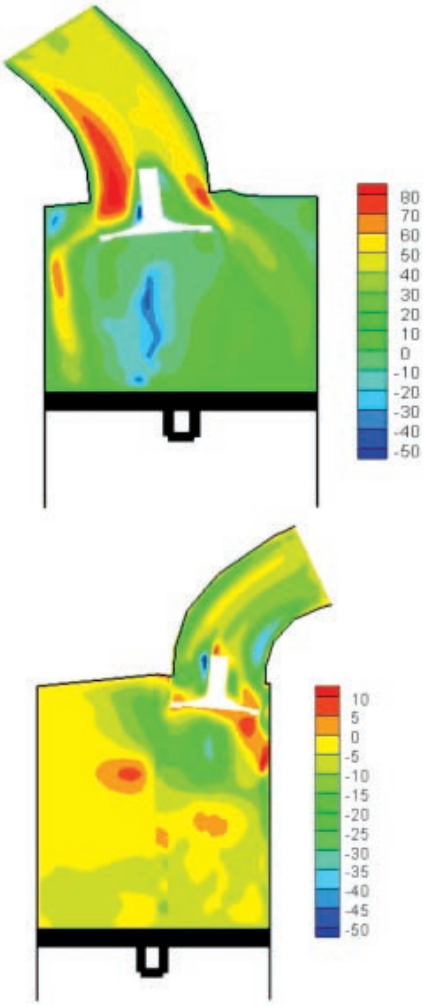

FIGURE 4. Cross-Section with Temperature Contours During Intake (Top) and Exhaust (Bottom)

A level two model which simplifies the system dynamics used for the nonlinear level one model analysis is shown in Figure 5.

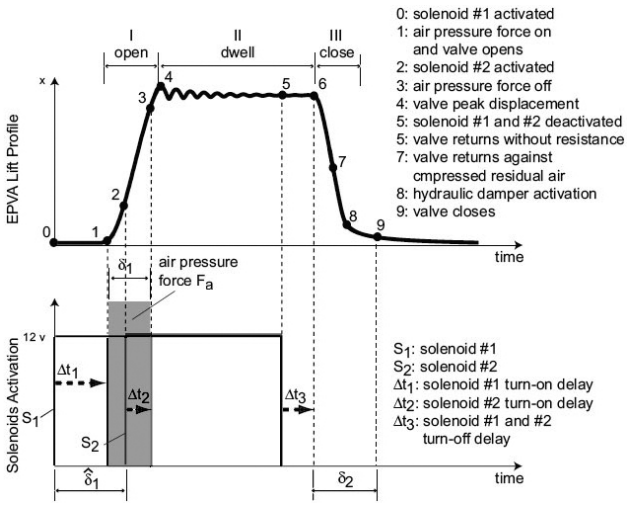

FIGURE 5. Valve Lift Profile with Solenoid Command Chart

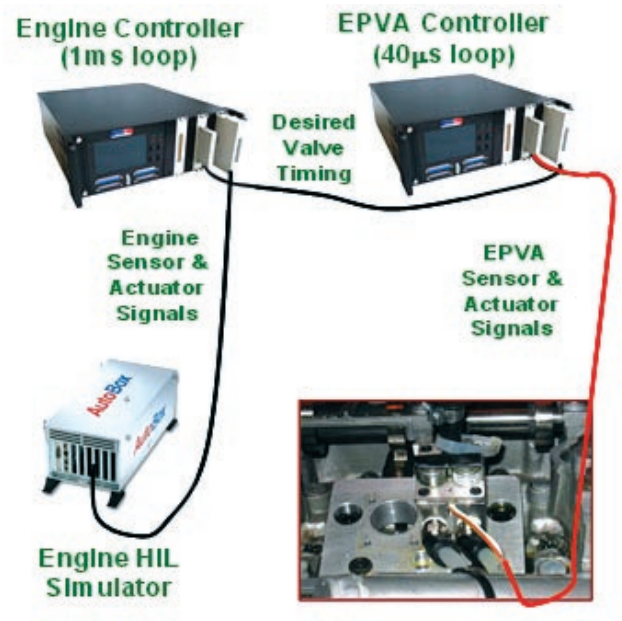

FIGURE 6. Decentralized Engine and EPVA Control Architecture

Decentralized Engine and EPVA Control Development

Communication between Opal-RT engine and EPVA controllers has been established and validated. The basic control principle is that the Opal-RT engine controller sends the crank synchronized desired valve lift, opening and closing signals to the EPVA Opal-RT controller; the EPVA controller conducts the valve lift, opening and closing timing control, based upon the reference signals from the engine controller, in a closed-loop.

Both engine and EPVA controllers have been validated using our engine HIL simulation station and EPVA test bench (see diagram in Figure 6). EPVA valve control strategy is under development using this setup. Dynamometer validation tests of both engine and EPVA control strategies are the last task to be completed.

Summary

The remaining component issue is validation of the performance of the pneumatic actuator for the HECC engine concept. Specifically, the closed-loop control system requires that a valve position sensor be capable of providing reliable feedback to the control system. Upon completion of this validated system engine performance can be ascertained. All other subsystems which were

part of this project are operational and have been experimentally validated. Final testing of the project is expected to be completed by the end of 2007.

FY 2007 Publications/Presentations

1. Ma, J., Stuecken, T., Schock, H., Zhu, G., Winkelman, J, "Model reference adaptive control of a pneumatic valve actuator for infinitely variable valve timing and lift," 2007 SAE World Congress (SAE 2007-01-1297), Detroit, MI, April, 2007.

2. Ma, J., Zhu, G., Schock, H., Winkelman, J., "Adaptive control of a pneumatic valve actuator for an internal combustion engine," 2007 American Control Conference, New York, NY, July, 2007.

3. Hung, D.L.S., Zhu, G., Winkelman, J., Stuecken, T., Schock, H., and Fedewa, A., "A High Speed Flow Visualization Study of Fuel Spray Pattern Effect on a Low Pressure Direct Injection Gasoline Engine," SAE Technical Paper No. 2007-01-1411, 2007.

4. Zhang, Y., Schock, H, and Hung, D.L.S., "Numerical Study of the Mixture Preparation Process in a 5.4L V8 GDI Engine," ILASS-Americas, 20th Annual Conference on Liquid Atomization and Spray Systems, Chicago, IL, 2007.

IV.8 On-Board Engine Exhaust Particulate Matter Sensor for HCCI and Conventional Diesel Engines

Matthew Hall (Primary Contact) and Ronald Matthews
The University of Texas (UT) at Austin
1 University Station, C2200
Austin, TX 78712-0292

DOE Technology Development Manager: Roland Gravel

NETL Project Manager: Ralph Nine

Subcontractor:
Cummins Engine Co., Columbus, IN

Objectives

- The primary goal of the research is to refine and complete development of an on-board particulate matter (PM) sensor, bringing it to a point where it can be commercialized and marketed. The work will be performed through a joint effort between the UT and the Cummins Engine Company. The research is to be completed in two phases.
- The objective of Phase 1 is to refine the current PM sensor system, adapting it to account for the velocity dependence of the PM sensor signal response, and to further improve and verify the accuracy, durability, and sensitivity of the sensor.
- The objectives of Phase 2 are to determine whether the sensor can be successfully used for diesel homogeneous charge compression ignition (HCCI) engines, including the diesel particulate filter (DPF) and determine if the sensor has the potential to provide useful sensing for individual cylinder control of HCCI engines. The sensor will also be tested upstream and downstream of a DPF to determine whether it would be useful as a diagnostic of the need for DPF regeneration and DPF failure.

Accomplishments

We have just completed the first year of this three-year and three-month project.

- The diesel engine and dynamometer rig for testing the particulate matter sensors was designed and set up in the UT Engine Combustion Laboratory.
- A particulate filter measurements system was designed and assembled to allow the sensors to be calibrated for non-volatile mass emissions of particulate matter. Using this system, the engine's PM emissions were determined as a function of engine operating condition.
- New sensor designs were developed, tested, and calibrated. A new air purged sensor design was created and evaluated. This design has led to much improved sensor durability. The lifetime of the first sensor of this type was in excess of 15 hours of operation, over an order of magnitude improvement over earlier designs. An hour-long test showed not change in sensor sensitivity.
- The response of the sensor to PM emissions created during engine transients has been assessed. The response time of the sensor was found to be less than 20 ms.
- We have established a relationship with an industrial partner to commercialize our PM sensor technology. The company is Emisense, Inc. a division of Ceramatec, Inc. We are currently pursuing joint development of the technology and are in the process of completing a licensing agreement for commercialization.

Future Directions

- Evaluate new sensor designs to further improve sensor durability
- Complete our analysis of the effects of exhaust gas velocity on sensor output
- Begin testing the sensor in a model-year 2007 6.7-liter Cummins diesel engine that we plan to install in the UT Combustion Laboratory

Introduction

In view of the tightening restrictions on engine emissions of particulate matter there has been increased interest in developing a fast, inexpensive sensor for measuring PM concentrations in engine exhaust flows. Numerous applications can be envisioned for diesel, HCCI, and direct-injection gasoline engines. These include: feedback for control of engine operating parameters, failure detection of DPFs, and as an indicator of the need for DPF regeneration.

Approach

The first 15 months of the project comprise Phase 1. A major focus has been the design and construction new sensor types, and testing them using our single-cylinder

diesel engine test rig to gain a better understanding of the sensor characteristics. Of particular interest is the sensitivity of the sensor, its response time, its accuracy, durability, and sensitivity to exhaust flow velocity. A procedure to calibrate the sensors for quantitative measurements has been established. We have built into the exhaust system a by-pass loop that allows us to direct a variable portion of the exhaust flow through to assess the velocity dependence of the sensor response. In addition an exhaust opacity meter system has been designed, constructed, and used as a metric against which to compare the PM sensor response.

Results

Eight tasks comprise the first budget period. In the first quarter of the research work was begun on Tasks 1.1–1.3. These tasks are listed below.

- Task 1.1. Assemble new PM sensors and sensor electronics and configure data acquisition.
- Task 1.2. Design external flow channel, order parts and materials, and order pitot tube system.
- Task 1.3. Complete set-up and instrumentation of existing single-cylinder diesel engine test stand.

In the second quarter of the research Tasks 1.1–1.3 were completed and progress was made on Task 1.4, given below.

- Task 1.4. Build external by-pass flow channel and test different blower/evacuation configurations with the single-cylinder diesel engine.

Also in the second quarter, an opportunity arose to work closely with a possible commercialization partner. This is Task 2.1 of the project (given below).

- Task 2.1. Identify qualified sensor commercialization partner.

This was not scheduled to occur until the second budget period, but we felt this task should be pursued now to take advantage of the opportunity presented to us since we feel it may help speed both the development and commercialization of the sensor system.

In the third and fourth quarters progress was made on tasks 1.5 and 1.6.

- Task 1.5. Evaluate the performance of the pitot tube velocity measurement system in the single-cylinder diesel engine.

We discovered that a pitot tube does not have sufficient response-time to follow the rapid changes in velocity associated with the pulsating flow of a single-cylinder engine. Fortunately we have found other methods of evaluating the effects of flow velocity on sensor response. These are mentioned below as part of the work we have done toward completion of Task 1.6.

- Task 1.6. Measure and document time-response, sensitivity, dynamic range, and durability of the best PM sensor system (from Tasks 1.4 and 1.5) in the exhaust of a single-cylinder engine, evaluating different sensor designs.

Figure 1 is an example of sensor response. It shows simultaneous measurements from two PM sensors located in the exhaust. The sensors show their response to momentary increases in fuel delivery known as tip-in events. The interesting aspect is the correlation between the outputs of the two sensors. Most of our measurements have since been done using two sensors because by observing two sensors it becomes much easier to distinguish between actual changes in PM concentration and noise artifacts in the signal. The strong correlation between the features in the signals is clear.

The analysis of these tip-in events were found important to quantifying sensor response and effects of exhaust velocity. Figure 2 shows the responses of two sensors to a pair of typical tip-in events. While the responses of the two sensors were qualitatively similar, features of the responses raised many interesting questions.

- The sensor response to the transient had a curious double hump; the signal envelope first rose and then decreased before rising again and finally falling to the baseline level.
- Pronounced spikes in the signal were evident which were especially large in the first hump.

The spikes seen in Figure 2 have a period of 70-80 ms, equal to the duration of one engine cycle.

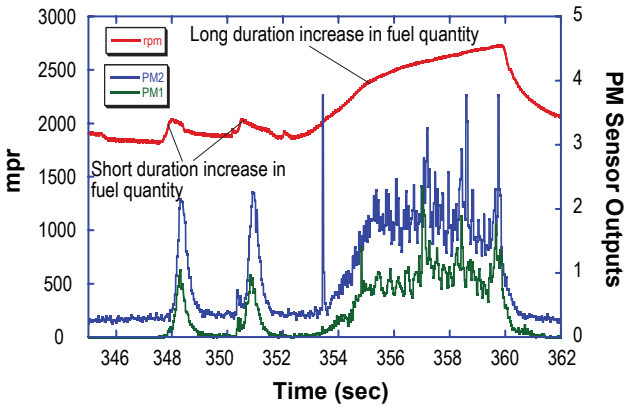

FIGURE 1. Simultaneous Measurements with Two PM Sensors During Two Short and One Long Engine Transient, Along with Engine Speed

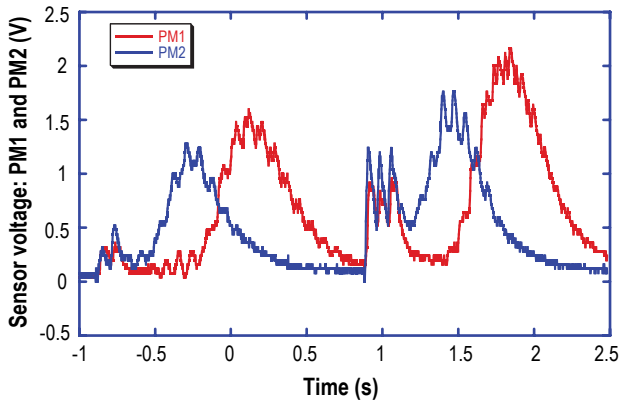

FIGURE 2. Response of Sensors PM1 and PM2 to a Double Tip-In Event

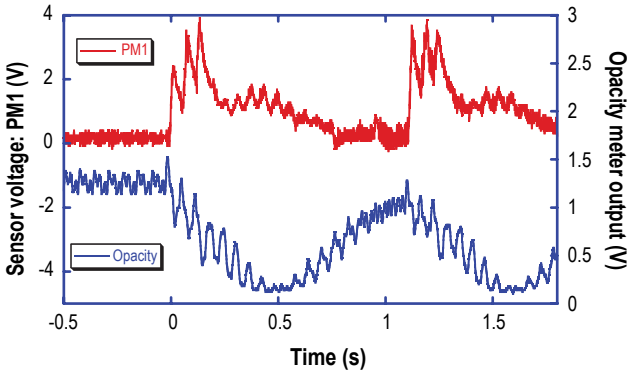

FIGURE 3. Response of Sensor PM1 and Opacity Sensor to a Pair of Tip-In Events

An especially curious aspect is that the first hump appeared to occur simultaneously in the two signals, but there is a time lag between the second humps of the two sensors.

We measured the time-resolved exhaust gas opacity while simultaneously measuring the PM sensor signal. The two signals were recorded on the oscilloscope for the same type tip-in events as above. An example of one set of results for a pair of tip-in events is shown in Figure 3.

These results were especially elucidating. The upper trace is the PM sensor output while the lower trace is the opacity signal. The opacity signal decreases as the light intensity reaching the detector drops due to attenuation by soot particles in the optical path.

- The most important observation is that the opacity signal begins to fall at the same moment the PM sensor signal begins its rise at the beginning of the tip-in. This demonstrates that the first hump in the PM sensor signal is indeed a reaction to the presence of particulate matter and is not a spurious signal.
- The second important observation is that the high PM concentration flow reached the two measurement locations very fast, on the order of 10 ms. At an engine speed of 1,500 rpm the duration of the exhaust stroke from bottom dead center to top dead center is 20 ms.

The data suggest that the first three engine or four cycles during a tip-in event receive large amounts of fuel and have very strong blow-down events. These blow-down events are strong enough to eject a portion of the cylinder contents more than 2 meters downstream of the exhaust port in a time shorter than the duration of the exhaust stroke. The PM in the second hump move through the exhaust at a velocity close to the time-averaged exhaust flow velocity.

As a test of sensor durability and signal stability, the engine was run for about one hour. No change in sensitivity was observed.

Conclusions

Development of the UT electronic particulate matter sensor is proceeding on schedule. New, more durable sensors having a longer life by at least an order of magnitude have been designed, built, calibrated, and tested. The sensor has a response time of less then 20 ms. Long-duration testing has demonstrated a stable baseline output for the sensor is possible. The use of a pitot tube in a by-pass line in the exhaust to measure velocity was found not to be practical due to the strongly pulsating exhaust flow. It was found that the effect of velocity on sensor sensitivity can be studied from engine transient. The velocity sensitivity can also be studied by comparing sensors located in sections of the exhaust pipe having different internal diameters. Over a range of a few m/s the velocity sensitivity is very small, but can be considerable for velocities on the order of 100 m/s. This velocity sensitivity, while complicating calibration, may have advantages for such applications as individual cylinder control of engines during HCCI operation.

In summary, the UT PM sensor is fast, portable, inexpensive to build, and shows promise for use in closed-loop control of particulate emissions from diesel and HCCI engines. Future work will refine its design and test its operation in a modern, heavy-duty diesel engine of an order of magnitude larger displacement.

FY 2007 Publications/Presentations

1. Diller, T.T., Hall, M.J., and Matthew, R.D. "Further Development of an Electronic Particulate Matter Sensor and Its Application to Diesel Engine Transients," Society of Automotive Engineers Paper 08PFL-401, submitted for the 2008 SAE Congress and Exposition, April, 2008.

2. Hall, M.J., poster presentation, U.S. DOE Merit Review Meeting, Washington, D.C., June 19, 2007.

Special Recognitions & Awards/Patents Issued

Patent Pending: 2443 - A Sensor to Measure Time-Resolved Particulate (soot) Exhaust Emissions from Internal Combustion Engines has been patented with coverage in the US in the form of a PCT that was nationalized in the US.

Provisional: 7/19/2002

PCT conversion: 7/18/2003

Nationalization in the US: 1/19/2005

V. NEW PROJECTS

V.1 Light-Duty Efficient Clean Combustion

Cummins Inc. – Columbus, IN

This project will focus on developing advanced combustion system technology for a light-duty diesel engine application to demonstrate in-cylinder combustion technologies for light-duty diesel engines that realize 10.5 percent efficiency improvements over today's state-of the art diesel engine while meeting U.S. Environmental Protection Agency light-duty emissions standards (Tier 2, Bin 5) in a robust and cost effective manner. The work will integrate the areas of low temperature combustion, air handling, advanced fuel systems, and closed-loop controls to support high efficiency, low emission combustion concepts. The planned approach centers around a multi-step development process including analysis led design, concept integration, advanced system development and demonstration of the combined elements of the combustion system on the Cummins light duty diesel engine platform. The work will target maintaining power density comparable to that of current conventional engines for the applicable vehicle class and will evaluate fuel sensing technology and the potential benefits of combustion system adaptation to fuel type.

V.2 Advanced Boost System Development for Diesel HCCI Application

Ford Motor Company – Dearborn, MI

This project will focus on complete and optimal system solutions to address boost system challenges in diesel combustion/emission control system development, and to enable commercialization of advanced diesel combustion technologies, such as homogeneous charge compression ignition (HCCI) and low-temperature combustion. This work will explore and analytically quantify benefits of various advanced boost technologies in turbine and compressor design for better efficiency, wider operational range and yet be compatible with diesel aftertreatment requirement, provide and validate turbine and compressor maps for diesel system integration and evaluation, demonstrate diesel performance and emission benefits on engine dynamometer, and explore cost and commercial feasibility of the advanced diesel boost system.

VI. Acronyms and Abbreviations

τ_{id}	Ignition delay time
η	Effectiveness
°C	Degrees Celsius
ΔP	Pressure drop
Φ	Fuel/air equivalence ratio
°F	Degrees Fahrenheit
0-D	Zero-dimensional
1-D	One-dimensional
3-D	Three-dimensional
4Q	Fourth quarter
A	Availability
a.u.	Arbitrary units
A/cm^2	Amps per square centimeter
A75	Near peak torque speed & 75% engine load point of ESC Test Procedure
AC	Air compressor
AC	Alternating current
A/C	After cooler
ACE	Advanced Combustion in Engines
ACES	Advanced Collaborative Emissions Study
AEC	Advanced Emission Controls Working Group
AEI	After end of injection
AETEG	Automobile exhaust thermoelectric generator
Ag	Silver
AHRR	Apparent heat release rate
AIChE	American Institute of Chemical Engineers
A/F	Air to fuel ratio
AFR	Air/fuel ratio
Al	Aluminum
Al_2O_3	Aluminum oxide
AM	Air motor
AMDC	Advanced mode diesel combustion
ANN	Artificial neural network
ANL	Argonne National Laboratory
ANSI	American National Standards Institute
APA	Air-power-assist
APU	Auxiliary power unit
ASI	Time after the start of injection
ASME	American Society of Mechanical Engineers
AT	Aftertreatment
atdc	After top dead center
ATDC	After top dead center
atm	Atmosphere
Au	Gold
B	Boron
B100	100% biodiesel
B100	Mid-speed & 100% engine load point of ESC Test Procedure
B25	Mid-speed & 25% engine load point of ESC Test Procedure
B75	Mid-speed & 75% engine load point of ESC Test Procedure
Ba	Barium
$BaAl_2O_4$	Barium aluminate
$Ba(NO_3)_2$	Barium nitrate
BaO	Barium oxide
BC	Black carbon
BDC	Bottom dead center
BES	Basic Energy Sciences
BET	Named after Brunauer, Emmett and Teller, this method for determining the surface area of a solid involves monitoring the adsorption of nitrogen gas onto the solid at low temperature and, from the isotherm generated, deriving the volume of gas required to form one monolayer adsorbed on the surface. This volume, which corresponds to a known number of moles of gas, is converted into a surface area though knowledge of area occupied by each molecule of adsorbate.
bhp-hr	Brake horsepower hour
Bi_2Te_3	Bismuth Telluride
BMEP	Brake mean effective pressure
bmep	Brake mean effective pressure
BOI	Beginning of injection
BP	formerly British Petroleum
BSDPM	Brake specific dry particulate matter
Bsfc	Brake specific fuel consumption
BSFC	Brake specific fuel consumption
bsNOx	Brake specific NOx emissions
btdc	Before top dead center
BTE	Brake thermal efficiency
C/N	Carbon to nitrogen ratio
C:N	Ratio of carbon to nitrogen
C_1	Carbon content in the exhaust or reformer in terms of carbon atoms
C_2H_6	Ethane

C_3H_6	Propylene
CA	Crank angle
CA50	Crank angle at which 50% of the combustion heat release has occurred
CAC	Charge air cooler
CAD	Computer-aided design
CAD	Crank angle degrees
CAFE	Corporate average fuel economy
CAI	Controlled autoignition
CAP	Critical adjustable parameter
CARB	California Air Resources Board
CBM	Carbon balance method
cc	Cubic centimeter
CDI	Compression direct injection
CDPF	Catalytic diesel particulate filter
CeO_2	Cerium oxide
CFD	Computational fluid dynamics
CFR	Waukesha Cooperative Fuel Research Engine
CFR	Coordinating Fuel Research
CFR	Critical functional response
Cg,i	Gas species concentration
CGIC	Clean gas induction cooler
CHEMKIN	Sandia chemical kinetics code
CI	Compression ignition
CIDI	Compression ignition direct injection
CIMAC	International Council on Combustion Engines
CINL	Cycle integrated natural luminosity
CLD	Chemi-luminescence detector
CLEAN	Trademark for Detroit Diesel low-temperature combustion strategy
CLEERS	Cross-Cut Lean Exhaust Emissions Reduction Simulations
CLOSE	Collaborative Lubricating Oil Study on Emissions
cm	Centimeter
cm^3	Cubic centimeters
CNC	Computer numerically controlled
CNG	Compressed natural gas
CO	Carbon monoxide
CO_2	Carbon dioxide
COV	Coefficient of variation
CO_x	Oxides of carbon
CP	Chevron Phillips
CPER	Counterflow preheating with near-equilibrium reaction
cpi	Cells per inch
CPF	Catalyzed particulate filter
CPU	Central processing unit
Cr	Chromium
CR	Compression ratio
CRADA	Cooperative Research and Development Agreement
CRC	Coordinating Research Council
CR-DPF	Continuously regenerating diesel particle filter
CRF	Combustion Research Facility
CRS	Common Rail System
Cs,i	Solid species concentration
Cu	Copper
CVT	Continuously variable transmission
CWLR	Constant weight loss rate
d	Nozzle diameter
DAQ	Data acquisition
DC	Direct current
DCSF	Diesel combustion simulation facility
DDC	Detroit Diesel Corporation
DECSE	Diesel Emission Control Sulfur Effects
DEER	Diesel Engine Emissions Reduction
deg	Degrees
DELTA	Diesel Engine for Light Truck Application
DEM	Delayed extended main
$DeNO_x$	Oxides of nitrogen reduction
DGE	Diethylene glycol diethyl ether (CAS 112-36-7)
DI	Direct injection, direct injected
DIB	Di-isobutylene
DIL	Dual in-line
dm	Decimeter
DME	Dimethyl ether
DNS	Direct numerical simulation
DNPH	2,4-dinitorophenylhydorazine
DOC	Diesel oxidation catalyst
DoE	Design of experiment
DOE	U.S. Department of Energy
DOHC	Double overhead camshaft
DOM	Discrete ordinates method
DP	Pressure differiential
DPF	Diesel particulate filter
DPNR	Diesel Particulate NOx Reduction
DPV	Differential pulse voltammetry
DRIFTS	Diffuse reflectance infrared Fourier-transform spectroscopy

DTTEG	Diesel truck thermoelectric generator
e^-	Electron
E10	10% ethanol, 90% gasoline fuel blend
E85	85% ethanol, 15% gasoline fuel blend
ECM	Engine control module
ECU	Engine control unit
EERE	Energy Efficiency and Renewable Energy
EDS	Energy dispersive spectroscopy
EDX	Energy dispersive X-ray
EGR	Exhaust gas recirculation
EINOx	Emissions index of NOx
ELPI	Electrical low pressure impactor
ELS	Elastic light scattering
ELSLII	Elastic laser scattering with laser-induced incandescence
EMD	Electro-Motive Division of General Motors Corporation
EO	Engine-out
EOI	End of injection
EPA	U.S. Environmental Protection Agency
EPVA	Electro-pneumatic valve actuator
ER	Expansion ratio
ERC	Engine Research Center
ESC	European Steady State Cycle
η	Effectiveness
ETC	Electric turbocompound
EVC	Exhaust valve closing
EVO	Exhaust valve opening
EWHR	Exhaust waste heat recovery
f	Fuel/Air Equivalence Ratio
FBMAFS	Forward-backward mass air flow sensor
FCVT	FreedomCAR and Vehicle Technologies
FEA	Finite-element analysis
Fe	Iron
f_{FO}	Fuel oxygen equivalence ratio
FHWA	Federal Highway Administration
FLC	Federal Laboratory Consortium
FIE	Fuel Injection Equipment
FLRS	Full load rated speed engine condition
FMEA	Failure mode and effects analysis
fmep	Friction mean effective pressure
FSN	Filter smoke number
FSNR	Fuel specific NOx reduction
FTIR	Fourier transform infrared
ft-lb	Foot-pound
FTP	Federal Test Procedure
FTP-75	Federal Test Procedure for light-duty vehicles
FVVA	Full variable valve actuation
FWHM	The full width at half the maximum activity as a function of temperature
FY	Fiscal year
G	Gram
g	Gram
g/hphr	Grams per horsepower-hour
g/bhp-hr	Grams per brake horsepower-hour
gIMEP	Gross indicated mean effective pressure
g/kWh	Grams/kilowatt-hour
g/mi	Grams per mile
GA	Genetic algorithm
GATE	Graduate Automotive Technology Education
GC	Gas Chromatography
GC-MS	Gas chromatography – mass spectrometry
GDC	Gadolinium-doped cerium oxide
GDI	Gasoline direct injection
GE	General Electric
Ge	Germanium
GHSV	Gas hourly space velocity
GM	General Motors
GRC	GE Global Research Center
GT-Power	Gamma Technologies engine modeling software
GUI	Graphical user interface
GVWR	Gross vehicle weight rating
h	Convective heat transfer coefficient
H	Enthalpy
H_2	Diatomic (molecular) hydrogen
H_2CO	Formaldehyde
H_2O	Water
H_2O_2	Hydrogen peroxide
H2-ICE	Hydrogen-fueled internal combustion engine
H2-SpaciMS	Hydrogen-calibrated spatially resolved capillary inlet mass spectrometry
HC	Hydrocarbons
HCCI	Homogeneous charge compression ignition
HCN	Hydro-cyanic acid
HC-SCR	Hydrocarbon selective catalytic reduction
HCT	Hydrodynamics, Chemistry, Thermodynamics code

HD	Heavy-duty
HDCC	Heavy-duty corporate composite
He	Helium
HECC	High-efficiency clean combustion
HEI	Health Effects Institute
HELD	High-energy laser diagnostics
HEV	Hybrid electric vehicle
HFPE	Hydrogen free piston engine
HHV	Higher heating value
HIL	Hardware-in-loop
HMO	Hydrous metal oxide
hp	Horsepower
HP	High pressure
HPCR	High-pressure common rail
HPL	High pressure loop
HR	Heat release
hr	Hour
HRR	Heat release rate
HSDI	High-speed direct-injection
HTCD	Heavy truck clean diesel
HTML	High Temperature Materials Laboratory
HVA	Hydraulic valve actuator
HWFET	Highway Fuel Economy Test
HXN	Heat excahnger
Hz	Hertz
IC	Internal combustion
I/C	Intercooler
ICCD	Intensified charged-coupled device
ICDEM	Individual cylinder delayed extended main
ICE	Internal combustion engine
ID	Injection delay
ID	Injection duration
ID	Internal diameter
IDD	Interstage duct difuser
IEA	International Energy Agency
IEEE	Institute of Electrical and Electronics Engineering
IMEP	Indicated mean effective pressure
I/O	Input-output
IR	Infrared
IS	Integrated system
ISFC	Indicated specific fuel consumption
ISU	Iowa State University
ISX	Cummins Inc. 15-liter displacement, inline, 6-cylinder heavy-duty diesel engine
ITEC	International Truck and Engine Corporation
ITH	Intake throttle valve
IVA	Intake valve actuation
IVC	Intake valve closing
IVO	Intake valve opening
J	Joule
JPL	Jet Propulsion Laboratory
JW	Jacket water
JWHR	Jacket water heat rejection
k	thousand
k	Mass transfer coefficient
K	Kelvin
K	Potassium
kg	Kilogram
kHz	Kilohertz
KIVA	Combustion analysis software developed by Los Alamos National Laboratory
KIVA-CTC	KIVA characteristic time combustion
KIVA-RIF	KIVA representative interactive flamelet
kJ	Kilojoules
kJ/L	Kilojoules per liter
kJ/m^3	Kilojoules per cubic meter
KL	Soot optical thickness
kPa	Kilopascal
KS	Converging hydroground nozzle
kW	Kilowatt
L	Liter
L/D	Length-to-diameter ratio
La	Lanthanum
Lambda	Ratio of the actual air/fuel ratio to the stiochiometric air/fuel ratio
LANL	Los Alamos National Laboratory
LAST	Lead, antimony, silver, and tellurium, an n-type TE material
LAST/T	LAST/Tin, a p-type TE material
LB	Lattice-Boltzmann
lb ft	Pound foot
lb/min	Pounds per minute
lbs	Pounds
lbs/sec	Pounds per second
LD	Light-duty
LDA	Laser doppler anemometry
LDT	Light-duty truck
LEM	Linear eddy model

LEP	Low Emissions Technologies Research and Development Partnership (often abbreviated to Low Emissions Partnership); a consortium between Ford, General Motors and DaimlerChrysler
LES	Large eddy simulation
LEVII	Low Emission Vehicle II
LHV	Lower heating value
LIBS	Laser-induced breakdown spectroscopy
LIDAR	Light detection and ranging
LIDELS	Laser-induced desorption with elastic light scattering
LIF	Laser-induced fluorescence
LII	Laser-induced incandescence of soot
LLNL	Lawrence Livermore National Laboratory
LNT	Lean NOx trap
LO	Light-off temperature – the minimum temperature at which half the maximum catalyst activity is identified
LP	Low pressure
LPEGR	Low pressure exhaust gas recirculation
LPL	Low pressure loop
LQHCCI	Lean quasi-homogeneous charge compression ignition
LRRI	Lovelace Respiratory Research Institute
LSA	Low solidity airfoil
LSC	Lanthanum strontium chromite
LTC	Low-temperature combustion
LTC-D	Low-temperature combustion-diesel
M/G	Motor/generator
m^2	Square meters
m^2/gm	Square meters per gram
m^3	Square meters
mA	Milliamps
MAS	Magic-angle spinning
MB	Mercedes-Benz
mbar	Millibar
MBE	Molecular beam epitaxy
MBT	Minimum for best torque
MCE	Multi-cylinder engine
MCH	Methylcyclohexane
MCRS	Modular Common Rail System
MD	Medium-duty
MDO	Mechanism design option
MECA	Manufacturers of Emission Controls Association
MeOH	Methanol
MET	More Electric Truck
mg/cm^2	Milligrams per square centimeter
mg/min	Milligram per mile
mg/mm^2	Micrograms per square millimeter
mg/scf	Milligrams per standard cubic foot
mi	Mile
min	Minute
MIT	Massachusetts Institute of Technology
MK	Modulated Kinetics
ML	Monolayer
MLQWF	Multi-layer quantum well films
MLR	Multivariable local regression
μm	Micrometer
mm	Millimeter
mmols	Micro-moles
Mn	Manganese
Mo	Molybdenum
mol	Mole
mol/s	Moles per second
MOU	Memorandum of Understanding
MPa	Megapascals
mph	Miles per hour
ms	Millisecond
MSATs	Mobile source air toxics
MSU	Michigan State University
MTU	Michigan Technological University
MVCO	Micro-variable circular oriface
MY	Model year
N_2	Diatomic nitrogen
N_2O	Nitrous oxide
N_2O_3	Nitrogen trioxide
Na	Sodium
NACS	North American Catalysis Society
NAHRR	Normalized apparient heat release rate
NAM	North American Meeting
NCO	Isocyanate
NEA	Nitrogen-enriched air
NEDC	New European Drive Cycle
NETL	National Energy Technology Laboratory
NH_3	Ammonia
NLCAT	National Laboratory Catalysis Conference
nm	Nanometer
Nm	Newton meter
NMEP	Net mean effective pressure
NMHC	Non-methane hydrocarbon

NMOG	Non-methane organic gases
NMR	Nuclear magnetic resonance
NO	Nitric oxide
NO_2	Nitrogen dioxide
NOx	Oxides of nitrogen (NO and NO_2)
NRE	NOx reduction efficiency
NRT	NOx reduction technology
ns	Nanosecond
NSLS	National Synchrotron Light Source
NSR	Normalized stoichiometric ratio
NSR	NOx storage and reduction
NTE	Negative temperature effect
NTE	Not-to-exceed
NTP	Non-thermal plasma
NTP	National Toxicology Program
NTRC	National Transportation Research Center
NVO	Negative valve overlap
NZ-50	Near-Zero Emissions at 50% Thermal Efficiency
O_2	Diatomic (molecular) oxygen
O_3	Ozone
OEM	Original Equipment Manufacturer
OFCVT	Office of FreedomCAR and Vehicle Technologies
OH	Hydroxyl
OH*	Hydroxyl radical that emits ultraviolet photons
OH PLIF	Planar laser-induced fluorescence of OH
OMS	Octahedral molecular sieve
ORC	Organic Rankine Cycle
ORNL	Oak Ridge National Laboratory
OS	Office of Science
OSC	Oxygen storage capacity
OTR	Over-the-road
P	Pressure
P-V	Pressure-volume
P2P	Ratio of the peak activity of a new material to the peak activity of a reference material
PAC	Plasma-assisted catalyst
PC	Personal computer
PCI	Partially premixed compression ignition
PCM	Power control module, powertrain control module
PCP	Peak cylinder pressure
PCCI	Premixed charge compression ignition
PCS	Power control subsystem
PD	Photodiode
PDF	Probability density function
PE	Power electronics
PEMS	Portable emissions measurement system
PFI	Port fuel injection, port fuel injected
PFI-DI	Port fuel injection/direct injection
PhosphorT	Phosphor thermography instrument
PHX	Primary heat exchanger
PID	Proportional, integral, and derivative
PIV	Particle image velocimetry
PLII	Planar laser-induced incandescence
PLIF	Planar laser induced fluorescence
PLRS	Planar laser Rayleigh scattering
PM	Particulate matter
PM	Permanent magnet
PMT	Photomultiplier tube
PNGV	Partnership for a New Generation of Vehicles
PNNL	Pacific Northwest National Laboratory
Post80	Late cycle injection after the main fuel pulse at 80° after top dead center
POx	Partial oxidation
ppb	Parts per billion
PPCI	Partially premixed compression ignition
ppi	Pores per square inch
ppm	Parts per million
PRF	Primary Reference Fuels (iso-octane and n-heptane),
PRF80	PRF mixture with an octane number of 80 (i.e., 80% iso-octane and 20% n-heptane)
PRR	Pressure rise rate
psi	Pounds per square inch
psig	Pounds per square inch gauge
Pt	Platinum
PWM	Pulse width modulated
Q	Heat
Q1, Q2, Q3, Q4	First, second, third and fourth quarters
QSB5.9	Quantum System B Series 5.9Liter (Midrange Industrial Product)
QSC8.3/QSL9	Quantum System C Series 8.3 Liter, Quantum System L Series 9 Liter
QSK19	Quantum System K Series 19 Liter
QSX15	Quantum System X Series 15 Liter
OTR	Over-the-road
QW	Quantum well
R&D	Research and development
RANS	Reynolds Averaged Navier Stokes
RASP	Rotating arc spark plug

RCF	Rapid compression facility
RDG-PFA	Rayleigh-Debye-Gans polydisperse fractal aggregate
RGF	Residual gas fraction
RGR	Residual gas recirculation
Rh	Rhodium
RIF	Representative interactive flamelet
RMS	Root mean square
ROHR	Rate of heat release
ROI	Rate of injection
rpm	Revolutions per minute
RSM	Response surface method
RT	Room temperature
RUS	Resonant ultrasound spectrography
s	Conductivity $(Wcm)^{-1}$
S	Entropy
S	Seebeck coefficient
S	Sulfur
S/N	Signal-to-noise ratio
SAE	Society of Automotive Engineers
SBCE	Set-based concurrent engineering
SCAQMD	South Coast Air Quality Management District
sccm	Standard cubic centimeters
SCE	Single-cylinder engine
SCF/min	Standard cubic feet per minute
SCI	Stoichiometric compression ignition
SCORE	Sandia Compression-ignition Optical Research Engine
SCORE	Single cylinder optical research engine
SCOT	Staged combustion with oxygen transfer
SCR	Selective catalytic reduction
SCTE	Single-cylinder test engine
sec	Second
SEM	Scanning electron microscopy
SGS	Subgrid-scale
Si	Silicon
SI	Spark ignition
SiC	Silicon carbide
SICM	System Integration Configuration Matrix
SIDI	Spark ignition direct injection
SINL	Spatially integrated natural luminosity
SF	Scaling factor
SFC	Specific fuel consumption
SFTP	Supplemental Federal Test Procedure
SLPM	Standard liters per minute
SMPS	Scanning mobility particle scanner
SMR	Steam methane reformation
SMSI	Strong metal support interaction
SNL	Sandia National Laboratories
SNR	Signal-to-noise ratio
SO_2	Sulfur dioxide
SOC	State of charge
SOC	Start of combustion
SOF	Soluble organic fraction
SOI	Start of injection
SO_x	Oxides of sulfur
S_p	Mean piston speed
SpaciMS	Spatially resolved capillary inlet mass spectrometer
SPS	Spark plasma sintering
Sr	Strontium
SR	Steam reforming
sS^2T	Power factor (mV/ºC)
SU	Stanford University
SUV	Sports utility vehicle
SV	Space velocity
SVOC	Semivoltaic organic compound
SwRI	Southwest Research Institute
T	Temperature
T70	A fuel blend containing the oxygenate tetraethoxy-propane
TACOM	Tank Automotive Armaments Command
TAGS	Tellurium, antimony, germanium and silver
TAP	Temporal Analysis of Products
TC	Turbocompund
TCI	Turbulence/chemistry interactions
TCR	Thermo-chemical recuperation
TDC	Top dead center
TDI	Turbocharged direct injection
TDL	Tunable diode laser
TE	Thermoelectric
TEG	Thermoelectric generator
TEM	Transmission electron spectroscopy
TEOM	Tapered element oscillating microbalance
TGA	Thermal gravimetric analysis
TGM	Thermoelectric generator module
THC	Total hydrocarbon
Ti:Si	Ratio of titanium to silicon
TP	Tailpipe
TPD	Temperature-programmed desorption
TPGME	Tri-propylene glycol monomethyl ether
TPM	Total particulate matter

TPR	Temperature-programmed reduction
TPRX	Temperature-programmed reaction
TPS	Throttle position sensor
TP-XRD	Temperature programmed X-ray diffraction
TR-XRD	Time resolved X-ray diffraction
TRLC	Top-ring-land crevice
TWC	Three-way catalyst
u	Gas velocity
U	Internal energy
UCB	University of California Berkeley
UEGO	Universal exhaust gas oxygen
UHC	Unburned hydrocarbons
UIS	Unit injector system
ULSD	Ultra-low sulfur diesel
UM	University of Michigan
UNIBUS	Uniform bulky combustion system
UPS	Unit pump system
USCAR	U.S. Cooperative Automotive Research
US06	High-speed portion of the Supplemental Federal Test Procedure (SFTP)
UTM	Universal Transverse Mercator (mapping projection methodology)
UTRC	United Technologies Research Center
UV	Ultraviolet
V	Volt
VAC	Volts, alternating current
VAT	Variable admission turbine
VCO	Valve-covering orifice
VCR	Variable compression ratio
VCT	Variable cam timing
VDC	Volts, direct current
VGC	Variable geometry compressor
VGS	Variable geometry spray
VMS	Vehicle mission simulation
VNT	Variable nozzle turbine
VOCs	Volatile organic compounds
VPTNA	Volvo Powertrain North America
VTG	Variable turbine geometry
VVA	Variable valve actuation
VVT	Variable valve timing
W	Work
WAVE	Ricardo engine and one-dimensional gas dynamics simulation software
W	Watt
W/cmK	Watts per centimeter-Kelvin
WGS	Water-gas-shift
WGSR	Water-gas-shift reaction
WHR	Waste heat recovery
WOT	Wide open throttle
WREL	Watt Road Environmental Laboratory
wt%	Weight percent
XAFS	X-ray aborption fine structure
XANES	X-ray absorption near-edge spectroscopy
XPS	X-ray photoelectron spectroscopy
XRD	X-ray diffraction
Y	Yttrium
yr	Year
Zn	Zinc
YSZ	Ytrria-stabilized zirconia
ZT	Dimensionless thermoelectric figure of merit; equal to: (electrical conductivity)(Seebeck coefficient)^2(temperature)/(thermal conductivity)

VII. Index of Primary Contacts

A Strong Energy Portfolio for a Strong America

Energy efficiency and clean, renewable energy will mean a stronger economy, a cleaner environment, and greater energy independence for America. Working with a wide array of state, community, industry, and university partners, the U.S. Department of Energy's Office of Energy Efficiency and Renewable Energy invests in a diverse portfolio of energy technologies.

For more information contact:
EERE Information Center
1-877-EERE-INF (1-877-337-3463)
www.eere.energy.gov